Review

Adventures with Heterocycles[1)]

Rolf HUISGEN

Department of Chemistry, Ludwig-Maximilians University of München, Butenandtstr. 13, D-31377 München, Germany.

Received February 9, 2000

Elucidation of mechanisms and discovery of novel reactions are interconnected, as four research chapters from the Munich laboratory demonstrate. 1) In a new opening of the furan ring, 2-methoxyfuran and tetra-acceptor-substituted ethylenes furnish methyl acrylates, which are *cis*-3-substituted by a cyclopropyl ring that bears the four acceptor groups. Experiments with *trans*- and *cis*-1,2-bis(trifluoromethyl)-1,2-dicyanoethylenes (BTE) clarify the role of zwitterionic intermediates. 2) The concerted nature of 1,3-dipolar cycloaddition is well established. On reacting thiocarbonyl *S*-ylides as electron-rich 1,3-dipoles with tetra-acceptor-substituted ethylenes, the switching to a two-step pathway *via* zwitterion was diagnosed from a loss of stereospecificity and the formation of strained 7-membered cyclic ketene imines. 3) Stable as crystals, these ketene imines rearrange to 5-membered thiolanes in solution. In contrast to open-chain ketene imines, the cyclic representatives add vinyl ether at the C=N bond and show a novel pathway of dimerization. 4) Cycloadducts of isoquinolinium *N*-phenylimide with ethylenic dipolarophiles undergo an acid-catalyzed [3.3] sigmatropic hydrazo rearrangement. An exception is the conversion of the dimethyl maleate adduct ($C_{21}H_{20}N_2O_4$) by acid into a yellow compound $C_{24}H_{22}N_2O_6$; the structure and the astounding mechanism were clarified.

Key words rearrangement; cycloaddition; furan ring-opening; cyclic ketene imine; zwitterionic intermediate; 1,2-dihydroisoquinoline derivative

1. Introduction

Two hundred years ago, the chemical science was an undivided field; around 1900 a division into inorganic, organic, and physical chemistry became necessary. The increase of factual material enforced a progressive segmentation into subdisciplines. A map shows countries and regions neatly separated; similarly, the uninformed observer may regard chemistry as a side-by-side of numerous disciplines and specialties. The comparison is fallacious, however, because broad overlap is thwarting clear divisions.

Heterocyclic chemistry offers an example for the lack of distinct demarcations; in fact, it pervades the plurality of the other chemical disciplines. Heterocycles are inextricably woven into the life processes. Nucleic acids, carbohydrates, macrocyclic dyes, coenzymes, and alkaloids may be quoted. The vital interest of the pharmaceutical and agrochemical industries in heterocycles is often connected with their natural occurrence. Synthetic chemistry provides a cornucopia of heterocyclic systems. Carbocycles tolerate many other elements in variable numbers as ring members. The world of metal chelates strengthens the impression of boundlessness and heterogeneity of heterocyclic chemistry.

This heterogeneity is reflected in the following assortment of short stories. They concern problems with which my young associates and I recently dealt in the Munich laboratory. If there is a common denominator, it may be the fascinating influence of the heteroatom on chemical reactivity.

2. Ring Opening of Donor-Substituted Furans with Highly Electrophilic Ethylenes

It deserves more praise to synthesize heterocycles than to destroy them. This chapter describes the demolition of the furan ring.

When 2-methoxyfuran was treated with tetracyanoethylene (TCNE), the violet charge transfer color disappeared in a few seconds, and a crystalline 1 : 1 product was isolated. 2-*p*-Tolyloxyfuran reacted slower, but furnished a higher product yield.[2)] Careful NMR analyses indicated that we were not dealing with Diels–Alder adducts, but rather with acrylic esters, which are substituted in *cis*-3-position by a tetracyanocyclopropyl group (Chart 1).

How does the opening of the furan ring come about? Electrophilic attack by TCNE at the nucleophilic 5-position gives rise to a zwitterion. The cationic portion is a carbodioxonium ion, whereas much of the carbanionic charge is transferred to the cyano groups. The key step of the novel conversion is an intramolecular nucleophilic substitution with the carboxylic ester as leaving group. It is one and the same reaction step, which is responsible for the closure of the three-membered ring and the cleavage of the furan ring.

Nothing is without precedent. In 1986, Ibata and associates reacted 5-alkoxyoxazoles with TCNE.[3)] The initial electrophilic attack gave likewise a zwitterion and the ring opening provided the methyl ester group (Chart 1, lower part). The concluding step was different: it is a 1,5-cyclization to give a dihydropyrrole derivative.

Deeper insight was expected from applying a *trans,cis* pair of tetra-acceptor-substituted ethylenes as a stereochemical

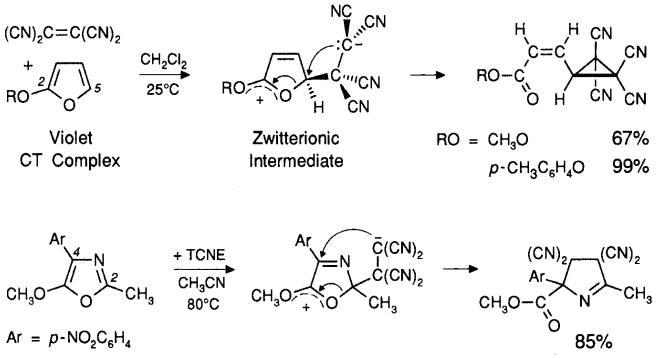

Chart 1. Donor-Substituted Furans and Tetracyanoethylene

© 2000 Pharmaceutical Society of Japan

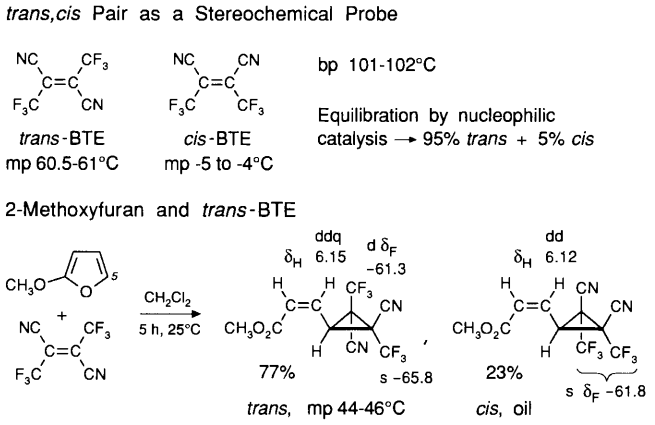

Chart 2. 1,2-Bis(trifluoromethyl)ethylene-1,2-dicarbonitrile

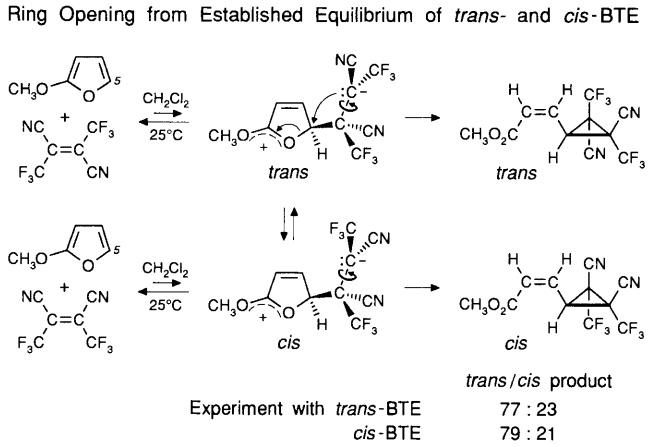

Chart 3. Reaction of 2-Methoxyfuran with BTE

probe. In the last decade, we repeatedly made use of the 1,2-bis(trifluoromethyl)-1,2-dicyanoethylenes (BTE) (Chart 2), which were first described by Proskow, Simmons, and Cairns.[4] *Trans*- and *cis*-BTE, as the long name is abbreviated, boil at *ca.* 100 °C and can be stored in the refrigerator. The disadvantage of an inconvenient access is more than made up for by the superb product analysis with fluorine NMR. Nucleophilic catalysts equilibrate the geometrical isomers to a 95 : 5 mixture.

Trans-BTE is less reactive than TCNE. In contact with 2-methoxyfuran, the orange charge-transfer color faded in 5 h. Fluorine NMR analysis revealed the quantitative formation of diastereoisomeric methyl acrylates, which contain *trans*- or *cis*-located CF_3 groups in the cyclopropane ring.[5] The two 1 : 1 products were separated, and the combination of proton and fluorine NMR parameters allowed an elegant structural assignment (Chart 2). The *trans* form is chiral, whereas the *cis* isomer has a plane of symmetry. The reaction was studied by my associates Urrutia-Desmaison and Mloston.

When the reaction was monitored by fluorine NMR, it turned out that equilibration of *trans*- and *cis*-BTE was faster than product formation. The donor furan is an efficient catalyst for this equilibration. A simple explanation consists in the formation of the zwitterion, rotation about the marked bond and reversal to the ethylenic reactants (Chart 3).

In the reaction with 2-methoxyfuran, *trans*- and *cis*-BTE afforded the same *trans*/*cis* ratio of the two 1 : 1 products, within the analytical limits. That means, the intramolecular substitution takes place from an established rotational equilibrium of the two zwitterionic conformations, *trans* and *cis*. Thus, the intermediate zwitterion rests in a trough of the energy profile and can do three things: rotation, dissociation, and furan ring cleavage. There is even a fourth reaction: Mloston observed a rapid equilibration of the zwitterion with (2+2) cycloadducts (four with *trans*-CF_3, one with *cis*-CF_3 groups)[6] that will not be discussed here.

Time-dependent concentration measurements by ^{19}F-NMR provided the rate constants for the ring opening of donor furans with BTE. 2-Methoxyfuran is more nucleophilic than 2-*p*-tolyloxyfuran, as reflected by an 87 times higher rate constant k_2 (Chart 4).

The zwitterion has a higher polarity than the reactants; due to enhanced solvation, its equilibrium concentration should be greater in polar solvents than in nonpolar ones. For 2-*p*-tolyloxyfuran, k_2 is in nitromethane 1200 times faster than in benzene. That leaves no doubt that k_i/k_{-i}, *i.e.*, the equilibrium constant of the zwitterion, increases with solvent polarity.[5]

When the donor furan reacted with BTE in the presence of 0.5 M pyridine, the furan aromaticity was restored. The proton in position 5 of the zwitterion is picked up by the base and delivered at the carbanionic center. The ring cleavage of

Born 1920 in Gerolstein, Eifel (Germany), Rolf Huisgen studied chemistry at Bonn and München. In 1943 he obtained the Ph. D. at the University of München; his thesis, directed by Heinrich Wieland, dealt with strychnine alkaloids. Huisgen served as assoc. prof. at the University of Tübingen, 1949—1952, and as full prof. at the University of München, 1952—1988; professor emeritus since 1988.

Rolf Huisgen's research activity (>560 publications) concerned topics of physical organic chemistry, reaction mechanisms, and cycloadditions.

Huisgen obtained many awards, e.g., the Roger Adams Award of the Am. Chem. Soc. (1975) and the Otto Hahn Prize in Chemistry and Physics from the German Chem. Soc. and the German Phys. Soc. (1979); he received honorary Ph. D. degrees from six universities. Rolf Huisgen is member of many academies, among them the Nat. Acad. Sci., Washington (1989), and honorary member of many learned societies, e.g., the Royal Soc. Chem., London (1981) and the Pharmaceutical Society of Japan (1985).

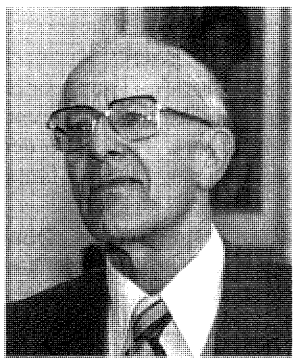

Rolf Huisgen

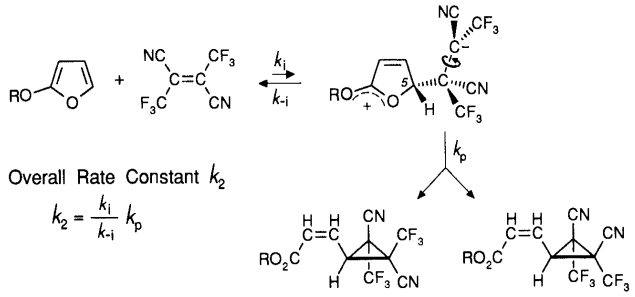

Variation of RO ($CDCl_3$, 25°C)

RO	$10^6 k_2 (M^{-1} s^{-1})$
CH_3O	6 600
p-$CH_3C_6H_4O$	76
$k_{CH_3O}/k_{C_7H_7O}$ =	*87*

Variation of solvent for RO = p-$CH_3C_6H_4O$, (25°C)

	$10^6 k_2 (M^{-1} s^{-1})$
C_6D_6	2.0
$CDCl_3$	76
CD_3NO_2	2 400

Chart 4. Dependence of Rate on Donor Substituent and Solvent

the furan was suppressed in favor of the substitution product which occurs in *threo* and *erythro* configuration. The NMR spectra disclose 2,5-disubstituted furans with the β-H hydrogen-bonded to the oxygen (Chart 5).[5]

Dimethyl 2,3-dicyanofumarate and dimethyl 2,3-dicyanomaleate constitute a second *trans,cis* pair of tetra-acceptor-substituted ethylenes which opened the ring of donor furans. The *trans,cis* equilibration (87 : 13), catalyzed by the nucleophilic furan derivative, was likewise fast; the zwitterion entered into substitution and ring opening in parallel reactions.[7]

Reaction in $CDCl_3$, 0.5 M in Pyridine, at 25°C

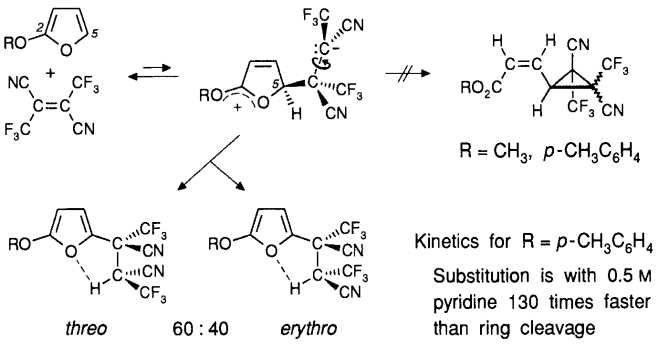

Chart 5. Substitution by BTE *vs.* Cyclopropane Formation

3. 1,3-Dipolar Cycloadditions: Switching from Concerted to Two-Step Pathway

Concerted or stepwise is a central question of cycloaddition chemistry. All evidence for concertedness is indirect. Every single criterion may be countered with objections. In contrast, the dip in the energy profile, due to the occurrence of an intermediate in a two-step reaction, invites to interference. As a mechanistic criterion, the capturing of an intermediate has the power of conviction.

The term concerted defines the simultaneous formation of the two new σ-bonds in a cycloaddition. Synchronous is the rare case of equal strength of the incipient bonds in the transition state; it is more or less limited to symmetrical systems like butadiene+ethylene. Bond formation in concert embraces all cases of unequal development of the new bonds in the transition state.

In the language of the MO theory, two π-HOMO–LUMO interactions are responsible for establishing the two new σ-bonds. A limiting case is foreseen when one HO–LU interaction strongly dominates and the second becomes negligibly small. That means: The second HO–LU pair contributes so little bond energy to the transition state, that it cannot outweigh the higher entropy requirements of the concerted process. A unilateral electron flow should establish one bond between the reactants; a zwitterionic intermediate would be generated.[8]

We searched for such a switch from the concerted to the two-step mechanism among 1,3-dipolar cycloadditions. It turned out that a second condition has also to be fulfilled: Strong steric hindrance at one terminus of the 1,3-dipole.

1,3-Dipoles are allyl anions with an onium function as middle center. Since sulfur has the same electronegativity as carbon, thiocarbonyl ylides should have high π-MO energies, approaching those of the allyl anion itself. The MO energies of acceptor-substituted ethylenes are low. The consequence is one large and one small HO–LU interaction.

Preparation of a Thiocarbonyl Ylide

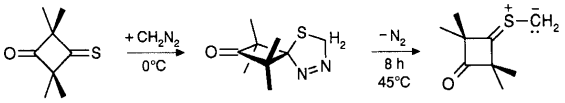

In situ Reactions with Dipolarophiles

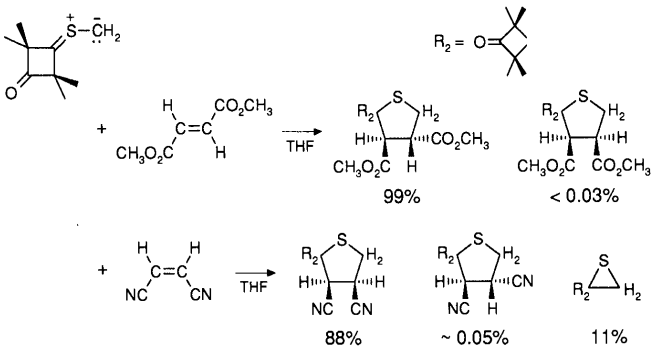

Analytical limits were determined by 500 MHz ^{1}H NMR in artificial mixtures. Occurrence of thiirane indicates low dipolarophilic activity.

Chart 6. Retention of Configuration as Criterion for Concertedness

Thioketones and diazomethane furnish 2,5-dihydro-1,3,4-thiadiazoles, as exemplified in Chart 6 for 3-thioxo-2,2,4,4-tetramethylcyclobutanone. Such thiadiazolines eliminate N_2 and provide thiocarbonyl ylides. These highly reactive 1,3-dipoles are not isolable, but easily interceptible by suitable dipolarophiles[9]; thiolanes are formed with C=C double bonds. The tetramethylcyclobutanone system is an accidental choice. Other thiocarbonyl ylides react similarly.

The addition with dimethyl fumarate proceeded with retention of the *trans* configuration; the *cis* spiroadduct remained below the analytical limit of 0.03%, as observed by Langhals. Thus, the stereospecificity amounts to >99.9%.[10]

Cis disubstituted ethylenes are less active dipolarophiles than the *trans* isomers. The capturing of the 1,3-dipole with maleonitrile was incomplete, and 11% of the thiocarbonyl ylide entered into electrocyclization, providing the thiirane

(Chart 6). Nevertheless, the stereospecificity of thiolane formation still amounted to 99.9%, well in accordance with concertedness.

Mloston and Langhals observed a violation of the retention principle for the reaction of our thiocarbonyl ylide with dimethyl dicyanofumarate and dicyanomaleate. Four acceptor substituents lower the π-MO energies. Ratios of *trans* and *cis* spirothiolanes of 61 : 39 and 25 : 75 were observed (Chart 7). Under the reaction conditions, hardly any isomerization of the excess of dipolarophile was noticed. Rotation in a zwitterionic intermediate is responsible for the loss of stereochemical integrity. The two-step pathway has been reached, and one bond is established here between the two reactants.[10] It is worth mentioning, that the borderline case of a two-step mechanism has also been reported by Quast *et al.* for the reaction of an electron-deficient 1,3-dipole with an electron-rich dipolarophile.[11]

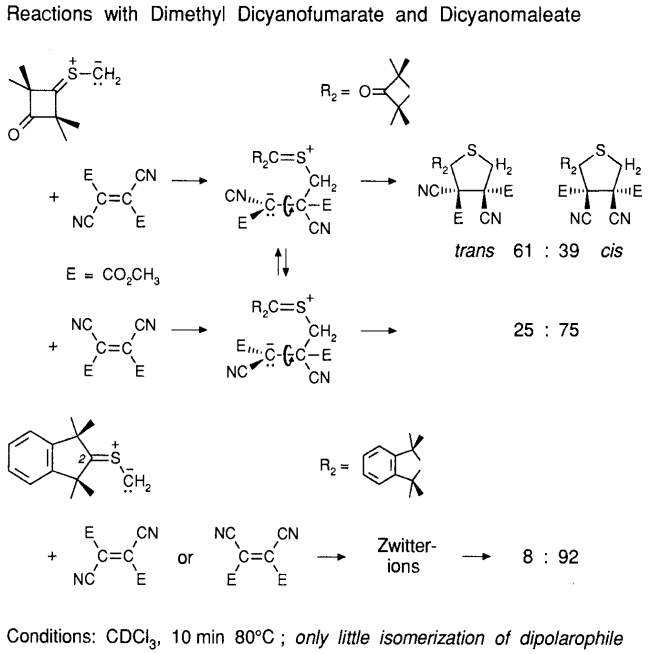

Chart 7. Violation of Retention Principle in Two-Step Cycloadditions

An extreme, *i.e.*, a complete equilibration of *trans* and *cis* zwitterion, was attained with 1,1,3,3-tetramethylindane-2-thione *S*-methylide as a 1,3-dipole. The additions with dimethyl dicyanofumarate or dicyanomaleate furnished one and the same 8 : 92 thiolane mixture without preceding dipolarophile isomerization, as found by Giera (Chart 7).[12] Oddly enough, it is the *cis* compound, which is preferred; the X-ray structures of both adducts, carried out by Polborn, left no doubt.

The reaction of the thiocarbonyl ylide of the tetramethylcyclobutanone series with tetracyanoethylene in absolute tetrahydrofuran at 45 °C provided 84% of the cycloadduct, the tetracyanospirothiolane. Nobody would suspect any complication. However, a reaction drama was brought to light, when Mloston repeated the experiment in tetrahydrofuran (THF) that contained 1.2% of methanol. The yield of the thiolane sank to 33%, and 64% of a crystalline compound was isolated which contains an additional molecule of methanol. It turned out to be the 7-membered lactim ether, an *S,N*-acetal (Chart 8).[13] The spirothiolane of the upper line is stable

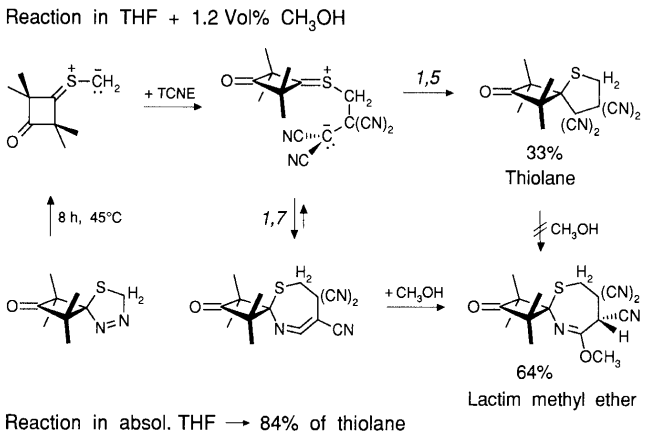

Chart 8. Thiocarbonyl Ylide and Tetracyanoethylene: Two Intermediates

to refluxing methanol and cannot occur on the pathway to the 7-membered ring.

Two intermediates are assumed in the reaction course. In the carbanionic portion of the zwitterion, the negative charge is distributed by resonance over carbon and nitrogen atom. Competing with the 1,5-cyclization is a 1,7 ring closure, in which the terminal nitrogen slips into the electron gap of the carbosulfonium ion. The product is a strained cyclic ketene imine that adds methanol to give the lactim ether.

The cyclic ketene imine must be connected with the zwitterion by an equilibrium. Otherwise, the high yield of the thiolane in the absence of methanol could not be explained. Is this a wild speculation?

Not so. BTE has been mentioned above. Its interaction with the thiocarbonyl ylide gave rise to two products in 84 : 16 ratio. The major compound, pale-yellow crystals, is in fact the cyclic ketene imine, and the colorless minor product is the thiolane (Chart 9). The ketene imine reacts with methanol affording the lactim ether, and with water the spirolactam. Oshima succeeded first in isolating the ketene imine in our laboratory.[14]

What makes the 7-membered cyclic ketene imine remarkable? The cumulated system creates high strain in a 7-membered ring. Allene type bond systems want to be linear. Here it must be twisted and deflected to fit into a 7-membered ring.

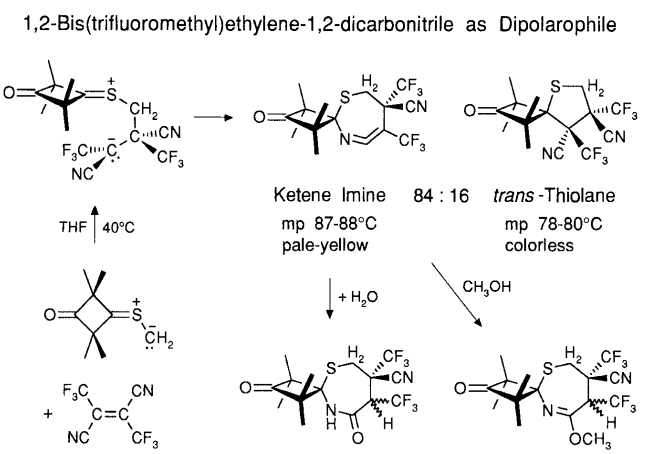

Chart 9. Isolation of a Cyclic Ketene Imine

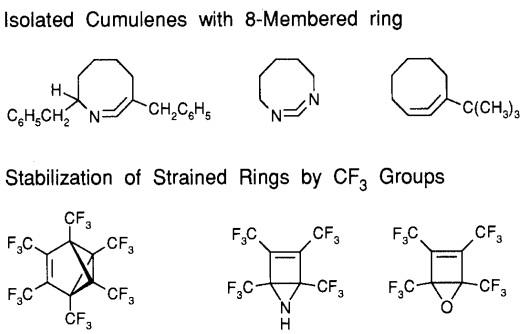

Chart 10. Why are 7-Membered Cyclic Ketene Imines Remarkable?

Only few compounds with cumulated double bonds in an 8-membered ring have been isolated (Chart 10). A dibenzylketene imine was described as an unstable oil which could not be obtained analytically pure.[15] The carbodiimide, prepared from pentamethylenethiourea, gave correct analyses, but slowly oligomerized.[16] The *tert*-butyl group appears to protect the 8-membered cyclic allene, which was spectroscopically characterized.[17]

Our ketene imine is the first stable cumulene embedded into a 7-membered ring. The stabilization comes from the perfluoroalkyl effect.[18] Strained rings gain kinetic stability and become isolable when they contain a sufficient number of CF_3 groups (Chart 10).[19,20] Hexakis(trifluoromethyl)benzvalene exceeds the parent substance in stability.[21]

In splendid work, Dewar-pyrroles, Dewar-furan, and thiophene were prepared by Kobayashi.[22] The origin of the trifluoromethyl effect is still unclear.

4. The Chemistry of Strained Seven-Membered Cyclic Ketene Imines

Besides the ketene imine with the tetramethylcyclobutanone ring, the interaction of BTE with three more thiocarbonyl ylides furnished crystalline ketene imines (Chart 11). They are storable in the deep-freeze under argon; quick handling in the open air causes no losses. The cyclic ketene imines show the strong IR absorption of cumulated systems. Two X-ray analyses confirmed the structures, and that of the ketene imine with the tetramethylindane residue is illustrated. The bond lengths of the ketene imine group are rather normal, but the angles are strongly deformed. The linear system of open-chain ketene imines has shrunk from 180° to 163°.[23]

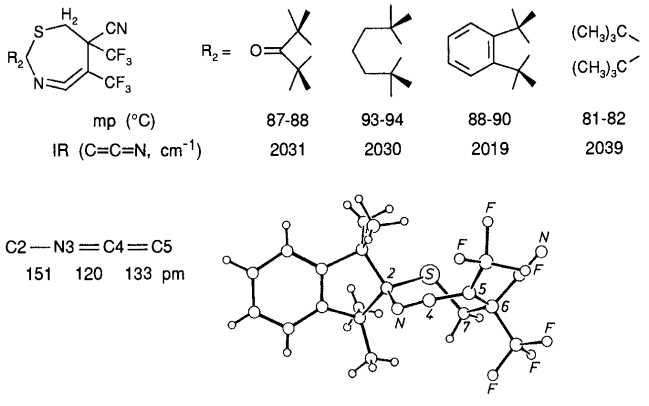

Chart 11. Stable Ketene Imines with 7-Membered Ring

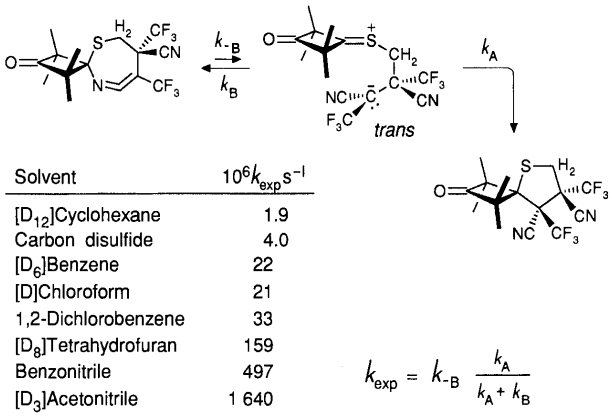

Chart 12. Ring Contraction of Ketene Imine at 60 °C *via* Zwitterion

How does the strain influence the reactivity of the cyclic ketene imine?

The ring strain is responsible for the slow isomerization to the thiolanes in solution. Compared with the short-lived ketene imine which occurs in the TCNE reaction of Chart 8, a kind of slow-motion picture is watched here (Chart 12).

According to measurements by Langhals, the rate of isomerization follows the first order. The half-life at 60 °C amounts to 100 h in cyclohexane and to 7 min in the highly polar acetonitrile. The rate increase by three powers of ten indicates an enhancement of charge separation in the transition state; that is in harmony with the intermediacy of the open-chain zwitterion in this rearrangement.[24]

Despite the steric hindrance by four methyl groups, the cyclic ketene imines react rapidly with diazomethane. The spiroindane compound on the first line of Chart 13 added the 1,3-dipole at the C=N double bond and afforded the triazole derivative in 80% yield. An X-ray analysis revealed the structure with the difluoromethylene group. Formally, the initial 1,3-cycloadduct has lost hydrogen fluoride, but the sequence of steps may be more complex.[12]

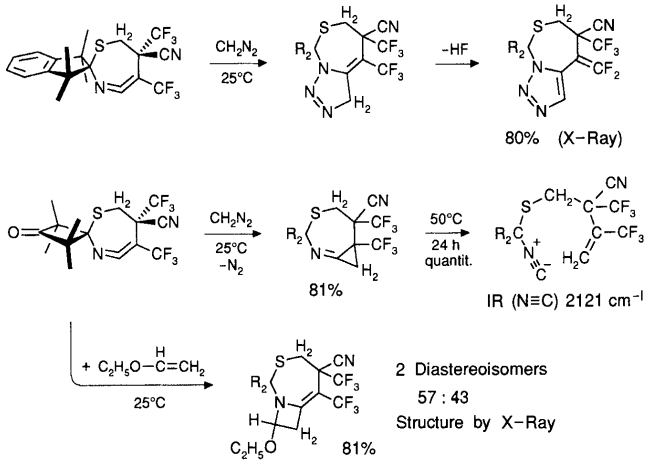

Chart 13. Cycloadditions of Cyclic 7-Membered Ketene Imines with Diazomethane and Ethyl Vinyl Ether

Amusingly, the corresponding triazole was only a minor product in the reaction of the ketene imine, which is spiro-annulated with the tetramethylcyclobutanone. The major product was the iminocyclopropane, the formal CH_2-adduct at the C=C double bond. Giera noticed that this is not the

final product; a cheletropic elimination leads to the ring-opened isonitrile.[12] Cyclopropanimines without the tether of an additional ring have been described; they undergo the cleavage to olefin+isonitrile at 150 °C.[25] In our example, the release of ring strain promotes the reaction.

Normal open-chain ketene imines do not react with vinyl ethers. Ring strain and CF_3-substitution accelerate the (2+2) cycloaddition of our cyclic ketene imines with ethyl vinyl ether (Chart 13). ^{13}C-NMR and an X-ray analysis established the addition to the C=N double bond, probably in a two-step process.[12]

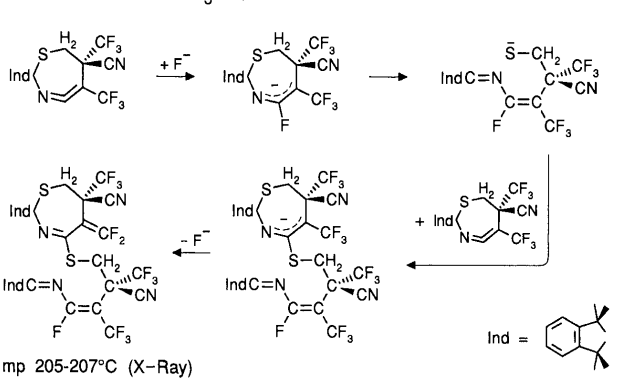

Chart 14. Base-Catalyzed Dimerization of Strained Ketene Imine

The propensity of ketenes to dimerize is not shared by open-chain ketene imines. However, the cyclic ketene imine of the spiro-indane series was converted to a dimer by nucleophilic catalysis (Chart 14), as observed by Langhals.[26] A few crystals of potassium cyanide in acetonitrile induced a rapid dimerization that furnished two diastereoisomers in 1 : 1 ratio, both crystalline. The X-ray diffraction brought to light an unusual structure that is not related to the two well-known types of ketene dimerization. Thus, relief of ring strain appears to be again the driving force.

A plausible, but speculative, pathway is formulated in Chart 14 for the fluoride anion as chain-transfer agent. The primarily generated allylic anion flips the ring open. The thiolate generated attacks a second molecule of ketene imine. The new cyclic anion transfers a fluoride ion, which initiates the next reaction cycle.

5. Astounding Reactivity of a 2-Amino-1,2-dihydroisoquinoline Derivative

Isoquinolines belong to the best studied heterocycles. Nevertheless, surprises do occur.

Isoquinolinium *N*-phenylimide shows the bond system $C=N^+-N^-$, which characterizes an azomethine imine in the classification of 1,3-dipoles.[27]

The colorless solution of *N*-anilinoisoquinolinium chloride became deep-red when triethylamine was added. The *N*-phenylimide was not isolable, but easily reacted *in situ* with dipolarophiles. A neutral source of the 1,3-dipole was offered by the crystalline adduct of carbon disulfide. Its red color in organic solvents indicated a dissociation equilibrium that is rapidly established (Chart 15).[28,29]

The red color disappeared on addition of dimethyl fumarate, and two diastereoisomeric *trans*-diesters were

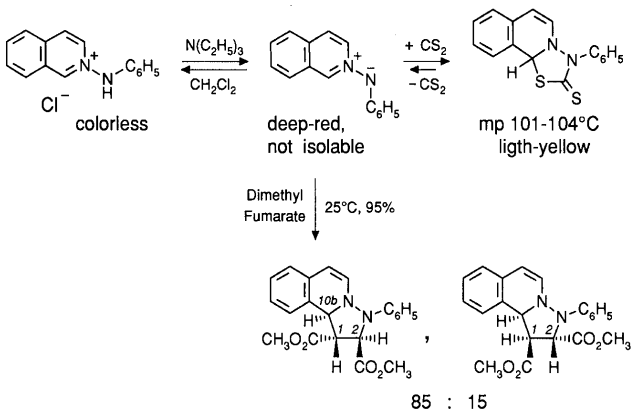

Chart 15. Isoquinolinium *N*-Phenylimide as 1,3-Dipole

formed.[28,30] The retention of dipolarophile structure is a criterion of concertedness. The adducts are derivatives of phenylhydrazine in which the β-nitrogen bears an ethylenic system. Such compounds are amenable to Fischer's indole synthesis.

This textbook procedure was discovered in 1883.[31] In acidic media, ketone phenylhydrazones are converted to substituted indoles. The mechanistic scheme was devised by Robinson and Robinson in 1918 (Chart 16).[32]

The phenylhydrazone is equilibrated with the vinylphenylhydrazine. The protonated species undergoes a [3.3]-sigmatropic shift, as it would be called it today. The weak N–N bond is broken and a strong C–C bond established in a

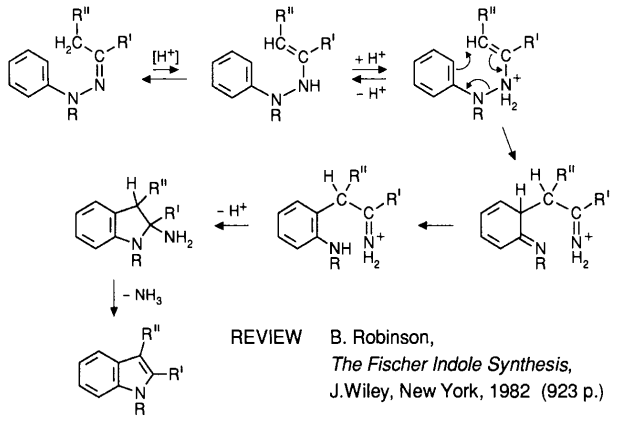

Chart 16. Emil Fischer's Indole Synthesis

cyclic electron shift. The lost aromaticity is restored by prototropy in the next step. The addition of the amine function to the iminium ion gives rise to a dihydroindole, and elimination of ammonia affords the aromatic heterocycle.

Our cycloadduct with dimethyl fumarate harbors a fixed ene-phenylhydrazine system. On acid treatment, it started to move on the Fischer pathway. The thick bonds will help to recognize the [3.3]-sigmatropic rearrangement in this polycyclic system (Chart 17).[33] After the intramolecular addition of the amino to the iminium function, the process got arrested. The aminal was isolated in 84% yield. Its structure was established by X-ray.[34]

Why is the last step, the formation of the indole, blocked? On looking at the 8-membered ring of the tetracyclic indole, a derivative of the strained (*E*,*Z*)-1,3-cyclooctadiene is iden-

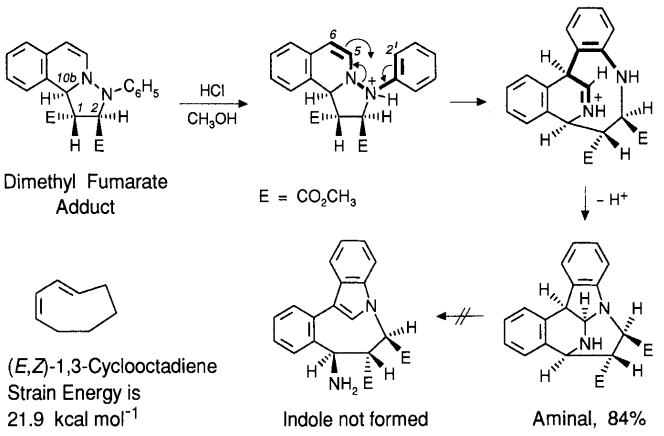

Chart 17. Hydrazo Rearrangement of a Tricylic Ene-phenylhydrazine

tified. The inclusion of the planar nitrogen increases the strain further. The final gain in aromaticity cannot compensate the increase of strain energy.

Numerous cycloadducts of isoquinolinium *N*-phenylimide were subjected to acid treatment by Temme; high yields of the tetracyclic aminals were the products. The cycloaddition to dimethyl maleate afforded the two *cis*-diesters in a 10 : 90 ratio. The Fischer reaction of the minor cycloadduct did not even require acid catalysis (Chart 18).[33]

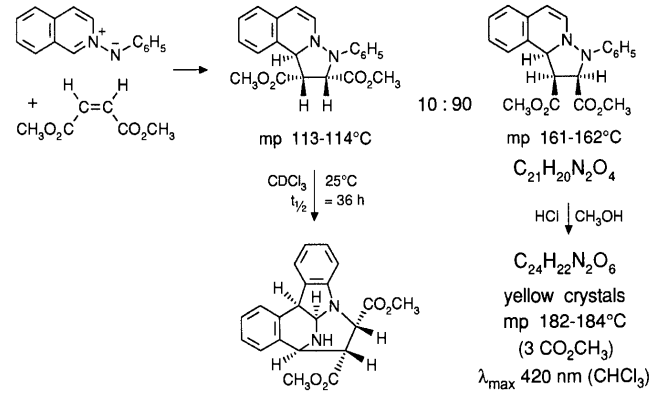

Chart 18. Acid Reactions of Dimethyl Maleate Adducts

To our amazement, the major isomer entered a completely different process with acid. When chemists study a reaction and vary the substrate, they expect generality. Then all on a sudden, like a thunderbolt, the generality fails.

In natural product synthesis, many chemists check new reactions by first using simple models. Woodward, the magician of organic synthesis, was a sworn enemy of model experiments. He commented once—half in joke:

> "One finds that there are no general reactions. That's the glory of chemistry—that it is an experimental science."

A conversion which has been successful in simple molecules, might fail in the synthetically important case.[35]

When the major cycloadduct of maleic ester was treated with HCl in methanol, bright yellow crystals of a compound $C_{24}H_{22}N_2O_6$ were formed. Embarassingly, it contained three carbon atoms more than the starting material; the NMR spectrum showed three different ester groups (Chart 18). Obviously, two molecules of the original cycloadduct participate in the formation of the yellow compound.

Tony Durst, a postdoc from the University of Western Ontario, Canada, spent the year 1965 in Munich. He carried out the described experiment, and recognized the C_{24} formula. The unexpected result of a sideline remained in the drawer for several decades, until a fascinating sequence of steps was brought to light.[36]

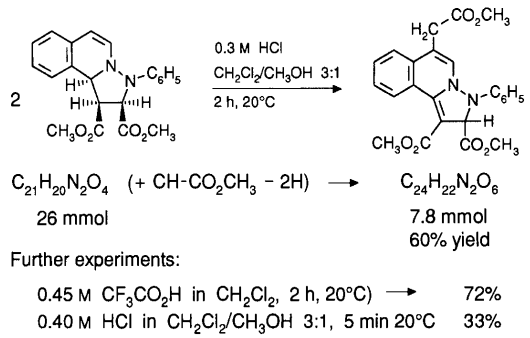

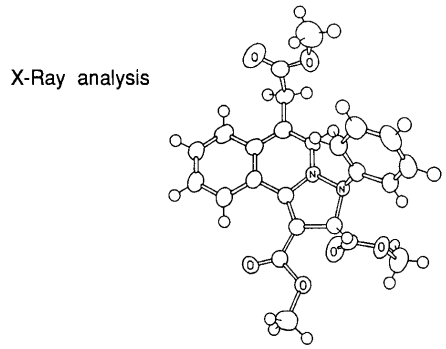

Chart 19. Structure of the Yellow Compound

The structure elucidation by X-ray was carried out by Karle and Flippen-Anderson.[34] The *N*-phenyl-substituted tricyclic system is still the same as in the cycloadduct (Chart 19), but a solution of the mechanistic puzzle was not obvious. The fragment CH–CO_2CH_3 has to be added to the molecular formula of the cycloadduct and 2 hydrogens deducted to arrive at $C_{24}H_{22}N_2O_6$.

In the experiment sketched in Chart 19, 60% of the C_{24} compound was produced, based on the consumption of two C_{21} molecules. The yield fluctuated; in the experiment with trifluoroacetic acid as a catalyst, it reached 72%. Finke showed that in 5 min at 20 °C already 33% of the yellow

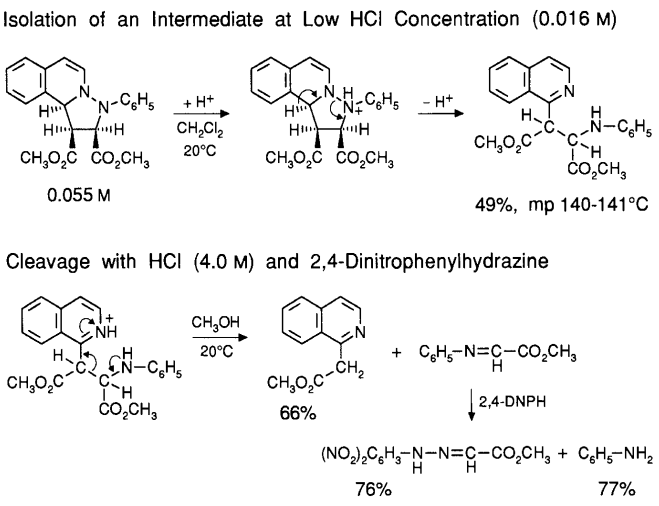

Chart 20. Key Experiments for Elucidation of Mechanism

compound is formed. What are the side products? What is the fate of the second molecule which has spent three C-atoms? The cracking of hard nuts is a favorite sport of many scientists.

When the dimethyl maleate adduct was treated with a low concentration of HCl, *i.e.*, only a third equivalent of acid, an isomer was obtained, which turned out to be an isoquinoline substituted in position 1 by an α-anilinosuccinic ester group. Thus, the pyrazolidine ring was cleaved by β-elimination (Chart 20).

The key experiment, the eye-opener, was the treatment of that open-chain isomer with strong acid in the presence of 2,4-dinitrophenylhydrazine. The isoquinoline-1-acetic ester was isolated in 66% yield. The dinitrophenylhydrazone of glyoxylic acid methyl ester precipitated, and aniline was isolated from the mother liquor (Chart 20). Thus, the anil of methyl glyoxylate must be the original fragment.[37]

This anil or—more correctly—its protonated form attacks the enamine group of a second molecule of the cycloadduct and converts it to the yellow C_{24} compound.

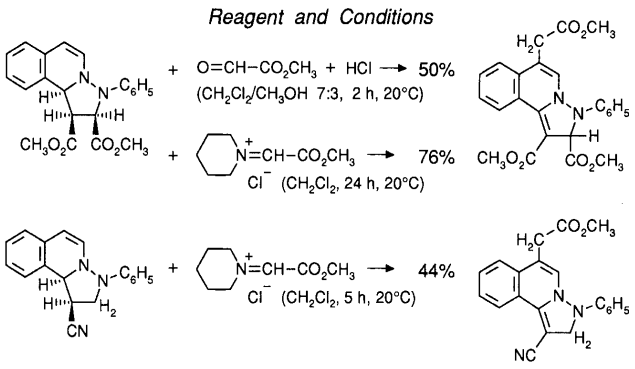

Chart 21. Synthesis of the Yellow Compound: Experimental

Indeed, a synthetic specimen of glyoxylic ester anil was capable of converting the cycloadduct into the yellow compound in acid medium. Since the anil is unstable, an experiment with methyl glyoxylate itself is recorded in Chart 21. The acid protonates the carbonyl oxygen, thus increasing its electrophilic character. The piperidinioglyoxylic ester chloride[38] produced 76% of the yellow compound; no acid is required here.[37]

The second molecule of the dimethyl maleate adduct can be replaced by the cycloadducts of acrylonitrile or dimethyl fumarate; what matters now, is only the ene-hydrazine group as nucleophilic reagent. The reaction with the piperidinio derivative of methyl glyoxylate provided the corresponding yellow products, as illustrated in Chart 21 by the nitrile.

A new problem is looming. The oxidation state of the aldehyde group in glyoxylic ester ends up with that of acetic ester in the C_{24} compound, and two hydrogen atoms of the pyrazolidine ring must be the reducing agent. How does this intramolecular redox reaction come about?

In a plausible scheme, the protonated glyoxylic ester anil binds to the β-position of the enehydrazine group. The iminium ion loses the β-proton; for simplicity, the proton is transferred to the anilino residue in Chart 22. The loss of aniline furnishes an α,β-unsaturated iminium ion. Removal of the 10*b*-proton establishes the aromatic isoquinolinium ion.

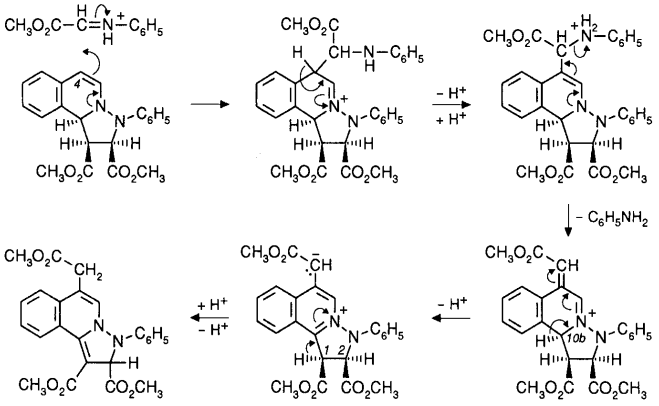

Chart 22. Synthesis of the Yellow Compound: Mechanism

Finally, a formal proton migration from position 1 to the carbanionic side chain furnishes our yellow compound. The electron flow from the lower to the upper part of the molecule demonstrates the redox process.

Our cycloadducts are derivatives of 1,2-dihydroisoquinoline. The mechanistic postulate presented in Chart 22 is supported by the fine work of Brown, Dyke, and Sainsbury.[39] A dimethoxy-1,2-dihydroisoquinoline reacted with benzaldehyde under acid catalysis (Chart 23). The not isolated intermediate eliminates water. Again, the upwards directed flow of electrons signals the intramolecular redox reaction; the side chain is formally reduced to benzyl by the hydrogen of the 1,2-dihydroisoquinoline ring.

The interaction of glyoxylic acid with *N*-methyl-1,2-dihydroisoquinoline constitutes a second example.

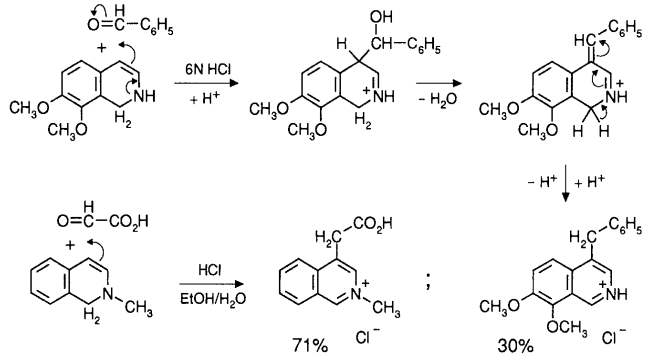

Chart 23. 1,2-Dihydroisoquinolines and Aldehydes as Redox Model

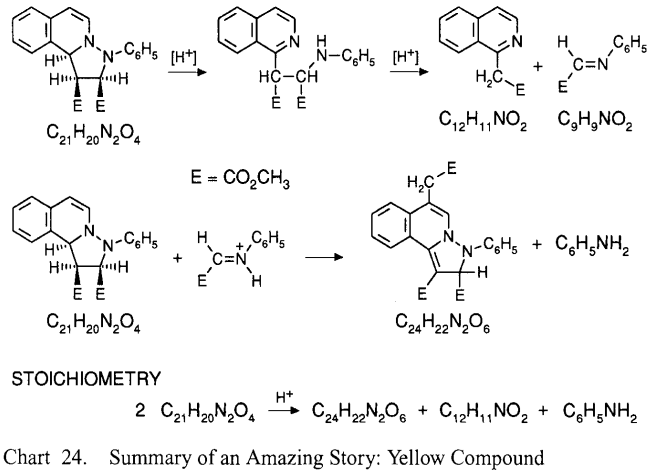

Chart 24. Summary of an Amazing Story: Yellow Compound

Chart 24 summarizes the amazing story that is a drama in two parts. In the first, the stepwise cleavage furnished methyl isoquinoline-1-acetate and the anil of glyoxylic ester. The proton adduct of the latter converted a second molecule of cycloadduct in a polystep sequence to the yellow C_{24} compound. The overall stoichiometry is displayed on the bottom line.

Nearly twenty cycloadducts of isoquinolinium *N*-phenylimide with C=C double bonds as dipolarophiles have been tested; they undergo the [3.3]-sigmatropic shift with acids. The conversion of the major dimethyl maleate adduct into the yellow C_{24} compound was unique and did not find an analogue. Obviously, the success depends on a fine tuning of the rate constants of all reaction steps, especially between part 1 and part 2 of the reaction drama.

Scientists proudly present new synthetic methods of wide scope. The last chapter demonstrates just the opposite: the anatomy of a singular case. Still shadowy, the contours of new reactions are recognized.

Heterocyclic chemistry has many frontiers of active research. In the new millenium, heterocycles will be as important as ever.

Acknowledgments It is the author's pleasure to express his sincere gratitude to excellent young associates who carried out the experiments and contributed so much with discussions and suggestions: Tony Durst, Henry Giera, Jürgen Finke, Elke Langhals, Grzegorz Mloston, Takumi Oshima, Kurt Polborn, Robert Temme, and Gonzalo Urrutia-Desmaison. The major role of Grzegorz Mloston may be singled out; in the meantime, he became full professor at the University of Lodz, Poland. Thanks for advice and help in NMR spectroscopy go to Helmut Huber and David S. Stephenson; Helmut Schulz carried out the elemental analyses.

The support of the projects by the Deutsche Forschungsgemeinschaft, Bonn, and the Fonds der Chemischen Industrie, Frankfurt, is gratefully acknowledged.

References and Notes

1) Based on a lecture presented at the 30th Symposium on Heterocyclic Chemistry, Tokyo University of Pharmacy & Life Science, Hachioji, on 25 November 1999.
2) Mloston G., Huisgen R., *J. Heterocycl. Chem.*, **31**, 1279—1282 (1994).
3) Ibata T., Isogami Y., Nakano S., Nakawa H., Tamura H., *J. Chem. Soc., Chem. Commun.*, **1986**, 1692—1693; Ibata T., Isogami Y., Nakawa H., Tamura H., Suga H., Shi X., Fujieda H., *Bull. Chem. Soc. Jpn.*, **65**, 1771—1778 (1992).
4) Proskow S., Simmons H. E., Cairns T. L., *J. Am. Chem. Soc.*, **88**, 5254—5266 (1966).
5) Urrutia-Desmaison G., Mloston G., Huisgen R., *Tetrahedron Lett.*, **35**, 4977—4980 (1994).
6) Huisgen R., Mloston G., *Tetrahedron Lett.*, **35**, 4981—4984 (1994).
7) Huisgen R., Mloston G., *Bull. Soc. Chim. Belg.*, **103**, 349—354 (1994).
8) General considerations: Huisgen R., *J. Heterocycl. Chem.*, **24**, S1—S11 (1987); *idem*, *Adv. Cycloadditions*, **1**, 1—31 (1988).
9) Reviews: Kellogg R. M., *Tetrahedron*, **32**, 2165—2184 (1976); Huisgen R., Fulka C., Kalvinsh I., Li X., Mloston G., Moran J. R., Pröbstl A., *Bull. Soc. Chim. Belg.*, **93**, 511—532 (1984).
10) Huisgen R., Mloston G., Langhals E., *J. Am. Chem. Soc.*, **108**, 6401—6402 (1986); Mloston G., Langhals E., Huisgen R., *Tetrahedron Lett.*, **30**, 5373—5376 (1989).
11) Quast H., Regnat D., Peters E.-M., Peters K., Schnering H. G. von, *Angew. Chem. Int. Ed. Engl.*, **29**, 695—697 (1990).
12) Giera H., Polborn K., Huisgen R., unpublished; Ph. Thesis H. Giera, University of Munich, 1991.
13) Huisgen R., Mloston G., Langhals E., *J. Org. Chem.*, **51**, 4085—4087 (1986).
14) Huisgen R., Langhals E., Mloston G., Oshima T., *Heterocycles*, **29**, 2069—2074 (1989).
15) Firl J., Schink K., Kosbahn W., *Chem. Lett.*, **1981**, 527—530.
16) Richter R., Tucker B., Ulrich H., *J. Org. Chem.*, **48**, 1694—1700 (1983).
17) Price J. D., Johnson R. P., *J. Org. Chem.*, **56**, 6372—6376 (1991).
18) Lemal D. M., Dunlap L. H., *J. Am. Chem. Soc.*, **94**, 6562—6564 (1972).
19) Smart B., "Fluorinated Organic Molecules" in Molecular Structure and Energetics, ed. by Liebman J. F., Greenberg A., Vol. 3, VCH, Weinheim, **1986**, pp. 141—191.
20) Greenberg A., Liebman J. F., Van Vechten D., *Tetrahedron*, **36**, 1161—1166 (1980).
21) Lemal D. M., Staros J. V., Austel V., *J. Am. Chem. Soc.*, **91**, 3373—3374 (1969).
22) Review: Kobayashi Y., Kumadaki I., *Acc. Chem. Res.*, **14**, 76—82 (1981); *Topics Curr. Chem.*, **123**, 103—150 (1984).
23) Huisgen R., Langhals E., Nöth H., *J. Org. Chem.*, **55**, 1412—1414 (1990).
24) Huisgen R., Langhals E., Oshima T., *Tetrahedron Lett.*, **29**, 2075—2078 (1989).
25) Quast H., Schmitt E., Frank R., *Angew. Chem. Int. Ed. Engl.*, **10**, 651 (1971).
26) Langhals E., Polborn K., Huisgen R., unpublished.
27) Huisgen R., *Angew. Chem. Int. Ed. Engl.*, **2**, 565—598 (1963).
28) Lecture abstract: Huisgen R., *Chimia*, **35**, 344—346 (1981).
29) Bast K., Behrens M., Durst T., Grashey R., Huisgen R., Schiffer R., Temme R., *Eur. J. Org. Chem.*, **1998**, 379—385.
30) Huisgen R., Temme R., *Eur. J. Org. Chem.*, **1998**, 387—401.
31) Fischer E., Jourdan F., *Ber. Dtsch. Chem. Ges.*, **16**, 2241—2245 (1883).
32) Robinson G. M., Robinson R., *J. Chem. Soc.*, **1918**, 639—645.
33) Bast K., Durst T., Huisgen R., Lindner K., Temme R., *Tetrahedron*, **54**, 3745—3764 (1998).
34) Karle I. L., Flippen-Anderson J. L., Huisgen R., *Acta Cryst.*, **C41**, 1095—1100 (1985).
35) Woodward R. B., *Proc. R. A. Welch Foundation Conferences*, **XII**, 3—6 (1969).
36) Preliminary account: Huisgen R., "The Adventure Playground of Mechanisms and Novel Reactions," Am. Chem. Soc., Washington, D.C., 1994, pp. 59—60.
37) Durst T., Finke J., Huisgen R., Temme R., to be submitted.
38) Gross H., Gloede J., Freiberg J., *Justus Liebigs Ann. Chem.*, **702**, 68—74 (1967).
39) Brown D. W., Dyke S. F., Sainsbury M., *Tetrahedron*, **25**, 101—117 (1969).

Four New Terpenes from the Pericarp of *Platycladus orientalis*

Yueh-Hsiung KUO,*,[a] Wen-Chin CHEN, and Ching-Kuo LEE[b]

Department of Chemistry, National Taiwan University,[a] Taipei, Taiwan, R.O.C. and China Junior of Medical Technology,[b] Tainan, Taiwan. Received July 22, 1999; accepted December 18, 1999

A new monoterpene, platydiol (1), and three new diterpenes, platyclolactonic acid (2), 14,15-bisnor-8(17)-labdene-16,19-dioic acid (3), and 6,7-dehydrosandaracopimaric acid (4), were isolated from the pericarp of *Platycladus orientalis*. Their structures were elucidated by spectral and chemical methods.

Key words *Platycladus orientalis*; Cupressaceae; platydiol; platyclolactonic acid; bisnor-8(17)-labdene-16,19-dioic acid; 6,7-dehydrosandaracopimaric acid

Many chemical components from the different parts of *Platycladus orientalis* FRANCO (=*Biota orientalis* Endl.) (Cupressaceae) have been studied. Sesquiterpenoids and diterpenoids from heartwood,[1—5] flavonoids from leaves,[6] bisnor- and trinorlabdane-type diterpenoids from seeds,[7] and two monolignol derivatives from pollen[8] have been reported. Because we are interested in labdane and norlabdane type diterpenoids, we investigated the components of the pericarp of this species and found a new diterpene acid, 15-hydroxypinusolic acid.[9] We have now reinvestigated the same extract from the pericarp of the same plant and found four new compounds, a monoterpene, platydiol (**1**), and three diterpenes, platyclolactonic acid (**2**), 14,15-bisnor-8(17)-labdene-16,19-dioic acid (**3**), and 6,7-dehydrosandaracopimaric acid (**4**). In this paper, we describe the structural elucidation of these new compounds.

Platydiol (**1**)[10] reported in the previous communication was elucidated in detail as follows. The molecular formula $C_{10}H_{18}O_2$, based on elemental analysis, indicated an index of hydrogen deficiency (IHD) of two. Analysis of the IR spectrum of **1** suggested that it contained a hydroxyl (3295 cm^{-1}) and geminal dimethyl groups (1387, 1367 cm^{-1}). The ^{1}H-NMR spectrum of **1** exhibited three singlet methyl groups (δ 0.80, 0.80, 1.02), a methine proton [δ 1.70 (t, J=4.8 Hz)], two carbinol methine protons [δ 4.20 (dd, J=12.2, 3.0 Hz)], and four methylene protons [δ 2.42 (td, 2H, J=12.2, 4.8 Hz), 1.30 (dd, 2H, J=12.2, 3.0 Hz)]. Only seven signals were observed in its ^{13}C-NMR spectrum [δ_C 11.6, 19.7 (CH_3), 39.3 (CH_2), 43.2, 80.0 (CH), 49.0, 49.2 (C)]. This result together with zero specific rotation suggested that compound **1** is a symmetric bicyclomonoterpene and a derivative of bornane. In the ^{1}H–^{13}C correlated spectroscopy (COSY) spectrum, δ_H 1.02 and 11.6, δ_H 0.80 and 19.7, δ_H 1.30, 2.42 and 39.3, δ_H 1.70 and 43.2, and δ_H 4.20 and 80.0 exhibited strong correlation. Irradiation at δ 1.30 (H_α-3, H_α-5) caused H_β-3 and H_β-5 to collapse to a doublet at δ 2.42 (dd, J=12.2, 4.8 Hz) and H-2, -6 to collapse to a doublet at 4.20 (d, J=12.2 Hz). Irradiation at δ 1.70 (H-4) simplified H_β-3 and H_β-5 at δ 2.42 to a triplet (J=12.2 Hz). When irradiation was made at δ 4.20, the signals at δ 1.30 and δ 2.42 collapsed to a doublet (J=12.2 Hz) and a doublet of doublets (J=12.2, 4.8 Hz), respectively. The coupling between H-6 and H_β-5 shows a large coupling constant (J=12.2 Hz).[11] This evidence suggested the hydroxyl group must be located in a α-endo orientation. From the above physical evidence, the structure of platydiol (**1**) could be assigned as 2α,6α-dihydroxybornane.

The chemical evidence supporting the structure of **1** is as follows. The reaction of Ac_2O and **1** in pyridine at room temperature overnight gave a diacetate **1a** [ν_{max} 1722 cm^{-1}; δ 0.90, 0.92, 0.92, 2.04, 2.04 (s, each 3H); δ 5.08 (dd, 2H, J=10.1, 3.6 Hz)]. Compound **1** and phenyl boronic acid dissolved in dry benzene were heated in a Dean and Stark apparatus, and phenyl boronate **1b** [ν_{max} 3050, 1597, 1490 cm^{-1}; δ 4.33 (2H, dd, J=8.4, 1.0 Hz)] was isolated. That the two hydroxyl groups are located in an α-endo orientation could be deduced from this result.

Platyclolactonic acid (**2**) was isolated as its methyl ester (**2a**) after treatment with diazomethane. Compound **2a** melted at 121—122 °C and has the molecular formula $C_{22}H_{32}O_5$ on the basis of elemental analysis. Analysis of the IR spectrum of **2a** suggested that it contained a lactone (1760 cm^{-1}), an ester (1708 cm^{-1}), and a terminal methylene group (3053, 1643, 874 cm^{-1}). The UV absorption of λ_{max} 230 nm was consistent with the presence of a conjugated lactone. The ^{1}H-NMR spectrum (Table 1) of **2a** revealed two singlet methyl groups (δ 0.49, 1.15), one singlet vinylic methyl group (δ 1.95), one methyl ester and one methoxy group (δ 3.58, 3.10), a terminal methylene group (δ 4.48, 4.83), and a vinyl proton vicinal to carbonyl (δ 5.87). Compound **2a** displayed twenty signals together with two methoxy signals in its ^{13}C-NMR spectrum, indicating a diterpenoid. The MS fragment ion (Chart 1) at m/z 121 (72%, structure **i**)[12] and the presence of the C-10 methyl signal at high field (δ 0.49 due to a shielding effect from the C-19 ester) showed that **2a** is a labdane-type diterpene with methyl carboxylate in a C-19 axial orientation.[9] The base peak in the MS spectrum (Chart 1) at m/z 127 (structure **ii**) was attributed to cleavage of side chain. This moiety was also confirmed from its UV, ^{1}H-NMR, and ^{13}C-NMR [δ_C 111.3, 166.0, 120.4, 169.9, 13.8 (C-12, -13, -14, -15, -16, respectively)] spectral data. Nuclear Overhauser enhancement and exchange spectroscopy (NOESY) correlations were observed between H-5 and H_α-7, -9, and H-14 and H_3-16 which indicate the relative stereochemistry of **2a**. This structure was also confirmed by the proton detected heteronuclear multiple-bond correlation (HMBC) technique.

Compound **3** was also isolated as its methyl ester (**3a**) (an amorphous solid). The methyl ester **3a** showed a molecular ion peak at m/z 336 and elemental analysis indicated the molecular formula $C_{20}H_{32}O_4$. It displayed IR absorption bands at 1719, 1220, 1151 (–COOR), and 3040 1639 and 890 cm^{-1} (terminal methylene). The ^{1}H-NMR spectrum of **3a** showed

* To whom correspondence should be addressed. e-mail: yhkuo@ccms.ntu.edu.tw

© 2000 Pharmaceutical Society of Japan

signals for two singlet methyl groups (δ 0.50, 1.18), two terminal methylene protons [δ 4.48, 4.84 (br s, each 1H)], and two singlet methyl carboxylates (δ 3.59, 3.62). The MS fragment ion (Chart 1) at *m/z* 121 (100%, structure **i**) and the presence of the C-10 methyl signal at higher field at δ 0.50 due to a shielding effect from the C-19 axial methyl carboxylate group, indicated that **3** was a labdane diterpene. After omitting the two methoxyl ^{13}C-NMR signals (Table 1, δ_C 51.2, 51.6), compound **3a** displayed eighteen signals. The ^{13}C chemical shifts from C-1 to C-11 of **3a** are very close to those of **2a**, which indicated that the difference between **2a** and **3a** was only in the side chain. Compound **3a** has two methyl carboxylate signals at δ_C 51.2, 51.6, 177.6 and 182.8, which suggest that **3a** is a 14,15-bisnorlabane diterpene with a methyl carboxylate in the side chain. Therefore, **3** can be assigned as 14,15-bisnor-8(17)-labdene-16,19-dioic acid.

The fourth new diterpene **4** has a molecular formula $C_{20}H_{28}O_2$ on the basis of high resolution (HR)-MS and ^{13}C-NMR data. The IR spectrum indicated the presence of a carboxylic acid and tri- and monosubstituted double bonds, as indicated by the absorption bands at 3300—2500, 3035, 1689, 1635, 1000, 910, and 860 cm^{-1}. The ^{1}H-NMR spectrum of **4** exhibited signals for three singlet methyl groups (δ_C 0.74, 1.06, 1.21), one vinyl group [δ 4.85 (dd, 1H, J= 10.5, 1.3 Hz), 4.93 (dd, 1H, J=17.4, 1.3 Hz), 5.79 (dd, J= 17.4, 10.5 Hz)], a trisubstituted double bond (δ 5.31, br s), and a *cis*-disubstituted double bond [δ 5.37 (dd, 1H, J=10.9, 2.5 Hz), δ 5.99 (dd, 1H, J=10.9, 3.0 Hz)]. The UV absorption band at λ_{max} 235 nm coincides with trisubstituted and monoexocyclic conjugated double bonds. Methylation of **4** with diazomethane in methanol yielded the methyl ester **4a** [mp 131—132 °C; ν_{max} 1723 cm^{-1}; δ 3.64 (s, 3H)]. By inspection of the ^{1}H- (see Experimental) and ^{13}C-NMR data

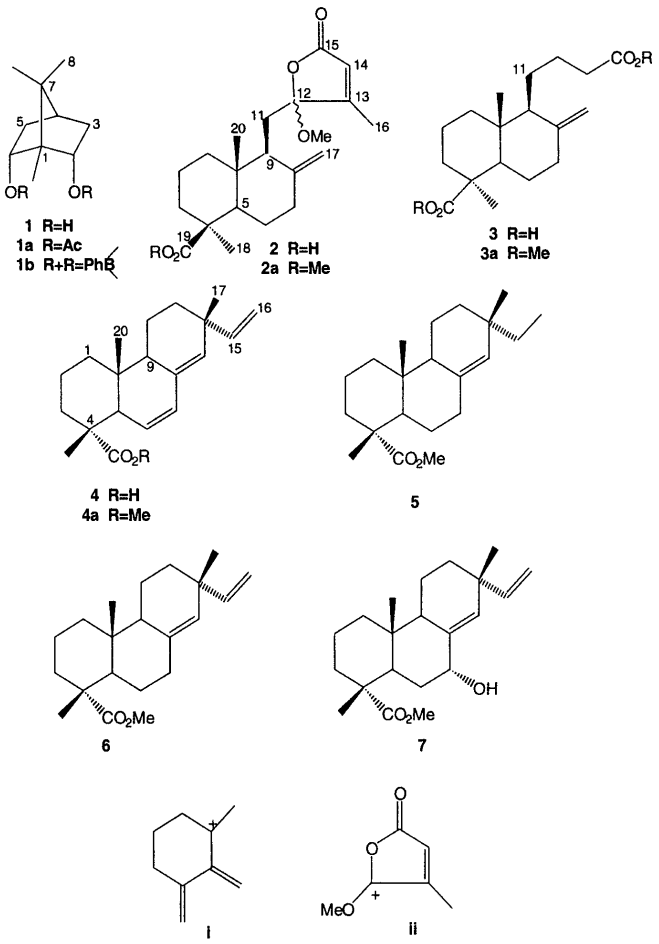

Chart 1

Table 1. ^{1}H- and ^{13}C-NMR Data for **2a**, **3a**, **4** and **4a** (300 and 75 MHz in $CDCl_3$)

No.	**2a** δ_C	**2a** δ_H	**3a** δ_C	**4a** δ_C	**4** δ_H
1	38.7	1.19 m, 1.75 m	39.0	36.4	
2	19.8	1.28 m	19.8	18.1	
3	38.7	1.03 m	38.0	35.9	
4	44.4		44.2	46.3	
5	56.2	1.32 dd (12.0, 2.7)	55.9	50.3	2.70 br s
6	26.3	1.74 m	25.8	133.4	5.37 dd (10.9, 2.5)
7	38.7	2.12 ddd (14.5, 12.0, 2.1) 2.36 dt (14.5, 2.3)	38.1	127.9	5.99 dd (10.9, 3.0)
8	148.5		147.2	135.2	
9	49.8	1.78[a)]	51.9	50.3	2.05 m
10	40.6		39.5	38.3	
11	29.8	2.01[a)]	30.8	18.5	
12	111.3		29.7	34.7	
13	166.0		32.6	36.8	
14	120.4	5.87 s		130.8	5.31 br s
15	169.9			148.5	5.79 dd (17.4, 10.5)
16	13.7	1.95 s	182.8	110.2	4.85 dd (10.5, 1.3) 4.93 dd (17.4, 1.3)
17	106.4	4.48 s, 4.83 s	106.3	17.1	1.06 s
18	28.6	1.15 s	28.8	178.7	
19	177.6		177.6	26.4	1.21 s
20	12.6	0.49 s	12.7	13.7	0.74 s
$CO_2\underline{C}H_3$	51.1	3.58 s	51.2	52.0	
$-O\underline{C}H_3$	50.2	3.10 s			
$CO_2\underline{C}H_3$			51.6		

a) Overlapped with other signals.

(Table 1) of **4a**, its structure was proposed as methyl 6,7-dehydrosandaracopimarate. Hydrogenation of **4a** with 10% Pd–C as catalyst in ethyl acetate produced methyl 15,16-dihydrosandaracopimarate (**5**) [mp 119—120 °C; δ 0.78 (t, 3H, J=6.6 Hz), 5.14 (1H, br s)] which was identified with the product obtained from methyl sandaracopimarate (**6**) by hydrogenation under similar conditions. Compound **4a** could be prepared from methyl sandaracopimarate (**6**) as follows. Oxidation of **6** with selenium dioxide in ethanol at room temperature give methyl 7α-hydroxysandaracopimarate (**7**),[13] which was then treated with methanesulfonyl chloride in triethylamine to yield compound **4a**. From the above spectral and chemical evidence, the structure of **4** can be assigned as 6,7-dehydrosandaracopimaric acid.

Experimental

Melting points were determined on a Yanagimoto micro melting point apparatus, ^{1}H- and ^{13}C-NMR spectra were obtained on a Bruker AM 300 in $CDCl_3$ solution with tetramethylsilane (TMS) as internal standard. Chemical shifts are given in hertz (Hz). Electron impact (EI)-MS and UV spectra were taken on JEOL-JMS-100 and Hitachi RMS-4 spectrometers, respectively.

Extraction and Isolation The air dried pericarps of *Platycladus orientalis* Franco (4.2 kg) were extracted at room temperature with acetone four times. The residues were successively extracted with methanol (60 l) (5 d×3). The combined methanolic extracts was evaporated *in vacuo* to yield a viscous residue (105 g), which was subsequently chromatographed over silica gel with hexane/EtOAc gradient solvent. Four products, platydiol (**1**) (1.3 g), crude platyclolactonic acid (**2**), crude 14,15-bisnor-8(17)-labdene-16,19-dioic acid (**3**), and crude 6,7-dehydrosandaracopimaric acid (**4**) (1.1 g) were isolated by using 50% EtOAc/hexane, 50% EtOAc/hexane, 80% EtOAc/hexane and EtOAc, respectively. Compounds **2** and **3** were purified as their methyl ester forms, **2a** (0.6 g) and **3a** (0.1 g), respectively.

Platydiol (**1**): mp 175—176 °C, $[\alpha]_D^{23}$ 0° (c=0.7, $CHCl_3$). IR ν_{max} cm^{-1}: 3295, 1387, 1367, 1133, 1059, 981, 901. EI-MS (70 eV) *m/z* (rel. int. %): 171 [$(M+H)^+$, 2], 153 [$(M+H-H_2O)^+$, 5], 135 (3), 108 (100), 93 (43). *Anal.* Calcd for $C_{10}H_{18}O_2$: C, 70.53; H, 10.66. Found: C, 70.48; H, 10.63.

Platyclolactonic Acid Methyl Ester (**2a**): mp 121—122 °C, $[\alpha]_D^{30}$ +56.2° (c=1.0 in MeOH). UV λ_{max} (log ε) nm: 230 (3.19). IR ν_{max} cm^{-1}: 3053, 1760, 1708, 1643, 1379, 1260, 1160, 1108, 874. ^{1}H- and ^{13}C-NMR data see Table 1. EI-MS (70 eV) *m/z* (rel. int. %): 376 (M^+, 7), 285 (15), 249 (43) 189 (70), 127 (100), 121 (72). *Anal.* Calcd for $C_{22}H_{32}O_5$: C, 70.17; H, 8.57. Found: C, 70.20; H, 8.59.

14,15-Bisnoar-8(17)-labdene-16,19-dioic Acid Dimethyl Ester (**3a**): Amorphous solid, $[\alpha]_D^{15}$ +13.4° (c=0.5 in $CHCl_3$). IR ν_{max} cm^{-1}: 3040, 1719, 1639, 1220, 1151, 890. ^{13}C-NMR data see Table 1. EI-MS (70 eV) *m/z* (rel. int. %) 336 (M^+, 2), 276 [$(M-HCO_2CH_3)^+$, 9], 262 (13), 248 (30), 121 (100). *Anal.* Calcd for $C_{20}H_{32}O_4$: C, 71.38; H, 9.59. Found: C, 71.46; H, 9.52.

6,7-Dehydrosandarapimaric Acid (**4**): Amorphous solid, $[\alpha]_D^{14}$ +15.3° (c=0.4 in $CHCl_3$). IR ν_{max} cm^{-1}: 3300—2500, 3035, 1689, 1635, 1381, 1239, 1000, 910, 860. ^{1}H-NMR data see Table 1. EI-MS (70 eV) *m/z* (rel. int. %) 300 (M^+, 57), 285 [$(M-CH_3)^+$, 100], 239 [$(M-HCO_2H)^+$, 40], 158 (38), 143 (27). HR-EI-MS *m/z* $[M]^+$ Calcd for $C_{20}H_{28}O_2$: 300.2089. Found: 300.2086.

Methyl 6,7-Dehydrosandaracopimarate (**4a**): mp 131—132 °C, $[\alpha]_D^{18}$ +8.2° (c=0.4 in $CHCl_3$). IR ν_{max} cm^{-1}: 3078, 1723, 1628, 1242, 4072, 994, 911, 865. ^{1}H-NMR ($CDCl_3$) δ: 0.74, 1.06, 1.19, 3.64 (s, each 3H), 2.09 (m, 1H, H-9), 2.69 (br s, 1H, H-5), 4.88 (dd, 1H, J=10.5, 1.2 Hz, H-16), 4.93 (dd, 1H, J=17.4, 1.2 Hz, H-16), 5.30 (m, 2H, H-6, -14), 5.79 (dd, 1H, J=17.4, 10.5 Hz), 5.99 (dd, 1H, J=10.9, 3.0 Hz, H-7). ^{13}C-NMR data see Table 1.

Acetylation of 1 with Ac_2O-Pyridine Compound **1** (10 mg) was allowed to react with Ac_2O (0.5 ml) and pyridine (0.5 ml) at room temperature overnight. Usual work-up gave diacetate **1a** (10 mg) [mp 60—61 °C. IR ν_{max} cm^{-1}: 1722. ^{1}H-NMR ($CDCl_3$) δ: 0.90, 0.92, 0.92, 2.04, 2.04 (s, each 3H), 5.08 (dd, 2H, J=10.1, 3.6 Hz, H-2, -6). HR-MS *m/z*: 254.1525 (M^+, Calcd for $C_{14}H_{22}O_4$: 254.1519].

Reaction of 1 with $PhB(OH)_2$ in Dry Benzene under Reflux A solution of **1** (15 mg) and $PhB(OH)_2$ (10 mg) in 20 ml of dry benzene was refluxed in a Dean–Stark apparatus for 3 h. The reaction mixture was directly subjected to chromatography on SiO_2 to afford **1b** [mp 70—71 °C; IR ν_{max} cm^{-1}: 3050, 1597, 1490; ^{1}H-NMR ($CDCl_3$) δ: 0.90, 0.90, 0.94, (s, each 3H), 4.33 (dd, 2H, J=8.4, 1.0 Hz, H-2, -6), 7.79 (dd, 2H, J=7.8, 1.2 Hz), 7.37 (m, 3H)].

Hydrogenation of 4a with 10% Pd–C in EtOAc Compound **4a** (20 mg) was hydrogenated in EtOAc (30 ml) with 10% Pd–C (10 mg) at room temperature for 10 h. The product was purified to afford methyl 15,16-dihydrosandaracopimarate (**5**) (18 mg) [mp 119—120 °C; δ 0.77, 0.84, 1.15, 3.62 (s, each 3H), 0.78 (t, 3H, J=6.6 Hz), 5.14 (br s, 1H)].

Allylic Hydroxylation of 6 with SeO_2 in EtOH Methyl sandaracopimarate (**6**) and SeO_2 (211 mg) was dissolved in 30 ml of ethanol and stirred at room temperature for 20 h. After remove of ethanol, 50 ml of H_2O was added to the residue, which was extracted with ether (30 ml ×3). The organic layer was purified by SiO_2 chromatography to afford methyl 7α-hydroxysandaracopimarate (**7**) (70 mg) [mp 79—80 °C, lit. viscous oil;[13] IR ν_{max} cm^{-1}: 3427, 3040, 1723, 1630, 1383, 1149, 1110, 1060, 1006, 911; ^{1}H-NMR ($CDCl_3$) δ: 0.78, 1.01, 1.22, 3.64 (s, each 3H), 4.12 (t, 1H, J=2.8 Hz), 4.89 (dd, 1H, J=10.8, 1.3 Hz), 4.91 (dd, 1H, J=17.3, 1.3 Hz), 5.48 (d, J=1.5 Hz), 5.75 (dd, 1H, J=17.3, 10.8 Hz)].

Dehydration of 7 with Methanesulfonyl Chloride in Triethylamine Methanesulfonyl chloride (30 mg) was added to a solution of **7** dissolved in 3 ml of triethylamine at 5—10 °C and then stirred 30 min at the same temperature. The reaction mixture was then stirred at room temperature for 4 h. The usual work-up and purification on SiO_2 chromatography gave **4a** (42 mg).

Acknowledgements This research was supported by the National Science Council of the Republic of China.

References

1) Erdtman H., Pelchowicz Z., *Chem. Ber.*, **89**, 341—343 (1956).
2) Dev S., Chetty G. L., *Tetrahedron Lett.*, **1964**, 73—76.
3) Hirose Y., Nakatsuka T., *Mokuzai-shi*, **4**, 26—31 (1958).
4) Tomita B., Hirose Y., Nakatsuka T., *Tetrahedron Lett.*, **1968**, 843—846.
5) Tomita B., Hirose Y., Nakatsuka T., *Mokuzai-shi*, **15**, 46—50 (1969).
6) Khabir M., Khatoon F., Ansari W. H., *Curr. Sci.*, **54**, 1180—1185 (1985).
7) Inoue M., Hasegawa S., Hirose Y., *Phytochemistry*, **24**, 1602—1604 (1985).
8) Ohmoto T., Yamaguchi K., *Chem. Pharm. Bull.*, **36**, 807—811 (1988).
9) Kuo Y. H., Chen W. C., *Heterocycles*, **31**, 1705—1709 (1990).
10) Kuo Y. H., Chen W. C., Shih K. S., *Chem. Express*, **4**, 511—514 (1989).
11) Jackman L. M., Sternhell S., "Application of Nuclear Magnetic Resonance Spectroscopy in Organic Chemistry," 2nd ed., Macmillan, New York, 1969, p. 289.
12) Kuo Y. H., Yu M. T., *Chem. Pharm. Bull.*, **44**, 1242—1244 (1996).
13) Teresa J. D. P., Barrero A.F., Muriel L., Feliciano A. S., Grande M., *Phytochemistry*, **19**, 1153—1156 (1980).

The Effects of Adsorbed Water on Tensile Strength and Young's Modulus of Moldings Determined by Means of a Three-Point Bending Method

Tomokatsu TSUKAMOTO, Cheng Yu CHEN, Hirokazu OKAMOTO, and Kazumi DANJO*

Faculty of Pharmacy, Meijo University, 150 Yagotoyama, Tempaku-ku, Nagoya 468–8503, Japan.
Received August 4, 1999; accepted March 2, 2000

Young's moduli (*E*) of three representative tableting excipients and their mix powders were measured for compressed rectangular beam specimens over a range of porosities using a three-point bending technique. We also examined the effects of the amount of water adsorbed on the tensile strength of these specimens. The maximal tensile strength (σ_{max}) decreased with increasing water vapor adsorption for microcrystalline cellulose (MCC) and mixed powders of lactose and MCC. σ_{max} increased with increasing compression stress and specimen weight for all samples. σ_{max} of an α-lactose and cornstarch mixture with a ratio of 7 : 3 showed a large value.

Young's modulus (*E*) and the crushing energy (*CE*) of MCC were larger than those of the other samples. Young's modulus of specimens decreased as the proportion of α-lactose increased.

Disintegration time (*DT*) of tablets comprised of lactose and MCC mixture was much faster than those of tablets comprised of individual powders. This appeared to demonstrate the effect of MCC swelling on the disintegration time of the tablet. The disintegration time of the lactose/cornstarch series increased only when Young's modulus increased sharply.

Key words bending test; excipient; tensile strength; Young's modulus; disintegration time

Microcrystalline cellulose (MCC), α-lactose and cornstarch are widely used as tableting excipients. In addition to the established range of amount in formulation for these excipients, other chemically equivalent ingredients with a similar range of particle sizes from alternative sources have recently been introduced. The mechanical properties of materials can be characterized by a variety of methods, the choice of test often being closely related to the intended use of the material.[1—7] Pharmaceutically, as powders are subjected to compression in punch and die systems during tablet formation, these systems are often used to assess the mechanical behavior of powders, *e.g.* for their resistance to change in volume.[8] The method described by Fell and Newton[9] can be used to characterize the formed compact tablet by its tensile strength and its tensile strength variability. Ress and Rue[10] used cylidrical specimens to determine the "work of failure" of some direct-compressible excipients. Another means of characterizing pharmaceutical materials is the four-point beam bending tests as reported by Church and Kennerley[11] who found a decrease in porosity of Avicel beams resulted in an increase in the mean tensile fracture stress and mean Young's modulus. The Young's modulus of materials is the stress required to produce a corresponding unit of strain. It can be estimated from the linear region of a stress–strain curve, irrespective of whether the material exhibits elastic or plastic behavior. An elastic material will completely recover its strain when the applied stress has been removed. A plastic material, however, will show permanent deformation on removal of stress greater than the yield stress of the material.

In this study, Young's moduli of three excipients *i.e.* MCC, α-lactose and cornstarch, and their mixtures were measured using a three-point bending technique using rectanglar beams with a range of beam porosities to determine the tensile strength.

Materials and Methods

Materials The powders used to prepare the rectangular beams were MCC (Asahi Chemical, Avicel PH-101), α-lactose monohydrate (DMV, 200 mesh) and corn starch (Nihonshokuhin). Table 1 shows the physicochemical properties of samples used.

Moisture Adsorption Measurement Samples were placed in a desiccator in a constant temperature incubator at 25 °C and left for various periods. The relative humidity in the desiccator was manipulated using saturated solutions of inorganic salts. Following their removal from the desiccator, the moisture content of the samples was determined by weighing.

Preparation of Beam Specimens Rectangular beams with dimensions of $2.0\times1.0\times h$ cm, where h is the thickness, were prepared by direct uniaxial compression using a rectangular hardened steel punch and die unit. Powder samples of a known weight were compressed using a universal tension and compression tester (Shimadzu Autograph AG 5000D) at loads up to 150 MPa. Beams of differing final porosities were obtained by compression at various loads. Beams were stored at 25 °C under eight different conditions of humidity for one week prior to testing, unless otherwise stated.

Three-Point Bending Test A granule hardness tester (Okadaseiko GRANO, granule strength tester) was adapted for three-point beam testing as shown in Fig. 1. Applied load (P) and beam deflection (δ) were monitored using a calibrated (50 kg) load cell and linear voltage displacement transducer. Load was applied at 0.5 mm/min. Young's modulus (E) and tensile strength (σ_{max}) were calculated by the following equations:[12]

$$\sigma_{max}=(12/bh^3)(PL/4)(h/2)=3PL/2bh^2 \quad (1)$$

$$E=PL^3/(48I\delta) \quad (2)$$

$$I=bh^3/12 \quad (3)$$

where b is the beam width, h is the beam thickness, L is the distance between the outer contact points, I is the geometric second moment of area and δ is the vertical deflection of the midpoint relative to the outer contact points. The values shown represent the means of five measurements.

Measurement of Crushing Energy Crushing energy of moldings was estimated from the product of compression stress and area under the curve in the compression stress–displacement curve of the three-point test. The

Table 1. Physicochemical Properties of Samples Used

Sample	Mean particle diameter (μm)	True density (g/cm^3)[a]
MCC (Avicel PH101)	34.3[b]	1.58
α-Lactose (DMV)	106—150[c]	1.55
Cornstarch (Nihon Shokuhin)	106 pass[c]	1.53

a) Density was measured with a Shimadzu-Micromeritics type 1302 helium-air hydrometer. *b*) Mean particle diameter was measured with a laser diffraction particle size analyzer (Seishin Enterprise type). *c*) Mean particle diameter was measured by the sieve method.

* To whom correspondence should be addressed. e-mail: danjo@meijo-u.ac.jp
© 2000 Pharmaceutical Society of Japan

values shown represent the means of five measurements.

Measurement of Disintegration Time Disintegration time was carried out according to the JP XIII, except purified water was used as the disintegration fluid. Disintegration time was determined at the point at which the tablet disintegrated completely and passed through the screen. The values shown represent the means of three measurements.

Results and Discussion

Water Vapor Adsorption Isotherms of Samples Water vapor adsorption isotherms of samples at 25 °C are shown in Fig. 2. All results are shown as BET type isotherms. Water adsorption of α-lactose was the lowest as compared with MCC and cornstarch. Water vapor adsorption of mixed powders decreased when the ratio of α-lactose increased.

Effects of Water Vapor Adsorption on the Maximal Flexure of Rectangular Samples Figure 3 shows the effects of water vapor adsorption on the maximal tensile strength, α_{max}, at a compression stress of 100 MPa and sample weight of 500 mg. For mixed powders, σ_{max} tended to decrease with increases in the ratio of α-lactose. α_{max} of MCC and mixed samples tended to show the maximal value and subsequently decreased with increasing water vapor adsorption due to the small amount of water vapor adsorbed on α-lactose. However, σ_{max} of α-lactose increased sharply with slight increases in water vapor adsorption.

The cornstarch–lactose system showed results approximately similar to those of the MCC–lactose system (data not shown). However, the tensile strength of the corn starch–lactose system was about 1/10 of that in the MCC–lactose system. The amount of moisture adsorption of cornstarch can explain the approximately 10-fold higher values of this as opposed to the MCC–lactose system as shown in Fig. 2.

We examined the effects of the water vapor adsorption on the interparticle adhesion force. Our results indicated that the adhesion force increased with increasing amounts of water adsorption when the adsorbed amount increased from the monolayer to the 2-triad layer, as previously reported.[13] Schubert[14] and Rumpf[15] reported that the adhesion force reached a maximum value at a water bridge angle of 10° when the particle diameter to interparticle distance ratio is 10^{-3}. Since the space between particles also increases with increases in the amount of the interparticle moisture, this is regarded as a decrease in the interparticle atractive force.

Only in the case of α-lactose, since the moisture was low content, could the increase in the adhesion of α-lactose be

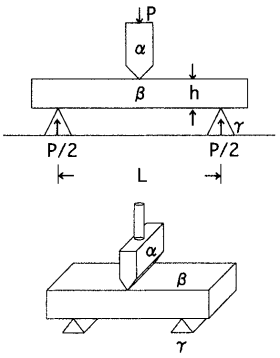

Fig. 1. Schematic Diagram of Three-point Bending Test

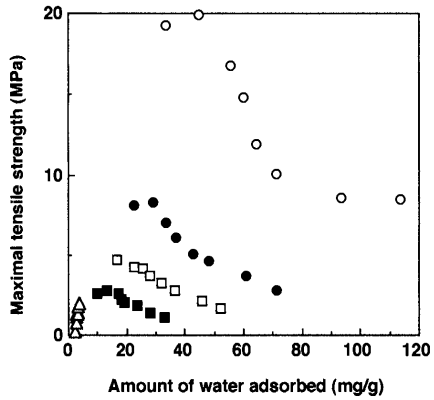

Fig. 3. Relationship between Amount of Water Adsorbed and Maximal Strength at Compression Stress of 100 MPa and Beam Weight of 500 mg

○, MCC; ●, lac/MCC=3/7; □, lac/MCC=1/1; ■, lac/MCC=7/3; △, lactose.

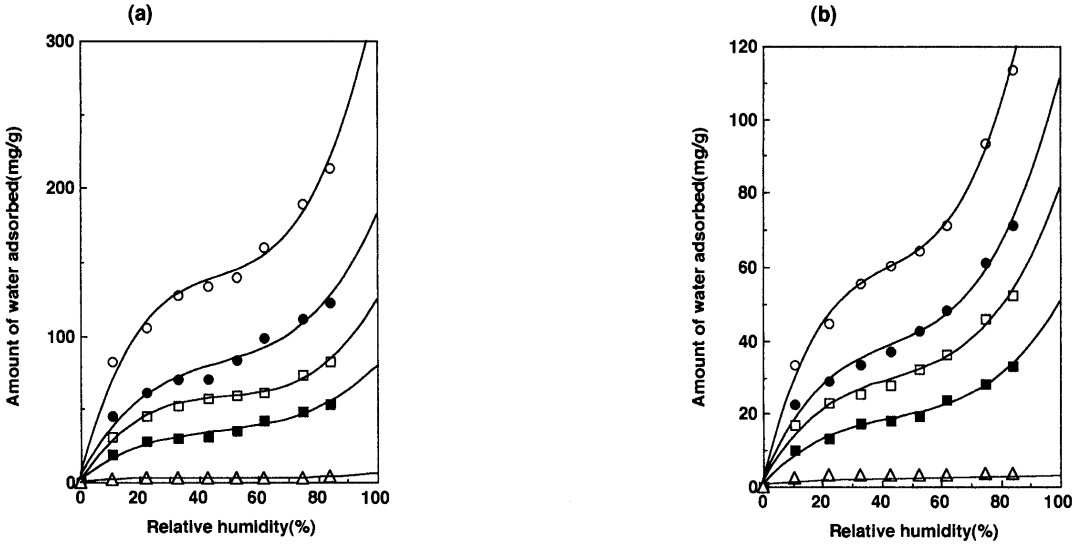

Fig. 2. Water Vapor Adsorption Isotherms at 25±0.5 °C

(a) Cornstarch and lactose ○, cornstarch; ●, lac/sta=3/7; □, lac/sta=1/1; ■, lac/sta=7/3; △, lactose. (b) MCC and lactose ○, MCC; ●, lac/MCC=3/7; □, lac/MCC=1/1; ■, lac/MCC=7/3; △, lactose.

Table 2. Porosity of Samples at Different Relative Humidities

Sample	ε							
	R.H.=10.6%	=22.2%	=32.7%	=42.8%	=52.7%	=61.8%	=75.0%	=84.0%
MCC	0.138	0.126	0.131	0.136	0.161	0.168	0.170	0.165
Lac/MCC=3/7	0.242	0.242	0.248	0.243	0.249	0.252	0.253	0.247
Lac/MCC=1/1	0.266	0.265	0.263	0.264	0.260	0.262	0.260	0.255
Lac/MCC=7/3	0.245	0.250	0.245	0.240	0.240	0.243	0.247	0.247
Lac	0.183	0.191	0.162	0.161	0.183	0.185	0.191	0.176
Lac/Sta=3/7	0.159	0.154	0.150	0.166	0.157	0.163	0.153	0.150
Lac/Sta=1/1	0.189	0.200	0.186	0.183	0.196	0.185	0.191	0.196
Lac/Sta=7/3	0.242	0.236	0.225	0.232	0.246	0.225	0.230	0.232
Sta	0.237	0.231	0.230	0.238	0.220	0.210	0.226	0.176

Compression stress=100 MPa; sample weight=500 mg.

Table 3. Porosity of Samples for Each Compression Stress and Sample Weight

Sample	ε					
	50 MPa	100 MPa	150 MPa[a)]	300 mg	500 mg	800 mg[b)]
MCC	0.241	0.131	0.115	0.160	0.131	0.158
Lac/MCC=3/7	0.356	0.248	0.182	0.283	0.248	0.228
Lac/MCC=1/1	0.349	0.263	0.202	0.282	0.263	0.245
Lac/MCC=7/3	0.312	0.245	0.201	0.252	0.245	0.241
Lac	0.220	0.162	0.130	0.166	0.162	0.152
Lac/Sta=3/7	0.295	0.150	0.110	0.213	0.150	0.151
Lac/Sta=1/1	0.280	0.186	0.110	0.203	0.186	0.177
Lac/Sta=7/3	0.305	0.225	0.183	0.235	0.225	0.217
Sta	0.299	0.230	0.168	0.183	0.230	0.215

a) Sampel weight=500 mg; relative humidity=32.7%. *b*) Compression stress=100 MPa; relative humidity=32.7%.

regarded as being due to the increase in the micro contact point number by hydrogen bonds due to water adsorption between the particles. Additional adhesive force between particles increases with interfacial tension and capillary negative pressure due to the greater numbers of water molecules caused by capillary condensation at the contact points between particles at relative humidity above 60%.[16,17]

The porosity tended to reach minimal values when the relative humidity was close to 32.7%. Table 2 shows the porosity of samples at a sample weight of 500 mg and compression stress of 100 MPa. The porosity of most samples was below 26%, except for the 1/1 complex of Lac/MCC, in the lactose–starch system which showed a very low value. It is well known that capping usually occurs at very low porosity. In this experiment, however, capping did not occur.

Effects of Specimen Weight and Compression Stress on Maximal Tensile Strength Table 3 shows the influence of sample weight and compression stress on porosity. The porosity decreased with increases in compression stress, in agreement with previous reports. On the other hand, porosity tended to decrease with increases in the amount of sample except in the case of starch. We previously reported[18] that the effects of the amount of sample on the porosity was independent in compression experiments using a manual hydraulic press. However, the density of specimens showed a tendency to increase in density with increases in the amount of sample when compressed by the present method.

Figure 4 shows the effects of specimen weight on the maximal tensile strength, σ_{max}, at 32.7% R. H. For all samples, as the specimen weight increased, σ_{max} increased indicating a greater resistance to flexure. According to Eq. 1, σ_{max} should be independent of the thickness of the specimen, yet σ_{max} was affected by thickness as shown in Fig. 4. Maximal tensile strength (σ_{max}) increased with increasing compression stress (P) for all samples as shown in Fig. 5. As the specimens became more dense with increasing compression stress, σ_{max} became greater than that of loose specimens at lower compression load.

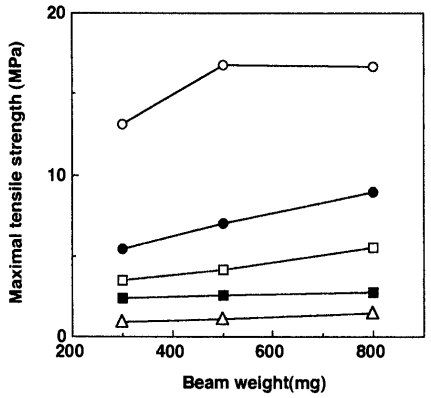

Fig. 4. Relationship between Beam Weight and Maximal Tensile Strength at Compression Stress of 100 MPa and Relative Humidity of 32.7%

○, MCC; ●, lac/MCC=3/7; □, lac/MCC=1/1; ■, lac/MCC=7/3; △, lactose.

Effects of Water Vapor Adsorption on Young's Modulus and Crushing Energy Figure 6 shows the relationship between water vapor adsorption and Young's modulus. The values of Young's modulus of specimens decreased with increasing proportion of α-lactose in the same manner as the

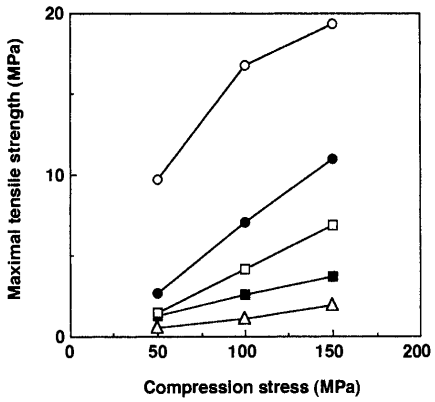

Fig. 5. Relationship between Compression Stress and Maximal Tensile Strength at Beam Weight of 500 mg and Relative Humidity of 32.7%

○, MCC; ●, lac/MCC=3/7; □, lac/MCC=1/1; ■, lac/MCC=7/3; △, lactose.

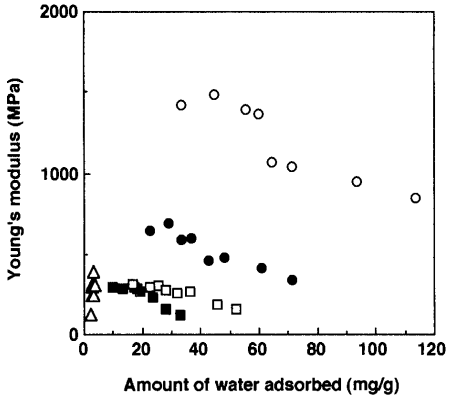

Fig. 6. Relationship between Amount of Water Adsorbed and Young's Modulus at Compression Stress of 100 MPa and Beam Weight of 500 mg

○, MCC; ●, lac/MCC=3/7; □, lac/MCC=1/1; ■, lac/MCC=7/3; △, lactose.

relationship between water vapor adsorption and the maximal tensile strength. The interparticle adhesion force decreased as a result of the increased interparticle water film formation, when moisture content increased. Therefore, the deformation of the powder layer was considered to increase even at low stress because both the interparticle adhesion force and Young's modulus decreased. The changes in crushing energy due to moisture adsorption showed a similar tendency to those in Young's modulus. That is, the crushing energy of MCC was greater than those of the other samples. In particular, α-lactose showed a very low value. Therefore, the crushing energy of mixed samples decreased with increasing ratio of α-lactose. The interparticle adhesion decreased, since the distance between particles increased with greater moisture content. The crushing energy also increased because of the increased displacement between particles. However, no marked effect of displacement was observed, because the thickness of specimens was small in the present experiment.

Relationship between Porosity and Maximal Tensile Strength We examined the changes in maximal tensile strength, σ_{max}, with increases in the porosity of each specimen. Figure 7 shows the relationship between porosity and the logarithmic maximal tensile strength, σ_{max}, for a beam weight of 500 mg at 10.6% R. H. As all the data yielded straight line plots, we considered that extrapolation of σ_{max} to the zero value of porosity was a characteristic value of

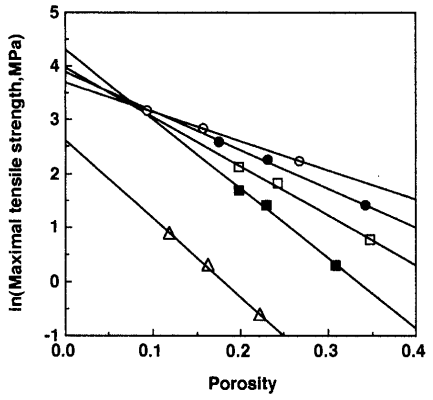

Fig. 7. Relationship between Porosity and ln (Maximal Tensile Strength) at Relative Humidity of 22.2% and Beam Weight of 800 mg

○, MCC; ●, lac/MCC=3/7; □, lac/MCC=1/1; ■, lac/MCC=7/3; △, lactose.

Table 4. Maximal Tensile Strength at Zero Porosity

Sample	$\sigma_{\varepsilon=0}$ (MPa)
Cornstarch	16.837
Lac : Sta=3 : 7	18.541
Lac : Sta=1 : 1	18.200
Lac : Sta=7 : 3	81.207
Lactose	13.849
Lac : MCC=7 : 3	49.789
Lac : MCC=1 : 1	53.807
Lac : MCC=3 : 7	73.611
MCC	40.149

Relative humidity=22.2%, beam weight=800 mg.

Table 5. Young's Modulus (E), Crushing Energy (CE) and Disintegration Time (DT) of Tablets at $\varepsilon=0$ and sample weight of 300 mg

Sample	E (MPa)	CE (10^{-4} J)	DT (s)
Cornstarch	569.4	2.606	35
Lac/Sta=3/7	984.2	0.830	45
Lac/Sta=1/1	903.3	1.128	51
Lac/Sta=7/3	1091	2.255	60
Lactose	919.5	1.238	59
Lac/MCC=7/3	2013	3.482	19
Lac/MCC=1/1	3132	6.683	19
Lac/MCC=3/7	3520	12.84	20
MCC	3914	18.08	131

these materials. The values of σ_{max} when extrapolated to zero porosity are shown in Table 4. MCC showed a large value of σ_{max} than the other samples such as cornstarch, lactose and mixtures containing these substances. However, a 7 : 3 mixture of lactose and cornstarch also showed a large σ_{max} value. These results confirmed that the most suitable ratio of lactose and cornstarch was as previously reported elsewhere.[19]

Relationship among Young's Modulus, Crushing Energy and Disintegration Time of Tablets Table 5 shows Young's modulus, crushing energy at zero porosity and disintegration time of tablets for each sample. Crushing energy tended to increase with increases in Young's modulus as shown in Table 5. Tablet disintegration time was correlated with increases in Young's modulus in the Lac–Sta system. Young's modulus also increased when the interparticle binding force increased. This indicated that the interparticle bind-

ing force had a signifcant effect on disintegration time in the Lac–Sta system. In the Lac–MCC system, MCC improved tablet compressibility and disintegration time in comparison with the Lac–Sta system. However, Fort *et al.*[20] reported that disintegration time of tablets prepared using MCC at high compression was decreased.

Conclusions

Young's modulus of elasticity of excipients as determined by 3-point beam bending can predict the disintegration time of single excipient tablets. Disintegration time of the lactose/cornstarch series increased only when Young's modulus increased sharply. However, the disintegration of the lactose/MCC series was more rapid than that of the other mixtures or single excipients. Young's modulus of MCC was large because the degree of swelling was high.

References

1) Church M. S., Kennerley J. W., *J. Pharm. Pharmacol.*, **34**, 50 (1982); *idem*, *ibid.*, **35**, 43 (1983).
2) Kerridge J. C., Newton J. M., *J. Pharm. Pharmacol.*, **38**, 79 (1986).
3) Mashad A, B., Newton J. M., *J. Pharm. Pharmacol.*, **39**, 961—965 (1987).
4) Bassam F., York P., Rowe R. C., Roberts R. J., *J. Pharm. Pharmacol.*, **40**, 68 (1988).
5) Bassam F., York P., Rowe R. C., Roberts R. J., *Int. J. Pharm.*, **64**, 55—60 (1990).
6) York P., Bassam F., Rowe R. C., Roberts R. J., *Int. J. Pharm.*, **66**, 143—148 (1990).
7) Roberts R. J., Rowe R. C., York P., *Int. J. Pharm.*, **91**, 173—182 (1993).
8) Roberts R. J., Rowe R. C., *J. Pharm. Pharmacol.*, **37**, 377—394 (1985), *idem*, *ibid.*, **38**, 567—571 (1986).
9) Fell J. T., Newton J. M., *J. Pharm. Sci.*, **59**, 688—691 (1970).
10) Ress J. E., Rue P. J., *Drug Dev. Ind. Pharm.*, **4**, 131—156 (1981).
11) Church M. S., Kennerley J. W., *J. Pharm. Pharmacol.*, **36**, Suppl. 44 (1984).
12) Yamaguchi U., Nishimatsu Y., "Elementary of Rock Dynamics," Publication of Tokyo University, 1977, p. 126.
13) Otsuka A., Danjo K., *J. Socie. Powder Techn. Japan*, **17**, 184—191 (1980).
14) Schubert H., *Chemie-Ing. Techn.*, **45**, 396—401 (1973).
15) Rumpf H., *J. Res. Assoc. Powder Techn. Japan*, **9**, 3—26 (1972).
16) Zimon A. D., "Adhesion of Dust and Powder," Plenum Press, New York, London, 1969, p. 63.
17) Pietsch W., Rumpf H., *Chemie. Ing. Tech.*, **39**, 885—893 (1967).
18) Danjo K., Ertel C., Carstensen J. T., *Drug Dev. Ind. Pharm.*, **15**, 1—5 (1989).
19) Sunada H., The 4th Symposium on Particulate Preparations and Designs, 1987.
20) Fot C. D., Richman M. D., Lia G. E., Chigraw R., *Abiseru Jihou* (in Japan), **1**, 5—11(1963).

Single Strand Conformation Polymorphism Analysis of Ras Oncogene by Capillary Electrophoresis with Laser-Induced Fluorescence Detector

Akiko NISHIMURA and Mitsutomo TSUHAKO*

Department of Functional Molecular Chemistry, Kobe Pharmaceutical University, Motoyama, Kitamachi, Higashinada-ku, Kobe 658–8558, Japan. Received August 30, 1999; accepted February 22, 2000

Single strand conformation polymorphism (SSCP) analysis of the N-ras oncogene was achieved by capillary electrophoresis with a laser-induced fluorescence detector (CE-LIF) using methylcellulose as a molecular sieving agent. The PCR-amplified N-ras oncogene, which is known to have a point mutation at codon 61 in the neuroblastoma, was investigated by CE-LIF combined with SSCP (SSCP-CE-LIF). A mixture of wild- and mutant-type single strand DNA fragments (103 bp) of the N-ras oncogene was separated by buffer solution containing 1.0% methylcellulose and 0.2 μM fluorescent dye (YO-PRO-1) at 25 °C.

The SSCP-CE-LIF technique gave good resolution for wild- and mutant-type single strand DNA fragments with separation completed within 7 min. SSCP analysis using a CE system with a LIF detector was successfully applied to the detection of the one point mutation on the N-ras oncogene.

Key words capillary electrophoresis; single strand conformation polymorphism; ras oncogene; PCR

Capillary electrophoresis (CE) is rapidly becoming an important tool for the analysis of the polymerase chain reaction (PCR) amplified products of DNA and for DNA sequencing in place of slab gel electrophoresis, owing to its high resolving power and high speed separation.[1—7] We have reported a technique for gene diagnosis of heart disease through human apolipoprotein B genotyping using CE with a laser-induced fluorescence detector (CE-LIF).[8] CE-LIF is an important technique for the highly sensitive analysis of DNA fragments of low concentration offering high sensitivity, resolution, accuracy, and speed. We applied the CE-LIF technique to the single strand conformation polymorphism (SSCP) analysis of the N-ras oncogene. Although SSCP analysis by capillary gel electrophoresis (CGE) was reported by Arakawa *et al.*[9] CGE with a UV detector has many disadvantages in sensitivity, reproducibility, and manipulation to fill the capillary with gel compared with CE-LIF using methylcellulose (MC) solution. Several groups have also demonstrated that SSCP analysis can be performed by CE-LIF.[10—15] In their systems, however, samples were amplified using primers labeled with one or two dyes,[10—14] or using samples post-labeled with two different dyes.[15] In the present study, N-ras gene was amplified without primer labeled with fluorescent dye. Furthermore, we used MC as polymer solution instead of linear polyacrylamide (LPA) which is conventionally used in SSCP analysis.[10—12,16] MC solution is superior to LPA in terms of handling because of low viscosity, repeatability, and easy preparation.

The N-ras oncogene is mapped to the short arm of chromosome 1 and is known to have a point mutation in codon 12 and 61, which are observed in various tumors such as leukemia and neuroblastoma. As shown in Fig. 1, the wild-type DNA has a codon CAA coding for glutamine (Gln), while the mutant-type DNA has a codon coding for various amino acids due to the difference of one base between the wild- and mutant-types. The mutation of the N-ras oncogene is now considered critical to human leukemogenesis.[17,18]

The SSCP method is a superior technique for the detection of mutation of DNA.[19] This method is based on the fact that a single strand DNA (ssDNA) molecule has a hold structure, which depends on its size and its sequence. A DNA molecule containing a mutation, even a single base substitution, will have a mobility shift during electrophoresis different to that of the wild type. Because the electrophoretic mobility of the ssDNA molecule in non-denaturing conditions strongly depends on its conformation, mutant- and wild-type ssDNA molecules would be separated by the CE-LIF technique in MC solution. Thus, we attempted the separation of SSCP containing a point mutation using the CE-LIF technique in polymer solution including intercalating dye. To improve the separation of ssDNA molecules, we investigated several parameters, electric field, running temperature, MC concentration, and intercalating dye concentration, which are known to have an influence on the electrophoretic mobility of ssDNA.

We have established a technique for the high performance DNA diagnosis of tumors through point mutation of the N-ras oncogene by the CE-LIF technique using an intercalating dye and a polymer solution. This technique is superior to slab gel electrophoresis and conventional SSCP analysis by the CE technique in sensitivity, reproducibility, speed, and handling.

Experimental

Wild-type and some mutant-type DNA fragments (103 bp) of N-ras oncogene, which have different mutations in codon 61, were amplified by PCR using the N-ras gene primer set (Takara). The genomic DNA of N-ras gene

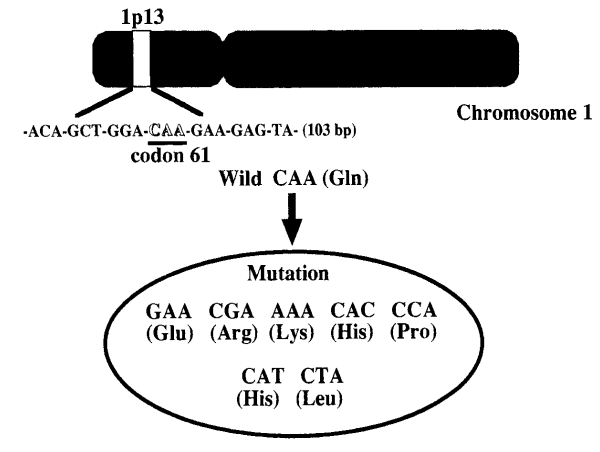

Fig. 1. Mutation of N-ras Oncogene

* To whom correspondence should be addressed. e-mail: mtsuhako@kobepharma-u.ac.jp

© 2000 Pharmaceutical Society of Japan

was the contents of the ras mutant set purchased form Takara. The oligonucleotide primers were 20 nucleotides in length. The sequence of the 5′-PCR primer was 5′-GGTGAAACCTGTTTGTTGGA-3′. That of the 3′-PCR primer was 5′-ATACACAGAGGAAGCCTTCG-3′. The PCR mixture (100 μl) contained 20 pmol of each primer, 2.5 mM of the four deoxynucleotide triphosphates (dNTPs), and 2.5 U of Taq DNA polymerase. PCR was performed on a thermal cycler (PHC-3, Techne Inc., Princeton, NJ, U.S.A.) with 35 cycles of amplification (denaturation: 1 min at 94 °C, annealing: 2 min at 55 °C, and extension: 1 min at 72 °C). The length of the generated PCR fragment was checked by CE using a 20 bp DNA ladder (Gensura Laboratories Inc., CA).

The PCR products were purified using SUPREC™-02 (Takara) to remove excess primers and dNTPs. The purified DNA samples were diluted 10—100 fold with MilliQ water and stored at −18 °C until use. Prior to CE separation the sample DNA (double strand DNA; dsDNA) was heated at 99 °C for 5 min, quenched, and kept on ice for more than 5 min to give ssDNA. All other chemicals were of analytical reagent or electrophoretic grade from Wako (Osaka, Japan).

A P/ACE 2050 CE system equipped with a LIF (Beckman Instruments, Inc., Fullerton, CA, U.S.A.) was used with negative source polarity. The laser source was operated at a power of 3 mW, excitation was at 488 nm and a 520 nm band pass filter was used as an emission cut off filter. A DB-17 coated capillary (360 μm o.d., 100 μm i.d.; J & W Scientific, Folsom, CA) of 20 cm effective length and 27 cm total length was used. The running buffer solution used in the present study was 50 mM Tris–borate (TB). To 10 ml of the buffer solution were added 0.5—1.0% MC and 1—10 μl of fluorescent dye 1-(4-[3-methyl-2,3-dihydro-(benzo-1,3-oxazole)-2-methylidene]-quinolinium)-3-trimethyl-ammonium propane diiodide (YO-PRO-1) which was intercalated into part of the double strand of SSCP. Denatured samples were electrophoretically introduced into the capillary at a negative polarity of 5.4 kV for 10—20 s and were run with running buffer solution containing MC and YO-PRO-1 at a negative polarity of 2.16—6.75 kV (80—250 V/cm). The temperature of the capillary was altered at 15—40 °C. DNA fragments were detected at 520 nm (Ex.; 488 nm).

Results and Discussion

Figure 2 shows the results of SSCP analysis of the wild- and three mutant-type ssDNA fragments of N-ras oncogene by the CE-LIF technique. Two peaks corresponding to ssDNA were observed at around 7 min in each electropherogram. The peaks indicate the sense and anti-sense ssDNA obtained by the denaturation of the N-ras oncogene. The peak at around 7.5 min in Figs. 2B, C, and D corresponded to the residual double strand DNA (dsDNA). The peak of dsDNA is thought to be due to the incomplete thermal denaturation of crude dsDNA at 99 °C and the formation of double strand DNA on cooling. However, the ssDNAs of the wild- and mutant-type N-ras oncogenes were completely separated by CE-LIF. Furthermore, only two peaks were also obtained in the analysis of ssDNA of other mutants, except dsDNA. The discrepancy in the peak height of the two ssDNA in Figs. 2B, C, and D is considered due to the difference in the amount of YO-PRO-1 intercalated into the double strand of ssDNA, since the same peak height was obtained by UV detection without YO-PRO-1. These results indicate that the

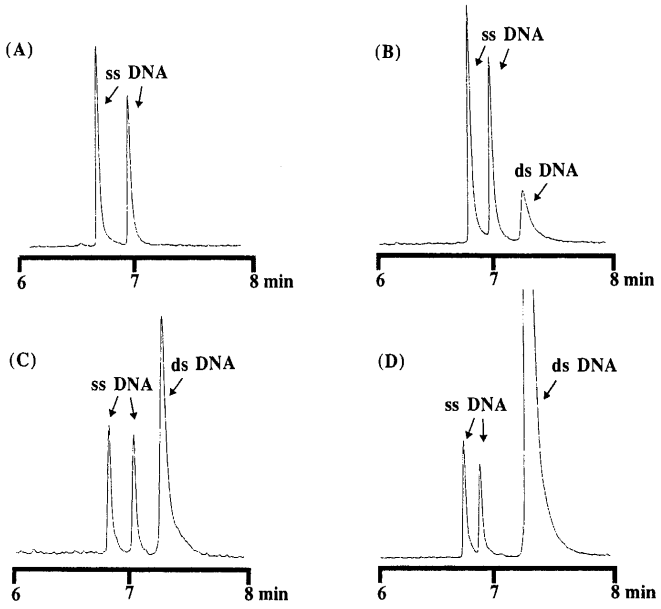

Fig. 2. CE Separation of ssDNA Obtained from N-ras Oncogene

Capillary; 100 μm i.d., 375 μm o.d., total length 27 cm, effective length 20 cm. Running buffer; 50 mM Tris–boric acid, 1.0% MC and 0.2 μM YO-PRO-1. Temperature; 25 °C. Field; 200 V/cm. Injection; 5.4 kV for 15 s. Detection; Ex., 488 nm, Em., 520 nm. Sample; A) wild-type ssDNA, B) mutant (proline)-type ssDNA, C) mutant (arginine)-type ssDNA, D) mutant (leucine)-type ssDNA.

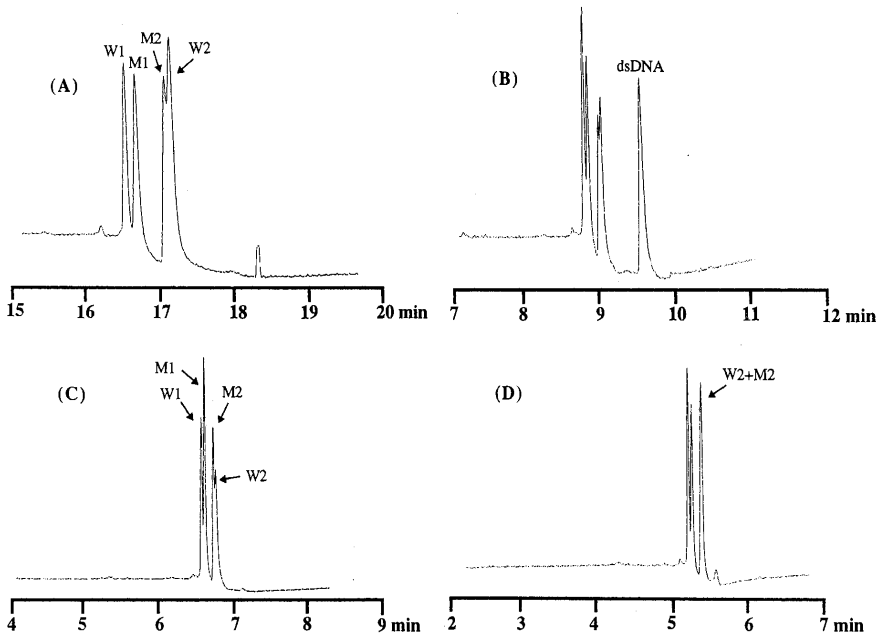

Fig. 3. Effect of Electric Field on the Separation of the Mixture of Wild- and Mutant-Type ssDNAs

Field; A) 80 V/cm, B) 150 V/cm, C) 200 V/cm, D) 250 V/cm. Sample; wild-type ssDNA + mutant (proline)-type ssDNA. Other conditions are as in Fig. 2.

one point mutation of N-ras oncogene can be detected, if there is a difference in the mobility of wild- and mutant-type ssDNAs. Thus, we examined the separation conditions for SSCP analysis of N-ras oncogene by the CE-LIF technique in detail to achieve high performance gene diagnosis for cancer through the mutation of N-ras oncogene.

The Effect of Electric Field on the Separation of ssDNA To begin with, we investigated the effect of the electric field on the CE separation. Figure 3 shows the effect of the applied fields (80—250 V/cm) on the separation of the mixture of wild- and mutant-type ssDNAs. Four peaks were assigned by changing the mixing ratio (wild-type ssDNA *vs.* Pro mutant-type ssDNA). As can be seen, the migration time of each ssDNA decreased with the increase of applied field. If the mixture of wild- and mutant-type ssDNAs can be completely separated, four peaks should be obtained in the electropherogram. The separation of ssDNAs was completed within only 18 min in the range of 80—200 V/cm although the resolution was poor at electric fields of more than 250 V/cm. At 200 V/cm, however, only 7 min was required to separate the four ssDNAs. Consequently, an electric field of 200 V/cm was used in subsequent experiments.

The Effect of Temperature on the Separation of ssDNA It is known that temperature is a potent influence on the higher-order structure of ssDNA. Thus, it is predicted that the separation of ssDNA of N-ras oncogene varies with the temperature. Figure 4 illustrates the effect of temperature (15—40 °C) on the separation of ssDNAs. Four peaks corresponding to the mixture of wild- and mutant-type ssDNAs were observed at a temperature of 30 °C and below, whereas the mixture was not separated at more than 35 °C. This is because the higher-order structure (conformation) of ssDNA changes with increasing temperature and the viscosity of the buffer solution containing MC decreases with temperature, resulting in poor resolution. As can be seen from Fig. 4, the wild- and mutant-type ssDNAs can be separated at 15—30 °C, and the migration time is reduced by increasing the temperature.

Thus, in the following experiments the temperature was set up at 25 °C in consideration of migration time, resolution, and experimental conditions such as temperature control and buffer handling.

The Effect of MC Concentration on the Separation of ssDNA We next examined the influence of the MC concentration on the separation of ssDNAs. Figure 5 demonstrates the influence of the concentration (0.5—1.0%) of MC on the separation of ssDNAs. As can be seen from Figs. 5A and B,

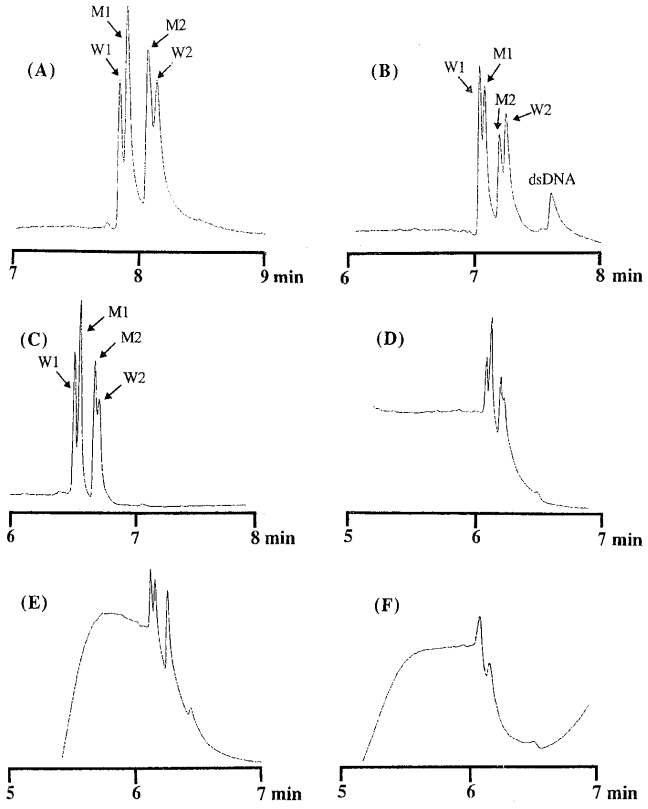

Fig. 4. Effect of Temperature on the Separation of the Mixture of Wild- and Mutant-Type ssDNAs

Temperature; A) 15 °C, B) 20 °C, C) 25 °C, D) 30 °C, E) 35 °C, F) 40 °C. Sample; wild-type ssDNA+mutant (proline)-type ssDNA. Other conditions are as in Fig. 2.

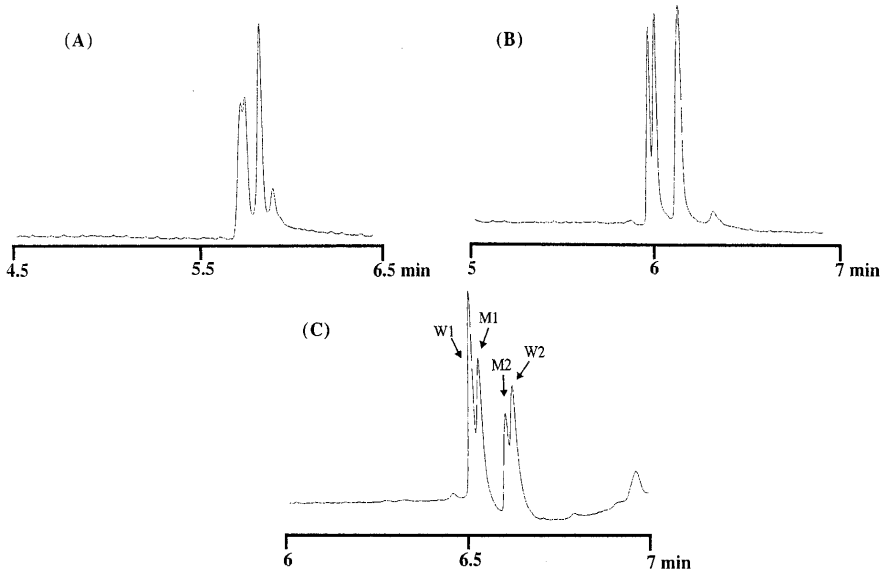

Fig. 5. Effect of MC Concentration on the Separation of the Mixture of Wild- and Mutant-Type ssDNAs

MC concentration; A) 0.5%, B) 0.7%, C) 1.0%. Sample; wild-type ssDNA+mutant (proline)-type ssDNA. Other conditions are as in Fig.2.

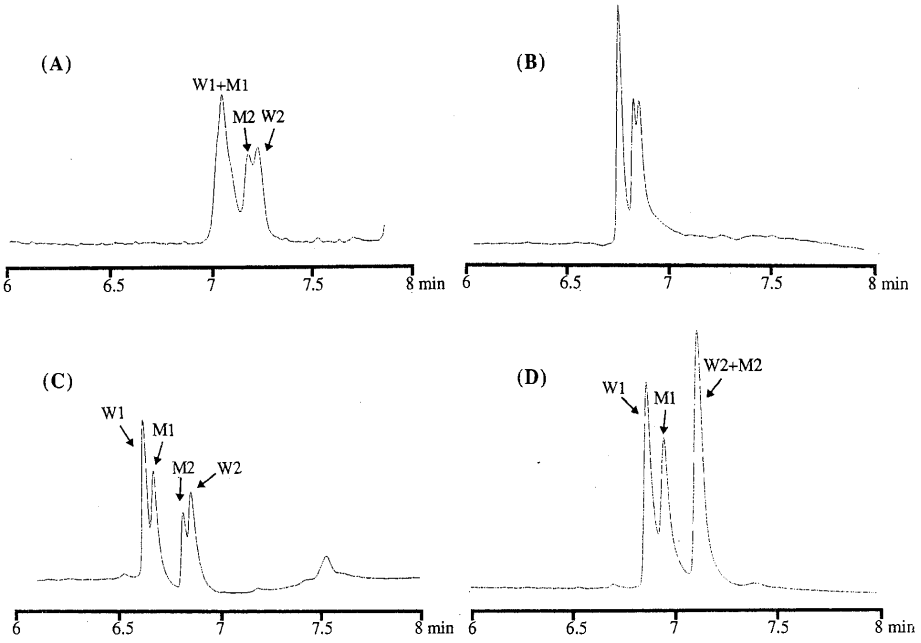

Fig. 6. Effect of YO-PRO-1 Concentration on the Separation of the Mixture of Wild- and Mutant-Type ssDNAs

YO-PRO-1 concentration; A) 1.0 μM, B) 0.5 μM, C) 0.2 μM, D) 0.1 μM. Sample; wild-type ssDNA+mutant (proline)-type ssDNA. Other conditions are as in Fig. 2.

the mixture of wild- and mutant-type ssDNAs could not be separated by MC solutions of less than 0.7%. However, four peaks corresponding to wild- and mutant-type ssDNAs were resolved using the 1.0% MC solution. It is conceivable that the polymer network in 0.5—0.7% MC is too large to detect the delicate difference in SSCP of N-ras oncogene. Also, it was difficult to fill the capillary with more than 1.2% MC solution because of high viscosity. Thus, the optimal MC concentration was determined to be 1.0% for subsequent experiments.

The Effect of YO-PRO-1 Concentration on the Separation of ssDNA One of the factors which has a great influence on the higher-order structure of ssDNA is the cation concentration. Figure 6 illustrates the effect of the concentration (0.1—1.0 μM) of the cationic intercalating dye YO-PRO-1 on the separation of ssDNAs. The intercalation of YO-PRO-1 into dsDNA expands the spacing of successive base pairs, distorts the regular sugar–phosphate backbone, and decreases the pitch of the double helix. As can be seen from Figs. 6A and B, three peaks were present with 1.0 and 0.5 μM YO-PRO-1 concentrations. However, the separation of the four ssDNA peaks could be achieved within 7 min by using 0.2 μM YO-PRO-1. As shown in Fig. 6D, poor resolution was obtained below 0.1 μM YO-PRO-1. From the results, the optimal concentration of YO-PRO-1 was found to be 0.2 μM. Broad peaks were obtained at higher YO-PRO-1 concentrations, indicating less difference in the higher-order structure of the ssDNAs, therefore, the resolution power was decreased at higher concentration. YO-PRO-1 is intercalated into DNA to delay the migration time, resulting in good separation. On the other hand, we could not achieve a good separation using other intercalating dyes such as 1,1′-(4,4,7,7-tetramethyl-4,7-diazundecamethylene)-bis-4-[3-methyl-2,3-dihydro(benzo-1,3-oxazole)-2-methylidene]-quinolinium tetraiodide (YO-YO-1) and quinolinium 4-[(3-methyl-2(3*H*)-benzothiazolyi-dene)methyl]-1-[3-(trimethylammonio)propyl]-diiodide (TO-PRO-1), which are optimally excited by the argon ion laser (488 nm), although the detection sensitivity of these fluorescent dyes is not very different from YO-PRO-1.

Table 1. Repeatability (n=9) of Migration Time, Mobility, and Relative Mobility for ssDNA Obtained from N-ras Oncogene

Peak	Migration time (min)	R.S.D. (%)	Mobility ($cm^2 V^{-1} s^{-1}$)	R.S.D. (%)	Relative mobility	R.S.D. (%)
W1	6.78	0.53	2.47×10^{-4}	0.51	1	—
M1	6.83	0.47	2.45×10^{-4}	0.50	0.993	0.07
M2	6.94	0.48	2.41×10^{-4}	0.54	0.975	0.22
W2	6.98	0.42	2.39×10^{-4}	0.45	0.969	0.19

From these results, the mixture of wild- and mutant-type ssDNAs could be separated with high resolution within 7 min (electric field; 200 V/cm) at 25 °C using a 27 cm capillary, 50 mM TB-buffer containing 1.0% MC and 0.2 μM YO-PRO-1.

Repeatability in SSCP Analysis We next examined the repeatability of the SSCP analysis by the CE-LIF technique. The analysis of the mixture of wild- and mutant-type ssDNAs was carried out 9 times using the same sample and buffer. The average migration time, mobility, and relative mobility of the peaks W2, M1, and M2 in Fig. 6C for the peak W1 of the wild-type ssDNA are summarized in Table 1. The repeatability of the migration time and the mobility of each ssDNA was about 0.5% relative standard deviation (R.S.D., n=9), but that of the relative mobility of each ssDNA for the peak W1 was in the range of 0.07—0.22% R.S.D., indicating that SSCP analysis by the CE-LIF technique has satisfactory precision for the detection of one point mutation of the N-ras oncogene.

SSCP Analysis of the N-ras Oncogene Figure 7 shows the CE separation of the mixture of wild- and other mutant-type ssDNAs. In this figure, peaks W1 and W2 show the ssDNA obtained from the wild-type, and peaks M1 and M2 from the mutant-type. Figure 7 indicates that six in seven mutant-type samples could be resolved. However, the mix-

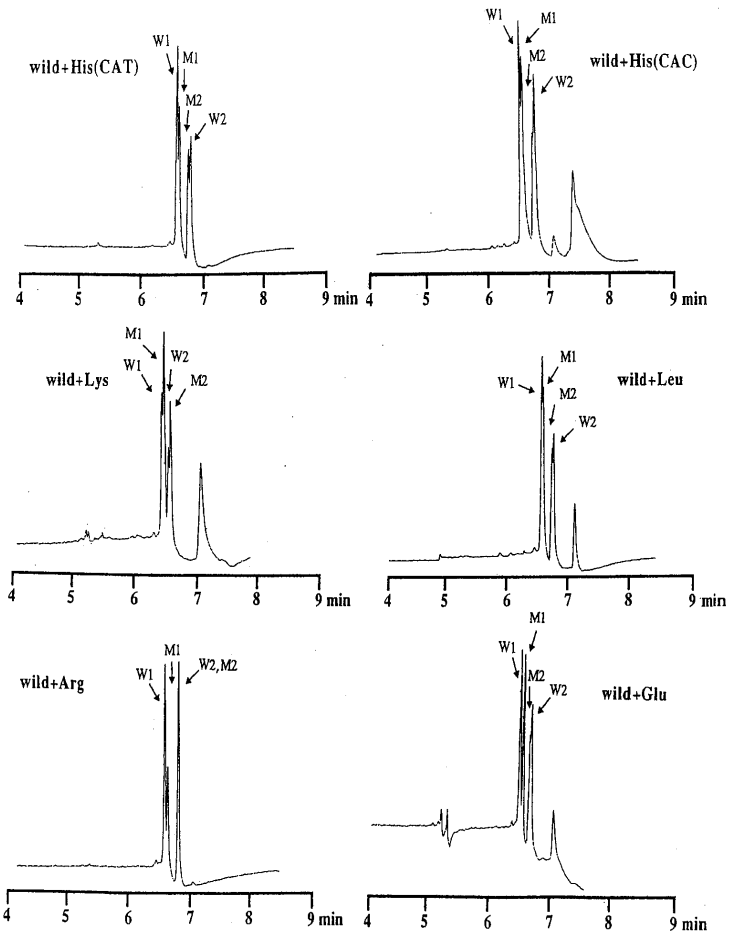

Fig. 7. SSCP Analysis of the N-ras Oncogene by the CE-LIF Technique

Conditions are as in Fig. 2. Peaks W1 and W2 are ssDNA obtained from wild-type DNA. Peaks M1 and M2 are ssDNA obtained from mutant-type DNA.

ture of wild- and mutant (arginine)-type ssDNAs could not be separated using the present experimental conditions. However, from the appearance of three peaks, it is clear that this sample contains the mutant-type DNA, which is different from wild-type DNA.

Conclusion

We reported the effects of electric field, temperature, MC concentration, and YO-PRO-1 concentration on the separation of ssDNAs by the SSCP-CE-LIF technique. N-ras oncogene containing one point mutation could be resolved by the SSCP-CE-LIF technique with high sensitivity.

The SSCP-CE-LIF technique using the intercalating dye, YO-PRO-1, can be used to genetically screen for cancer through the detection of the one point mutation of the N-ras oncogene. This technique offers excellent resolving power, high-speed separation, and good repeatability. In SSCP analysis with the CE-LIF technique using MC polymer solution it is very easy to prepare a buffer solution and refill the capillary with the buffer solution, and it is possible to reuse the capillary any number of times.

Acknowledgements This work was supported by the Scientic Research Promotion Fund of the Japan Private School Promotion Foundation.

References

1) Baba Y., Tomisaki R., Sumita C., Tsuhako M., Miki T., Ogihara T., *Electrophoresis*, **16**, 437—440 (1995).
2) McCord B. R., McClure D. L., Jung J. M., *J. Chromatogr.*, **652**, 75—82 (1993).
3) Srinvasan K., Girard J. E., Williams P., Roby R. K., Weedn V. M., Morris S. C., Kline M. C., Reeder D. J., *J. Chromatogr.*, **652**, 83—91 (1993).
4) Gelfi C., Orsi A., Righetti P. G., Brancolinni V., Cremonesi L., Ferrai M., *Electrophoresis*, **15**, 640—643 (1994).
5) Baba Y., Ishimaru N., Samata K., Tsuhako M., *J. Chromatogr.*, **653**, 329—335 (1993).
6) Sumita C., Baba Y., Hide K., Ishimaru N., Samata K., Tanaka A., Tsuhako M., *J. Chromatogr.*, **661**, 297—303 (1994).
7) Baba Y., Tomisaki R., Sumita C., Tsuhako M., Miki T., Ogihara T., *Biomedical Chromatogr.*, **8**, 291—293 (1994).
8) Nishimura A., Tsuhako M., Miki T., Ogihara T., Baba Y., *Chem. Pharm. Bull.*, **46**, 294—297 (1998).
9) Arakawa H., Nakashiro S., Maeda M., Tsuji A., *J. Chromatogr. A.*, **722**, 359—368 (1996).
10) Hebembrock K., Williams P. M., Karger B. L., *Electrophoresis*, **16**, 1429—1436 (1995).
11) Katsuragi K., Kitagishi K., Chiba K., Ikeda S., Kinoshita M., *J. Chromatogr. A.*, **744**, 311—320 (1996).
12) Ren J., Ulvik A., Ueland P. M., Refsum H., *Anal. Biochem.*, **245**, 79—84 (1997).
13) Arakawa H., Tsuji A., Maeda M., Kamahori M., Kambara H., *Pharm J. Biomed. Anal.*, **15**, 1537—1544 (1997).
14) Geisel J., Walz T., Bodis M., Nauck M., Oette K., Herrmann W., *J. Chromatogr. B.*, **724**, 239—247 (1999).
15) Inazuka M., Wenz H., Sakabe M., Tahira T., Hayashi K., *Genome Res.*, **7**, 1094—1103 (1997).
16) Kuypers A. W. H. M., Willems P. M. W., Schans M. J., Linssen P. C. M., Wessels H. M. C., Bruijn C. H., M. M., Everaerts F. M., Mensink E. J. B. M., *J. Chromatogr.*, **621**, 149—156 (1993).
17) Gambke C., Signer E., Moroni C., *Nature* (London), **307**, 476—478 (1984).
18) Gambke C., Hall A., Moroni C., *Proc. Natl. Acad. Sci. U.S.A.*, **82**, 879—882 (1985).
19) Orita M., Iwahana H., Kanazawa H., Hayashi K., Sekiya T., *Proc. Natl. Acad. Sci. U.S.A.*, **86**, 2766—2770 (1989).

Characteristics of Complexes Composed of Sodium Hyaluronate and Bovine Serum Albumin

Shouhong XU, Junpei YAMANAKA, Shizuko SATO, Isamu MIYAMA, and Masakatsu YONESE*

Faculty of Pharmaceutical Sciences, Nagoya City University, 3–1 Tanabe-dori, Mizuho-ku, Nagoya 467–8603, Japan.
Received September 10, 1999; accepted February 11, 2000

Complexes composed of sodium hyaluronate (NaHA) and bovine serum albumin (BSA) were studied to elucidate the exact composition of the complex, the phase separation, the electrophoretic mobility and the size using dynamic light scattering (DLS) and electrophoretic light scattering (ELS), *etc.* The phase diagram of the mixed solutions was determined. The complexes were soluble in neutral or weakly acidic pH regions and showed phase separation in the more acidic pH region. From the concentration of Na^+ released from NaHA when it binds to BSA, the ratios of BSA to NaHA of the complexes were determined. In the region of soluble complexes, one BSA molecule was determined to bind with 15 carboxylic groups of NaHA and in the region of insoluble complexes to bind with 6 carboxylic groups. At the phase separation point, 117 BSA molecules bound with one NaHA molecule and 17% of the carboxylic groups of NaHA did not contribute to the binding of BSA. The sizes of the complexes decreased from several μm to several hundred nm as the binding ratio of BSA increases. Decreases in the viscosities of the mixed solutions were consistent with the decreases of the sizes. From these results, a model of complex formation is proposed.

Key words sodium hyaluronate; bovine serum albumin; complex; light scattering

Complexes of polyelectrolytes and proteins have been studied to understand the structures and the mechanism of their formation from basic and applied points of view.[1—12] Complex formation due to electrostatic interactions between oppositely charged groups depends on pH, ion strength, concentration and temperature. According to Kokufuta E. *et al.*,[3] the complexes are grouped into intra- and inter-polymer complexes. The former is a soluble complex and the latter is formed by the bindings of the intra-polymer complexes. The inter-polymer complexes bring about a phase separation, and precipitated aggregations or coacervations are formed. Polyanions and proteins form soluble complexes in neutral or weak acidic pH region, and in the more acidic pH region, a phase separation occurrs.

Complexes composed of a mucopolysaccharide and a protein have been widely studied to elucidate the functions in the living and as basic studies of the interaction between polyelectrolytes. Hyaluronate (HA) is widely distributed in living tissue, such as skin, bone, glass body fluid, *etc.* It does not exist alone and usually combines with protein to maintain the shape of the tissues and to control the permeability of ions and water. The structure of HA is a linear polysaccharide whose repeating disaccharide units are composed of *N*-acetyl-D-glucosamine and D-glucuronic acid, and there is only one carboxylic group per one repeating unit.[13,14] HA is well known to moisturize skin to prevent aging and is used widely in the cosmetics and pharmaceutical industry.[15]

In our laboratory, the characteristics of polysaccharides have been studied not only in solutions but also at interfaces to elucidate the effects of charge densities and the kinds of charged groups. Recently, NaHA was reported to form two-dimensional auto-organized hexagonal-like networks on a bovine serum albumin (BSA) monolayer resulting from interfacial interactions.[16] In this paper, the interactions of sodium hyaluronate (NaHA) and BSA in solution were studied as the basis of interfacial interactions. Their complex formation, the composition, the size and the phase separation were studied using dynamic light scattering (DLS) and electrophoretic light scattering (ELS) which are powerful techniques in the study of macromolecular solutions.[17,18]

Experimental

Materials and Sample Preparation NaHA obtained from Seikagaku Kogyo Co. Ltd. was used without any purification. The weight averaged molecular weight M_w was determined to be 8.50×10^5 g·mol^{-1} using static light scattering (Otsuka Electronics Co., DLS-700Ar).

BSA was purified by delipidizing a BSA Fraction V (Seikagaku Kogyo) as follows: 1) To the BSA solution (10 w/v%, 100 cm^3), an activated carbon (5 g, Darco Ci.Ltd., G-60) was added. 2) After adjusting the solution to pH=3, the solution was stirred in an ice bath for 2 h, and then centrifuged under 24000×***g*** for 30 min. 3) The supernatant was filtered and adjusted to pH=5 by adding NaOH (0.2 mol·dm^{-3}). 4) The above solution was passed through a mixed column (cation exchange resin: anion exchange resin=1 : 1) and then freeze-dried. Cation and anion exchange resins were of Amberlite IR-120B and IRA-400 (Organo Co.). The isoionic point of BSA was 5.2 and the value of M_w was 70000 g·mol^{-1}.

Preparing sample solutions composed of NaHA and BSA, concentration of NaHA (C_{NaHA}) was 0.1 w/v% (1.2 μmol·dm^{-3}) and various concentrations of BSA were added.

Measurement of Activities of Na^+ and pH of Mixed Solutions Composed of NaHA and BSA The activities of Na^+ ion of NaHA solution and of NaHA–BSA mixed solutions were measured at 25 °C using a pH/ion meter (Orion 920A), which was connected with a double junction reference electrode (Orion Co., No. 900200). The pH value was obtained by using a digital pH/mV meter (Orion model 701A). The ionic strengths J of the solutions were 0.001 mol·dm^{-3}, which was adjusted by NaCl.

Measurement of Viscosity and Transparency The viscosities of NaHA–BSA mixed solutions were measured at 25 °C under the condition of J=0.001 mol·dm^{-3} using an Ostward-type viscometer of which the falling time of the solvent was 92 s. The transparencies of the solutions were measured in the region from neutral to acidic pH region using a spectrophotometer (Hitachi Electronics Co., U-3000) at λ=700 nm.

Measurement of Electrophoretic Mobility, Apparent Diffusion Coefficient and Hydrodynamic Diameter The electrophoretic mobilities of NaHA–BSA mixed solutions were measured at 25 °C using an electrophoretic light scattering photometer (Otsuka Electronics Co., LEZA-600, λ=632.8 nm) at a fixed scattering angle of 20°. The true mobility U was obtained by correcting for the electro-osmotic effects. The apparent diffusion coefficients of the NaHA–BSA mixed solutions were measured at 25 °C in the region of scattering angle λ=30—90° using a DLS (DLS700Ar: Otsuka Electronics Co., λ=488 nm).

* To whom correspondence should be addressed. e-mail: yonese@phar.nagoya-cu.ac.jp
© 2000 Pharmaceutical Society of Japan

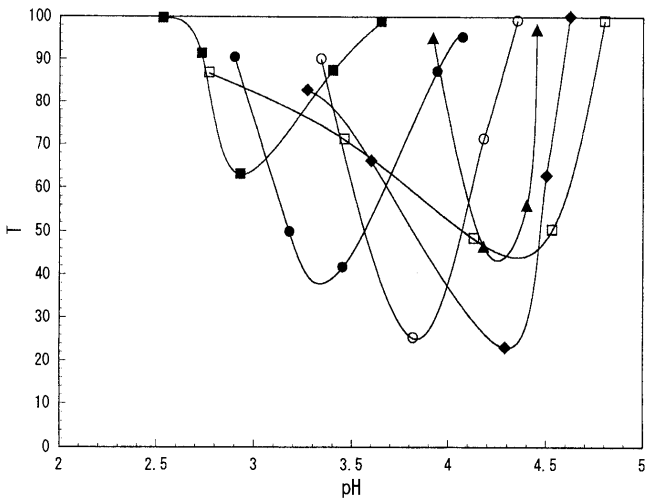

Fig. 1. Transparencies of NaHA–BSA Mixed Solutions Plotted against pH Value

C_{NaHA}=1.2 μmol·dm^{-3}, J=0.001 mol·dm^{-3}. C_{BSA} (μmol·dm^{-3}): ■, 15; ●, 29; ○, 42; ▲, 57; ◆, 85; □, 128.

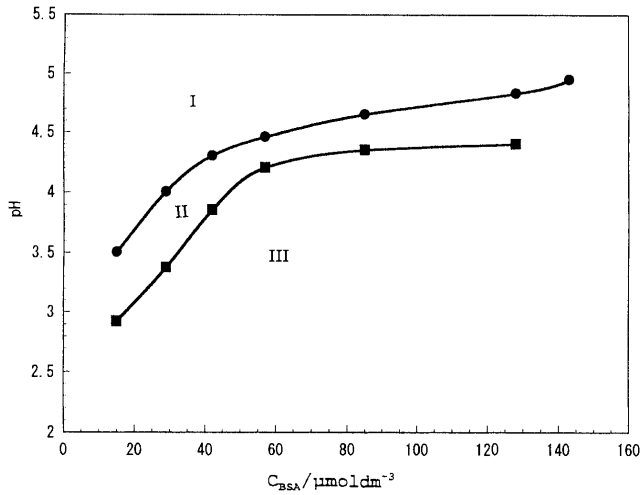

Fig. 2. Phase Diagram of Soluble and Insoluble Complexes

■, $pH_{pr.}$, pH which the insoluble complex begins to precipitate; ●, $pH_{ps.}$, pH which the phase separation begins to occur. I, soluble complex; II, suspended complex; III, precipitating complex.

Results

Soluble and Insoluble Complexes Various amounts of BSA (C_{BSA}=0—128 μmol·dm^{-3}) were added to NaHA solution (C_{NaHA}=1.2 μmol·dm^{-3}, J=0.001mol·dm^{-3}) and then the mixed solutions were titrated by using HCl (1 mol·dm^{-3}).[2] The transparency (T) of the solutions was measured under stirring at 25 °C. As shown in Fig. 1, with decreasing pH the solutions became turbid due to the formation of the insoluble complexes and the T of the mixed solutions showed minima at which the complexes started to precipitate. In the more acidic pH region, the precipitation increased and became more bulky. As a result, the solutions became less turbid. The pH value at which T began to decrease was defined as the phase separation pH ($pH_{ps.}$), and the pH value at which T showed a minimum was defined as the precipitation pH ($pH_{pr.}$). The values of $pH_{ps.}$ and $pH_{pr.}$ depended significantly on C_{BSA} and increased with increasing C_{BSA}.[3]

Complex formations and the states depended on pH and the compositions. The values of $pH_{ps.}$ and $pH_{pr.}$ are shown in Fig. 2 as a function of C_{BSA}. In the region of III, the precipitation of the complex occurs and in the region of II the insoluble complexes are dispersed. In the region of I, the soluble complexes are considered to be formed. In the more alkaline region, the complexes cannot be formed although the boundary was not determined.

Concentration of Na^+ Ion Released Due to Complex Formation In the formation of the complexes between NaHA and BSA, the complexes are considered to be formed by an electrostatic interaction between carboxylic groups of NaHA and BSA. When BSA binds to NaHA, Na^+ ions should be released. The activities of Na^+ ion of the mixed solutions composed of NaHA (C_{NaHA}=1.2 μmol·dm^{-3}) and BSA (C_{BSA}=0—171 μmol·dm^{-3}) were measured under J=0.001 mol·dm^{-3} by using a Na^+ ion electrode at 25 °C. The activity coefficients were approximated to be 1 because of the low concentration.

Figure 3 shows the concentration of Na^+ ion of the mixed solutions (C_{Na^+}), released by the binding of BSA to NaHA as a function of C_{BSA}. The value of C_{Na^+} at C_{BSA}=0 is the contribution of NaHA and NaCl. With increasing C_{BSA}, C_{Na^+} increased due to the increases in the binding amounts of BSA. In the region of C_{BSA}≧141 μmol·dm^{-3}, the solutions became a little turbid due to the formation of the insoluble complex. An arrow in Fig. 3 shows the phase separation point. The slopes of C_{Na^+} changed at C_{BSA}=141 μmol·dm^{-3} and in the region of C_{BSA}≧141 μmol·dm^{-3} the slope decreased significantly. These results show the binding states of BSA change at the phase separation point, *i.e.*, the numbers of carboxylic group of NaHA binding to one BSA molecule changed. At C_{BSA}=141 μmol·dm^{-3}, the ratio of C_{BSA} to C_{NaHA} (C_{BSA}/C_{NaHA})^{ps} was 117.

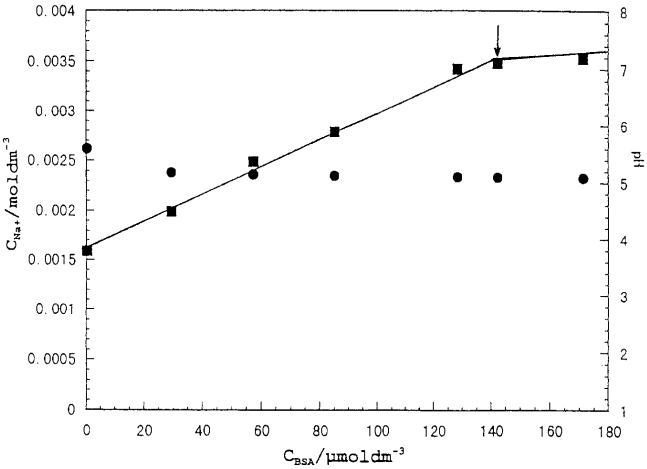

Fig. 3. Concentration of Na^+ Ion Released from NaHA by Adding BSA

■, concentration of Na^+ ion; ●, the pH value of mixed solution. C_{NaHA}=1.2 μmol·dm^{-3}, J=0.001 mol·dm^{-3} (NaCl). The arrow shows C_{BSA} at which the solution became turbid.

The values of pH of the mixed solutions are also shown in Fig. 3. As C_{BSA} increased, pH of the solutions decreased slightly from the value of pH of NaHA solution (pH=5.6) to pH=5.0.

Viscosity of Mixed Solutions Effects of the complex formation on the viscosity of the mixed solutions were studied by using an Ostward-type viscometer under the same conditions mentioned above. The relative viscosities of the soluble solutions ($\eta_{rel.}$) were measured and the results are

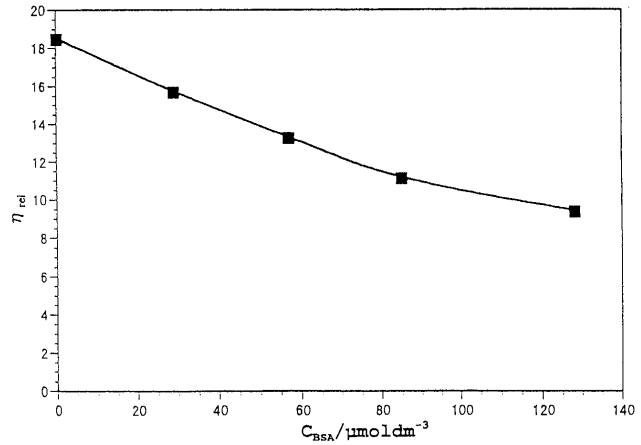

Fig. 4. Relative Viscosity of Soluble Complexes Plotted against C_{BSA}
$C_{NaHA}=1.2\,\mu mol\cdot dm^{-3}$, $J=0.001$ mol·dm^{-3}.

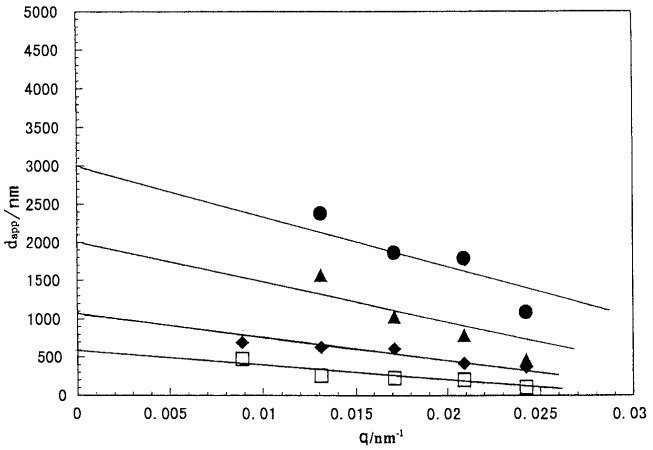

Fig. 5. Apparent Diameter of Complex Particles Plotted against Scattering Vector q
$C_{NaHA}=1.2\,\mu mol\cdot dm^{-3}$, $J=0.001$ mol·dm^{-3}. C_{BSA}(μmol·dm^{-3}): ●, 29; ▲, 57; ◆, 85; □, 128.

shown in Fig. 4 as a function of C_{BSA}. In the region of $C_{BSA} \geqq 141\,\mu mol\cdot dm^{-3}$, the viscosities were not measured because of the phase separation of the solutions. The values of $\eta_{rel.}$ were found to decrease with increasing C_{BSA}, *i.e.*, in spite of the increases of the binding amounts of BSA to NaHA the values of $\eta_{rel.}$ were found to decrease. NaHA molecules are known to have a worm like structure[19] in solution due to electrostatic repulsion. Thus, with increasing C_{BSA}, NaHA–BSA complexes are considered to change from the extended worm like structure to a shrunken random coil structure.

Apparent Diffusion Coefficient and Diameter of Complexes To estimate the sizes of the NaHA–BSA complexes, their apparent diffusion coefficients ($D_{app.}$) were measured using DLS in the region of scattering angle $\theta=30$—$90°$. The values of $D_{app.}$ were obtained by the cumulant method. The variances were in the range of 0.3—0.7 which were much more than 0.02 and the size distributions of the complexes were found to be inhomogeneous. Assuming that all the complexes are sphere-like structures, their mean apparent diameters ($d_{app.}$) were estimated by using the Einstein–Stokes' equation. The results of $d_{app.}$ are shown in Fig. 5 as a function of scattering vector (q) ($q=4\pi n/\lambda \sin(\theta/2)$), where λ is wavelength. The values of $d_{app.}$ depended on q and decreased

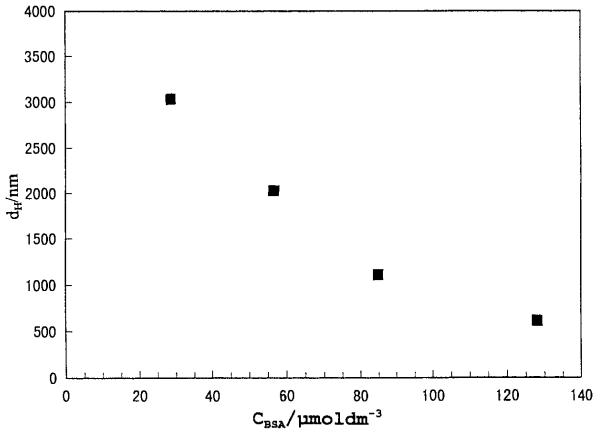

Fig. 6. Hydrodynamic Diameter of Complex Particles Plotted against C_{BSA}

with increasing q. The dependence results from long range interactions between the complexes and the hydrodynamic diameter d_H can be obtained from the extrapolated value of $d_{app.}$ to $q=0$.[20] As shown in Fig. 6, the values of d_H decreased from 3 μm to 600 nm with increasing C_{BSA}. The decrease of d_H with increasing C_{BSA} was consistent with the results of decreasing $\eta_{rel.}$ shown in Fig. 4. As to the point at $C_{BSA}=0$, the value of $D_{app.}$ could not be measured. The size of the NaHA molecule is considered to be too large to be measured.

Electrophoretic Mobility of Complexes The electrophoretic mobilities (U) of the complexes in the same mixed solutions mentioned above were measured using ELS at 25 °C. The spectra U of $C_{BSA}=57\,\mu mol\cdot dm^{-3}$ is shown in Fig. 7(a) as a typical result in the region of $C_{BSA}<C^{ps}_{BSA.}$ The spectra showed one sharp peak. As shown in a previous paper,[21] the isoelectric point of BSA was pH=5.2 and the values of U of BSA were almost 0 in the region of pH=5.6—5.0. The peak of BSA was not found near 0. The spectrum of $C_{BSA}=128\,\mu mol\cdot dm^{-3}$, which is a little less than C^{ps}_{BSA}, is shown in Fig. 7 (b) and showed a slightly broad peak with several small shoulders at the region near $U=0$. The shoulders show the presence of the complexes containing more BSA being just before the phase separation. However, the peak of BSA could be neglected. From these results, almost all BSA molecules added to NaHA solutions are considered to bind to NaHA molecules in the region of $C_{BSA}<C^{ps}_{BSA}$.[4,5]

The results U of the complexes are shown in Fig. 8 as a function of C_{BSA}. The results of U were negative and the absolute values of U decreased with increasing C_{BSA} in the region of $C_{BSA}<C^{ps}_{BSA.}$ The value of $C_{BSA}=0$ is that of NaHA ($U=-4.982\times10^4\,cm^2\cdot V^{-1}\cdot s^{-1}$). In the region of $C_{BSA}\geqq C^{ps}_{BSA}$, in which the phase separation occurred, the mobilities were measured after filtrating out insoluble complexes through a 0.8 μm filter. However, several peaks appeared near the main peaks in the filtrates. The values of U of the main peak are shown in Fig. 8 as an open square and the results increased slightly. Even after filtering, inhomogeneous complexes were found to exist and the values of U of the main complexes are considered to increases due to the slight increases of binding BSA in $C_{BSA}\geqq C^{ps}_{BSA}$ as shown in Fig. 3. It should be noted that the value of U of C^{ps}_{BSA} was negative $-1.9\times10^4\,cm^2\cdot V^{-1}\cdot s^{-1}$.

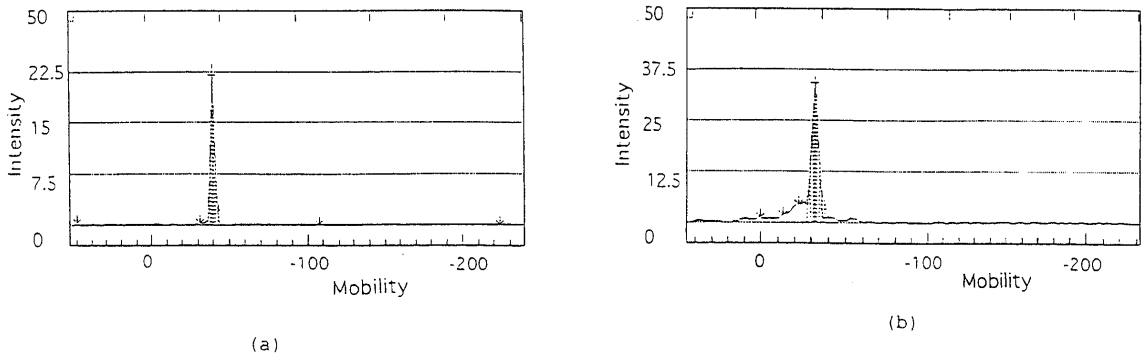

Fig. 7. Spectra of Mobility of Soluble NaHA–BSA Complexes

(a) $C_{NaHA}=1.2\,\mu mol\cdot dm^{-3}$, $C_{BSA}=57\,\mu mol\cdot dm^{-3}$, $n_{BSA}/n_{NaHA}=47$. (b) $C_{NaHA}=1.2\,\mu mol\cdot dm^{-3}$, $C_{BSA}=128\,\mu mol\cdot dm^{-3}$, $n_{BSA}/n_{NaHA}=107$.

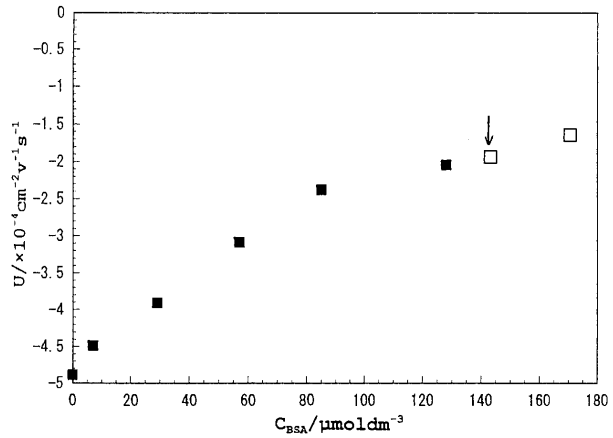

Fig. 8. Electrophoretic Mobility of Soluble Complexes Plotted against C_{BSA}

$C_{NaHA}=1.2\,\mu mol\cdot dm^{-3}$, $J=0.001 mol\cdot dm^{-3}$ (NaCl). The arrow shows C_{BSA} at which the solution became turbid.

Discussion

The Composition of Soluble Complexes The formation of the complex between NaHA and BSA brings about the release of Na^+ ions according to the following reaction.[6]

$$n(\text{HA-COO-Na})+\text{BSA}\rightarrow \text{BSA(HA-COO)}_n+n\text{Na}^+ \quad (1)$$

Where n is the molar numbers of the carboxylic groups of NaHA bound to one mole BSA. Assuming all BSA molecules added to NaHA solution bind to NaHA molecules in the region of $C_{BSA}\geqq C^{ps}_{BSA}$, n can be obtained from Eq. 2,

$$n=\Delta C^{f}_{Na^+}/\Delta C_{BSA} \quad (C_{BSA}<C^{ps}_{BSA}) \quad (2)$$

where $\Delta C^{f}_{Na^+}$ is the released concentration of Na^+ ion and ΔC_{BSA} is the increase of BSA concentration.

In the region of $C_{BSA}<C^{ps}_{BSA}$, approximating that almost all BSA molecules added to the NaHA solution bind to NaHA molecules and free BSA molecules can be neglected from the results of Fig. 7, the values of n can be obtained from the slope of C_{Na^+} shown in Fig. 3. The slope was constant in the region of $C_{BSA}<C^{ps}_{BSA}$ and the value of n was found to be 15. One BSA molecule binds with 15 carboxylic groups of NaHA. Since the molecular weight of a repeating unit of NaHA is $401\,g\cdot mol^{-1}$, there are 2119 carboxylic groups in one NaHA molecule. Then, assuming all carboxylic groups of NaHA bind to BSA, 141 BSA molecules should bind to 1 NaHA molecule for the saturated complex, *i.e.*, $(C_{BSA}/C_{NaHA})^{sat}_{cal.}=141$. The experimental result of $(C_{BSA}/C_{NaHA})^{ps}$ (=117) was smaller than the calculated value and 17% of the carboxylic groups were found not to contribute to the formation of the complexes. These free carboxylic groups are considered to contribute to the negative mobility of the complexes ($C_{BSA}\geqq C^{ps}_{BSA}$) shown in Fig. 8.

In the region of $C_{BSA}\geqq C^{ps}_{BSA}$, the value of n obtained was 6 from the slight increase of C_{Na^+} shown in Fig. 3. BSA molecules were found to bind furthermore to the complex. The charge densities of the complexes approach to zero due to the extra binding to BSA. The decrease in the electrostatic repulsion between the complexes brings about the inter-polymer complex, which is followed by the phase separation.

The Model of Complex Formation The NaHA molecule is a rod- or worm-like structure and the BSA molecule is a prolate ellipsoid one. BSA molecules bind to the carboxylic groups of the NaHA molecules by electrostatic attraction and form intra-polymer complexes. With increasing the binding amounts of BSA, the apparent charge amounts decrease due to the shielding effects and the extensions of NaHA contract, *i.e.*, NaHA molecules are entangled by the bindings of BSA, which induces a decrease in the viscosity and the diffusion coefficients. In the region of $C_{BSA}\geqq C^{ps}_{BSA}$, the interactions between complexes are enhanced due to the decreases of the electrostatic repulsion, and inter-polymer complexes are formed and a phase separation occurs. The model of the complex formation is shown in Fig. 9.

The complexes of sodium chondroitin sulfate C (ChS) and BSA were studied using a static light scattering and the shape was reported to be a rod-like structure just like ChS alone. With increasing the binding amounts of BSA, the length was 30% longer and 6 times thicker in diameter than the ChS molecule at the saturated binding state.[9] Acid mucopolysaccharides are a rod or worm like structure in aqueous solutions due to the electrostatic repulsion of the negative charges and the stiffness of sugar chains. The charge density of ChS is two times as much as NaHA, which might induce the rod-like structure of the complexes of ChS and BSA even at the saturated binding state. On the other hand, the sizes of the complexes of HA and BSA decreased with increasing the binding amounts of BSA. The differences of the shape from the complexes of ChS and BSA are considered to result from the smaller charge densities and the much higher molecular masses of NaHA (M_w of NaHA, $850\times10^3\,g\cdot mol^{-1}$, M_w of NaChS, $70.9\times10^3\,g\cdot mol^{-1}$).

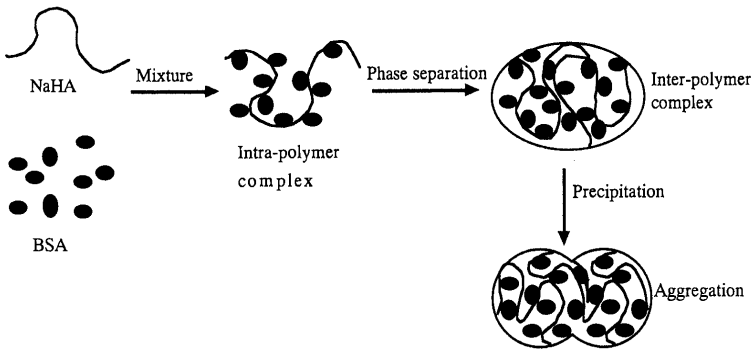

Fig. 9. Model of NaHA–BSA Complex Formation

References

1) Chen R. F., *J. Biol. Chem.*, **242**, 173—180 (1967).
2) Yonese M., Yano M., *Bull. Chem. Soc. Jpn.*, **64**, 1814—1820 (1991).
3) Kokufuta E., Dubin P. L., *Surface*, **32**, 460—479 (1994).
4) Yonese M., Xu S. H., Kugimiya S., Sato S., Miyata I., *Prog. Colloid Polym. Sci.*, **106**, 252—256 (1997).
5) Makino K., Ikekita M., Kondo T., Tanuma S., Ohshima H., *Colloid Polym. Sci.*, **272**, 478—492 (1994).
6) Xia J. L., Dubin P. L., Kim Y., Muhoberac B. B., Klimkowski V. J., *J. Phys. Chem.*, **97**, 4528—4534 (1993).
7) Tsuboi A., Izumi T., Hirata M., Xia J. L., Dubin P. L., Kokufuta E., *Langmuir*, **12**, 6295—6303 (1996).
8) Yamaguchi K., Hachiya K., Moriyama Y., Takeda K., *J. Colloid Interface Sci.*, **179**, 249—254 (1996).
9) Nakagaki M., Sano Y., *Bull. Chem. Soc. Jpn.*, **45**, 1011—1018 (1972).
10) Sano Y., *Bull. Natl. Inst. Agrobiol. Resour.*, **2**, 1—12 (1986).
11) Lyon M., Nieduszynski I. A., *Biochem. J.*, **213**, 445—450 (1983).
12) Izumi T., Hirata M., *J. M. S.-Pureappl. Chem.*, **A31**, 39—51 (1994).
13) Anno K., *Comparative Biochemistry of Mucopolysaccharides*, **14**, 167—170 (1977).
14) Pouyani T., Harbison G. S., Prestiwich G. D., *J. Am. Chem. Soc.*, **166**, 7515—7522 (1994).
15) Isogai Z., Yoneda M., Itan N., Kimata K., *Nagoya Med. J.*, **41**, 27—37 (1997).
16) Nonogaki T., Xu S. H., Kugimiya S., Sato S., Miyata I., Yonese M., *Langmuir*, accepted.
17) Pecora R., Dynamic Light Scattering: Application of Photon Correlation Spectroscopy, Plenum Press, New York, 1976.
18) Schmitz K. S., An Introduction to Dynamic Light Scattering by Macromolecules, Academic Press, New York, 1990.
19) Kratky O., Porod G., *Recl. Trav. Chim. Pays-Bas.*, **68**, 1106 (1949).
20) Nakajima A., Shinoda K., *J. Colloid Interface Sci.*, **55**, 126—132 (1976).
21) Hagiwara T., Kumagai H., Nakamura K., *Biosci. Biotech. Biochem.*, **60**, 1757—1763 (1996).

ESR Study on the Antioxidant Activity of TAK-218 in Biological Model Membranes

Morio MURAKAMI,*,[a] Kohji FUKATSU,[b] Shigenori OHKAWA,[b] Fumiko KASAHARA,[a] and Tohru SUGAWARA[c]

Discovery Research Laboratories V,[a] Discovery Research Division and Medicinal Chemistry Research Laboratories,[b] Research Management Department,[c] Pharmaceutical Research Division, Takeda Chemical Industries, Ltd., 17–85, Jusohonmachi 2-chome, Yodogawa-ku, Osaka 532–8686, Japan. Received October 6, 1999; accepted February 22, 2000

TAK-218 has a 2,3-dihydrobenzofuran-5-amine (coumaran) structure which resembles α-tocopherol, and is a promising candidate as an agent for central nervous system (CNS) trauma and ischemia. The radical scavenging activity of TAK-218 was studied using electron spin resonance (ESR) spectroscopy.

TAK-218 exhibited a more potent scavenging activity towards the hydroxyl radical than did the well-known hydroxyl radical scavengers, mannitol and dimethylsulfoxide. Towards the superoxide radical, TAK-218 showed equal potency to glutathione. TAK-218 reacted rapidly with stable radicals, such as galvinoxyl and 2,2-diphenyl-1-picrylhydrazyl hydrate (DPPH), and gave the quinone as a two-electron oxidized product in analogy with α-tocopherol.

To exhibit an excellent antioxidative activity in living systems, the compounds should not only have the intrinsic radical scavenging activity but also good distribution in the biological lipid-bilayer membrane. To examine the antioxidant activity of TAK-218, the inhibition of lipid peroxidation by α-tocopherol and TAK-218 in liposomal membranes was studied using an ESR spin-label technique.

Both α-tocopherol and TAK-218 completely inhibited lipid peroxidation by radicals generated in an aqueous layer using a water-soluble radical initiator, 2,2′-azobis-(2-amidinopropane) hydrochloride (AAPH). At a high incubation temperature (45 °C), α-tocopherol scavenged radicals more effectively than TAK-218 on the surface of the membrane, while TAK-218 scavenged radicals more effectively in the interior of the membrane. The difference between TAK-218 and α-tocopherol for radical scavenging in the membrane system derives from the different distribution pattern of these compounds. TAK-218 can penetrate the membrane freely and can scavenge the radical in the membrane interior.

Furthermore, TAK-218 was shown to inhibit lipid peroxidation initiated by a lipid soluble radical initiator, 2,2′-azobis-(2,4-dimethylvaleronitrile) (AMVN), in a membrane more effectively than α-tocopherol.

Key words TAK-218; ESR; biological model membrane; spin-label technique; antioxidant activity; α-tocopherol

TAK-218 ((*S*)-2,3-dihydro-2,4,6,7-tetramethyl-2-[(4-phenyl-1-piperidinyl)methyl]-5-benzofuranamine dihydrochloride) shown in Fig. 1, is a promising candidate as an agent for central nervous system (CNS) trauma and ischemia.[1] TAK-218 exhibits two functions in living systems: one is the inhibition of dopamine release and the other is the scavenging of free radicals. Cell injury and cell death are caused by the lack of oxygen during brain ischemia and the mechanical damage in traumatic injuries (primary injury), followed by the generation of free radicals after reperfusion.[2—4] The resulting free radicals attack the normal cells surrounding the primary injured cell and cause secondary injury.[2] By inhibiting lipid peroxidation, TAK-218 prevents secondary injury and minimizes the damage. TAK-218 has not only intrinsic radical scavenging activity but also good distribution in the biological lipid-bilayer membrane, which leads to its excellent antioxidative activity in living systems.[5]

In this paper, the scavenging activity for the hydroxyl and the superoxide radical was initially estimated in homogeneous solution using a spin-trapping method. Next, the inhibition of lipid peroxidation by TAK-218 and α-tocopherol in liposomal membranes was studied using an ESR spin-label technique. Two systems were adopted to estimate the inhibition of lipid peroxidation. One was an 2,2′-azobis-(2-amidinopropane) hydrochloride (AAPH) system to simulate the attack of free radicals from the aqueous region and the other was 2,2′-azobis-(2,4-dimethylvaleronitrile) (AMVN) system to simulate the attack of free radicals in membranes. The former is the model of the initial stage of injury, in which the free radicals emanating from the damaged cell attack the membrane of the normal cell. The latter is the model of the progressing stage of injury, in which the chain reaction of the lipid peroxidation starts in the membrane.

The effect of TAK-218 on the membrane fluidity of the liposomes was also examined to estimate the interaction between TAK-218 and the membranes. Finally, ESR spectra of the aminyl radicals derived from TAK-218 were measured and the stability and the electronic structure of this radical are discussed.

Experimental

Radical Scavenging Activities Stable Radical Scavenging Activity: The stable free radicals, galvinoxyl and 2,2-diphenyl-1-picrylhydrazyl hydrate (DPPH) were used to assay the radical scavenging activity.[6,7] The reaction mixture consisted of galvinoxyl (1.0 mM, 1.0 ml) and TAK-218 (1.0 mM, 1.0 ml) dissolved in methanol. The ESR signal intensity of galvinoxyl in this mixture was measured using an ESR spectrometer. DPPH was used as a stable radical in the same manner as galvinoxyl (1.0 mM, 1.0 ml).

Hydroxyl Radical Scavenging Activity: We used the ESR spin-trapping method to evaluate the hydroxyl radical scavenging activity.[8,9] Hydroxyl radicals (·OH) were produced using Fenton's reaction involving Fe^{2+} and hydrogen peroxide. The resulting hydroxyl radicals were trapped by 5,5-di-

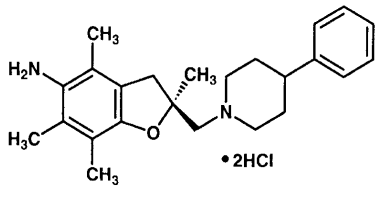

Fig. 1. Chemical Structure of TAK-218

* To whom correspondence should be addressed. e-mail: Murakami_Morio@takeda.co.jp

© 2000 Pharmaceutical Society of Japan

methyl-1-pyrroline-*N*-oxide (DMPO).

In the standard experiment, each of the following stock solutions was added in the following order, up to a total volume of 1.0 ml:

a) ADP (adenosine 5′-diphosphate sodium salt, from equine muscle grade X, Sigma) as a chelating agent, 20.0 mM, 0.1 ml; b) $FeCl_2$ dissolved in 0.001 N HCl, 1.0 mM, 0.1 ml; c) the test substance dissolved in distilled water, 1.0—10.0 mM, 0.1 ml; d) buffer solution (100.0 mM NaCl+25 mM $NaHCO_3$, pH=3.0); e) DMPO as the spin trap (Aldrich), 500 mM, 0.1 ml; and f) H_2O_2, 0.3%, 0.1 ml.

After addition of H_2O_2, the sample was transferred into a quartz flat cell and put into the standard cavity of the ESR spectrometer. Recording of the spectrum was started 2 min after the addition of H_2O_2. The method to calculate the 50% inhibitory concentration (IC_{50}) is the same as shown below for superoxide radical scavenging activity.

Superoxide Radical Scavenging Activity: The basic methodology and the preparation of the reagents used for these experiments were essentially the same as described in our previous article.[10] Superoxide radicals ($O_2^{-\cdot}$) were produced from hypoxanthine (HPX) and xanthine oxidase (XOD). The generation of $O_2^{-\cdot}$ radicals by the HPX–XOD system was followed by trapping these radicals on DMPO, and detecting the DMPO–O_2^- spin adduct. All the reagents were dissolved in phosphate buffer solution (60.0 mM Na_2HPO_4+6.67 mM KH_2PO_4, pH=7.8). In the standard experiment, each of the following stock solutions was added in the following order, to make up the total volume to 0.2 ml:

a) HPX (Sigma), 2.0 mM, 0.05 ml; b) DETAPAC (diethylene triamine-*N*,*N*,*N*′,*N*″,*N*″-pentaacetic acid, Sigma) as a chelating agent, 5.5 mM, 0.03 ml; c) the test substance dissolved in DMF (*N*,*N*-dimethylformamide), 2.0—10.0 mM, 0.05 ml; d) DMPO as the spin trap (Aldrich), 500 mM, 0.02 ml; and e) XOD (from buttermilk, Grade I, Sigma), 0.25 units/ml, 0.05 ml.

After the last solution, XOD, was added, the sample was transferred into a quartz flat cell and put into the standard cavity of the ESR instrument. Recording of the spectrum was started 2 min after the addition of XOD, when the maximum ESR signal intensity of DMPO–O_2^- was expected.

The reactivity of the test substances with $O_2^{-\cdot}$ radicals was estimated from the signal intensities of DMPO–O_2^- relative to the control intensity. The $O_2^{-\cdot}$ scavenging activity was represented as the IC_{50} for the formation of DMPO–O_2^- and used to obtain the rate constants of the reactions between the $O_2^{-\cdot}$ radicals and the scavengers, in the kinetic competition model.[10,11] Assuming the validity of the kinetic competition model, we can consider two main reactions competing in our system as described by Eqs. 1 and 2:

$$O_2^{-\cdot} + S \xrightarrow{k} S - O_2^- \quad (1)$$

$$O_2^{-\cdot} + DMPO \xrightarrow{k'} DMPO - O_2^- \quad (2)$$

where S means the scavenger being tested. Since $k'=17.9\ M^{-1}s^{-1}$ [10,11] and we know the final concentration of the scavenger under test as well as the $[IC_{50}]_{final}$ and the final concentration of DMPO, $[DMPO]_{final}$, we can approximate the value of k ($M^{-1}s^{-1}$).

$$k=k'\times[DMPO]_{final}/[IC_{50}]_{final}=3.58\times10^3/IC_{50} \quad (3)$$

where IC_{50} means the same as in Fig. 4 and Table 2.

IC_{50} was calculated as described[10] using the following equation:

$$V=(I_{control}/I_{test})-1 \quad (4)$$

where $I_{control}$ and I_{test} are the spin adduct signal intensities observed in the absence and in the presence of the tested antioxidant, respectively. After we plotted V against the concentration of the added TAK-218, we linearized the V values using the least-squares method. So the reliability of our data was confirmed using the square of regression coefficient (R^2) derived from a curve fitting calculation. The ESR signal intensities used for the calculation of IC_{50} values were those with the best R^2 values obtained from duplicate measurements. IC_{50} is the concentration of the tested substance at which $V=1$.

Inhibition of Lipid Peroxidation The inhibition of lipid peroxidation of TAK-218 in a phosphatidylcholine liposome was studied using a spin label technique. A liposome of phosphatidylcholine was used for the model membrane and azo compounds were adopted as initiators for lipid peroxidation. The amount of radicals in the liposomal membrane was estimated from the time–course of the ESR signal intensity of the DOXYL-stearic acid spin label.

AAPH and AMVN were used as hydrophilic and lipophilic radical initiators, respectively. These azo compounds enabled us to generate radicals that might initiate lipid peroxidation of the liposomal membrane at a constant and known rate, either in the aqueous phase or in the lipid region.[5,6,12,13] AAPH, AMVN and α-tocopherol were purchased from Wako. Four kinds of DOXYL-stearic acid, 5-DOXYL-stearic acid (5DSA), 7DSA, 12DSA and 16DSA were used as spin labels, where the nitroxide group is attached at various positions along the fatty acid chain to locate it at different depths in the lipid bilayer. All the spin label agents were purchased from Aldrich.

The liposome used in this investigation as a model membrane was made from L-α-phosphatidylcholine. It is generally accepted that phospholipids spontaneously form bilayers when dispersed in water, and that these can serve as excellent models for real biological membranes. Commercial L-α-phosphatidylcholine, from egg yolk purchased from Sigma, was used without further purification.

Spin labeled liposome containing antioxidants was prepared by the thin-film method of Niki and his colleagues[12—14] and the ESR spectra were measured as follows.

1) The phosphatidylcholine (100 mg/ml, 0.4 ml) and lipophilic additives such as antioxidants (TAK-218 or α-tocopherol) and spin label agents, or AMVN when necessary, were dissolved in chloroform (5 ml).

2) This chloroform solution was transferred to a round-bottom flask and the solvent was slowly evaporated under reduced pressure to obtain a thin film of phosphatidylcholine on the glass wall.

3) HEPES buffer solution (*N*-2-hydroxyethylpiperazine-*N*′-2-ethanesulfonic acid+NaOH, pH=7.76, 5.0 ml) was added to the flask. The mixture was vigorously mixed with a Vortex mixer for 2 min and sonicated for 15 min under nitrogen atmosphere using a Branson Sonifier Model 450 (450 W, 20 kHz) to convert it into small unilamellar vesicles. The final concentration was as follows: L-α-phosphatidylcholine, 10.0 mM; spin label agent, 0.1 mM; AMVN, 10.0 mM; antioxidant (TAK-218 or α-tocopherol), 0.1 mM.

4) When AMVN was used as a radical initiator, liposomal suspensions containing AMVN were incubated at 50 °C in air. The reaction mixture was taken into the quartz flat cell to measure the ESR spectra of the liposome at various time intervals.

5) When AAPH (final concentration; 20.0 mM) was used in experiments, it was added to the solution at the beginning of the measurement, and oxidation was carried out at 40 °C or 45 °C.

Interaction between TAK-218 and Liposomal Membranes: Measurement of the Membrane Fluidity The spin label, 16DSA was incorporated into the liposomal membranes using the above thin-film method. Final concentration was as follows; L-α-phosphatidylcholine (from egg yolk), 10.0 mM; 16DSA, 0.1 mM; TAK-218 or α-tocopherol, 1.0—5.0 mM (molar ratio to lipid, 10—50%); phosphate buffer solution (60.0 mM KH_2PO_4 +6.67 mM Na_2HPO_4, pH=7.8). The additive effect of the antioxidants on the membrane fluidity was monitored by the correlation time (τ_R) calculated from the following equation[15—17]:

$$\tau_R=7.1\times10^{-10}\delta H(0)\{R(-1)+R(+1)-2\} \quad (1)$$

where $R(-1)$, $R(+1)$ are given by

$$R(m)=\delta H(m)/\delta H(0)=\sqrt{I(0)/I(m)} \quad (m=-1,0,1) \quad (2)$$

where $I(m)$ and $\delta H(m)$ are the peak intensity and line width of the ESR signal, respectively.

ESR Spectra of TAK-218 Radical Since it became clear from our studies that TAK-218 radicals play an important role in the radical scavenging activity, we measured the ESR spectrum of this radical. The radical was obtained by the oxidation of TAK-218 with H_2O_2 at 40—80 °C. The reaction mixture consisted of TAK-218 (50.0 mM, 0.1 ml) and H_2O_2 (1.5%wt, 0.1 ml) dissolved in distilled water (H_2O) or deuterium oxide (D_2O) under air.

ESR Measurements ESR spectra were recorded on an X-band JEOL JES-RE3X spectrometer (JEOL Co., Ltd., Tokyo) operating at 9.20 GHz with a 100 KHz high-frequency modulation amplitude ranging from 0.5 G to 1.0 G. The specification of this spectrometer was as follows: magnetic field, 327 mT; microwave power, 4.0 mW; sweep width, ±5.0 mT; sweep time, 5—10 mT/min; response time, 0.03 s; and receiver gain, ×100—×2000. JEOL digital variable temperature accessories and an X-band universal cavity (cylindrical TE011 mode) were used. For the ESR measurement, the temperature was monitored and controlled using a copper–constantan thermocouple that was placed in the sample just below the active volume of the cavity.

Results and Discussion

Radical Scavenging Activities Stable Radical Scavenging Activity: TAK-218 reacted with stable radicals, galvi-

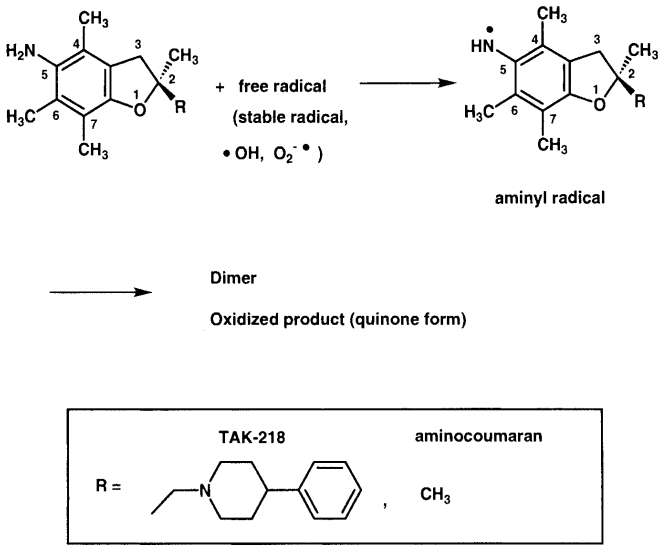

Fig. 2. Mechanism of the Free Radical Scavenging Reaction of TAK-218

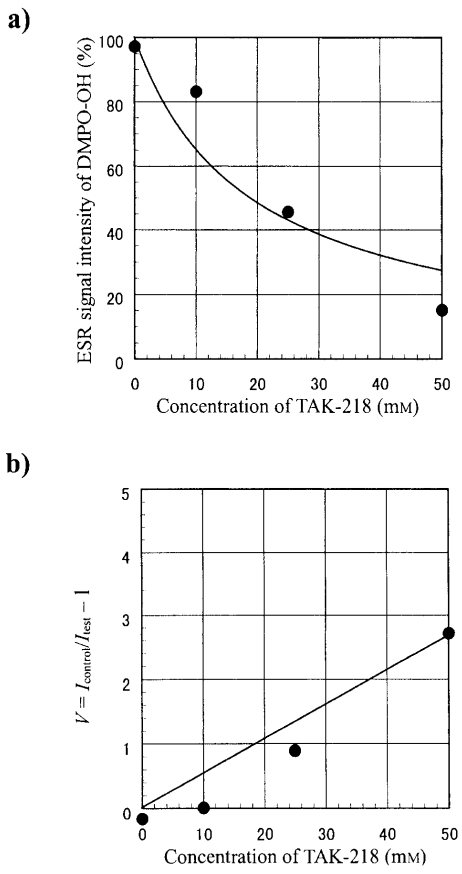

Fig. 3. Hydroxyl Radical Scavenging Activities of TAK-218 Obtained by the Spin Trapping Method in the ADP–Fe(II)–H_2O_2–DMPO System

a) The ESR signal intensity (%) of DMPO–OH adduct as plotted against the concentration of the added TAK-218. The function used for curve fitting is $y=100/(5.33\times10^{-2}x+1)$.

b) The same as shown in a) but linearized by the least-squares method in order to calculate IC_{50} values. The function used for curve fitting is $y=5.33\times10^{-2}x$, $R^2=0.97$.

noxyl and DPPH to rapidly quench their ESR signals. TAK-218 exhibited radical scavenging activity towards both substances, which are model radicals for the lipid radicals generated during lipid peroxidation.

When α-tocopherol reacted with galvinoxyl, the ESR signal of α-tocopheroxyl radical was observed, but the aminyl radical derived from TAK-218 was not detected by ESR measurement. By analogy with α-tocopherol,[18,19] it was presumed that TAK-218 reacted rapidly with stable radicals to give a quinone as a two-electron oxidized product (Fig. 2).

Table 1. Hydroxyl Radical Scavenging Activities Obtained by the Spin Trapping Method in the ADP–Fe(II)–H_2O_2–DMPO System

Compound	IC_{50} (mM)
Ascorbic acid	0.26
TAK-218	19
Aminocoumaran	38
DMSO	>100
Mannitol	>100

Hydroxyl Radical Scavenging Activity: Addition of TAK-218 to the ADP+Fe(II)+H_2O_2+DMPO system significantly reduced the ESR signal of DMPO–OH in proportion to the amount of TAK-218 added (Fig. 3). The 50% inhibition concentration (IC_{50}) of TAK-218 to the DMPO–OH is 19 mM. IC_{50} values of the other antioxidants are shown in Table 1; as indicated, TAK-218 exhibited stronger scavenging activity towards the hydroxyl radical than did the well-known hydroxyl radical scavengers, mannitol and dimethylsulfoxide (DMSO).

Superoxide Radical Scavenging Activity: Addition of TAK-218 to the XOD+HPX+DMPO system reduced the ESR signal of DMPO–O_2^- in proportion to the added TAK-218 (Fig. 4). Nevertheless, even if the concentration of TAK-218 was increased, its effect tended to show a saturation-like curve, *i.e.*, it could not achieve complete inhibition of the formation of DMPO–O_2^- adduct. The same phenomenon was observed, when we used another antioxidants, superoxide dismutase (SOD).[10] The IC_{50} of TAK-218 to the DMPO–O_2^- is 6.9 mM. IC_{50} values of the other antioxidants are shown in Table 2. Towards the superoxide radical, TAK-218 showed equal potency to glutathione.

Inhibition of Lipid Peroxidation Lipid Peroxidation of Liposomal Membrane Initiated by an Azo Compound: In the absence of a radical initiator, the rate of autooxidation of phosphatidylcholine was quite slow, but the addition of an azo compound as an initiator could induce accelerative oxidation. AAPH and AMVN were used as water-soluble and lipid-soluble initiators, respectively. These azo compounds enable us to simulate the attack of free radicals from outside or inside the membrane.

Oxidation of lipids initiated by the pyrolysis of an azo compound, A–N=N–A, can be represented by the following scheme.[6]

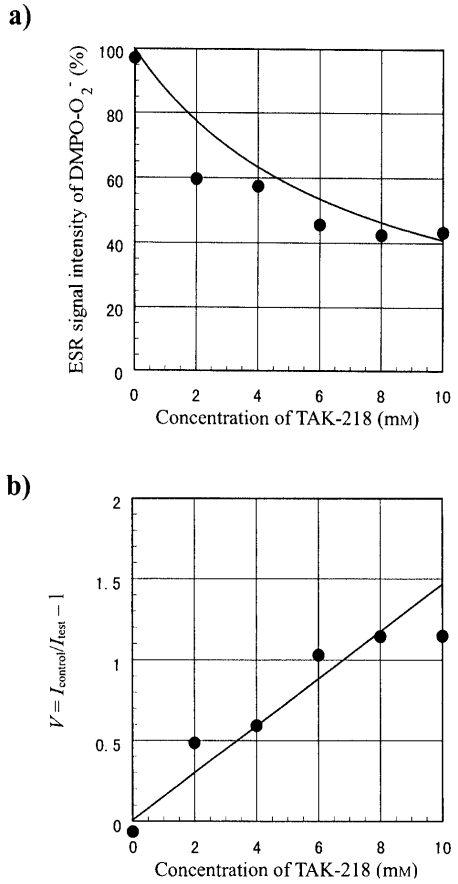

Fig. 4. Superoxide Radical Scavenging Activities of TAK-218 Obtained by the Spin Trapping Method in the XOD–HPX–DMPO System

a) The ESR signal intensity (%) of DMPO–O_2^- adduct as plotted against the concentration of the added TAK-218. The function used for curve fitting is $y=100/(1.46\times10^{-1}x+1)$.

b) The same as shown in a) but linearized by the least-squares method in order to calculate IC_{50} values. The function used for curve fitting is $y=1.46\times10^{-1}x$, $R^2=0.90$.

Table 2. Superoxide Radical Scavenging Activities Obtained by the Spin Trapping Method in the XOD–HPX–DMPO System

Compound	IC_{50} (mM)	Rate consatant k ($\times10^2$ M^{-1} s^{-1})
Aminocoumaran 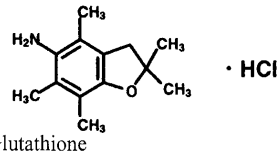 · HCl	4.9	7.3
Glutathione 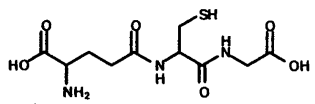	6.4	5.6
TAK-218 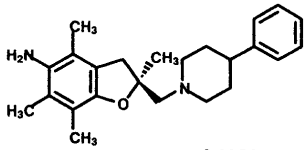 · 2 HCl	6.9	5.2

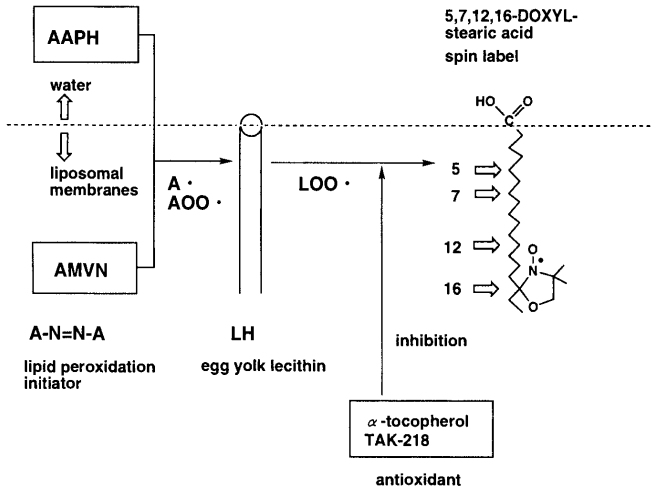

Fig. 5. Evaluation of the Inhibition of the Lipid Peroxidation by TAK-218 Using the ESR Spin-Label Technique

Schematic diagram of the experiment shows the reaction in the liposomal membranes.

Initiation:

$$A\text{–}N{=}N\text{–}A \rightarrow (1-e)A\text{–}A+2eA^{\cdot}+N_2$$
$$A^{\cdot}+O_2 \rightarrow AOO^{\cdot}$$
$$AOO^{\cdot}+LH \xrightarrow{O_2} AOOH+LOO^{\cdot}$$

Propagation:

$$LOO^{\cdot}+LH \rightarrow LOOH+L^{\cdot}$$
$$L^{\cdot}+O_2 \rightarrow LOO^{\cdot}$$

Termination:

$$LOO^{\cdot}+IH \rightarrow LOOH+I^{\cdot}$$
$$(n-1)LOO^{\cdot}+I^{\cdot} \rightarrow \text{nonradical products}$$

In this scheme, "LH" represents lipid, "IH" is antioxidant, "L˙" and "LOO˙" are alkyl and alkylperoxy radicals, respectively, "e" is efficiency of radical production and "n" is the stoichiometric number of radicals trapped by each antioxidant.

Free radicals generated in liposomal membranes react with spin labels in the membranes to reduce their ESR signals with the passage of time. If antioxidants co-exist with spin labels in the membrane, they partially scavenge the free radicals due to lipid peroxidation and decrease the rate of the consumption of the spin labels.

Figure 5 is a schematic diagram of the assay system used in this study to evaluate the inhibition of the lipid peroxidation by the antioxidant, showing the reaction in the liposomal membranes.

Figure 6 shows the ESR spectra of the four spin labels 5DSA,7DSA,12DSA and 16DSA, incorporated into the liposomes. The ESR spectra show an apparent large anisotropy of g and hyperfine splitting values in the order 16DSA< 12DSA<7DSA<5DSA, suggesting a decrease in the molecular mobility of the spin label. In this study, a half-life period, $T_{1/2}$, represents the rates of consumption of the spin label. Increase in the $T_{1/2}$ of the spin label co-existing with the antioxidant would suggest that this antioxidant could inhibit lipid peroxidation.

Attack of Free Radicals Induced by AAPH from the Aqueous Region: AAPH was used as a water-soluble radical ini-

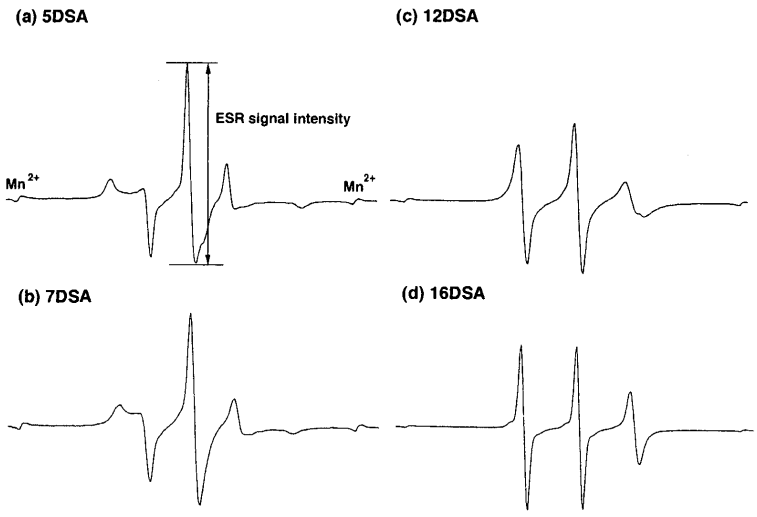

Fig. 6. ESR Spectra of 5DSA, 7DSA, 12DSA, 16DSA Spin Labels Incorporated into the Membranes at Room Temperature (T=20 °C)

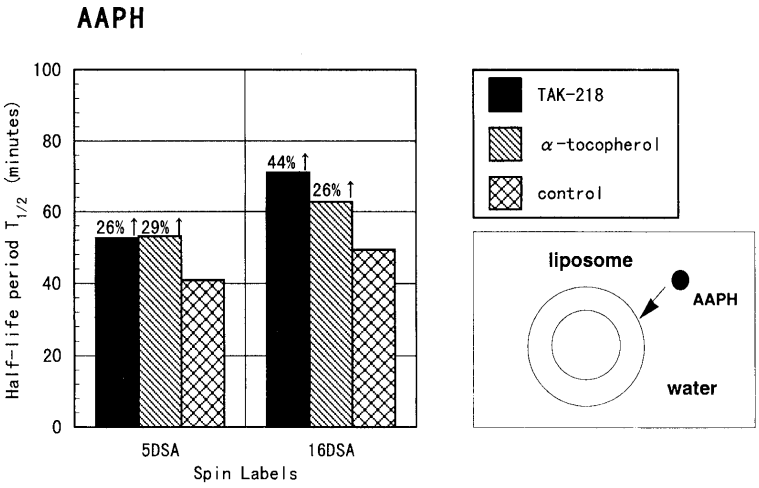

Fig. 7. $T_{1/2}$ of Spin Labels (5DSA, 16DSA) Incorporated into the Liposomes in the Presence of Antioxidants (TAK-218 or α-Tocopherol)
The oxidation was initiated with AAPH at 45 °C.

tiator to simulate radical attack from outside of the membrane. 5DSA and 16DSA were adopted as the spin labels. When the oxidation was initiated with AAPH at 40 °C, both α-tocopherol and TAK-218 completely suppressed the decrease of ESR signal of 5DSA and 16DSA during 5-hours of incubation (data not shown). This indicated that both antioxidants completely inhibited the lipid peroxidation by radicals generated in an aqueous phase using AAPH.

At a higher incubation temperature (45 °C), addition of α-tocopherol exhibited slightly longer $T_{1/2}$ than did the addition of TAK-218 for 5DSA as a spin label, while addition of TAK-218 exhibited longer $T_{1/2}$ than did the addition of α-tocopherol for 16DSA as a spin label (Fig. 7). This result showed that α-tocopherol scavenged the free radicals produced in aqueous regions near the membrane's surface. In contrast, TAK-218 could scavenge the radicals more effectively in the interior of the membrane than α-tocopherol. The difference between TAK-218 and α-tocopherol in radical scavenging activity in the membrane system is due to the different mobility of these compounds in the liposomal membrane. Although the phytyl side chain of α-tocopherol is required for retention by the biomembranes, it appears that this side chain reduces the mobility of α-tocopherol within the membranes.[12—14] The benzpiperidine group in TAK-218, however, does not prevent the mobility in the biomembranes, and thus TAK-218 can move through the membrane freely and scavenge the radical in the membrane interior.

Attack of Free Radicals Induced by AMVN in the Membranes: AMVN was used as a lipid-soluble radical initiator to simulate radical attack inside the membrane. Figure 8 shows the half-life period ($T_{1/2}$) of spin labels (5DSA, 7DSA, 12DSA, 16DSA) incorporated into the liposomes in the absence or presence of antioxidants (TAK-218 or α-tocopherol), when the oxidation was initiated by AMVN at 50 °C under air. Calculations of the $T_{1/2}$ in the case of 5DSA and 16DSA are demonstrated in Figs. 9 and 10. The ESR signal intensities used for the calculation of the $T_{1/2}$ values were those with the best R^2 values obtained from duplicate measurements.

Interestingly, it was found that the increment rate of 5DSA spin label's $T_{1/2}$, when co-existing with α-tocopherol, was the greatest among all of the spin labels (see Fig. 8), which suggests that α-tocopherol scavenges radicals near the surface more efficiently than it does in the inner region of the mem-

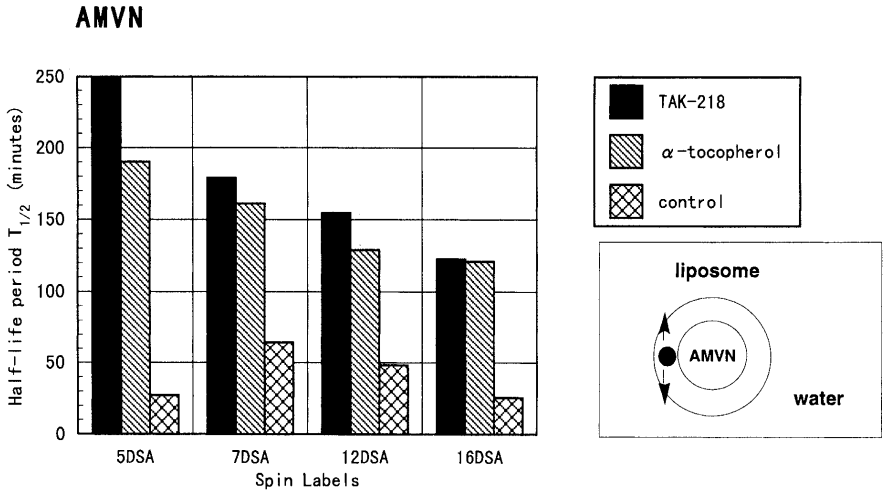

Fig. 8. $T_{1/2}$ of Spin Labels (5DSA, 7DSA, 12DSA, 16DSA) Incorporated into the Liposomes in the Presence of Antioxidants (TAK-218 or α-Tocopherol)

The oxidation was initiated with AMVN at 50 °C. The increment rates of the $T_{1/2}$ co-existing with TAK-218 or α-tocopherol to the $T_{1/2}$ in the control system are: 920% (5DSA), 290% (7DSA), 330% (12DSA) and 460% (16DSA) co-existing with TAK-218, or 700% (5DSA), 260% (7DSA), 270% (12DSA) and 450% (16DSA) co-existing with α-tocopherol.

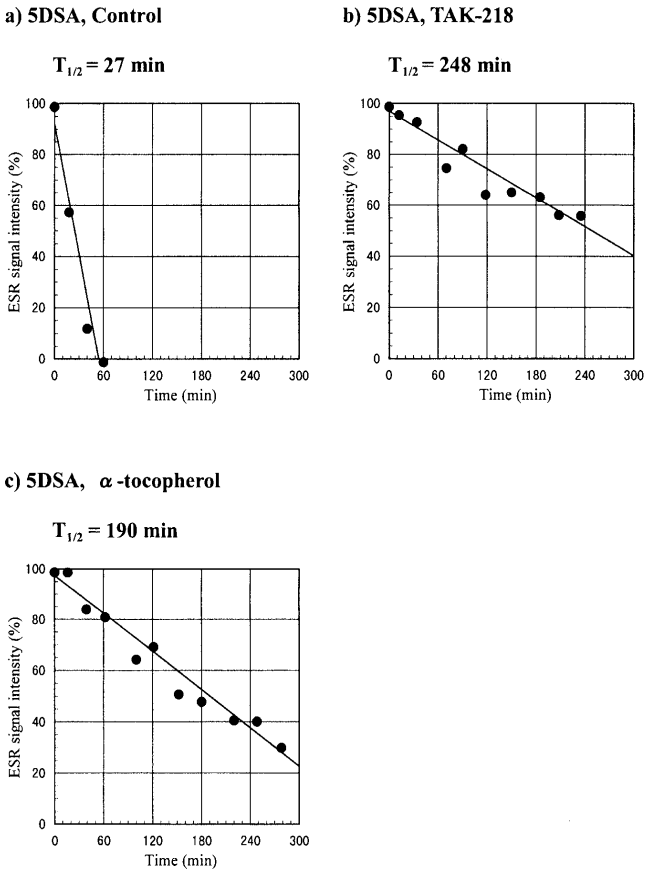

Fig. 9. Decrease of ESR Signal Intensities of 5DSA Spin Label Incorporated into the Liposomes in the Presence of Antioxidants (TAK-218 or α-Tocopherol)

The oxidation was initiated with AMVN at 50 °C. After we plotted ESR signal intensities, we linearized them using the least-squares method. Calculated R^2 values are as follows: a) R^2=0.95, b) R^2=0.91 and c) R^2=0.96.

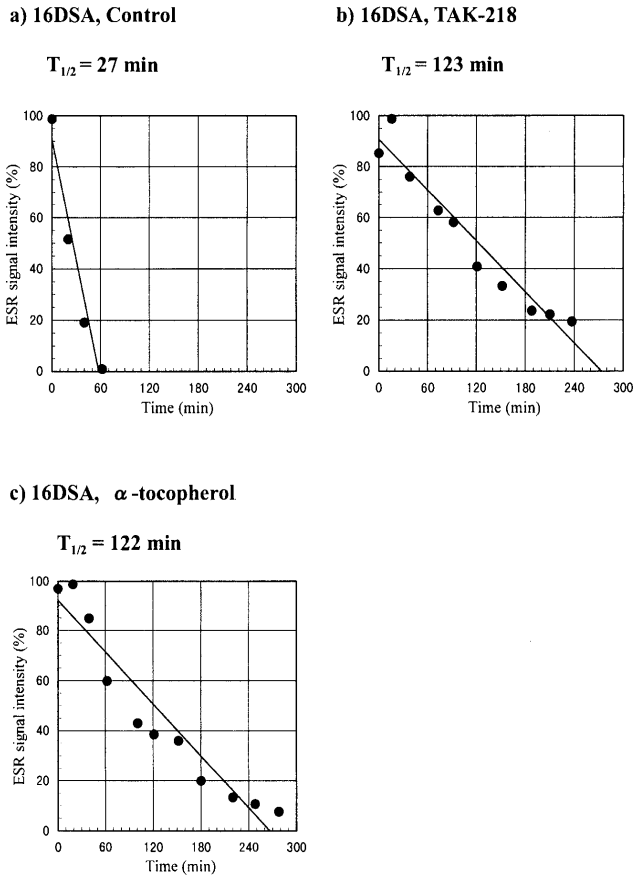

Fig. 10. Decrease of ESR Signal Intensities of 16DSA Spin Label Incorporated into the Liposomes in the Presence of Antioxidants (TAK-218 or α-Tocopherol)

The oxidation was initiated with AMVN at 50 °C. After we plotted ESR signal intensities, we linearized them using the least-squares method. Calculated R^2 values are as follows: a) R^2=0.95, b) R^2=0.94 and c) R^2=0.92.

branes. This result is in accord with Niki's reports.[12—14] The $T_{1/2}$ of spin labels containing TAK-218 also decreased in the order 5DSA≫16DSA>12DSA, 7DSA, in a similar manner to α-tocopherol. TAK-218, however, exhibited a longer $T_{1/2}$ value than α-tocopherol with all the spin labels. Comparing these results, it can be said that TAK-218 scavenges radicals more easily within the membranes than α-tocopherol.

Interaction between TAK-218 and Liposomal Membranes. Measurement of the Membrane Fluidity The result of the liposomal experiment clearly shows that the inhibition of lipid peroxidation by TAK-218 is more effective than that by α-tocopherol. It is assumed that this is mainly

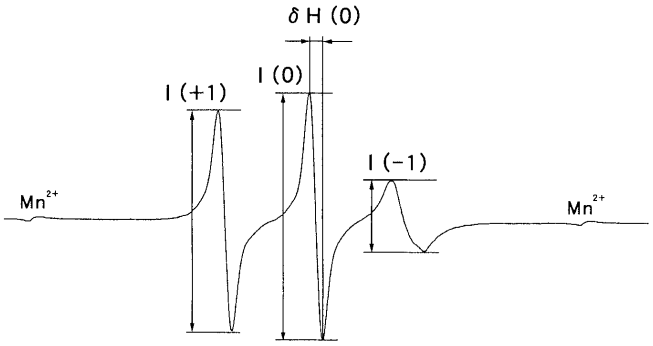

Fig. 11. Calculation of the Correlation Time (τ_R) of Rotational Diffusion Using ESR Spectrum of 16DSA in L-α-Phosphatidylcholine Liposomal Membranes

Temperature=20 °C.

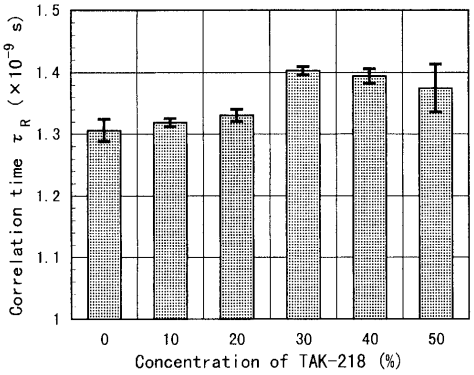

Fig. 12. The Effect of TAK-218 on the ESR Correlation Time (τ_R) of 16DSA in the Liposomal Membranes of L-α-Phosphatidylcholine

Temperature=20 °C.

because TAK-218 can easily move through the membrane and scavenge the radicals in the interior. However, the C log P value (calculated partition coefficient between aqueous and membrane regions) for α-tocopherol (C log P=12.1) shows it to be more hydrophobic than TAK-218 (C log P=5.58), which would generally suggest that the total distribution of TAK-218 in the membrane region will be smaller than that of α-tocopherol. To confirm that TAK-218 can penetrate to the membrane interior, we examined the interaction between TAK-218 and the membrane.

The ESR spectra of 16DSA in the membrane, which is used for the calculation of τ_R, is shown in Fig. 11. The effect of TAK-218 and α-tocopherol on the correlation time, τ_R, of 16DSA in the L-α-phosphatidylcholine liposomal membranes is shown in Figs. 12 and 13, respectively. In this experiment, ESR spectra were measured at room temperature (T=20 °C). Since the phase transition temperature of this liposome is about 0 °C, τ_R was measured at above the phase transition temperature (liquid-crystal region). The τ_R of 16DSA in the liposomes increased with an increase in the additive concentration of TAK-218 and α-tocopherol to the liposomes, indicating that the membranes exhibited rigidity and reduced fluidity. The effect of α-tocopherol on reducing τ_R is more remarkable than that of TAK-218, when compared at the same additive concentration.

These results suggest that the phytyl side chain of α-tocopherol causes the stronger interaction with the membrane.

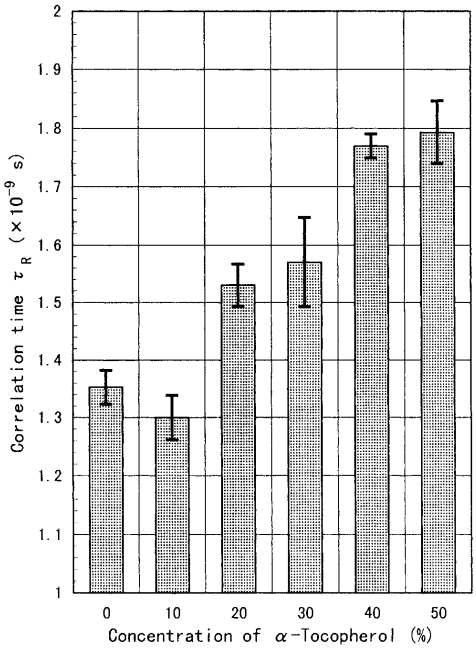

Fig. 13. The Effect of α-Tocopherol on the ESR Correlation Time (τ_R) of 16DSA in the Liposomal Membranes of L-α-Phosphatidylcholine

Temperature=20 °C.

We have confirmed that TAK-218 can reside in the interior of the membrane, since it has an effect on the τ_R of 16DSA in the interior.

ESR Spectra of TAK-218 Radical The experimental results described above definitely indicate: a) that TAK-218 exhibits strong radical scavenging activity in a homogeneous solution and b) demonstrates the remarkable inhibition of lipid peroxidation in liposomal membrane. Though the radical scavenging reaction mechanism of TAK-218, shown in Fig. 2, is proposed, it has not been confirmed experimentally.

It is assumed that the aminyl radical is derived from TAK-218, when TAK-218 scavenges free radicals such as the model radicals (DPPH, galvinoxyl), hydroxyl radical and superoxide radical, as shown in Fig. 2. Since the aminyl radicals play an important role in the realization of the radical scavenging activity of TAK-218, we determined the hyperfine splitting constant of the aminyl radicals in well-resolved ESR spectra produced by several methods.

As soon as the TAK-218 solution was mixed with H_2O_2 at room temperature, the ESR signal of the radicals derived from TAK-218 was observed at the minimum detection level. When the temperature of the mixture was raised from 40 °C to 80 °C, the ESR signal of the TAK-218 radical exhibited a stronger intensity. The concentration of the generating radicals at 40 °C and 80 °C was about 1.80×10^{-7} and 5.50×10^{-7} M, respectively. The ESR spectra of the TAK-218 radical, obtained by oxidation using H_2O_2 at 80 °C, is shown in Fig. 14. When TAK-218 was reacted with H_2O_2 in D_2O solution, the NH group in the TAK-218 radical underwent a change to ND (D: deuterium). The ESR spectrum of the TAK-218 radical in D_2O solution is shown in Fig. 15; it was measured at high resolution with a modulation width of 0.5 G. The ESR spectrum of the TAK-218 radical consists of twenty-seven peaks, whose hyperfine structure (hfs) is 1.82 G. The ESR spectrum changes in hfs (0.97 G), when the hydrogen in the amino group is substituted by deuterium,

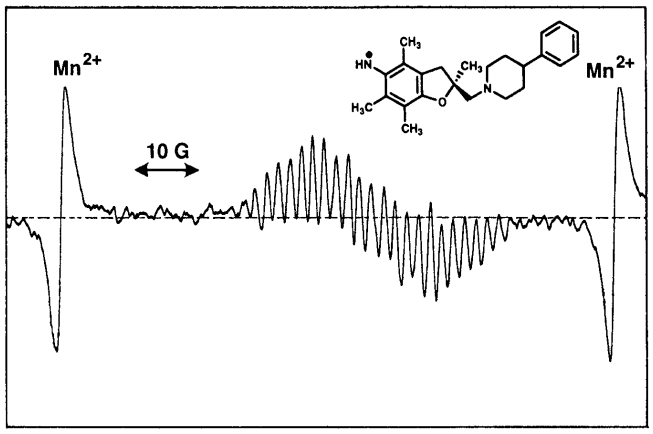

Fig. 14. ESR Spectrum of TAK-218 Radical at 80 °C

The reaction mixture contained 25 mM TAK-218 and 0.5% H_2O_2 in H_2O solution. The specification of this spectrometer was as follows: sweep width, 100 G; mod. width 1.0 G; sweep time, 2.0 min; time constant, 0.3 s; and receiver gain, ×2000.

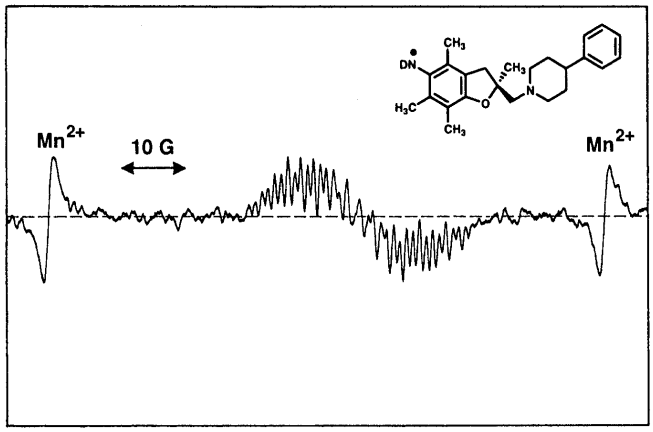

Fig. 15. ESR Spectrum of TAK-218 Radical at 80 °C

The reaction mixture contained 25 mM TAK-218 and 0.5% H_2O_2 in D_2O solution. The specification of this spectrometer was as follows: sweep width, 100 G; mod. width 0.50 G; sweep time, 2.0 min; time constant, 0.3 s; and receiver gain, ×2000.

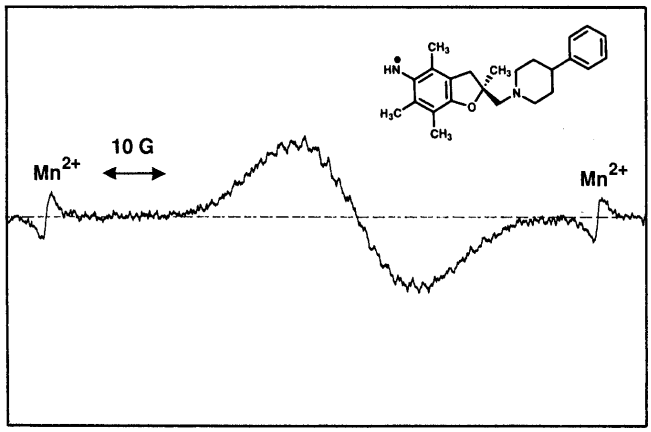

Fig. 16. ESR Spectrum of TAK-218 Radical at 20 °C

The reaction mixture contained 0.1 M TAK-218 and PbO_2 in CH_3OH solution. The specification of this spectrometer was as follows: sweep width, 100 G; mod. width 1.0 G; sweep time, 2.0 min; time constant, 0.1 s; and receiver gain, ×1000.

which indicates that the TAK-218 radical has an exchangeable hydrogen in its molecule. The structure of the aminyl radical is shown in Fig. 2 and the same aminyl radical was observed using PbO_2 as an oxidation reagent, as shown in Fig. 16. However, the spectra did not exhibit the hyperfine structure due to the presence of atmospheric oxygen in the solvent.

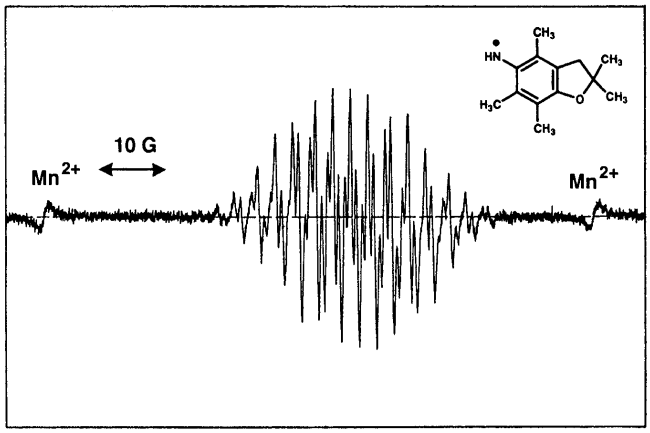

Fig. 17. ESR Spectrum of Aminocoumaran Radical at 50 °C

The reaction mixture contained 25 mM aminocoumaran and 0.5% H_2O_2 in H_2O solution. The specification of this spectrometer was as follows: sweep width, 100 G; mod. width 0.50 G; sweep time, 4.0 min; time constant, 0.03 s; and receiver gain, ×630.

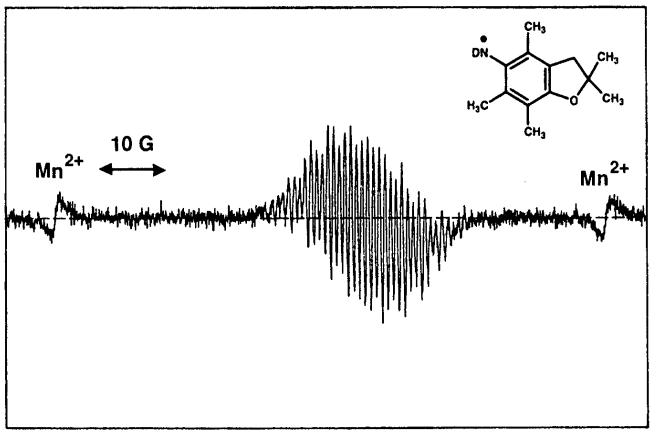

Fig. 18. ESR Spectrum of Aminocoumaran Radical at 80 °C

The reaction mixture contained 25 mM aminocoumaran and 0.5% H_2O_2 in D_2O solution. The specification of this spectrometer was as follows: sweep width, 100 G; mod. width 0.50 G; sweep time, 2.0 min; time constant, 0.03 s; and receiver gain, ×1000.

ESR spectra of the other aminocoumaran compound, whose chemical structure is shown in Fig. 2, are shown in Figs. 17 and 18. The hyperfine structure of the spectra arise from the coupling with four groups of protons: with coupling constants of a_{N5}=8.96 G (5-position NH_2, nitrogen), a_{H5}=5.97 G (5-position NH_2 proton), a_{H4}=2.99 G (4-position CH_3 proton) and a_{H6}=2.99 G (6-position CH_3 proton). The hyperfine structure was assigned by referring to other aminyl radicals in the literature.[18—20] We have thus identified the aminyl radicals derived from TAK-218 by the direct measurement of ESR spectra.

By analogy with α-tocopherol, TAK-218's radical must be a stable radical in order for it to exhibit the excellent antioxidant activity in the radical chain reaction which occurs in the membrane during lipid peroxidation. According to the hfs of the aminyl radicals, the spin density is observed not only at the 5-position nitrogen atom but also at the two ortho carbon atoms, at the 4- and 6-position of the benzofuran ring. These results suggest that the TAK-218 radical is a stable radical with delocalization of the unpaired π-electron.

Conclusion

The radical scavenging activities of TAK-218, which are very important for its protective effects against CNS trauma and ischemia, were studied using ESR spectroscopy and the following conclusions were deduced.

First, towards the hydroxyl radical in homogeneous solution, TAK-218 exhibited stronger scavenging activity than did the well-known scavengers, mannitol and DMSO. Towards the superoxide radicals, TAK-218 was comparable in activity to glutathione.

Second, the inhibition of lipid peroxidation by α-tocopherol and TAK-218 in the liposomal membranes was studied using an ESR spin-label technique. When the lipid peroxidation was initiated by radicals generated in an aqueous region using a water-soluble radical initiator (AAPH), both α-tocopherol and TAK-218 completely suppressed the lipid peroxidation in the model membranes. When the amount of radicals generated from AAPH was increased by raising the incubation temperature, α-tocopherol scavenged the radicals more effectively than TAK-218 near the surface of the membranes, while TAK-218 scavenged radicals more effectively in the interior of the membrane. The difference between TAK-218 and α-tocopherol in radical scavenging activity in the model membrane system is due to the different distribution pattern of these compounds. When the lipid peroxidation was initiated using a lipid-soluble radical initiator (AMVN), both compounds inhibited the lipid peroxidation, however, TAK-218 exhibited more potent inhibitory activity than α-tocopherol.

Further, the additive effect of TAK-218 and α-tocopherol on the liposomes was examined by monitoring the correlation time of spin labels (16DSA). Since the effect of α-tocopherol on the correlation time was greater than that of TAK-218, it was presumed that α-tocopherol exhibited stronger interaction with the lipid in the model membranes.

Based on these experimental results, TAK-218 is believed to be beneficial not only at the initial stage of an injury, but also the progressing stages of an injury, in which the injury progresses into the interior of the membrane.

References

1) Ohkawa S., Fukatsu K., Miki S., Hashimoto T., Sakamoto J., Doi T., Nagai Y., Aono T., *J. Med. Chem.*, **40**, 559—573 (1997).
2) Faden A. I., Salzman S., *Trends Pharmacol. Sci.*, **13**, 29—35 (1992).
3) Halliwell B., Gutteridge J. M. C., "Free Radicals in Biology and Medicine," Clarendon Press, Oxford, 1985.
4) Pryor W. A., "Free Radicals in Biology," Vol. 4, Academic Press, London, 1980.
5) Horan K. L., Lutzke B. S., Cazers A. R., McCall J. M., Epps D. E., *Free Radical Biology & Medicine*, **17**, 587—596 (1994).
6) Niki E., Kawakami A., Saito M., Yamamoto Y., Tsuchiya J., Kamiya Y., *J. Bio. Chem.*, **260**, 2191—2196 (1985).
7) Niki E., *Ann. N.Y. Acad. Sci.*, **498**, 186—199 (1987).
8) Floyd R. A., Lewis C. A., *Biochemistry*, **22**, 2645—2649 (1983).
9) Zs.-Nagy I., Floyd R. A., *Arch. Gerontol. Geriatr.*, **11**, 215—231 (1990).
10) Murakami M., Zs.-Nagy I., *Arch. Gerontol. Geriatr.*, **11**, 199—214 (1990).
11) Mitsuta K., Mitzuta Y., Kohno M., Hiramatsu M., Mori A., *Bull. Chem. Soc. Jpn.*, **63**, 187—191 (1990).
12) Takahashi M., Tsuchiya J., Niki E., *J. Nutr. Sci. Vitaminol.*, **34**, 25—34 (1988).
13) Takahashi M., Tsuchiya J., Niki E., *J. Am. Chem. Soc.*, **111**, 6350—6353 (1989).
14) Takahashi M., Tsuchiya J., Niki E., "Medical Biochemical and Chemical Aspects of Free Radicals," ed. by Hayaishi O., Niki E., Kondo M., Yoshikawa T., Elsevier, Amsterdam, 1989, pp. 833—836.
15) Berliner L. J., Reuben J. (ed.), "Spin Labeling, Theory and Applications, Biological Magnetic Resonance," Vol. 8, Plenum Press, New York, 1989.
16) Berliner L. J., (ed.), "Spin Labeling II, Theory and Applications," Academic Press, New York, 1979.
17) Subczynsk W. K., Kusumi A., *Biochim. Biophys. Acta.*, **854**, 318—320 (1986).
18) Denisov E. T., Khudyakov I. V., *Chem. Rev.*, **87**, 1313—1357 (1987).
19) Nelsen S. F., Landis II. R. T., *J. Am. Chem. Soc.*, **95**, 8707—8713 (1973).
20) Iwatsuki M., Komuro E., Niki E., *Bull. Chem. Soc. Jpn.*, **68**, 620—624 (1995).

Study of Tolbutamide–Hydroxypropyl-γ-cyclodextrin Interaction in Solution and Solid State

María-Dolores VEIGA* and Fakhrul AHSAN

Departamento de Farmacia y Tecnología Farmacéutica, Facultad de Farmacia, Universidad Complutense de Madrid, 28040-Madrid, Spain. Received November 8, 1999; accepted February 15, 2000

Tolbutamide–hydroxypropyl-γ-cyclodextrin (TBM–HPGCD) interaction has been investigated in an aqueous environment and in the solid state. The solubility of TBM was increased in accord with the amount of HPGCD added to the aqueous medium forming a soluble inclusion compound. The phase solubility diagram obtained was of A_L type. Physical mixtures and kneaded systems of the drug and cyclodextrin derivative were prepared in 1 : 1 and 1 : 2 drug/cyclodextrin mol/mol ratio. All solid binary systems were characterised by hot-stage microscopy (HSM), differential scanning calorimetry (DSC), thermogravimetry (TG) and X-ray powder diffractometry (XRD). An inclusion complex was formed in both of the kneaded systems. In the 1 : 2 kneaded system, the entire drug was included in the cyclodextrin cavity, while, in the 1 : 1 kneaded system only a part of the drug formed an inclusion complex with the cyclodextrin. A significant improvement in the dissolution of the drug was obtained from the kneaded systems in comparison with that of the pure TBM and physical mixtures. However, there was no significant difference between the dissolution profiles of the two kneaded systems. The study suggests that an inclusion complex was obtained both in aqueous solution and in solid state.

Key words tolbutamide; hydroxypropyl-γ-cyclodextrin; solubility; inclusion complex; dissolution; characterisation tolbutamide–hydroxypropyl-γ-cyclodextrin inclusion compound in solid state

Hydroxypropyl-cyclodextrins have found considerable interest as parenteral drug carriers because of their low toxicity and high tolerance. Their excellent solubilizing capacity enables poorly water-soluble drugs to dissolve fully and rapidly in water and in consequence improves the bioavailability significantly. Among the hydroxypropyl-cyclodextrins, hydroxypropyl-β-cyclodextrin (HPBCD) has been studied extensively.[1—3] However, hydroxypropyl-γ-cyclodextrin (HPGCD) has been studied to a lesser extent, although its parent compound γ-cyclodextrin (GCD) is a potent solubilizer. Because of its large cavity size, GCD can effectively encapsulate bulky drug molecules such as prostaglandins, steroid hormones, and benzodiazepines.[4] Like GCD, which has been used as bonding materials of the stationary phase of chiral chromatography, especially to separate enantiomers containing three benzene rings,[5] HPGCD has been used as a chiral resolving agent in enantioseparation by capillary electrophoresis. In a recent study, 30 racemic drugs were separated by electrophoresis using HPGCD as a chiral resolving agent.[6] As HPGCD is much more soluble than its parent molecule, it has also been found promising in enhancing solubility and dissolution of poorly water soluble drugs. These properties of HPGCD have been exploited by several authors. The poor aqueous solubility of carbamazepine, an anticonvulsant agent, was dramatically increased *via* complexation with HPGCD.[7] An enhanced dissolution of spironolactone was obtained from its inclusion complex with HPGCD prepared by spray drying.[8] However, studies about the interaction of this cyclodextrin derivative with poorly watersoluble drugs, especially in the solid state, have not been extensive in nature.

Tolbutamide (TBM) is well known for its inclusion compound with cyclodextrins. Its molecular geometry allows it to form inclusion compound with β-cyclodextrin (BCD) and HPBCD.[9] The drug forms a 1 : 2 inclusion compound with BCD[10] and a 1 : 1 inclusion compound with HPBCD.[9] The interactions of TBM with BCD and HPBCD, both in solution and solid state, were studied by several authors.[9—11]

In this paper, TBM was selected as a substrate to study its interaction with HPGCD in solution and in the solid state. Hot stage microscopy (HSM), differential scanning calorimetry (DSC) and X-ray powder diffractometry (XRD) were employed in studying the interaction between TBM and HPGCD in the solid state.

Experimental

Materials TBM, 1-butyl-3-*p*-tolylsulphonylurea, was purchased from Sigma Chemicals Co. (St. Luis, MO, U.S.A.) and 2-hydroxypropyl-γ-cyclodextrin (HPGCD), with a substitution degree of 0.6, was a gift from Wacker-Chemie GmbH (München, Germany).

Phase Solubility Study A phase solubility study was performed according to the method reported by Higuchi and Connors.[12] An excess (20 mg) of TBM was weighed out into a series of test tubes. A constant volume of demineralized water or aqueous solutions of cyclodextrin containing increasing concentration of HPGCD (0.002—0.02 M) were added to each test tube. Test tubes were then closed and placed in an oscillating water bath (15 oscillation per minute) and solutions were brought to solubility equilibrium at room temperature (25 °C), with constant shaking for 5 d. After attainment of equilibrium, the contents of the test tubes were filtered through Whatman filter paper (type 42). The drug concentration in the filtered solutions was determined from the absorbance at 228 nm using a Beckman DU-6 spectrophotometer and three replicates were made for each assay. To nullify the absorbance due to the presence of the cyclodextrin, each time the apparatus was calibrated with the corresponding blank.

Preparation of Binary Systems Two types of binary systems were prepared: physical mixtures and kneaded systems. In both physical mixtures and kneaded systems, drug–HPGCD ratios were 1 : 1 (14.64% w/w of TBM and 85.36% w/w of HPGCD) and 1 : 2 mol/mol (7.32% w/w of TBM and 92.68% w/w of HPGCD). Physical mixtures were prepared by homogeneous intermingling of previously sieved and weighed drug and cyclodextrin in a suitable container.

Kneaded systems were prepared from physical mixtures by adding a small volume of distilled water. After moistening, the resultant systems were kneaded to produce a homogeneous dispersion. Once a homogeneous slurry was obtained, samples were dried at 40 °C for 24 h; all of the dried systems were crushed and sieved, and fractions smaller than 100 μm were collected for further study. Pure TBM and HPGCD have also been kneaded in the same manner to reveal if the kneading method has any influence on the physical characteristics of the pure substances.

Drug concentration in physical mixtures and kneaded systems was deter-

* To whom correspondence should be addressed. e-mail: mdveiga@eucmos.sim.ucm.es

© 2000 Pharmaceutical Society of Japan

mined by UV spectrometry (228 nm), to confirm that the drug–HPGCD ratios were not changed during the treatment.

HSM Analysis About 1 mg of sample was placed on a microscopic slide with cover and heated at a rate of 2 °C/min on a Kofler stage and samples were carried out by using a Thermogalen microscope fitted with the Kofler stage.

DSC Analysis DSC curves of pure materials (kneaded and without any treatment) and all binary systems were recorded on a Mettler TA 3000 differential scanning calorimeter (model DSC 20). About 5—10 mg of sample was placed in a pinholed aluminum sample pan with lid and heated at a rate of 10 °C/min between 30 and 350 °C. The instrument was periodically calibrated with a standard sample of indium.

Termogravimetry (TG) Analysis TG curves were obtained by using a Mettler TA 3000 thermogravimetric analyzer (TG 50). Samples (10 mg) were placed in a crucible of alumina and heated at a rate of 10 °C/min between 30 and 600 °C.

XRD Analysis The powder X-ray diffraction patterns of pure ingredients, their kneaded counterparts, and all binary systems were recorded by using an automated Philips X'Pert X-ray diffractometer. Samples were irradiated with monochromatized Cu$K\alpha$ radiation and analysed between 2θ angles of 5 and 40°. The voltage, current, and time per step used were 40 kV, 55 mA, and 1 s, respectively.

Dissolution Study A Sotax AT-7 dissolution apparatus with paddles was employed to carry out all of the tests. The volume of the dissolution medium, experimental temperature, and paddle speed were 1000 ml, 37± 0.1 °C, and 75 rpm, respectively. Previously powdered and sieved (particle size lower than 100 μm) samples (250 mg of TBM or equivalent amount of binary systems) were used for all dissolution studies. All of the systems were assayed in demineralized water and the duration of assay was 3 h, the samples were withdrawn at measured time interval and filtered with a Whatman filter paper (type 42). Dissolved drug was assayed at a wavelength of 228 nm in a Beckman DU-6 spectrophotometer and three replicates of each dissolution assay were carried out.

Results and Discussion

Phase Solubility Study The phase solubility diagram (Fig. 1) indicates that the drug solubility increases linearly in accord with the amount of cyclodextrin added. It seems that in the range of concentration studied, at least, a soluble TBM–HPGCD was formed giving rise to a phase solubility diagram of A_L type.[12] The apparent stability constant of the inclusion complex can be calculated from the slope and intercept of the linear phase solubility diagram by using the equation.[13]

$$K_s = \frac{\text{slope}}{\text{intercept}\,(1-\text{slope})}$$

The stability constant (K_s) obtained was 38.12 M^{-1}. The value for the stability constant was lower in comparison with that obtained for the TBM–HPBCD inclusion complex (144.8 M^{-1}).[9] This lower value of stability constant indicates that although HPGCD can form an inclusion complex with TBM, the complex between HPBCD and TBM is more stable. This maybe due to the larger cavity size of HPGCD and the binding forces between the guest and host are not sufficient to hold firmly the TBM molecule in the cavity of the cyclodextrin.

HSM Analysis The examinations of both pure TBM and its kneaded counterpart revealed that the samples were constituted of laminar crystalline particles and both of the samples appeared as coloured particles even without polarised light. No change in the particle aspect was observed until the melting of the substance (115—118 °C); the melting process was followed by the decomposition of the material. Under microscopic view, the sample of pure HPGCD was constituted of spherical particles, while all the particles of the kneaded HPGCD sample were of irregular shape. The thermal behaviour of both HPGCD (pure and kneaded) was similar. Upon heating, melting was the first change detected (250—255 °C). Immediately after the fusion, decomposition of the melted particles begins, which was detected from the darkening of the droplets.

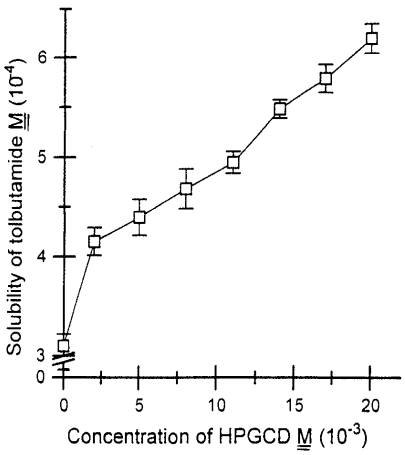

Fig. 1. TBM–HPGCD Phase Solubility Diagram

Each point is the average of three measurements; error bars indicate±standard deviation.

In the physical mixtures (1 : 1 and 1 : 2), TBM and HPGCD particles were easily distinguishable from each other. The drug melted in the range of 115—120 °C; afterwards, the melted mass of the drug mixed with the HPGCD particles and a partial dissolution of the cyclodextrin in the melted TBM was observed. The decomposition of melted TBM was not observed. The melting of undissolved HPGCD particles begins at 220 °C. The completion of the fusion of the system was observed at 250 °C and this process was followed by the decomposition of the system.

The 1 : 1 kneaded system sample consisted of irregular particles. In polarised light some coloured particles, similar to that of pure TBM, were observed and upon heating, melting of the coloured particles took place at 125 °C. This melt mixed with the rest of the particles of the system. The sample melted completely in the range 220—250 °C and immediately afterwards, the decomposition of the system started (darkening of the droplets). The 1 : 2 kneaded system appeared as a homogeneous sample formed by particles of irregular shape. In this system, no isolated particles of TBM were observed as in the 1 : 1 kneaded system. Unlike the sample of the 1 : 1 kneaded system, the entire sample of the 1 : 2 kneaded system melted in the range of 220—250 °C without any prior transition. After the sampled melted it decomposed.

DSC Analysis The analysis of pure and kneaded TBM by DSC gives rise to a curve of three endotherms. The first endotherm is for melting of the drug and the remaining two could indicate the decomposition of the melted drug (Fig. 2, Graphs A and B); this behaviour is in accord with the HSM observation of the drug. DSC traces of pure and kneaded HPGCD consists of two peaks: a dehydration endotherm and a decomposition endotherm (Fig. 2, Graphs C and D). The melting process of this cyclodextrin derivative was not detected by DSC. Because of its amorphous nature, the transition for fusion takes place with the absorption of a lower

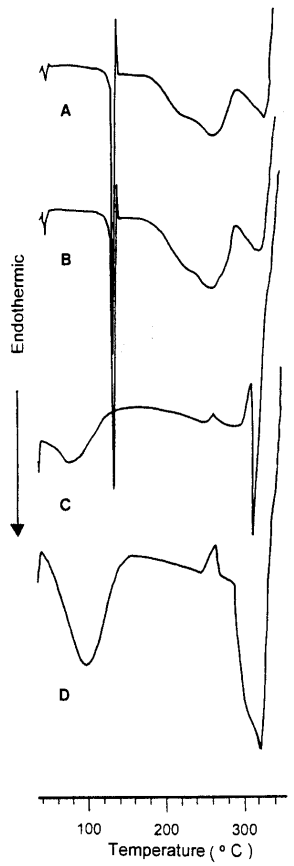

Fig. 2. DSC Curves of TBM and 2-HPGCD

(A) Pure TBM, (B) kneaded TBM, (C) pure HPGCD and (D) kneaded HPGCD.

Table 1. Thermal Data from DSC Analysis of pure TBM and HPGCD and Their kneaded Counterparts

Transition	Pure TBM	Kneaded TBM	HPGCD	Kneaded HPGCD
Dehydration	—	—	76[a]	93[a]
	—	—	91[b]	157[b]
Melting	126[a]	125[a]	—	—
	86[b]	87[b]	—	—
Decomposition	251[a], 318[a]	246[a], 315[a]	308[a]	316[a]
	249[b], 109[b]	313[b], 114[b]	193[b]	293[b]

a) Peak temperature (°C). *b*) Enthalpy (J g^{-1}).

Table 2. Thermal Data from DSC Analysis of TBM–HPGCD Physical Mixtures (PM) and Kneaded Systems (KS)

Transition	PM (1 : 1)	PM (1 : 2)	KS (1 : 1)	KS (1 : 2)
Dehydration from the system	84[a]	78[a]	92[a]	97[a]
	107[b]	103[b]	67[b]	160[b]
Melting of TBM	127[a]	127[a]	126[a]	—
	8[b]	5[b]	3[b]	—
Decomposition of the system	297[a]	311[a]	303[a]	298[a]
	485[b]	399[b]	482[b]	140[b]

a) Peak temperature (°C). *b*) Enthalpy (J g^{-1}).

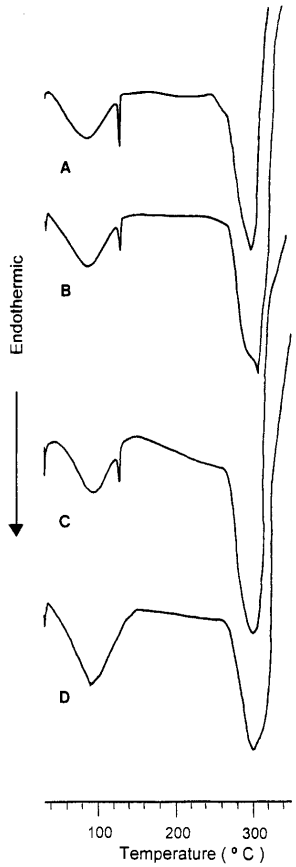

Fig. 3. DSC Curves of TBM–HPGCD Binary Systems

(A) TBM–HPGCD physical mixture 1 : 1, (B) TBM–HPGCD physical mixture 1 : 2, (C) TBM–HPGCD kneaded system 1 : 1 and (D) TBM–HPGCD kneaded system 1 : 2.

amount of energy, as it was observed with other cyclodextrins of amorphous nature.[14] The thermal data from the DSC analysis of TBM and HPGCD, and their kneaded counterparts, presented in Table 1, indicate that the possible changes produced by the kneading process were insignificant, and these minor changes may be attributed to the partial dissolution followed by the re-crystallisation of the materials.

The DSC profiles of the physical mixtures (1 : 1 and 1 : 2) show identical traces (Table 2; Fig. 3, Graphs A and B). In both traces, there are three endotherms and these can be attributed to dehydration of HPGCD, melting of TBM and decomposition of the system. The DSC scan of the 1 : 1 kneaded system (Fig. 3, Graph C) shows similar behaviour to that of the physical mixtures: the peak of the dehydration from the system, peak of TBM melting and the peak of the decomposition of the system. Conversely, the DSC curve of the 1 : 2 kneaded system (Fig. 3, Graph D) exhibits only two endothermic peaks corresponding to the dehydration from the system and decomposition of the system. Like that of pure HPGCD, the fusion process corresponding to the complex was not detected in the kneaded system. Instead, the decomposition of the system was detected.

The absence of the TBM melting peak indicates that in the 1 : 2 kneaded system the entire drug forms a complex with the cyclodextrin. Comparing the scan of the 1 : 2 kneaded system with that of the 1 : 1 kneaded system (in which a small peak is observed in the melting range of TBM) it can be deduced that in the latter system, only a part of the drug forms a complex with the cyclodextrin and the rest of the drug remains free. This free part of the drug melts when the sample reaches the melting point of TBM.

The absence of the two endothermic peaks, corresponding to the TBM decomposition, in all binary systems could indicate that during heating an inclusion complex could have

Table 3. Data from Thermogravimetric Analysis of TBM and HPGCD, Their Kneaded Counterparts, TBM–HPGCD Physical Mixtures (PM), and Kneaded Systems (KS)

Sample	Ranges (°C)	Weight loss (%)	Inference
Pure TBM	121—294	100	Decomposition
Kneaded TBM	127—324	100	Decomposition
Pure HPGCD	52—94	6	Dehydration
	288—481	83	Decomposition
Kneaded	49—122	8	Dehydration
HPGCD	260—489	88	Decomposition
PM 1 : 1	49—92	6	Dehydration from HPGCD
	268—501	88	Decomposition of system
PM 1 : 2	41—99	8	Dehydration from HPGCD
	283—487	82	Decomposition of system
KS 1 : 1	48—105	7	Dehydration from system
	255—505	78	Decomposition of system
KS 1 : 2	46—99	8	Dehydration from system
	264—486	79	Decomposition of system

formed; the melted drug could have occupied the cyclodextrin cavity at higher temperature[15] and in this way the complexed TBM remained protected from the decomposition. This theory is in agreement with the observation of HSM and indicates that the inclusion of TBM into the HPGCD cavity has a stabilizing effect for tolbutamide.

Thermogravimetry Results of the thermogravimetric study are shown in Table 3. Data from both pure and kneaded TBM reveals that both materials lose 100% of their weight in a single step, which begins at 121—127 °C. Both pure HPGCD and its kneaded counterpart lose their weights in two steps. The first step corresponds to the loss of water of hydration and the second step is due to the decomposition of the sample (Table 3).

Thermogravimetric behaviour of all solid binary systems is similar, showing two steps of weight loss attributed to dehydration from HPGCD and decomposition of the system. The temperature at which the decomposition process begins is higher than that of the pure TBM. This behaviour could confirm the hypothesis suggested in the explanation of the results obtained from DSC curves. The formation of a TBM–HPGCD inclusion compound during the kneading process or heating process (thermal analysis) impedes the characteristic decomposition of TBM at temperatures above its melting point.

XRD Analysis The X-ray profiles of TBM and HPGCD (pure and kneaded) are shown in Fig. 4. There was no change in the profiles of the two X-ray patterns of TBM and its kneaded counterparts suggesting that the kneading process has no influence on the crystal structure of pure TBM (Fig. 4, Graphs 1 and 2). On the other hand, both X-ray profiles of HPGCD were of halo pattern indicating its amorphous nature. There was no change in the amorphous nature of HPGCD due to the kneading process (Fig. 4, Graphs 3 and 4).

The X-ray patterns of the two physical mixtures show the characteristic peaks of TBM, although they were of lower intensity in the 1 : 2 physical mixture in comparison with that of the 1 : 1 physical mixture (Fig. 5, Graphs 1 and 3). However, compared with that of pure TBM, the intensities of some of the important peaks of TBM were lower in the profiles of the physical mixtures. This behaviour is due to the

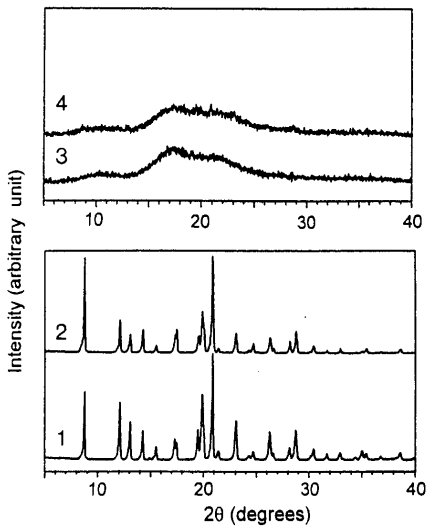

Fig. 4. X-Ray Diffraction Profiles of TBM and HPGCD

(1) Pure TBM, (2) kneaded tolbutamide, (3) pure HPGCD and (4) kneaded HPGCD.

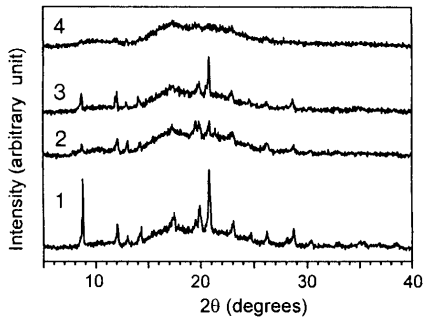

Fig. 5. X-Ray Diffraction Profiles of TBM–HPGCD Binary Systems

(1) TBM–HPGCD physical mixture 1 : 1, (2) TBM–HPGCD kneaded system 1 : 1, (3) TBM–HPGCD physical mixture 1 : 2 and (4) TBM–HPGCD kneaded system 1 : 2.

presence of proportionately (% w/w) higher amount of the carrier in the systems.

The X-ray patterns of the two kneaded systems are of dissimilar type. In the X-ray pattern of the 1 : 1 kneaded system (Fig. 5, Graph 2), some of the TBM peaks are present and this behaviour indicates that some of the drug particles remained in uncomplexed form. In other words, a complete inclusion was not obtained in this system. On the other hand, like that HPGCD, the profile of the 1 : 2 kneaded system is of halo pattern (Fig. 5, Graph 4). The absence of any peaks corresponding to the drug indicates that the entire drug was included in the cavity of this cyclodextrin.

Dissolution Assay The results of the dissolution assay are presented in Table 4 and Fig. 6. Both the 1 : 1 and 1 : 2 kneaded systems showed significant improvement in dissolution in comparison with the physical mixtures and the drug alone. The release of the drug from the kneaded systems was almost instantaneous. Because the formation of TBM–HPGCD inclusion complex increases solubility and dissolution of the drug (Fig. 6). The profiles from the physical mixtures were similar to those obtained from the pure drug. Comparable dissolution profiles from the physical mixtures and pure TBM indicate that the rate of the formation of the TBM–HPGCD inclusion complex in solution was not so fast as to give rise to an *in situ* inclusion complex during the period of assay. This is because the dissolution profiles from

Table 4. Dissolution Efficiency Obtained from Pure TBM and TBM–HPGCD Binary Systems

Systems	Dissolution efficiency (%)		
	30 min	90 min	180 min
Pure TBM	14.94	23.43	29.27
TBM–HPGCD physical mixture 1 : 1	12.61	22.59	30.25
TBM–HPGCD physical mixture 1 : 2	21.36	28.71	34.83
TBM–HPGCD kneaded system 1 : 1	42.05	47.56	48.85
TBM–HPGCD kneaded system 1 : 2	45.72	50.04	51.37

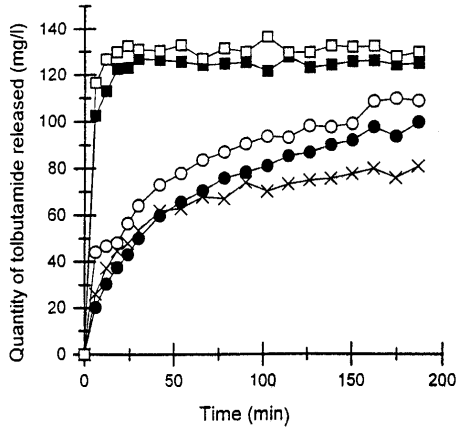

Fig. 6. Dissolution Profiles of TBM and TBM–HPGCD Binary Systems

(×) Pure TBM, (●) TBM–HPGCD physical mixture 1 : 1, (○) TBM–HPGCD physical mixture 1 : 2, (■) TBM–HPGCD kneaded system 1 : 1 and (□) TBM–HPGCD kneaded system 1 : 2.

the physical mixtures cannot reach the profiles from the kneaded system during the three hours of the assay.

The results of the physical characterisation and dissolution studies demonstrate that a TBM–HPGCD inclusion compound was formed due to the kneading process. The improvement in the dissolution of TBM from this inclusion complex was not, however, as promising as those from the TBM–BCD and TBM–HPBCD inclusion compound.[9] Nevertheless, by the preparation of a TBM–HPGCD kneaded system, a dissolution rate better than that from the solid dispersion with PEGS 6000[11] was obtained. Analysing the results of this study along with other studies about complexation phenomena between TBM and different cyclodextrins,[9,16] it can be concluded that the preparation of a TBM-cyclodextrin inclusion compound using any cyclodextrin (BCD, HPBCD and HPGCD) could be the best procedure to obtain an adequate drug dissolution from a solid dosage form of TBM.

Acknowledgements F. Ahsan gratefully acknowledges the Spanish Agency for International Co-operation, Ministry of Foreign Affairs of the government of Spain for providing him with a Full-bright scholarship to do his Ph.D. at the Complutense University of Madrid.

References

1) Torres-Labandeira J. J., Davignon P., Pitha J., *J. Pharm. Sci.*, **80**, 384—386 (1990).
2) Bauer J. A., Fung H. L., *Pharm. Res.*, **8**, 1329—1334 (1991).
3) Brewster M. E., Hora M. S., Simpkins J. W., Bodor N., *Pharm. Res.*, **8**, 792—795 (1991).
4) Uekama K., Otagiri M., *CRC Crit. Rev. Ther. Drug Carrier Syst.*, **3**, 1—40 (1987).
5) Snyder L. R., Kirkland J. J., Glajch J. L., "Practical HPLC Method Development," John Wiley and Sons Inc., New York, 1997, pp. 600—615.
6) Koppenhoefer B., Epperlein U., Xiaofeng Z., Bingcheng L., *Electrophoresis*, **18**, 924—930 (1987).
7) Brewster M. E., Anderson W. R., Estes K. S., Bodor N., *J. Pharm. Sci.*, **80**, 380—383 (1991).
8) Soliman O. A. E., Kimura K., Hiryama F., Uekama K., El-Sabbagh H. M., El-Gawad A. E. H. A., Hashim F. M., *Int. J. Pharm.*, **149**, 73—83 (1997).
9) Veiga F., Teixeira-Dias J. J. C., Kedzierewicz F., Sousa A., Maincent P., *Int. J. Pharm.*, **129**, 63—71 (1996).
10) Nozawa Y., Nawa H., Sadzuka Y., Miyagishima A., Hirota S., *Pharm. Acta Helv.*, **72**, 37—42 (1997).
11) Kedzierewicz F., Hoffman M., Maincent P., *Int. J. Pharm.*, **58**, 221—227 (1990).
12) Higuchi T., Connors K. A., "Advances in Analytical Chemistry and Instrumentation," Interscience Publishers, New York, pp. 117—212, 1965.
13) Thompson D. O., *CRC Crit. Rev. Ther. Drug Carrier Syst.*, **14**, 1—104 (1997).
14) Veiga M. D., Díaz P.J., Ahsan F., *J. Pharm. Sci.*, **87**, 891—900 (1998).
15) Frömming K., Szejtli J., "Cyclodextrins in Pharmacy," Vol. 5, Kluwer Academic Publishers, Dordrecth, 1994, p. 86.
16) Gandhi R. B., Karara A. H., *Drug Dev. Ind. Pharm.*, **14**, 657—682 (1988).

Absorption, First-Pass Metabolism, and Disposition of Itraconazole in Rats

Sun Dong Yoo,* Eunhee Kang, Hun Jun, Beom Soo Shin, Kang Choon Lee, and Kyu Hyun Lee

College of Pharmacy, Sungkyunkwan University, 300 Chonchon-dong, Jangan-ku, Suwon, Kyunggi-do, 440–746, Korea.
Received November 12, 1999; accepted February 7, 2000

This study examined the pharmacokinetic disposition, oral absorption and hepatic extraction of itraconazole and its active metabolite, hydroxyitraconazole, in rats. After i.v. injection, serum itraconazole concentrations decreased biexponentially, with an average terminal elimination half-life, volume of distribution and systemic clearance of 4.9 h, 6.0 l/kg and 14.2 ml/min/kg, respectively. When given orally, its absorption was low, with a mean absolute bioavailability of 16.6%. The metabolite to parent drug area under the curve (*AUC*) ratio was higher after oral administration compared with i.v. injection (mean ratio, 2.7 *vs.* 0.9). The hepatic drug extraction ratio determined after femoral and portal vein administration averaged 18.5%. When hydroxyitraconazole was injected i.v., the elimination half-life, volume of distribution and systemic clearance of itraconazole averaged 10.0 h, 2.4 l/kg and 3.4 ml/min/kg, respectively. The fraction of the systemically available itraconazole that was metabolized to hydroxyitraconazole was 21.0% and 76.0% after i.v. and oral administration, respectively. In summary, this study is the first reporting the hepatic extraction of itraconazole and the i.v. disposition characteristics of hydroxyitraconazole in rats. Itraconazole is a drug with a low hepatic extraction ratio and its systemic clearance appears to be largely accounted for by hepatic metabolism.

Key words itraconazole; hydroxyitraconazole; hepatic first-pass metabolism; bioavailability; metabolite kinetics

Itraconazole is an orally active triazole antifungal agent indicated for the treatment of blascomycosis, histoplasmosis, aspergillosis, oropharynea and esophageal candidiases. It is a weak base with a pK_a of 3.7 and a low aqueous solubility ($<5\ \mu g/ml$).[1] Studies have shown that the dissolution and absorption of itraconazole is pH-dependent, with higher serum levels being obtained at lower gastric pH levels.[2] When taken with food, its oral absorption is enhanced due to a reduced gastric pH and increased gastric emptying time.[3,4] Alternatively, administration with gastric acid-suppressants reduces the oral bioavailability of itraconazole and this reduction can be counteracted by ingestion of acidic cola beverages.[2] Being lipophilic (o/w partition coefficient 5.66), itraconazole is distributed extensively to tissues and its tissue levels are many times higher than in plasma.[5] It is extensively biotransformed to more than 30 metabolites, with hydroxyitraconazole being the major active metabolite in human and rats.[1,6,7] There are a number of publications reporting the oral absorption kinetics of itraconazole in healthy volunteers[8—10] and in disease states,[11—13] as well as interactions with food[3,4,14—16] and other drugs.[17,18] Itraconazole is a potent inhibitor of CYP3A and, when given concomitantly with other drugs such as quinidine,[19] midazolam,[20] bromperidol,[21] oxybutynin,[22] and methylprednisolone[23] that are metabolized by this enzyme system, can significantly increase their serum levels. To our knowledge, no information has been published on the hepatic extraction of itraconazole and the i.v. disposition characteristics of hydroxyitraconazole in human and animals.

The present study was conducted to characterize the hepatic first-pass metabolism of itraconazole and the i.v. pharmacokinetics of hydroxyitraconazole in rats. The absorption kinetics, oral bioavailability and disposition of itraconazole were further investigated.

Experimental

Chemicals Acetonitrile, methylene chloride and methanol (HPLC grades) were purchased from J. T. Baker (Phillipsburg, NJ, U.S.A.). Ketamine, xylazine, diethylamine, *tert*-butyl methyl ether and acetic acid were obtained from Sigma Chem. Co. (St. Louis, MO, U.S.A.). Polyethylene glycol (PEG) 400 was purchased from Yakuri Pure Chem. Co. Ltd. (Osaka, Japan). Itraconazole, hydroxyitraconazole and ketoconazole were synthesized at Choongwae Pharma Co. and were used without further purification (purity >99.2%). All other chemicals used in the study were of analytical grade.

Animals Male Sprague Dawley rats (7—9 weeks of age, 250—325 g, SPF) were obtained from Japan SLC Inc. (Shizuoka, Japan). The rats were kept in plastic rat cages and housed in an animal facility (temperature 23±2 °C) with a light/dark cycle of 12/12 h and relative humidity of 50±10%. The animals were fed with standard rat diet (DaeJong Co., Seoul, Korea) and had free access to water. At least one week of acclimatization was allowed prior to experimentation.

I.v. Injection Study Rats were anesthetized with an i.m. injection of ketamine and xylazine (90/10 mg/kg) and then cannulated with PE tubing (0.58 mm i.d. and 0.96 mm o.d., Natsume Co., Tokyo, Japan) in the right jugular and left femoral vein. Itraconazole and hydroxyitraconazole dissolved in PEG 400 (2 mg/ml) were injected into the femoral vein (5 mg/kg doses) in two groups of rats ($n=4$ each). Serial blood samples (approximately 0.3 ml each) were taken *via* the jugular vein catheter at 0, 5, 10, 15, 30 and 45 min, and 1, 1.5, 2, 4, 8, 12, 24, 36 and 48 h after dosing. Equal volumes of saline were given as a replacement after each sampling. Serum samples were obtained by centrifugation at 1500 ***g*** for 10 min and kept at −20 °C until drug analysis.

Oral Absorption Study Rats were anesthetized and cannulated with PE tubing in the right jugular vein ($n=6$). After surgery, at least a 2 d recovery period was allowed prior to drug administration. Two mini-capsules filled with the contents of Sporanox® capsules were administered orally (itraconazole 2.5 mg per mini-capsule) with the aid of a mini-capsule injector (Natsume Co.). Immediately after capsule administration, 0.4 ml distilled water was given to facilitate swallowing. The mini-capsules had an external diameter of 2.55 mm, length 7.3 mm and a minimum capacity of 30 mm^2 (Natsume Co.). Serial blood samples (approximately 0.3 ml each) were taken from the jugular vein at 0, 5, 10, 15, 30 and 45 min, and 1, 1.5, 2, 4, 8, 12, 24, 36 and 48 h after dosing. Equal volumes of saline were replaced after each sampling. Serum samples were obtained by centrifugation at 1500 ***g*** for 10 min and kept at −20 °C until drug analysis.

Hepatic Extraction Study Rats were anesthetized with an i.m. injection of ketamine and xylazine and were cannulated with PE tubing in the femoral artery and the portal vein or in the femoral artery and vein. Itraconazole dissolved in PEG 400 was administered *via* the femoral or portal vein on separate occasions in two groups of animals ($n=3$ each). The drug was given by simultaneous bolus injection (0.57 mg/kg) followed by infusion (0.26 mg/h/kg) for 90 min in both studies. Serial blood samples (approximately

* To whom correspondence should be addressed. e-mail: sdyoo@skku.ac.kr

© 2000 Pharmaceutical Society of Japan

0.3 ml each) were taken from the femoral artery at 0, 30, 60 and 90 min. Serum samples were obtained by centrifugation at 1500 ***g*** for 10 min and kept at −20 °C until drug analysis.

Drug Analysis Serum concentrations of itraconazole and hydroxyitraconazole were assayed by a validated HPLC method. Briefly, to 100 μl serum in borosilicate tubes (Scientific Glass Inc., Rockwood, TN, U.S.A.) was added 10 μl internal standard solution (ketoconazole 15 μg/ml in mobile phase) and 100 μl 1 M carbonate buffer (pH 10) and the mixture was mixed on a vortex mixer for 10 s. The mixture was extracted with 2 ml of *tert*-butyl methyl ether on a vortex mixer for 70 s and centrifuged at 4000 ***g*** for 10 min. The resulting supernatant was transferred to a fresh tube and dried at 45 °C under nitrogen gas. The residue was reconstituted with 125 μl mobile phase on a vortex mixer for 90 s and the reconstituted solution was centrifuged at 1500 ***g*** for 30 s and a portion (40 μl) was injected onto the chromatograph. Chromatographic separations were achieved on a Hewlett Packard 1100 series HPLC (Hewlett Packard, Santa Clara, CA, U.S.A.) using a Lichrospher 100 RP 8 (4.0×250 mm, 5 μm, Merck, Darmstadt, Germany) and a guard column (4.0×4.0 mm, 5 μm, Hewlett Packard). The mobile phase consisted of acetonitrile : 0.05% diethylamine in deionized water (6 : 4, v/v) (Milli Q Plus System, Millipore, Milford, MA, U.S.A.), with the pH adjusted to 6.0 by drop-wise addition of 30% acetic acid. The mobile phase was filtered and degassed by ultra sonication under vacuum before use. The flow rate of the mobile phase was maintained at 2.0 ml/min at ambient temperature and the effluent was monitored at a UV detection wavelength of 263 nm. Itraconazole, hydroxyitraconazole and ketoconazole (internal standard) were eluted with retention times of 2.8, 3.3 and 5.4 min, respectively. The standard curves were linear over the concentration range 10—2000 ng/ml, with a typical correlation coefficient of r=0.9995. The extraction recovery was >87% and >93% for itraconazole and hydroxyitraconazole, respectively, and the intra- and inter-day assay variability was <5.0% and <2.1% for itraconazole and hydroxyitraconazole, respectively, over the concentration range studied.

Data Analysis Serum itraconazole and hydroxyitraconazole concentration *vs.* time data obtained after i.v. and oral administration were analyzed by compartmental and noncompartmental methods, respectively, using the nonlinear least squares regression program WinNonlin (Scientific Consulting Inc., Cary, NC, U.S.A.). The absolute oral bioavailability of itraconazole was determined as the ratio of $AUC_{oral} \cdot D_{i.v.}/AUC_{i.v.} \cdot D_{oral}$, where the AUCs were the mean values of two groups. The steady-state drug levels after femoral and portal venous infusions were calculated as the mean of the drug concentrations determined at 30, 60 and 90 min. Pharmacokinetic parameters were expressed as the mean±S.D. Statistical differences in the pharmacokinetic parameters of itraconazole and hydroxyitraconazole after their respective i.v. injections were tested by the unpaired Student's t-test (p<0.05).

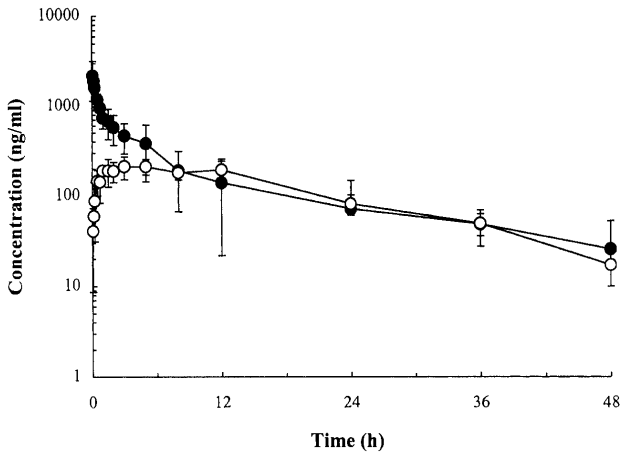

Fig. 1. Average Serum Concentration *vs.* Time Curves of Itraconazole (●) and Hydroxyitraconazole (○) after i.v Injection of Itraconazole (5 mg/kg Doses, n=4)

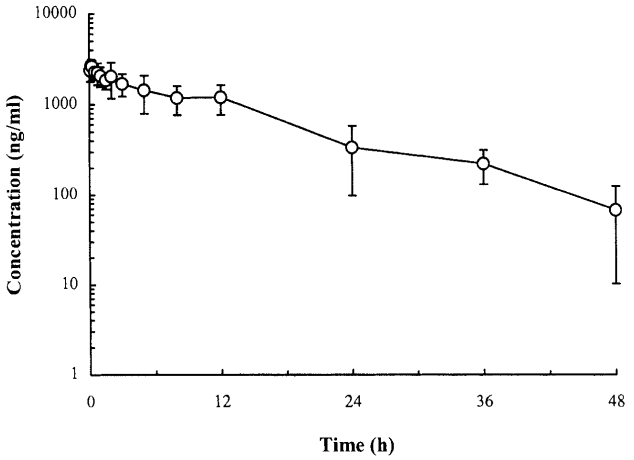

Fig. 2. Average Serum Concentration *vs.* Time Curves of Hydroxyitraconazole after i.v. Injection (5 mg/kg Doses, n=4)

Results and Discussion

The average serum concentration *vs.* time curves of itraconazole and hydroxyitraconazole after their respective i.v. injections are shown in Figs. 1, 2. The serum concentrations of itraconazole declined biphasically, with mean initial distribution and elimination half-lives of 0.2 and 4.9 h, respectively (Table 1). The elimination half-life of itraconazole was significantly shorter than that of hydroxyitraconazole (4.9 *vs.* 10.0 h) following i.v. injection. Consistent with its lipophilic nature (o/w partition ratio 5.66),[1] itraconazole exhibited a large distribution volume (V_{ss} 6.0±2.5 l/kg). The mean systemic clearance of itraconazole was 14.2±7.6 ml/min/kg and the metabolite-to-parent drug *AUC* ratio (AUC_M/AUC_D) averaged 0.9±0.5. A significant correlation (r=0.999) was found between the systemic clearance of itraconazole and the AUC_M/AUC_D ratio in individual rats. This correlation indicates that the variations seen in the systemic clearance of itraconazole may be due to differences in the formation of hydroxyitraconazole. The elimination half-life of hydroxyitraconazole (10.0±3.4 h) after i.v. injection was comparable with that (12.4±2.0 h) found after administration of the parent drug. The systemic clearance (3.4±2.0 ml/min/kg) and distribution volume (2.4±0.7 l/kg) of hydroxyitraconazole were less than that of the parent drug. The fraction of hydroxyitraconazole formed after i.v. injection of the parent drug, calculated as $CL_M \cdot AUC_M/CL_D \cdot AUC_D$, was 21.0% of the administered dose.

Table 1. Pharmacokinetic Parameters (Mean±S.D.) Obtained after i.v. Injection of Itraconazole and Hydroxyitraconazole in Rats (5 mg/kg Doses)

Parameter	Drug i.v.		Metabolite i.v.
	Itraconazole	Hydroxyitraconazole	Hydroxyitraconazole
Weight (g)	318±30	318±30	320±38
$t_{1/2,\lambda 1}$ (h)	0.2±0.1	—	0.6±0.5
$t_{1/2,\lambda z}$ (h)	4.9±5.6	12.4±2.0	10.0±3.4
C_{max} (ng/ml)	—	254±24	—
T_{max} (h)	—	12.0±5.4	—
MRT (h)	8.8±4.9	19.1±1.7	14.0±4.7
AUC (ng/h/ml)	7385±3991	5523±204	31279±14289
AUMC (ng/h/ml)	78560±76167	105717±11689	477923±305789
CL (ml/min/kg)	14.2±7.6	—	3.4±2.0
V_c (l/kg)	1.9±1.0	—	1.9±0.5
V_{ss} (l/kg)	6.0±2.5	—	2.4±0.7

Figure 3 shows the average serum concentration *vs.* time curves of itraconazole and hydroxyitraconazole after oral administration of itraconazole (5 mg doses). Itraconazole was

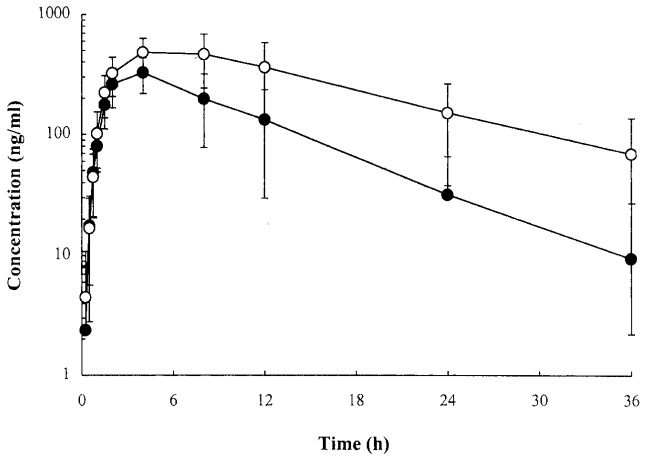

Fig. 3. Average Serum Concentration *vs.* Time Curves of Itraconazole (●) and Hydroxyitraconazole (○) after Oral Administration of 50 mg Doses of Itraconazole (n=6)

Table 2. Pharmacokinetic Parameters (Mean±S.D.) of Itraconazole and Hydroxyitraconazole after Oral Administration of Itraconazole (5 mg Doses) in Rats

Parameter	Itraconazole	Hydroxyitraconazole
Weight (g)	317±29	317±29
$t_{1/2,\lambda z}$ (h)	6.0±2.3	10.4±2.8
C_{max} (ng/ml)	328±107	527±197
T_{max} (h)	4.0±1.1	6.7±3.3
MRT (h)	9.7±3.1	16.4±4.9
AUC (ng/h/ml)	3864±2381	10178±5807
AUMC (ng/h^2/ml)	42280±37856	181719±147702
CL/F (ml/min/kg)	89.4±47.3	—
V_z/F (l/kg)	40.7±16.9	—

slowly absorbed, with a T_{max} being reached at 4.0 and 6.7 h for the parent drug and metabolite, respectively (Table 2). Serum levels of the metabolite exceeded that of the parent drug from approximately 2 h after administration and remained elevated thereafter. The peak concentrations (C_{max}) were higher for the metabolite than for the parent drug (mean 527 *vs.* 328 ng/ml). The apparent elimination half-lives of the drug and metabolite (6.0 and 10.4 h, respectively) were comparable with those (4.9 and 10.0 h, respectively) after i.v. injection (Table 1). These elimination half-lives of itraconazole are comparable with that reported in rats previously (6.5 h).[1] The mean AUC_M/AUC_D ratio after oral administration was higher than that after i.v. injection (2.7 *vs.* 0.9). The absolute bioavailability of itraconazole was low (16.6%) and most (76.0%) of the absorbed drug was converted to hydroxyitraconazole, as calculated from the drug and metabolite *AUC* and clearance values. In human, the relative oral bioavailability of itraconazole from capsules over solution is 39.8%[3] and the absolute oral bioavailability from solution is 55%.[7] It is not known whether the low oral bioavailability of itraconazole in rats and human is due to poor dissolution and absorption, hepatic first-pass metabolism or extensive gut wall metabolism.

The extent of hepatic drug extraction was determined by comparing the arterial serum drug levels after separate femoral and portal venous infusions[24] of itraconazole. There were no statistical differences in the arterial drug concentrations determined at 30, 60 and 90 min, indicating that steady-state was achieved within 30 min of infusion. The mean steady-state hepatic extraction of itraconazole averaged 18.5%. The systemic clearance of itraconazole obtained after femoral venous infusion averaged 15.5 ml/min/kg, which was comparable with that determined in the i.v. bolus injection study (14.2 ml/min/kg). Assuming an even distribution of itraconazole between serum and erythrocytes, its systemic clearance accounts for <30% of the hepatic blood flow (55.2 ml/min/kg) in rats.[25] Therefore, the hepatic clearance of itraconazole (10.5 ml/min/kg), calculated as the product of the hepatic blood flow and hepatic extraction ratio, appears to account for most of its systemic clearance.

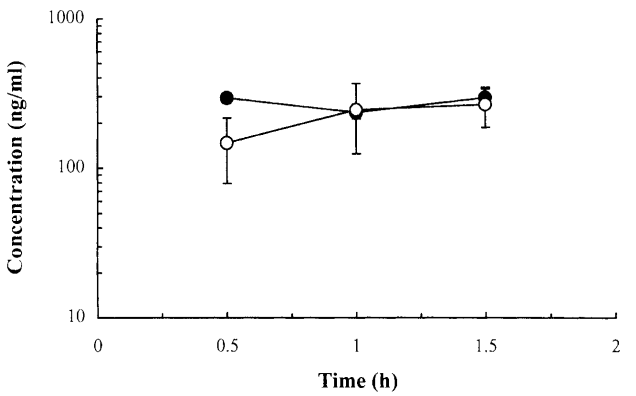

Fig. 4. Average Arterial Serum Concentrations of Itraconazole Following Simultaneous i.v. Bolus Injection (0.57 mg/kg) Plus Infusion (0.26 mg/h/kg) into the Femoral Vein (●) and the Portal Vein (○) on Separate Occasions (n=3 each)

Summary and Conclusions

This study examined the pharmacokinetic disposition of itraconazole and hydroxyitraconazole in rats. Itraconazole exhibited a greater systemic clearance (14.2 *vs.* 3.4 ml/min/kg), greater steady-state volume of distribution (6.0 *vs.* 2.4 l/kg) and shorter elimination half-life (4.9 *vs.* 10.0 h) compared with hydroxyitraconazole. The absolute oral bioavailability (16.6%) and hepatic extraction (18.5%) of itraconazole were low. Nevertheless, the systemic clearance of itraconazole appears to be largely due to its hepatic clearance.

References

1) Heykants J., Michiels M., Meuldermans W., Monbaliu J., Lavrijsen K., Van Peer A., Levron J. C., Woestenborghs R., Cauwenbergh G., "Recent Trends in the Discovery, Development and Evaluation of Antifungal Agents," ed. by Fromtling R. A., J. R. Prous Science Publishers, Barcelona, 1987, pp. 223—249.
2) Lange D., Pavao J. H., Wu J., Klausner M., *J. Clin. Pharmacol.*, **37**, 535—540 (1997).
3) Van Peer A., Woestenborghs R., Heykants J., Gasparini R., Cauwenbergh G., *Eur. J. Clin. Pharmacol.*, **36**, 423—426 (1989).
4) Barone J. A., Koh J. G., Bierman R. H., Colaizzi J. L., Swanson K. A., Gaffar M. C., Moskovitz B. L., Mechlinski W., Van de Velve V., *Antimicrob. Agents Chemother.*, **37**, 778—784 (1993).
5) Heykants J., Van Peer A., Lavrijsen K., Meuldermans S.W., Woestenborghs R., Cauwenbergh G., *Br. J. Clin. Pract.*, **71**, S50—S56 (1990).
6) Dupont B., Drouhet E., *Rev. Infect. Dis.*, **9**, S71—S76 (1987).
7) Heykants J., Van Peer A., Van de Velve V., Van Rooy P., Meuldermans W., Lavrijsen K., Woestenborghs R., Van Cutsem J., Cauwenbergh G., *Mycoses*, **32**, 67—87 (1989).
8) Hardin T. C., Graybill J. R., Fetchick R., Woestenborghs R., Rinaldi M.

G., Kuhn J., *Antimicrob. Agents Chemother.*, **32**, 1310—1313 (1988).
9) Christensen K. J., Gubbins P. O., Gurley B. J., Bowman J. L., Buice R. G., *Am. J. Health Syst. Pharm.*, **55**, 261—265 (1998).
10) Barone J. A., Moskovitz B. L., Guarnieri J., Hassell A. E., Colaizzi J. L., Bierman H. R., Jessen L., *Antimicrob. Agents Chemother.*, **42**, 1862—1865 (1998).
11) Boelaert J., Schurgers M., Matthys E., Daneels R., Van Peer A., De Beule K., Woestenborghs R., Heykants J., *Antimicrob. Agents Chemother.*, **32**, 1595—1597 (1988).
12) Smith D., Van de Velde V., Woestenborghs R., Gazzard B. G., *J. Pharm. Pharmacol.*, **44**, 618—619 (1992).
13) Patterson T. F., Peters J., Levine S. M., Anzueto A., Bryan C. L., Sako E. Y., Miller O. L., Calhoon J. H., Rinaldi M. G., *Antimicrob. Agents Chemother.*, **40**, 2217—2220 (1996).
14) Zimmermann T., Yeates R.A., Laufen H., Pfaff G., Wildfeuer A., *Eur. J. Clin. Pharmacol.*, **46**, 147—150 (1994).
15) Zimmermann T., Yeates R.A., Albrecht M., Laufen H., Wildfeuer A., *Int. J. Clin. Pharm. Res.*, **14**, 87—93 (1994).
16) Van de Velde V. J., Van Peer A.P., Heykants J. J., Woestenborghs R. J., Van Rooy P., De Beule K. L., Cauwenbergh G. F., *Pharmacotherapy*, **16**, 424—428 (1996).
17) Ducharme M. P., Slaughter R. L., Warbasse L. H., Chandrasekar P. H., Van de Velde V., Mannens G., Edwards D. J., *Clin. Pharmacol. Ther.*, **58**, 617—624 (1995).
18) Neuvonen P. J., Suhonen R., *J. Am. Acad. Dermatol.*, **33**, 134—135 (1995).
19) Kaukonen K. M., Olkkala K. T., Neuvonen P. J., *Clin. Pharmacol. Ther.*, **62**, 510—517 (1997).
20) Backman J. T., Kivisto K. T., Olkkala K. T., Neuvonen P .J., *Eur. J. Clin. Pharmacol.*, **54**, 53—58 (1998).
21) Furukori H., Kondo T., Yasui N., Otani K., Tokinaga N., Nagashima U., Kaneko S., Inoue Y., *Psychopharmacology*, **145**, 189—192 (1999).
22) Lukkari E., Juhakoski A., Aranko K., Neuvonen P. J., *Eur. J. Clin. Pharmacol.*, **52**, 403—406 (1997).
23) Varis T., Kaukonen K. M., Kivisto K. T., Neuvonen P. J., *Clin. Pharmacol. Ther.*, **64**, 363—368 (1998).
24) Kumar S., Riggs K. W., Rurak D. W., *Drug Metab. Dispos.*, **27**, 297—302 (1999).
25) Davies B., Morris T., *Pharm. Res.*, **10**, 1093—1095 (1993).

Phosphorylation of D-Glucose Derivatives with Inorganic Cyclo-Triphosphate: Substituent Effect at the 5-CH_2OH or 2-OH Group

Hideko INOUE, Mari WATANABE, Hirokazu NAKAYAMA, and Mitsutomo TSUHAKO*

Department of Functional Molecular Chemistry, Kobe Pharmaceutical University, Kobe 658–8558, Japan.
Received December 6, 1999; accepted February 18, 2000

The phosphorylation of several D-glucose derivatives has been achieved using inorganic sodium cyclo-triphosphate hexahydrate (P_{3m}), $Na_3P_3O_9 \cdot 6H_2O$, in aqueous solution. In the phosphorylation of D-glucuronic acid, 6-phosphoryl-D-glucose and D-xylose, β-D-glucuronic acid 1-triphosphate, 6-phosphoryl-β-D-glucose 1-triphosphate and β-D-xylose 1-triphosphate were synthesized stereoselectively with maximum yields of 43.5, 32.8 and 41.9%, respectively. In the case of D-glucosamine and 2-deoxy-D-glucose, the main phosphorylated products were assigned to β-D-glucosamine 1-triphosphate and 2-deoxy-β-D-glucose 1-triphosphate by ^1H-, ^{13}C- and ^{31}P-NMR, and the yields were 13.9 and 13.4%, respectively.

Key words phosphorylation; β-D-glucose 1-triphosphate; cyclo-triphosphate hexahydrate; multinuclear NMR; HPLC

Sodium cyclo-triphosphate (P_{3m}), which is a simple inorganic condensed phosphate having a six-membered ring, is a very attractive phosphorylation reagent for synthesizing biologically important compounds in one step in aqueous solution. The reaction proceeds well for organic compounds having an amino or a hydroxyl group. Feldmann demonstrated the phosphorylation of ammonia[1] and alcohols[2] with P_{3m}. Later on, the phosphorylation reactions of amino acids,[3,4] alkyldiamine,[5] nucleosides,[6] sugar,[7,8] phenols,[9] and cellulose[10] were examined in detail. Recently, we have reported that D-glucose (**1**) reacts with P_{3m} to stereoselectively form β-D-glucose 1-triphosphate (**5**)[8] in aqueous solution, and that the optimum condition for the phosphorylation is a molar ratio of P_{3m} and **1**=1 : 5, pH 12, and room temperature.[7] In order to clarify the mechanism of the stereoselective reaction at 1-OH of **1**, the phosphorylation of D-glucose derivatives in which the neighbor of the reaction site, that is, the CH_2OH group at C-5 or OH group at C-2, is exchanged by other function groups, was examined in detail.

Results and Discussion

Phosphorylation of D-Glucuronic Acid (2), 6-Phosphoryl-D-glucose (3) and D-Xylose (4) with P_{3m} D-Glucose (**1**) and its derivatives used in the present study are shown in Chart 1. The phosphorylation was carried out essentially according to the previous method.[8] Figure 1 shows HPLC profiles for the reaction mixture of D-glucuronic acid (**2**) (1.25 $mol \cdot dm^{-3}$) and P_{3m} (0.25 $mol \cdot dm^{-3}$) incubated at room temperature and pH 12. A peak of the main phosphorylated product (**6**) appeared at the retention time of about 50 min, predicting that the product (**6**) is a triphosphate derivative of **2**. A peak at the retention time of about 21 min (reaction time of 72 h) was assigned as a by-product. The other chromatographic peaks were assigned to P_{3m} and its hydrolytic products, *i.e.*, monophosphate (P_1), diphosphate (P_2), and triphosphate (P_3), respectively.

Figure 2 shows changes in the amounts of the products in the reaction of **2** (1.25 $mol \cdot m^{-3}$) and P_{3m} (0.25 $mol \cdot m^{-3}$) at pH 12 and room temperature. The yield of **6** increased with the passage of reaction time, reaching about 30% after 8 h, then it decreased gradually. This decrease is due to the hydrolysis of **6** to form a monophosphate derivative (by-product). At the same time, P_{3m} was gradually hydrolyzed to P_2 and P_1. Therefore, P_2 increased monotonously (Fig. 2). Table

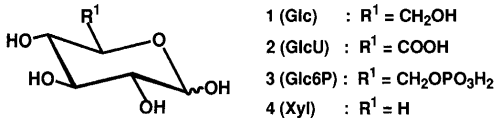

1 (Glc) : $R^1 = CH_2OH$
2 (GlcU) : $R^1 = COOH$
3 (Glc6P) : $R^1 = CH_2OPO_3H_2$
4 (Xyl) : $R^1 = H$

Chart 1

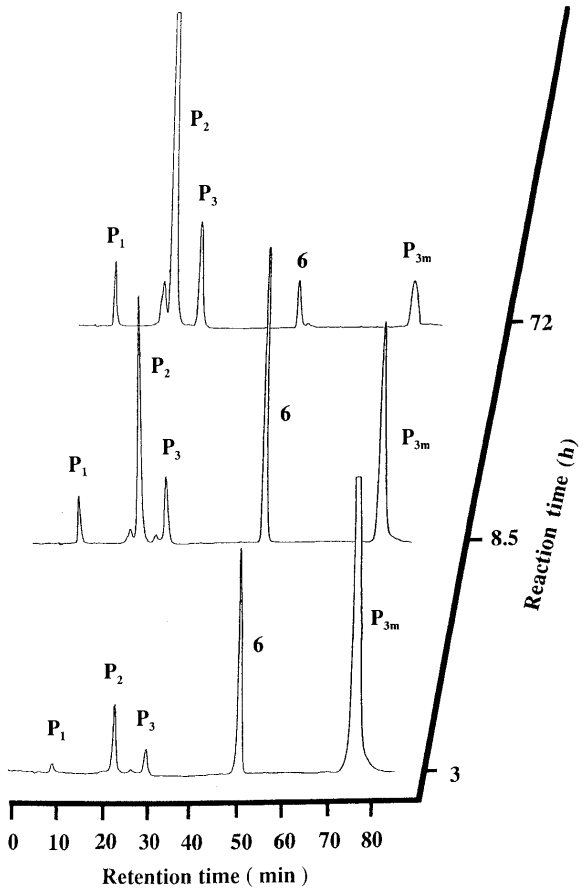

Fig. 1. HPLC Profiles for the Reaction Mixture of **2** and P_{3m}

2: P_{3m}=1.25 $mol \cdot dm^{-3}$: 0.25 $mol \cdot dm^{-3}$, pH 12, and room temperature. P_1, monophosphate; P_2, diphosphate; P_3, triphosphate; P_{3m}, cyclo-triphosphate.

* To whom correspondence should be addressed. e-mail: mtsuhako@kobepharma-u.ac.jp
© 2000 Pharmaceutical Society of Japan

1 summarizes the yields of the product **6** in the reactions of **2** with P_{3m} under various mixing ratios. The yield of **6** increased with the increase of initial concentration of **2**. The maximum yield and its time suggest that the optimum condition for the phosphorylation of **2** with P_{3m} is pH 12 and a molar ratio of P_{3m} : **2**=1 : 7.

To identify the main product (**6**), ^{31}P-, ^{1}H- and ^{13}C-NMR spectra were measured. Figure 3(A) shows the ^{31}P-NMR spectrum of the P_α region in the reaction product of **2** with P_{3m}. The spectrum showed one doublet of doublets at −11.4 ppm, which became doublet on ^{1}H-decoupling, indicating the characteristic peak of P_α in triphosphate derivatives[9,11] of D-aldose.

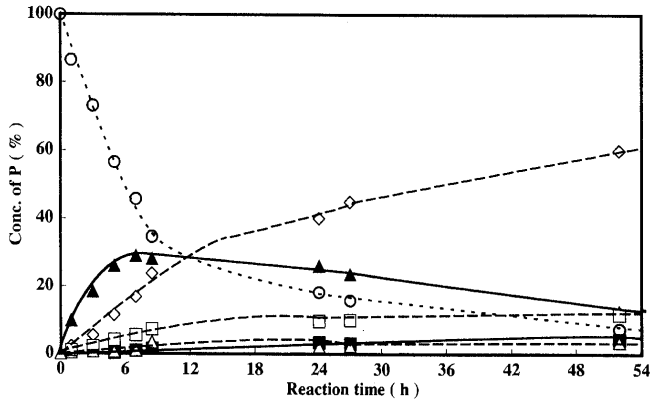

Fig. 2. Changes in the Amounts of the Products in the Reaction of **2** (1.25 mol·dm^{-3}) and P_{3m} (0.25 mol·dm^{-3}) at pH 12 and Room Temperature

▲, 6; ■, by-product; △, P_1; ◇, P_2; □, P_3; ○, P_{3m}.

Table 1. Yields in the Phosphorylation of D-Glucose Derivatives

Reaction conditions		Yield (%) (product)
Mixing ratio	Time (h)	
P_{3m}: **2**		
=1 : 10 (0.25 M : 2.5 M)	3.0	43.4 (**6**)
=1 : 7 (0.25 M : 1.75 M)	4.5	43.5 (**6**)
=1 : 5 (0.25 M : 1.25 M)	6.5	29.9 (**6**)
P_{3m}: **3**		
=1 : 10 (0.2 M : 2.0 M)	6.0	31.8 (**7**)
=1 : 7 (0.2 M : 1.4 M)	20.5	32.8 (**7**)
=1 : 5 (0.2 M : 1.0 M)	23.5	28.6 (**7**)
P_{3m}: **4**		
=1 : 10 (0.5 M : 5.0 M)	6.5	41.9 (**8**)
=1 : 7 (0.5 M : 3.5 M)	8.5	38.1 (**8**)
=1 : 5 (0.5 M : 2.5 M)	30.0	31.3 (**8**)

Figure 3(B) shows ^{1}H-NMR spectra in the region of H-1 of the reaction mixture. The doublet of doublets at 4.92 ppm was assigned to H-1 of **6**. The $^{3}J_{1,2}$ value of **6** is 7.8 Hz, which is typical for β-D-glucose 1-triphosphate (**5**),[8] β-D-aldose 1-monophosphates[12] and β-D-glucuronic acid.[13] The $^{3}J_{P_\alpha H\text{-}1}$ value from ^{1}H-NMR is consistent with that deduced from ^{31}P-NMR data and also with data of **5**[8] and β-D-aldose 1-phosphates.[12] Thus, these results suggest that **6** is β-D-glucuronic acid 1-triphosphate.

^{13}C-NMR chemical shift values and coupling constants of **6** also confirmed this identification. The chemical shift values of **6** are close to those of the β-anomer of **2**,[13] although δ in C-1 shows a down-field shift as a result of the phosphorylation. This tendency is observed in β-D-aldose 1-phosphates.[12] Also, the $^{2}J_{P_\alpha C\text{-}1}$ and $^{3}J_{P_\alpha C\text{-}2}$ values of **6** were close to those of **5**[8] and β-D-aldose 1-phosphates.[12] Therefore, **2** reacts with P_{3m} to form β-D-glucuronic acid 1-triphosphate (**6**) stereoselectively, as shown in Chart 2.

The reactions of 6-phosphoryl-D-glucose (**3**) and D-xylose (**4**) with P_{3m} were carried out under the same reaction condition as **2**. The results of HPLC indicated that the products are their triphosphate derivatives. The experiment at different mixing ratios showed that maximum yields of **7** and **8** were

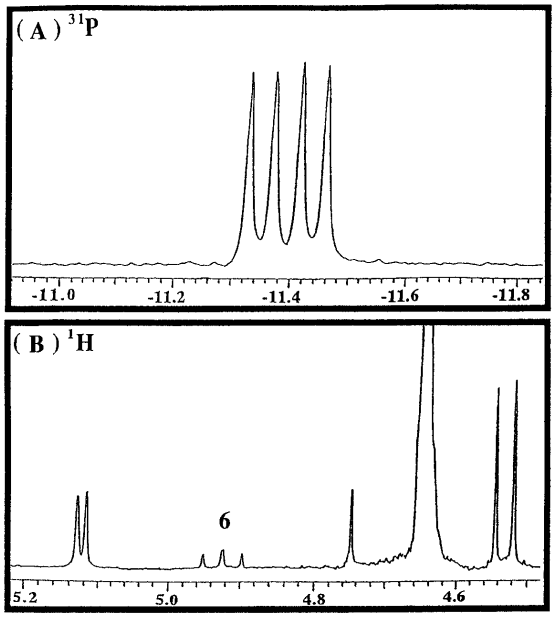

Fig. 3. ^{31}P-NMR Spectrum of the P_α Region (A), and ^{1}H-NMR Spectrum of the H-1 Region (B) in the Reaction Mixture

2: P_{3m}=1.25 mol·dm^{-3}: 0.25 mol·dm^{-3}, pH 12, and room temperature, after 6.5 h.

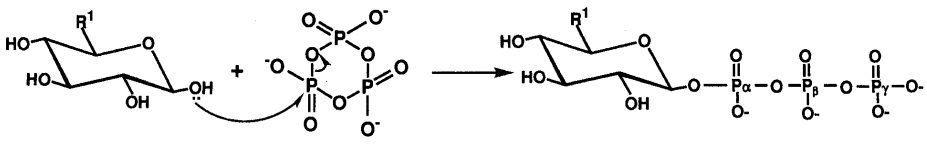

1 - 4 **5 - 8**

1, 5 : R^1 = CH_2OH
2, 6 : R^1 = COOH
3, 7 : R^1 = $CH_2OPO_3H_2$
4, 8 : R^1 = H

Chart 2

32.8 and 41.9% at molar ratios of 1 (P_{3m}) : 7 (**3**) and 1 (P_{3m}) : 10 (**4**), respectively (Table 1).

Similar to **6**, ^{31}P-, ^{1}H- and ^{13}C-NMR spectra of **7** and **8** suggest them to be β-D-aldose 1-triphosphates.[12,14,15] Therefore, **3** and **4** stereoselectively react with P_{3m} to form 6-phosphoryl-β-D-glucose 1-triphosphate (**7**) and β-D-xylose 1-triphosphate (**8**). The phosphorylation of D-glucose derivatives, in which the 5-CH_2OH group is substituted with other functional groups, *i.e.*, COOH, $CH_2OPO_3H_2$ and H, proceeds by a mechanism similar to that of **1** (Chart 2).

Phosphorylation of D-Glucosamine (9), 2-Deoxy-D-glucose (10) and 2-Fluoro-2-deoxy-D-glucose (11) with P_{3m}

Chart 3 shows D-glucose derivatives substituted at 2-OH. Figure 4 shows HPLC profiles for the reaction mixture of D-glucosamine (**9**) (1.25 mol·dm^{-3}) and P_{3m} (0.25 mol·dm^{-3}) incubated at room temperature and pH 12. Two peaks due to the phosphorylated products (**12** and **13**) appeared at retention times of about 23 and 32 min, respectively. The amount of **12** increased with the passage of reaction time and reached 11.6% after 3 d; the maximum amount remained more than 7 d. The formation rate of **13** was slow compared with that of **12** and the yield was about 5.0% at 5 d. The reaction of **9** with P_{3m} was carried out under various reaction conditions. The yields of **12** and **13** did not increase by an increase of the initial concentration of **9** (Table 2).

To identify the phosphorylated products **12** and **13**, ^{31}P- and ^{1}H-NMR spectra for the reaction mixture were measured because of the difficulty of isolation due to low yields. Figure 5 shows the ^{31}P-NMR spectra for the reaction mixture of **9** and P_{3m}. A proton-decoupling spectrum showed characteristic signals assigned to two triphosphate derivatives of **9** in addition to the signals of P_2 (−4.3 ppm) and P_3 (−4.0 and −18.2 ppm). At this reaction condition, the yields of **12** and **13** were 10.3 and 2.2%, respectively, indicating that the signal of **12** would mainly be observed. When the pH of the reaction mixture was changed to 3 (acidic), the peaks at 0.62, −4.2 and −19.6 ppm disappeared, and the peak at 32 min in

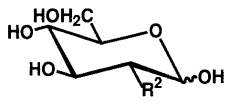

9 (GlcN) : R^2= NH_2
10 (2dGlc) : R^2 = H
11 (2F2dGlc) : R^2 = F

Chart 3

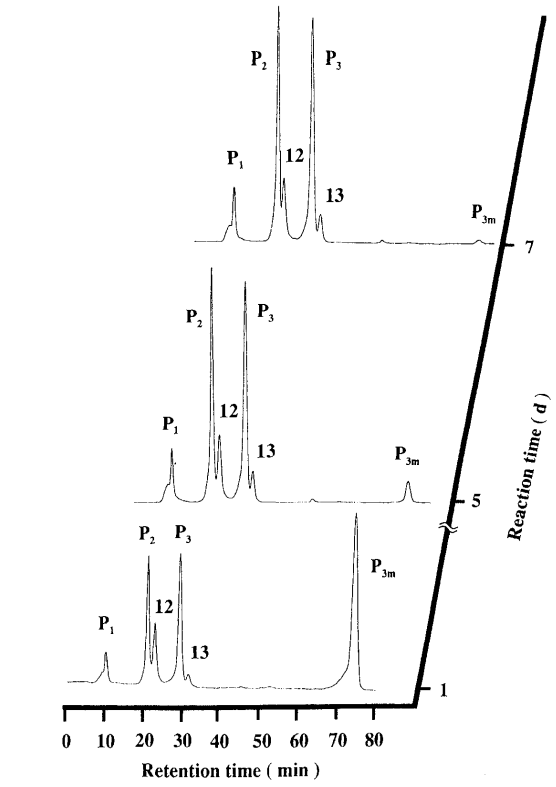

Fig. 4. HPLC Profiles for the Reaction Mixture of **9** and P_{3m}

9: P_{3m}=1.25 mol·dm^{-3}: 0.25 mol·dm^{-3}, pH 12, and room temperature.

Table 2. Yields in the Phosphorylation of D-Glucose Derivatives

Reaction conditions		Yield (%) (product)
Mixing ratio	Time (h)	
P_{3m}: **9**		
=1 : 7 (0.25 M : 1.75 M)	48	13.9 (**12**)
	48	4.1 (**13**)
=1 : 5 (0.25 M : 1.25 M)	72	11.6 (**12**)
	120	5.0 (**13**)
P_{3m}: **10**		
=1 : 5 (0.2 M : 1.0 M)	144	7.9 (**14**)
=1 : 4 (0.5 M : 2.0 M)	24	13.4 (**14**)
P_{3m}: **11**		
=1 : 5 (0.02 M : 0.1 M)	—	0

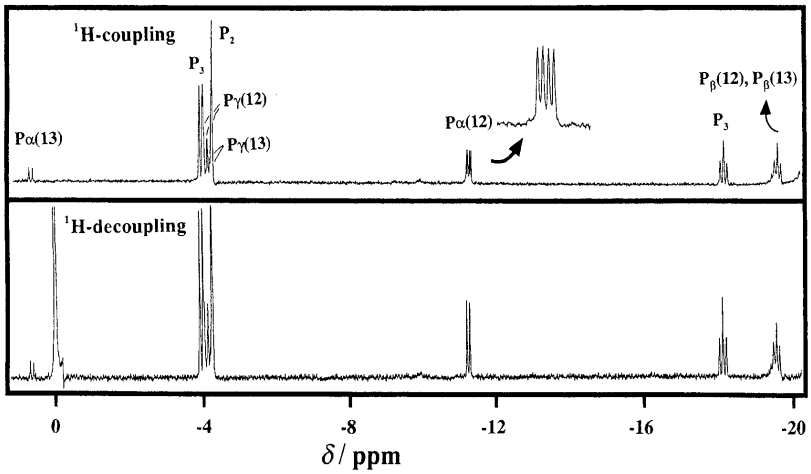

Fig. 5. ^{31}P-NMR Spectra for the Reaction Mixture of **9** (1.25 mol·dm^{-3}) and P_{3m} (0.25 mol·dm^{-3}) Incubated at pH 12 and Room Temperature for 1 d

The big signal at 0 ppm on ^{1}H-decoupling spectrum is an external reference (H_3PO_4).

HPLC profile disappeared as well. Therefore, the peaks at −4.1, −11.3, and −19.7 ppm were assigned to **12**. The doublet at −11.3 ppm was assigned to the signal of the P_α atom in **12** because the proton coupling spectrum shows that the doublet was split into a doublet of doublets ($^3J_{P_\alpha H\text{-}1}$=8.5 Hz). The triplet at −19.7 ppm and the doublet at −4.1 ppm were assigned to the middle (P_β in **12**) and end phosphorus (P_γ in **12**) atoms, respectively.[9,11]

Figure 6 illustrates ^{1}H-NMR spectra in the region of H-1 of the reaction mixture at 14 h (A), 1 d (B) and 3 d (C). At 14 h (A), a signal due to **12** was observed because the amounts of **12** and **13** were 7.7 and 1.8%, respectively. As the reaction time elapsed, the signal due to **13** increased gradually. In Figs. 6(A) and (B), the doublet of doublets at about 5.27 ppm is assigned to H-1 of β-D-glucosamine 1-triphosphate (**12**). The $^3J_{1,2}$ value of **12** is 8.5 Hz, which is equal to that of β-D-glucosamine.[16] The triplet is due to the accidental coincidence of $^3J_{1,2}$ and $^3J_{P_\alpha H\text{-}1}$. The latter is consistent with $^3J_{P_\alpha H\text{-}1}$ deduced from ^{31}P-NMR (Fig. 5). Furthermore, the ^{31}P–^{1}H 2D-NMR (heteronuclear multiple bond correlation spectroscopy (HMBC)) experiment also showed a correlation of P_α at −11.3 ppm and the ^{1}H signal at 5.27 ppm, confirming the above conclusion. Therefore, the main phosphorylated product in the reaction of **9** with P_{3m} was proved to be β-D-glucosamine 1-triphosphate (**12**).

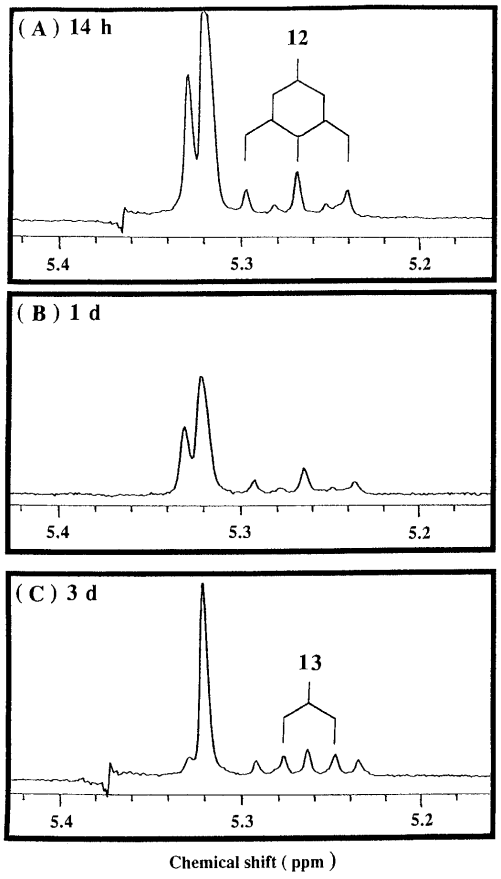

Fig. 6. The 300 MHz ^{1}H-NMR Spectra in the Region of H-1 of the Main Product in the Reaction of D-Glucosamine (**9**) (1.25 mol·dm^{-3}) with P_{3m} (0.5 mol·dm^{-3}) at pH 12 for 14 h (A), 1 d (B) and 3 d (C)

The previous works indicated that the phosphorylation products of alkylamines[17] and alkyldiamine[5] with P_{3m} are alkylamido- and alkylimidotriphosphates with a P–N bond. These products show a characteristic P_α signal[4] of ^{31}P-NMR at around 0 ppm, and are easily recyclized to P_{3m} under an acidic condition. From these facts, **13**, which shows ^{31}P-NMR signals at 0.62, −19.6 and −4.2 ppm, is considered to be β-D-glucosamine 2-triphosphate with a P–N bond. From the previous work,[18] the amino group is predicted to be more easily phosphorylated with P_{3m} than the OH group. However, this is not the case in the phosphorylation of **9** with P_{3m}, probably because the 1-OH group in **9** has an aldehyde character and shows higher reactivity than the 2-NH_2 group (Chart 4).

The reactions of 2-deoxy-D-glucose (**10**) and 2-fluoro-2-deoxy-D-glucose (**11**) with P_{3m} were carried out with mixing ratios of 5 : 1 and 4 : 1 at pH 12 and room temperature. The maximum yield of the main phosphorylated product (**14**) of **10** was 13.4%, whereas **11** did not react with P_{3m} at all (Table 2). A ^{31}P–^{1}H 2D HMBC correlation experiment showed correlation between P_α at −12.4 ppm and the ^{1}H signal at 5.25 ppm, indicating that the main product is confirmed to be 2-deoxy-β-D-glucose 1-triphosphate (**14**), as shown in Chart 5.

Mechanism of the Reaction of D-Glucose Derivatives with P_{3m} In the phosphorylation of D-glucose derivatives (**2**—**4**) substituted at the 5-CH_2OH of **1** with P_{3m}, β-D-aldopyranose 1-triphosphates (**6**—**8**), they were stereoselectively synthesized with yields of more than 32%. On the other hand, the reactions of D-glucose derivatives (**9** and **10**) substituted at 2-OH of **1** with P_{3m} produced their triphosphate derivatives in low yields with poor selectivity. 2-Fluoro-2-

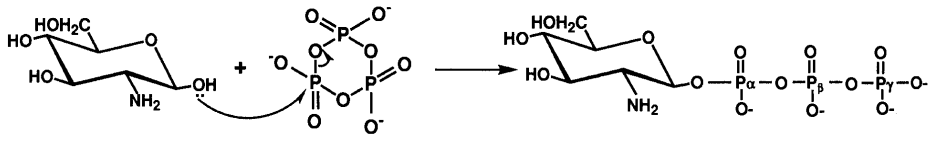
HOH2C
HO
HO
NH2
OH
+
O
O
P
O
O
O

Table 3. Population of Anomers in H_2O at Room Temperature

Monosaccharide	α (%)	β (%)
1	36	64
2	35	65
3	35	65
4	37	63
9	31	69
10	35	65
11	33	67

a) See ref. 20.

deoxy-D-glucose (**11**) did not react with P_{3m} at all.

The stereoselectivity of the reactions of D-glucose derivatives substituted at 5-CH_2OH with P_{3m} will be explained by the following mechanism. At pH 12, P_{3m} is easily attacked by nucleophilic reagents such as amine,[5,17] alcohol,[2] amino acid,[3,4] and nucleoside.[6] In the present study, thus, the lone electron pair on the anomeric hydroxyl group of β-D-aldose nucleophilically attacks a phosphorus atom on P_{3m} to open its six-membered ring. It is noteworthy that the formation of hydrogen bonding between the hydroxyl group at C-2 and the oxygen atom on P_{3m} would make the attack of cyclo-triphosphate easier. No attack of α-D-aldose must be due to the steric hinderance of the *cis* conformation of the hydroxyl groups at C-1 and C-2, or to the 1,3-diaxial interaction[19] between H-3 and the triphosphate group. Table 3 shows the population[20] of each anomer of D-aldose used in this study, as estimated from ^{1}H-NMR. From these results, it is suggested that the main anomer, that is, the energetically stable β-anomer, is selectively phosphorylated. Furthermore, the population of the β-anomer increases in the reaction condition (pH 12), inducing the yields of more than 32%.

No noteworthy difference in the reactivity of the hydroxyl group at C-1 of D-glucose derivatives, that is, CH_2OH, COOH, $CH_2OPO_3H_2$ and H groups at C-5, was observed, although the polarities of these functional groups are different. This is probably because the bond between O-5 and C-1 is not so strong under anomer equilibrium, thus, the effect of these functional groups on the phosphorylation of β-D-aldose is small.

The reactions of D-glucose derivatives substituted at 2-OH with P_{3m} produced their triphosphate derivatives with low yield and poor selectivity. In spite of the *trans* conformation of the hydroxyl group at C-1 and the amino group at C-2 in β-D-glucosamine, its reactivity with P_{3m} is low. P_{3m} is known to react with ammonia,[1,21] alkylamine,[17] 1,6-hexanediamine,[22] and amino acids[3,4] to yield new compounds with a P–N bond in their molecules. In the case of alkylamines, the yields are more than 80%. Furthermore, ^{13}C-NMR showed that **9** decomposes gradually in an alkaline solution. Therefore, the reactivity at 1-OH in **9** is low, with poor stereoselectivity. In the cases of 2-deoxy-β-D-glucose and 2-fluoro-2-deoxy-β-D-glucose, high yields and stereoselectivity are expected because the population of their β-anomers is nearly equal to those of **1**, **2**, **3** and **4** (Table 3). However, 2-deoxy-β-D-glucose and 2-fluoro-2-deoxy-β-D-glucose showed low yield. Although the reason for this is not clear at present, the OH group at C-2 will be essential to obtaining a stereoselective phosphorylated product. The substituent effect in 2-OH in the phosphorylation of D-glucose derivatives with P_{3m} is noteworthy.

In conclusion, the phosphorylation of D-glucose derivatives (**2**—**4**) substituted at 5-CH_2OH with P_{3m} proceeds stereoselectively, with a yield of more than 32%, whereas the phosphorylation of D-glucose derivatives (**9** and **10**) substituted at 2-OH with P_{3m} proceeds with low yield and poor selectivity.

Experimental

Materials and Methods Sodium cyclo-triphosphate (P_{3m}), $Na_3P_3O_9 \cdot 6H_2O$, was prepared as described in a previous paper.[3] 6-Phosphoryl-D-glucose (**3**), D-xylose (**4**), 2-fluoro-2-deoxy-D-glucose (**11**), and sodium 2,2-dimethy-2-silapentane-5-sulfonate (DSS) were purchased from Sigma (St. Louis, U.S.A.). Unless otherwise stated, guaranteed grade reagents from Wako Chemical Industries, Ltd. (Osaka, Japan), were used. ^{13}C-NMR spectra with broad band ^{1}H-decoupling and ^{1}H-NMR spectra were measured with Varian Gemini 300 and 200 spectrometers. Samples were dissolved in D_2O (99.9%) to avoid the effect of ^{1}H in water. DSS was used as an external standard for ^{13}C and ^{1}H-NMR spectra. ^{31}P-NMR spectra with and without broad band ^{1}H-decoupling and ^{31}P–^{1}H 2D HMBC spectra were obtained with a Varian VXR-500 spectrometer. As an external standard, 85% H_3PO_4 was used. HPLC analysis was carried out with a JASCO GULLIVER HPLC system (Tokyo, Japan), coupled with a JASCO DU-4F flow injection system to detect phosphate by a post-column reaction. A column (150×6.0 mm i.d.) packed with a polystyrene-based anion-exchanger (TSK gel, SAX, 5 μm, TOSOH, Japan), was used for the analysis of phosphate. The column temperature was maintained at 40 °C. A convex gradient elution technique using 0.17 and 0.45 mol·dm^{-3} potassium chloride solutions was employed for the analysis of phosphate. Determination of phosphorus was carried out by spectrophotometry of a phosphorus–molybdenum heteropoly blue complex at 830 nm. The flow rate of the eluent was 1.0 ml·min^{-1}.

The Procedure for the Syntheses of β-D-Glucuronic Acid 1-Triphosphate (6), 6-Phosphoryl-β-D-glucose 1-Triphosphate (7), and β-D-Xylose 1-Triphosphate (8) The reaction of D-glucuronic acid (**2**) (1.25—2.5 mol·dm^{-3}) with P_{3m} (0.25 mol·dm^{-3}) was carried out at pH 12 and room temperature. The yields and the structures of the products were determined by HPLC and NMR measurements. Because the reaction was performed under a P_{3m} deficient condition, that is, an aldose rich condition, the yield was calculated based on the amount of P_{3m}. Similar procedures were used for the syntheses of **7** and **8**.

Compounds **6** and **8** were isolated as crystalline barium salts. The reactions of **2** and **4** (2.5 mol·dm^{-3}) with P_{3m} (0.25 mol·dm^{-3}) were carried out at pH 12 and room temperature. After 3 h, the reaction mixture was neutralized using *ca.* 5 mol·dm^{-3} HCl. The addition of 1 mol·dm^{-3} $BaCl_2$ aqueous solution precipitated barium diphosphate, $Ba_2P_2O_7$, which was separated by filtration. When 1 mol·dm^{-3} $BaCl_2$ aqueous solution was added to the filtrate, **6** and **8** precipitated out. They were separated from the solution, then washed with distilled water and ethanol.

β-D-Glucuronic Acid 1-Triphosphate (**6**): ^{1}H-NMR (D_2O) δ: 5.04 (1H, dd, $J_{1,2}$=7.8 Hz, $J_{P_\alpha H\text{-}1}$=8.6 Hz, H-1), 3.39 (1H, dd, $J_{1,2}$=7.8 Hz, $J_{2,3}$=7.5 Hz, H-2), 3.52 (1H, dd, $J_{2,3}$=7.5 Hz, $J_{3,4}$=9.0 Hz, H-3), 3.56 (1H, dd, $J_{3,4}$=9.0 Hz, $J_{4,5}$=9.4 Hz, H-4), 3.79 (1H, d, $J_{4,5}$=9.4 Hz, H-5). ^{13}C-NMR (D_2O) δ: 99.8 (1C, d, $J_{P_\alpha C\text{-}1}$=5.6 Hz, C-1), 75.7 (1C, d, $J_{P_\alpha C\text{-}2}$=8.5 Hz, C-2), 78.2 (1C, s, C-3), 73.9 (1C, s, C-4), 77.4 (1C, s, C-5), 178.1 (1C, s, C-6). ^{31}P-NMR (D_2O) δ: −11.4 (1P, dd, $J_{P_\alpha P_\beta}$=18.2 Hz, $J_{P_\alpha H\text{-}1}$=8.6 Hz, P_α) −20.5 (1P, dd, $J_{P_\alpha P_\beta}$=18.2 Hz, $J_{P_\beta P_\gamma}$=20.8 Hz, P_β), −4.8 (1P, d, $J_{P_\beta P_\gamma}$=20.8 Hz, P_γ).

6-Phosphoryl-β-D-glucose 1-Triphosphate (**7**): ^{1}H-NMR (D_2O) δ: 4.91 (1H, dd, $J_{1,2}$=8.2 Hz, $J_{P_\alpha H\text{-}1}$=8.6 Hz, H-1). ^{13}C-NMR (D_2O) δ: 100.4 (1C, d, $J_{P_\alpha C\text{-}1}$=5.6 Hz, C-1), 76.2 (1C, d, $J_{P_\alpha C\text{-}2}$=7.8 Hz, C-2), 77.0 (1C, s, C-3), 71.2 (1C, s, C-4), 78.3 (1C, s, C-5), 67.0 (1C, s, C-6). ^{31}P-NMR (D_2O) δ: −11.6 (1P, dd, $J_{P_\alpha P_\beta}$=17.7 Hz, $J_{P_\alpha H\text{-}1}$=8.6 Hz, P_α) −20.0 (1P, dd, $J_{P_\alpha P_\beta}$=17.7 Hz, $J_{P_\beta P_\gamma}$=19.4 Hz, P_β), −4.7 (1P, d, $J_{P_\beta P_\gamma}$=19.4 Hz, P_γ).

β-D-Xylose 1-Triphosphate (**8**): ^{1}H-NMR (D_2O) δ: 4.85 (1H, dd, $J_{1,2}$=7.5 Hz, $J_{P_\alpha H\text{-}1}$=8.6 Hz, H-1), 3.23 (1H, dd, $J_{1,2}$=7.5 Hz, $J_{2,3}$=9.0 Hz, H-2), 3.37 (1H, dd, $J_{2,3}$=9.0 Hz, $J_{3,4}$=9.0 Hz, H-3), 3.50 (1H, ddd, $J_{3,4}$=9.0 Hz, $J_{4,5}$=5.3 Hz, $J_{4,5'}$=10.2 Hz, H-4), 3.84 (1H, dd, $J_{4,5}$=5.3 Hz, $J_{5,5'}$=11.5 Hz, H-5), 3.25 (1H, dd, $J_{4,5'}$=10.2 Hz, $J_{5,5'}$=11.5 Hz, H-5′). ^{13}C-NMR (D_2O) δ: 100.9 (1C, d, $J_{P_\alpha C\text{-}1}$=5.9 Hz, C-1), 75.8 (1C, d, $J_{P_\alpha C\text{-}2}$=8.2 Hz, C-2), 77.6 (1C, s, C-3), 71.5 (1C, s, C-4), 68.0 (1C, s, C-5). ^{31}P-NMR (D_2O) δ: −11.7 (1P, dd, $J_{P_\alpha P_\beta}$=17.7 Hz, $J_{P_\alpha H\text{-}1}$=8.6 Hz, P_α) −19.9 (1P, dd, $J_{P_\alpha P_\beta}$=17.7 Hz, $J_{P_\beta P_\gamma}$=19.0 Hz, P_β), −4.6 (1P, d, $J_{P_\beta P_\gamma}$=19.0 Hz, P_γ).

The Procedure for the Syntheses of β-D-Glucosamine 1-Triphosphate

(12), β-D-Glucosamine 2-Triphosphate (13), and 2-Deoxy-β-D-glucose 1-Triphosphate (14) The reaction of D-glucosamine (1.25—1.75 mol·dm^{-3}) with P_{3m} (0.25 mol·dm^{-3}) was carried out at pH 12 and room temperature. The yields and structures of the products were determined by the above mentioned procedures. The separation of **12** from the reaction mixture was accomplished by anion-exchange chromatography with a 2×80 cm column filled with Dowex 1-X2 resin (100—200 mesh, chloride form). Elution was carried out with 0.3 mol·dm^{-3} KCl aqueous solution, and each 100 ml fraction was measured by HPLC. The solution fractionated was concentrated at −113 °C *in vacuo* (freeze-drying). An aliquot of the obtained product was dissolved in D_2O for HPLC, and ^{1}H-, ^{13}C- and ^{31}P-NMR measurements. In the case of **13** and **14**, the isolation could not be performed because of low yield.

β-D-Glucosamine 1-Triphosphate (**12**): ^{1}H-NMR (D_2O) δ: 5.27 (1H, dd, $J_{1,2}$=8.5 Hz, $J_{P_\alpha H\text{-}1}$=8.5 Hz, H-1), 3.09 (1H, dd, $J_{1,2}$=8.5 Hz, $J_{2,3}$=11.0 Hz, H-2), 3.67 (1H, dd, $J_{2,3}$=11.0 Hz, $J_{3,4}$=9.5 Hz, H-3), 3.39 (1H, dd, $J_{3,4}$=9.5 Hz, $J_{4,5}$=9.5 Hz, H-4), 3.53 (1H, ddd, $J_{4,5}$=9.5 Hz, $J_{5,6}$=2.0 Hz, $J_{5,6'}$=6.0 Hz, H-5), 3.82 (1H, dd, $J_{5,6}$=2.0 Hz, $J_{6,6'}$=11.5 Hz, H-6), 3.64 (1H, dd, $J_{5,6'}$=6.0 Hz, $J_{6,6'}$=11.5 Hz, H-6′). ^{13}C-NMR (D_2O) δ: 96.7 (1C, d, $J_{P_\alpha C\text{-}1}$=5.2 Hz, C-1), 58.6 (1C, d, $J_{P_\alpha C\text{-}2}$=9.1 Hz, C-2), 74.0 (1C, s, C-3), 71.8 (1C, s, C-4), 79.3 (1C, s, C-5), 63.0 (1C, s, C-6). ^{31}P-NMR (D_2O) δ: −11.3 (1P, dd, $J_{P_\alpha P_\beta}$=17.1 Hz, $J_{P_\alpha H\text{-}1}$=8.5 Hz, P_α) −19.7 (1P, dd, $J_{P_\alpha P_\beta}$=17.1 Hz, $J_{P_\beta P_\gamma}$=18.4 Hz, P_β), −4.1 (1P, d, $J_{P_\beta P_\gamma}$=18.4 Hz, P_γ).

β-D-Glucosamine 2-Triphosphate (**13**): ^{1}H-NMR (D_2O) δ: 5.27 (1H, d, $J_{1,2}$=8.6 Hz, H-1). ^{31}P-NMR (D_2O) δ: 0.62 (1P, d, $J_{P_\alpha P_\beta}$=19.0 Hz, P_α), −19.6 (1P, dd, $J_{P_\alpha P_\beta}$=19.0 Hz, $J_{P_\beta P_\gamma}$=17.2 Hz, P_β), −4.2 (1P, d, $J_{P_\beta P_\gamma}$=17.2 Hz, P_γ).

2-Deoxy-β-D-glucose 1-Triphosphate (**14**): ^{1}H-NMR (D_2O) δ: 5.25 (H-1). ^{31}P-NMR (D_2O) δ: −12.4 (1P, dd, $J_{P_\alpha P_\beta}$=17.6 Hz, $J_{P_\alpha H\text{-}1}$=8.0 Hz, P_α), −20.2 (1P, dd, $J_{P_\alpha P_\beta}$=17.6 Hz, $J_{P_\beta P_\gamma}$=18.8 Hz, P_β), −4.5 (1P, d, $J_{P_\beta P_\gamma}$=18.8 Hz, P_γ).

Acknowledgements The authors thank assistant professor M. Sugiura of Kobe Pharmaceutical University for the measurements of ^{31}P- and ^{31}P–^{1}H 2D (HMBC) NMR spectra. This work was partly supported by the Science Research Promotion Fund from the Japan Private School Promotion Foundation.

References

1) Feldmann W., *Z. Chem.*, **5**, 26—27 (1965).
2) Feldmann W., *Chem. Ber.*, **100**, 3850—3860 (1967).
3) Tsuhako M., Fujita N., Nakahama A., Matsuo T., Kobayashi M., Ohashi S., *Bull. Chem. Soc. Jpn.*, **53**, 1968—1972 (1980).
4) Inoue H., Baba Y., Furukawa T., Maeda Y., Tsuhako M., *Chem. Pharm. Bull.*, **41**, 1895—1899 (1993).
5) Tsuhako M., Nakahama A., Ohashi S., Nariai H., Motooka I., *Bull. Chem. Soc. Jpn.*, **56**, 1372—1377 (1983).
6) Tsuhako M., Fujimoto M., Ohashi S., Nariai H., Motooka I., *Bull. Chem. Soc. Jpn.*, **57**, 3274—3280 (1984).
7) Tsuhako M., Sueyoshi C., Baba Y., Miyajima T., Ohashi S., Nariai H., Motooka I., *Chem. Lett.*, **1987**, 1431—1434.
8) Inoue H., Watanabe M., Nakayama H., Tsuhako M., *Chem. Pharm. Bull.*, **46**, 681—683 (1998).
9) Inoue H., Baba Y., Miyajima T., Tsuhako M., *Chem. Pharm. Bull.*, **40**, 3127—3132 (1992).
10) Inoue H., Baba Y., Tsuhako M., *Chem. Pharm. Bull.*, **43**, 677—678 (1995).
11) Cohn M., Hughes T. R., *J. Biol. Chem.*, **235**, 3250—3253 (1960).
12) O'Connor J. V., Nunez H. A., Baker R., *Biochemistry*, **18**, 500—507 (1979).
13) Jaques L. W., Macaskill J. B., Weltner W., *J. Phys. Chem.*, **83**, 1412—1421 (1979).
14) Bock K., Thogenson H., *Ann. Rep. NMR Spect.*, **13**, 1—57 (1982).
15) Benesi A. J., Falzone C. J., Benerjee S., Farber G. K., *Carbohydr. Res.*, **258**, 27—33 (1994).
16) Bunel S., Ibarra C., Moraga E., Blasko A., Bunton C. A., *Carbohydr. Res.*, **244**, 1—14 (1993).
17) Feldmann W., Thilo E., *Z. Anorg. Allg. Chem.*, **327**, 159—164 (1964).
18) Tsuhako M., Sueyoshi C., Miyajima T., Ohashi S., Nariai H., Motooka I., *Bull. Chem. Soc. Jpn.*, **59**, 3091—3095 (1986).
19) David S., "The Molecular and Supramolecular Chemistry of Carbohydrates," Oxford University Press, Oxford, 1997, p. 12.
20) Angyal S. J., *Adv. Carbohydr. Chem. Biochem.*, **42**, 15—68 (1984).
21) Quimby O. T., Flautt T. J., *Z. Anorg. Allg. Chem.*, **296**, 220—228 (1958).
22) Dombrovskii N. M., Dorosh A. I., *Russ. J. Inorg. Chem.*, **17**, 981—984 (1972).

Study of Synthesis and Cardiovascular Activity of Some Furoxan Derivatives as Potential NO-Donors

Li Mu,[a,b] Si-shen Feng,*[,a,c] and Mei Lin Go[d]

Department of Chemical and Environmental Engineering,[a] National University of Singapore, 10 Kent Ridge Crescent, Singapore 119260, Division of Medicinal Chemistry, China Pharmaceutical University,[b] Tongjiaxiang 24#, Nanjing 210009, P. R. China, Institute of Materials Research and Engineering (IMRE),[c] 3 Research Link, Singapore 117602, and Department of Pharmacy, National University of Singapore,[d] 10 Kent Ridge Crescent, Singapore 119260.
Received December 10, 1999; accepted February 28, 2000

A series of hybrid molecules incorporating the furoxan and nicorandil moieties were designed as potential NO donors with cardiovascular and cerebrovascular activities. Thirty-six target molecules were successfully synthesized by conventional methods and characterized by infrared spectroscopy, ^{1}H-NMR spectroscopy and high resolution mass spectra. The compounds were tested for their effects on KCl-induced contraction of rabbit thoracic aorta whose endothelium was denuded. Eight compounds were found to reduce KCl-induced contraction by more than 30% at 10 μM. All except one of these compounds are characterized by the presence of electron withdrawing groups in the phenyl ring attached *via* an amide or ester linkage to the furoxan moiety. The nature of the terminal carbonyl linkage (ester or amide) and the length or type of the alkyl chain bridging the two carbonyl functions have little effect on the activity. One of the active compounds, *N*-(4-methoxy-benzoyl)-*N'*-[3-methylfuroxanyl-4-carbonyl)piperazine (17i) was tested for hypotensive effects on anaesthesized rats at 1.5 mg/kg, and found to demonstrate a gradual and sustained hypotensive effect. The results suggest that the furoxan-nicorandil derivatives are a useful lead in the design of NO-donor compounds for hypertension.

Key words furoxan derivatives; vasodilation; nitric oxide; NO-donor; synthesis; hypertension

Nitric oxide (NO) is an important messenger involved in many pathological and physiological processes which occur in the mammalian body. It has been shown to play a key role in neurotransmission, control of blood pressure and cellular defence mechanisms.[1] The increasing awareness of the involvement of NO in numerous bioregulatory pathways has also opened up new therapeutic avenues for organic nitrates and NO donors, and underscored the importance of such compounds in mimicking an endogenous NO-related response or substituting for an endogenous NO deficiency.[2] A variety of acute and chronic circulatory diseases are known which are associated with a marked degree of endothelial dysfunction and characterized by a significant attenuation of endothelial derived NO.[3,4] An emerging therapeutic strategy is to administer physiological amounts of NO in the bloodstream or at the site of the local tissue and injured cells in order to improve diminished supplies of NO for the maintenance of cardiovascular homeostasis. The furoxan ring system (1,2,5-oxadiazole-2-oxide, furazan oxide) has been widely used as an intermediate for the synthesis of various heterocyclic compounds,[5] owing to its mysterious structure or intricate chemistry. It has been reported to possess a wide spectrum of pharmacological activities, including vasodilatory activity.[6—12] Studies have shown that furoxan derivatives are NO donors,[10—16] which generate NO or related *N*-oxide species in a controlled manner. These findings have prompted the inclusion of the furoxan ring in the design of NO releasing drugs. The furoxan derivatives CAS 1609 and CHF 2206 are notable examples of furoxan derivatives which have demonstrated the success of such an approach (Fig. 1). They exert vasodilating activity with a pharmacological potency suggestive of NO donating pro-drugs (so-called NO donors).[3,16] CHF 2206 (3-phenylsulfonyl-4-phenylfuroxan) was able to inhibit rabbit aortic ring contraction induced by norepinephrine and KCl, and the activity was independent of endothelium integrity. CAS 1609 (2-hydroxymethyl-furoxan-3-carboxamide) relaxed both potassium-depolarized and phenylephrine-contracted guinea pig vessel strips in a concentration-dependent manner.

The combination of a nitrate moiety with another pharmacologically active substructure in a single molecule has recently received particular attention.[2,17,18] Nicorandil is an antianginal drug, which shares properties of K^+ channel openers and NO donors. It causes vascular smooth muscle relaxation *via* two main mechanisms: increasing membrane K^+ conductance through the opening of ATP-dependent K^+ channels leading to hyperpolarization and releasing NO elevating cyclic GMP levels by stimulating soluble guanylate cyclase.[17] Nicorandil may be the prototype of the hybrid drugs with K^+ channel opening properties mixed with NO-dependent vasodilating activities. Structurally, it is a nicotinamide derivative with a nitrate group in its chemical structure (Fig. 1). The O–NO_2 moiety is responsible for the group's action as nitrates and also influences their potency as K^+-chan-

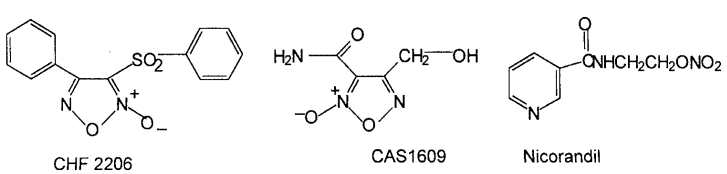

CHF 2206 CAS1609 Nicorandil

Fig. 1. Structures of CHF 2206, CAS 1609 and Nicorandil

* To whom correspondence should be addressed. e-mail: chefss@nus.edu.sg

© 2000 Pharmaceutical Society of Japan

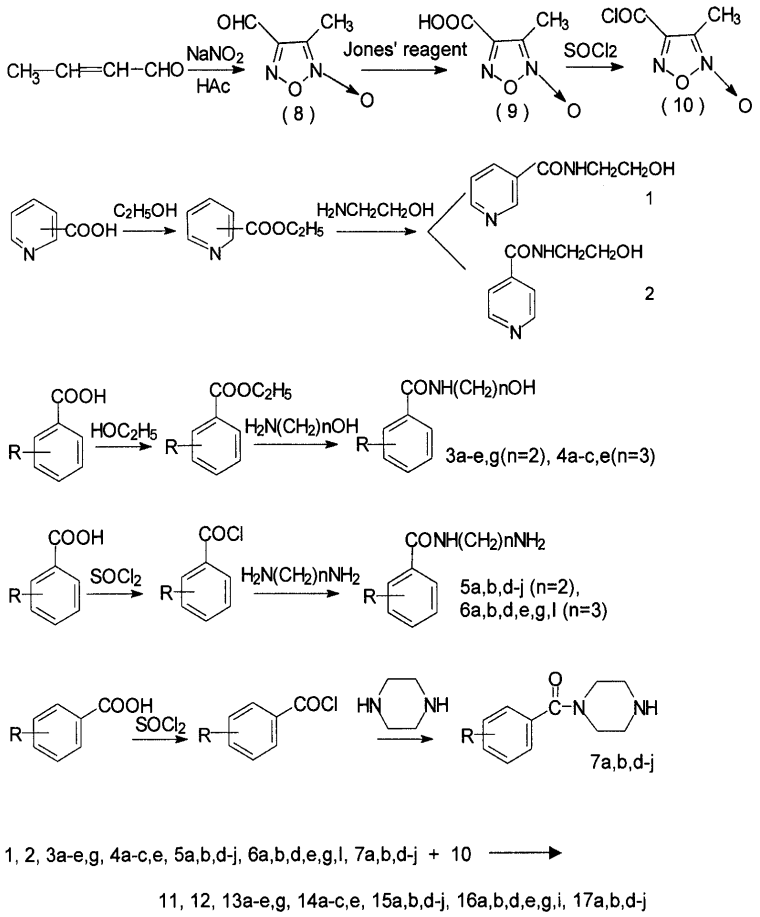

Chart 1

nel activators.

The synthesizing of hybrid molecules of furoxan and nicorandil derivatives may prove to be a useful approach in moderating the NO releasing properties,[18,19] so as to achieve an ideal cardiovascular drug with good selectivity, efficiency, acceptable duration of action and low toxicity.

Based on this idea, we synthesized in the present paper a series of "hybrid" drugs designed by linking the furoxan ring to nicorandil analogues and investigated their NO donating properties. The compounds are evaluated for their ability to inhibit KCl-induced contraction of rabbit aortic strips which have been denuded of endothelium. Eight compounds were identified to possess good vasodilatory activity and one of them was further tested for its hypotensive effects in anaesthesized rats. This compound was found able to significantly reduce blood pressure 3 h after administration. Its hypotensive effects can prevail for a further 3 h. The results indicate that the present approach of molecular hybridization is a viable step in designing active NO releasing compounds.

Results and Discussion

Chemistry The furoxan-nicorandil derivatives were synthesized according to the pathways shown in Chart 1. 3-Methylfuroxan-4-carbaldehyde (**8**) was synthesized from the reaction of dinitrogen trioxide (generated from sodium nitrite and acetic acid) on crotonaldehyde.[19,20] The aldehyde was oxidized to the acid (3-methylfuroxan-4-carboxylic acid (**9**) using Jones' reagent, and the resulting acid was converted to the reactive acid chloride using thionyl chloride. The acid

Table 1. Chemical Structures of Synthesized Furoxan Derivatives **11**—**17**

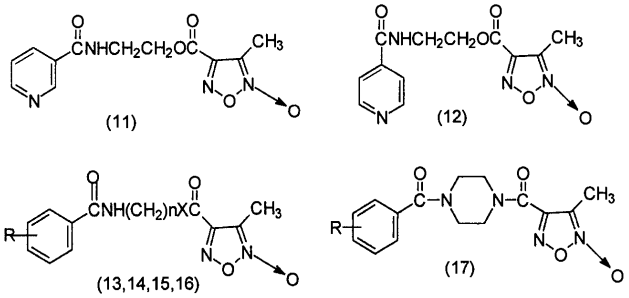

Compounds					R
X=O		X=NH			
13 (n=2)	**14** (n=3)	**15** (n=2)	**16** (n=3)	**17**	
13a	**14a**	**15a**	**16a**	**17a**	3-NO_2
13b	**14b**	**15b**	**16b**	**17b**	4-NO_2
13c	**14c**				3,4-di-NO_2
13d		**15d**	**16d**	**17d**	3-Cl
13e	**14e**	**15e**	**16e**	**17e**	4-Cl
		15f		**17f**	3-Br
13g		**15g**	**16g**	**17g**	4-Br
		15h		**17h**	3-OCH_3
		15i	**16i**	**17i**	4-OCH_3
		15j		**17j**	H

Table 2. Physical Data of Synthesized Compounds

Compound	Yield (%)	mp (°C)	IR (cm^{-1})	^{1}H-NMR (δ ppm)	HR-MS
11	54.5	112—114	3250, 3060 (N-H); 1730, 1650 (C=O); 1100 (O=C−O)	8.98 (d,1H, pyridine-C_2H), 8.75—8.66 (s+dd, 2H, pyridine-C_6-H, CONH), 8.23—8.09 (tt, 1H, pyridine-C_4-H), 7.56—7.34 (q, 1H, pyridine-C_5-H), 4.61—4.48 (t, 2H, CH_2OCO), 3.79—3.60 (q, 2H, $NHCH_2$), 2.26 (S, 3H, CH_3)	Formula $C_{12}H_{12}N_4O_5$ $(M+H)^+$ Calcd 293.088047. Found 293.089550. MS (SCI, *m/z*):293 (MH^+, base peak), 149 ($C_5H_4NCONHCH_2CH_2^+$), 121 ($C_5H_4NCONH^+$)
12	50.5	168—170	3200, 3050 (N-H); 1750, 1650 (C=O); 1100 (O=C−O)	8.85 (s, 1H, CONH), 8.37—8.67 (dd, 2H, pyridine-C_2,C_6-2H), 7.79—7.72 (dd, 2H, pyridine-C_3, C_5-2H), 4.60—4.54 (t, 2H, CH_2OCO), 3.80—3.70 (q, 2H, $NHCH_2$), 2.31 (s, 3H, CH_3)	Formula $C_{12}H_{12}N_4O_5$ $(M+H)^+$ Calcd 293.088047. Found 293.088075. MS (SCI, *m/z*): 293 (MH^+, base peak), 214 ($CONHCH_2CH_2$−Furoxan), 149 ($C_5H_4NCONHCH_2CH_2^+$)
13a	33.2	112—114	3260, 3100 (N-H); 1730, 1640 (C=O); 1120 (O=C−O)	8.95 (s, br, 1H, CONH), 8.789—8.748 (t, 1H, ArH), 8.392—8.253 (m, 2H, ArH), 7.768—7.680 (q, 1H, ArH), 4.681—4.558 (t, 2H, CH_2OCO), 3.825—3.762 (m, 2H, N-CH_2C), 2.332 (s, 3H, CH_3)	Formula $C_{13}H_{12}N_4O_7$ $(M+H)^+$ Calcd 337.077877. Found 337.079630. MS (SCI, *m/z*): 337 (MH^+), 193 ($C_6H_4NO_2CONHCH_2CH_2^+$) 176 ($C_6H_4NO_2CONHCH_2CH^+$), 150 (C_6H_4-NO_2CO^+), 89 ($C_6H_5Cl^+$)
13b	36.6	122—124	3300, 3100 (N-H); 1730, 1630 (C=O); 1100 (O=C−O)	8.321—7.996 (m, 4H, ArH), 4.640 (t, 2H, CH_2OCO), 3.95—3.75 (m, 2H, NCH_2C), 2.362 (s, 3H, CH_3)	Formula $C_{13}H_{12}N_4O_7$ $(M+H)^+$ Calcd 337.077877. Found 337.079630. MS (SCI, *m/z*): 193 ($C_6H_4NO_2NHCH_2CH_2^+$), 176 ($C_6H_4NO_2$-$CONHCH_2CH^+$).
13c	30.6	172—174	3300, 3100 (N-H); 1740, 1650 (C=O); 1100 (O=C−O)	9.35 (br, 1H, CONH), 9.160—9.043 (m, 3H, ArH), 4.626—4.563 (t, 2H, CH_2OCO), 3.836—3.779 (q, 2H, NCH_2C), 2.326 (s, 3H, CH_3)	Formula $C_{13}H_{11}N_5O$ $(M+H)^+$ Calcd 382.062956. Found 382.061212. MS (SCI, *m/z*): 382 (MH^+), 238 (base peak, $C_6H_3N_2O_4CO$ $NHCH_2$–CH_2^+), 193 ($C_6H_4NO_2$ $CONHCH_2$-CH_2^+)
13d	20.2	96—98	3250, 3080 (N-H); 1730, 1630 (C=O); 1100 (O=C−O)	8.60 (br, 1H, CONH), 7.877—7.789 (m, 2H, ArH), 7.462—7.370 (m, 2H, ArH), 4.648—4.525 (t, 2H, CH_2OCO), 3.779—3.719 (m, 2H, NCH_2C), 2.324 (s, 3H, CH_3)	Formula $C_{13}H_{12}N_3O_5Cl$ $(M+H)^+$ Calcd 326.053825. Found 326.056041. MS (SCI, *m/z*): 326 (MH^+), 214 ($CONHCH_2CH_2$Furoxan$^+$), 182 (base peak, $C_6H_4ClCONHCH_2CH_2^+$), 139 ($C_6H_4ClCO^+$), 89 ($C_6H_5CO^+$)
13e	23.9	152—154	3400, 3100 (N-H); 1730, 1640 (C=O); 1100 (O=C-O)	8.50 (br, 1H, CONH), 7.887—7.792 (m, 2H, ArH), 7.438—7.343 (m, 2H, ArH), 4.642—4.520 (t, 2H, CH_2COC), 3.776—3.716 (m, 2H, NCH_2), 2.310 (s, 3H, CH_3)	Formula $C_{13}H_{12}N_3O_5Cl$ $(M+H)^+$ Calcd 326.053825. Found 326.053883. MS (SCI, *m/z*): 326 (MH^+), 182 (base peak, $C_6H_4ClCONH$-$CH_2CH_2^+$), 139 (C_6H_4Cl CO^+)
13g	22.6	160—162	3400, 3080 (N-H); 1740, 1650 (C=O); 1100 (O=C−O)	8.50 (br, 1H, CONH), 7.817—7.490 (m, 4H, ArH), 4.651—4.528 (t, 2H, CH_2COC), 3.787—3.727 (m, 2H, NCH_2), 2.318 (s, 3H, CH_3)	Formula $C_{13}H_{12}N_3O_5Br$ $(M+H)^+$ Calcd 370.003309. Found 370.002949. MS (SCI, *m/z*): 370 (MH^+), 226 (base peak, $C_6H_4BrCONH$-$CH_2CH_2^+$), 183 ($C_6H_4BrCO^+$)
14a	19.9	114—116	3300, 3080 (N-H); 1730, 1640 (C=O); 1100 (O=C−O)	8.781—8.759 (t, 1H, ArH), 8.60 (br, 1H, CONH), 8.351—8.247 (m, 2H, ArH), 7.727—7.588 (q, 1H, ArH), 4.601—4.463 (t, 2H, CH_2O), 3.610—3.547 (m, 2H, NCH_2C), 2.373 (s, 3H, CH_3), 2.212—2.070 (q, 2H, CCH_2C).	Formula $C_{14}H_{14}N_4O_7$ $(M+H)^+$ Calcd 351.093527. Found 351.094320. MS (SCI, *m/z*): 351 (MH^+), 207 (base peak, $C_6H_4NO_2CONH$ $(CH_2)_3^+$), 150 ($C_6H_4NO_2$ CO^+)
14b	22.6	106—108	3300 (N-H); 1730, 1640 (C=O); 1100 (C=O)	8.318—7.966 (m, 4H, ArH), 4.498 (t, 2H, CH_2OCO), 3.50 (m, 2H, NCH_2), 2.343 (s, 3H, CH_3), 2.05 (t, 2H, CCH_2C)	Formula $C_{14}H_{14}N_4O_7$ $(M+H)^+$ Calcd 351.093527. Found 351.093360. MS (SCI, *m/z*): 351 (MH^+), 207 (base peak, $C_6H_4NO_2CONH$ $(CH_2)_3^+$), 150 ($C_6H_4NO_2$ CO^+)
14c	20.5	114—116	3380, 3080 (N-H); 1740, 1640 (C=O); 1100 (O=C−O)	9.233—9.075 (m, 3H, ArH), 4.618—4.479 (t, 2H, CH_2OCO), 3.659—3.593 (m, 2H, NCH_2), 2.247—2.103 (t, 2H, CCH_2C)	Formula $C_{14}H_{13}N_5O_9$ $(M+H)^+$ Calcd 396.078606. Found 396.079600. MS (SCI, *m/z*): 396 (MH^+), 252 (base peak, $C_6H_3N_2O_4CO$-$NH(CH_2)_3^+$), 195 ($C_6H_3N_2O_4CO^+$)
14e	18.8	108—110	3400, 3100 (N-H); 1730, 1640 (C=O); 1100 (O=C−O)	8.60 (br, 1H, CONH), 7.886—7.464 (m, 4H, ArH), 3.359—3.234 (m, 4H, NCH_2, CH_2N), 2.253 (s, 3H, CH_3), 1.866—1.713 (m, 2H, CCH_2C)	Formula $C_{14}H_{14}N_3O_5Cl$ $(M+H)^+$ Calcd 340.078825; Found 340.078883. MS (SCI, *m/z*): 340 (MH^+), 196 (base peak, $C_6H_4ClCONH$-$(CH_2)_3^+$), 139 (C_6H_4Cl CO^+)

Table 2. (Continued)

Compound	Yield (%)	mp (°C)	IR (cm^{-1})	^{1}H-NMR (δ ppm)	HR-MS
15a	20.6	190	3300, 3100 (N-H); 1660, 1640 (C=O)	8.787—8.743 (t, 1H, ArH), 8.381—8.247 (m, 2H, ArH), 7.740—7.566 (q, 1H, ArH), 3.642 (br, 4H, NCH_2–CH_2N), 2.359 (s, 3H, CH_3)	Formula $C_{13}H_{13}N_5O_6$ $(M+H)^+$ Calcd 336.093861. Found 336.095230. MS (SCI, *m/z*): 336 (MH^+, base peak), 318 ($MH+H_2O$), 236 ($C_6H_4NO_2$ $CONHCH_2CH_2NH$ CO^+), 170 (CH_2CH_2–Furoxan$^+$)
15b	23.3	154—155	3300 (N-H); 1670, 1630 (C=O)	8.70 (br, 1H, CONH), 8.45 (br, 1H,CONH), 8.299—8.010 (m, 4H, ArH), 3.642 (br, 4H, NCH_2CH_2N), 2.356 (s, 3H, CH_3)	Formula $C_{13}H_{13}N_5O_6$ $(M+H)^+$ Calcd 336.093861. Found 336.095859. MS (SCI, *m/z*): 336 (MH^+, base peak), 318 (MH^+H_2O), 236 ($C_6H_4NO_2CONC(CH_2)_2NHCO^+$), 170 ($CH_2$-$CH_2$–Furoxan), 150 ($C_6H_4NO_2CO^+$), 104 ($C_6H_4CO^+$)
15d	17.5	154—156	3300, 3060 (N-H); 1670, 1630 (C=O)	8.75 (br, m, CONH), 8.25 (br, 1H, CONH), 7.868—7.729 (m, 2H, ArH), 7.449—7.356 (m, 2H, ArH), 3.599—3.572 (br, 4H, NCH_2CH_2N), 2.340 (s, 3H, CH_3)	Formula $C_{13}H_{13}N_4O_4Cl$ $(M+H)^+$ Calcd 325.069809. Found 325.071878. MS (SCI, *m/z*): 325 (MH^+), 307 (MH^+H_2O), 170 (CH_2CH_2–Furoxan$^+$), 139 (base peak, $C_6H_4ClCO^+$), 111 ($C_6H_4Cl^+$)
15e	24.5	122—124	3350 (N-H); 1670, 1630 (C=O)	8.55 (br, 1H, CONH), 8.00 (br, 1H, CONH), 7.857—7.759 (m, 2H, ArH), 7.416—7.318 (m, 2H, ArH), 3.612 (br, 4H, NCH_2–CH_2N), 2.348 (s,3H,CH_3)	Formula $C_{13}H_{13}N_4O_4Cl$ $(M+H)^+$ Calcd 325.069809. Found 325.071709. MS (SCI, *m/z*): 325 (MH^+), 307 ($MH+H_2O$), 139 (base peak, $C_6H_4ClCO^+$), 111 ($C_6H_4Cl^+$)
15f	15.7	162—168	3300 (N-H); 1670, 1630 (C=O)	8.85 (br, 1H, CONH), 8.35 (br, 1H, CONH), 8.018—7.318 (m, 4H, ArH), 3.640 (br, 4H, NCH_2CH_2N), 2.351 (s, 3H, CH_3)	Formula $C_{13}H_{13}N_4O_4Br$ $(M+H)^+$ Calcd 369.019293. Found 369.020400. MS (SCI, *m/z*): 369 (MH^+), 351 (MH^+H_2O), 183 (base peak, $C_6H_4ClCO^+$), 170 (CH_2CH_2–Furoxan$^+$), 155 ($C_6H_4Br^+$)
15g	20.5	196—198	3350 (N-H); 1670 (C=O)	8.70 (br, 1H, CONH), 7.795—7.468 (m, 4H, ArH), 3.569 (br, 4H, NCH_2–CH_2N), 2.343 (s, 3H, CH_3).	Formula $C_{13}H_{13}N_4O_4Br$ $(M+H)^+$ Calcd 369.019293. Found 369.020727. MS (SCI, *m/z*): 369 (MH^+), 183 (base peak, $C_6H_4BrCO^+$), 170 (CH_2CH_2–Furoxan$^+$), 155 ($C_6H_4Br^+$)
15h	14.5	106—108	3300 (N-H), 1670, 1630 (C=O)	8.65 (br, 1H, CONH), 8.15 (br, 1H, CONH), 7.85—6.95 (m, 4H, ArH), 3.836 (s, 3H, OCH_3), 3.659—3.612 (br, 4H, NCH_2–CH_2N), 2.356 (s, 3H, CH_3)	Formula $C_{14}H_{16}N_4O_5$ $(M+H)^+$ Calcd 321.119347. Found 321.121080. MS (SCI, *m/z*): 321 (MH^+), 303 ($MH+H_2O$), 170 (CH_2CH_2–Furoxan$^+$), 151 ($C_6H_4OCH_3C^+$), 135 (base peak, $C_6H_4OCH_3$ CO^+), 107 ($C_6H_4OCH_3^+$)
15i	23.6	128—130	3300 (N-H); 1660, 1630 (C=O)	7.789—7.691 (m, 2H, ArH), 6.958—6.858 (m, 2H, ArH), 3.844 (s, 3H, OCH_3), 3.716—3.681 (br, 4H, NCH_2CH_2N), 2.365 (s, 3H, CH_3)	Formula $C_{14}H_{16}N_4O_5$ $(M+H)^+$ Calcd 321.119347. Found 321.117630. MS (SCI, *m/z*): 321 (MH^+), 303 ($MH+H_2O$), 170 (CH_2CH_2–Furoxan$^+$), 151 ($C_6H_4OCH_3C^+$), 135 (base peak, $C_6H_4OCH_3CO^+$), 107 ($C_6H_4OCH_3^+$)
15j	13.6	164—166	3400, 3310 (N-H); 1670, 1640 (C=O)	8.72 (br, 1H, CONH), 8.06 (br, 1H, CONH), 7.896—7.381 (m, 5H, ArH), 3.629—3.615 (br, 4H, CH_2CH_2), 2.348 (s, 3H, CH_3)	Formula $C_{13}H_{14}N_4O_4$ $(M+H)^+$ Calcd 291.08782. Found 291.08510. MS (SCI, *m/z*): 291(MH^+), 273 (MH^+H_2O), 170 (CH_2CH_2–Furoxan$^+$), 134 (C_6H_5CONH CH_2^+), 105 (base peak, C_6H_5 CO^+), 77 ($C_6H_5^+$)
16a	18.6	152—154	3360, 3320 (N-H); 1670, 1640 (C=O)	8.784 (t, 1H, ArH), 8.394—8.280 (q, 2H, ArH), 7.739—7.550 (t,1H,ArH), 3.501 (br, 4H, NCH_2CH_2N), 2.397 (s, 3H, CH_3), 1.95—1.85 (m, 2H, CCH_2C)	Formula $C_{14}H_{15}N_5O_6$ $(M+H)^+$ Calcd 350.109511. Found 350.108110. MS (SCI, *m/z*): 350 (MH^+), 332 (MH^+H_2O), 250 ($C_6H_4NO_2$ $CONH(CH_2)_3NHCO^+$), 150 (base peak, $C_6H_4NO_2CO^+$), 104 ($C_6H_4CO^+$), 76 ($C_6H_4^+$)
16b	21.8	156—158	3350 (N-H); 1660, 1620 (C=O)	8.386—8.288 (m, 2H, ArH), 8.013—7.912 (m, 2H, ArH), 4.280—4.117 (t, 2H, CH_2H), 3.610—3.495 (q, 2H, NCH_2), 2.320 (s, 3H, CH_3), 2.182 (m, 2H, CCH_2C)	Formula $C_{14}H_{15}N_5O_6$ $(M+H)^+$ Calcd 336.109511. Found 350.108410. MS (SCI, *m/z*): 350 (MH^+), 250 ($C_6H_4NO_2CONC$ ($(CH_2)_3$-$NHCO^+$), 207 (C_6H_4CONH-$(CH_2)_3^+$), 184 $(CH_2)_3$–Furoxan$^+$), 150 (base peak, $C_6H_4NO_2CO^+$), 104 ($C_6H_4CO^+$), 76 ($C_6H_4^+$)

Table 2. (Continued)

Compound	Yield (%)	mp (°C)	IR (cm^{-1})	^{1}H-NMR (δ ppm)	HR-MS
16d	19.6	154—156	3360, 3260 (N-H); 1670, 1630 (C=O)	8.95 (br, 1H, CONH), 8.45 (br, 1H, CONH), 7.896—7.454 (m, 4H, ArH), 3.359—3.234 (m, 4H, NCH_2, CH_2N), 2.253 (s, 3H, CH_3), 1.866—1.713 (m, 2H, CCH_2C)	Formula $C_{14}H_{15}N_4O_4Cl$ $(M+H)^+$ Calcd 339.094809. Found 339.096818. MS (SCI, *m/z*): 339 (MH^+), 321 ($MH+H_2O$), 184 ($(CH_2)_3$–Furoxan$^+$), 139 (base peak, $C_6H_4ClCO^+$), 111 ($C_6H_4Cl^+$)
16e	24.5	166—168	3400, 3270 (N-H); 1670, 1640 (C=O)	8.95 (br, 1H, CONH), 8.45 (br, 1H, CONH), 7.896—7.454 (m, 4H, ArH), 3.359—3.234 (m, 4H, NCH_2CH_2N), 2.253 (s, 3H, CH_3), 1.866—1.713 (m, 2H, CCH_2C)	Formula $C_{14}H_{15}N_4O_4Cl$ $(M+H)^+$ Calcd 339.094809. Found 339.096709. MS (SCI, *m/z*): 339 (MH^+), 321 (MH^+H_2O), 139 (base peak, $C_6H_4ClCO^+$), 111 ($C_6H_4Cl^+$)
16g	21.5	188—190	3400, 3260 (N-H); 1670, 1640 (C=O)	8.95 (br, 1H, CONH), 8.45 (br, 1H, CONH), 7.844—7.533 (m, 4H, ArH), 3.343 (m, 4H, NCH_2, CH_2N), 2.302 (s, 3H, CH_3), 1.822 (m, 2H, CCH_2C)	Formula $C_{14}H_{15}N_4O_4Br$ $(M+H)^+$ Calcd 383.034943. Found 383.033280. MS (SCI, *m/z*): 383 (MH^+), 365 (MH^+H_2O), 256 ($C_6H_4BrCONHCH(CH_2)_3NHCO^+$), 187 ($(CH_2)_3$–Furoxan$^+$), 183 (base peak, $C_6H_4BrCO^+$), 155 ($C_6H_4Br^+$)
16i	11.5	140—142	3400, 3240 (N-H); 1670, 1630 (C=O)	8.94 (br,1H,CONH), 8.14 (br, 1H, CONH), 7.868—7.773 (m, 2H, ArH), 6.964—6.866 (m, 2H, ArH), 3.833 (s, 3H, OCH_3), 3.457—3.305 (m, 4H, NCH_2–CH_2N), 2.318 (s, 3H, CH_3), 1.822 (m, 2H, CCH_2C)	Formula $C_{15}H_{18}N_4O_5$ $(M+H)^+$ Calcd 335.134997. Found 335.133950. MS (SCI, *m/z*): 335 (MH^+), 317 ($MH+H_2O$), 184 ($(CH_2)_3$–Furoxan$^+$), 135 (base peak, $C_6H_4OCH_3CO^+$),
17a	28.6	108—110	1640 (C=O)	8.288 (m, 2H, ArH), 7.754—7.656 (m, 2H, ArH), 3.820 (br, 8H, NC_4H_8N), 2.299 (s, 3H, CH_3). 107 ($C_6H_4OCH_3^+$)	Formula $C_{15}H_{15}N_5O_6$ $(M+H)^+$ Calcd 362.109511. Found 362.107139. MS (SCI, *m/z*): 362 (MH^+, base peak), 344 (MH^+H_2O), 262 ($C_6H_4NO_2CONC_4H_8N^+$), 150 ($C_6H_4NO_2$-CO^+)
17b	29.9	170—172	1640, 1630 (C=O)	8.356—8.258 (m, 2H, ArH),7.661—7.561 (m, 2H, ArH), 3.790 (br, 8H, NC_4H_8N), 2.299 (s, 3H, CH_3)	Formula $C_{15}H_{15}N_5O_6(M+H)^+$ Calcd 362.109511. Found 362.111748. MS (SCI, *m/z*): 362 (MH^+, base peak), 344 (MH^+H_2O), 262 ($C_6H_4NO_2CONC_4H_8NCO^+$), 150 ($C_6H_4NO_2CO^+$)
17d	19.5	60—62	1640, 1630 (C=O)	7.441—7.280 (m, 4H, ArH), 3.770 (br, 8H, NC_4H_8N), 2.294 (s, 3H, CH_3)	Formula $C_{15}H_{15}N_4O_4Cl$ $(M+H)^+$ Calcd 351.08459. Found 351.085840. MS (SCI, *m/z*): 351 (MH^+), 333 (MH^+H_2O), 139 (base peak, $C_6H_4ClCO^+$), 111 ($C_6H_4Cl^+$)
17e	22.6	132—134	1640, 1630 (C=O)	7.40 (s, 4H, ArH), 3.88—3.77 (br, 8H, NC_4H_8N), 2.29 (s, 3H, CH_3)	Formula $C_{15}H_{15}N_4O_4Cl$ $(M+H)^+$ Calcd 351.08459. Found 351.085840. MS (SCI, *m/z*): 351 (MH^+), 333 (MH^+H_2O), 139 (base peak, $C_6H_4ClCO^+$), 111 ($C_6H_4Cl^+$)
17f	20.6	78—80	1650, 1640 (C=O)	7.566—7.303 (m, 4H, ArH), 3.773 (br, 8H, NC_4H_8N), 2.288 (s, 3H, CH_3)	Formula $C_{15}H_{15}N_4O_4Br$ $(M+H)^+$ Calcd 395.034943. Found 395.0331790. MS (SCI, *m/z*): 395 (MH^+), 377 (MH^+H_2O), 267 ($C_6H_4BrCONC_4H_8N^+$), 211 (NC_4H_8N–Furoxan$^+$), 183 (base peak, $C_6H_4BrCO^+$), 155 ($C_6H_4Br^+$)
17g	29.8	156—158	1650, 1630 (C=O)	7.645—7.310 (m, 4H, ArH), 3.798 (m, 8H, NC_4H_8N), 2.294 (s, 3H, CH_3)	Formula $C_{15}H_{15}N_4O_4Br$ $(M+H)^+$ Calcd 395.034943. Found 395.033597. MS (SCI, *m/z*): 395 (MH^+), 377 (MH^+H_2O), 267 ($C_6H_4BrCONC_4H_8N^+$), 183 (base peak, $C_6H_4BrCO^+$), 155 ($C_6H_4Br^+$)
17h	19.5	112—114	1640, 1630 (C=O)	7.441—6.931 (m, 4H, ArH), 3.830 (br, 8H, NC_4H_8N), 2.286 (s, 3H, CH_3)	Formula $C_{16}H_{18}N_4O_5$ $(M+H)^+$ Calcd 347.134997. Found 347.134790. MS (SCI, *m/z*): 347 (MH^+), 135 (base peak, $C_6H_4OCH_3CO^+$), 107 ($C_6H_4OCH_3^+$), 77 ($C_6H_5^+$)
17i	21.2	104—106	1650, 1630 (C=O)	7.545—7.299 (m, 2H, ArH), 6.975—6.879 (m, 2H, ArH), 3.841—3.773 (m, 3H+8H, OCH_3+NC_4H_8N), 2.286 (s, 3H, CH_3)	Formula $C_{16}H_{18}N_4O_5$ $(M+H)^+$ Calcd 347.134997. Found 347.137267. MS (SCI, *m/z*): 347 (MH^+), 135 (base peak, $C_6H_4OCH_3$-CO^+)
17j	16.6	118—120	1650, 1630 (C=O)	7.427 (s, 5H, ArH), 3.762—3.563 (m, 8H, NC_4H_8N), 2.283 (s, 3H, CH_3)	Formula $C_{15}H_{16}N_4O_4$ $(M+H)^+$ Calcd 317.124432. Found 317.124366. MS (SCI, *m/z*): 317 (MH^+, base peak), 105 ($C_6H_5CO^+$)

chloride (**10**) was reacted quickly with the following alcohols (**1**, **2**, **3a**—**e**, **g**; **4a**—**c**, **e**) and amines (**5a**, **b**, **d**—**j**; **6a**, **b**, **d**, **e**, **g**, **i**; **7a**, **b**, **d**—**j**) to give the desired compounds (**11**; **12**; **13a**—**e**, **g**; **14a**—**c**, **e**; **15a**, **b**, **d**—**j**; **16a**, **b**, **d**, **e**, **g**, **i**; **17a**, **b**, **d**—**j**) (Table 1).

The alcohols *N*-(2-hydroxyethyl)nicotinamide (**1**) and *N*-(2-hydroxyethyl)iso-nicotinamide (**2**) were synthesized by reacting the ethyl esters of nicotinic acid and isonicotinic acid with ethanolamine in chloroform. The alcohols in the **3**(**a**—**e**, **g**) series are *N*-(2-hydroxyethyl)benzamides, with mono- or di-substitution on the phenyl ring. The substituents on the ring were predominantly electron withdrawing groups (nitro, chloro, bromo) at the 3, 4 or 3, 4 positions, with the exception of the methoxy substituent. These were prepared from the reaction of ethanolamine and the ethyl ester of the substituted benzoic acid in refluxing chloroform. The alcohols in the **4**(**a**—**c**, **e**) series are ring substituted *N*-(3-hydroxypropyl)-benzamides and these were prepared from the reaction of propanolamine and the ethyl ester of the substituted benzoic acid in refluxing chloroform. The amines in series **5**, **6**, **7** are substituted *N*-(2-aminoethyl)benzamides, *N*-(3-aminopropyl)-benzamides and *N*-benzoylpiperazines, respectively. They were prepared from the reaction of ethylenediamine, 1,3-diaminopropane or piperazine with substituted benzoyl chlorides. The main difficulty encountered in the synthesis of these compounds is the reactivity of the amino groups in ethylenediamine, diaminopropane and piperazine, resulting in acylation of both amino groups by acid chloride. Various approaches can be used to prevent this from happening: one of the amino groups can be protected by formylation or with an ethoxycarbonyl group, or by conversion to a salt. All of these methods necessitate additional reaction steps and careful control of reaction conditions. Alternatively, the diamine may be titrated with the acyl chloride to ensure that the reaction is terminated only after 1 eq of the reagent has been consumed, or by reacting the diamine with the substituted benzoic acid using dicyclohexylcarbodiimide (DCC) as condensing agent. However, both approaches present considerable difficulties and it was not possible to obtain the monoacylated product by these techniques; this may be due to the fact that both amino groups are of very similar reactivity. It was subsequently found that the problem could be averted by converting the diamino compound into the monoamine salt form, or by carrying out the reaction in a weakly acidic solvent like acetic acid which serves to reduce the nucleophilicity of the amino group by salt formation. After numerous trials, it was found that monoacylation could be achieved if the reaction was carried out using a ratio of 2 parts acyl chloride to 3 parts diamine compound in acetic acid as solvent, and at room temperature. The monoacylated compounds were obtained as hydroscopic solids which were used immediately for the next step of the reaction.

Condensation of the alcohols (**1**, **2**, **3a**—**e**, **g**, **4a**—**c**, **e**) and amines (**5a**, **b**, **d**—**j**, **6a**, **b**, **d**, **e**, **g**, **i**; **7a**, **b**, **d**—**j**) with the furoxan (**10**) was carried out in either chloroform or dichloromethane in the presence of triethylamine, which served a catalytic function or reacted with HCl released during the reaction. The final compounds were characterized by IR, ^{1}H-NMR, and high resolution mass spectroscopy (HR-MS), and the analytical results were compatible with the proposed structures (Table 2).

Table 3. Inhibitory Effects of Furoxan Derivatives on Rabbit Aortia Strips Precontracted with KCl

Compound	Concentration (μM)	Inhibitory percentage (%, ±SE)			
		Low [K^+] (30 mM)		High [K^+] (80 mM)	
11	10	24.5	±3.1	0	
12	10	12.1	±14.8	0	
13a	10	31.9	±15.3	0	
13b	10	16.3	±8.3	3.0	±3.5
13c	10	16.4	±11.6	0	
13d	10	3.9	±3.9	3.0	±0.5
13e	10	0.4	±0.8	2.7	±4.1
13g	10	25.7	±24.8	0	
14a	10	12.4	±6.5	4.4	±1.3
14b	10	0.9	±1.6	1.3	±1.5
14c	10	30.3	±17.0	1.1	±2.0
14e	10	24.8	±4.4	2.1	±2.8
15a	10	34.8	±22.3	6.0	±7.1
15b	10	0		0.4	±0.7
15d	10	24.4	±17.7	9.2	±2.9
15e	10	30.4	±21.1	1.9	±2.4
15f	10	3.8	±4.8	0	
15g	10	39.6	±1.4	5.6	±2.3
15h	10	25.2	±4.9	2.5	±3.3
15i	10	13.1	±18.9	0.2	±0.4
15j	10	16.0	±12.9	0	
16a	10	40.1	±9.8	0.5	±0.8
16b	10	22.4	±7.5	0	
16e	10	40.6	±9.4	0.2	±0.4
16g	10	17.7	±7.9	0	
16i	10	28.7	±19.7	0.8	±1.7
17a	10	13.9	±13.8	2.2	±3.6
17b	10	15.6	±6.7	0	
17e	10	24.6	±12.2	5.2	±1.0
17f	10	28.8	±23.6	2.3	±3.9
17g	10	21.0	±10.7	4.2	±3.9
17h	10	0		0	
17i	10	36.3	±19.2	0.2	±0.4
17j	10	28.9	±23.8	0	

(Notes: Biological data are not available for compounds **16d** and **17d**).

Structure–Activity Relationship To investigate the vasorelaxing action of the synthesized compounds, different KCl-induced contraction systems were proposed. The inhibitory effect at high KCl concentration (80 mM) was not strong and the highest inhibition was only 9.2±2.9. Thus, a low KCl concentration (30 mM) system was used, and it was found that most of the compounds demonstrated the ability to cause a relaxation in the aorta precontracted with KCl; the highest inhibition was 40.6±9.4. The pharmacological data are shown in Table 3. Eight compounds reduced the KCl (30 mM)-induced contraction by at least 30%. They were **13a**, **14c**, **15a**, **15e**, **15g**, **16a**, **16e**, **17i**, all are substituted phenyl derivatives. The pyridyl derivatives **11** and **22** demonstrated significantly less activity. Of the 8 substituted phenyl derivatives, there is a significant preponderance of rings substituted with electron withdrawing groups (nitro or halogen) at the *meta* and/or *para* positions. The only exception is **17i** which has an electron donating methoxy function at the *para* position. Other than this feature, the presence of an amide or ester function in the side chain, the number of methylene units (2 or 3) between the carbonyl groups or the presence of a piperazine ring did not appear to be important determinants of activity.

Following the demonstration of functional vasodilatory ac-

tivity on the thoracic aorta whose endothelium was denuded, the effects of the compounds were investigated on the blood pressure of anaesthesized rats. Compound **17i** was chosen as a representative compound for this investigation and was found to cause a gradual reduction in the blood pressure (systolic, diastolic and mean arterial pressures) of the animal, which reached a plateau after 3 h. The reductions in these three arterial pressures were 30, 20 and 26 mmHg, respectively, after 3 h. The reduction in blood pressure was maintained over a period of 6 h thereafter. Therefore, it can be concluded that **17i** demonstrates a gradual and sustained hypotensive action which may be related to a measured release of NO from the furoxan moiety. This is a desirable feature which could be exploited in the drug design of potential NO donors.

Conclusion

Thirty six furoxan-nicorandil derivatives have been synthesized successfully by conventional chemical methods, and were investigated for their ability to reduce KCl-induced contraction in the isolated rabbit thoracic aorta. All except 2 of the compounds were found to cause a relaxation in the aorta precontracted with KCl to varying degrees. Of the active compounds, 8 analogues caused at least 30% reduction of the control KCl-induced contraction; the most active compound was **16e** which reduced the contraction by 40.6% (30 mM KCl). A representative compound **17i** (which caused 36.3% reduction in the KCl-induced contraction) was tested for hypotensive effects in the anesthesized rat. It was seen that **17i** caused a gradual and sustained reduction in blood pressure. Based on these preliminary results, it would seem that the furoxan-nicorandil derivatives are a useful lead in the design of NO-donor compounds for hypertesion.

Experimental

General Melting points were determined with a capillary apparatus and were uncorrected. The compounds were routinely characterised by IR spectrophotometry (Perkin-Elmer Model 983, KBr tablet). The ^{1}H-NMR spectra were recorded in acetone-d_6, chloroform-d_6/$CDCl_3$ or dimethyl sulfoxide-d_6/DMSO-d_6. Chemical shifts were expressed in δ (ppm) units (JEDL-FX-90Q Fourier transform NMR spectrometer, $Si(Me)_4$/TMS as internal standard). For all final compounds, HR-MS spectra were carried out on a Finnigan FTMS-2000 instrument and were in agreement with the proposed structures. Column chromatography was performed on silica gel (China Qingdao Marine Chemical Company, 100—200 mesh ASTM) with the indicated solvent system. Thin layer chromatography (TLC) was carried out on 5×20 cm plates and 2.5×7.5 cm microscope slides, which were coated with Qingdao Marine silica gel GF_{254} (400 mesh) and 0.8%—1% CMC-Na, activated and dried for 1—2 h at 100—110 °C, then stored in a dryer. Anhydrous magnesium sulphate was used as drying agent for the organic layers. Petroleum ether (30—60 °C) and dicholoromethane were used for chromatography purification and crystallization. Solvent was removed under reduced pressure at room temperature. Intermediates **8**—**10** were synthesised according to methods reported in the literature.[19,20]

***N*-(2-Hydroxyethyl)nicotinic Amide (1)** Concentrated sulphuric acid (5 ml) was added dropwise to a stirred mixture of nicotinic acid (0.2 mol, 25 g) in anhydrous ethanol and cyclohexane (1 : 1, 200 ml). A water separator condensor was attached. The temperature was raised slowly and the mixture was refluxed for 3—6 d with stirring. Removal of the solvent under reduced pressure gave a light-yellow oil which was added to saturated Na_2CO_3 solution with stirring until a pH value of 7 was reached. The mixture was then extracted with ethoxyethane, and the combined organic phase was washed with saturated NaCl, dried with $MgSO_4$ and evaporated. The nicotinic acid ester was obtained as pure colourless oil after vacuum distillation. Then nicotinic acid ester (0.05 mol, 7.2 g) and ethanolamine (5 ml) were added to chloroform with stirring. The mixture was refluxed for 3—4 h, and allowed to stand overnight before the solvent $CHCl_3$, ethanol formed from reaction and the excess of ethanolamine were evaporated under reduced pressure. A white hard solid was obtained, which gave white crystals when recrystallized with acetone. Yield 96%, mp 90—92 °C.

3-Methyl-4-[2(3-pyridineformamido)ethoxycarbonyl]furoxan (11) 1 (0.02 mol, 3.3 g), CH_2Cl_2 (80 ml) and triethylamine (3 ml) were mixed and stirred at a temperature below 30 °C. A light-yellow solution was obtained. A solution of compound (**10**) (0.02 mol) in tetrahydrofuran (THF) was added dropwise at room temperature and a colour change (yellow to black-brown) was observed. The reaction was exothermic and heat was exuded. The mixture was stirred at room temperature for 16 h, after which water was added. The organic phase was washed with water, decolourised with active carbon and filtered. The solution was evaporated to dryness under reduced pressure to give (**11**) as a pure brown solid. Yield 54.5%. mp 112—114 °C. ^{1}H-NMR (DMSO-d_6) δ: 8.98 (d, 1H, pyridine-C_2-H), 8.75—8.66 (s+dd, 2H, pyridine-C_6-H, CONH), 8.23—8.09 (tt, 1H, pyridine-C_4-H), 7.56—7.34 (q, 1H, pyridine-C_5-H), 4.61—4.48 (t, 2H, CH_2OCO), 3.79—3.60 (q, 2H, $NHCH_2$), 2.26 (S, 3H, CH_3). Formula $C_{12}H_{12}N_4O_5$; $(M+H)^+$ Calcd: 293.088047. Found: 293.089550. MS (SCI, *m/z*): 293 (MH^+, base peak), 149 ($C_5H_4NCONHCH_2$–CH_2^+), 121 (C_5H_4N–$CONH^+$). IR (KBr, cm^{-1}): 3250, 3060 (N–H); 1730, 1650 (C=O); 1100 (O=C–O).

***N*-(2-hydroxyethyl)isonicotinic Amide (2)** Concentrated sulphuric acid (1.5 ml) was added dropwise to a stirred mixture of isonicotinic acid (0.1 mol, 13.0 g) in absolute ethanol (30 ml). The mixture was refluxed for 10 d. A hard white solid was formed after the ethanol was evaporated *in vacuo*. The solid dissolved with the addition of saturated Na_2CO_3, and the alkaline solution was then extracted with ethoxyethane. The organic layer was washed with saturated NaCl solution, dried, evaporated and then vacuum distilled, resulting in a pale-yellow oil of ethyl isonicotinate. A mixture of the ethyl isonicotinate (0.02 mol, 3.3 g), ethanolamine (3.0 ml) and chloroform (10 ml) were refluxed for 3—4 h with stirring, after which the solvent chloroform and ethanol were removed *in vacuo*. Ethoxyethane and acetone were then added and a white precipitate was obtained, filtered off, washed with chloroform, acetic ester, acetone, and dried to give the title compound. Yield 96%, mp 130—132 °C.

3-Methyl-4-[2(4-pyridineformamido)ethoxycarbonyl]furoxan (12) A solution of compound (**10**) (0.01 mol) in THF was added dropwise to a stirred mixture of **2** (0.01 mol, 1.6 g) in THF (50 ml) and triethylamine (1 ml) at room temperature. The stirring was continued for 6 h, after which the solvent was evaporated *in vacuo* to give a brown sticky paste, which was poured into water. The solution was filtered to remove some pale brown precipitate. The aqueous solution was extracted with CH_2Cl_2, and the combined organic solution was washed with saturated NaCl, decolorized with 400 mesh silica gel, dried and evaporated to give the title compound as a white solid. It was then purified by washing with ethanol and ethoxythane. Yield 50.5%. mp 168—170 °C. ^{1}H-NMR ($CDCl_3$+DMSO-d_6) δ: 8.85 (s, 1H, CONH), 8.37—8.67 (dd, 2H, pyridine-C_2,C_6-2H), 7.79—7.72 (dd, 2H, pyridine-C_3, C_5-2H), 4.60—4.54 (t, 2H, CH_2OCO), 3.80—3.70 (q, 2H, $NHCH_2$), 2.31 (s, 3H, CH_3). Formula $C_{12}H_{12}N_4O_5$ $(M+H)^+$ Calcd: 293.088047. Found: 293.088075. MS (SCI, *m/z*): 293 (MH^+, base peak), 214 ($CONHCH_2$–CH_2-furoxan), 149 (C_5H_4NCONH–$CH_2CH_2^+$). IR (KBr, cm^{-1}): 3200, 3050 (N–H); 1750, 1650 (C=O); 1100 (O=C–O).

General Method for the Preparation of *N*-Substituted Benzoylpiperazine (7a,b, d—j) Hydrate piperazine (0.006 mol, 0.62 g) and acetic acid (50 ml) were mixed, immediately producing some gaseous fumes and heat was released. The mixture was then stirred until a colourless solution was obtained as it cooled. A solution of the substituted benzoic acid chloride (0.006 mol) in THF (2 ml) obtained by refluxing the relating substituted benzoic acid in thionyl chloride was then added dropwise to the stirred mixture which became turbid. The stirring was continued for about 60 min at room temperature, water was added and the pH was adjusted with NaOH solution to 12. The solution was filtered to remove some white or pale-brown undissolved substances. The aqueous solution was extracted with chloroform, the organic solution was then washed with water or saturated NaCl solution, dried and evaporated *in vacuo* to give the desired compound (**7a**, **b**, **d**—**j**), which was then processed quickly for the next step of the reaction.

General Method for the Preparation of *N*-(3/4-Substituted-benzoyl)-*N'*-[3-methylfuroxanyl-4-carbonyl]piperazine (17a, b, d—j) A solution of compound **10** (0.006 mol) in THF was added dropwise to a stirred mixture of **7a**, **b**, **d**—**j** (0.006 mol) in CH_2Cl_2 (60 ml) and N $(C_2H_5)_3$ (1 ml). Stirring was continued for about 6 h at room temperature, after which the resulting mixture was washed several times with water, 10% HCl and saturated $NaHCO_3$ consecutively. The organic layer was then decolorized with active carbon, dried and evaporated to afford a solid compound which was further purified with acetone or ethanol to give the final compounds (**17a**, **b**, **d**—**j**).

The physical data of the synthesised compounds (**17a, b, d—j**) are given in Table 2. The compounds are *N*-(3-nitrobenzoyl)-*N'*-[3-methyl furoxanyl-4-carbonyl]piperazine (**17a**), *N*-(4-nitrobenzoyl)-*N'*-[3-methyl furoxanyl-4-carbonyl]piperazine (**17b**), *N*-(3-chlorobenzoyl)-*N'*-[3-methyl furoxanyl-4-arbonyl]piperazine (**17d**), *N*-(4-chlorobenzoyl)-*N'*-[3-methyl furoxanyl-4-carbonyl]piperazine (**17e**), *N*-(3-bromobenzoyl)-*N'*-[3-methyl furoxanyl-4-carbonyl]piperazine (**17f**), *N*-(4-bromobenzoyl)-*N'*-[3-methyl furoxanyl-4-carbonyl]piperazine (**17g**), *N*-(3-methoxybenzoyl)-*N'*-[3-methylfuroxanyl-4-carbonyl]piperazine (**17h**), *N*-(4-methoxybenzoyl)-*N'*-[3-methylfuroxanyl-4-carbonyl]piperazine (**17i**), *N*-benzoyl-*N'*-[3-methylfuroxanyl-4-carbonyl]-piperazine (**17j**).

General Method for the Preparation of 3-Methyl-4-[2-(3/4-substituted benzoyl amino) ethylaminocarbonyl]furoxan (15a, b, d—j) Ethylene diamine (0.017 mol, 1.0 g) and acetic acid (50 ml) were slowly mixed together, a large amount of white gas was produced and the reaction was exothermic. A white solid was initially formed but dissolved gradually to form a colourless solution, as it cooled to room temperature. The corresponding benzoic acid chloride derivative (0.01 mol) was then added dropwise with stirring over 30 min at room temperature. After 2 h water was added to the mixture, and the pH adjusted to 12 with NaOH solution. The solution was filtered to remove some white precipitate and the aqueous filtrate was extracted with chloroform, the organic phase was washed with saturated NaCl, dried and evaporated under reduced pressure to afford the intermediate *N*-(2-aminoethyl)-substituted benzoylamide (**5a, b, d—j**) which was used immediately for the next step of the reaction. A solution of compound **10** (0.01 mol) in THF (2 ml) in the presence of triethylamine (0.5 ml) was added dropwise at room temperature to a stirred solution of **5a, b, d—j** in CH_2Cl_2. The stirring was continued 3—6 h and then the reaction mixture was poured into water. The organic layer was washed several times with water, decolorised with active carbon, dried and evaporated under reduced pressure to give the desired derivatives (**15a, b, d—j**) which were recrystallized with ethanol. The physical data of the synthesized compounds (**15a, b, d—j**) are given in Table 2. The compounds are 3-methyl-4-[2-(3-nitrobenzoylamino)-ethylaminocarbonyl]furoxan (**15a**), 3-methyl-4-[2-(4-nitrobenzoylamino)-ethylaminocarbonyl] furoxan (**15b**), 3-methyl-4-[2-(3-chlorobenzoylamino)-ethylaminocarbonyl]furoxan (**15d**), 3-methyl-4-[2-(4-chlorobenzoylamino)-ethylaminocarbonyl]furoxan (**15e**), 3-methyl-4-[2-(3-bromobenzoylamino)-ethylaminocarbonyl]furoxan (**15f**), 3-methyl-4-[2-(4-bromobenzoylamino)-ethylaminocarbonyl]furoxan (**15g**), 3-methyl-4-[2-(3-methoxybenzoylamino)-ethylaminocarbonyl]furoxan (**15h**), 3-methyl-4-[2-(4-methoxybenzoylamino)-ethylaminocarbonyl]furoxan (**15i**), 3-methyl-4-(2-benzoyl aminoethyl aminocarbonyl)furoxan (**15j**).

General Method for the Preparation of 3-Methyl-4-[3(3/4-substituted-benzoyl aminopropyl aminocarbonyl)furoxan (16a, b, d, e, g, i) 1,3-Diaminopropane (0.02 mol, 1.50 g) and acetic acid (50 ml) were reacted together as described for the preparation of 3-methyl-4-[2(3/4-substituted-benzoylamino) ethylaminocarbonyl]furoxan (**15a, b, d—j**). The intermediate *N*-(3-aminopropyl)-substituted-benzoylamide (**6a, b, d, e, g, i**) was first obtained. A mixture of **6** (**a, b, d, e, g, i**) in $CHCl_3$ was similarly reacted with compound **10** (0.02 mol) as described earlier. The physical data of the synthesised compounds (**16a, b, d, e, g, i**) are given in Table 2. The compounds are 3-methyl-4-[3-(3-nitrobenzoylamino)propylaminocarbonyl]furoxan (**16a**), 3-methyl-4-[3-(4-nitrobenzoylamino)propylaminocarbonyl]furoxan (**16b**), 3-methyl-4-[3-(3-chlorobenzoylamino)propylaminocarbonyl]furoxan (**16d**), 3-methyl-4-[3-(4-nitrobenzoylamino)propylaminocarbonyl]furoxan (**16e**), 3-methyl-4-[3-(4-bromobenzoylamino)propylaminocarbonyl]furoxan (**16g**), 3-methyl-4-[3-(4-methoxylbenzoylamino)propylaminocarbonyl]furoxan (**16i**).

General Method for the Preparation of 3-Methyl-4-[2(3/4-substituted-benzoyl amino)ethoxylcarbonyl]furoxan (13a—e, g) Concentrated sulphuric acid (1 ml) was added dropwise to a stirred mixture of the substituted benzoic acid (0.02 mol) in absolute ethanol (100 ml). After refluxing for 8 h, the solution was cooled to room temperature, and cyclohexane (60 ml) was added. The mixture was distilled to evaporate the water formed from the reaction, as well as the solvents cyclohexane and ethanol. A pale-yellow sticky residue was exuded, water was added and the mixture was extracted with ethoxyethane. The organic solution was washed several times with saturated NaCl and water, dried and evaporated *in vacuo* to give the substituted benzoic acid ester. The ester was reacted with ethanolamine (0.02 mol, 1.3 g) in chloroform with stirring. The mixture was then refluxed for 8 h, after which the organic solvents were removed *in vacuo* to give a pale-brown oil which became a sticky solid on cooling in the refrigerator. Subsequent grinding of the sticky solid with some acetone and ethoxyethane gave a white solid which was the intermediate *N*-(2-hydroxyethyl)-substituted-benzoylamides (**3a—e, g**). These intermediates were recrystallized with one of the following solvents: acetone, acetic ester, ethoxyethane, or petroleum ether. A solution of **10** (0.01 mol) in THF (2 ml) was added dropwise to a stirred mixture of **3a—e, g** in dichloromethane (60 ml) in the presence of triethylamine (1 ml). The stirring was continued for 3—6 h, after which the reaction mixture was poured into water. The separated organic solution was washed several times with water, decolorized with active carbon, dried and evaporated under reduced pressure. The expected final derivatives 3-methyl-4-[(2/3-substituted benzoylamino)alkyloxylcarbonyl]furoxan (**13a—e, g**) were obtained after recrystallization with ethanol or ethoxyethane. The physical data of the synthesized compounds (**13a—e, g**) are given in Table 2. The compounds are 3-methyl-4-[2(3-nitrobenzoylamino)ethoxylcarbonyl]furoxan (**13a**), 3-methyl-4-[2(4-nitrobenzoyl amino)ethoxylcarbonyl]furoxan (**13b**), 3-methyl-4-[2(3,4-dinitrobenzoylamino)ethoxylcarbonyl]furoxan (**13c**), 3-methyl-4-[2(3-chlorobenzoylamino)ethoxylcarbonyl]furoxan (**13d**), 3-methyl-4-[2(4-chlorobenzoylamino)ethoxylcarbonyl]furoxan (**13e**), 3-methyl-4-[2(4-bromobenzoylamino)ethoxylcarbonyl]furoxan (**13g**).

General Method for the Preparation of 3-Methyl-4-[3(3/4-substituted-benzoyl-amino)propyloxylcarbonyl]furoxan (14a—c, e) Propanoamine (0.015 mol, 1.03 g) and acetic acid (50 ml) were reacted together as described for the preparation of 3-methyl-4-[2(3/4-substitutedbenzoylamino)-ethoxylcarbonyl]furoxan (**13a—e, g**). The intermediate *N*-(3-hydroxypropyl)-3/4-substituted-benzoylamide (**4a—c, e**) were first obtained. A mixture of **4a—c,e** in CH_2Cl_2 was similarly reacted with compound **10** (0.01 mol) as described earlier. The physical data of the synthesised compounds (**14a—c, e**) are given in Table 2. The compounds are 3-methyl-4-[3(3-nitrobenzoylamino)propyloxylcarbonyl]furoxan (**14a**), 3-methyl-4-[3(4-nitrobenzoylamino)propyloxylcarbonyl]furoxan (**14b**), 3-methyl-4-[3(3,4-dinitrobenzoylamino)propyloxylcarbonyl]furoxan (**14c**), 3-methyl-4-[3(4-chlorobenzoylamino)propyloxylcarbonyl]furoxan (**14e**).

Pharmacology. Experiments on Denuded Thoracic Aorta Isolated from Rabbits The thoracic aorta was isolated from male or female rabbits weighting 1.8—2.5 kg, which were sacrificed by a sharp blow on the head. Helicoid strips were prepared according to known methods and mounted in an organ bath containing Krebs–Henseleit buffer solution pH 7.4 of the following composition: NaCl, 120; KCl, 4.8; $CaCl_2$, 2.5; $MgSO_4 \cdot 7H_2O$, 1.4; KH_2PO_4, 1.2; $NaHCO_3$, 25; glucose 11 mmol/l; Na_2EDTA 13.4 μmol/l. The tissue was maintained at 37 °C and aerated with 95% O_2—5% CO_2. After an equilibrium period of 2 h, the aortic strips were contracted by addition of either 30 or 80 mM KCl solution. The sample (10 μM) was then added and its effect on KCl-induced contraction was monitored. Each experiment was repeated 3 times. The drug was dissolved in DMSO–saline, and the volume ratio of DMSO did not exceed 0.5% of the bath volume. The effect of the drug on the aorta precontracted with KCl was expressed as an inhibitory ratio which is given as Eq. 1.

$$\%\ \text{inhibition of KCl-induced contraction} = \frac{\left(\begin{matrix}\text{height of control}\\ \text{KCl contraction}\end{matrix}\right) - \left(\begin{matrix}\text{height of KCl contraction}\\ \text{in presence of drug}\end{matrix}\right)}{\text{height of control KCl contraction}} \quad (1)$$

Effect of Blood Pressure in Anaesthesised Rats Male or female rats weighting about 250 g were anesthesised and carefully dissected to expose the carotid artery. The artery was cannulated and a pressure transducer connected to a Grass Polygraph recorder was attached. The systolic, diastolic and mean arterial (MAP) pressures were monitored until steady values were obtained. The drug was administered *via* intravenous injection at a dose of 1.5 mg/kg and the pressures were monitored over a period of 6 h.

Acknowledgments The first author would like to thank Professor Sixun Peng and Professor Wei-yi Hua, China Pharmaceutical University, Nanjing, China, for their guidance of the original work of this paper. This work was supported by NUS Research Grant RP3970637.

References

1) Boucher J. L., Moali C., Tenu J. P., *Cell. Mol. Life Sci.*, **55**, 1015—1028 (1999).
2) Feelisch M., *Naunyn-Schmiederg's Arch. Pharmacol.*, **358**, 113—122 (1998).
3) Civelli M., Caruso P., Giossi M., Bergamaschi M., Razzetti R., Bongrani S., Gasco A., *Eur. J. Pharmacol.*, **255**: 17—24 (1994).
4) Lefer A. M., Lefer D., *Drugs Future*, **19**, 665—672 (1994).
5) Gasco A., *Adv. Heterocyclic Chem.*, **29**, 251—253 (1981).
6) Bolt A. G., Ghosh P. B., Sleigh M. J., *Biochem Pharmacol.*, **23**, 1963 (1974).

7) Keisei D., Belton J. G., *Cancer Res.*, **35**, 3735—3743 (1975).
8) Ghosh P. B., *J. Med. Chem.*, **17**, 203 (1974).
9) Schonafinger K., Beyer R., Mogilev A., Eu.r Pat. Appl. 54 872, 54 873 (1982).
10) Calvino R., Fruttero R., Ghigo D., *J. Med. Chem.*, **35**, 3296—3300 (1992).
11) Gasco A. M., Boschi D., Di Stilo A., Medana C., Gasco A., Martorana P. A., Schonafinger K., *Arzneim.-Forsch. Drug Res.*, **48**, 212—218 (1998).
12) Ghigo D., Heller R., Calrino R., Alessio P., Fruttero R., Gasco A., Bosia A., Pescarmona G., *Biochem. Pharmacol.*, **43**, 1281—1288 (1992).
13) Feelisch M., *J. Cardiovasc. Pharmacy*, **17** (Suppl. 3), S25—28 (1991).
14) Feelisch M., Schonafinger K., Noack E., *Biochem Pharmacol.*, **44**, 1149—1157 (1992)
15) Medana C., Ermondi G., Fruttero R., Di Stilo A., Ferrelli C., Gasco A., *J. Med. Chem.*, **37**, 4412—4416 (1994).
16) Bohn H., Brendel J., Martorana P. A., Schonafinger K., *Br. J. Pharmacol.*, **114**, 1605—1612 (1995).
17) Magnon M., Durand I., Cavero I., *J. Pharmacol. Exp. Ther.*, **268**, 1411—1416 (1994).
18) Di Stilo A., Visentin S., Cena C., Gasco A. M., Ermondi G., Gasco A., *J. Med. Chem.*, **41**, 5393—5401 (1998).
19) Di Stilo A., Fruttero R., Boschi D., *Med. Chem. Res.*, **3**, 554—557 (1993).
20) Fruttero R., Ferrarotti B., Serafino A., *J. Heterocyclic. Chem.*, **26**, 1345—1349 (1989).

Bioavailable Acyl-CoA : Cholesterol Acyltransferase Inhibitor with Anti-peroxidative Activity: Synthesis and Biological Activity of Novel Indolinyl Amide and Urea Derivatives

Shoji KAMIYA,[a] Hiroaki SHIRAHASE,*,[a] Akihisa YOSHIMI,[a] Shohei NAKAMURA,[a] Mamoru KANDA,[a] Hiroshi MATSUI,[a] Masayasu KASAI,[a] Kenji TAKAHASHI,[a] and Kazuyoshi KURAHASHI[b]

Research Laboratories, Kyoto Pharmaceutical Industries, Ltd.,[a] 38 Nishinokyo, Tsukinowa-cho, Nakakyo-ku, Kyoto 604–8444, Japan and Pharmacology Division, Radioisotope Research Center, Kyoto University,[b] Yoshida-Konoe-cho, Sakyo-ku, Kyoto 606–8501, Japan. Received December 14, 1999; accepted February 28, 2000

We synthesized a series of indoline derivatives with an amide or urea moiety and examined their inhibitory effects on acyl-CoA : cholesterol acyltransferase (ACAT) activity, lipid-peroxidation and serum cholesterol levels in experimental animals. Among the derivatives synthesized, a series of *N*-(1-alkyl-4,6- dimethylindolin-7-yl)-2,2-dimethylpropanamides potently inhibited rabbit intestinal ACAT activity and lipid-peroxidation of rat brain homogenate. The effect on ACAT activity was related to the length of the alkyl chain at the 1-position of indoline. *N*-(4,6-Dimethyl-1-octylindolin-7-yl)-2,2-dimethylpropanamide hydrochloride (55) showed inhibitory effects on intestinal and hepatic ACAT activity slightly weaker than those of YM-750, and an inhibitory effect on low density lipoprotein (LDL)-peroxidation similar to that of probucol. Compound 55 also reduced serum cholesterol at 10 mg/kg/d in hyperlipidemic rats and 20 mg/kg/d in normolipidemic hamsters. The plasma concentration of 55 reached 716 ng/ml in dogs (10 mg/kg, *p.o.*), which is an effective concentration against hepatic ACAT activity and LDL-peroxidation. In conclusion, compound 55 is a novel bioavailable ACAT inhibitor with anti-peroxidative activity and is thus a promising anti-atherosclerotic and anti-hyperlipidemic drug. Indoline proved to be a useful pharmacophore for molecular design of new anti-peroxidative drugs.

Key words indoline derivative; acyl-CoA : cholesterol acyltransferase inhibitor; anti-oxidant; anti-hyperlipidemic drug; anti-atherosclerotic drug

Acyl-CoA : cholesterol acyltransferase (ACAT) plays a key role in intestinal absorption of dietary cholesterol, incorporation of hepatic cholesterol into very low density lipoprotein (VLDL) and vascular accumulation of cholesterol in hyperlipidemia and atherosclerosis.[1] Thus, inhibition of ACAT has been believed to lower serum cholesterol level and also directly prevent deposition of cholesterol in atherosclerotic plaques. There have been a number of attempts to develop ACAT inhibitors as a novel type of anti-atherosclerotic drug,[2,3] however, none has been successfully developed for clinical use. Most of the early ACAT inhibitors with high lipophilicity showed low oral bioavailability and had adrenal and/or hepatic toxicity. Adrenotoxicity is a critical problem for ACAT inhibitors, and early studies reported that it may be due to their nonspecific cytotoxicity rather than to ACAT inhibitory activity.[3,4] Rapid and strong ACAT inhibition has recently been suggested to increase the intracellular free cholesterol level, which causes damage to adrenal plasma membrane.[3] It may be difficult to completely inhibit vascular and macrophage ACAT without affecting adrenal ACAT, since a recent monoclonal antibody study showed that adrenal and vascular ACAT are both the same subtype, ACAT-1.[5] Bioavailable and weak ACAT inhibitors such as CI-1011 have been reported to show little adrenotoxicity.[3,6] However, these weak ACAT inhibitors without adrenotoxicity may not effectively prevent cholesterol deposition in atherosclerotic plaques. There have been only a few reports on the effects of ACAT inhibitor on atherosclerosis in Watanabe Heritable Hyperlipidemic (WHHL) rabbits, which are a reliable genetic model of familial hyperlipidemia. E5324 significantly reduced the atherosclerotic area in WHHL rabbits,[7] while FR145237 had no significant effect on atherosclerosis in these rabbits but had adrenotoxic effects in cholesterol-fed rabbits.[8,9]

On the other hand, oxidized but not native low density lipoprotein (LDL) is taken up into macrophages in a non-regulated manner and then cholesterol is accumulated *via* re-esterification by ACAT.[10] Therefore, anti-oxidant therapy is effective to prevent atherosclerosis.[11] Indeed, probucol reduces atherosclerotic area and xantoma by inhibition of LDL-peroxidation without affecting blood cholesterol levels in WHHL rabbits.[12] We hypothesized that bioavailable moderate ACAT inhibitors with inhibitory effects on LDL-oxidation would be safe and effective anti-atherosclerotic drugs.

The aim of this study was synthesis of a novel effective anti-atherosclerotic drug with dual inhibitory activity against ACAT and lipid-peroxidation. Two types of ACAT inhibitors have been reported to date (Fig. 1): compounds such as YM-750 and RP64477 with a urea or amide structure incorporated between two aromatic rings (Ar–Ar type), and those such as E5324, CI-976 and TEI-6522 with a urea or amide structure incorporated between an aromatic ring and an aliphatic chain (Ar–Al type).[1,13—16] Most of the known ACAT inhibitors are very potent but show poor oral bioavailability probably due to their high lipophilicity and/or high molecular weight. An indoline structure was reported to act as a pharmacophore responsible for the inhibitory effect of indapamide on lipid-peroxidation.[17,18] We synthesized a series of indoline derivatives with an amide or urea moiety to find an effective anti-atherosclerotic drug with inhibitory effects on ACAT and lipid-peroxidation, and to determine whether the indoline structure is a useful pharmacophore in the molecular design of anti-peroxidative drugs.

Chemistry As shown in Chart 1, indole derivatives **1**, *i.e.* 6-methylindole[19] (**1b**), 4,6-dimethylindole[20] (**1c**), 4,6-diethylindole[21,22] (**1d**), and 4,6-dimethoxyindole[23] (**1e**), were

* To whom correspondence should be addressed. e-mail: shirahase@kyoto-pharm.co.jp

© 2000 Pharmaceutical Society of Japan

prepared according to the previously described methods. 1-Acetylindoline derivatives **2a**—**2e** were obtained from corresponding indole derivatives **1a**—**1e** by reduction with sodium cyanoborohydride in AcOH followed by acetylation with Ac_2O. 1-Acetylindoline derivatives **2a**—**2e** were brominated to give 1-acetyl-5-bromoindoline derivatives **3a**—**3e**, which were nitrated with fuming nitric acid in H_2SO_4 and AcOH to give 1-acetyl-5-bromo-7-nitroindoline derivatives[24] **4a**—**4e**. Removal of the acetyl group of **4a**—**4e** was performed using NaOH, and the resulting indolines were alkylated by treatment with NaH and alkyl iodide in *N*,*N*-dimethylformamide (DMF) to afford 1-alkyl-5-bromo-7-nitroindoline derivatives **5a**—**5e**. Catalytic reduction of **5a**—**5e** using 5% Pd–C gave corresponding 1-alkyl-7-aminoindoline derivatives, which were condensed with the appropriate isocyanate or acyl chloride, then deprotected if necessary, to afford the indoline derivatives (**20**—**25**, **27**, **32**—**48**, **58**—**61**). 1-Acetyl-5-bromo-4,6-dimethyl-7-nitroindoline (**4c**) was reduced using 5% Pd–C to give 1-acetyl-7-amino-4,6-dimethylindoline, which was condensed with pivaloyl chloride to afford **6c** followed by hydrolysis of its acetyl group and condensation with the appropriate bromide, then deprotected if necessary to give the indoline derivatives (**49**—**57**, **62**—**66**).

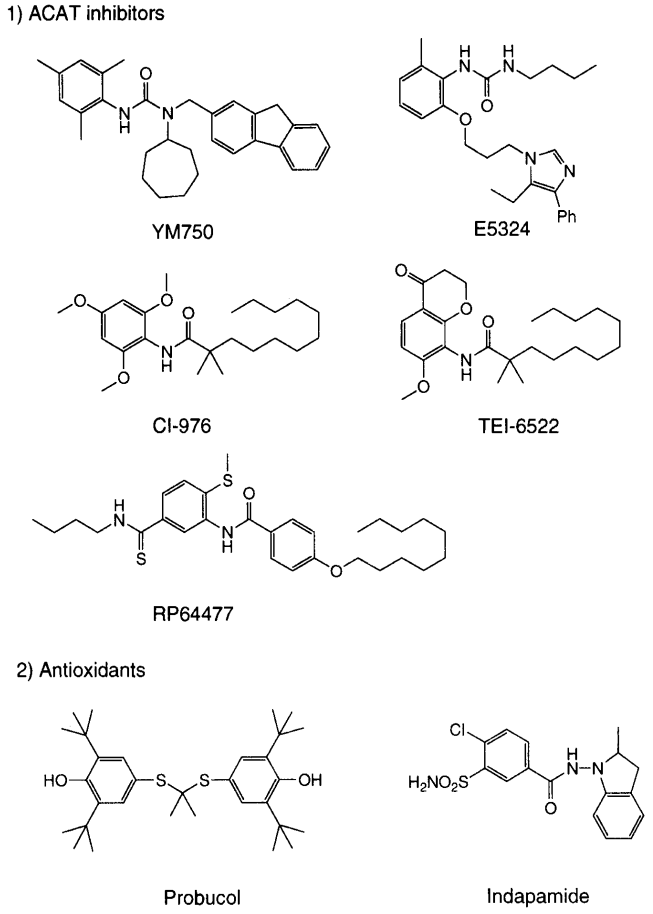

Fig. 1

As shown in Chart 2, nitration of indoline derivatives (**2a**, **2c**) with fuming nitric acid in Ac_2O gave 1-acetyl-5-nitroindoline derivatives (**7a**, **7c**), then hydrolysis of **7a** and **7c** provided 5-nitroindoline derivatives (**8a**, **8c**), which were alkylated by treatment with NaH and hexyliodide in DMF to afford 1-hexyl-5-nitroindoline derivatives (**9a**, **9c**). Catalytic reduction of **9a** and **9c** using 5% Pd–C gave the corresponding amines which were condensed with the appropriate isocyanate or pivaloyl chloride to afford the indoline derivatives (**19**, **26**, **30**).

As shown in Chart 3, 5,7-dimethylindole (**11**) was synthesized from 2,4-dimethylaniline (**10**) according to the procedure described by Demerson *et al.*[22] Compound **11** was reduced with sodium cyanoborohydride in AcOH and nitrated with fuming nitric acid in H_2SO_4[25] to give 5,7-dimethyl-6-nitroindoline (**13**), which was alkylated by treatment with NaH and hexyl iodide in DMF to afford 1-hexyl-5,7-dimethyl-6-nitroindoline (**14**). Catalytic reduction of **14** using 5% Pd–C gave the corresponding amine, which was condensed with pivaloyl chloride to afford the indoline derivative **28**.

As shown in Chart 4, 1-acetyl-5-hydroxyindoline[26] (**15**) was alkylated by treatment with K_2CO_3 and alkyl bromide in EtOH to afford 1-acetyl-5-alkyloxyindolines (**16a**, **16b**), which were nitrated with fuming nitric acid in Ac_2O to give 1-acety-5-alkyloxy-6-nitroindoline derivatives **17a** and **17b**. Removal of the acetyl groups of **17a** and **17b** was performed

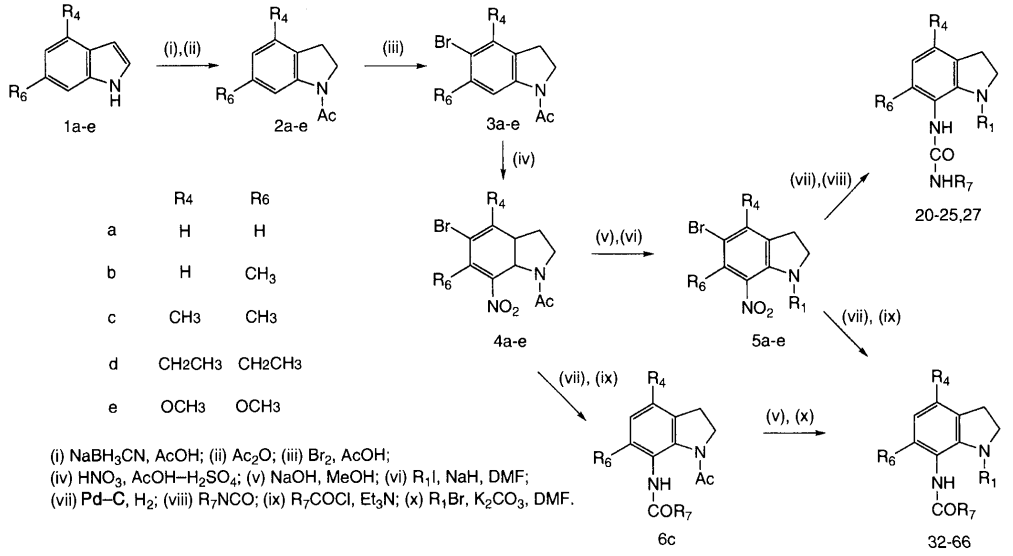

Chart 1

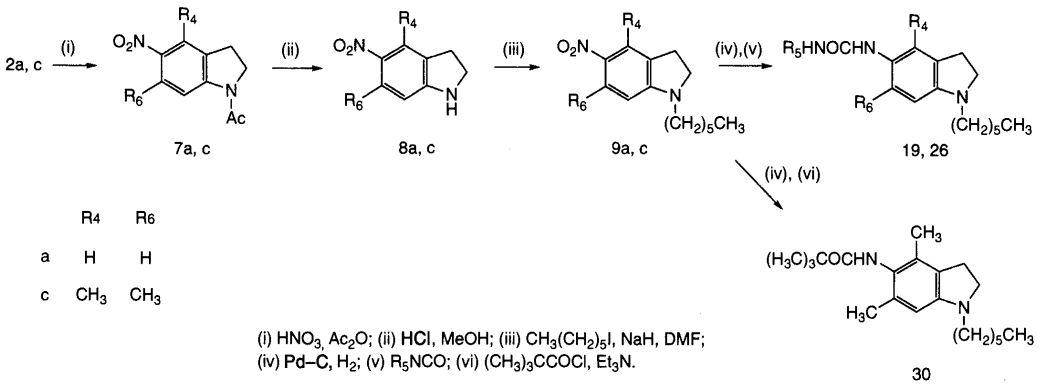

Chart 2

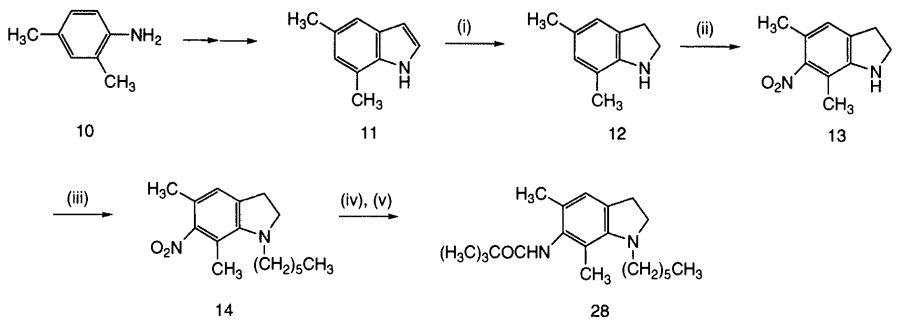

Chart 3

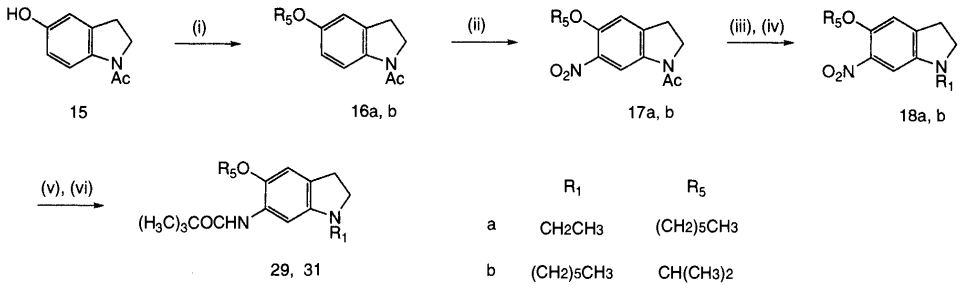

Chart 4

using HCl, and the resulting indolines were alkylated by treatment with K_2CO_3 and alkyl iodide in DMF to afford 1-alkyl-5-alkyloxy-6-nitroindoline derivatives (**18a**, **18b**). Catalytic reduction of **18a** and **18b** using 5% Pd–C gave the corresponding 1-alkyl-6-aminoindoline derivatives, which were condensed with pivaloyl chloride to afford the indoline derivatives (**29**, **31**).

Results and Discussion

We designed and synthesized a series of Ar–Ar type urea derivatives and Ar–Al type urea and amide derivatives based on the indoline structure, the molecular weights of which were limited to around 400, and examined their *in vitro* activity against rabbit intestinal ACAT and lipid-peroxidation of rat brain homogenate.

In the first set of experiments, indoline derivatives with a substituted urea moiety were synthesized, and the biological results are shown in Table 1. Compound **19** with 2,4,6-trimethylphenyl urea at the 5-position and a hexyl group at the 1-position had little effect on ACAT. Compound **20**, an isomer of **19**, with the same urea moiety at the 7-position had weak ACAT inhibitory activity. Furthermore, decreases in size of the 1-alkyl chain resulted in reduction of the activity (**20** *vs.* **21**). Compounds **23** and **24** with 2-(hexyloxy)phenyl urea showed relatively potent ACAT inhibition, while compound **25** with 4-(hexyloxy)phenyl urea, which is an isomer of **23**, showed lower activity. Compound **26** with *n*-butylurea at the 5-position and a hexyl group at the 1-position was about 3-fold weaker than that of its 7-positional isomer **27**. These results demonstrated that introduction of a lipophilic and bulky substituent(s) into a position close to the urea moiety enhanced the inhibitory effect on ACAT activity. In a series of *N*-(substituted phenyl)ureas, the introduction of bulky substituents isopropyl and ethyl into the *ortho*-position has

Table 1. Structure and Biological Activities of Indoline Substituted Ureas

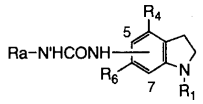

No.	R_1	R_4	R_6	Ra	Position	ACAT inhibition[a] IC_{50} (μM)	LPO inhibition[b] (%)
19	$(CH_2)_5CH_3$	H	H		5	>10	96.8
20	$(CH_2)_5CH_3$	H	H		7	3.26	26.7
21	CH_2CH_3	H	H		7	8.39	35.2
22	$(CH_2)_5CH_3$	H	H		7	2.76	97.9
23	CH_2CH_3	H	H	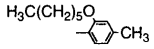	7	0.68	97.3
24	$(CH_2)_5CH_3$	H	H	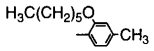	7	0.36	95.7
25	CH_2CH_3	H	H	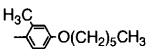	7	1.63	97.1
26	$(CH_2)_5CH_3$	CH_3	CH_3	$(CH_2)_3CH_3$	5	9.50	98.1
27	$(CH_2)_5CH_3$	CH_3	CH_3	$(CH_2)_5CH_3$	7	3.51	95.2
YM-750						0.02	—
Probucol						—	23.1

a) Rabbit intestinal mucosal microsomes were used as ACAT preparations. *b*) % Inhibition at 10 μM in lipid-peroxidation (LPO) of rat brain homogenate.

been reported to markedly increase the activity against ACAT.[27] The compounds listed in Table 1 showed inhibitory effects on lipid-peroxidation comparable to or greater than that of probucol, indicating that introduction of an indoline structure could confer anti-peroxidative activity. The most potent compound, **24**, showed about 18-fold weaker ACAT-inhibitory activity than that of YM-750 and more potent anti-peroxidative activity than that of probucol.

In the next set of experiments, we attempted to design Ar–Al type indolinyl amide derivatives to find a lead compound smaller than **24** (M.W. 451.6). Known typical Ar–Al type ACAT inhibitors such as CI-976 and TEI-6522 have a long alkyl amide chain.[15,16] However, of the TEI-6522 derivatives (oxochroman derivatives), a compound with 2,2-dimethylpropanamide combined with the *ortho*-decyloxy group showed a relatively strong inhibitory activity against ACAT.[16] Thus, we synthesized indoline derivatives with a small alkylamide moiety and a hexyl or hexyloxy chain. The chemical structures and results are shown in Table 2. Compounds **28**—**30** with an amide moiety at the 5- or 6-position and a hexyl group at the 1-position showed weak ACAT inhibitory activity. The activity of **31** with an amide moiety at the 6-position and a hexyloxy group at the 5-position was relatively high compared with **28**—**30**. A bulky and lipophilic substituent (hexyloxy) flanking the amide moiety enhanced the ACAT inhibitory activity as shown in the urea derivatives (Table 1). Among **32**—**36** with an amide moiety at the 7-position, **32**—**35** showed moderate ACAT inhibitory activity and **36** relatively weak activity. These results implied that methyl, methoxy or ethyl substituents at the 4- and/or 6-position (**33**—**36**) did not increase the activity. In fatty acid anilide derivatives including CI-976, the substituents methyl, methoxy, ethyl or isopropyl at the *ortho*-position of alkylamide effectively increased the ACAT inhibitory activity.[15] Unlike CI-976, our system had a bicyclic structure (indoline) and a bulky moiety at the 1-position on the ring. Thus, additional substituents at 4- and 6-positions may have failed to further increase the activity. Interestingly, despite the similar *in vitro* activity, compound **34** showed a markedly more potent *in vivo* anti-hyperlipidemic effect than **32**, **33**, **35** and **36**. When administered orally to rats fed a high-cholesterol diet, compounds **32**—**36** lowered serum cholesterol levels by 14.1% at 10 mg/kg, 11.7% at 30 mg/kg, 42.0% at 10 mg/kg, 19.2% at 30 mg/kg and 4.0% at 10 mg/kg, respectively. These differences of *in vivo* activity may have been attributable to absorption and/or metabolic resistance of the compounds. The compounds listed in Table 2 all showed more potent anti-peroxidative activity than probucol. Compound **34** was then chosen as a lead compound for structural optimization to enhance the inhibitory activity on ACAT.

Derivatives of **34** with various substituents at the 1-position (R_1) and at the terminal of the amide (R_7) were synthesized (Table 3). Of the 1-hexyl derivatives, compound **37** was a weaker ACAT inhibitor than **34**, but **38**—**43** were roughly equipotent to **34**, indicating that the ACAT inhibitory activity is not highly dependent on size of R_7. In other Ar–Al type ACAT inhibitors such as CI-976 and TEI-6522, ACAT inhibitory activity is closely related to the length of the alkyl

Table 2. Structure and Biological Activities of Indoline Substituted Amides

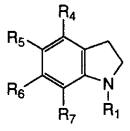

A = $-NHCOC(CH_3)_3$

No.	R_1	R_4	R_5	R_6	R_7	ACAT inhibition[a] IC_{50} (μM)	LPO inhibition[b] (%)
28	$(CH_2)_5CH_3$	H	CH_3	A	CH_3	3.44	62.7
29[c]	$(CH_2)_5CH_3$	H	$OCH(CH_3)_2$	A	H	33.2	99.5
30	$(CH_2)_5CH_3$	CH_3	A	CH_3	H	4.33	98.0
31[c]	CH_2CH_3	H	$O(CH_2)_5CH_3$	A	H	0.96	99.3
32	$(CH_2)_5CH_3$	H	H	H	A	0.33	92.9
33[c]	$(CH_2)_5CH_3$	H	H	CH_3	A	0.44	95.7
34[c]	$(CH_2)_5CH_3$	CH_3	H	CH_3	A	0.26	96.9
35[c]	$(CH_2)_5CH_3$	OCH_3	H	OCH_3	A	0.35	91.5
36	$(CH_2)_5CH_3$	CH_2CH_3	H	CH_2CH_3	A	1.03	96.7

a) Rabbit intestinal mucosal microsomes were used as ACAT preparations. *b*) % Inhibition at 10 μM in lipid-peroxidation (LPO) of rat brain homogenate. *c*) Hydrochloride salt.

amide chain.[15,16] In compounds **34** and **37**—**43**, the 1-hexyl chain but not alkylamide moiety appeared to be important for interaction with the hydrophobic region of the enzyme. ACAT is considered to have one large hydrophobic interaction area, and thus only one lipophilic group in the ACAT inhibitor can interact with the enzyme, as previously described in a series of oxochroman derivatives which also have a long alkyl chain near the alkylamide moiety.[16]

In compounds **44**—**46** with an ethyl instead of a hexyl group at the 1-position, ACAT inhibitory activity was moderately related to the carbon number of R_7. Increase of the carbon number by 8 at R_7 resulted in only 8-fold enhancement of ACAT inhibitory activity (**44** *vs.* **46**). In contrast, comparison among **44**, **47**—**57** with 2,2-dimethylpropanamide at the 7-position demonstrated that the ACAT inhibitory activity was notably dependent on carbon number of the alkyl moiety at the 1-position (R_1). Increase of the carbon number by 8 at R_1 resulted in 43-fold enhancement of the ACAT inhibitory activity (**44** *vs.* **56**). These results clearly demonstrated that the 1-alkyl moiety interacted more effectively with ACAT than the alkyl amide moiety in the indoline derivatives. With respect to length of R_1, the activity appeared to reach the maximal level in octyl (**55**), since **55**—**57** showed similar IC_{50} values. Comparison among **48**—**51**, between **34** and **52** and between **53** and **54** showed that introduction of a branched, cyclic structure, or a double bond into the 1-alkyl moiety tended to decrease ACAT inhibitory activity. The indoline structure with 2,2-dimethylpropanamide and 1-long alkyl chain was identified as a new system favorable for ACAT inhibition. All compounds listed in Table 3 showed anti-peroxidative activity greater than that of probucol.

To decrease the lipophilicity of compound **55** which showed 5-fold weaker ACAT inhibitory activity than YM-750 and more potent anti-peroxidative activity than probucol, we introduced the polar groups hydroxy, amine, carboxylic acid or basic heterocycles into R_1 or R_7 (Table 4). However, R_1 or R_7 bearing polar groups reduced ACAT inhibitory activity in **58**—**66**. Basic but not acidic groups have been successfully introduced into some ACAT inhibitors.[14,28,29] In compounds **59** and **62**, anti-peroxidative activity was also markedly reduced.

Finally, we selected compound **55** for further evaluation and the results are shown in Table 5. This compound was about 2-fold weaker than YM-750 against hepatic ACAT and about 3-fold safer with regard to hepatic/adrenal ACAT selectivity. Compound **55** and YM-750 lowered serum cholesterol levels to similar degrees not only in hyperlipidemic rats fed a high cholesterol diet but also in normolipidemic hamsters fed a regular diet, suggesting the contribution of hepatic

Table 3. Structure and Biological Activities of *N*-(4,6-Dimethylindolin-7-yl)amides

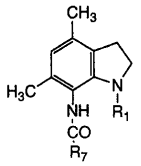

No.	R_1	R_7	ACAT inhibition[a] IC_{50} (μM)	LPO inhibition[b] (%)
34[c]	$(CH_2)_5CH_3$	$C(CH_3)_3$	0.26	96.9
37	$(CH_2)_5CH_3$	CH_3	1.19	91.7
38[c]	$(CH_2)_5CH_3$	$CH(CH_3)_2$	0.38	95.3
39	$(CH_2)_5CH_3$	c-C_3H_6	0.27	94.3
40	$(CH_2)_5CH_3$	$(CH_2)_3CH_3$	0.58	93.6
41	$(CH_2)_5CH_3$	$CH_2C(CH_3)_3$	0.49	96.3
42	$(CH_2)_5CH_3$	$C(CH_3)_2(CH_2)_3CH_3$	0.35	96.3
43	$(CH_2)_5CH_3$	$C(CH_3)_2(CH_2)_5CH_3$	0.40	90.9
44[c]	CH_2CH_3	$C(CH_3)_3$	2.15	24.5
45	CH_2CH_3	$C(CH_3)_2(CH_2)_5CH_3$	0.48	98.1
46	CH_2CH_3	$C(CH_3)_2(CH_2)_8CH_3$	0.26	98.9
47[c]	$(CH_2)_3CH_3$	$C(CH_3)_3$	0.68	65.2
48[c]	$(CH_2)_4CH_3$	$C(CH_3)_3$	0.41	93.2
49[c]	$(CH_2)_2CH(CH_3)_2$	$C(CH_3)_3$	0.52	85.2
50[c]	$CH_2CH=C(CH_3)_2$	$C(CH_3)_3$	1.40	60.3
51	c-C_5H_{10}	$C(CH_3)_3$	0.52	78.6
52	$CH_2CH(CH_2CH_3)_2$	$C(CH_3)_3$	1.10	94.4
53[c]	$(CH_2)_6CH_3$	$C(CH_3)_3$	0.13	97.1
54	CH_2⬡	$C(CH_3)_3$	0.64	96.1
55[c]	$(CH_2)_7CH_3$	$C(CH_3)_3$	0.09	97.9
56[c]	$(CH_2)_9CH_3$	$C(CH_3)_3$	0.05	96.8
57[c]	$(CH_2)_{11}CH_3$	$C(CH_3)_3$	0.07	96.9

a) Rabbit intestinal mucosal microsomes were used as ACAT preparations. *b*) % Inhibition at 10 μM in lipid-peroxidation (LPO) of rat brain homogenate. *c*) Hydrochloride salt.

and intestinal ACAT inhibitory activity. Compound **55**, but not YM-750, showed an inhibitory effect on LDL-oxidation comparable to that of probucol. The peak plasma concentration of **55** in dogs after oral administration at 10 mg/kg was 716 ng/ml, which is an effective concentration against hepatic ACAT and LDL-peroxidation. These observations indicated that compound **55** is a bioavailable ACAT inhibitor with anti-lipidperoxidative activity. In future studies, direct anti-atherosclerotic effects of these dual actions and adreno-safety will be determined using reliable hyperlipidemic and atherosclerotic models such as WHHL rabbits.

Conclusions

A novel series of indolinyl amide and urea derivatives were synthesized to find a new ACAT inhibitor with anti-lipid-peroxidative activity. Among the compounds synthesized, *N*-(4,6-dimethyl-1-octylindolin-7-yl)-2,2-dimethylpropanamide hydrochloride (**55**) showed moderate ACAT inhibitory activity compared to YM-750, potent anti-peroxidative activity comparable to probucol and oral bioavailability sufficient for both effects. Thus, **55** is a promising anti-atherosclerotic drug. The indoline structure was shown to be a pharmacophore responsible for anti-peroxidative activity and to be useful for molecular design of anti-peroxidative drugs.

Table 4. Structure and Biological Activities of *N*-(4,6-Dimethylindolin-7-yl)amide

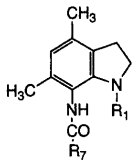

No.	R_1	R_7	ACAT inhibition[a] IC_{50} (μM)	LPO inhibition[b] (%)
58[c]	$(CH_2)_5CH_3$	$C(CH_3)_2CH_2OH$	2.54	89.8
59	$(CH_2)_5CH_3$	$CH_2C(CH_3)_2CH_2CO_2H$	>10	15.2
60	$(CH_2)_5CH_3$		1.51	97.4
61	$(CH_2)_5CH_3$		3.68	92.4
62	$(CH_2)_5CO_2H$	$C(CH_3)_3$	>10	1.9
63		$C(CH_3)_3$	1.10	86.4
64		$C(CH_3)_3$	3.14	13.4
65[c]	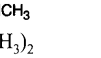	$C(CH_3)_3$	3.12	76.0
66[c]	$(CH_2)_8N(CH_3)_2$	$C(CH_3)_3$	2.88	81.7

a) Rabbit intestinal mucosal microsomes were used as ACAT preparations. *b*) % Inhibition at 10 μM in lipid-peroxidation (LPO) of rat brain homogenate. *c*) Hydrochloride salt.

Experimental

Melting points were measured on a Yamato capillary melting-point apparatus and are uncorrected. IR spectra were taken with a JASCO IR-800 spectrometer. ^{1}H-NMR spectra were recorded at 90 MHz on a Hitachi R-1900 spectrometer using tetramethylsilane as an internal standard. For column chromatography, silica gel (Daisogel No.1001W, Daiso) was used.

***N*-Acetyl-4,6-dimethylindoline (2c)** To a solution of 4,6-dimethylindole **1c** (16.0 g) in AcOH (80 ml) was added sodium cyanoborohydride (13.8 g) portionwise at 5 °C. The reaction mixture was stirred at the same temperature for 1 h, then was poured into ice water and neutralized with 5 N aq. NaOH. 4,6-Dimethylindoline was extracted with AcOEt (200 ml) and the extracts were washed with water and dried. The solvent was removed *in vacuo* to give 4,6-dimethylindoline as an oil which was used for the next reaction without purification. To the solution of 4,6-dimethylindoline in $CHCl_3$ (100 ml) was added Ac_2O (13.5 g) followed by stirring at 20 °C for 1 h. The reaction mixture was washed with aq. $NaHCO_3$ and dried. The solvent was removed *in vacuo* to afford a solid, which was purified by column chromatography (benzene–AcOEt) to yield **2c** (19 g, yield 91%). ^{1}H-NMR ($CDCl_3$) δ: 2.18 (s, 6H), 2.30 (s, 3H), 3.01 (t, 2H, J=8.3 Hz), 4.04 (t, 2H, J=8.3 Hz), 6.66 (s, 1H), 7.90 (s, 1H). IR (Nujol): 1652, 1595 cm^{-1}.

The following compounds **2a**, **2b**, **2d** and **2e** were prepared in a manner similar to that described for *N*-acetyl-4,6-dimethylindoline **2c**.

N-Acetylindoline (**2a**): Yield 95%. ^{1}H-NMR [dimethyl sulfoxide-d_6 (DMSO-d_6)] δ: 2.15 (s, 3H), 3.08 (t, 2H, J=8.5 Hz), 3.99 (t, 2H, J=8.5 Hz), 6.8—7.4 (m, 3H), 8.00 (d, 1H, J=8.0 Hz). IR (Nujol): 1645, 1595 cm^{-1}.

N-Acetyl-6-methylindoline (**2b**): Yield 90%. ^{1}H-NMR ($CDCl_3$) δ: 2.21 (s, 3H), 2.33 (s, 3H), 3.12 (t, 2H, J=8.5 Hz), 4.04 (t, 2H, J=8.5 Hz), 6.82 (d, 2H, J=8.4 Hz), 7.06 (d, 2H, J=8.4 Hz), 8.05 (s, 1H). IR (Nujol): 1625, 1595 cm^{-1}.

N-Acetyl-4,6-diethylindoline (**2d**): Yield 92%. ^{1}H-NMR ($CDCl_3$) δ: 1.20 (t, 3H, J=7.0 Hz), 1.22 (t, 3H, J=7.0 Hz), 2.20 (s, 3H), 2.54 (q, 2H, J=7.0 Hz), 2.62 (q, 2H, J=7.0 Hz), 3.06 (t, 2H, J=8.4 Hz), 4.05 (t, 2H, J=8.4 Hz), 6.72 (s, 1H), 7.95 (s, 1H). IR (Nujol): 1630, 1595 cm^{-1}.

N-Acetyl-4,6-dimethoxyindoline (**2e**): Yield 97%. ^{1}H-NMR ($CDCl_3$) δ: 2.20 (s, 3H), 3.01 (t, 2H, J=8.4 Hz), 3.79 (s, 6H), 4.05 (t, 2H, J=8.4 Hz), 6.17 (s, 1H), 7.54 (s, 1H). IR (Nujol): 1625, 1587 cm^{-1}.

***N*-Acetyl-5-bromo-4,6-dimethyl-7-nitroindoline (4c)** To a stirred solution of **2c** (5.5 g) in AcOH (110 ml), Br_2 (2.0 ml) was added dropwise. The reaction mixture was stirred for a few minutes and then was poured into ice water. The suspension was treated with sodium bisulfite to remove the excess Br_2, and the solid was collected and recrystallized from MeOH to give **3c** as white crystals (6.5 g, yield 83%). mp 170—172 °C. ^{1}H-NMR ($CDCl_3$) δ: 2.19 (s, 3H), 2.28 (s, 3H), 2.39 (s, 3H), 3.06 (t, 2H, J=8.4 Hz), 4.03 (t, 2H, J=8.4 Hz), 7.99 (s, 1H). IR (Nujol): 1659, 1635 cm^{-1}.

3c (6.5 g) was added portionwise to a mixture of fuming nitric acid (1.4 ml), AcOH (25 ml) and H_2SO_4 (25 ml) at 5 °C. The reaction mixture was stirred at the same temperature for 6 h, and then poured into ice water. The precipitate was collected and washed with water to give **4c** (7.0 g, yield 93%). ^{1}H-NMR ($CDCl_3$) δ: 2.22 (s, 3H), 2.36 (s, 3H), 2.46 (s, 3H), 3.13 (t, 2H, J=8.2 Hz), 4.17 (t, 2H, J=8.2 Hz). IR (Nujol): 1672 cm^{-1}.

N-Acetyl-5-bromo-7-nitroindoline (**4a**): Yield 66%. ^{1}H-NMR (DMSO-d_6) δ: 2.20 (s, 3H), 3.20 (t, 2H, J=8.5 Hz), 4.23 (t, 2H, J=8.5 Hz), 7.75 (s, 2H).

N-Acetyl-5-bromo-6-methyl-7-nitroindoline (**4b**): Yield 46%. ^{1}H-NMR ($CDCl_3$) δ: 2.20 (s, 3H), 2.40 (s, 3H), 3.20 (t, 2H, J=8.4 Hz), 4.03 (t, 2H, J=8.4 Hz), 7.45 (s, 1H).

N-Acetyl-5-bromo-4,6-diethyl-7-nitroindoline (**4d**): Yield 50%. ^{1}H-NMR

Table 5. Biological Activities of Compound **55**, YM-750 and Probucol

Compound	ACAT (IC_{50}, μM)[a]		% change in serum TC[b]		LDL-oxidation[c] (% inhibition)
	Liver	Adrenal	Rat (10 mg/kg/d)	Hamster (20 mg/kg/d)	
55	0.058	2.22	−59.5*	−38.8*	50.0
YM-750	0.029	0.38	−46.4*	−36.1*	N.T.
Probucol	N.T.	N.T.	−9.4	N.T.	49.2

a) Liver and adrenal microsomes of rabbits fed a high-cholesterol diet were used as ACAT preparations. *b*) % Changes in serum total cholesterol (TC). Test compounds were orally administered to rats fed a high-cholesterol diet at 10 mg/kg/day (n=6) and to hamsters fed a regular diet at 20 mg/kg/day (n=5). *p<0.01, *vs.* control animals treated with vehicle, Student's t-test. *c*) LDL isolated from rabbits fed a high-cholesterol diet was oxidized with $CuSO_4$ (5 μM). N.T.: not tested.

($CDCl_3$) δ: 1.14 (t, 3H, J=7.5 Hz), 1.21 (t, 3H, J=7.5 Hz), 2.20 (s, 3H), 2.4—2.9 (m, 4H), 3.15 (t, 2H, J=8.5 Hz), 4.16 (t, 2H, J=8.5 Hz).

N-Acetyl-5-bromo-4,6-dimethoxy-7-nitroindoline (**4e**): Yield 49%. ^{1}H-NMR ($CDCl_3$) δ: 2.21 (s, 3H), 3.16 (t, 2H, J=8.5 Hz), 3.83 (s, 3H), 3.89 (s, 3H), 4.07 (t, 2H, J=8.5 Hz).

***N*-Hexyl-5-bromo-4,6-dimethyl-7-nitroindoline (5c)** A solution of **4c** (5.0 g) and NaOH (3.2 g) in 80% MeOH (50 ml) was refluxed for 2 h. After removal of the solvent *in vacuo*, the residue was diluted with $CHCl_3$. The solution was washed with water and dried. The solvent was removed *in vacuo* to give a solid, which was purified by column chromatography (hexane) to give 5-bromo-4,6-dimethyl-7-nitroindoline (3.0 g, yield 69%). ^{1}H-NMR ($CDCl_3$) δ: 2.30 (s, 3H), 2.66 (s, 3H), 3.10 (t, 2H, J=8.5 Hz), 3.82 (t, 2H, J=8.5 Hz). IR (Nujol): 1610, 1576 cm^{-1}.

To a solution of 5-bromo-4,6-dimethyl-7-nitroindoline (3.0 g) in dry DMF (50 ml) was added NaH (*ca.* 60%, 530 mg) followed by stirring at 20 °C for 0.5 h. To the reaction mixture was added *n*-hexyl iodide (2.5 g) and the whole was stirred for 10 h at the same temperature. It was then poured into ice water and **5c** was extracted with AcOEt (100 ml). The extracts were washed with water and dried. The solvent was removed *in vacuo* to give an oil, which was purified by column chromatography (toluene–AcOEt) to yield **5c** as an oil (3.1 g, yield 79%). ^{1}H-NMR ($CDCl_3$) δ: 0.92 (brt, 3H), 1.0—1.7 (m, 8H), 2.25 (s, 3H), 2.30 (s, 3H), 2.92 (t, 2H, J=8.5 Hz), 2.94 (t, 2H, J=6.8 Hz), 3.58 (t, 2H, J=8.5 Hz). IR (Nujol): 1600 cm^{-1}.

N-Hexyl-5-bromo-7-nitroindoline (**5a**): Yield 67%. ^{1}H-NMR ($CDCl_3$) δ: 0.87 (brt, 3H), 1.0—1.7 (m, 8H), 3.05 (t, 2H, J=8.6 Hz), 3.11 (t, 2H, J=7.5 Hz), 3.73 (t, 2H, J=8.6 Hz), 7.18 (d, 1H, J=1.5 Hz), 7.73 (d, 1H, J=1.5 Hz).

N-Hexyl-5-bromo-6-methyl-7-nitroindoline (**5b**): Yield 60%. ^{1}H-NMR ($CDCl_3$) δ: 0.89 (brt, 3H), 1.1—1.7 (m, 8H), 2.26 (s, 3H), 2.8—3.2 (m, 4H), 3.57 (t, 2H, J=8.3 Hz), 7.20 (s, 1H).

N-Hexyl-5-bromo-4,6-diethyl-7-nitroindoline (**5d**): Yield 48%. ^{1}H-NMR ($CDCl_3$) δ: 0.88 (brt, 3H), 1.13 (t, 3H, J=7.5 Hz), 1.21 (t, 3H, J=7.5 Hz), 1.0—1.7 (m, 8H), 2.66 (q, 2H, J=7.5 Hz), 2.68 (q, 2H, J=7.5 Hz), 2.7—3.2 (m, 4H), 3.57 (t, 2H, J=8.4 Hz).

N-Hexyl-5-bromo-4,6-dimethoxy-7-nitroindoline (**5e**): Yield 70%. ^{1}H-NMR ($CDCl_3$) δ: 0.88 (brt, 3H), 1.1—1.8 (m, 8H), 2.98 (t, 2H, J=7.5 Hz), 3.05 (t, 2H, J=8.5 Hz), 3.63 (t, 2H, J=8.5 Hz), 3.83 (s, 3H), 3.90 (s, 3H).

***N*-(1-Hexyl-4,6-dimethylindolin-7-yl)-*N'*-butylurea (27)** A solution of **5c** (2.0 g) in benzene (50 ml) was hydrogenated at 3 atm in the presence of 5% Pd–C (500 mg) at 30 °C for 10 h. After removal of the catalyst by filtration, the filtrate was concentrated *in vacuo*. The residue was diluted with $CHCl_3$ (50 ml) and the solution was washed with aq. $NaHCO_3$ and dried. To the solution was added *n*-butyl isocyanate (550 mg) and the mixture was stirred at 20 °C under N_2 for 20 h. The reaction mixture was concentrated *in vacuo* to give an oil, which was purified by column chromatography ($CHCl_3$–MeOH) to give **27** as a solid (850 mg, yield 42%). mp 192—199 °C: ^{1}H-NMR ($CDCl_3$) δ: 0.88 (brt, 6H), 1.1—1.7 (m, 12H), 2.14 (s, 6H), 2.83 (t, 2H, J=8.3 Hz), 3.0—3.6 (m, 6H), 4.80 (br, 1H), 5.52 (br, 1H), 6.40 (s, 1H). IR (Nujol): 1625, 1603 cm^{-1}.

The following compounds **20**—**25** were prepared in a manner similar to that described for **27** from *N*-hexyl-5-bromo-7-nitroindoline (**5a**) and the appropriate isocyanate.

N-(1-Hexylindolin-7-yl)-*N'*-(2,4,6-trimethylphenyl)urea (**20**): Yield 40%. mp 252—253 °C. ^{1}H-NMR ($CDCl_3$) δ: 0.92 (brt, 3H), 1.1—2.0 (m, 8H), 2.22 (s, 9H), 2.96 (t, 2H, J=7.9 Hz), 3.30 (t, 2H, J=7.0 Hz), 3.40 (t, 2H, J=7.9 Hz), 6.20 (br, 2H), 6.76 (t, 1H, J=7.5 Hz), 6.88 (s, 2H), 6.90 (d, 1H, J=7.5 Hz), 7.15 (d, 1H, J=7.5 Hz). IR (Nujol): 3370, 1615 cm^{-1}.

N-(1-Ethylindolin-7-yl)-*N'*-(2,4,6-trimethylphenyl)urea (**21**): Yield 45%. mp 273—275 °C. ^{1}H-NMR ($CDCl_3$) δ: 1.04 (t, 3H, J=7.0 Hz), 2.27 (s, 9H), 2.96 (t, 2H, J=7.9 Hz), 3.31 (q, 2H, J=7.0 Hz), 3.40 (t, 2H, J=7.9 Hz), 6.30 (br, 2H), 6.78 (t, 1H, J=7.5 Hz), 6.88 (s, 2H), 6.90 (d, 1H, J=7.5 Hz), 7.08 (d, 1H, J=7.5 Hz). IR (Nujol): 3370, 1630 cm^{-1}.

N-(1-Hexylindolin-7-yl)-*N'*-(2,4-difluorophenyl)urea (**22**): Yield 60%. mp 162—163 °C. ^{1}H-NMR ($CDCl_3$) δ: 0.81 (brt, 3H), 1.0—1.7 (m, 8H), 3.03 (t, 2H, J=7.9 Hz), 3.37 (t, 2H, J=7.2 Hz), 3.48 (t, 2H, J=7.9 Hz), 6.6—7.1 (m, 6H), 7.8—8.3 (m, 2H). IR (Nujol): 3290, 1640 cm^{-1}.

N-(1-Ethylindolin-7-yl)-*N'*-(2-hexyloxy-4-methylphenyl)urea (**23**): Yield 30%. mp 119—120 °C. ^{1}H-NMR ($CDCl_3$) δ: 0.86 (brt, 3H), 1.07 (t, 3H, J=7.2 Hz), 1.1—2.0 (m, 8H), 2.27 (s, 3H), 2.97 (t, 2H, J=7.9 Hz), 3.34 (q, 2H, J=7.2 Hz), 3.42 (t, 2H, J=7.9 Hz), 3.79 (t, 2H, J=6.4 Hz), 6.33 (s, 1H), 6.5—7.1 (m, 5H), 7.37 (br, 1H), 8.06 (br, 1H). IR (Nujol): 3280, 1658 cm^{-1}.

N-(1-Hexylindolin-7-yl)-*N'*-(2-hexyloxy-4-methylphenyl)urea (**24**): Yield 31%. mp 104—105 °C. ^{1}H-NMR ($CDCl_3$) δ: 0.6—2.0 (m, 22H), 2.27 (s, 3H), 2.98 (t, 2H, J=7.9 Hz), 3.39 (t, 2H, J=7.0 Hz), 3.43 (t, 2H, J=7.9 Hz), 3.78 (t, 2H, J=7.0 Hz), 6.18 (s, 1H), 6.5—7.1 (m, 5H), 7.34 (br, 1H), 8.07 (br, 1H). IR (Nujol): 3260, 1682, 1640 cm^{-1}.

N-(1-Ethylindolin-7-yl)-*N'*-(4-hexyloxy-2-methylphenyl)urea (**25**): Yield 49%. mp 165—166 °C. ^{1}H-NMR ($CDCl_3$) δ: 0.90 (brt, 3H), 1.06 (t, 3H, J=7.0 Hz), 1.2—1.9 (m, 8H), 2.11 (s, 3H), 2.97 (t, 2H, J=7.9 Hz), 3.30 (q, 2H, J=7.0 Hz), 3.42 (t, 2H, J=7.9 Hz), 3.90 (t, 2H, J=7.1 Hz), 6.6—7.5 (m, 8H). IR (Nujol): 3280, 1640, 1610 cm^{-1}.

***N*-(1-Hexyl-4,6-dimethylindolin-7-yl)-2,2-dimethylpropanamide Hydrochloride (34)** A solution of **5c** (2.0 g) in benzene (50 ml) was hydrogenated at 3 atm in the presence of 5% Pd–C (500 mg) at 30 °C for 10 h. After removal of the catalyst by filtration, the filtrate was concentrated *in vacuo*. The residue was diluted with $CHCl_3$ (50 ml) and the solution was washed with aq. $NaHCO_3$ and dried. To the solution were added pivaloyl chloride (670 mg) and triethylamine (620 mg) followed by stirring at 20 °C for 1 h. The reaction mixture was washed with 5% aq. citric acid, water and dried. The solvent was removed *in vacuo*. The residue was purified by column chromatography ($CHCl_3$–MeOH) to give an oil, which was converted to HCl salt and was recrystallized from EtOH to give **34** (700 mg, yield 34%). mp 184—186 °C. ^{1}H-NMR ($CDCl_3$) δ: 0.90 (brt, 3H), 1.1—1.8 (m, 8H), 1.42 (s, 9H), 2.15 (s, 3H), 2.25 (s, 3H), 2.9—3.3 (m, 4H), 3.5—4.2 (m, 2H), 7.11 (s, 1H), 9.20 (br, 1H). IR (Nujol): 3220, 1670, 1635 cm^{-1}.

The following compounds **32**—**48** were prepared in a manner similar to that described for **34** from **4a**—**4e** and the appropriate acylchloride.

N-(1-Hexylindolin-7-yl)-2,2-dimethylpropanamide (**32**): Yield 46%. mp 92—93 °C. ^{1}H-NMR ($CDCl_3$) δ: 0.82 (brt, 3H), 1.1—1.8 (m, 8H), 1.32 (s, 9H), 2.93 (t, 2H, J=7.9 Hz), 3.02 (t, 2H, J=7.0 Hz), 3.41 (t, 2H, J=7.9 Hz), 6.75 (t, 1H, J=7.7 Hz), 6.90 (d, 2H, J=7.7 Hz), 7.20 (br, 1H), 7.47 (d, 1H, J=7.7 Hz). IR (Nujol): 3250, 1658 cm^{-1}.

N-(1-Hexyl-6-methylindolin-7-yl)-2,2-dimethylpropanamide Hydrochloride (**33**): Yield 34%. mp 173—175 °C. ^{1}H-NMR ($CDCl_3$) δ: 0.86 (brt, 3H), 1.1—2.0 (m, 8H), 1.42 (s, 9H), 2.19 (s, 3H), 2.9—3.5 (m, 4H), 3.5—4.2 (m, 2H), 7.18 (d, 1H, J=7.7 Hz), 7.31 (d, 1H, J=7.7 Hz), 9.36 (br, 1H). IR (Nujol): 3200, 1685, 1635 cm^{-1}.

N-(1-Hexyl-4,6-dimethoxyindolin-7-yl)-2,2-dimethylpropanamide Hydrochloride (**35**): Yield 28%. mp 167—168 °C. ^{1}H-NMR (DMSO-d_6) δ: 0.83 (brt, 3H), 1.1—1.8 (m, 8H), 1.24 (s, 9H), 3.04 (t, 2H, J=7.7 Hz), 3.12 (t, 2H, J=7.0 Hz), 3.77 (t, 2H, J=7.7 Hz), 3.78 (s, 3H), 3.86 (s, 3H), 6.30 (br, 1H), 6.63 (s, 1H), 8.72 (br, 1H). IR (Nujol): 3230, 1665, 1640 cm^{-1}.

N-(4,6-Diethyl-1-hexylindolin-7-yl)-2,2-dimethylpropanamide (**36**): Yield 48%. mp 133—135 °C. ^{1}H-NMR ($CDCl_3$) δ: 0.86 (brt, 3H), 1.15 (t, 3H, J=7.0 Hz), 1.17 (t, 3H, J=7.0 Hz), 1.1—1.7 (m, 8H), 1.34 (s, 9H), 2.42 (q, 2H, J=7.0 Hz), 2.46 (q, 2H, J=7.0 Hz), 2.91 (t, 2H, J=8.1 Hz), 3.09 (t, 2H, J=7.2 Hz), 3.48 (t, 2H, J=8.1 Hz), 6.56 (s, 1H), 7.20 (br, 1H). IR (Nujol): 3240, 1648 cm^{-1}.

N-(1-Hexyl-4,6-dimethylindolin-7-yl)acetamide (**37**): Yield 86%. mp 138—139 °C. ^{1}H-NMR ($CDCl_3$) δ: 0.88 (brt, 3H), 1.0—1.7 (m, 8H), 1.81 (s, 3H), 2.11 (s, 6H), 2.74 (t, 2H, J=7.8 Hz), 3.17 (t, 2H, J=6.7 Hz), 3.38 (t, 2H, J=7.8 Hz), 6.39 (s, 1H), 6.64 (br, 1H). IR (Nujol): 3260, 1645 cm^{-1}.

N-(1-Hexyl-4,6-dimethylindolin-7-yl)-2-methylpropanamide Hydrochloride (**38**): Yield 43%. mp 158—160 °C. ^{1}H-NMR ($CDCl_3$) δ: 0.86 (brt, 3H), 1.33 (d, 3H, J=6.8 Hz), 1.37 (d, 3H, J=6.8 Hz), 1.0—2.0 (m, 8H), 2.19 (s, 3H), 2.26 (s, 3H), 2.6—3.0 (m, 1H), 3.0—3.4 (m, 4H), 3.5—4.3 (m, 2H), 7.12 (s, 1H), 9.48 (br, 1H). IR (Nujol): 3159, 1675, 1630 cm^{-1}.

N-(1-Hexyl-4,6-dimethylindolin-7-yl)cyclopropanecarboxamide (**39**): Yield 50%. mp 157—158 °C. ^{1}H-NMR ($CDCl_3$) δ: 0.6—1.7 (m, 15H), 2.0—2.9 (m, 1H), 2.13 (s, 3H), 2.16 (s, 3H), 2.82 (t, 2H, J=7.8 Hz), 3.1—3.7 (m, 4H), 6.35 (s, 1H), 6.53 (br, 1H). IR (Nujol): 3269, 1649 cm^{-1}.

N-(1-Hexyl-4,6-dimethylindolin-7-yl)pentanamide (**40**): Yield 35%. mp 116—118 °C. ^{1}H-NMR ($CDCl_3$) δ: 0.83 (brt, 6H), 1.0—1.8 (m, 12H), 2.10 (s, 6H), 2.38 (t, 2H, J=6.8 Hz), 2.85 (t, 2H, J=7.9 Hz), 3.22 (t, 2H, J=6.8 Hz), 3.47 (t, 2H, J=7.9 Hz), 6.49 (s, 1H), 7.0 (br, 1H). IR (Nujol): 3267, 1651 cm^{-1}.

N-(1-Hexyl-4,6-dimethylindolin-7-yl)-3,3-dimethylbutanamide (**41**): Yield 46%. mp 107—109 °C. ^{1}H-NMR ($CDCl_3$) δ: 0.95 (brt, 3H), 1.0—1.7 (m, 8H), 1.12 (s, 9H), 2.09 (s, 6H), 2.22 (s, 2H), 2.79 (t, 2H, J=8.1 Hz), 3.12 (t, 2H, J=6.8 Hz), 3.39 (t, 2H, J=8.1 Hz), 6.38 (s, 1H), 6.70 (br, 1H). IR (Nujol): 3340, 1660 cm^{-1}.

N-(1-Hexyl-4,6-dimethylindolin-7-yl)-2,2-dimethylhexanamide (**42**): Yield 51%. mp 71—74 °C. ^{1}H-NMR ($CDCl_3$) δ: 0.90 (brt, 6H), 1.0—1.8 (m, 14H), 1.30 (s, 6H), 2.08 (s, 3H), 2.12 (s, 3H), 2.83 (t, 2H, J=8.2 Hz), 3.14 (t, 2H, J=6.8 Hz), 3.52 (t, 2H, J=8.2 Hz), 6.44 (s, 1H), 6.90 (br, 1H). IR (Nujol): 3280, 1640 cm^{-1}.

N-(1-Hexyl-4,6-dimethylindolin-7-yl)-2,2-dimethyloctanamide (**43**): Yield 71%. Oil. ^{1}H-NMR ($CDCl_3$) δ: 0.88 (brt, 6H), 1.0—1.8 (m, 18H), 1.34 (s, 6H), 2.11 (s, 3H), 2.17 (s, 3H), 2.95 (t, 2H, J=8.1 Hz), 3.09 (t, 2H,

J=6.8 Hz), 3.60 (t, 2H, J=8.1 Hz), 6.72 (s, 1H), 7.90 (br, 1H). IR (neat): 3280, 1650, 1645 cm^{-1}.

N-(1-Ethyl-4,6-dimethylindolin-7-yl)-2,2-dimethylpropanamide Hydrochloride (**44**): Yield 34%. mp 208—210 °C. ^{1}H-NMR ($CDCl_3$) δ: 1.42 (s, 9H), 1.43 (t, 3H, J=7.0 Hz), 2.15 (s, 3H), 2.25 (s, 3H), 3.0—3.5 (m, 4H), 3.6—4.2 (m, 2H), 7.12 (s, 1H), 9.20 (br, 1H). IR (Nujol): 3380, 3240, 1675 cm^{-1}.

N-(1-Ethyl-4,6-dimethylindolin-7-yl)-2,2-dimethyloctanamide (**45**): Yield 24%. mp 70—72 °C. ^{1}H-NMR ($CDCl_3$) δ: 0.87 (brt, 3H), 1.0—1.8 (m, 13H), 1.29 (s, 6H), 2.08 (s, 3H), 2.12 (s, 3H), 2.82 (t, 2H, J=7.8 Hz), 3.26 (q, 2H, J=7.3 Hz), 3.42 (t, 2H, J=7.8 Hz), 6.44 (s, 1H), 6.75 (br, 1H). IR (Nujol): 3230, 1640 cm^{-1}.

N-(1-Ethyl-4,6-dimethylindolin-7-yl)-2,2-dimethylundecanamide (**46**): Yield 38%. mp 55—57 °C. ^{1}H-NMR ($CDCl_3$) δ: 0.88 (brt, 3H), 1.0—1.9 (m, 19H), 1.34 (s, 6H), 2.13 (s, 3H), 2.19 (s, 3H), 2.99 (t, 2H, J=7.8 Hz), 3.22 (q, 2H, J=7.3 Hz), 3.65 (t, 2H, J=7.8 Hz), 6.80 (s, 1H), 8.10 (br, 1H). IR (Nujol): 3210, 1660, 1640 cm^{-1}.

N-(1-Butyl-4,6-dimethylindolin-7-yl)-2,2-dimethylpropanamide Hydrochloride (**47**): Yield 64%. mp 205—207 °C. ^{1}H-NMR ($CDCl_3$) δ: 0.92 (t, 2H, J=7.0 Hz), 1.0—2.0 (m, 4H), 1.42 (s, 9H), 2.15 (s, 3H), 2.25 (s, 3H), 2.9—3.4 (m, 4H), 3.6—4.2 (m, 2H), 7.12 (s, 1H), 9.21 (br, 1H). IR (Nujol): 3320, 1665, 1630 cm^{-1}.

N-(4,6-Dimethyl-1-pentylindolin-7-yl)-2,2-dimethylpropanamide Hydrochloride (**48**): Yield 50%. mp 205—206 °C. ^{1}H-NMR ($CDCl_3$) δ: 0.89 (brt, 3H), 1.0—2.0 (m, 6H), 1.42 (s, 9H), 2.15 (s, 3H), 2.25 (s, 3H), 2.8—3.3 (m, 4H), 3.5—4.2 (m, 2H), 7.11 (s, 1H), 9.20 (br, 1H). IR (Nujol): 3230, 1670, 1645 cm^{-1}.

***N*-(1-Hexyl-4,6-dimethylindolin-7-yl)-3-hydroxy-2,2-dimethylpropanamide Hydrochloride (58)** After condensation of *N*-hexyl-7-amino-4,6-dimethylindoline with 3-acetoxy-2,2-dimethylpropionyl chloride in a manner similar to that described for **34**, the resulting *N*-(1-hexyl-4,6-dimethylindolin-7-yl)-3-acetoxy-2,2-dimethylpropanamide was hydrolyzed with NaOH and converted to HCl salt (**58**). Yield 96%. mp 150—152 °C. ^{1}H-NMR ($CDCl_3$) δ: 0.88 (brt, 3H), 1.0—1.8 (m, 8H), 1.19 (s, 6H), 1.99 (s, 3H), 2.08 (s, 3H), 2.78 (t, 2H, J=8.1 Hz), 3.10 (t, 2H, J=7.0 Hz), 3.37 (t, 2H, J=8.1 Hz), 3.48 (s, 2H), 4.00 (br, 1H), 6.35 (s, 1H), 7.81 (br, 1H). IR (Nujol): 3340, 1660 cm^{-1}.

N-(1-Hexyl-4,6-dimethylindolin-7-yl)-4-carboxy-3,3-dimethylbutanamide (**59**): After condensation of *N*-hexyl-7-amino-4,6-dimethylindoline with 4-methoxycarbonyl-3,3-dimethylbutyryl chloride in a manner similar to that described for **34**, the resulting *N*-(1-hexyl-4,6-dimethylindolin-7-yl)-4-methoxycarbonyl-3,3-dimethylbutanamide was hydrolyzed with NaOH to give **59**. Yield 50%. Oil. ^{1}H-NMR ($CDCl_3$) δ: 0.82 (brt, 3H), 1.0—1.8 (m, 8H), 1.21 (s, 6H), 2.17 (s, 6H), 2.48 (s, 2H), 2.53 (s, 2H), 3.01 (t, 2H, J=8.1 Hz), 3.10 (t, 2H, J=7.2 Hz), 3.54 (t, 2H, J=8.1 Hz), 6.70 (s, 1H), 7.70 (br, 1H), 8.70 (br, 1H). IR (neat): 1725, 1650 cm^{-1}.

N-(1-Hexyl-4,6-dimethylindolin-7-yl)nicotinamide (**60**): Yield 85%. mp 88—90 °C. ^{1}H-NMR ($CDCl_3$) δ: 0.82 (brt, 3H), 1.0—2.0 (m, 8H), 2.15 (s, 6H), 2.82 (t, 2H, J=8.1 Hz), 3.13 (t, 2H, J=7.2 Hz), 3.50 (t, 2H, J=8.1 Hz), 6.45 (s, 1H), 7.3—7.6 (m, 2H), 8.1—8.3 (m, 1H), 8.7—8.9 (m, 1H), 9.10 (br, 1H). IR (Nujol): 3340, 1660 cm^{-1}.

N-(1-Hexyl-4,6-dimethylindolin-7-yl)-1-ethylpiperidine-4-carboxamide (**61**): Yield 58%. mp 173—177 °C. ^{1}H-NMR ($CDCl_3$) δ: 0.89 (brt, 3H), 1.11 (t, 3H, J=7.0 Hz), 1.0—1.7 (m, 8H), 2.05 (s, 3H), 2.11 (s, 3H), 1.7—2.6 (m, 9H), 2.85 (t, 2H, J=8.2 Hz), 2.8—3.3 (m, 4H), 3.41 (t, 2H, J=8.2 Hz), 6.39 (br, 1H), 6.70 (s, 1H). IR (Nujol): 3270, 1650 cm^{-1}.

***N*-(1-Acetyl-4,6-dimethylindolin-7-yl)-2,2-dimethylpropanamide (6c)** A suspension of **4c** (10 g) in MeOH (300 ml) was hydrogenated at 3 atm in the presence of 5% Pd–C (500 mg) at 30 °C for 10 h. After removal of the catalyst by filtration, the filtrate was concentrated *in vacuo*. The residue was diluted with $CHCl_3$ (200 ml) and the solution was washed with aq. $NaHCO_3$ and dried. To this solution were added pivaloyl chloride (3.9 g) and triethylamine (3.2 g) followed by stirring at 20 °C for 1 h. The reaction mixture was washed with 5% aq. citric acid, water and dried. The solvent was removed *in vacuo* to give a solid, which was purified by column chromatography ($CHCl_3$–MeOH) to give **6c** (6.6 g, yield 71%). ^{1}H-NMR ($CDCl_3$) δ: 1.27 (s, 9H), 2.17 (s, 6H), 2.29 (s, 3H), 2.94 (t, 2H, J=7.7 Hz), 4.09 (t, 2H, J=7.7 Hz), 6.87 (s, 1H), 9.10 (br, 1H). IR (Nujol): 3194, 1677, 1639, 1610 cm^{-1}.

***N*-(4,6-Dimethyl-1-octylindolin-7-yl)-2,2-dimethylpropanamide Hydrochloride (55)** A solution of **6c** (3.7 g) and NaOH (2.6 g) in 60% MeOH (20 ml) was refluxed for 7 h. After removal of the solvent *in vacuo*, the residue was diluted with $CHCl_3$ (100 ml), washed with water and dried. The solvent was removed *in vacuo* to give *N*-(4,6-dimethylindolin-7-yl)-2,2-dimethylpropanamide (2.1 g, yield 65%), which was used for the following reaction without further purification. A mixture of *N*-(4,6-dimethylindolin-7-yl)-2,2-dimethylpropanamide (2.1 g), *n*-octyl bromide (4.1 g) and K_2CO_3 (2.3 g) in DMF (30 ml) was stirred under N_2 at 40 °C for 10 h. The reaction mixture was poured into water and extracted with AcOEt (100 ml). The extracts were washed with water and dried. The solvent was removed *in vacuo*. The residue was purified by column chromatography ($CHCl_3$–MeOH) to give an oil, which was converted to HCl salt and was recrystallized from EtOH to give **55** (2.0 g, yield 59%). mp 123—124 °C. ^{1}H-NMR ($CDCl_3$) δ: 0.87 (brt, 3H), 1.1—1.9 (m, 12H), 1.42 (s, 9H), 2.16 (s, 3H), 2.26 (s, 3H), 2.9—3.3 (m, 4H), 3.5—4.2 (m, 2H), 7.11 (s, 1H), 9.21 (br, 1H). IR (Nujol): 3200, 1660, 1625 cm^{-1}. *Anal.* Calcd for $C_{23}H_{38}N_2O \cdot HCl \cdot 0.7H_2O$: C, 67.77; H, 9.99; N, 6.87. Found: C, 67.78; H, 9.99; N, 6.86.

The following compounds **49**—**57** and **62**—**66** were prepared in a manner similar to that described in **55** from **6c** and the corresponding halide.

N-(1-Isopentyl-4,6-dimethylindolin-7-yl)-2,2-dimethylpropanamide Hydrochloride (**49**): Yield 39%. mp 205—206 °C. ^{1}H-NMR ($CDCl_3$) δ: 0.84 (brd, 6H), 1.2—1.9 (m, 3H), 1.37 (s, 9H), 2.11 (s, 3H), 2.21 (s, 3H), 2.9—3.3 (m, 4H), 3.6—4.2 (m, 2H), 7.08 (s, 1H), 9.14 (br, 1H). IR (Nujol): 3600, 3210, 1680 cm^{-1}.

N-[4,6-Dimethyl-1-(3-methyl-2-butenyl)indolin-7-yl]-2,2-dimethylpropanamide Hydrochloride (**50**): Yield 18%. mp 185—187 °C. ^{1}H-NMR ($CDCl_3$) δ: 1.42 (s, 9H), 1.67 (s, 3H), 1.81 (s, 3H), 2.16 (s, 3H), 2.25 (s, 3H), 2.9—3.2 (m, 2H), 3.4—4.2 (m, 4H), 5.44 (brt, 1H), 7.12 (s, 1H), 9.27 (br, 1H). IR (Nujol): 3200, 1670, 1630 cm^{-1}.

N-(1-Cyclopentyl-4,6-dimethylindolin-7-yl)-2,2-dimethylpropanamide (**51**): Yield 22%. mp 172—174 °C. ^{1}H-NMR ($CDCl_3$) δ: 1.23 (s, 9H), 1.3—1.9 (m, 8H), 2.06 (s, 3H), 2.10 (s, 3H), 2.89 (t, 2H, J=8.3 Hz), 3.42 (t, 2H, J=8.3 Hz), 4.1—4.5 (m, 1H), 6.40 (s, 1H), 6.77 (br, 1H). IR (Nujol): 3300, 1650 cm^{-1}.

N-[1-(2-Ethylbutyl)-4,6-dimethylindolin-7-yl]-2,2-dimethylpropanamide (**52**): Yield 42%. mp 171—172 °C. ^{1}H-NMR ($CDCl_3$) δ: 0.89 (t, 6H, J=6.5 Hz), 1.1—1.9 (m, 5H), 1.32 (s, 9H), 2.04 (s, 3H), 2.11 (s, 3H), 2.80 (t, 2H, J=8.3 Hz), 3.09 (d, 2H, J=6.6 Hz), 3.34 (t, 2H, J=8.3 Hz), 6.38 (s, 1H), 6.67 (br, 1H). IR (Nujol): 3270, 1645 cm^{-1}.

N-(1-Heptyl-4,6-dimethylindolin-7-yl)-2,2-dimethylpropanamide Hydrochloride (**53**): Yield 24%. mp 145—147 °C. ^{1}H-NMR ($CDCl_3$) δ: 0.90 (brt, 3H), 1.1—1.9 (m, 10H), 1.42 (s, 9H), 2.15 (s, 3H), 2.25 (s, 3H), 2.9—3.3 (m, 4H), 3.5—4.2 (m, 2H), 7.11 (s, 1H), 9.21 (br, 1H). IR (Nujol): 3230, 1670 cm^{-1}.

N-(1-Cyclohexylmethyl-4,6-dimethylindolin-7-yl)-2,2-dimethylpropanamide (**54**): Yield 62%. mp 174—175 °C. ^{1}H-NMR ($CDCl_3$) δ: 0.6—2.0 (m, 11H), 1.34 (s, 9H), 2.04 (s, 3H), 2.10 (s, 3H), 2.81 (t, 2H, J=8.3 Hz), 3.01 (d, 2H, J=7.0 Hz), 3.39 (t, 2H, J=8.3 Hz), 6.36 (s, 1H), 6.69 (br, 1H). IR (Nujol): 3280, 1645 cm^{-1}.

N-(1-Decyl-4,6-dimethylindolin-7-yl)-2,2-dimethylpropanamide Hydrochloride (**56**): Yield 40%. mp 136—138 °C. ^{1}H-NMR ($CDCl_3$) δ: 0.87 (brt, 3H), 1.1—1.8 (m, 16H), 1.42 (s, 9H), 2.15 (s, 3H), 2.25 (s, 3H), 2.9—3.3 (m, 4H), 3.5—4.2 (m, 2H), 7.11 (s, 1H), 9.21 (br, 1H). IR (Nujol): 3165, 1674 cm^{-1}.

N-(1-Dodecyl-4,6-dimethylindolin-7-yl)-2,2-dimethylpropanamide Hydrochloride (**57**): Yield 54%. mp 124—126 °C. ^{1}H-NMR ($CDCl_3$) δ: 0.91 (brt, 3H), 1.1—1.9 (m, 20H), 1.42 (s, 9H), 2.15 (s, 3H), 2.25 (s, 3H), 2.9—3.3 (m, 4H), 3.5—4.2 (m, 2H), 7.11 (s, 1H), 9.21 (br, 1H). IR (Nujol): 3170, 1662 cm^{-1}.

N-[1-(5-Carboxypentyl)-4,6-dimethylindolin-7-yl]-2,2-dimethylpropanamide (**62**): *N*-[1-(5-Methoxycarbonylpentyl)-4,6-dimethylindolin-7-yl]-2,2-dimethylpropanamide was hydrolyzed with NaOH to give **62** as an oil. Yield 60%. ^{1}H-NMR ($CDCl_3$) δ: 1.2—1.8 (m, 6H), 1.32 (s, 9H), 2.07 (s, 3H), 2.18 (s, 3H), 2.29 (t, 2H, J=6.8 Hz), 2.84 (t, 2H, J=7.9 Hz), 3.04 (t, 2H, J=6.8 Hz), 3.42 (t, 2H, J=7.9 Hz), 5.50 (br, 1H), 6.52 (s, 1H), 7.28 (br, 1H). IR (neat): 3300, 1720 cm^{-1}.

N-[1-(8-1*H*-Imidazolyloctyl)-4,6-dimethylindolin-7-yl]-2,2-dimethylpropanamide (**63**): Condensation of *N*-[1-(8-bromooctyl)-4,6-dimethylindolin-7-yl]-2,2-dimethylpropanamide with imidazole gave **63** as an oil. Yield 90%. ^{1}H-NMR ($CDCl_3$) δ: 1.1—1.9 (m, 12H), 1.32 (s, 9H), 2.06 (s, 3H), 2.11 (s, 3H), 2.82 (t, 2H, J=8.1 Hz), 3.14 (t, 2H, J=6.8 Hz), 3.41 (t, 2H, J=8.1 Hz), 3.91 (t, 2H, J=6.8 Hz), 6.40 (s, 1H), 6.70 (br, 1H), 6.89 (s, 1H), 7.04 (s, 1H), 7.44 (s, 1H). IR (neat): 3300, 1660 cm^{-1}.

N-[4,6-Dimethyl-1-(3-morpholinopropyl)indolin-7-yl]-2,2-dimethylpropanamide (**64**): Condensation of *N*-[1-(3-bromopropyl)-4,6-dimethylindolin-7-yl]-2,2-dimethylpropanamide with morpholine gave **64** as a crystal. Yield 60%. mp 125—126 °C. ^{1}H-NMR ($CDCl_3$) δ: 1.5—2.0 (m, 2H), 1.34 (s, 9H), 2.05 (s, 3H), 2.11 (s, 3H), 2.1—2.6 (m, 2H), 2.3—2.6 (m, 4H), 2.82 (t, 2H, J=7.7 Hz), 3.32 (t, 2H, J=6.8 Hz), 3.42 (t, 2H, J=7.7 Hz), 3.6—3.8

(m, 4H), 6.40 (s, 1H), 6.95 (br, 1H). IR (neat): 3250, 1642 cm^{-1}.

N-{4,6-Dimethyl-1-[8-(*N*-methylpiperazinyl)octyl]indolin-7-yl}-2,2-dimethylpropanamide Trihydrochloride (**65**): Condensation of *N*-[1-(8-bromooctyl)-4,6-dimethylindolin-7-yl]-2,2-dimethylpropanamide with *N*-methylpiperazine and conversion to HCl salt gave **65** as a white powder. Yield 94%. ^{1}H-NMR (DMSO-d_6) δ: 1.1—1.9 (m, 12H), 1.30 (s, 9H), 2.06 (s, 3H), 2.28 (s, 3H), 2.50 (s, 3H), 2.9—4.4 (m, 16H), 7.10 (s, 1H), 9.35 (br, 1H), 12.0 (br, 3H). IR (Nujol): 3410, 1670 cm^{-1}.

N-{4,6-Dimethyl-1-[8-(*N*,*N*-dimethylamino)octyl]indolin-7-yl}-2,2-dimethylpropanamide Dihydrochloride (**66**): Condensation of *N*-[1-(8-bromooctyl)-4,6-dimethylindolin-7-yl]-2,2-dimethylpropanamide with dimethylamine and conversion to HCl salt gave **66** as a white powder. Yield 90%. ^{1}H-NMR (DMSO-d_6) δ: 1.1—2.0 (m, 12H), 1.31 (s, 9H), 2.07 (s, 3H), 2.25 (s, 3H), 2.65 (s, 3H), 2.71 (s, 3H), 2.8—3.4 (m, 6H), 3.7—4.0 (m, 2H), 7.18 (s, 1H), 9.46 (br, 1H), 11.0 (br, 2H). IR (Nujol): 3420,1670 cm^{-1}.

1-Hexyl-4,6-dimethyl-5-nitroindoline (9c) Fuming nitric acid (0.87 ml) was added dropwise to a solution of *N*-acetyl-4,6-dimethylindoline **2c** (2.6 g) in Ac_2O (35 ml) at 5 °C. The mixture was stirred at 20 °C for 1 h, neutralized with aq. $NaHCO_3$ and **7c** was extracted with $CHCl_3$ (100 ml). The extracts were washed with water and dried. The solvent was removed *in vacuo* to give **7c** as a solid (2.4 g, yield 73%). ^{1}H-NMR ($CDCl_3$) δ: 2.17 (s, 3H), 2.24 (s, 3H), 2.30 (s, 3H), 3.08 (t, 2H, J=8.6 Hz), 4.12 (t, 2H, J=8.6 Hz), 8.00 (s, 1H). IR (Nujol): 1680, 1595 cm^{-1}.

A solution of **7c** (2.4 g) and conc. HCl 10 ml in MeOH (100 ml) was refluxed for 10 h. After removal of the solvent *in vacuo*, the residue was diluted with $CHCl_3$ (200 ml). The solution was washed with water, aq. $NaHCO_3$ and dried. The solvent was removed *in vacuo* to give an oil which was purified by column chromatography (hexane) to give **8c** as a solid (1.8 g, yield 99%). ^{1}H-NMR ($CDCl_3$) δ: 2.19 (s, 3H), 2.25 (s, 3H), 2.96 (t, 2H, J=8.5 Hz), 3.64 (t, 2H, J=8.5 Hz), 3.8 (br, 1H), 6.24 (s, 1H). IR (Nujol): 3390, 1615 cm^{-1}.

To a solution of **8c** (1.8 g) in dry DMF (20 ml) was added NaH (*ca.* 60%, 450 mg) followed by stirring at 20 °C for 0.5 h. To the reaction mixture was added *n*-hexyl bromide (1.8 g) followed by stirring at the same temperature for 5 h. The mixture was then poured into ice water and **9c** was extracted with AcOEt (300 ml). The extracts were washed with water and dried. The solvent was removed *in vacuo* to give an oil, which was purified by column chromatography (toluene–AcOEt) to give **9c** as an oil (2.5 g, yield 88%). ^{1}H-NMR ($CDCl_3$) δ: 0.90 (br t, 3H), 1.1—1.8 (m, 8H), 2.18 (s, 3H), 2.30 (s, 3H), 2.99 (t, 2H, J=8.4 Hz), 3.09 (t, 2H, J=7.0 Hz), 3.51 (t, 2H, J=8.4 Hz), 5.99 (s, 1H). IR (Nujol): 1605 cm^{-1}.

***N*-(1-Hexyl-4,6-dimethylindolin-5-yl)-*N'*-butylurea (26)** A solution of **9c** (1.0 g) in benzene (25 ml) was hydrogenated at 3 atm in the presence of 5% Pd–C (250 mg) at 30 °C for 10 h. After removal of the catalyst by filtration, the filtrate was concentrated *in vacuo*. To the residue dissolved in $CHCl_3$ (20 ml) was added *n*-butyl isocyanate (400 mg) followed by stirring under N_2 at 20 °C for 20 h. The reaction mixture was washed with water and dried. The solvent was removed *in vacuo* to give a solid, which was purified by column chromatography ($CHCl_3$–MeOH) and was recrystallized from EtOH to give **26** (650 mg, yield 52%). mp 143—145 °C. ^{1}H-NMR ($CDCl_3$) δ: 0.90 (br t, 6H), 1.0—1.9 (m, 12H), 2.09 (s, 3H), 2.19 (s, 3H), 2.86 (t, 2H, J=8.6 Hz), 3.03 (t, 2H, J=7.0 Hz), 3.19 (t, 2H, J=7.0 Hz), 3.48 (t, 2H, J=8.6 Hz), 4.30 (br, 1H), 5.45 (br, 1H), 6.18 (s, 1H). IR (Nujol): 3300, 1638, 1610 cm^{-1}.

N-(1-Hexylindolin-5-yl)-*N'*-(2,4,6-trimethylphenyl)urea (**19**): **19** was prepared from **2a** in a manner similar to that described for **26**. Yield 44%. mp 201—202 °C. ^{1}H-NMR (DMSO-d_6) δ: 0.87 (br t, 3H), 1.1—1.8 (m, 8H), 2.15 (s, 6H), 2.21 (s, 3H), 2.6—3.0 (m, 4H), 3.20 (t, 2H, J=7.6 Hz), 6.37 (d, 1H, J=8.3 Hz), 6.85 (s, 2H), 6.85 (d, 1H, J=8.3 Hz), 7.14 (s, 1H), 7.36 (br, 1H), 8.09 (br, 1H). IR (Nujol): 3290, 1640 cm^{-1}.

***N*-(1-Hexyl-4,6-dimethylindolin-5-yl)-2,2-dimethylpropanamide (30)** A solution of **9c** (1.0 g) in benzene (25 ml) was hydrogenated at 3 atm in the presence of 5% Pd–C (250 mg) at 30 °C for 10 h. After removal of the catalyst by filtration, the filtrate was concentrated *in vacuo*. To the residue dissolved in $CHCl_3$ (20 ml) was added pivaloyl chloride (470 mg) and triethylamine (395 mg) followed by stirring at 20 °C for 1 h. The reaction mixture was washed with 5% aq. citric acid, water and dried. The solvent was removed *in vacuo* to give an oil, which was purified by column chromatography ($CHCl_3$–MeOH) and was recrystallized from EtOH to give **30** (900 mg, yield 76%). mp 122—123 °C. ^{1}H-NMR ($CDCl_3$) δ: 0.85 (br t, 3H), 1.1—1.8 (m, 8H), 1.33 (s, 9H), 2.00 (s, 3H), 2.11 (s, 3H), 2.82 (t, 2H, J=8.1 Hz), 2.99 (t, 2H, J=7.0 Hz), 3.33 (t, 2H, J=8.1 Hz), 6.16 (s, 1H), 6.70 (br, 1H). IR (Nujol): 3270, 1640, 1610 cm^{-1}.

5,7-Dimethyl-6-nitroindoline (13) To a solution of 5,7-dimethylindole **11** (3.4 g) in AcOH (340 ml) was added sodium cyanoborohydride (2.9 g) at 10 °C, and the reaction mixture was stirred at the same temperature for 1 h. The mixture was poured into ice water and neutralized with 5 N aq. NaOH. 5,7-Dimethylindoline **12** was extracted with AcOEt (200 ml). The extracts were washed with water and dried and the solvent was removed *in vacuo* to give **12** as an oil (2.5 g, yield 73%). ^{1}H-NMR ($CDCl_3$) δ: 2.09 (s, 3H), 2.24 (s, 3H), 2.99 (t, 2H, J=8.3 Hz), 3.15 (br, 1H), 3.53 (t, 2H, J=8.3 Hz), 6.68 (s, 1H), 6.80 (s, 1H). IR (Nujol): 3370, 1615 cm^{-1}.

Fuming nitric acid (0.78 ml) in H_2SO_4 (5 ml) was added dropwise to a solution of **12** (2.5 g) in H_2SO_4 (25 ml) at 5 °C. After stirring at the same temperature for 1 h, the reaction mixture was poured into water and neutralized with aq. NaOH, and **13** was extracted with $CHCl_3$ (100 ml). The extracts were washed with water and dried. The solvent was removed *in vacuo* to give an oil, which was purified by column chromatography ($CHCl_3$–MeOH) to give **13** as an oil (2.3 g, yield 70%). ^{1}H-NMR ($CDCl_3$) δ: 2.02 (s, 3H), 2.17 (s, 3H), 3.03 (t, 2H, J=8.1 Hz), 3.40 (br, 1H), 3.60 (t, 2H, J=8.1 Hz), 6.83 (s, 1H).

***N*-(1-Hexyl-5,7-dimethylindolin-6-yl)-2,2-dimethylpropanamide (28)** To a solution of **13** (2.3 g) in dry DMF (23 ml) was added NaH (*ca.* 60%, 530 mg), and the mixture was stirred at 20 °C for 0.5 h. To the reaction mixture was added *n*-hexyl iodide (2.8 g) followed by stirring at the same temperature for 15 h. The mixture was poured into ice water and **14** was extracted with AcOEt (100 ml). The extracts were washed with water and dried. The solvent was removed *in vacuo* to give an oil, which was purified by column chromatography (toluene–AcOEt) to give **14** as an oil (1.0 g, yield 30%). ^{1}H-NMR ($CDCl_3$) δ: 0.89 (br t, 3H), 1.1—1.9 (m, 8H), 2.16 (s, 6H), 2.94 (t, 2H, J=8.3 Hz), 3.13 (t, 2H, J=6.8 Hz), 3.44 (t, 2H, J=8.3 Hz), 6.79 (s, 1H).

A solution of **14** (1.0 g) in benzene (40 ml) was hydrogenated at 3 atm in the presence of 5% Pd–C (250 mg) at 30 °C for 10 h. After removal of the catalyst by filtration, the filtrate was concentrated *in vacuo*. To the residue dissolved in $CHCl_3$ (20 ml) were added pivaloyl chloride (470 mg) and triethylamine (400 mg) followed by stirring at 20 °C for 1 h. The reaction mixture was washed with 5% aq. citric acid, water and dried. The solvent was removed *in vacuo* to give an oil which was purified by column chromatography ($CHCl_3$–MeOH) and was recrystallized from EtOH to give **28** (100 mg, yield 8.4%). mp 117—118 °C. ^{1}H-NMR ($CDCl_3$) δ: 0.88 (br t, 3H), 1.1—1.8 (m, 8H), 1.35 (s, 9H), 2.09 (s, 6H), 1.8—2.2 (m, 4H), 3.39 (t, 2H, J=8.1 Hz), 6.81 (s, 1H). IR (Nujol): 3370, 1640 cm^{-1}.

***N*-Acetyl-5-hexyloxy-6-nitroindoline (17a)** The mixture of *N*-acetyl-5-hydroxyindoline **15** (5.0 g), *n*-hexyl bromide (5.6 g) and K_2CO_3 (8.0 g) in EtOH (50 ml) was refluxed for 10 h. After removal of EtOH *in vacuo*, the residue was diluted with AcOEt (100 ml). The solution was washed with water and dried. The solvent was removed *in vacuo* to give an oil, which was purified by column chromatography (toluene–AcOEt) to give **16a** as a solid (5.2 g, yield 58%). ^{1}H-NMR ($CDCl_3$) δ: 0.85 (br t, 3H), 1.1—1.9 (m, 8H), 2.19 (s, 3H), 3.14 (t, 2H, J=8.4 Hz), 3.92 (t, 2H, J=8.4 Hz), 4.03 (t, 2H, J=6.5 Hz), 6.70 (d, 1H, J=9.4 Hz), 6.74 (s, 1H), 8.10 (d, 1H, J=9.4 Hz). IR (Nujol): 1652, 1615 cm^{-1}.

Fuming nitric acid (0.99 ml) was added dropwise to the solution of **16a** (5.2 g) in Ac_2O (52 ml) at 5 °C. After stirring at 20 °C for 1 h, the reaction mixture was neutralized with aq. $NaHCO_3$ and **17a** was extracted with $CHCl_3$ (200 ml). The extracts were washed with water and dried. The solvent was removed *in vacuo* to give **17a** as a solid (2.9 g, yield 47%). ^{1}H-NMR ($CDCl_3$) δ: 0.90 (br t, 3H), 1.1—2.0 (m, 8H), 2.20 (s, 3H), 3.21 (t, 2H, J=8.0 Hz), 4.02 (t, 2H, J=6.8 Hz), 4.09 (t, 2H, J=8.0 Hz), 6.87 (s, 1H), 8.57 (s, 1H). IR (Nujol): 1640, 1620 cm^{-1}.

***N*-(1-Ethyl-5-hexyloxyindolin-6-yl)-2,2-dimethylpropanamide Hydrochloride (31)** A solution of **17a** (2.0 g) and conc. HCl (6 ml) in MeOH (40 ml) was refluxed for 4 h. After removal of the MeOH *in vacuo*, the residue was neutralized with aq. $NaHCO_3$. 5-Hexyloxy-6-nitroindoline was extracted with AcOEt (100 ml). The extracts were washed with water and dried. The solvent was removed *in vacuo* to give an oil, which was purified by column chromatography (hexane) to give 5-hexyloxy-6-nitroindoline as an oil (1.6 g, yield 92%). ^{1}H-NMR ($CDCl_3$) δ: 0.89 (br t, 3H), 1.1—1.9 (m, 8H), 3.05 (t, 2H, J=7.9 Hz), 3.10 (br, 1H), 3.60 (t, 2H, J=7.9 Hz), 4.00 (t, 2H, J=6.3 Hz), 6.88 (s, 1H), 7.04 (s, 1H). IR (Nujol): 3370 cm^{-1}.

The mixture of 5-hexyloxy-6-nitroindoline (1.6 g), ethyl iodide (1.0 g) and K_2CO_3 (1.7 g) in dry DMF (16 ml) was stirred at 20 °C for 10 h. The reaction mixture was poured into ice water, and **18a** was extracted with AcOEt (200 ml). The extracts were washed with water and dried. The solvent was removed *in vacuo* to give an oil, which was purified by column chromatography (toluene–AcOEt) to give **18a** as oil (1.3 g, yield 73%). ^{1}H-NMR ($CDCl_3$) δ: 0.90 (br t, 3H), 1.18 (t, 3H, J=7.2 Hz), 1.1—1.9 (m, 8H), 2.97 (t,

2H, J=8.1 Hz), 3.06 (q, 2H, J=7.2 Hz), 3.36 (t, 2H, J=8.1 Hz), 4.00 (t, 2H, J=6.4 Hz), 6.86 (s, 2H). IR (Nujol): 1582 cm^{-1}.

A solution of **18a** (1.2 g) in benzene (40 ml) was hydrogenated at 3 atm in the presence of 5% Pd–C (120 mg) at 30 °C for 10 h. After removal of the catalyst by filtration, the filtrate was concentrated *in vacuo*. To the residue dissolved in $CHCl_3$ (10 ml) were added pivaloyl chloride (490 mg) and triethylamine (410 mg) followed by stirring at 20 °C for 1 h. The reaction mixture was washed with 5% aq. citric acid, water and dried. The solvent was removed *in vacuo* to give an oil, which was purified by column chromatography ($CHCl_3$–MeOH), converted to HCl salt and was recrystallized from EtOH to give **31** (470 mg, yield 33%). mp 165—167 °C. ^{1}H-NMR ($CDCl_3$) δ: 0.92 (br t, 3H), 1.1—2.0 (m, 11H), 1.31 (s, 9H), 3.1—3.8 (m, 6H), 3.98 (t, 2H, J=6.8 Hz), 6.82 (s, 1H), 8.17 (br, 1H), 8.54 (s, 1H). IR (Nujol): 3430, 1678 cm^{-1}.

N-(1-Hexyl-5-isopropyloxyindolin-6-yl)-2,2-dimethylpropanamide Hydrochloride (**29**): Yield 40%. mp 173—176 °C. ^{1}H-NMR ($CDCl_3$) δ: 0.93 (br t, 3H), 1.1—2.1 (m, 8H), 1.30 (s, 9H), 1.40 (d, 6H, J=6.8 Hz), 3.1—4.2 (br, 6H), 4.58 (q, 1H, J=6.8 Hz), 6.83 (s, 1H), 8.21 (br, 1H), 8.55 (s, 1H). IR (Nujol): 3410, 1682, 1615 cm^{-1}.

In Vitro* ACAT Activity** Intestinal, hepatic and adrenal microsomes were prepared according to the method of Field and Mathur.[30] Briefly, the intestinal mucosa, liver and adrenal isolated from male Japanese White rabbits fed a high cholesterol diet for a month were homogenized in a buffered sucrose solution (250 mM sucrose, 5 mM KH_2PO_4, 1 mM EDTA, 1 mM dithioerythritol, pH 7.4) using a Teflon homogenizer. The homogenate was spun at 12000 ***g for 15 min at 4 °C. The resulting supernatant was centrifuged at 105000 ***g*** for 30 min at 4 °C. The microsomal pellet obtained was re-homogenized in cold buffered sucrose solution and used as the ACAT preparation. ACAT activity was determined according to the method described by Heider *et al.*[31] The microsomes of the intestine, adrenal or liver were incubated in phosphate buffer (pH 7.4) containing 500 μl of 30 nmol bovine serum albumin (BSA). Test compounds were applied and preincubated at 37 °C for 5 min, then 30 nmol [1-^{14}C]oleoyl-CoA (222000 dpm) was added. The reaction mixture was incubated at 37 °C for a specified period (7.5 min for intestinal mucosa, 20 min for liver and 10 min for adrenal). The reaction was terminated by the addition of 12.5 ml of chloroform–methanol (2 : 1) and 2.5 ml distilled water. After shaking, the chloroform phase was evaporated to dryness and the residue was separated by thin-layer chromatography (TLC glass sheets, Silica gel 60, Merck Co.) using hexane–ethyl acetate (9 : 1). The cholesterol ester zone was cut out and placed directly in a scintillation vial for counting. Amounts of cholesterol ester produced in the microsomes treated with vehicle and test compounds were determined. IC_{50} values were calculated using data from duplicate assay tubes at each concentration of test drugs.

Lipid Peroxidation in Rat Brain Homogenate Production of lipid-peroxide was determined as malondialdehyde (MDA) in rat brain homogenate as reported previously.[17,18] Briefly, the cerebral cortex isolated from male SD rats (6-week old) was homogenized in ice-cold 50 mM phosphate-buffered saline (pH 7.4). The homogenate was centrifuged at 1300 ***g*** for 10 min at 4 °C. The supernatant was incubated at 37 °C for 30 min in the presence of vehicle or test compounds. The reaction was terminated by addition of 20% trichloroacetic acid, and the mixture was immediately centrifuged at 2000 ***g*** for 15 min at 4 °C. The supernatant was heated at 100 °C for 15 min with thiobarbituric acid solution at pH 7.0. The optical absorbance of MDA was measured at 532 nm. MDA level in medium before the assay was determined, and the net production of MDA during the incubation period in the presence of vehicle or test compounds was determined. % Inhibition of lipid peroxidation was calculated by comparison of MDA produced in the presence of vehicle and test compounds.

Lipid Peroxidation in Rabbit LDL The effects of test compounds on LDL-oxidation were determined according to the method of Breugnot *et al.*[32] Briefly, the LDL fraction was isolated from plasma of Japanese white rabbits (2.4—2.7 kg) fed a high-cholesterol diet for a month and incubated with $CuSO_4$ (5 μM) at 37 °C for 10 h in the presence of vehicle or test compound. Oxidized LDL was determined as MDA.

Serum Total Cholesterol Level in Rats Male Wistar rats (8—9 weeks old) were fed a high-cholesterol diet (1% cholesterol, 0.5% cholic acid) for 3 d, during which period test compounds suspended in 5% arabic gum solution and vehicle were orally administered at a dose of 1—30 mg/kg once a day (n=6/group). The animals were fasted for 5 h after the last administration, and blood samples were collected from the abdominal aorta under ether-anesthesia. Serum total cholesterol levels (TC) were measured by an enzymatic method using a commercial assay kit (Wako Pure Chemicals Ind.). % Decrease in serum TC was calculated from comparison between rats treated with vehicle and test compounds.

Serum Total Cholesterol in Hamsters Male Golden Syrian hamsters (8 weeks old) fed a regular diet were used (n=5/group). Test compounds suspended in 5% arabic gum solution and vehicle were orally administered at a dose of 10 mg/kg twice a day for 4 d. The animals were anesthetized with 50 mg/kg of sodium pentobarbital 18 h after the last administration, and blood samples were collected from the abdominal aorta. Serum TC was measured enzymatically using a commercial assay kit (Wako Pure Chemicals Industries).

Pharmacokinetics in Dogs Compound **55** suspended in 5% arabic gum solution was orally administered to fasted male beagle dogs (n=3). Blood samples was taken from the jugular vein using a heparinized syringe at 0.5, 1, 2, 4, 6 and 8 h after administration. Blood was centrifuged at 3000 rpm for 10 min and the plasma samples were used for HPLC analysis. To 100 μl of each plasma sample were added 200 μl of 0.1 N NaOH and 1.0 ml of ethyl acetate. After shaking vigorously for 5 min, the mixture was centrifuged at 3000 rpm for 10 min. The organic layer (800 μl) was dried under a stream of N_2 at 35 °C and was reconstituted in 200 μl of the mobile phase; 25 μl of the sample was injected into the HPLC system. The calibration sample was prepared by spiking into the blank plasma and was processed similarly. The HPLC system consisted of a pump (LC-6A ,Shimadzu, Kyoto), electrochemical detector (L-ECD 6A, Shimadzu), autoinjector (851-AS, Jasco, Tokyo), recorder (C-R3A, Shimadzu) and STR ODS-II column (5 μm, 4.6 mm×150 mm, Shimadzu Techno-research Inc.). The analysis of **55** was carried out using 0.02 M KH_2PO_4–H_3PO_4 (pH 2.4) : acetonitrile (1 : 1) as a mobile phase at a flow rate of 0.7 ml/min, and the potential of the detector was +0.7 V.

References

1) Sliskovic D. R., White A. D., *Trends Pharmacol. Sci.*, **12**, 194—199 (1991).
2) Matsuda K., *Med. Res. Rev.*, **14**, 271—305 (1994).
3) Roth B. D., *DDT*, **3**, 19—25 (1998).
4) Dominick M. A., McGuire E. J., Reindel J. F., Bobrowski W. F., Bocan T. M. A., Gough A. W., *Fund. Appl. Tox.*, **20**, 217—224 (1993).
5) Lee O., Chang C. C. Y., Lee W., Chang T.-Y., *J. Lipid. Research*, **39**, 1722—1727 (1998).
6) Lee H. T., Sliskovic D. R., Picard J. A., Roth B. D., Wierenga W., Hicks J. L., Bousley R. F., Hamelehle K. L., Homan R., Speyer C., Stanfield R. L., Krause B. R., *J. Med. Chem.*, **39**, 5031—5034 (1996).
7) Kogushi M., Tanaka H., Ohtsuka I., Yamada T., Kobayashi H., Saeki T., Takada M., Hiyoshi H., Yanagimachi M., Kimura T., Yoshitake S., Saito I., *Atherosclerosis*, **124**, 203—210 (1996).
8) Matsuo M., Ito F., Konto A., Aketa M., Tomoi M., Shimomura K., *Biochem. Biophys. Acta*, **1259**, 254—260 (1995).
9) Matsuo M., Hashimoto M., Suzuki J., Iwanami K., Tomoi M., Shimomura K., *Toxicol. Appl. Pharmacol.*, **140**, 387—392 (1996).
10) Holvoet P., Collen D., *Atherosclerosis*, **137**, 33—38 (1998).
11) Jackson R. L., Ku G., Thomas C. E., *Med. Res. Rev.*, **13**, 161—182 (1993).
12) Nagano Y., Nakamura T., Matsuzawa Y., Cho M., Ueda Y., Kita T., *Atherosclerosis*, **92**, 131—140 (1992).
13) Bello A. A., Bright C., Burton B. J., Bush R. C., Casey J. H., Dron D. I., Facchini V., Joannou P. P., Parrott D. P., Riddell D., Roberts S. A., Williams R. J., *Biochem. Pharmacol.*, **51**, 413—421 (1996).
14) Kimura T., Watanabe N., Matsui M., Hayashi K., Tanaka H., Ohtsuka I., Saeki T., Kogushi M., Kabayashi H., Akasaka K., Yamagishi Y., Saitou I., Yamatsu I., *J. Med. Chem.*, **36**, 1641—1653 (1993).
15) Roth B. D., Blankley C. J., Hoefle M. L., Holmes A., Roark W. H., Trivedi B. K., Essenburg A. D., Kieft K. A., Krause B. R., Stanfield R. L., *J. Med. Chem.*, **35**, 1609—1617 (1992).
16) Kataoka K., Shiota T., Takeyasu T., Mochizuki T., Taneda K., Ota M., Tanabe H., Yamaguchi H., *J. Med. Chem.*, **38**, 3174—3186 (1995).
17) Uehara Y., Shirahase H., Nagata T., Ishimitsu T., Morishita S., Osumi S., Matsuoka H., Sugimoto T., *Hypertens.*, **15**, 216—224 (1990).
18) Nakamura S., Shirahase H., Uehara Y., Wada K., Kamiya S., Matsui H., "Frontiers of Reactive Oxygen Species in Biology and Medicine," ed. by Asada K., Yoshikawa T., Excerpta Medica, Amsterdam, 1994, pp. 347—348.
19) Clark R. D., Repke D. B., *Heterocycles*, **22**, 195—221 (1984).
20) Nordlander J. E., Catalane D. B., Kotian K. D., Stevens R. M., Haky J. E., *J. Org. Chem.*, **46**, 777—782 (1981).
21) Kovacic P., Field K. W., Roskos P. D., Scalzi F. V., *J. Org. Chem.*, **32**, 585—588 (1967).

22) Demerson C. A., Humber L. G., Philipp A. H., *J. Med. Chem.*, **19**, 391—395 (1976).
23) Brown V. H., Skinner W. A., DeGraw J. I., *J. Heterocycl. Chem.*, **6**, 539—543 (1969).
24) Gall W. G., Astill B. D., Boekelheide V., *J. Org. Chem.*, **20**, 1538—1544 (1955).
25) Ikan R., Hoffmann E., Bergmann E. D., Galun A., *Israel J. Chem.*, **2**, 37—42 (1964).
26) Hunt R. R., Rickard R. L., *J. Chem. Soc.*, **1966**, 344—345.
27) Trivedi B. K., Holmes A., Stoeber T. L., Blankley C. J., Roark W. H., Picard J. A., Shaw M. K., Essenburg A. D., Stanfield R. L., Krause B. R., *J. Med. Chem.*, **36**, 3300—3307 (1993).
28) Trivedi B. K., Purchase T. S., Holmes A., Augelli-Szafran C. E., Essenburg A. D., Hamelehle K. L., Stanfield R. L., Bousley R. F., Krause B. R., *J. Med. Chem.*, **37**, 1652—1659 (1994).
29) Tanaka A., Terasawa T., Hagihara H., Sakuma Y., Ishibe N., Sawada M., Takasugi H., Tanaka H., *J. Med. Chem.*, **41**, 2390—2410 (1998).
30) Field F. J., Mathur S., *J. Lipid Research*, **24**, 409—417 (1983).
31) Heider J. G., Pickens C. E., Kelly L. A., *J. Lipid. Research*, **24**, 1127—1134 (1983).
32) Breugnot C., Iliou J. P., Privat S., Robin F., Vilaine J. P., Lenaers A., *J. Cardiovasc. Pharmacol.*, **20**, 340—347 (1992).

Four New Triterpene Glycosides from *Thalictrum squarrosum*

Hitoshi YOSHIMITSU,*,[a] Makiko NISHIDA,[a] Zhong-Zhi QIAN,[b] Zhen-Huan LEI,[b] and Toshihiro NOHARA[b]

Faculty of Engineering, Kyushu Kyoritsu University,[a] 1–8 Jiyugaoka Yahata-nishi-ku, Kitakyushu 807–8585, Japan and Faculty of Pharmaceutical Sciences, Kumamoto University,[b] 5–1 Oe-honmachi, Kumamoto 862–0973, Japan.
Received December 17,1999; accepted March 7, 2000

Four new triterpene glycosides were isolated from the dried aerial parts of *Thalictrum squarrosum* (Ranunculaceae). They were designated as squarroside I, being a cycloartane-type glycoside, and squarrosides II, III and IV, being oleanene-type glycosides. Their structures were established by using two dimensional (2D) NMR techniques.

Key words *Thalictrum squarrosum*; squarroside; Ranunculaceae; cycloartane glycoside; oleanene glycoside

Thalictrum squarrosum STEPH. is a ranunculaceous plant distributed from the northern area of China to east Siberia. Its dried whole plant has been used as an antacid in traditional Chinese medicine.

As regards its constituents, cycloartane-type glycosides named squarrosides A1, A2, B1, B2, B3 and B4 have been isolated.[1)] As part of our continuing investigation on the chemical constituents in the genus *Thalictrum* plants,[2)] this paper deals with structural elucidation of four new triterpene glycosides, named squarrosides I (**1**), II (**2**), III (**3**) and IV (**4**).

The methanolic extract of the dried aerial parts of *Thalictrum squarrosum* STEPH. collected in Heilungkiang province of China was partitioned into a benzene–water solvent system. A styrene polymer MCI gel CHP20P column chromatography of the water soluble portion provided the glycosidic constituents, which were purified by using a combination of silica gel and octadecyl silica gel (ODS) column chromatography to furnish four new glycosides, designated squarrosides I (**1**), II (**2**), III (**3**) and IV (**4**), together with a known cycloartane-type glycoside, named thalictoside C (**5**).[2a)]

Squarroside I (**1**) was obtained as a white powder, $[\alpha]_D$ −2.7° (MeOH), and displayed a peak at *m/z* 911 $[M-H]^-$ in the neg. FAB-MS. The ^{1}H-NMR spectrum of **1** showed a couple of doublet signals at δ 0.24 and 0.55, which is characteristic of a cyclopropane methylene, four tertiary methyls at δ 0.91, 1.03, 1.23 and 1.29, an olefinic methyl at δ 2.01, three secondary methyls at δ 1.15 (d, J=6.7 Hz), 1.60 (d, J=6.1 Hz) and 1.63 (d, J=6.1 Hz), an olefinic proton at δ 5.66 (1H, dd, J=6.7, 7.3 Hz) and three anomeric protons at δ 4.70 (1H, d, J=7.9 Hz), 5.06 (1H, d, J=7.9 Hz) and 6.37 (1H, br s). The above ^{1}H-NMR data of **1** were similar to those of thalictoside C (**5**). In the ^{13}C-NMR spectrum of **1**, the signals due to the aglycone moiety were in good agreement with those of **5**, although the signals due to the sugar moiety were not identical. Furthermore, a nuclear Overhauser effect (NOE) was observed between the olefinic methyl proton at δ 2.01 and the olefinic proton at δ 5.66. On acid hydrolysis, **1** afforded D-glucose, D-fucose and L-rhamnose, together with several unidentified artificial sapogenols.[3)] The ^{1}H- and ^{13}C-NMR spectrum of **1**, which could be assigned with the aid of ^{1}H–^{1}H correlation spectroscopy (COSY) and heteronuclear multiple quantum coherence (HMQC) techniques, showed that the signals due to the trisaccharide moiety consisted of one glucopyranosyl moiety, one fucopyranosyl moiety and one rhamnopyranosyl moiety. In the heteronuclear multiple bond correlation spectroscopy (HMBC) experiment, the anomeric proton signals at δ 4.70 (2,4-di-substituted fucosyl moiety), 5.06 (terminal glucosyl moiety) and 6.37 (terminal rhamnosyl moiety) showed long-range correlations with the ^{13}C signals at δ 88.4 (C-3 of aglycone), 84.8 (C-4 of 2,4-di-substituted fucosyl moiety) and 76.5 (C-2 of 2,4-di-substituted fucosyl moiety), respectively. From the above evidence, the structure of **1** was concluded to be (22*S*,24*Z*)-cycloart-24-en-3β,22,26-triol 3-*O*-β-D-glucopyranosyl-(1→4)-[α-L-rhamnopyranosyl-(1→2)]-β-D-fucopyranoside.

Squarroside II (**2**) was obtained as a white powder, $[\alpha]_D$ −4.8° (MeOH), and exhibited a $[M-H]^-$ peak at *m/z* 1057 in the neg. FAB-MS. The ^{1}H-NMR spectrum of **2** displayed seven tertiary methyls at δ 0.87, 0.89, 0.92, 1.08, 1.08, 1.16 and 1.25, an olefinic proton at δ 5.43 (1H, br s) and four anomeric protons at δ 4.76 (1H, d, J=6.1 Hz), 5.12 (1H, d, J=7.9 Hz), 6.12 (1H, br s) and 6.24 (1H, d, J=7.9 Hz). The ^{13}C-NMR spectrum revealed the presence of six quaternary carbon signals at δ 30.8, 37.0, 39.5, 39.9, 42.1 and 47.0, a set of olefinic carbon signals at δ 122.9 and 144.1, one ester carbonyl carbon signal at δ 176.4 and four anomeric carbon signals at δ 95.7, 101.7, 104.9 and 106.3. These spectral data indicated that **2** was the 3,28-bisdesmoside of oleanolic acid (**6**),[4)] having four monosaccharide units. On acid hydrolysis, **2** afforded oleanolic acid, D-glucose, D-xylose and L-rhamnose.[3)] The ^{1}H- and ^{13}C-NMR spectrum of the sugar moiety were assigned by the ^{1}H–^{1}H COSY and HMQC techniques. In the HMBC experiment, long-range correlations were observed between the anomeric proton [δ 4.76 (d, J=6.1 Hz)] of 2,4-di-substituted xylosyl moiety and the C-3 (δ 88.7) of aglycone, the anomeric proton [δ 5.12 (d, J=7.9 Hz) H-1′] of terminal glucosyl moiety and the C-4 (δ 79.4) of 2,4-di-substituted xylosyl moiety, the anomeric proton [δ 6.12 (br s)] of terminal rhamnosyl moiety and the C-2 (δ 76.4) of 2,4-di-substituted xylosyl moiety and the anomeric proton [δ 6.24 (d, J=7.9 Hz) H-1″] of terminal glucosyl moiety and the C-28 (δ 176.4) of aglycone. Based on the above evidence, the structure of **2** was elucidated as 3-*O*-β-D-glucopyranosyl-(1→4)-[α-L-rhamnopyranosyl-(1→2)]-β-D-xylopyranosyl oleanolic acid 28-β-D-glucopyranosyl ester.

Squarroside III (**3**) was obtained as a white powder, $[\alpha]_D$ −14.1° (MeOH), and exhibited a $[M-H]^-$ peak at *m/z* 1219 in the neg. FAB-MS. The ^{1}H-NMR spectrum of **3** displayed seven tertiary methyls at δ 0.89, 0.89, 0.89, 1.09, 1.09, 1.16

* To whom correspondence should be addressed. e-mail: yoshimt@kyukyo-u.ac.jp
© 2000 Pharmaceutical Society of Japan

and 1.25, an olefinic proton at δ 5.42 (1H, br s) and five anomeric protons at δ 4.76 (1H, d, J=6.1 Hz), 5.01 (1H, d, J=7.9 Hz), 5.12 (1H, d, J=7.9 Hz), 6.12 (1H, br s) and 6.24 (1H, d, J=7.9 Hz). The above ^{1}H-NMR data of **3** were similar to those of **2** except for the new additional anomeric proton at δ 5.01. In the ^{13}C-NMR spectrum of **3**, the signals due to the aglycone moiety were in good agreement with those of **2**, although the signals due to the sugar moiety were not identical. On acid hydrolysis, **3** afforded oleanolic acid, D-glucose, D-xylose and L-rhamnose.[3] Meanwhile, the neg. FAB-MS of **3** gave a quasi-molecular peak at *m/z* 1219, which was higher by 162 mass units than that of **2**. Furthermore, a comparative study of the ^{13}C-NMR spectrum of **3** with that of **2** indicated the presence of an additional glucosyl unit in **3**, which was linked to the C-6 hydroxy group of the ester linked glucopyranosyl moiety according to the glycosylation shifts.[5] The ^{1}H- and ^{13}C-NMR spectrum of **3**, which could be assigned with the aid of ^{1}H–^{1}H COSY, HMQC and total correlation spectroscopy (TOCSY) techniques, showed that the signals due to the pentasaccharide moiety consisted of three glucopyranosyl moieties, one xylopyranosyl moiety and one rhamnopyranosyl moiety. In the HMBC experiment, long-range correlations were observed between the anomeric proton [δ 4.76 (d, J=6.1 Hz)] of 2,4-di-substituted xylosyl moiety and the C-3 (δ 88.7) of aglycone, the anomeric proton [δ 5.01 (d, J=7.9 Hz) H-1‴] of terminal glucosyl moiety and the C-6 (δ 69.4) of 6-substituted glucosyl moiety, the anomeric proton [δ 5.12 (d, J=7.9 Hz) H-1′] of terminal glucosyl moiety and the C-4 (δ 79.5) of 2,4-di-substituted xylosyl moiety, the anomeric proton [δ 6.12 (br s)] of terminal rhamnosyl moiety and the C-2 (δ 76.4) of 2,4-di-substituted xylosyl moiety and the anomeric proton [δ 6.24 (d, J=7.9 Hz) H-1″] of 6-substituted glucosyl moiety and the C-28 (δ 176.5) of aglycone. Based on the above data, **3** was formulated as 3-*O*-β-D-glucopyranosyl-(1→4)-[α-L-rhamnopyranosyl-(1→2)]-β-D-xylopyranosyl oleanolic acid 28-β-D-glucopyranosyl-(1→6)-β-D-glucopyranosyl ester.

Squarroside IV (**4**) was obtained as a white powder, $[\alpha]_D$ −4.2° (MeOH), and showed the same ion peak at *m/z* 1219 due to $[M-H]^-$ as that of **3** in the neg. FAB-MS. The ^{1}H-NMR spectrum of **4** displayed seven tertiary methyls at δ 0.87, 0.90, 0.92, 1.10, 1.15, 1.27 and 1.33, an olefinic proton at δ 5.44 (1H, br s) and five anomeric protons at δ 4.71 (1H, d, J=6.7 Hz), 5.13 (1H, d, J=7.9 Hz), 5.45 (1H, d, J=7.9 Hz), 6.14 (1H, br s) and 6.33 (1H, d, J=7.9 Hz). The above ^{1}H-NMR data of **4** were similar to those of **2** except for the new additional anomeric proton at δ 5.45. In the ^{13}C-NMR spectrum of **4**, the signals due to the aglycone moiety were in good agreement with those of **3**, although the signals due to the sugar moiety were not identical. On acid hydrolysis, **4** afforded oleanolic acid, D-glucose, D-xylose and L-rhamnose.[3] Furthermore, a comparative study of the ^{13}C-NMR spectrum of **4** with that of **2** indicated the presence of an additional glucosyl unit in **4**, which was linked to the trisaccharide moiety. The ^{1}H- and ^{13}C-NMR spectrum of **4**, which could be assigned by using 2D NMR techniques (^{1}H–^{1}H COSY, HMQC, TOCSY), showed that the signals due to the pentasaccharide moiety consisted of three glucopyranosyl moieties, one xylopyranosyl moiety and one rhamnopyranosyl moiety. In the HMBC experiment, long-range correlations were observed between the anomeric proton [δ 4.71 (d, J=6.7 Hz)] of 2,4-di-substituted xylosyl moiety and the C-3 (δ 88.7) of aglycone, the anomeric proton [δ 5.13 (d, J=7.9 Hz) H-1′] of terminal glucosyl moiety and the C-4 (δ 80.1) of 2,4-di-substituted xylosyl moiety, the anomeric proton [δ 5.45 (d, J=7.9 Hz) H-1⁗] of terminal glucosyl moiety and the C-3 (δ 83.2) of 3-substituted rhamnosyl moiety, the anomeric proton [δ 6.14 (br s)] of 3-substituted rhamnosyl moiety and the C-2 (δ 76.2) of 2,4-di-substituted xylosyl moiety and the anomeric proton [δ 6.33 (d, J=7.9 Hz) H-1″] of terminal glucosyl moiety and the C-28 (δ 176.4) of aglycone. Consequently, the structure of **4** was determined to be 3-*O*-β-D-glucopyranosyl-(1→4)-[β-D-glucopyranosyl-(1→3)-α-L-rhamnopyranosyl-(1→2)]-β-D-xylopyranosyl oleanolic acid 28-β-D-glucopyranosyl ester.

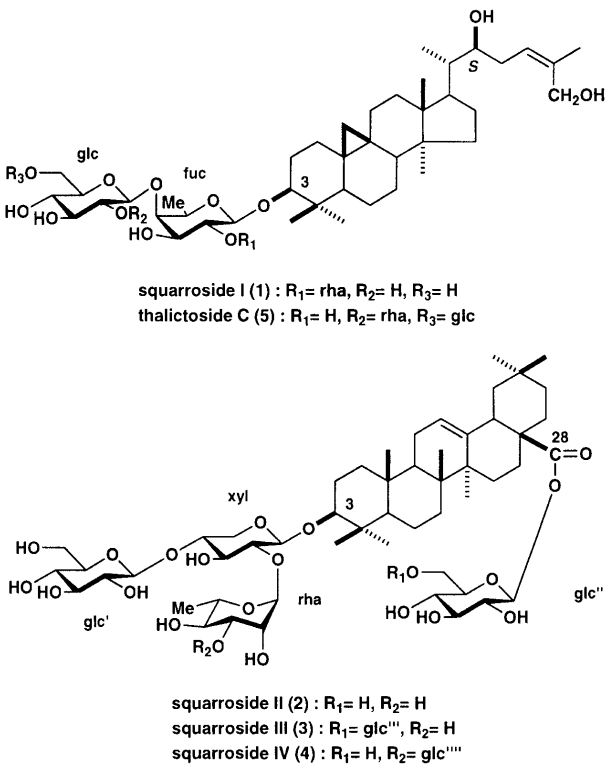

squarroside I (1) : R_1= rha, R_2= H, R_3= H
thalictoside C (5) : R_1= H, R_2= rha, R_3= glc

squarroside II (2) : R_1= H, R_2= H
squarroside III (3) : R_1= glc‴, R_2= H
squarroside IV (4) : R_1= H, R_2= glc⁗

Fig. 1

Experimental

Optical rotations were taken with a JASCO DIP-1000 automatic digital polarimeter. The ^{1}H- and ^{13}C-NMR spectra were measured with a JEOL alpha 500 NMR spectrometer and chemical shifts are given on a δ (ppm) scale with tetramethylsilane (TMS) as the internal standard. The FAB-MS was measured with a JEOL DX-303 HF spectrometer and taken in a 3-nitrobenzyl alcohol matrix. HPLC was carried out using a TSK gel-120A (7.8 mm i.d.×30 cm) column with a Tosoh CCPM pump and Tosoh RI-8010 differential refractometer as detector. TLC was performed on pre-coated Kiesel gel 60 F_{254} (Merck) and detection was achieved by spraying with 10% H_2SO_4 followed by heating. Column chromatography was carried out on Kieselgel (230—400 mesh, Merck), ODS (PrePAK-500/C_{18}, Waters) and MCI gel CHP20P (Mitsubishi Chemical Ind.)

Extraction and Separation The fresh aerial parts of *Thalictrum squarrosum* Steph. were collected in Heilungkiang province of China. The dried aerial parts (4.1 kg) of this plant were extracted with MeOH under reflux, and the extract (511 g) was partitioned in benzene and water (1 : 1). The water soluble portion (402 g) was subjected to MCI gel CHP-20P column chromatography with MeOH–H_2O (30→40→50→60→70→80→90%) to afford nine fractions (fr. 1—fr. 9). Fraction 7 (6.5 g) was further separated by ODS column chromatography with MeOH–H_2O (40→50→60→70→80→90%) to afford four fractions (fr. 10—fr. 13). Fraction 11 (533 mg) was

Table 1. ^{13}C-NMR Data for **1** and **5** (Pyridine-d_5)

	1	5		1	5
C- 1	32.3	32.0	3-*O*-		
C- 2	30.0	29.7	Fuc-1	105.1	107.0
C- 3	88.4	89.1	Fuc-2	76.5	74.9
C- 4	41.2	41.1	Fuc-3	77.1	75.6
C- 5	47.9	47.5	Fuc-4	84.8	77.8
C- 6	21.1	20.6	Fuc-5	70.3	72.7
C- 7	26.1	27.8	Fuc-6	17.4	17.8
C- 8	47.7	47.8	Rha-1	101.9	101.7
C- 9	19.9	19.8	Rha-2	72.3	72.1
C-10	26.3	26.1	Rha-3	72.4	72.3
C-11	26.7	26.0	Rha-4	74.1	74.1
C-12	33.4	35.6	Rha-5	69.5	70.4
C-13	45.4	45.2	Rha-6	18.7	18.5
C-14	49.1	48.9	Glc-1	107.0	102.7
C-15	35.8	33.2	Glc-2	75.7	78.5
C-16	28.0	26.5	Glc-3	78.7	78.2
C-17	49.0	48.9	Glc-4	71.5	71.4
C-18	18.2	19.4	Glc-5	78.5	76.6
C-19	29.6	29.5	Glc-6	62.8	69.8
C-20	41.7	41.4	Glc-1		105.3
C-21	12.1	11.9	Glc-2		75.6
C-22	72.7	72.6	Glc-3		78.2
C-23	34.8	34.6	Glc-4		71.7
C-24	125.2	124.9	Glc-5		78.2
C-25	137.7	137.4	Glc-6		62.5
C-26	61.1	60.8			
C-27	22.7	22.0			
C-28	19.5	18.1			
C-29	25.6	25.6			
C-30	15.5	15.1			

separated by silica gel column chromatography with $CHCl_3$–MeOH–H_2O (6 : 4 : 1), followed by HPLC with MeOH–H_2O (7 : 3), to furnish squarroside III (**3**) (34 mg). Fraction 12 (814 mg) was separated by silica gel column chromatography with $CHCl_3$–MeOH–H_2O (12 : 8 : 1), followed by HPLC with MeOH–H_2O (7 : 3), to furnish squarroside II (**2**) (311 mg). Fraction 13 (1.6 g) was separated by silica gel column chromatography with $CHCl_3$–MeOH–H_2O (6 : 4 : 1), followed by HPLC with MeOH–H_2O (7 : 3), to furnish squarroside IV (**4**) (655 mg). Fraction 9 (2.7 g) was further separated by ODS column chromatography with MeOH–H_2O (40→50→60→70→80→90%) to afford four fractions (fr. 14—fr. 17). Fraction 15 (393 mg) was separated by silica gel column chromatography with $CHCl_3$–MeOH–H_2O (12 : 8 : 1), followed by HPLC with MeOH–H_2O (4 : 1), to furnish thalictoside C (**5**) (135 mg). Fraction 16 (165 mg) was separated by silica gel column chromatography with $CHCl_3$–MeOH–H_2O (14 : 6 : 1), followed by HPLC with MeOH–H_2O (4 : 1), to furnish squarroside I (**1**) (43 mg).

Squarroside I (**1**): A white powder, $[\alpha]_D^{25}$ −2.7° (c=0.90, MeOH). Neg. FAB-MS (*m/z*): 911 $[M-H]^-$, 749 $[M-H-hexose]^-$. ^{1}H-NMR (pyridine-d_5): δ 0.24, 0.55 (each 1H, d, J=3.7 Hz, H2-19), 0.91 (3H, s, H_3-28), 1.03 (3H, s, H_3-18), 1.15 (3H, d, J=6.7 Hz, H_3-21), 1.23 (3H, s, H_3-30), 1.29 (3H, s, H_3-29), 2.01 (3H, s, H_3-27), 3.38 (1H, dd, J=4.3, 11.6 Hz, H-3), 4.01 (1H, br s, H-22), 5.66 (1H, dd, J=6.7, 7.3 Hz, H-24); fuc-1 to fuc-6, 4.70 (1H, d, J=7.9 Hz), 4.46 (1H, overlapped), 4.10 (1H, br d, J=9.2 Hz), 3.98 (1H, overlapped), 3.74 (1H, m), 1.60 (3H, d, J=6.1 Hz); rha-1 to rha-6, 6.37 (1H, br s), 4.78 (1H, br d, J=3.7 Hz), 4.62 (1H, dd, J=3.7, 9.2 Hz), 4.27 (1H, dd, J=9.8, 9.2 Hz), 4.75 (1H, m), 1.63 (3H, d, J=6.1 Hz); glc-1 to glc-6, 5.06 (1H, d, J=7.9 Hz), 3.98 (1H, dd, J=7.9, 9.2 Hz), 4.14 (1H, dd, J=9.2, 8.6 Hz), 4.18 (1H, dd, J=8.6, 8.6 Hz), 4.00 (1H, m), 4.33 (1H, dd, J=4.9, 11.6 Hz), 4.48 (1H, overlapped). ^{13}C-NMR (pyridine-d_5): Table 1.

Squarroside II (**2**): A white powder, $[\alpha]_D^{25}$ −4.8° (c=0.90, MeOH). Neg. FAB-MS (*m/z*): 1057 $[M-H]^-$, 895 $[M-H-hexose]^-$, 733 $[M-H-hexose-hexose]^-$, 587 $[M-H-hexose-hexose-deoxyhexose]^-$, 455 $[M-H-hexose-hexose-deoxyhexose-pentose]^-$. ^{1}H-NMR (pyridine-$d_5$): δ 0.87(3H, s, H_3-25), 0.89 (3H, s, H_3-30), 0.92 (3H, s, H_3-29), 1.08 (3H, s, H_3-24), 1.08 (3H, s, H_3-26), 1.16 (3H, s, H_3-23), 1.25 (3H, s, H_3-27), 3.19 (1H, dd, J=11.4, 4.6 Hz, H-3), 5.43 (1H, br s, H-12); xyl-1 to xyl-5, 4.76 (1H, d, J=6.1 Hz), 4.47 (1H, overlapped), 4.25 (1H, overlapped), 4.27 (1H, m), 3.80 (1H, br d, J=10.4 Hz), 4.18 (1H, overlapped); rha-1 to rha-6, 6.12 (1H, br s), 4.70 (1H, br s), 4.57 (1H, br d, J=9.2 Hz), 4.27 (1H, dd, J=9.2, 9.2 Hz), 4.59 (1H, m), 1.63 (3H, d, J=6.1 Hz); glc-1′ to glc-6′, 5.12 (1H, d, J=7.9 Hz), 4.10 (1H, dd, J=7.9, 8.6 Hz), 4.19 (1H, overlapped), 4.21 (1H, overlapped), 3.89 (1H, m), 4.37 (1H, overlapped), 4.48 (1H, overlapped); glc-1″ to glc-6″, 6.24 (1H, d, J=7.9 Hz), 4.18 (1H, dd, J=7.9, 8.5 Hz), 4.34 (1H, overlapped), 4.37 (1H, overlapped), 4.01 (1H, m), 4.37 (1H, overlapped), 4.48 (1H, overlapped). ^{13}C-NMR (pyridine-d_5): Table 2.

Squarroside III (**3**): A white powder, $[\alpha]_D^{25}$ −14.1° (c=0.55, MeOH). Neg. FAB-MS (*m/z*): 1219 $[M-H]^-$, 1057 $[M-H-hexose]^-$, 895 $[M-H-hexose-hexose]^-$, 733 $[M-H-hexose-hexose-hexose]^-$, 587 $[M-H-hexose-hexose-hexose-deoxyhexose]^-$, 455 $[M-H-hexose-hexose-hexose-deoxyhexose-pentose]^-$. ^{1}H-NMR (pyridine-$d_5$): δ 0.89(3H, s, H_3-25), 0.89 (3H, s, H_3-30), 0.89 (3H, s, H_3-29), 1.09 (3H, s, H_3-24), 1.09 (3H, s, H_3-26), 1.16 (3H, s, H_3-23), 1.25 (3H, s, H_3-27), 3.20 (1H, br d, J=15.2 Hz, H-3), 5.42 (1H, br s, H-12); xyl-1 to xyl-5, 4.76 (1H, d, J=6.1 Hz), 4.47 (1H, overlapped), 4.25 (1H, overlapped), 4.27 (1H, m), 3.80 (1H, br d, J=10.4 Hz), 4.39 (1H, br d, J=11.6 Hz); rha-1 to rha-6, 6.12 (1H, br s), 4.70 (1H, br s), 4.57 (1H, br d, J=9.2 Hz), 4.27 (1H, overlapped), 4.58 (1H, m), 1.63 (3H, d, J=6.1 Hz); glc-1′ to glc-6′, 5.12 (1H, d, J=7.9 Hz), 4.01 (1H, dd, J=7.9, 8.5 Hz), 4.18 (1H, overlapped), 4.17 (1H, overlapped), 3.87 (1H, m), 4.34 (1H, overlapped), 4.50 (1H, br d, J=11.6 Hz); glc-1″ to glc-6″, 6.24 (1H, d, J=7.9 Hz), 4.13 (1H, dd, J=7.9, 8.6 Hz), 4.25 (1H, overlapped), 4.27 (1H, overlapped), 4.10 (1H, m), 4.35 (1H, overlapped), 4.69 (1H, br d, J=9.2 Hz); glc-1‴ to glc-6‴, 5.01 (1H, d, J=7.9 Hz), 3.98 (1H, dd, J=7.9, 8.6 Hz), 4.16 (1H, overlapped), 4.17 (1H, overlapped), 3.88 (1H, m), 4.33 (1H, overlapped), 4.46 (1H, overlapped). ^{13}C-NMR (pyridine-d_5): Table 2.

Squarroside IV (**4**): A white powder, $[\alpha]_D^{25}$ −4.2° (c=0.85, MeOH). Neg. FAB-MS (*m/z*): 1219 $[M-H]^-$, 1057 $[M-H-hexose]^-$, 895 $[M-H-hexose-hexose]^-$, 733 $[M-H-hexose-hexose-hexose]^-$, 587 $[M-H-hexose-hexose-hexose-deoxyhexose]^-$, 455 $[M-H-hexose-hexose-hexose-deoxyhexose-pentose]^-$. ^{1}H-NMR (pyridine-$d_5$): δ 0.87(3H, s, H_3-25), 0.90 (3H, s, H_3-30), 0.92 (3H, s, H_3-29), 1.10 (3H, s, H_3-26), 1.15 (3H, s, H_3-24), 1.27 (3H, s, H_3-27), 1.33 (3H, s, H_3-23), 3.25 (1H, br d, J=15.8 Hz, H-3), 5.44 (1H, br s, H-12); xyl-1 to xyl-5, 4.71 (1H, d, J=6.7 Hz), 4.42 (1H, dd, J=6.7, 8.6 Hz), 4.18 (1H, overlapped), 4.23 (1H, m), 3.74 (1H, br d, J=11.0 Hz), 4.41 (1H, overlapped); rha-1 to rha-6, 6.14 (1H, br s), 4.97 (1H, br s), 4.81 (1H, dd, J=3.7, 9.2 Hz), 4.48 (1H, overlapped), 4.64 (1H, m), 1.56 (3H, d, J=6.1 Hz); glc-1′ to glc-6′, 5.13 (1H, d, J=7.9 Hz), 4.03 (1H, dd, J=7.9, 9.2 Hz), 4.22 (1H, overlapped), 4.21 (1H, overlapped), 3.90 (1H, m), 4.36 (1H, overlapped), 4.50 (1H, overlapped); glc-1″ to glc-6″, 6.33 (1H, d, J=7.9 Hz), 4.22 (1H, overlapped), 4.29 (1H, dd, J=9.2, 9.2 Hz), 4.36 (1H, overlapped), 4.03 (1H, m), 4.42 (1H, overlapped), 4.48 (1H, overlapped); glc-1⁗ to glc-6⁗, 5.45 (1H, d, J=7.9 Hz), 4.09 (1H, dd, J=7.9, 8.5 Hz), 4.22 (1H, overlapped), 4.21 (1H, overlapped), 3.97 (1H, m), 4.36 (1H, overlapped), 4.50 (1H, overlapped). ^{13}C-NMR (pyridine-d_5): Table 2.

Sugar Analysis of 1, 2, 3 and 4 A solution of each compound (**1**, **2**, **3** or **4**) (2 mg) in 2 N HCl–dioxane (1 : 1, 2 ml) was heated at 100 °C for 1 h. The reaction mixture was diluted with H_2O and evaporated to remove dioxane. The solution was neutralized with Amberlite MB-3 and passed through a SEP-PAK C_{18} cartridge to give the sugar fraction. A solution of the sugar fraction analyzed by TLC [CH_3CN–MeOH–H_2O (6 : 4 : 1), **1**: glucose, *Rf* 0.29; rhamnose, *Rf* 0.54; fucose, *Rf* 0.38; **2**: rhamnose, *Rf* 0.54; xylose, *Rf* 0.40; glucose, *Rf* 0.29; **3**: rhamnose, *Rf* 0.54; xylose, *Rf* 0.40; glucose, Rf 0.29; **4**: rhamnose, *Rf* 0.54; xylose, *Rf* 0.40; glucose, *Rf* 0.29]. A solution of the sugar fraction in 1 ml of H_2O was treated with a solution of L-(−)-α-methylbenzylamine (150 ml) and $NaBH_3CN$ (8 mg) in 1 ml of EtOH, and the mixture was kept at 40 °C for 3 h. Then several drops of acetic acid were added and the mixture was concentrated to dryness. The residue dissolved in Ac_2O–C_5H_5N (1 : 1, 2 ml) was treated with 4-dimethylaminopyridine (DMAP) (20 mg), and the whole mixture was left at room temperature overnight. After removal of excess Ac_2O and C_5H_5N, the residue dissolved in 20% CH_3CN was loaded into a SEP-PAK C_{18} cartridge and eluted with 20% CH_3CN (total 7 ml) and 100% CH_3CN. The fraction eluted with 100% CH_3CN was analyzed by normal-phase HPLC. Conditions of HPLC : column, Develosil 60-3, 3 μm (4.6 mm i.d.×150 mm); solvent, *n*-hexane–EtOH (19 : 1); flow rate, 1.20 ml/min; detection, ultraviolet (UV) (230 nm). t_R (min) of 1-(*N*-acetyl-L-α-methylbenzylamino)-1-deoxyalditol acetates were as follows. **1**: L-rhamnose 16.9, D-fucose 17.5, D-glucose 30.8. **2**: L-rhamnose 17.1, D-xylose 30.6, D-glucose 30.6. **3**: L-rhamnose 17.2, D-xylose 30.8, D-glucose 30.8. **4**: L-rhamnose 16.8, D-xylose 30.8, D-glucose 30.8 (reference: L-rhamnose 17.0, D-fucose 17.8, D-xylose 30.7, D-glucose 30.8).

Table 2. ^{13}C-NMR Data for **2**—**4** and **6** (Pyridine-d_5)

	2	**3**	**4**	**6**		**2**	**3**	**4**
C- 1	38.9	38.9	38.9	39.0	3-*O*-			
C- 2	26.6	26.6	26.7	28.1	Xyl-1	104.9	104.9	105.4
C- 3	88.7	88.7	88.7	78.2	Xyl-2	76.4	76.4	76.2
C- 4	39.5	39.5	39.6	39.4	Xyl-3	73.9	73.8	74.4
C- 5	56.0	56.0	56.0	55.9	Xyl-4	79.4	79.5	80.1
C- 6	18.5	18.5	18.5	18.8	Xyl-5	64.4	64.3	65.4
C- 7	32.5	32.6	32.5	33.3	Rha-1	101.7	101.8	101.5
C- 8	39.9	39.9	39.9	39.8	Rha-2	72.2	72.2	71.6
C- 9	48.1	48.1	48.0	48.2	Rha-3	72.5	72.5	83.2
C-10	37.0	37.0	37.0	37.5	Rha-4	74.1	73.9	62.9
C-11	23.8	23.8	23.8	23.8	Rha-5	69.8	69.8	69.8
C-12	122.9	122.9	122.9	122.7	Rha-6	18.6	18.6	18.6
C-13	144.1	144.1	144.1	145.0	Glc-1′	106.3	106.3	106.6
C-14	42.1	42.1	42.1	42.2	Glc-2′	75.4	75.4	75.5
C-15	28.2	28.3	28.2	28.4	Glc-3′	78.8	78.5	78.9
C-16	23.4	23.4	23.4	23.8	Glc-4′	71.3	71.3	71.3
C-17	47.0	47.0	47.0	46.7	Glc-5′	78.7	78.7	78.7
C-18	41.7	41.7	41.7	42.1	Glc-6′	62.5	62.5	62.5
C-19	46.2	46.3	46.2	46.6	Glc-1′′′′			106.9
C-20	30.8	30.8	30.8	31.0	Glc-2′′′′			75.9
C-21	34.0	34.0	34.0	34.3	Glc-3′′′′			78.5
C-22	33.1	33.1	33.1	33.3	Glc-4′′′′			71.5
C-23	28.1	28.1	28.1	28.8	Glc-5′′′′			78.5
C-24	17.0	17.0	17.2	16.6	Glc-6′′′′			62.6
C-25	15.6	15.7	15.6	15.6	28-*O*-			
C-26	17.5	17.5	17.5	17.4	Glc-1″	95.7	95.7	95.8
C-27	26.1	26.1	26.1	26.2	Glc-2″	74.0	7.40	74.1
C-28	176.4	176.5	176.4	180.3	Glc-3″	78.5	78.4	78.4
C-29	33.1	33.1	33.1	33.3	Glc-4″	71.1	71.0	71.1
C-30	23.7	23.7	23.7	23.8	Glc-5″	79.3	78.0	79.3
					Glc-6″	62.2	69.4	62.2
					Glc-1‴		105.3	
					Glc-2‴		75.1	
					Glc-3‴		78.4	
					Glc-4‴		71.5	
					Glc-5‴		78.7	
					Glc-6‴		62.6	

Acknowledgments We are grateful to Mr. K. Takeda and Mr. T. Iriguti of Kumamoto University for measurement of the mass and NMR spectra.

References

1) *a*) Khamidullina E. A., Gromova A. S., Lutsky V. I., Vereshchagin A. L., Semenov A. A., Larin M. F., *Khim. Prirod. Soed.*, **1989**, 516; *b*) Khamidullina E. A., Gromova A. S., Lutsky V. I., Zinchenko S. V., Semenov A. A., *Izv. Akad. Nauk, Ser. Khim.*, **1996**, 1547—1551.
2) *a*)Yoshimitsu H., Hayashi K., Shingu K., Kinjo J., Yahara S., Nakano K., Murakami, K., Tomimatsu T., Nohara T., *Chem. Pharm. Bull.*, **40**, 2465—2468 (1992); *b*) Yoshimitsu H., Nishida M., Yahara S., Nohara T., *Tetrahedron Lett.*, **39**, 6919—6920 (1998).
3) Oshima R., Yamauchi Y., Kumanotani J., *Carbohydr. Res.*, **107**, 169—176 (1982).
4) Kizu H., Kitayama S., Nakatani F., Tomimori T., Namba T., *Chem. Phram. Bull.*, **33**, 3324—3329 (1985).
5) *a*) Kasai R., Suzuo M., Asakawa J., Tanaka O., *Tetrahedron Lett.*, **1977**, 175—178; *b*) Tori K., Seo S., Yoshimura Y., Arita H., Tomita Y., *ibid.*, **1977**, 179—182.

Bicyclo[3.2.1]octane and 6-Oxabicyclo[3.2.2]nonane Type Neolignans from *Magnolia denudata*

Masanori KUROYANAGI,*,[a] Kenichi YOSHIDA,[b] Atsushi YAMAMOTO,[b] and Masao MIWA[b]

School of Bioresources, Hiroshima Prefectural University,[a] 562, Nanatsukacyo, Shobara-shi, Hiroshima, 727–0023, Japan and School of Pharmaceutical Sciences, University of Shizuoka,[b] 52–1, Yada, Shizuoka-shi, 422–8526, Japan.
Received December 20, 1999; accepted March 3, 2000

From the ethyl acetate soluble fraction of twigs of *Magnolia denudata* (Magnoliaceae), seven new neolignan derivatives, 1—7, were isolated along with eighteen known lignan and neolignan derivatives, 8—25. The structures of the new neolignans were elucidated by means of spectral methods, especially by ^{1}H-NMR and ^{13}C-NMR spectra, and two dimensional NMR methods such as ^{1}H-detected heteronuculear multiple bond connectivity (HMBC), ^{1}H-detected multiple quantum coherence (HMQC) and ^{1}H–^{1}H-correlation spectroscopy (COSY). Compounds 1—4 have novel structures possessing a 6-oxabicyclo[3.2.2]nonane skeleton and compounds 5—8 also have novel structures possessing a bicyclo[3.2.1]octane skeleton. The anti-platelet-activating factor (PAF) activity of these compounds was tested by measurement of inhibition activity against acetyl transferase to *lyso*-PAF.

Key Words *Magnolia denudata*; Magnoliaceae; neolignane; bicyclo[3.2.1]octane; 6-oxa-bicyclo[3.2.2]nonane; anti-platelet-activating factor activity

Platelet-activating factor (PAF) is a potent lipid mediator in inflammation and asthma. A neolignan, kazurenone, isolated from *Piper futokadsura*, was reported as a potent anti-PAF constituent.[1] Miwa and his coworkers proposed a new method based on inhibition of acetyl transferase activity to *lyso*-PAF for testing anti-PAF activity.[2] The new method has been applied to many kinds of natural products, two of which, the neolignan derivatives magnolol and honokiol, isolated as main constituents from *Magnolia obovata*, showed potent anti-PAF activity.[2] So it was promising that lignan and neolignan derivatives were anti-PAF reagents. So, we planned to isolate some lignan and neolignan derivatives and test their anti-PAF activity by the Miwa method. *Magnolia* sp. and *Piper* sp.[3] plants are well known as sources of lignans and neolignans. Isolation of the constituents of *M. denudata* was carried out by repeated silica gel column chromatography and HPLC using a reversed phase (octadecyl silica (ODS)) column to give new neolignan derivatives, compounds **1**—**7**, along with known lignan and neolignan derivatives, compounds **8**—**25**. The structures of the new compounds were determined by spectral methods such as ^{1}H-NMR, ^{13}C-NMR , ^{1}H-detected heteronuculear multiple bond connectivity (HMBC), nuclear Overhauser effect (NOE) and circular dichroism (CD) spectrum. This paper deals with the structural elucidation of these neolignan derivatives and their anti-PAF activity.

Results and Discussion

The methanol extract of powdered twigs of *M. denudata* was partitioned between EtOAc and water to give the EtOAc soluble fraction. The EtOAc soluble fraction gave seven new neolignan derivatives, named as denudanolides A (**1**), B (**2**), C (**3**), D (**4**), denudadiones A (**5**), B (**6**) and C (**7**) along with known lignan and known neolignan compounds by repeated silica gel column chromatography and HPLC using ODS column. The structures of the known compounds, **9**—**25**, were examined from spectral data and identified with known compounds, denudatin B (**9**),[4] denudatin A (**10**),[4] **11**,[5] kadsurin A (**12**),[6] **13**,[7] **14**,[8] burcellin (**15**),[9] **16**,[10] nirandin A (**17**),[11] licarin B (**18**),[12] acuminatin (**19**),[13] veraguensin (**20**),[14] grandisin (**21**),[15] yangambin (**22**),[16] syringresinol (**23**),[17] isodihydrofutoquinol A (**24**)[18] and isodihydrofutoquinol B (**25**),[18] respectively.

Denudanolide A (**1**) gave the molecular formula, $C_{20}H_{20}O_6$, from hi-resolution electron impact (HR-EI)-MS (*m/z* 356.1220 $[M]^+$). The IR spectrum of **1** showed absorption bands due to a lactone carbonyl (1752 cm^{-1}) and an α,β-unsaturated ketone (1681 cm^{-1}). The ^{1}H-NMR spectrum of **1** showed the presence of a methoxyl group [δ 3.56 (s)], a vinyl group [δ 5.80 (ddt, J=16.8, 10.0, 6.8 Hz), 5.18 (md, J=10.0 Hz), 5.15 (md, J=16.8 Hz), 3.10 (dd, J=16.4, 6.8 Hz), 3.01 (dd, J=16.4, 6.8 Hz)], an olefin proton [δ 6.71 (br s)], a doublet methyl group [δ 1.07 (d, J=8.0 Hz)], a methylenedioxy group [δ 5.96 (s)], a singlet proton [δ 3.87 (s), H-1], a doublet proton [δ 2.59 (d, J=8.4 Hz, H-7)], multiplet methine proton [δ 2.93 (dq, J=8.4, 8.0 Hz, H-8)] and 3,4-dioxophenyl group [δ 6.75 (d, J=8.0 Hz, H-5′), 6.64 (d, J=1.6 Hz, H-2′), 6.62 (dd, J=8.0, 1.6 Hz, H-6′)]. The ^{13}C-NMR spectrum of **1** showed the presence of a methoxyl group (δ 50.9), a conjugated carbonyl group (δ 189.3), lactone carbonyl group (δ 166.0), ketal carbon (δ 106.6), a methylenedioxy group (δ 101.4), two double bond (δ 143.6, 140.7, 133.7, 118.5) and a phenyl group (δ 148.5, 147.3, 134.6, 120.7, 108.7, 107.4). These NMR data suggested the planar structure having a bicyclo ring for **1**. The HMBC experiment indicated the presence of a 6-oxabicyclo[3.2.2]-nonane skeleton and the relative position of the functional groups of **1** as shown in Fig. 1. The relative configuration of **1** was elucidated from coupling constants and difference NOE experiments as shown in Fig. 2. The coupling constant between H-1 and H-9 was almost 0 Hz. This indicated that the dihedral angle between H-1 and H-9 was approximately 90°. The Dreiding molecular model of **1** indicated the presence of two conformations in **1** and one of them had the 90° dihedral angle between H-1 and H-9. In the difference NOE experiment, H-1 correlated with H-2′ and H-6′. H-9 correlated with Me-8. OMe at C-5 correlated with H-8. H-8 correlated with H-2′ and H-6′. These NOE experiments indicated the relative configuration of **1** as shown in Fig. 2. The absolute configuration of **1** was determined by the CD spec-

* To whom correspondence should be addressed. e-mail: kuroyang@bio.hiroshima-pu.ac.jp
© 2000 Pharmaceutical Society of Japan

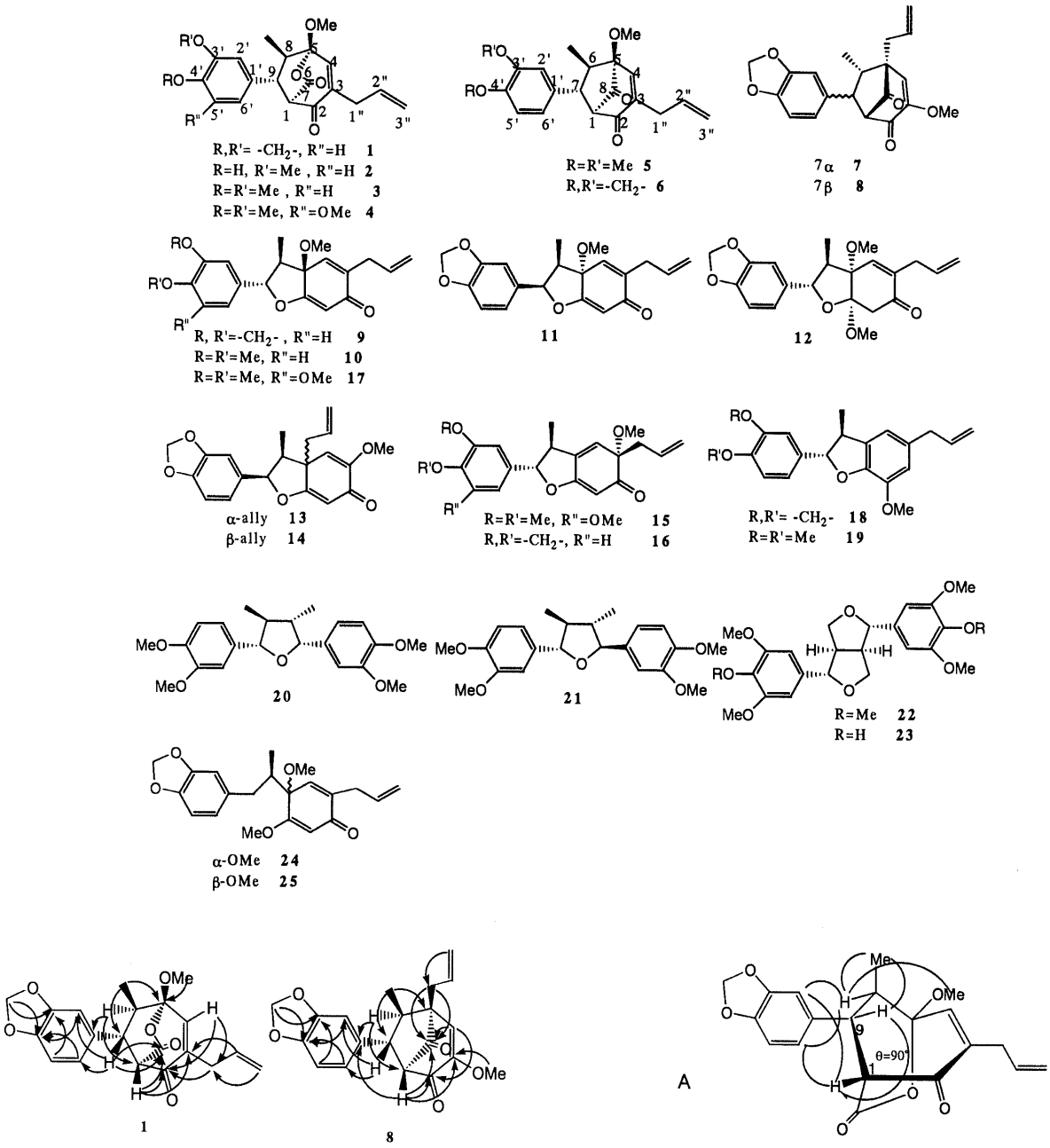

Fig. 1. Significant HMBC Correlations of **1** and **8**

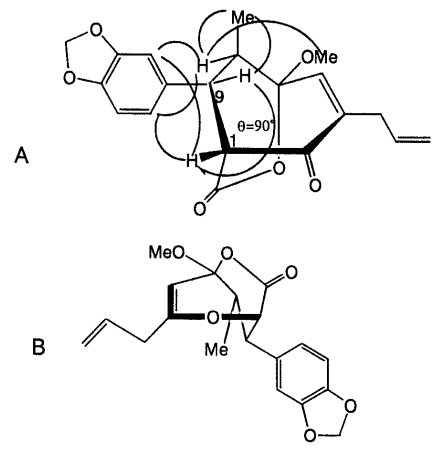

Fig. 2. Difference NOEs and Dihedral Angle between H-1 and H-9 (A) and Octant Projection of **1** (B)

A) Dihedral angle between H-1 and H-9 was predicted to be 90 degrees from the coupling constant of H-1 (J=0 Hz) and was supported from Dreiding model. B) Octant projection of α,β-unsaturated ketone of **1** was deduced from CD data ($[\theta]_{343}$−3465; n→π*, $[\theta]_{238}$+28182; π→π*).

trum of **1**, in which CD Cotton effects based on n→π* and π→π* transition of the α,β-unsaturated ketone chromophore was observed at 343 nm (−3465) and 238 nm (+28182), respectively . The CD Cotton effects were applied to the empirical rule[19, 20] for an α,β-unsaturated ketone as shown in Fig. 2, which determined the absolute configuration to be (1*R*,5*S*,8*R*,9*R*). Thus, the structure of **1** was elucidated to be (1*R*,5*S*,8*R*,9*R*)-3-allyl-8-methyl-5-methoxy-9-(3,4-methylenedioxyphenyl)-6-oxabicyclo[3.2.2]non-3-en-2,7-dione.

The molecular formula of denudanolide B (**2**) was assumed to be $C_{20}H_{22}O_6$ from the EI-MS (*m/z* 358 $[M]^+$). The ^{13}C-NMR data showed the presence of twenty carbon signals, from which the molecular formula of **2** was determined to be $C_{20}H_{22}O_6$. The ^{1}H-NMR spectrum of **2** was very similar (see Table 1) with those of **1** except the presence of 4-hydroxy-3-methoxyphenyl [δ 3.87 (s)] instead of a 3,4-methylenedioxyphenyl group. These facts were indicated from the ^{13}C-NMR spectrum (see Table 2) and the molecular formula of **2**. The position of the methoxyl group on the phenyl moiety was confirmed by the difference NOE experiment. Irradiation at the methoxyl group (δ 3.87) on the aromatic ring gave a correlation with H-2 [δ 6.62 (d, J=2.0 Hz)]. The CD spec-

Table 1. ^{1}H-NMR Data of 6-Oxabicyclo[3.2.2]nonane and Bicyclo[3.2.1]octane Type Neolignans (400 MHz, in $CDCl_3$)

	1	2	3	4
H-1	3.87 s	3.91 s	3.91s	3.93 s
4	6.71 br s	6.73 br s	6.73 br s	6.74 br s
6				
7				
8	2.39 dq (J=8.4, 8.0)	2.41 dq (J=8.4, 6.8)	2.43 dq (J=8.0, 6.8)	2.45 dq (J=8.8, 6.8)
9	2.59 d (J=8.4)	2.60 d (J=8.4)	2.62 d (J=8.0)	2.66 d (J=8.8)
2′	6.64 d (J=1.6)	6.62 d (J=2.0)	6.65 d (J=2.0)	6.35 s
5′	6.75 d (J=8.0)	6.86 d (J=7.6)	6.81 d (J=8.4)	
6′	6.62 dd (J=8.0, 1.6)	6.66 dd (J=7.6, 2.0)	6.72 dd (J=8.4, 2.0)	6.35 s
1″	3.10 mdd (J=16.4, 6.8)	3.11 mdd (J=16.0, 5.2)	3.11 mdd (J=16.8, 6.8)	3.11 mdd (J=16.0, 6.8)
	3.01 mdd (J=16.4, 6.8)	3.04 mdd (J=16.0, 6.8)	3.05 md (J=16.8, 6.8)	3.05 mdd (J=16.0, 7.2)
2″	5.80 ddt (J=16.8, 10.0, 6.8)	5.81 ddt (J=17.2, 10.4, 6.8)	5.81 ddt (J=17.2, 10.4, 6.8)	5.81 ddt (J=17.2, 10.6, 6.8)
3″	5.18 md (J=10.0)	5.19 md (J=10.4)	5.19 md (J=10.4)	5.19 md (J=10.4)
	5.15 md (J=16.8)	5.16 md (J=17.2)	5.16 md (J=17.2)	5.17 md (J=17.2)
Me	1.07 d (J=8.0)	1.08 d (J=6.8)	1.09 d (J=6.8)	1.11 d (J=6.8)
OMe	3.56 s	3.75 s	3.57 s	3.58 s
		3.87 s	3.86 s	3.84 s×2
			3.87 s	3.83 s
O–CH_2–O	5.96 s			

	5	6	7	8
H-1	3.52 s	3.59 s	3.74 d(J=7.2)	3.54 s
4	7.04 br s	7.03 br s	6.26 s	5.78 s
6	2.46 over lap	2.41 dq (J=8.0, 6.5)	2.53 dq (J=6.0, 7.2)	2.10 quin (J=7.2)
7	2.46 over lap	2.45 d (J=8.0)	3.11 dd (J=6.0, 7.2)	2.50 over lap
8				
9				
2′	6.57 d (J=2.0)	6.58 d (J=2.0)	6.52 d (J=2.0)	6.53 d (J=2.0)
5′	6.79 d (J=8.0)	6.73 d (J=8.0)	6.70 d (J=7.6)	6.72 d (J=8.4)
6′	6.66 dd (J=8.0, 2.0)	6.57 dd (J=8.0, 2.0)	6.54 dd (J=7.6, 1.6)	6.53 dd (J=8.4, 2.0)
1″	3.20 mdd (J=16.4, 7.2)	3.12 mdd (J=16.5, 7.0)	2.61 dd (J=14.8, 7.2)	2.50 over lap
	3.07 mdd (J=16.4, 6.8)	3.07 mdd (J=16.5, 7.0)	2.44 dd (J=14.8, 6.8)	
2″	5.86 ddt (J=16.0, 10.8, 6.8)	5.85 ddt (J=16.5, 10.5, 7.0)	5.95 ddt (J=16.8, 10.4, 7.0)	5.96 ddt (J=17.2, 10.0, 7.6)
3″	5.18 md (J=10.8)	5.18 md (J=10.5)	5.29 md (J=16.8)	5.19 md (J=17.2)
	5.17 md (J=16.0)	5.17 md (J=16.5)	5.27 md (J=10.4)	5.16 md (J=10.0)
Me	1.07 d (J=6.0)	1.06 d (J=6.5)	1.14 d (J=7.2)	1.05 d (J=6.8)
OMe	3.63 s	3.63 s	3.68 s	3.73 s
	3.84 s			
	3.85 s			
O–CH_2–O		5.94 s	5.91 s	5.94 s

trum of **2** was not measured because of a lack of sample amount. Similarities of the ^{1}H-NMR (Table 1) and ^{13}C-NMR data (Table 2) of the 6-oxabicyclo[3.2.2]-nonane part of **2** with those of **1** indicated that **2** had the same relative configuration with that of **1** and the absolute configuration of **2** was assumed to be the same as that of **1**. Thus, the structure of **2** was assumed to be 3-allyl-8-methyl-5-methoxy-9-(4-hydroxy-3-methoxyphenyl)-6-oxabicyclo-[3.2.2]non-3-en-2,7-dione and the absolute configuration of **2** was supposed to be (1*R*,5*S*,8*R*,9*R*).

Denudanolide C (**3**) gave the molecular formula, $C_{21}H_{24}O_6$, from HR-EI-MS (*m/z* 372.1573 $[M]^+$). The IR spectrum of **3** showed the absorption bands due to lactone carbonyl (1750 cm^{-1}) and an α,β-unsaturated ketone (1681 cm^{-1}). The ^{1}H-NMR spectrum of **3** showed similar signal patterns with those of **2** except for the presence of three methoxy groups [δ 3.57 (3H, s), 3.87 (6H, s)]. The ^{13}C-NMR spectrum of **3** also showed the same signal patterns with that of **1** except for two methoxy groups on the aromatic ring. These indicated the presence of a 6-oxabicyclo[3.2.2]nonane skeleton and a 3,4-dimethoxyphenyl group in **3**. The CD spectrum of **3** showed a similar Cotton effect ($[\theta]_{345}-3720$, $[\theta]_{236}+3054$) with those of **1**. From these data, the structure of **1** was determined to be (1*S*,5*R*,8*R*,9*R*)-3-allyl-9-methyl-5-methoxy-8-(3,4-dimethoxyphenyl)-6-oxabicyclo[3.2.2]non-3-en-2,7-dione.

Denudanolide D (**4**) gave the molecular formula $C_{22}H_{26}O_7$ from the HR-EI-MS (*m/z* 402.1704 $[M]^+$). The IR spectrum showed absorption bands due to a lactone carbonyl (1750 cm^{-1}) and an α,β-unsaturated ketone (1681 cm^{-1}). The ^{1}H-NMR spectrum showed the presence of a symmetrical 3,4,5-trimethoxyphenyl group [δ 3.83 (3H,s), 3.84 (6H, s), 6.35 (2H, s)]. The ^{1}H-NMR signal patterns of the other parts were identical with those of **1** (see Table 1). This was also seen in the ^{13}C-NMR data [δ 60.9 (MeO at C-4′), 56.3 (MeO at 3′ and 5′), 136.7 (at C-4′), 153.8 (at C-3′ and 5′), 104.4 (at C-2′ and 6′), 137.7 (at C-1′)]. From these data the structure of **4** was assumed to be a 6-(3,4,5-trimethoxyphenyl)-derivative of **1**. The CD spectrum of **4** also showed a similar Cotton effect ($[\theta]_{347}-4248$, $[\theta]_{248}+15624$) with that of **1**. These facts

Table 2. ^{13}C-NMR Data of 6-Oxabicyclo[3.2.2]nonane and Bicyclo[3.2.1]octane Type Neolignans (100 MHz, in $CDCl_3$)

C-No.	1	2	3	4	5	6	7	8
1	65.4	65.6	66.5	66.3	69.9	69.8	69	70.3
2	189.3	189.4	189.4	189.3	194.4	194.3	189.9	190.2
3	140.7	140.8	140.8	140.9	140.5	140.4	153.7	152.5
4	143.6	143.5	143.5	143.6	147.2	147.2	121.9[a)]	118.0
5	106.6	106.7	106.7	106.6	89.4	89.3	55.0	57.4
6					45.3	45.2	44.8	47.0
7	166	166.3	166.1	166.2	48.8	48.9	49.5	50.2
8	45.3	45.4	45.3	45.3	202.2	202	201.4	202.6
9	46.0	46.0	45.9	46.5				
Me	15.3	15.4	15.4	15.6	13.7	13.5	18.1	14.0
1′	134.6	132.8	133.5	137.7	133.9	135.0	131.6	135.3
2′	107.4	109.2	110.1	104.3	110.1	107.3	108.5[b)]	107.3
3′	147.3	145.3	148.7	153.8	148.5	148.3	147.1	148.3
4′	148.5	147.2	149.7	136.7	149.4	147	148.1	146.9
5′	108.7	114.8	111.7	153.8	111.5	108.5	108.6[b)]	108.6
6′	120.7	120.4	119.6	104.3	119.3	120.5	121.7[a)]	120.6
1″	34.1	34.2	34.2	34.2	32.7	32.7	32.6	35.5
2″	133.7	133.7	143.5	143.6	133.8	133.8	133.3	133.2
3″	118.5	118.5	118.5	118.6	118.1	118.1	119.6	119.1
OMe	50.9	50.9	50.9	51.0	54.0	53.9	55.7	55.7
		56.0	56.0 ×2	56.3×2	56.0			
				60.9	56.1			
O–CH_2–O	101.4					101.3	101.2	101.2

a,b) Assignments may be interchangeable.

indicated that the structure of **4** was (1*R*,5*S*,8*R*,9*R*)-3-allyl-8-methyl-5-methoxy-9-(3,4,5-trimethoxyphenyl)-6-oxabicyclo[3.2.2]non-3-en-2,7-dione.

Denudadione A (**5**) gave the molecular formula, $C_{21}H_{24}O_5$, from HR-EI-MS (*m/z* 356.1611 $[M]^+$). The IR spectrum of **5** showed absorption bands due to a strained ketone (1767 cm^{-1}) and an α,β-unsaturated ketone (1681 cm^{-1}). The ^{1}H-NMR spectrum of **5** showed the presence of two methoxyl groups [δ 3.84 (3H, s), 3.85 (3H, s)] on aromatic carbons, a methoxyl group [δ 3.63 (3H, s)] on an aliphatic carbon, an allyl group [δ 5.17 (md, J=16.0 Hz), 5.18 (md, J=10.8 Hz), 5.86 (ddt, J=16.0, 10.8, 6.8 Hz), 3.20 (mdd, J=16.4, 7.2 Hz), 3.07 (mdd, J=16.4, 6.8 Hz)], a doublet methyl group [δ 1.07 (d, J=6.0 Hz)], a 3,4-dioxyphenyl group [δ 6.79 (d, J=8.0 Hz), 6.66 (dd, J=8.0, 2.0 Hz), 6.57 (d, J=2.0 Hz)], a singlet methine proton (δ 3.49) and a singlet olefin proton [δ 7.04 (s)]. The ^{13}C-NMR spectrum of **5** showed the presence of two carbonyl carbons (δ 202.2 and 194.4), a 3,4-dioxyphenyl group (δ 148.5, 149.4, 133.9, 119.3, 111.5, 110.1), two double bonds (δ 140.5, 147.2, 133.8, 118.1), a carbinyl carbon (δ 89.4), a characteristicly lower shifted methine carbon (δ 69.9), two methoxyl carbons on an aromatic ring [δ 56.0 (MeO×2)] and a methoxyl group (δ 54.0) on an aliphatic carbon. From this NMR evidence, the planar structure was assumed to be a bicyclo[3.2.1]octane derivative, and its structure was confirmed by HMBC experiment as shown in Fig. 1. The H-1 proton appeared at δ 3.14 as singlet signal, from which the dihedral angle between H-1 and H-7 of **5** was assumed to be approximately 90°. The Dreiding molecular model of **5** showed the presence of only one conformation having approximately 90° dihedral angle between H-1 and H-9. Relative configuration of **5** was deduced by means of a difference NOE experiment (Fig. 2). The absolute configuration of **5** was assumed from reaction mechanism from bicyclo[3.2.1]octane derivatives into 6-oxabicyclo[3.2.2]-nonane derivatives (**1**—**4**). In the course of the Baeyer-Villiger oxidation of bicyclo[3.2.1]octane derivatives to 6-oxabicyclo[3.2.2]nonane derivatives, the configuration at C-4 was retained, so the absolute configuration of **5** turns out to be (1*R*,5*R*,6*R*,7*R*). The CD spectrum of **5** showed a negative Cotton effect ($[\theta]_{335}$−10252) and a positive Cotton effect ($[\theta]_{270}$+5553). These results were applied to the empirical rule[19,20] to give the same result as the above supposition. From these facts, the structure of **5** was determined to be (1*R*,5*R*,6*R*,7*R*)-3-allyl-6-methyl-5-methoxy-7(3,4-dimethoxyphenyl)-bicyclo[3.2.1]oct-2-en-2,8-dione.

Denudadione B (**6**) gave the molecular formula, $C_{20}H_{20}O_5$, from HR-EI-MS (*m/z* 340.1282 $[M]^+$). The ^{1}H-NMR spectrum of **6** showed a similar signal pattern with that of **5** except for the presence of a methylene dioxyphenyl group [δ 5.94 (s)] instead of the 3,4-dimethoxphenyl group in **5**. The ^{13}C-NMR spectrum also showed the presence of a 3,4-methylenedioxyphenyl group (δ 101.3). The ^{1}H- and ^{13}C-NMR spectra of the bicyclo[3.2.1]octane part of **6** were identical with those of **5** (Tables 1, 2). The CD spectrum ($[\theta]_{332}$−6195, $[\theta]_{262}$−12628) of **6** was identical with that of **5**. From these facts, the structure of **6** was determined to be (1*R*,5*R*,6*R*,7*R*)-3-allyl-6-methyl-5-methoxy-7-(3,4-methylendioxyphenyl)-bicyclo[3.2.1]oct-2-en-2,8-dione.

Compound **8** gave *m/z* 340 $[M]^+$ from EI-MS. The ^{13}C-NMR spectrum gave 20 carbon signals. From these data, the molecular formula of **8** was deduced to be $C_{20}H_{20}O_5$. The ^{1}H-NMR and ^{13}C-NMR spectra of **8** showed the presence of the same groups with those of **5**. But the signal patterns of the ^{1}H-NMR and ^{13}C-NMR spectra of **8** showed a small difference with those of **5**. This was assumed to depend on the difference of the position of the methoxyl group and the allyl group. So we assumed that the position of the methoxyl group and the allyl group should be interchanged. This was confirmed by the HMBC experiment. The relative configuration of **8** was discussed from the coupling constants (the coupling constant between H-1 and H-7 was 0 Hz) and a differ-

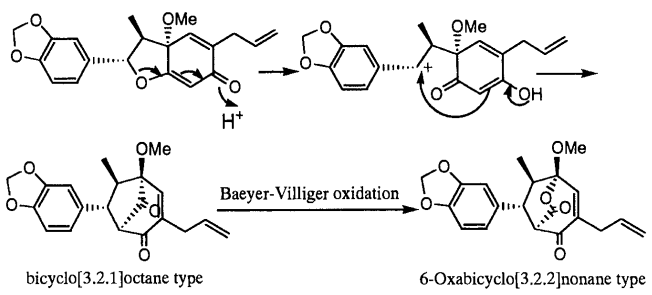

Fig. 3. Biogenesis of Denudanolides from Hydrobenzofurane Type Neolignan

ence NOE experiment. These indicated that **8** was a known compound isolated from *Mezilaurs itauba*[21] including the relative configuration. The racemate of this compound was synthesized as an intermediate to guianin.[22] The CD spectrum of **8** gave a opposite Cotton effect ($[\theta]_{350}+3825$ and $[\theta]_{250}-14025$) with that of **5**. Thus, the absolute stereochemistry of the 6-oxabicyclo[3.2.2]nonane skeleton of **8** was found to be antipodal with that of **5**.

Denudadione C (**7**) gave the molecular formula, $C_{20}H_{20}O_5$, from HR-EI-MS, *m/z* 340.1323 $[M]^+$. The ^{1}H-NMR and ^{13}C-NMR spectra of **7** showed the presence of a 7-(3,4-methylendioxyphenyl) group, a 5-allyl group, a 3-methoxy group and a bicyclo[3.2.1]oct-3-en-2,8-dione skeleton, the same as **8**. But, the H-1 proton appeared as doublet signal ($J=7.2$ Hz). This indicated that the relative configuration between H-1 and H-7 was different from that of **8**, and **7** was an epimer of **8** at C-7. Thus, the structure of **7** was found to be rel-(1*S*,5*S*,6*S*,7*R*)-5-allyl-6-methyl-3-methoxy-7-(3,4-methylenedioxyphenyl)-bicyclo[3.2.1]oct-3-en-2,8-dione.

Ten compounds, **1**, **9**, **12**—**14**, **17** and **19**—**22**, of the isolated neolignans were tested for anti-PAF activity by Miwa's method as described in the previous papers.[2] Of these tested compound, **1** and **9** showed moderate anti-PAF activity, 50% inhibition at 50 and 100 μg/ml, respectively.

The novel 6-oxabicyclo[3.2.2]nonane type neolignans might be synthesized from hydrobenzofuranoid type neolignanes through a bicyclo[3.2.1]octane type neolignan by protonation at the C-6 carbonyl, followed by skeleton rearrangement and Baeyer-Villiger oxidation as shown in Fig. 3.

Experimental

^{1}H-NMR and ^{13}C-NMR spectra were measured with a 400 MHz instrument (JEOL α-400), chemical shifts are given in δ value (ppm) with tetramethylsilane (TMS) as internal standard. Column chromatographies were carried out on silica gel (Merck). Semi-preparative HPLC was carried out on an ODS column (YMC R-ODS-7) using the CH_3CN–H_2O solvent system. EI-MS and HR-EI-MS were measured on JEOL JMS-AX505W mass spectrometer. IR spectra were obtained with a Perkin Elmer GX FT-IR spectrometer. UV spectra were obtained with a Hitachi U3410 spectrometer. CD spectra were obtained with JASCO J-20A spectroporalimeter. TLC was carried out using precoated Silica gel 60F_{254} plates (Merck).

Plant Source and Isolation Twigs of *Magnolia denudata* were collected at a private garden in Shizuoka city on July 1995. The twigs (1.5 kg) were powdered and extracted with hot MeOH under reflux. The MeOH extract was partitioned between AcOEt and water to give an AcOEt soluble fraction. The AcOEt soluble fraction (29 g) was chromatographed on a silica gel column using a gradient $CHCl_3$–MeOH solvent system to give ten fractions, fr. 1 (900 mg), fr. 2 (100 mg), fr. 3 (240 mg), fr. 4 (760 mg), fr. 5 (720 mg), fr. 6 (2.0 g), fr. 7 (2.1 g), fr. 8 (800 mg), fr. 9 (1.8 g) and fr. 10 (11 g). These fractions were further separated by repeated and precise HPLC using an ODS column and a CH_3CN–water solvent system. Fraction. 2 gave licarin B (**18**) (13 mg). Fraction 4 gave acuminatin (**19**) (10 mg), denudanolide A (**1**) (17 mg), denudadione A (**5**) (12 mg). Fraction 5 gave denudatin B (**9**) (290 mg), denudatin A (**10**) (40 mg), **11** (10 mg), kadsurin A (**12**) (36 mg) and denudadione B (**6**) (14 mg). Fraction 6 gave denudanolide B (**2**) (20 mg), C (**3**) (13 mg), D (**4**) (12 mg), denudadione C (**7**) (12 mg), **8** (5 mg), veraguensin (**20**) (27 mg), grandisin (**21**) (27 mg), isodihydrofutoquinol A (**24**) (7 mg) and isodihydrofutoquinol B (**25**) (12 mg). Fraction 7 gave mirandin-A (**17**) (20 mg) and yangambin (**22**) (50 mg). Fraction 8 gave **13** (150 mg), **14** (12 mg), burcellin (**15**) (11 mg) and **16** (10 mg). Fraction 10 gave syringresinol (**23**) (200 mg).

Denudanolide A (**1**) HR-EI-MS; *m/z* 356.1220 $[M]^+$ (Calcd for $C_{20}H_{20}O_6$; 356.1259), IR ν_{max} (KBr) cm^{-1}; 1752, 1681, 1490, 1249, 1038, CD; $[\theta]_{343}-3465$, $[\theta]_{280}-2541$, $[\theta]_{238}+28182$ (MeOH), ^{1}H-NMR data are shown in Table 1 and ^{13}C-NMR data are shown in Table 2.

Denudanolide B (**2**) EI-MS; *m/z* 358 $[M]^+$ $C_{20}H_{22}O_6$, ^{1}H-NMR data are shown in Table 1 and ^{13}C-NMR data are shown in Table 2.

Denudanolide C (**3**) HR-EI-MS; *m/z* 372.1546 $[M]^+$ (Calcd for $C_{21}H_{24}O_6$; 372.1573), IR ν_{max} (KBr) cm^{-1}; 1750, 1681, 1518, 1263, 1240, 1144, CD; $[\theta]_{345}-3720$, $[\theta]_{236}+30504$ (MeOH), ^{1}H-NMR data was shown in Table 1 and ^{13}C-NMR data was shown in Table 2.

Denudanolide D (**4**) HR-EI-MS; *m/z* 402.1704 $[M]^+$ (Calcd for $C_{22}H_{24}O_7$; 402.1678), IR ν_{max} (KBr) cm^{-1}; 1750, 1681, 1592, 1240, 1129, CD; $[\theta]_{347}-4248$, $[\theta]_{248}+15624$ (MeOH), ^{1}H-NMR data are shown in Table 1 and ^{13}C-NMR data was shown in Table 2.

Denudadione A (**5**) HR-EI-MS; *m/z* 356.1661 $[M]^+$ (Calcd for $C_{21}H_{24}O_5$; 356.1624), IR ν_{max} (KBr) cm^{-1}; 1768, 1681, 1518, 1263, 1144, CD; $[\theta]_{335}-10252$, $[\theta]_{305}+5553$, $[\theta]_{270}-11108$, $[\theta]_{230}+37288$ (MeOH), ^{1}H-NMR data are shown in Table 1 and ^{13}C-NMR data are shown in Table 2.

Denudadione B (**6**) HR-EI-MS; *m/z* 340.1282 $[M]^+$ (Calcd for $C_{20}H_{20}O_5$; 340.1311), IR ν_{max} (KBr) cm^{-1}; 1767, 1681, 1490, 1249, 1038, CD; $[\theta]_{332}-6195$, $[\theta]_{301}+3812$, $[\theta]_{262}-12628$, $[\theta]_{225}+27877$ (MeOH), ^{1}H-NMR data are shown in Table 1 and ^{13}C-NMR data are shown in Table 2.

Denudadione C (**7**) HR-EI-MS; *m/z* 340.1323 $[M]^+$ (Calcd for $C_{20}H_{20}O_5$; 340.1311), ^{1}H-NMR data are shown in Table 1, ^{13}C-NMR data are shown in Table 2.

(1*S*,5*S*,6*S*,7*S*)-5-Allyl-6-methyl-3-methoxy-7(3,4-methylendioxyphenyl)-bicyclo[3.2.1]oct-3-en-2,8-dione (**8**) EI-MS; *m/z* 340 $[M]^+$ $C_{20}H_{20}O_5$, IR ν_{max} (KBr) cm^{-1}; 1671, 1624, 1517, 1268, 1140, CD; $[\theta]_{350}+3825$, $[\theta]_{250}-14205$ (MeOH), ^{1}H-NMR data are shown in Table 1 and ^{13}C-NMR data are shown in Table 2.

Anti-PAF Activity Anti-PAF activity test was carried out according to the novel method for determination of acetyl-CoA : *lyso*-PAF acetyltransferase activity as previously mentioned.[2]

Acknowledgements We thank Dr. M. Uchida, the Central Analytical Center of University of Shizuoka, for his support of the HR-EI-MS measurement. We also thank Dr. Yahara of Kumamoto University, for kind discussions. This work was supported by a Research Fund of Shizuoka Prefectural Government, Japan.

References

1) Shen T. Y., Hwang S.-B., Chang M. N., Doebber T. W., Lan M.-H. T., Wu M. S., Wang X., Han G. Q., Li R. Z., *Proc. Natl. Acad. Sci. U.S.A.*, **82**, 672—676 (1985).
2) Yamazaki R., Sugatani J., Fujii I., Kuroyanagi M., Umerhara K., Ueno A., Suzuki Y., Miwa M., *Biochemical Pharmacology*, **47**, 995—1006 (1994).
3) Jensen S., Hansen J., Boll P. M., *Phytochemistry*, **33**, 523—530 (1993).
4) Iida T., Ichino K., Ito K., *Phytochemistry*, **21**, 2939—2941 (1982).
5) Han G., Li S., Li. C., Springer J. P., Hawng S. B., Cheng M. N., *Yaoxue Xuebao*, **21**, 361—365 (1986).
6) Chang M. N., Han G-Q., Arison B. H., Springer J. P., Hwang S-B., Shen T. Y., *Phytochemistry*, **24**, 2079—2082 (1985).
7) Jensen S., Olsen C. E., Tyagi O. D., Boll P. M., Hussaini F. A., Guputa S., Bisht K. S., Parmar V. S., *Phytochemistry*, **36**, 789—792 (1994).
8) Lima O. A., Gottlieb O. R., Magalhaes M. T., *Phytochemistry*, **11**, 2031—2037(1972).
9) Aiba C. J., Fernandes J. B., Gottlieb O. R., Maia J. G. S., *Phytochemistry*, **14**, 1597—1604 (1975).
10) Gottlieb O. R., da Silva M. L., Ferreira Z. S., *Phytochemistry*, **14**, 1825—1827 (1975).
11) Filho R. B., Figliuolo R. O., Gottlieb O. R., *Phytochemistry*, **19**, 659—662 (1980).
12) Dias D. A., Yoshida M., Gottlieb O. R., *Phytochemistry*, **25**, 2613—2616 (1986).

13) El-Feraly F. S., Cheatham S. F., Hufford S. D., Li W.-S., *Phytochemistry*, **21**, 1133—1135 (1982).
14) Barata L. E. S., Baker P. M., Gottlieb O. R., Ruveda E. A., *Phytochemistry*, **17**, 783—785 (1978).
15) Ma Y., Han G.-Q., Li C. L., Cheng J. L., Arison B. H., Hwang S. B., *Acta Pharm. Sin.*, **26**, 345—350 (1991).
16) Briggs L. H., Cambie R. C., Couch R. A. F., *J. Chem. Soc. C*, **1968**, 3042—3045.
17) Nawwar M. A. M., Buddrus J., Bauer H., *Phytochemistry*, **21**, 1755—1758 (1982).
18) Tyagi O. D., Jensen S. Boll., Sharma N. K., Bisht K. S., Parmar V. S., *Phytochemistry*, **32**, 445—448 (1993).
19) Snatzke G, *Tetrahedron*, **21**, 413—420, 421—438 (1965)
20) Djerassi C., Records R., Bunnenberg E., Mislow K., Moscowitz A., *J. Am. Chem. Soc.*, **84**, 870—872 (1962).
21) Xiomara R. Y., Aura M. P. de D., Pedero P. D. D., *Phytochemistry*, **25**, 1953—1956 (1986).
22) Angle S. R., Turnbull K. D., *J. Am. Chem. Soc.*, **112**, 3698—3700 (1990).

Four New Saponins from the Root Bark of *Aralia elata*

Shao-jiang SONG,[a,b] Norio NAKAMURA,[a] Chao-mei MA,[a] Masao HATTORI,*,[a] and Sui-xu XU[b]

Institute of Natural Medicine, Toyama Medical and Pharmaceutical University,[a] 2630 Sugitani, Toyama 930–0194, Japan and Department of Natural Product, Shenyang Pharmaceutical University,[b] Shenyang 110015, China.

Received December 22, 1999; accepted February, 24, 2000

Four new saponins, 3-*O*-[β-D-glucopyranosyl (1→3)-α-L-arabinopyranosyl]-16α-hydroxyoleanolic acid 28-*O*-β-D-glucopyranosyl ester (called aralia-saponin I), 3-*O*-[β-D-glucopyranosyl(1→3)-α-L-arabinopyranosyl]-16α-hydroxyhederagenin 28-*O*-β-D-glucopyranosyl ester (aralia-saponin II), 3-*O*-[β-D-glucopyranosyl(1→3)-β-D-glucopyranosyl(1→3)-α-L-arabinopyranosyl]-16α-hydroxyoleanolic acid 28-*O*-β-D-glucopyranosyl ester (aralia-saponin III), 3-*O*-[β-D-glucopyranosyl(1→3)-β-D-glucopyranosyl(1→3)-β-D-glucopyranosyl]-16α-hydroxyoleanolic acid 28-*O*-β-D-glucopyranosyl ester (aralia-saponin IV), were isolated from the root bark of *Aralia elata* (Miq.) Seem., together with nineteen known compounds including glycosides of (20*S*)-protopanaxadiol and (20*S*)-protopanaxatriol. Their structures were determined on the basis of chemical and spectroscopy methods.

Key words Araliaceae; *Aralia elata*; 16α-hydroxyhederagenin; 16α-hydroxyoleanolic acid; saponin

Aralia elata (Miq.) Seem. (Japanese name: Taranoki) (Araliaceae) is widely distributed in the northeast of China and Korea. Its root bark has been used as a folk medicine for rheumatism, diabetes and as a tonic in China, Japan and Russia.[1] Many saponins have been isolated from this plant, and reported to show anti-diabetic activity and a cytoprotective effect on carbon tetrachloride-induced hepatic injury.[2—7] The present paper deals with the isolation and structure elucidation of four new saponins, called aralia-saponins I—IV (**1**—**4**), and nineteen known compounds, including nine saponins (**14**, **16**—**23**) that were isolated for the first time from this plant.

Results and Discussion

The air-dried root bark of *A. elata* was extracted with methanol. The methanol extract was suspended in water, washed with petroleum ether and chloroform, and then extracted with butanol saturated with water. The butanol soluble part was repeatedly chromatographed over normal and reversed-phase silica gel to give 23 saponins. The structures of isolated saponins are shown in Chart 1. The known compounds were identified as 3-*O*-[β-D-glucopyranosyl (1→3)-α-L-arabinopyranosyl] hederagenin 28-*O*-β-D-glucopyranosyl ester (**5**),[3] congmuyenoside B (**6**),[4] 28-*O*-β-D-glucopyranosyloleanolic acid (**7**),[5] 3-*O*-[β-D-galactopyranosyl (1→6)-β-D-glucopyranosyl]oleanolic acid (**8**),[5] elatoside F (**9**),[6] calenduloside E (**10**),[6] spinasaponin A (**11**),[7] spinasaponin A 28-*O*-glucoside (**12**),[6] calenduloside G (**13**),[5] elatoside A (**14**),[7] elatoside C (**15**),[7] 3-*O*-{[β-D-glucopyranosyl (1→2)]-[α-L-arabinopyranosyl (1→3)]-β-D-glucuronopyranosyl}-oleanolic acid (**16**),[5] (20*S*)-protopanaxadiol 3-*O*-β-D-glucopyranosyl-20-β-D-glucopyranoside (**17**),[8] (20*S*)-protopanaxadiol 3-*O*-β-D-glucopyranosyl-20-α-L-arabinopyranosyl(1→6)-β-D-glucopyranoside (**18**),[8] ginsenoside Rb_2 (**19**),[9] (20*S*)-protopanaxadiol 3-*O*-[β-D-glucopyranosyl(1→2)-β-D-glucopyranosyl]-20-α-L-arabinopyranosyl(1→6)-β-D-glucopyranoside (**20**),[8] (20*S*)-protopanaxatriol-20-α-L-arabinopyranosyl(1→6)-β-D-glucopyranoside (**21**),[8] (20*S*)-protopanaxatriol 6-*O*-[β-D-glucopyranosyl (1→2)-β-D-glucopyranoside (**22**),[10] ginsenoside Re (**23**),[10] by comparing their spectral data with those reported previously.

Compound **1** (aralia-saponin I) showed quasi-molecular ion peaks at *m/z* 951 $[M+Na]^+$ in the positive ion electrospray ionization (ESI)-MS, and at *m/z* 927 $[M-H]^-$ in the negative ion ESI-MS, suggesting the molecular formula of $C_{47}H_{76}O_{18}$ [HR-FAB-MS, *m/z*: 951.4910 $[M+Na]^+$ (Calcd for $C_{47}H_{76}O_{18}Na$: 951.4931)]. The IR spectrum showed the presence of an ester carbonyl group at 1740 cm^{-1} and an olefinic group at 1640 cm^{-1}. The ^1H-NMR spectrum of **1** exhibited signals characteristic of seven singlet methyls at δ 0.87, 0.96, 0.99, 1.02, 1.12, 1.26 and 1.84, one trisubstituted olefinic proton at δ 5.59, and three anomeric protons at δ 6.33, 5.39 and 4.73. The ^{13}C-NMR spectrum of **1** showed signals of a pair of olefinic carbons at δ 122.7 and 144.4, three anomeric carbons at δ 107.3, 106.2 and 95.7, and a car-

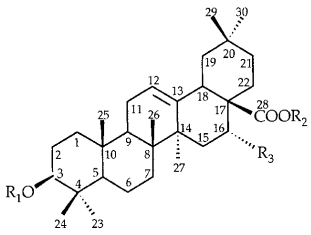

	R1	R2	R3
1	-ara^3-glc	glc	OH
3	-ara^3-glc^3-glc	glc	OH
4	-glc^3-glc^3-glc	glc	OH
7	H	glc	H
8	-glc^6-gal	H	H
9	-ara^3-glc (2 xyl)	glc	H
10	-glcA	H	H
11	-glcA^3-glc	H	H
12	-glcA^3-glc	glc	H
13	-glcA^3-gal	H	H
14	-glcA^3-gal (2 xyl)	H	H
15	-glcA^3-glc (2 xyl)	glc	H
16	-glcA^2-ara (3 glc)	H	H

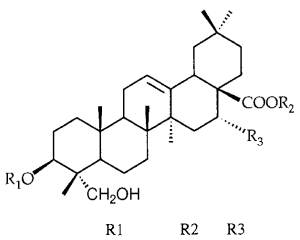

	R1	R2	R3
2	-ara^3- glc	glc	OH
5	-ara^3- glc	glc	H
6	-glc^3-glc^3-glc (2 glc)	H	H

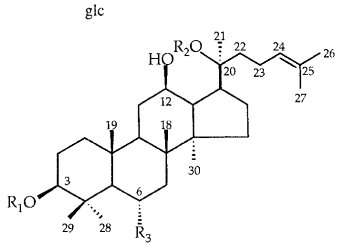

	R1	R2	R3
17	glc	glc	H
18	glc	-glc^6-ara	H
19	-glc^2-glc	glc	H
20	-glc^2-glc	-glc^6-ara	H
21	H	-glc^6-ara	OH
22	H	H	-O-glc^2-glc
23	H	glc	-O-glc^2-rha

Chart 1. Structures of Compounds Isolated from the Root Bark of *Aralia elata*

* To whom correspondence should be addressed. e-mail: saibo421@ms.toyama-mpu.ac.jp

© 2000 Pharmaceutical Society of Japan

Table 1. ^{1}H-NMR Spectrum Data of Compounds **1**—**4** in C_5D_5N (500 MHz)

	1	**2**	**3**	**4**
Aglycon				
3	3.34 (dd, J=4.0, 11.5 Hz)	4.25	3.34 (dd, J=4.0, 11.5 Hz)	3.35 (dd, J=4.0, 11.5 Hz)
12	5.59 (br s)	5.58 (br s)	5.59 (br s)	5.59 (br s)
16	5.31 (br s)	5.26 (br s)	5.31 (br s)	5.31 (br s)
18	3.51 (dd, J=4.5, 14.0 Hz)	3.48 (dd, J=4.0, 14.0 Hz)	3.51 (dd, J=4.0, 14.0 Hz)	3.51 (dd, J=4.0, 12.0 Hz)
23	1.26 (s)	3.66 (d, J=11 Hz)	1.28 (s)	1.26 (s)
		4.27 (d, J=11 Hz)		
24	0.96 (s)	0.91 (s)	0.97 (s)	0.98 (s)
25	0.87 (s)	0.96 (s)	0.88 (s)	0.85 (s)
26	1.12 (s)	1.34 (s)	1.12 (s)	1.12 (s)
27	1.84 (s)	1.75 (s)	1.83 (s)	1.84 (s)
29	0.99 (s)	0.95 (s)	0.98 (s)	0.98 (s)
30	1.02 (s)	1.00 (s)	1.02 (s)	1.02 (s)
3-*O*-Sugar	Ara	Ara	Ara	Glc
1′	4.73 (d, J=7.5 Hz)	4.93 (d, J=7.5 Hz)	4.70 (d, J=7.5 Hz)	4.85 (d, J=8.0 Hz)
2′	4.58[a]	4.56[a]	4.55[a]	4.02
3′	4.20[a]	4.05[a]	4.20[a]	4.19
4′	4.42[a]	4.35[a]	4.36[a]	3.92
5′	3.59 (d, J=11.5 Hz)	3.59 (d, J=11.5 Hz)	3.69 (dd, J=11.5, 2.5 Hz)	4.05
	4.13 (d, J=11 Hz)	4.13 (d, J=11 Hz)		
6′				4.52[a]
Glc				
1″	5.39 (d, J=8.0 Hz)	5.29 (d, J=8.0 Hz)	5.39 (d, J=8.0 Hz)	5.28 (d, J=8.0 Hz)
2″	4.02	4.01	4.14	4.06
3″	3.98	4.25	4.21	4.22
4″	4.21	4.35	4.11	4.16
5″	3.95	4.26	3.91	4.42
6″	4.45[a]	4.44[a]	4.51[a]	4.43[a]
Glc				
1‴			5.28 (d, J=8.0 Hz)	5.31 (d, J=8.0 Hz)
2‴			4.18	4.04
3‴			4.23	4.21
4‴			4.17	3.92
5‴			4.01	4.42
6‴			4.45[a]	4.52[a]
C-28-Glc				
1	6.33 (d, J=8.0 Hz)	6.31 (d, J=8.0 Hz)	6.32 (d, J=8.0 Hz)	6.35 (d, J=8.0 Hz)
2	4.13	4.12	4.15	4.14
3	4.24	4.25	4.25	4.25
4	4.30	4.31	4.30	4.28
5	4.00	3.99	4.02	4.01
6	4.53[a]	4.52[a]	4.32[a]	4.43[a]

a) Chemical shifts of these signals were determined by ^{1}H–^{1}H COSY, HOHAHA and HMQC.

bonyl carbon at δ 175.9. On acid hydrolysis, an aglycone of **1** was determined to be 16-hydroxyoleanolic acid by comparing the ^{1}H-NMR and ^{13}C-NMR spectra data with those reported.[11] The configuration of a hydroxyl group at C-16 was determined to be α, for a nuclear Overhauser effect (NOE) correlation was found between proton signals at δ 5.31 (H-16) and δ 1.12 (H_3-26) in the nuclear Overhauser enhancement and exchange spectroscopy (NOESY) spectrum. The monosaccharide units obtained were identified by co-TLC with authentic samples as arabinose and glucose; their absolute configurations were determined as L and D-forms, respectively, by a method developed by Hara *et al.*[12] The spin systems for sugars were assigned on the basis of spectroscopic evidence obtained by ^{1}H–^{1}H correlation spectroscopy (COSY), ^{1}H-detected multiple quantum coherence (HMQC) and homonuclear Harmann-Hahn (HOHAHA) experiments. The sugar components were identified as one arabinose and two glucose, their protons and carbons being assigned as shown in Tables 1 and 2. The sugar linkages were determined on the basis of the heteronuclear multiple-bond correlation (HMBC) spectrum. Long-range couplings ($^3J_{HCOH}$) were observed between a proton signal at δ 6.33 (glc-H-1) and a carbonyl carbon signal at δ 175.9 (C-28), between a proton signal at δ 4.73 (ara-H-1′) and a carbon signal at δ 88.5 (C-3), and between a proton signal at δ 5.39 (glc-H-1″) and a carbon signal at δ 84.0 (ara-C-3′), suggesting glycosylation at C-3 with a glc (1→3) ara moiety and at C-28 with a glucose moiety. Furthermore, the characteristic ion peaks at *m/z* 789 $[M+Na-glc]^+$ in the positive ion ESI-MS, and at *m/z* 765 $[M-H-glc]^-$, 603 $[M-H-glc-glc]^-$ and 461 $[M-H-glc-glc-ara]^-$ in the negative ion ESI-MS confirmed the sugar linkages. The anomeric configurations of the sugar moieties were determined to be β for glucose and α for arabinose, on the basis of the J_{H-H} values (8.0 and 7.5 Hz, respectively) . From the above evidence, the structure of **1** was concluded to be 3-*O*-[β-D-glucopyranosyl (1→3)-α-L-arabinopyranosyl]-16α-hydroxyoleanolic acid 28-*O*-β-D-glucopyranosyl ester.

Compound **2** (aralia-saponin II) with HR-FAB-MS *m/z*: 967.4868 $[M+Na]^+$ (Calcd for $C_{47}H_{76}O_{19}Na$: 967.4879),

Table 2. ^{13}C-NMR Spectrum Data of Compounds **1**—**4** in C_5D_5N (500 MHz)

C-position	1	2	3	4
1	38.9	38.8	38.8	38.8
2	26.7	26.2	27.1	27.2
3	88.5	81.9	88.7	88.9
4	39.6	43.5	39.6	39.5
5	55.9	47.8	55.9	55.8
6	18.5	18.1	18.5	18.5
7	33.4	32.2	33.2	33.2
8	40.1	41.9	40.1	40.0
9	47.2	47.3	49.1	47.1
10	37.1	36.9	37.0	36.9
11	23.8	23.8	23.8	23.8
12	122.7	122.7	122.7	122.7
13	144.4	144.3	144.4	144.4
14	42.1	40.1	42.1	42.0
15	35.9	36.1	36.1	36.1
16	74.1	74.5	74.5	74.5
17	49.1	48.9	49.1	49.1
18	41.3	41.1	41.2	41.3
19	47.2	47.0	47.1	47.5
20	30.8	30.7	30.8	30.8
21	36.1	35.9	33.4	36.9
22	32.2	32.2	32.2	32.1
23	28.1	64.1	28.0	28.1
24	16.9	13.6	16.9	17.0
25	15.7	16.3	15.7	15.6
26	17.6	17.5	17.5	17.5
27	27.2	27.1	27.2	27.2
28	175.9	175.9	175.9	175.9
29	33.2	33.1	33.2	33.2
30	24.6	24.5	24.5	24.5
3-*O*-Sugar	Ara	Ara	Ara	Glc
1′	107.3	106.5	107.4	106.3
2′	71.8	71.9	71.9	74.5
3′	84.0	84.1	83.3	88.2
4′	69.2	69.2	69.4	69.8
5′	66.9	67.0	67.1	78.2
6′				62.2
Glc				
1″	106.2	106.3	105.7	105.8
2″	75.6	75.8	74.3	74.4
3″	78.3	78.8	88.3	88.4
4″	71.5	71.4	69.6	69.8
5″	78.6	78.3	78.2	78.1
6″	62.2	62.1	62.1	62.2
Glc				
1‴			105.9	105.2
2‴			75.6	75.6
3‴			78.1	78.7
4‴			71.5	71.6
5‴			79.4	77.8
6‴			62.2	62.5
C-28-Glc				
1	95.7	95.7	95.8	95.9
2	74.4	74.1	74.0	74.3
3	78.8	78.6	78.3	78.9
4	71.1	70.1	70.9	71.1
5	79.3	79.3	78.1	79.3
6	62.6	62.6	62.5	62.5

showed quasi-molecular ion peaks at *m/z* 967 $[M+Na]^+$ in the positive ion ESI-MS, and at *m/z* 943 $[M-H]^-$ in the negative ion ESI-MS. The IR spectrum showed the presence of an ester carbonyl group at 1740 cm^{-1} and an olefinic group at 1640 cm^{-1}. The ^{1}H-NMR and ^{13}C-NMR spectra of **2** were similar to those of **1**, especially in the sugar region. The difference in chemical shift for the aglycone of **2** was that a methyl group at C-23 was replaced by a hydroxymethyl group (δ_H 3.66, 4.27, δ_C 64.1). The ^{1}H-NMR spectrum of **2** showed signals [δ 5.26 (br s. 16-H), δ 1.75 (s, 27-H$_3$)] characteristic of hederagenin bearing a 16-hydroxyl group.[13] The spin systems for sugars were assigned by detailed analysis of the two-dimensional (2D)-NMR (^{1}H–^{1}H COSY, HMQC, HOHAHA) spectra. The sugar linkages were determined on the basis of the HMBC spectrum, correlations were observed between a proton signal at δ 6.31 (glc-H-1) and a carbonyl carbon signal at δ 175.9 (C-28), whereas the proton signals at δ 4.93 (ara-H-1′) and 5.29 (glc-H-1″) showed correlations with the carbon signals at δ 81.9 (C-3) and δ 84.1 (ara-C-3′), respectively. The configuration of a hydroxyl group at C-16 was determined to be α, for an NOE correlation was found between proton signals at δ 5.26 (H-16) and δ 1.34 (H$_3$-26) in the NOESY spectrum. On acid hydrolysis, **2** yielded L-arabinose and D-glucose. Based on the above data, **2** was determined to be 16α-hydroxyhederagenin glycosylated at C-3 with a glc (1→3) ara moiety and at C-28 with a glucose moiety. Moreover, significant fragment ions observed at *m/z* 781 $[M-H-glc]^-$, 619 $[M-H-glc-glc]^-$ and 487 $[M-H-glc-glc-ara]^-$ in the negative ion ESI-MS confirmed the linkages of sugars. The anomeric configurations of the sugar moieties were determined to be β for glucose and α for arabinose, on the basis of the J_{H-H} values (8.0 and 7.5 Hz, respectively). From the above evidence, the structure of **2** was concluded to be 3-*O*-[β-D-glucopyranosyl(1→3)-α-L-arabinopyranosyl]-16α-hydroxyhederagenin 28-*O*-β-D-glucopyranosyl ester.

Compound **3** (aralia-saponin III), HR-FAB-MS *m/z*: 1113.5437 $[M+Na]^+$ (Calcd for $C_{53}H_{86}O_{23}Na$: 1113.5458), showed quasi-molecular ion peaks $[M+Na]^+$ at *m/z* 1113 in the positive ion ESI-MS, and at *m/z* 1089 $[M-H]^-$ in the negative ion ESI-MS. Compound **3** displayed four anomeric proton signals at δ 6.32, 5.39, 5.28 and 4.70 in the ^{1}H-NMR spectrum, and four anomeric carbon signals at δ 107.4, 105.9, 105.7 and 95.8 in the ^{13}C-NMR spectrum. Comparison of the spectral data between **1** and **3** showed that signals for an aglycone part were superimposable, indicating that the aglycone of **3** was also 16α-hydroxyoleanolic acid and the sugars were linked at both C-3 and C-28 positions. On acid hydrolysis, the monosaccharide units obtained were identified as L-arabinose and D-glucose by the method used for **1**. The spin systems for sugars were assigned on the basis of spectroscopic evidence obtained in ^{1}H–^{1}H-COSY, HMQC and HOHAHA experiments. The sugar components were identified as one arabinose and three glucose, and sugar linkages were determined by HMBC. Long-range coupling ($^3J_{HCOH}$) observed between a proton signal at δ 4.70 (ara-H-1′) and a carbon signal at δ 88.7 (C-3), between a proton signal at δ 5.39 (glc-H-1″) and a carbon signal at δ 83.3 (ara-C-3′), between a proton signal at δ 5.28 (glc-H-1‴) and a carbon signal at δ 88.3 (glc-C-3″), and between a proton signal at δ 6.32 (glc-H-1) and a carbon signal at δ 175.9 (C-28), confirmed glycosylation at C-3 with a glc(1→3)glc(1→3)-ara moiety and at C-28 with a glucose moiety. In addition, the significant fragment ions observed at *m/z* 928 $[M-glc]^-$, 766 $[M-glc-glc]^-$ and 604 $[M-glc-glc-glc]^-$ in the negative ion ESI-MS supported the linkages of sugars. The anomeric configurations of the sugar moieties were determined to be β for glucose and α for arabinose, on the basis

of the J_{H-H} values (8.0 and 7.5 Hz, respectively). From the above evidence, the structure of **3** was concluded to be 3-*O*-[β-D-glucopyranosyl(1→3)-β-D-glucopyranosyl(1→3)-α-L-arabinopyranosyl]-16α-hydroxyoleanolic acid 28-*O*-β-D-glucopyranosyl ester.

Compound **4** (aralia-saponin IV), HR-FAB-MS *m/z*: 1143.5583 $[M+Na]^+$ (Calcd for $C_{54}H_{88}O_{24}Na$: 1143.5564), showed quasi-molecular ion peaks $[M+Na]^+$ at *m/z* 1143 in the positive ion ESI-MS, and at *m/z* 1119 $[M-H]^-$ in the negative ion ESI-MS. Compound **4** displayed four anomeric proton signals at δ 6.35, 5.31, 5.28 and 4.85 in the ^{1}H-NMR spectrum, and four anomeric carbon signals at δ 106.3, 105.8, 105.2 and 95.9 in the ^{13}C-NMR spectrum. Signals for the aglycone part were similar to those of **3**, suggesting that the aglycone of **4** was also 16α-hydroxyoleanolic acid linked with sugars at C-3 and C-28 positions. On acid hydrolysis, the monosaccharide unit was identified to be D-glucose. By detailed analysis of the 2D-NMR (^{1}H–^{1}H COSY, HMQC, HOHAHA) spectra, all signals due to the sugar protons were assigned. In the HMBC spectrum, long-range correlations were observed between a proton signal at δ 4.85 (glc-H-1′) and a carbon signal at δ 88.9 (C-3 of the aglycone), between a proton signal at δ 5.28 (glc-H-1″) and a carbon signal at δ 88.2 (glc-C-3′), between a proton signal at δ 5.31 (glc-H-1‴) and a carbon signal at δ 88.4 (glc-C-3″), and between a proton signal at δ 6.35 (glc-H-1) and a carbon signal at δ 175.9 (C-28), indicating glycosylation at C-3 with a glc (1→3)glc(1→3)glc moiety and at C-28 with a glucose moiety. The anomeric configurations of the sugar moieties were determined to be β on the basis of the J_{H-H} values (8.0 or 7.5 Hz). From this evidence, the structure of **4** was determined to be 3-*O*-[β-D-glucopyranosyl(1→3)-β-D-glucopyranosyl(1→3)-β-D-gluco-pyranosyl]-16α-hydroxyoleanolic acid 28-*O*-β-D-glucopyranosyl ester.

Experimental

General Optical rotations were measured with a JASCO DIP-360 automatic polarimeter. IR spectra were measured with a JASCO FT/IR-230 IR spectrometer. ^{1}H- and ^{13}C-NMR spectra were measured with a JNM-LA400WB Lambda (JEOL) NMR (^{1}H, 400 MHz; ^{13}C, 100 MHz) or a Varian UNITY 500 (^{1}H, 500 MHz; ^{13}C, 125 MHz) spectrometer. ESI-MS were measured with a Perkin-Elmer SCIEX API III biomolecular mass analyzer. HR-FAB-MS were measured with a JEOL SX-102A mass spectrometer with a resolution of 5000 and glycerol containing a faint amount of NaCl. GC was performed on a Shimadzu GC-17A instrument.

Column chromatography was carried out on Silica-gel 60 (Merck,70—230 mesh). Medium pressure liquid chromatography (MPLC) was carried out on Lichroprep RP-18 (Merck, size A), Lichroprep Si 60 (Merck, size B). Preparative HPLC was carried out on a Gilson instrument with a 231XL injector, a 119 UV/VIS detector and a TSK-gel ODS-80Tm column (21.5×300 mm, Tosoh Co.). Spots were detected after spraying with ethanol–5% H_2SO_4.

Isolation of Compounds 1—23 from the Root Bark of *Aralia elata* The root bark of *A. elata* was collected at Xinbin (Liaoning, China), and its botanical source was confirmed by Professor Qishi Shun, Shenyang Pharmaceutical University (SPU), Shenyang, China. The specimen is deposited in the Department of Natural Products of SPU. Dried bark (3.5 kg) of A. elata was extracted three times with methanol (7 l each time) for 2 h under reflux, and the combined solutions were concentrated in vacuo to a syrup (1.25 kg), then suspended in water. The suspension was extracted with petroleum ether, chloroform and *n*-butanol saturated with water, successively, to give the respective extracts after removal of the solvent. The *n*-butanol-soluble part (100 g) was subjected to silica gel 60 column chromatography (10×100 cm) with $CHCl_3$–MeOH–H_2O (7 : 3 : 0.5) to give six fractions (fr. I—VI). Fraction III (15 g) was further separated by silica gel 60 column chromatography with a solvent system of $CHCl_3$–MeOH–H_2O (7 : 3 : 1) to yield **7** (30 mg), **8** (10 mg), **10** (7 mg) and a mixture. The mixture was then applied to RP-18 MPLC with MeOH–H_2O (7 : 3) and preparative HPLC [MeOH–0.1% trifluoroacetic acid (TFA)/H_2O (8 : 2→10 : 0), 5 ml/min, monitored at 205 nm] to afford **17** (12 mg), **18** (30 mg), **19** (400 mg), **20** (20 mg), **21** (8 mg), **22** (5 mg) and **23** (200 mg). Meanwhile, fraction V (10 g) was further separated by column chromatography on silica gel 60 with $CHCl_3$–MeOH–H_2O (6 : 4 : 1) to give three fractions (Va—Vc). Fraction Va (1.6 g) was applied to Si 60 MPLC with $CHCl_3$–MeOH–H_2O (65 : 35 : 10, lower phase) to yield **13** (20 mg) and **16** (23 mg). Fraction Vb (2.5 g) was applied to RP-18 MPLC with MeOH–H_2O (6 : 4) to yield **1** (25 mg), and then the residual mixture was applied to preparative HPLC [MeOH–0.1% TFA/H_2O (7 : 3→10 : 0), 5 ml/min, monitored at 205 nm] to afford **2** (15 mg), **3** (12 mg), **4** (4 mg), **5** (25 mg) and **6** (25 mg). Fraction Vc (1.2 g) was applied to preparative HPLC [MeOH–0.1% TFA/H_2O (7 : 3→10 : 0), 5 ml/min, monitored at 205 nm] to afford **9** (8 mg), **11** (12 mg), **12** (40 mg), **14** (7 mg) and **15** (35 mg).

3-*O*-[β-D-Glucopyranosyl(1→3)-α-L-arabinopyranosyl]-16α-hydroxyoleanolic Acid 28-*O*-β-D-Glucopyranosyl Ester (Aralia-saponin I, 1) Colorless amorphous powder, $[\alpha]_D$ −28.9° (*c*=0.15, pyridine). IR (KBr) cm^{-1}: 3400, 2950, 2880, 1740, 1640, 1464, 1394, 1300, 1278, 1030, 995. ^{1}H-NMR: Table 1. ^{13}C-NMR: Table 2. Positive ion ESI-MS *m/z*: 951 $[M+Na]^+$, 789 $[M+Na-glc]^+$. Negative ion ESI-MS *m/z*: 927 $[M-H]^-$, 765 $[M-H-glc]^-$, 603 $[M-H-glc-glc]^-$, 461 $[M-H-glc-glc-ara]^-$. HR-FAB-MS *m/z*: 951.4910 $[M+Na]^+$ (Calcd for $C_{47}H_{76}O_{18}Na$: 951.4931).

Acid Hydrolysis of 1 Compound **1** (5 mg) was refluxed with 7% HCl in H_2O–EtOH (1 : 1, 1 ml) for 3 h. The reaction mixture was partitioned between $CHCl_3$ and H_2O. The $CHCl_3$ layer was concentrated to dryness to afford 16-hydroxyoleanolic acid (1.5 mg) as an aglycone. The structure was determined by comparison of its ^{1}H-NMR and ^{13}C-NMR spectroscopic data with those of 16-hydroxyoleanolic acid.[11,13] The water layer was concentrated and checked by cellulose TLC [pyridine–ethyl acetate–acetic acid–water (36 : 36 : 7 : 21), *Rf*: L-arabinose, 0.61; D-glucose, 0.38]. The residual water layer was used to determine the absolute configuration of sugar as reported by Hara *et al.*[12] After being desalted with Amberlite MB-3 and dried, the residue was dissolved in pyridine (0.1 ml), then 0.1 M L-cysteine methyl ester hydrochloride in pyridine (0.2 ml) was added to the sugar solution. The mixture was kept at 60 °C for 1.5 h, dried *in vacuo*, and trimethylsilylated with hexamethyl disilazane–trimethyl chlorosilane (HMDS–TMCS) (0.1 ml) at 60 °C for 1 h. After partition with hexane (0.3 ml) and water (0.3 ml), the hexane layer was analyzed by GC [column, DB-1, J & W Scientific, 0.25 mm i.d.×30 m; column temperature, 50—230 °C, 15 °C/min then 230 °C, 18 min; carrier gas, He]. The sugar derivatives thus obtained showed retention times of 16.4 and 21.4 min, identical to those of authentic L-arabinose and D-glucose derivatives, respectively. Under the same conditions, derivatives of D-arabinose and L-glucose showed retention times of 17.0 and 22.0 min, respectively.

3-*O*-[β-D-Glucopyranosyl(1→3)-α-L-arabinopyranosyl]-16α-hydroxyhederagenin 28-*O*-β-D-Glucopyranosyl Ester (Aralia-saponin II, 2) Colorless amorphous powder, $[\alpha]_D$ −39.4° (*c*=0.22, pyridine). IR (KBr) cm^{-1}: 3400, 2920, 1740, 1640, 1550, 1460, 1394, 1300, 1260, 1030, 1260, 1080, 1035 and 995. ^{1}H-NMR: Table 1. ^{13}C-NMR: Table 2. Positive ion ESI-MS *m/z*: 967 $[M+Na]^+$. Negative ion ESI-MS *m/z*: 943 $[M-H]^-$, 781 $[M-H-glc]^-$, 619 $[M-H-glc-glc]^-$ and 487 $[M-H-glc-glc-ara]^-$. HR-FAB-MS *m/z*: 967.4868 $[M+Na]^+$ (Calcd for $C_{47}H_{76}O_{19}Na$: 967.4879).

Acid Hydrolysis of 2 Compound **2** (1 mg) was refluxed with 7% HCl in H_2O–EtOH (1 : 1, 1 ml) for 3 h. The reaction mixture was partitioned between $CHCl_3$ and H_2O. The water layer was concentrated and checked by cellulose TLC [pyridine–ethyl acetate–acetic acid–water (36 : 36 : 7 : 21), *Rf*: L-arabinose, 0.61; D-glucose, 0.38]. The residual water layer was desalted with Amberlite MB-3, treated with L-cysteine methyl ester hydrochloride and trimethyl-silylated with HMDS–TMCS then analyzed by GC in the same manner as described for **1**. The sugars were confirmed as L-arabinose and D-glucose, respectively.

3-*O*-[β-D-Glucopyranosyl(1→3)-β-D-glucopyranosyl(1→3)-α-L-arabinopyranosyl]-16α-hydroxyoleanolic Acid 28-*O*-β-D-Glucopyranosyl Ester (Aralia-saponin III, 3) Colorless amorphous powder, $[\alpha]_D$ −13.3° (*c*=0.2, pyridine). IR (KBr) cm^{-1}: 3400, 2920, 2850, 1740, 1640, 1550, 1464, 1380, 1310, 1080, 1030 and 890. ^{1}H-NMR: Table 1. ^{13}C-NMR: Table 2. Positive ion ESI-MS *m/z*: 1113 $[M+Na]^+$ and 951 $[M+Na-glc]^+$. Negative ion ESI-MS *m/z*: 1089 $[M-H]^-$, 927 $[M-H-glc]^-$, 765 $[M-H-glc-glc]^-$ and 603 $[M-H-glc-glc-glc]^-$. HR-FAB-MS *m/z*: 1113.5437 $[M+Na]^+$ (Calcd for $C_{53}H_{86}O_{23}Na$: 1113.5458).

Acid Hydrolysis of 3 Compound **3** (1 mg) was refluxed with 7% HCl in H_2O–EtOH (1 : 1, 1 ml) for 3 h. The reaction mixture was partitioned between $CHCl_3$ and H_2O. The water layer was concentrated and checked by cellulose TLC [pyridine–ethyl acetate–acetic acid–water (36 : 36 : 7 : 21),

Rf: L-arabinose, 0.61; D-glucose, 0.38] and the residual water layer was analyzed by GC as described above. The sugars were identified as L-arabinose and D-glucose, respectively.

3-*O*-[β-D-Glucopyranosyl(1→3)-α-D-glucopyranosyl(1→3)-β-D-glucopyranosyl]-16α-hydroxyoleanolic Acid 28-*O*-β-D-Glucopyranosyl Ester (Aralia-saponin IV, 4) Colorless amorphous powder, $[\alpha]_D$ −18.8° (*c*= 0.2, pyridine). IR (KBr) cm^{-1}: 3400, 2860, 1738, 1628, 1450, 1394, 1310, 1210, 1040, 890. ^{1}H-NMR: Table 1. ^{13}C-NMR: Table 2. Positive ion ESI-MS *m/z*: 1143 $[M+Na]^+$, 981 $[M+Na-glc]^+$. Negative ion ESI-MS *m/z*: 1119 $[M-H]^-$, 957 $[M-H-glc]^-$, 795 $[M-H-glc-glc]^-$, 633 $[M-H-glc-glc-glc]^-$ and 471 $[M-H-glc-glc-glc-glc]^-$. HR-FAB-MS *m/z*: 1143.5583 $[M+Na]^+$ (Calcd for $C_{54}H_{88}O_{24}Na$: 1143.5564).

Acid Hydrolysis of 4 Compound **4** (1 mg) was refluxed with 7% HCl in H_2O–EtOH (1 : 1, 1 ml) for 3 h. The reaction mixture was worked up as described above. The sugar component was identified as D-glucose alone.

Acknowledgements We are grateful to Miss Mari Ikurumi and Dr. Masako Takani of the Faculty of Pharmaceutical Science, Kanazawa University, Japan, for the measurement of HR-FAB-MS

References

1) New Medical College of Jiangsu (ed.), "Dictionary of Chinese Materia Medica," Shanghai Scientific and Technological Publishing Co., Shanghai, 1977, p. 2583.
2) Saito S., Ebashi J., Sumita S., Furumoto T., NagamuraY., Nishida K., Ishiguro I., *Chem. Pharm. Bull.*, **41**, 1935—1401 (1993).
3) Yang G., Zhou J., Song C., *Zhongcaoyao.*, **26**, 514—517 (1993).
4) Kuang H., San H., Zhang N., Okada Y., Okuyama T., *Chem. Pharm. Bull.*, **44**, 2183—2185 (1996).
5) Shao C., Kasai R., Xu J., Tanaka ., *Chem. Pharm. Bull.*, **37**, 311—314 (1989)
6) Yoshikawa M., Matsuda H., Harada E., *Chem. Pharm. Bull.*, **42**, 1354—1356 (1994).
7) Yoshikawa M., Murakami T., Harada E., Murakami N., *Chem. Pharm. Bull.*, **44**, 1923—1927 (1996).
8) Koizumi H., Sanada S., Ida Y., *Chem. Pharm. Bull.*, **30**, 2393—2398 (1982).
9) Tanaka O., Yahara S., *Phytochemistry*, **17**, 1353—1358 (1978).
10) Yahara S., Kaji K., Tanaka O., *Chem. Pharm. Bull.*, **27**, 88—92 (1979).
11) Nagao T., Tanaka R., Shimokawa H., Okabe H., *Chem. Pharm. Bull.*, **39**, 1719—1725 (1991).
12) Hara S., Okabe H., Mihashi K., *Chem. Pharm. Bull.*, **35**, 501—506 (1987).
13) Kitagawa I., Yoshikawa M., Yosioka I., *Tetrahedron Lett.*, **5**, 469—472 (1974).

Quantitative Structure–Activity Relationship Study of *N*-(3-Oxo-3,4-dihydro-2*H*-benzo[1,4]thiazine-6-carbonyl)guanidines as Potent Na/H Exchange Inhibitors

Takeshi YAMAMOTO,* Manabu HORI, Ikuo WATANABE, Kengo HARADA, Shoji IKEDA, and Hiroshi OHTAKA

R&D Laboratories, Nippon Organon K.K., 1–5–90, Tomobuchi-cho, Miyakojima-ku, Osaka 534–0016, Japan.
Received December 24, 1999; accepted February 15, 2000

We have previously reported that *N*-(4-isopropyl-2,2-dimethyl-3-oxo-3,4-dihydro-2*H*-benzo[1,4]oxazine-6-carbonyl)guanidine (4b) methanesulfonate salt (KB-R9032) is a potent and highly water-soluble Na/H exchange inhibitor. In a series of studies on Na/H exchange inhibitors, we designed and synthesized *N*-(3-oxo-3,4-dihydro-2*H*-benzo[1,4]thiazine-6-carbonyl)guanidines (5) as more potent inhibitors with high water-solubility. The design strategy for 5 was based on a quantitative structure–activity relationship (QSAR) study, involving the proportional relationship between the biological activity and hydrophobicity of the ring structure of compounds 4. As expected, compounds 5 showed more potent activity than 4. It was found by using the QSAR analysis that 5 were about five-fold more potent than 4. The increase in potency of compounds 5 well agreed with our previous QSAR analysis result. The most potent derivative was the methanesulfonate salt 5d of the 4-isopropyl derivative (IC_{50}=0.0091 μM). And in addition to the *in vitro* study, 5d showed significant protective activity against a rat acute myocardial infraction model.

Key words Na/H exchange inhibitor; quantitative structure–activity relationship; *N*-(2*H*-benzo[1,4]thiazine-6-carbonyl)guanidine

Changes in intracellular pH have been implicated in the pathophysiology of essential hypertension, myocardial ischemia, postischemic dysfunction and cellular death. However, the cells have some mechanisms which control and regulate intracellular pH. These mechanisms become vital, *e.g.*, for the correction of intracellular acidosis during and following a period of myocardial ischemia. One of the major alkalizing exchangers that exist in the myocardial cell is the Na/H exchanger which extrudes protons by the countertransport of Na^+ ions. There are many reports that the Na/H exchanger plays a key role in the pathophysiology of cardiac ischemia and reperfusion.[1)]

Although activation of the Na/H exchanger is essential for the restoration of normal intracellular pH, it results in a deleterious Na^+ overload after a prolonged period of ischemia. Due to the coupling via a Na/Ca exchanger, this causes a cellular Ca^{2+} overload, and finally, serious contractile dysfunction, arrhythmia, and cellular death. Recently, inhibition of the Na/H exchange has been experimentally shown to be a useful approach in limiting Ca^{2+} influx and avoiding its serious consequences during ischemia and reperfusion.[2)]

Some monocyclic aroylguanidines, EIPA (**1**),[3)] HOE-694 (**2a**)[4)] and HOE-642 (**2b**),[5)] are known to be typical Na/H exchange inhibitors (Chart 1), but there may still be some limitation for wide clinical application, because of their low water-solubility. Thus, we have started a new research project to discover more potent and highly water-soluble inhibitors. We have already reported the structural requirements for potent Na/H exchange inhibitors using the quantitative structure–activity relationship (QSAR) analysis of EIPA (**1**) and its derivatives.[6)] Namely, the structural requirements necessary for potent activity were as follows: 1) bicyclic aroylguanidines inhibited the Na/H exchanger, 2) the activity was proportionally related to the hydrophobicity of the bicyclic ring structure, and 3) a substituent having an appropriate length at the 5-position of 2-naphthoylguanidine enhanced the activity. In the series of study on Na/H exchange inhibitor design, we discovered *N*-(3-oxo-3,4-dihydro-2*H*-benzo[1,4]oxazine-7-carbonyl)guanidine (**3a**) as a lead compound for potent and highly water-soluble inhibitors.[7)] In this studies, we designed some compounds having moderate hydrophobicity (clog*P*[8)]), around 1.5—2, based on an optimum value necessary for good bioavailability.[9)] The QSAR analysis of **3** indicated that the lengths of the 2- and 4-substituents were parabolically related to the inhibitory activity, independently (Chart 2). The 2-ethyl-4-ethyl (or isopropyl) derivatives **3b** or **3c** (clog*P*=1.33 or 1.65) were biologically potent in *in vitro* study and highly water-soluble from a physicochemical view point.

Recently, we found that *N*-(2*H*-benzo[1,4]oxazine-6-carbonyl)guanidines **4** also had potent Na/H exchange inhibitory activity.[10)] The SAR of the 4-substituent of compounds **4** was similar to that of compounds **3**, although the relative positions of the guanidinocarbonyl group essential for potent activity were different from each other (Chart 2). With regard to the 2-substituent of compounds **3** and **4**, the SARs seemed to be somewhat different. Shorter and/or smaller substituents were tolerated, while longer and/or larger substituents reduced the activity. The most potent compound among **4** was the 2,2-dimethyl-4-isopropyl derivative **4b** (clog*P*=1.65). The methanesulfonate salt of **4b** (KB-R9032) showed high water-solubility and good bioavailability, so it was under further investigation as a promising Na/H exchange inhibitor candidate.

In addition, the QSAR analysis of **4** predicted that the isopropyl group of **4b** was significant for enhancement of the biological potency. However, it was not actually indicated that the 2,2-dimethyl moiety contributed to the increase of the activity in an *in vitro* assay, although this hydrophobic moiety would be important for adjustment of the clog*P* value

* To whom correspondence should be addressed. e-mail: Yamamoto.Takeshi@organon.co.jp
© 2000 Pharmaceutical Society of Japan

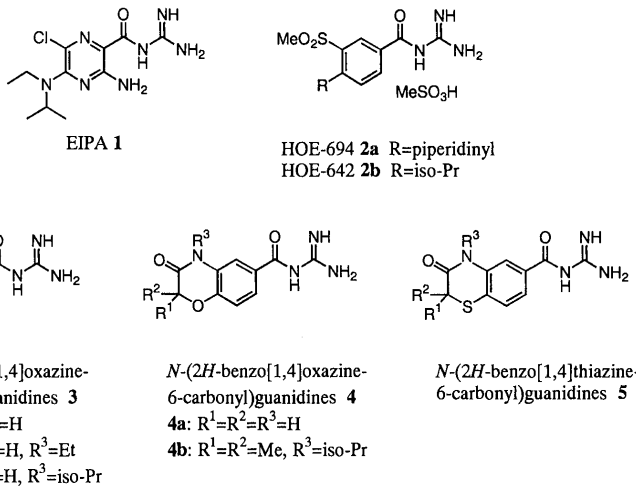

Chart 1. Na/H Exchange Inhibitors

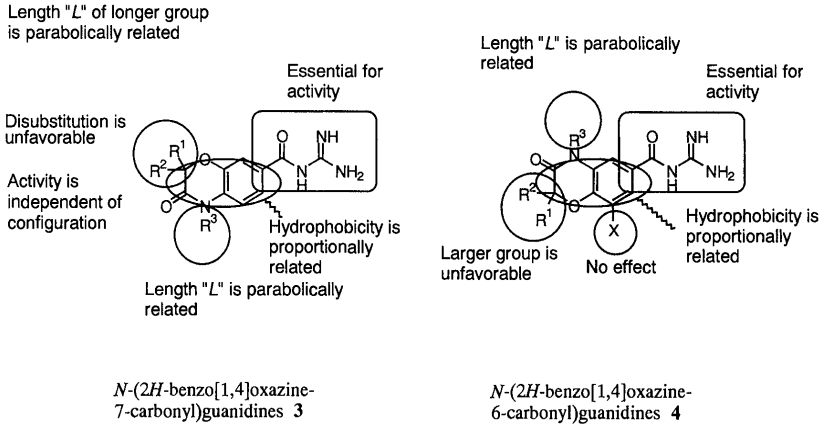

Chart 2. Structure–Activity Relationships of Benzoxazine Derivatives **3** and **4**

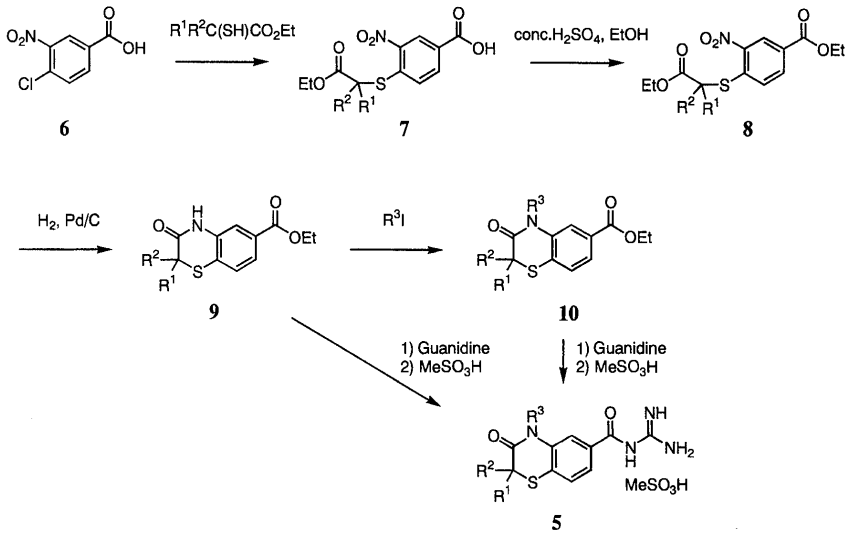

Chart 3. Synthesis of *N*-(2*H*-Benzo[1,4]thiazine-6-carbonyl)guanidines **5**

to the optimum range necessary for good bioavailability (around 1.5—2). As described before, hydrophobic fused-rings would be favorable for potent activity.[6] These results prompted us to design a more hydrophobic bicyclic ring by removal of the dimethyl moiety of **4b**. Consequently, we have designed *N*-(3-oxo-3,4-dihydro-2*H*-benzo[1,4]thiazine-6-carbonyl)guanidines **5a** as the new lead compound, with a clog*P* value appropriate for optimized compounds. The benzothiazine derivative **5a** was expected to be more potent than the benzoxazine derivative **4a**, because the clog*P* value of **5a** (0.20) was higher than that of **4a** (−0.36).[8]

In this paper, we describe the synthesis and SAR study of

Table 1. Physical Properties of *N*-(2*H*-Benzo[1,4]thiazine-6-carbonyl)guanidines **5**

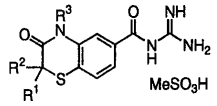

No.	R^1	R^2	R^3	Yield (%)	mp (°C) (Recryst. solvent)	Formula	Analysis Calcd (Found)		
							C	H	N
5a	H	H	H	5	263—264 (MeOH–H_2O)	$C_{10}H_{10}N_4O_2S \cdot CH_3SO_3H$	38.14 (38.14	4.07 4.23	16.18 16.28)
5b	H	H	Me	13	231—233 (MeOH–H_2O)	$C_{11}H_{12}N_4O_2S \cdot CH_3SO_3H$	39.99 (39.93	4.47 4.57	15.50 15.59)
5c	H	H	Et	7	232—234 (MeOH–H_2O)	$C_{12}H_{14}N_4O_2S \cdot CH_3SO_3H$	41.70 (41.68	4.85 4.88	14.96 15.09)
5d	H	H	iso-Pr	36	188—190 (EtOH)	$C_{13}H_{16}N_4O_2S \cdot CH_3SO_3H$	43.29 (43.07	5.19 5.28	14.42 14.36)
5e	H	H	Pr	44	228—230 (EtOH)	$C_{13}H_{16}N_4O_2S \cdot CH_3SO_3H$	43.29 (43.16	5.19 5.21	14.42 14.38)
5f	H	H	Butyl	41	193—195 (EtOH)	$C_{14}H_{18}N_4O_2S \cdot CH_3SO_3H$	44.76 (44.67	5.51 5.48	13.92 13.90)
5g	H	H	Pentyl	39	239—240 (EtOH)	$C_{15}H_{20}N_4O_2S \cdot CH_3SO_3H$	46.14 (46.02	5.81 5.85	13.45 13.51)
5h	H	Me	Et	28	169—171 (EtOH)	$C_{13}H_{16}N_4O_2S \cdot CH_3SO_3H$	43.29 (43.28	5.19 5.19	14.42 14.45)
5i	H	Me	iso-Pr	35	183—185 (EtOH)	$C_{14}H_{18}N_4O_2S \cdot CH_3SO_3H$	44.76 (44.68	5.51 5.48	13.92 13.93)

Table 2. Physical Properties of Methyl 2*H*-Benzo[1,4]thiazine-6-carboxylates **10**

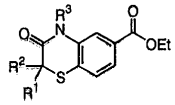

No.	R^1	R^2	R^3	Yield (%)	mp (°C) (Recryst. solvent)	Formula	Analysis Calcd (Found)		
							C	H	N
10a	H	H	Me	63	110—112 (IPE)	$C_{12}H_{13}NO_3S$	57.35 (57.35	5.21 5.20	5.57 5.64)
10b	H	H	Et	65	56—57 (Hexane)	$C_{13}H_{15}NO_3S$	58.85 (58.80	5.70 5.60	5.28 5.25)
10c	H	H	iso-Pr	50	Oil	$C_{14}H_{17}NO_3S$	60.19 (60.17	6.13 6.24	5.01 5.04)
10d	H	H	Pr	37	Oil	$C_{14}H_{17}NO_3S$	60.19 (60.58	6.13 6.37	5.01 4.84)
10e	H	H	Butyl	62	Oil	$C_{15}H_{19}NO_3S$	61.41 (61.45	6.53 6.65	4.77 4.64)
10f	H	H	Pentyl	44	Oil	$C_{16}H_{21}NO_3S$	62.52 (62.75	6.89 7.08	4.56 4.44)
10g	H	Me	Et	79	Oil	$C_{14}H_{17}NO_3S$	60.19 (60.45	6.13 6.26	5.01 4.95)
10h	H	Me	iso-Pr	83	Oil	$C_{15}H_{19}NO_3S$	61.41 (61.36	6.53 6.61	4.77 4.50)

Na/H exchange inhibitory activity of *N*-(3-oxo-3,4-dihydro-2*H*-benzo[1,4]thiazine-6-carbonyl)guanidines **5** in order to find potent Na/H exchange inhibitors.

Chemistry *N*-(2*H*-Benzo[1,4]thiazine-6-carbonyl)guanidines **5** listed in Table 1 were synthesized by the route shown in Chart 3. 4-Chrolo-3-nitrobenzoic acid (**6**) was allowed to react with ethyl mercaptoacetate or ethyl 2-mercaptopropionate to obtain 4-ethoxycarbonylmethyl (or 4-[(1-ethoxycarbony)ethyl])sulfanyl-3-nitrobenzoic acids **7**, which were converted to esters **8** by reflux with concentrated sulfuric acid in ethanol (EtOH). Compounds **8** were hydrogenated with palladium–charcoal (Pd–C), and the hydrogenated intermediates spontaneously cyclized to give ethyl 3-oxo-3,4-dihydro-2*H*-benzo[1,4]thiazine-6-carboxylates **9**, which were alkylated to give *N*-alkyl derivatives **10**. *N*-(2*H*-Benzo[1,4]thiazine-6-carbonyl)guanidines **5** were prepared from **9** or **10** by reflux with an excess amount of guanidine in dimethyl sulfoxide (DMSO) for several hours. The physical data for **5** and **10** are

Table 3. ^{1}H-NMR Spectral Data for *N*-(2*H*-Benzo[1,4]thiazine-6-carbonyl)guanidines **5**

No.	Spectral data (DMSO-d_6) δ
5a	2.40 (3H, s), 3.57 (2H, s), 7.52—7.60 (3H, m), 8.35 (4H, br), 10.77 (1H, br), 11.20 (1H, br)
5b	2.43 (3H, s), 3.43 (3H, s), 3.61 (2H, s), 7.60—7.71 (3H, m), 8.43 (4H, br), 11.35 (1H, br)
5c	1.18 (3H, t, *J*=7 Hz), 2.42 (3H, s), 3.58 (2H, s), 4.06 (2H, q, *J*=7 Hz), 7.59—7.68 (2H, m), 7.73 (1H, d, *J*=1 Hz), 8.43 (4H, br), 11.35 (1H, br)
5d	1.51 (6H, d, *J*=7 Hz), 2.45 (3H, s), 3.44 (2H, s), 4.58—4.64 (1H, m), 7.64—7.76 (3H, m), 8.42 (4H, br), 11.37 (1H, br)
5e	0.85 (3H, t, *J*=7 Hz), 1.52—1.64 (2H, m), 2.39 (3H, s), 3.61 (2H, s), 4.03 (2H, q, *J*=7 Hz), 7.61 (1H, dd, *J*=8, 2 Hz), 7.70 (1H, d, *J*=8 Hz), 7.73 (1H, d, *J*=2 Hz), 8.40 (4H, br), 11.31 (1H, br)
5f	0.88 (3H, t, *J*=7 Hz), 1.20—1.35 (2H, m), 1.46—1.58 (2H, m), 2.40 (3H, s), 3.61 (2H, s), 4.06 (2H, q, *J*=7 Hz), 7.62 (1H, dd, *J*=8, 1 Hz), 7.70 (1H, d, *J*=8 Hz), 7.75 (1H, d, *J*=1 Hz), 8.42 (4H, br), 11.33 (1H, br)
5g	0.84 (3H, t, *J*=7 Hz), 1.12—1.33 (4H, m), 1.46—1.60 (2H, m), 2.41 (3H, s), 3.61 (2H, s), 4.05 (2H, q, *J*=7 Hz), 7.62 (1H, d, *J*=8 Hz), 7.70 (1H, d, *J*=8 Hz), 7.75 (1H, s), 8.42 (4H, br), 11.34 (1H, br)
5h	1.18 (3H, t, *J*=7 Hz), 1.34 (3H, d, *J*=7 Hz), 2.41 (3H, s), 3.78 (1H, q, *J*=7 Hz), 4.07 (2H, q, *J*=7 Hz), 7.63 (1H, dd, *J*=8, 1 Hz), 7.69 (1H, d, *J*=8 Hz), 7.74 (1H, d, *J*=1 Hz), 8.44 (4H, br), 11.38 (1H, br)
5i	1.29(3H, d, *J*=7 Hz), 1.45 (3H, d, *J*=7 Hz), 1.46 (3H, d, *J*=7 Hz), 2.42 (3H, s), 3.57 (1H, q, *J*=7 Hz), 4.53—4.69 (1H, m), 7.59—7.67 (2H, m), 7.75 (1H, s), 8.43 (4H, br), 11.38 (1H, br)

Table 4. ^{1}H-NMR Spectral Data for Methyl 2*H*-Benzo[1,4]thiazine-6-carboxylates **10**

No.	Spectral data ($CDCl_3$) δ
10a	(DMSO-d_6) 1.40 (3H, t, *J*=7 Hz), 3.43 (2H, s), 3.49 (3H, s), 4.39 (2H, q, *J*=7 Hz), 7.41 (1H, d, *J*=8 Hz), 7.69 (1H, dd, *J*=8, 2 Hz), 7.75 (1H, d, *J*=2 Hz)
10b	(DMSO-d_6) 1.30 (3H, t, *J*=7 Hz), 1.40 (3H, t, *J*=7 Hz), 3.40 (2H, s), 4.10 (2H, q, *J*=7 Hz), 4.39 (2H, q, *J*=7 Hz), 7.41 (1H, d, *J*=8 Hz), 7.67 (1H, dd, *J*=8, 2 Hz), 7.81 (1H, d, *J*=2 Hz)
10c	1.39 (3H, t, *J*=7 Hz), 1.53 (6H, d, *J*=7 Hz), 3.31 (2H, s), 4.42 (2H, q, *J*=7 Hz), 4.63—4.74 (1H, m), 7.43 (1H, d, *J*=8 Hz), 7.67 (1H, dd, *J*=8, 1 Hz), 7.89 (1H, d, *J*=1 Hz)
10d	0.94 (3H, t, *J*=7 Hz), 1.42 (3H, t, *J*=7 Hz), 1.60—1.79 (2H, m), 3.41 (2H, s), 4.04 (2H, t, *J*=7 Hz), 4.39 (2H, q, *J*=7 Hz), 7.42 (1H, d, *J*=8 Hz), 7.68 (1H, dd, *J*=8, 1 Hz), 7.80 (1H, d, *J*=1 Hz)
10e	0.95 (3H, t, *J*=7 Hz), 1.36—1.42 (2H, m), 1.40 (3H, t, *J*=7 Hz), 1.60—1.64 (2H, m), 3.40 (2H, s), 4.05 (2H, t, *J*=7 Hz), 4.39 (2H, q, *J*=7 Hz), 7.42 (1H, d, *J*=8 Hz), 7.68 (1H, dd, *J*=8, 1 Hz), 7.81 (1H, d, *J*=1 Hz)
10f	0.88 (3H, t, *J*=7 Hz), 1.31—1.38 (4H, m), 1.41 (3H, t, *J*=7 Hz), 1.60—1.67 (2H, m), 3.40 (2H, s), 4.04 (2H, t, *J*=7 Hz), 4.38 (2H, q, *J*=7 Hz), 7.42 (1H, d, *J*=8 Hz), 7.68 (1H, dd, *J*=8, 2 Hz), 7.80 (1H, d, *J*=2 Hz)
10g	1.29 (3H, t, *J*=7 Hz), 1.41 (3H, t, *J*=7 Hz), 1.45 (3H, d, *J*=7 Hz), 3.49 (1H, q, *J*=7 Hz), 4.09 (2H, q, *J*=7 Hz), 4.40 (2H, q, *J*=7 Hz), 7.41 (1H, d, *J*=8 Hz), 7.68 (1H, dd, *J*=8, 2 Hz), 7.80 (1H, d, *J*=2 Hz)
10h	1.41 (3H, t, *J*=7 Hz), 1.43 (3H, d, *J*=7 Hz), 1.51 (3H, d, *J*=7 Hz), 1.54 (3H, d, *J*=7 Hz), 3.36 (1H, q, *J*=7 Hz), 4.39 (2H, q, *J*=7 Hz), 4.62—4.78 (1H, m), 7.43 (1H, d, *J*=8 Hz), 7.68 (1H, dd, *J*=8, 2 Hz), 7.88 (1H, d, *J*=8 Hz)

listed in Tables 1—4.

Biological Results and Discussion

The Na/H exchange inhibitory activities of *N*-(3-oxo-3,4-dihydro-2*H*-benzo[1,4]thiazine-6-carbonyl)guanidines **5** were tested by their ability to inhibit platelet swelling induced by sodium propionate, in accordance with the method of Rosskopf *et al.*[11] The results are given in Table 5.

As expected from the clog*P* values, **5a** was actually about five-fold more potent than **4a** in *in vitro* assay. Prompted by this result, we optimized the lead compound **5a**. Several substituents were introduced to the 2- and/or 4-positions of the benzothiazine ring. All the 4-substituted compounds **5** showed more potent activity than the corresponding 4-substituted benzoxazine derivatives **4**, and their activities were considered to be parabolically related to the length of the 4-substituent. On the other hand, the 2-substituent did not much affect the activity. In order to confirm the SAR in greater detail, compounds **5** were subjected to QSAR analysis. Eq. 1 was obtained as the best equation.

$$pIC_{50}=2.10(\pm1.25)L(R^3)-0.21(\pm0.13)L(R^3)^2-3.63(\pm2.78) \quad (1)$$

$$n=9,\ r=0.861,\ s=0.396,\ F=8.61,\ L(R^3)_{opt.}=4.91$$

In Eq. 1, L is Verloop's STERIMOL parameter[12] and is assumed to be in an extended conformation. The number in parentheses is the 95% confidence interval, n is the number of data points used in deriving the equation, r is the correlation coefficient, s is the standard deviation, and F is the F-ratio between the variances of calculated and observed activities. $L(R^3)_{opt.}$ is the calculated optimum values of $L(R^3)$.

Equation 1 suggested a parabolic relation between activity and the length $L(R^3)$ of the 4-substituent. This QSAR result was identical to the SAR (Eq. 2) of the benzoxazine derivastives **4**.[7]

$$pIC_{50}=1.42(\pm0.57)L(R^3)-0.15(\pm0.06)L(R^3)^2-2.87(\pm1.36) \quad (2)$$

$$n=20,\ r=0.806,\ s=0.361,\ F=15.72,\ L(R^3)_{opt.}=4.81$$

The optimum $L(R^3)$s are almost equal in these two equations. This result was reasonable, because compounds **5** and **4** would interact with the same region of the Na/H exchanger protein. However, the constants are different in spite of similar optimum $L(R^3)$s. Therefore, we supposed that the constants depended differences in the hydrophobicity between the ring structure of **5** and **4**. In order to confirm this hypothesis, compounds **5** and **4** were subjected to QSAR analysis using the indicator variable D, which takes one for compounds **5** and takes zero for **4**. And as a result, Eq. 3 was obtained.

Table 5. Na/H Exchange Inhibitory Activity of *N*-(2*H*-Benzo[1,4]thiazine-6-carbonyl)guanidines **5** and *N*-(2*H*-Benzo[1,4]oxazine-6-carbonyl)guanidines **4**

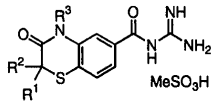

5

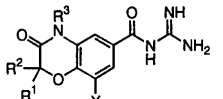

4

No.	R^1	R^2	R^3	X	$L(R^3)^{a)}$	Na/H exchange inhibitory activity				
						IC_{50} (μM)	pIC_{50}			
							Obsd.	Eq. 1	Eq. 2[b)]	Eq. 3
5a	H	H	H	—	2.06	2.1	−0.32	−0.20	—	0.10
5b	H	H	Me	—	3.00	0.19	0.72	0.75	—	0.83
5c	H	H	Et	—	4.11	0.051	1.29	1.40	—	1.32
5d	H	H	iso-Pr	—	4.11	0.0091	2.04	1.40	—	1.32
5e	H	H	Pr	—	5.05	0.086	1.07	1.53	—	1.41
5f	H	H	Butyl	—	6.17	0.11	0.96	1.20	—	1.15
5g	H	H	Pentyl	—	8.22	0.19	0.72	0.50	—	0.61
5h	H	Me	Et	—	4.11	0.070	1.15	1.40	—	1.32
5i	H	Me	iso-Pr	—	4.11	0.018	1.74	1.40	—	1.32
4a	H	H	H	H	2.06	10	−1.00	—	−0.57	−0.71
4b	H	H	Et	H	4.11	0.33	0.48	—	0.48	0.51
4c	H	H	iso-Pr	H	4.11	0.25	0.60	—	0.48	0.51
4d	H	Me	Et	H	4.11	0.29	0.54	—	0.48	0.51
4e	H	Et	iso-Pr	H	4.11	0.17	0.76	—	0.48	0.51
4f	H	Ph	iso-Pr	H	4.11	1.0	0.00	—	0.48	0.51
4g	Me	Me	iso-Pr	H	4.11	0.12	0.92	—	0.48	0.51
4h[c)]	Me	Me	H	H	2.06	7.4	−0.87	—	−0.57	−0.71
4i[c)]	Me	Me	Me	H	3.00	0.81	0.09	—	0.06	0.02
4j	Me	Me	Et	H	4.11	0.38	0.42	—	0.48	0.51
4k	Me	Me	Pr	H	5.05	0.74	0.13	—	0.55	0.61
4l[c)]	Me	Me	Butyl	H	6.17	1.3	−0.11	—	0.29	0.34
4m[c)]	Me	Me	$(CH_2)_2OEt$	H	6.99	5.6	−0.75	—	−0.13	−0.11
4n[c)]	Me	Me	Hexyl	H	8.22	3.7	−0.57	—	−1.13	−1.20
4o	H	H	Me	Cl	3.00	0.33	0.48	—	0.06	0.02
4p	H	H	Et	Cl	4.11	0.22	0.66	—	0.48	0.51
4q[c)]	H	H	iso-Pr	Cl	4.11	0.16	0.80	—	0.48	0.51
4r	H	H	Me	OMe	3.00	0.50	0.30	—	0.06	0.02
4s	H	H	Et	OMe	4.11	0.27	0.57	—	0.48	0.51
4t	Me	Me	iso-Pr	OMe	4.11	0.37	0.43	—	0.48	0.51

a) See reference 12. *b*) See reference 10. *c*) Hydrochloride.

$$pIC_{50} = 1.60(\pm 0.48)L(R^3) - 0.16(\pm 0.05)L(R^3)^2 + 0.81(\pm 0.30)D - 3.31(\pm 1.13) \quad (3)$$

$$n=29,\ r=0.875,\ s=0.367,\ F=27.26,\ L(R^3)_{opt.}=4.89$$

In Eq. 3, the indicator variable D is significant. The coefficient 0.81(±0.30) of D is statistically equal to the calculated factor (0.58) based on the difference of clog*P*s between **5a** (0.20) and **4a** (−0.36).[13] Thus, our hypothesis was confirmed and it was clarified that the benzothiazine derivatives **5** were about five-fold more potent than the benzoxazine derivatives **4**. In addition, the proportional relationship between the activity and the hydrophobicity of the ring structure was re-confirmed.

The most potent derivative was the methanesulfonate salt of the 4-isopropyl derivative **5d**, with an IC_{50} value of 0.0091 μM. The clog*P* (1.15) of the free base of **5d** was around the optimum value (around 1.5—2) for good bioavailability. Compound **5d** also showed good water-solubility. Therefore, **5d** was subjected to *in vivo* investigation. Anti-arrhythmia activity of **5d** was tested in terms of the duration of ventricular fibrillation (VF) using a rat acute myocardial infarction model, in accordance with the method of Tagliavini *et al.*[14] The duration of VF time for the control group was 171±5.8 s (mean±standard error). The administration of **5d** (0.3 mg/kg, i.v.) before occlusion significantly reduced the duration of VF (5.1±5.1 s).

Table 6. Na/H Exchange Inhibitory Activity and Duration of Ventricular Fibrillation of Compound **5d**

No.	Structure	Na/H exchange inhibitory activity IC_{50} (μM)	Duration(s) of ventricular fibrillation[a)] (Mean±S.E.)
Control	—	—	171.0±5.8
5d	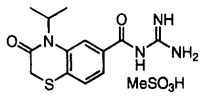	0.0091	5.1±5.1[b)]

a) i.v. administration of compound 0.3 mg/kg, reperfusion induced arrhythmia in anesthetized rats (n=5—7). Significantly different from the control group. *b*) $p<0.01$ (Mann–Whitney U-test).

Conclusion

In order to find potent Na/H exchange inhibitors, we designed and synthesized *N*-(3-oxo-3,4-dihydro-2*H*-benzo-

[1,4]thiazine-6-carbonyl)guanidines **5** and evaluated their inhibitory activities. The result of QSAR analysis indicated that the activity was parabolically related to the length of the 4-substituent. As expected from our previous SAR study, compounds **5** were about five-fold more potent than the benzoxazine derivatives **4**. The most potent derivative was the methanesulfonate salt of the 4-isopropyl derivative **5d** (IC_{50}=0.0091 μM). The hydrophobicity (clog$P$=1.15) of the free base of **5d** was at the optimum value (around 1.5—2) for good bioavailability. Compound **5d** also showed significant protective activity against a rat acute myocardial infarction model. This SAR-based methodology of drug design would be useful for the rapid optimization of lead candidates.

Experimental

Melting points were measured with a capillary melting point apparatus (Yamato MP-21) and are uncorrected. ^{1}H-NMR spectra were taken on a Bruker DPX-250 NMR (250 MHz) spectrometer with tetramethylsilane (TMS) as an internal standard. Chemical shifts are given as δ values (ppm). Elemental analysis was performed with a Yanagimoto CHN-CORDER MT-5.

4-Ethoxycarbonylmethylsulfanyl-3-nitrobenzoic Acid (7a) A mixture of 4-chloro-3-nitrobenzoic acid (**6**, 100 g, 496 mmol), ethyl mercaptoacetate (72 g) and pyridine (250 ml) was refluxed for 8 h. After cooling, the reaction mixture was acidified with diluted hydrochloric acid. The precipitates were collected by filtration and washed with water to give **7a** (121 g, 424 mmol, yield 85%). The analytical sample was obtained by recrystallization from EtOH, mp 159—161 °C. ^{1}H-NMR (DMSO-d_6) δ: 1.18 (3H, t, J=7 Hz), 4.12 (2H, q, J=7 Hz), 4.17 (2H, s), 7.70 (1H, d, J=9 Hz), 8.15 (1H, dd, J=9, 2 Hz), 8.63 (1H, d, J=2 Hz), 13.46 (1H, br). *Anal.* Calcd for $C_{11}H_{11}NO_6S$: C, 46.31; H, 3.89; N, 4.91. Found: C, 46.37; H, 3.95; N, 4.51.

4-(1-Ethoxycarbonylethylsulfanyl)-3-nitrobenzoic Acid (7b) A mixture of 4-chloro-3-nitrobenzoic acid (**6**, 62.6 g, 311 mmol), ethyl 2-methylmercaptoacetate (50 g) and pyridine (150 ml) was refluxed for 20 h. After cooling, the reaction mixture was acidified with diluted hydrochloric acid. The precipitates were collected by filtration and washed with water and diisopropyl ether (IPE) to give **7b** (78 g, 261 mmol, yield 84%). The analytical sample was obtained by recrystallization from IPE, mp 89—91 °C. ^{1}H-NMR ($CDCl_3$) δ: 1.25 (3H, t, J=7 Hz), 1.67 (3H, t, J=7 Hz), 4.07—4.28 (3H, m), 7.73 (1H, d, J=9 Hz), 8.24 (1H, dd, J=9, 2 Hz), 8.88 (1H, d, J=2 Hz). *Anal.* Calcd for $C_{12}H_{13}NO_6S$: C, 48.16; H, 4.38; N, 4.68. Found: C, 48.22; H, 4.40; N, 4.60.

Ethyl 4-Ethoxycarbonylmethylsulfanyl-3-nitrobenzoate (8a) A mixture of **7a** (30.0 g, 105 mmol), sulfuric acid (5 ml) and EtOH (300 ml) was refluxed for 5 h and concentrated *in vacuo*. Water was added to the residue. The precipitates were collected by filtration and washed with water to give **8a** (33.0 g, 105 mmol, yield 100%). The analytical sample was obtained by recrystallization from IPE, mp 66—67 °C. ^{1}H-NMR ($CDCl_3$) δ: 1.27 (3H, t, J=7 Hz), 1.42 (3H, t, J=7 Hz), 3.78 (2H, s), 4.23 (2H, q, J=7 Hz), 4.42 (2H, q, J=7 Hz), 7.58 (1H, d, J=9 Hz), 8.18 (1H, dd, J=9, 2 Hz), 8.85 (1H, d, J=2 Hz). *Anal.* Calcd for $C_{13}H_{15}NO_6S$: C, 49.83; H, 4.83; N, 4.47. Found: C, 49.81; H, 4.83; N, 4.22.

Ethyl 4-(1-Ethoxycarbonylethylsulfanyl)-3-nitrobenzoate (8b) A mixture of **7b** (73.0 g, 244 mmol), sulfuric acid (7.3 ml) and EtOH (730 ml) was refluxed for 22 h and concentrated *in vacuo*. Aqueous sodium carbonate was added to the residue. The mixture was extracted with ethyl acetate (AcOEt). The extract was concentrated *in vacuo* to give **8b** (74.0 g, 226 mmol, yield 93%) as an oil. The analytical sample was obtained by column chromatography on silica gel with chloroform–MeOH (10 : 1, v/v). ^{1}H-NMR ($CDCl_3$) δ: 1.23 (3H, t, J=7 Hz), 1.41 (3H, t, J=7 Hz), 1.66 (3H, d, J=7 Hz), 4.09 (1H, q, J=7 Hz), 4.12—4.26 (2H, m), 4.42 (2H, q, J=7 Hz), 7.68 (1H, d, J=9 Hz), 8.16 (1H, dd, J=9, 2 Hz), 8.79 (1H, d, J=2 Hz). *Anal.* Calcd for $C_{14}H_{17}NO_6S$: C, 51.37; H, 5.23; N, 4.28. Found: C, 51.16; H, 5.17; N, 4.31.

Ethyl 3-Oxo-3,4-dihydro-2*H*-benzo[1,4]thiazine-6-carboxylate (9a) A mixture of **8a** (31.0 g, 98.9 mmol), 10% Pd–C (3.1 g) and EtOH (300 ml) was stirred at 50 °C under a hydrogen atmosphere (4 kg/cm^2) for 2 h. The mixture was filtered. The filtrate was evaporated *in vacuo*. The residue was column chromatographed on silica gel with chloroform and triturated with hexane–AcOEt to give **9a** (7.80 g, 32.9 mmol, yield 33%). The analytical sample was obtained by recrystallization from hexane–AcOEt, mp 159—160 °C. ^{1}H-NMR ($CDCl_3$) δ: 1.39 (3H, t, J=7 Hz), 3.46 (2H, s), 4.37 (2H, q, J=7 Hz), 7.37 (1H, d, J=8 Hz), 7.50 (1H, d, J=2 Hz), 7.69 (1H, dd, J=8, 2 Hz), 7.92 (1H, br). *Anal.* Calcd for $C_{11}H_{11}NO_3S$: C, 55.68; H, 4.67; N, 5.90. Found: C, 55.76; H, 4.71; N, 5.75.

Ethyl 2-Methyl-3-oxo-3,4-dihydro-2*H*-benzo[1,4]thiazine-6-carboxylate (9b) A mixture of **8b** (40.0 g, 122 mmol), 10% Pd–C (4.0 g) and EtOH (400 ml) was stirred at 40 °C under a hydrogen atmosphere (4 kg/cm^2) for 16 h. The mixture was filtered. The filtrate was evaporated *in vacuo*. The residue was washed with IPE and recrystallized from AcOEt–IPE to give **9b** (18.85 g, 75.0 mmol, yield 61%), mp 155—157 °C. ^{1}H-NMR ($CDCl_3$) δ: 1.39 (3H, t, J=7 Hz), 1.51 (3H, d, J=7 Hz), 3.59 (1H, q, J=7 Hz), 4.39 (2H, q, J=7 Hz), 7.37 (1H, d, J=8 Hz), 7.56 (1H, d, J=2 Hz), 7.68 (1H, dd, J=8, 2 Hz), 8.38 (1H, br). *Anal.* Calcd for $C_{12}H_{13}NO_3S$: C, 57.35; H, 5.21; N, 5.57. Found: C, 57.46; H, 5.23; N, 5.38.

General Procedure for the Preparation of Methyl 3-Oxo-4-substituted-3,4-dihydro-2*H*-benzo[1,4]thiazine-6-carboxylates 10 An alkyl iodide (20 mmol) was added to a mixture of **9** (10 mmol), potassium *tert*-butoxide (15 mmol) and tetrahydrofuran (24 ml) at room temperature. The mixture was stirred at 60 °C for several hours. Water was added to the mixture and the whole was extracted with AcOEt. The extract was washed with water and dried over anhydrous magnesium sulfate. The solvent was removed *in vacuo*. The residue was chromatographed on silica gel with hexane–AcOEt or recrystallized to give **7**. Physical data are listed in Tables 2 and 4.

General Procedure for the Preparation of *N*-(3-Oxo-(4-substituted-)3,4-dihydro-2*H*-benzo[1,4]thiazine-6-carbonyl)guanidine Methanesulfonates 5 A mixture of **9** or **10** (5 mmol), guanidine hydrochloride (55 mmol), sodium methoxide (50 mmol), and DMSO (25 ml) was stirred at 120 °C for several hours, then diluted with water. The precipitates were collected by filtration, washed with water and dissolved in MeOH. Methanesulfonic acid was added to the solution. After concentration *in vacuo*, the residue was recrystallized to give **5**. Physical data are listed in Tables 1 and 3.

Na/H Exchange Inhibitory Activity Na/H exchange inhibitory activity was determined based on the ability to inhibit sodium propionate-induced swelling of platelets in accordance with the method of Rosskopf *et al.*[11] Platelet-rich plasma was prepared as described by Mammen and coworkers.[15] Male Wistar rats (230—300 g) were anesthetized with ether, and blood was taken from the abdominal aorta. To inhibit blood coagulation, acid citrate dextrose (ACD) solution (a mixture of 65 mM citric acid, 85 mM sodium citrate, and 11 mM dextrose) was added to the blood, and this treated blood was centrifuged at 90×g for 10 min. The supernatant was separated to prepare platelet-rich plasma. A solution of the test compound in DMSO was then added to 140 mM sodium propionate buffer solution. To this mixture was added the platelet-rich plasma prepared above, and the decrease in optical density was recorded at 37 °C using a platelet aggregometer (turbidimeter) and an X–Y recorder [decrease rate in optical density in the presence of the test compound (D)]. As a control, the solvent DMSO alone was used instead of a solution of test compound, and the decrease in optical density was recorded in a similar manner [control (C)]. The swelling inhibitory rate (Na/H exchange inhibitory rate, %) was calculated using Eq. 4.

$$\text{Swelling inhibitory rate (Na/H exchange inhibitory rate, \%)} = (1 - D/C) \times 100 \quad (4)$$

The concentration of the test compound which causes 50% inhibition (IC_{50}) was calculated by the least-squares method.

Inhibitory Activity against Reperfusion-Induced Arrhythmia Using a rat acute myocardial infarction model, compound **5d** was tested for inhibitory activity against reperfusion arrhythmia in accordance with the method of Tagliavini *et al.*[14] Male Sprague–Dawley rats (310—510 g) were anesthetized by intraperitoneal administration of sodium pentobarbital (50 mg/kg). The rats were cannulated *via* the trachea and the cannula was linked to a respirator. An electrocardiogram (lead II) was obtained from electrodes attached to limbs using a bioelectric amplifier, while body temperature was maintained at 37 °C. The chests of the rats were opened at the fifth intercostal space, and the pericardium was cut open to reveal the heart. A solution of the test compound in a mixed solvent of polyethylene glycol 400, ethanol and physiological saline [3 : 3 : 14 (v/v)] was then administered into the femoral vein. Ten minutes after administration of the compound, the origin of the left coronary was occluded. After occlusion for 5 min, reperfusion was carried out for 10 min and the duration (seconds) of ventricular fibrillation was assessed in accordance with the guidelines of the Lambeth Convention.[16] The mixed solvent of polyethylene glycol 400, ethanol and physio-

logical saline [3 : 3 : 14 (v/v)] was used as a control, and the duration (seconds) of ventricular fibrillation was measured in a similar manner.

References

1) *a*) Wakabayashi S., Shigekawa M., Pouyssegur J., *Physiol. Rev.*, **77**, 51—74 (1997); *b*) Fröhlich O., Karmazyn M., *Cardiovasc. Res.*, **36**, 138—148 (1997).
2) *a*) Garcia-Dorado D., González M. A., Barrabés J. A., Ruiz-Meana M., Solares J., Lidon R.-M., Blanco J., Puigfel Y., Piper H. M., Soler-Soler J., *Cardiovasc. Res.*, **35**, 880—889 (1997); *b*) Miura T., Ogawa T., Suzuki K., Goto M., Shimamoto K., *J. Am. Coll. Cardiol.*, **29**, 693—701 (1997).
3) Meng H.-P., Maddaford T. G., Pierce G. N., *Am. J. Physiol.*, **264**, H1831—H1835 (1993).
4) Yasutake M., Ibuki C., Hearse D. J., Avkiran M., *Am. J. Physiol.*, **267**, H2430—H2440 (1994).
5) Scholz W., Albus U., Counillon L., Gögelein H., Lang H.-J., Linz W., Weichert A., Schölkens B. A., *Cardiovasc. Res.*, **29**, 260—268 (1995).
6) Yamamoto T., Hori M., Watanabe I., Tsutsui H., Harada K., Ikeda S., Ohtaka H., *Chem. Pharm. Bull.*, **45**, 1282—1286 (1997).
7) Yamamoto T., Hori M., Watanabe I., Tsutsui H., Harada K., Ikeda S., Maruo J., Morita T., Ohtaka H., *Chem. Pharm. Bull.*, **45**, 1975—1983 (1997).
8) CLOGP program. Version 4.42, Daylight Chemical Information Systems, Inc., Irvine. The clog*P* of aroylguanidines was determined by subtraction of 0.3, due to the methyl group, from the calculated clog*P* value of the *N*-methyl-*N'*-carbonylguanidine derivatives. The value of 0.3 was calculated by averaging the difference (0.46) between guanidine (clog*P*=−1.50) and its methyl derivative (clog*P*=−1.04) and the difference (0.15) between phenethylamine (clog*P*=1.28) and its methyl derivative (clog*P*=1.43).
9) Lien E. J., "Drug Design," Vol. 5, ed. by Ariens E. J., Academic Press, Inc., New York, 1975, pp. 81—132.
10) Yamamoto T., Hori M., Watanabe I., Tsutsui H., Harada K., Ikeda S., Maruo J., Morita T., Ohtaka H., *Chem. Pharm. Bull.*, **46**, 1716—1723 (1998).
11) Rosskopf D., Morgenstern E., Scholz W., Osswald U., Siffert W., *J. Hypertension*, **9**, 231—238 (1991).
12) Verloop A., Hoogenstraaten W., Tipker J., "Drug Design," Vol. 7, ed. by Ariens E. J., Academic Press, Inc., New York, 1976, pp. 165—207.
13) The coefficient of clog*P* in the QSAR equation of various bicyclic ring compounds is 1.043.[6] Thus, the calculated factor based on the different rings is 0.58 (=1.043×[0.20−(−0.36)]).
14) Tagliavini S., Genedani S., Bertolini A., Bazzani C., *Eur. J. Pharmacol.*, **194**, 7—10 (1991).
15) Dunbar J. C., Reinholt L., Henry R. L., Mammen E., *Diabet. Res. Clin. Prac.*, **9**, 265—272 (1990).
16) Walker M. J. A., Curtis M. J., Hearse D. J., Campbell R. W. F., Janse M. J., Yellon D. M., Cobbe S. M., Coker S. J., Harness J. B., Harron D. W. G., Higgins A. J., Julian D. G., Lab J. J., Manning A. S., Northover B. J., Parratt J. R., Riemersma R. A., Riva E., Russell D. C., Sheridan D. J., Winslow E., Woodward B., *Cardiovasc. Res.*, **22**, 447—455 (1988).

Preparation and Characterization of Hyaluronate–Hydroxyethyl Acrylate Blend Hydrogel for Controlled Release Device

Masao INUKAI,[a] Yu JIN,[a] Chikako YOMOTA,[b] and Masakatsu YONESE*,[a]

Faculty of Pharmaceutical Sciences, Nagoya City University,[a] 3–1 Tanabe-dori, Mizuho-ku Nagoya 467–8603, Japan and National Institute of Health Sciences, Osaka Branch,[b] 1–1–43 Hoenzaka, Chuo-ku, Osaka 540–0006, Japan.
Received January 11, 2000; accepted March 11, 2000

Hyaluronate–hydroxyethyl acrylate blend hydrogels were investigated as matrices for controlled release devices. Glycidyl methacrylate (GMA) derivatized HA (GMA–HA) was synthesized by coupling of GMA to HA in the presence of a suitable catalyst. These hydrogels were prepared by a free radical copolymerization of GMA–HA and hydroxyethyl acrylate. The water content of these hydrogels at equilibrium swelling in water (Ww) was 0.978±0.0073 (n=18); however, these hydrogel was mechanically tough and could be used as disk shape. The hydrogels swelling were found to depend on ionic strength and pH. The dried hydrogels quickly regained their original condition in water, and they swelled to more than 90% of its initial water contents after 30 min. This swelling–deswelling behavior was reproducible. The release of chlorpromazine HCl as a model cationic drug from the gels was suppressed significantly in water. The release increased with increasing the ionic strength and decreasing pH of bulk solutions.

Key words hyaluronic acid; hydroxyethyl acrylate; hydrogel; swelling; drug release

Hydrogels are formed from hydrophilic synthetic polymers and many natural polymers such as proteins and polysaccharides, and their crosslinking mechanisms depend on their properties. Due to three-dimensional hydrophilic polymer networks, hydrogels are insoluble in water and hold much water in them under keeping equal the chemical potentials in the both phases *i.e.*, the gel and the bulk phases. They swell or deswell depending on various ambient conditions such as pH, ionic strength, solvent composition, temperature and pressure. Especially, hydrogels prepared from natural polymers are more suitable adequate than synthetic polymers because of their biocompatibility and biodegradability. Because of these advantages, natural polymers have been widely applied to pharmaceutical fields such as controlled delivery devices of various drugs.

Hyaluronate (HA) is a natural polysaccharide, and is an important component of connective tissues such as the intercellular matrixes of skin, muscle and cartilage cells. It is a linear block copolymer of repeating units composed of *N*-acetyl-D-glucosamine and D-glucuronic acid connected by alternate β(1–3) and β(1–4) glucosidic bonds. The important properties of HA solutions are high viscoelasticities resulting from the very high molecular weights and high preserving ability of water. Furthermore, as HA is highly transparent, it is used as a surgical tool in eye surgery and as a remedy for arthritis.

HA gels are reported[1—4] to maintain such properties as HA solutions. In this paper, the novel blend hydrogel obtained from the copolymerization of a methacrylate derivative of HA was prepared and the characteristics of the HA gel were investigated. The effects of ionic strength on the swelling, cationic drug releases and the reversibility of the swelling were elucidated.

Materials and Methods

Sodium HA (NaHA, M_W 2070000 g mol^{-1}) from *Streptococcus zooepidemicus* was purchased from Kibun food Chemifa Co. (Tokyo, Japan). Glycidyl methacrylate (GMA, 95%), ammonium peroxodisulfate (APS), 2-hydroxyethyl acrylate (HEA, 95%) and chlorpromazine hydrochloride (CPHCl) were purchased from Wako Pure Chemical Co. (Osaka, Japan). Other chemicals used were of analytical grades. Distilled and deionized water was used for the preparation of aqueous solutions.

Preparation of Glycidyl Methacrylated HA Glycidyl methacryl HA (GMA–HA) was prepared as follows[5—9]: 1) 2.0 g of NaHA was dissolved in 40 cm^3 of 0.05 mol·dm^{-3} carbonate buffer (pH 11). 2) GMA (1.0 cm^3, 7.6 mmol·dm^{-3}) was added to the NaHA solution and the mixture was gently stirred at room temperature. 3) After 7 d, the solution was adjusted to pH 7 with HCl. 4) The solution was purified by dialyzing against distilled and deionized water for 7 d. 5) After filtering to get rid of insoluble substances, the GMA–HA was freeze dried and stored at −20 °C. The chemical reaction of NaHA with GMA and the chemical formula of GMA–HA are shown in Fig. 1.

Preparation of HA–polyhydroxyethyl acrylate (PHEA) hydrogels GMA–HA (100 mg) and HEA (0.92 cm^3, 100 mg) were dissolved in 0.8 cm^3 of water, and APS solution (200 μmol·dm^{-3}, 0.1 cm^3) was added. After the reaction mixture was vigorously mixed and degassed, the sample solutions in a petri dish (diameter 3 cm) were allowed to react for 30 min at 60 °C and the blend gels composed of HA and PHEA were prepared. In the process of formation of HA–PHEA hydrogels, PHEA should be formed due to the polymerization of HEA. Due to the reactions of PHEA with GMA groups of GMA-HA, HA molecules are crosslinked by PHEA and simultaneously PHEA extended furthermore. Finally, HA and PHEA are crosslinked at the GMA groups of GMA–HA. Thus, the blend gels composed of HA and PHEA are formed as shown in Fig. 2.

After polymerization, the HA–PHEA hydrogels were removed from the mould. After washing in distilled water, they were dialyzed in distilled water for 3 d. The swollen hydrogel was cut into disks (diameter: 1.5 cm, thickness: 0.3 cm). The hydrogels were placed in vials contains 0.02 w/v% sodium azide solution to prevent bacterial contamination. The samples were equilibrated in water for 3 d. The water contents (W_w) of these hydrogels were measured as the ratios of the mass changes due to drying of the swollen gel to dry one,

$$W_w=(W_{SG}-W_{DG})/W_{SG} \quad (1)$$

where W_{SG} and W_{DG} are the weights of swollen gel and dried one.

Ionic Strength and pH-Responsive Swelling of HA–PHEA Hydrogels The equilibrium swellings of the HA–PHEA hydrogel were studied in NaCl and Na_2SO_4 solutions. Several samples were immersed in the solutions in the range of ionic strengths J=0.001−2.0 mol·dm^{-3} for 3 d at 25 °C. The effects of pH were measured in JP XIII 1st fluid (pH: 1.2, J=0.105 mol·dm^{-3}) and JP XIII 2nd fluid (pH: 6.8, J=0.074 mol·dm^{-3}). Relative swellings are shown as the percentages of the weights of the equilibrated hydrogel in the solutions to the initial equilibrated weights in water.

Recycles of Swelling and Drying States of HA–PHEA Hydrogels The HA–PHEA gels equilibrated in water were dried in a desiccator for 1 d at room temperature. The dried samples were immersed in vials containing water, JP XIII 1st and 2nd fluid. For the first 1 h at fixed time intervals and

* To whom correspondence should be addressed. e-mail: yonese@phar.nagoya-cu.ac.jp
© 2000 Pharmaceutical Society of Japan

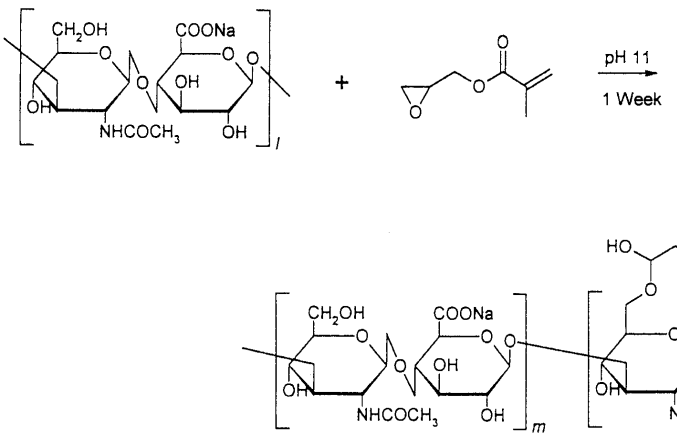

Fig. 1. Reaction of HA with GMA

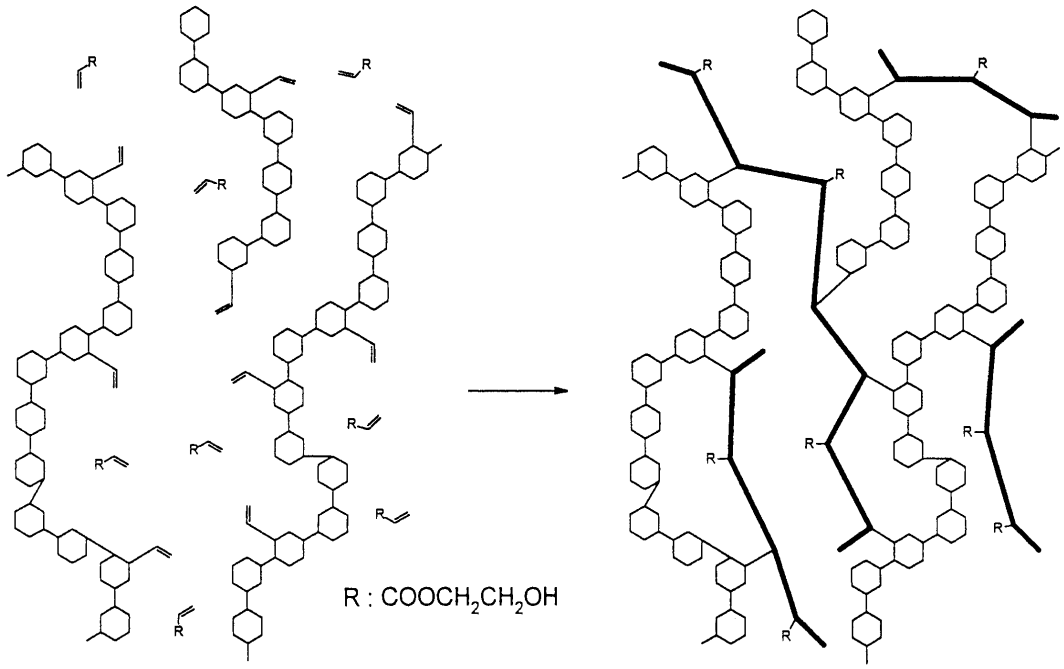

Fig. 2. Schematic Representation of the Formation of HA-PHEA Hydrogel

after 1 d gel samples were taken out, wiped dry using filter paper, and weighed.

Swelling reversibility of hydrogel was determined using the same samples swelling in water and desiccated in a desiccator for 1 d at room temperature, repeating 3 times. Relative swelling is the ratio of the swelling/diswelling of the hydrogel to the initial swelling of the hydrogel calculated as a percentage.

Measurements of Creep and the Analysis The creep of HA–PHEA gels measured using a creep meter (RE-33005; Yamaden Co., Tokyo). The front of the probe was a circular plate of diameter 0.8 cm and the creep can be measured with 0.001 cm accuracy. The results can be analyzed by Voigt models and the viscoelastic parameters are estimated by curve fitting methods. In the simplest 2 element model composed of a spring and a dashpot, a strain γ under a stress σ is expressed by Eq. 2

$$\gamma=\sigma/G_1(1-\exp(-tG_1/\eta))=\sigma/G_1(1-\exp(-t/\tau)) \quad (2)$$

where G_1 and η are an elastic modulus and viscosity coefficient, and τ is a delay time ($=\eta/G_1$).

Measurement and Determination of Drug Release of HA–PHEA Hydrogels CPHCl was used as a cationic model drug. The disks of the HA–PHEA gel were equilibrated in 0.01 mol·dm^{-3} CPHCl solution for 24 h at room temperature under shielding light as CPHCl is decomposed under light. Drug content of the HA–PHEA hydrogels C_0 was determined from absorbance before and after loading CPHCl using a spectro multi channel photo detector (MCPD-2000: Otsuka Electronics Co.) at 245 nm.

Measurements of CPHCl release were measured at 25 °C under shielding light using a diffusion cell (50 cm^3) made of a glass. The HA–PHEA gel was fixed in the manner of the releases from one surface of the disk. The releases of CPHCl were measured in water, NaCl solution or HCl solution. The bulk solutions were stirred continuously at 350 rpm. by a magnetic stirrer unit. Sample solutions were withdrawn at regular intervals of 20 min and replaced with equal volumes of the media. The absorbance of CPHCl in the sample solutions was determined using a spectro (MCPD-2000 Otsuka Electronics Co.) at 245 nm.

Total amount of CPHCl released till ith sampling time Q_i is obtained by Eq. 3[10]

$$Q_i=C_iV+\sum C_jV_s \quad (3)$$

where C_i is the concentration of CPHCl at ith sampling, V is the volume of the diffusion cell and V_s is the volume of the sample solution.

Results and Discussion

Characteristics of HA and HA–PHEA Hydrogels HA–PHEA hydrogels prepared from the polymerizations of HEA and GMA–HA were stable and transparent as shown in Fig. 3. The water contents (W_w) of the hydrogels were

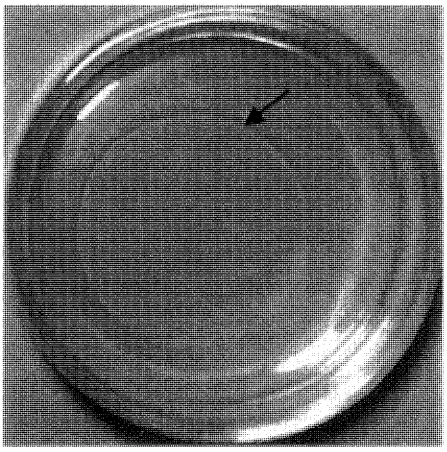

Fig. 3. Photograph of HA–PHEA Hydrogel
Arrow shows the transparent HA–PHEA gel.

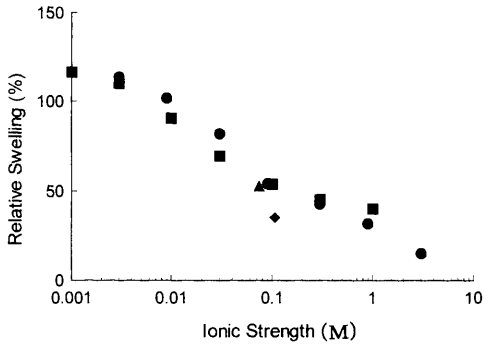

Fig. 4. Effect of Ionic Strength on Swelling of HA–PHEA Hydrogels
■: NaCl, ●: Na_2SO_4, ◆: 1st fluid and ▲: 2nd fluid.

0.978 ± 0.0073 ($n=18$). In spite of such high water contents, these hydrogels were mechanically tough and could be used as disk shape. However, HA hydrogels prepared from GMA–HA alone had much higher water contents ($W_W=0.996$) and were so brittle that they could not be used as gel samples. The HA–PHEA hydrogels were found to be useful for basic research of transparent hydrogels and applications to drug delivery system.

The viscoelastic properties of HA–PHEA hydrogel were measured in water using a creep meter at 25 °C. The creeps of the HA–PHEA hydrogels showed long relaxations and the results under the load of 50 g could be analyzed using the simplest 2 element Voigt model. Their viscoelastic parameters in Eq. 2 were $G_1=6.63\times10^4\,N\cdot m^2$, $\eta_1=2.10\times10^8\,N\cdot m^{-2}\cdot s$ and $\tau=3.165\times10^3\,s$. From these values, the HA–PHEA hydrogels were found to possess relatively high viscoelastic properties which were good enough for delivery experiments.

Effects of Added Salts on Swellings of HA–PHEA Hydrogels Effects of added salts on the swells of the HA–PHEA hydrogels were studied in NaCl and Na_2SO_4 solutions at 25 °C. Their swells were found to attain to the equilibrated states after 24 h. The relative weight percentages to the weight of the HA–PHEA gels equilibrated in water are defined as relative swells. The relative equilibrated swells after 24 h are shown as a function of ionic strengths (J) in Fig. 4. The relative swells were found not to depend on the kind of electrolyte but depend significantly on J. The relative swells decreased with increasing J as expected from the properties of charged gels and at $J=2\,mol\cdot dm^{-3}$ decreased to 20%. The decrease of the relative swells resulted from the decreases of the electrostatical repulsion between HA due to shielding effects of added salts on the carboxylic groups of HA. The two characteristic swelling behaviors of the HA–PHEA gels are as follows: 1) In the diluted added salt solutions ($J<0.01\,mol\cdot dm^{-3}$), the relative swellings were beyond 100% and showed 115% at $J=0.001\,mol\cdot dm^{-3}$. 2) In very high added salt solutions ($J=2\,mol\cdot dm^{-3}$), the relative swelling was 20 %, *i.e.*, the HA–PHEA gels shrink significantly in high ionic strength solutions.

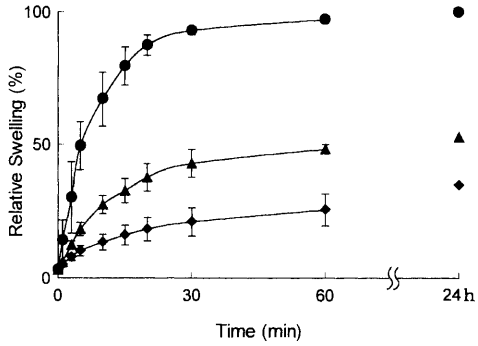

Fig. 5. Time Courses of Swelling of HA–PHEA Hydrogels
●: water, ◆: 1st fluid and ▲: 2nd fluid.

To examine the effects of pH of bulk solutions, the relative swellings were measured in 1st and 2nd fluid. As shown in Fig. 4, in the 2nd fluid the relative swelling was in accordance with the results of NaCl and Na_2SO_4 solutions. However, in the 1st fluid being strong acid the relative swelling was found to be smaller than the strong electrolyte solutions. As the HA–PHEA gels possess carboxylic groups, in the strong acidic region the carboxylic groups are not dissociated and the swellings become smaller than in other strong electrolyte solutions. The HA–PHEA gels equilibrated in the 1st fluid became brittle. HA is known to decompose in the strong acidic region. Thus, the brittleness is considered to result from the decomposition of HA.

Recycles of Swelling and Drying States of HA–PHEA Hydrogels The HA–PHEA gels equilibrated in water at 25 °C were dried at 80 °C for 24 h. The dried HA–PHEA gels were reswelled at 25 °C and the time courses of the reswelling processes in water, the 1st and the 2nd fluid are shown in Fig. 5. The ordinate shows the relative swelling on the basis of the original HA–PHEA gels equilibrated in water. The relative swellings were found to depend on pH and ionic strengths. The dried gels reswelled in the same solutions attained to almost 90% during 60 min and recovered to the original states after 24 h, and the relative swellings were found to depend on pH and J. The relative swelling in water was found to recover to the original one. However, the results of the 1st and the 2nd fluids were much smaller than 100 % and the former was found to be smaller than the latter.

The HA–PHEA gels equilibrated in water were dried at room temperature and reswelled to the equilibrium state. The cycles of dry and swell states were repeated. The relative swells to the original gel equilibrated in water are shown in Fig. 6 which shows 4 cycles. The cycles were found to be re-

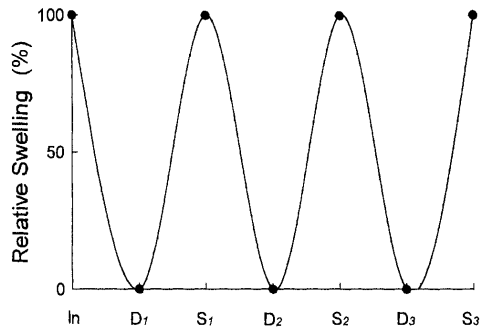

Fig. 6. Reversibility of Swelling–Drying Cycles of HA–PHEA Hydrogel
In: initial condition, D_n: nth drying condition and S_n: nth swelling condition.

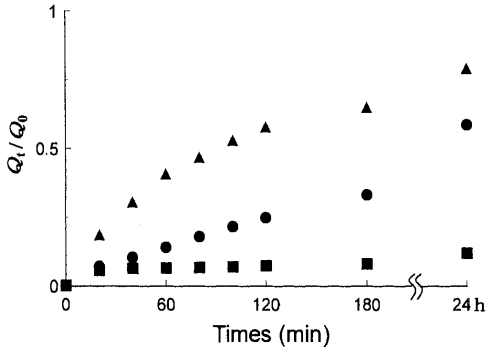

Fig. 7. Effect of Added NaCl on Release of CPHCl from HA–PHEA Hydrogels
■: water, ●: 0.01 mol·dm^{-3} and ▲: 0.1 mol·dm^{-3}.

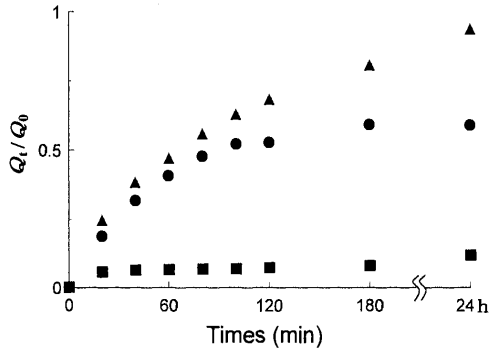

Fig. 8. Effect of Added HCl on Release of CPHCl from HA–PHEA Hydrogels
■: water, ●: 0.01 mol·dm^{-3} and ▲: 0.1 mol·dm^{-3}.

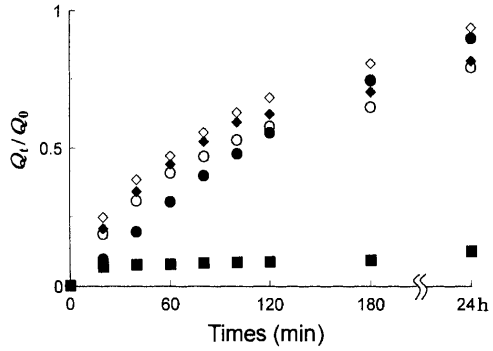

Fig. 9. Effect of Drying on Release of CPHCl from HA–PHEA Hydrogels
■: water, ●, ◆: dried gel (NaCl and HCl) and ○, ◇: original swelling gel (NaCl and HCl).

versible processes and the HA–PHEA gels were found to recover completely to the original swelling. In general, natural polymer gels such as an alginate and a gelatin do not recover to the original swelling states after drying and their relative swelling decreases with increasing the number of the recycles. The reversible recycles of HA–PHEA gels are considered to result from the high affinity of water for HA. The HA–PHEA gels were found to be recycling gels.

Characteristic Releases of CPHCl from HA–PHEA Hydrogels due to Added Ions As a cationic drug, CPHCl was used. The HA–PHEA gels equilibrated in CPHCl solution (0.01 mol·dm^{-3}) shrank significantly and became opaque. CPHCl is known to associate due to hydrophobic interactions. Thus, CPHCl does not interact only electrostatically with the carboxylic groups of HA but also hydrophobically. Furthermore, CPHCl molecules bound with the HA–PHEA matrixes interact with each others and form intraassociated aggregations.[11] Thus, the shrink of the HA–PHEA gels due to CPHCl is considered to result from electrostatic shielding and the formation of the intraassociation.

Releases of CPHCl from the HA–PHEA gels were measured in NaCl and HCl solutions at 25 °C and the time courses of the results are shown in Figs. 7 and 8. The ordinate is the relative released amounts to the original CPHCl Q_t/Q_0. In water, the releases were found to be very small and after 24 h only 10% was released. In NaCl solutions (C_{NaCl}= 0.01 and 0.1 mol·dm^{-3}), the values of Q_t/Q_0 after 24 h increased with increasing the concentration C_{NaCl} as shown in Fig. 7. Even in higher NaCl concentration C_{NaCl}=0.1 mol·dm^{-3}, all CPHCl could not be released and after 24 h the value of Q_t/Q_0 was found to reach only to 0.8. In lower concentration of NaCl C_{NaCl}=0.01 mol·dm^{-3}, a lower amount (Q_t/Q_0=0.6) was released.

The releases in HCl solutions are shown in Fig. 8. The release rates and Q_t/Q_0 after 24 h were more than those of the results in NaCl solutions. From these results, CPHCl bound electrostatically with carboxylic groups of HA is suggested to release due to the counterion exchanges and the dissociation equilibrium.

Effects of Drying on Releases of CPHCl from HA–PHEA Hydrogels The HA–PHEA gels equilibrated in CPHCl solution (0.01 mol·dm^{-3}) were dried in a desiccator for 1 d at room temperature. The weight ratio of dried weights was 0.055. The dried gels containing CPHCl showed also reversible swelling–drying processes in the same manner as in water. The releases of CPHCl from the dried HA–PHEA gels were studied in water, 0.1 mol·dm^{-3} NaCl and 0.1 mol·dm^{-3} HCl solutions at 25 °C. As shown in Fig. 9, the slight releases were found in water and by adding electrolytes the releases increased. The results in HCl solution were more than those in NaCl in the same manner as those from swollen gels. It should be noticed that the rates of releases were almost equal to the results from the swollen gels *i.e.*, in the releases, the HA–PHEA gels were recyclable.

Other natural polymer gels such as gelatin and alginate do not recover to their original states after a drying process. Recycling uses of these gels are difficult. Thus, the HA–PHEA gels are considered to be useful not only in pharmaceutical fields but in other fields.

Conclusion

1) The interpenetrating HA–PHEA gels composed of HA and PHEA were prepared from the copolymerization of GMA–HA and HEA.

2) The HA–PHEA gels were negative charged hydrogels of high water content and transparent.

3) The swells of the HA–PHEA gels responded to ionic strengths and pH as expected from the properties of charged gels.

4) The HA–PHEA gels were recyclable and reversible in the many swelling–drying cycles.

5) Releases of CPHCl as a model cationic drug from the HA–PHEA gels were suppressed significantly in water. The releases increased with increasing the ionic strength and decreasing pH of bulk solutions. However, all CPHCl in the gel could not be released. From these results, not only electrostatic interactions but also intraassociations were found to contribute to the releases. Even from the dried HA–PHEA gels, the rates of releases were almost equal to the results from the swollen gels.

References

1) Shah C. B., Barnett S. M., *J. Appl. Polym. Sci.*, **45**, 293—298 (1992).
2) Yui N., Nihira J., Okano T., Sakurai Y., *J. Control. Release*, **22**, 105—116 (1992).
3) Tomer R., Dimitrijevic D., Florence A. T., *J. Control. Release*, **33**, 405—413 (1995).
4) Vercruysse K. P., Marecak D. M., Marecek J. F., Prestwich G. D., *Bioconjugate Chem.*, **8**, 686—694 (1997).
5) Edman P., Ekman B., Sjöholm I., *J. Pharm. Sci.*, **69**, 838—842 (1980).
6) Simonsen L., Hovgaard L., Mortensen P. B., Brondsted H., *Eur. J. Pharm. Sci.*, **3**, 329—337 (1995).
7) Van Dijk-Wolthuis W. N. E., Franssen O., Talsma H., van Steenbergen M. J., Kettenes-van den Bosch J. J., Hennink W. E., *Macromolecules*, **28**, 6317—6322 (1995).
8) Hennink W. E., Talsma H., Borchert J. C. H., De Smedt S. C., Demeester J., *J. Control. Release*, **39**, 47—55 (1996).
9) Moriyama K., Yui N., *J. Control. Release*, **42**, 237—248 (1996).
10) Inukai M., Yonese M., *Chem. Pharm. Bull.*, **47**, 1059—1063 (1999).
11) Caram-Lelham N., Sundelöf L.-O., *Pharm. Res.*, **13**, 920—925 (1996).

Synthetic Studies of an 18-Membered Antitumor Macrolide, Tedanolide. 6. Synthesis of a Key Intermediate *via* a Highly Efficient Macrolactonization of Computer-Aid Designed Seco-Acid

Tomohiro MATSUSHIMA,[a] Noriyuki NAKAJIMA,[b] Bao-Zhong ZHENG,[c] and Osamu YONEMITSU*,[c]

Faculty of Pharmaceutical Sciences, Hokkaido University,[a] Sapporo 060–0812, Japan, Biotechnology Center, Toyama Prefectural University,[b] Kosugi, Toyama 939–0398, Japan, and Department of Chemistry, Okayama University of Science,[c] Okayama 700–0005, Japan. Received January 20, 2000; accepted February 28, 2000

A stereoselective synthesis is described of the 18-membered lactone (2) *via* an efficient macrolactonization of the conformation-controlled seco-acid (3); this was designed with the aid of molecular mechanics (MM)-calculation and synthesized by coupling between the C1—C12 (4) and C13—C23 (5) fragments.

Key words macrolide; 18-membered lactone; macrolactonization; seco-acid; aldol reaction; calculation

Tedanolide (**1**), a potent cytotoxic macrolide, was isolated from the Caribbean "fire sponge" *Tedania ignis* in 1984; its relative and absolute structure was determined by X-ray analysis[1] and revealed an unusual structural feature: four labile aldol units, an 18-membered lactone formed at a primary hydroxyl instead of the usual secondary hydroxyl,[2] and an α-epoxy alcohol. Because of its novel and complex structure as well as strong biological activity,[3] **1** has recently attracted considerable synthetic attention.[4]

In 1996, as part of our synthetic studies of **1** we reported in a preliminary communication[4b] on the synthesis of the 18-membered lactone (**2**), a key intermediate to **1**, *via* modified Yamaguchi macrolactonization[5,6] of the corresponding seco-acid (**3**). Quite recently, the synthesis of two fragments, C1—C12 (**4**)[4d] and C13—C23 (**5**)[4f] as precursors to **3** starting from methyl (*R*)- and (*S*)-3-hydroxy-2-methylpropionates was reported in detail. In this full paper we describe the synthesis of **2** *via* the quite efficient cyclization of **3**, which was carried out by coupling between **4** and **5**.

In macrolide synthesis the most crucial step to success is usually macrocyclization of a seco-acid to the corresponding lactone, and hence it is extremely important to design a seco-acid derivative suitable for macrolactonization, that is, on the basis of conformational analyses the seco-acid should be designed so that its global conformation is as close as possible to that of the corresponding lactone.[4a,5,7] Only recent computational chemistry can predict the significantly populated conformers of such complex molecules with considerable accuracy within a reasonable computation time. After careful calculations by virtue of a molecular mechanics (MM) method (CONFLEX-MM2),[8] we chose **3** and **2** as the most promising seco-acid and its cyclized lactone, respectively. The most dominant conformations of **3a** and **2a** as calculation models for **3** and **2**, respectively, are shown in Fig. 2.[4b]

Synthesis of the Seco-Acid (3) The kinetic enolate of the C1—C12 ketone (**4**)[9] was first prepared with a slight excess of lithium hexamethyldisilazide (LHMDS)[10] at −78 °C, and then allowed to react with *ca.* one-third equivalent of the

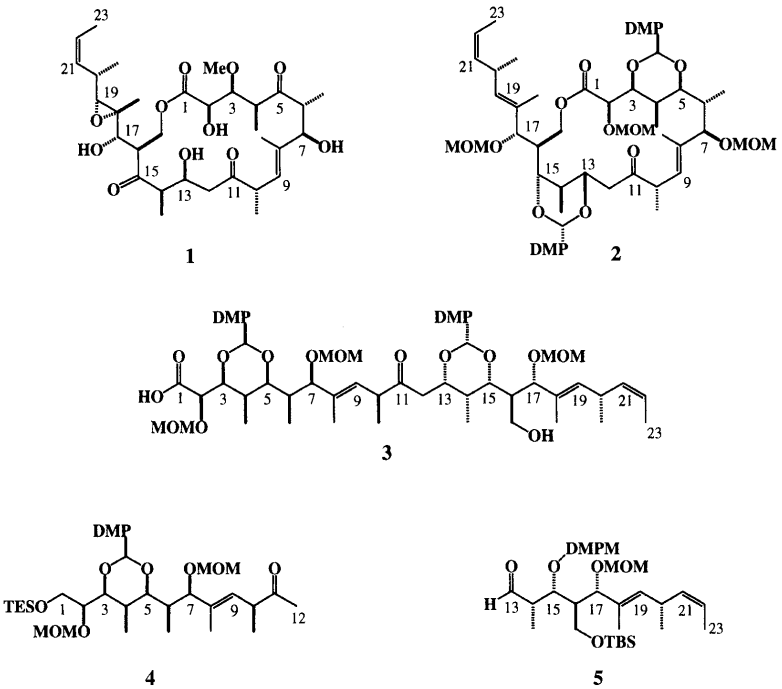

Fig. 1

* To whom correspondence should be addressed. e-mail: yonemit@high.ous.ac.jp

© 2000 Pharmaceutical Society of Japan

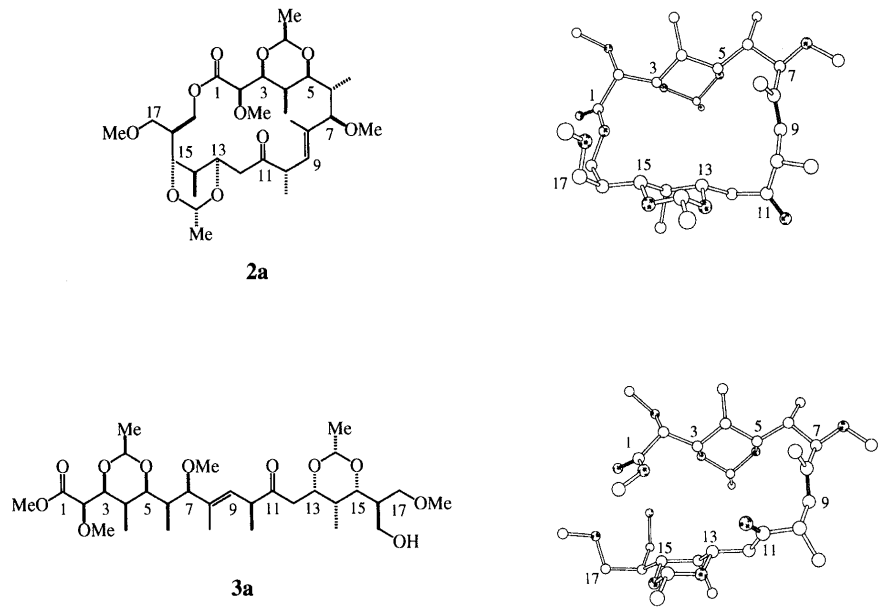

Fig. 2. The Most Stable Conformers of **2a** and **3a** Calculated by CONFLEX-MM2

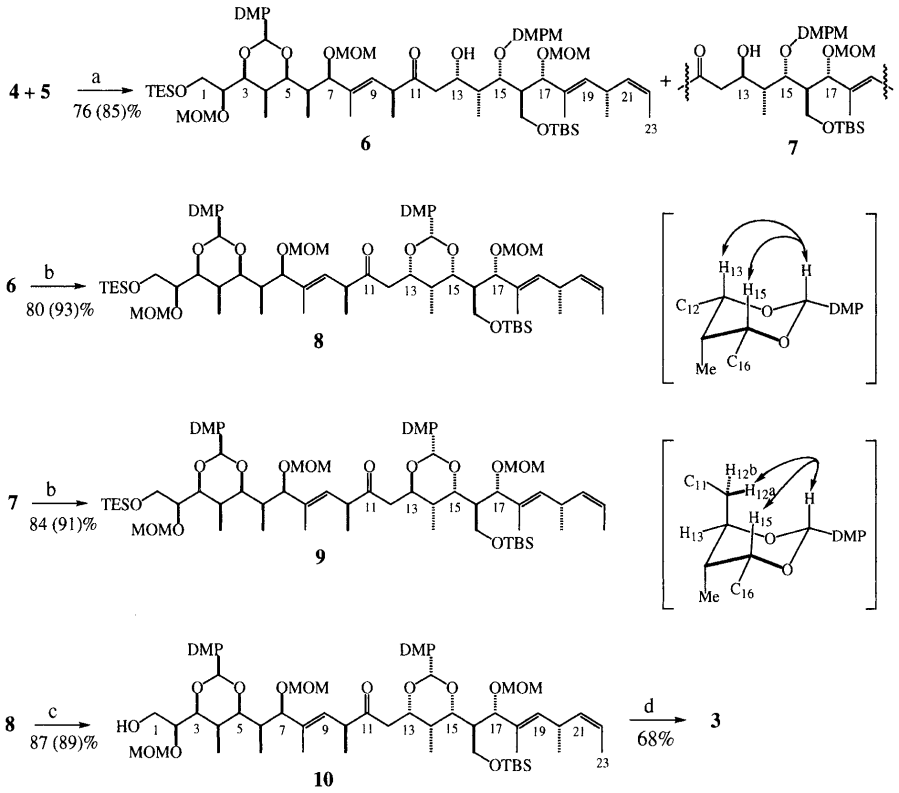

Values in paren theses are yields based on consumed starting materials.
(a) $LiN(TMS)_2$, THF, −78°C to −40°C (**6** : **7** = 1.0 : 1.9). (b) DDQ, CH_2Cl_2, −10°C. (c) TBAF, AcOH–THF, 0°C. (d) 1) Dess–Martin reagent, pyridine, CH_2Cl_2, r.t.; 2) $NaClO_2$, NaH_2PO_4, 2-methyl-butene, *tert*-BuOH–H_2O, r.t.; 3) *n*-Bu_4NF, AcOH–THF, r.t.

Chart 1

C13—C23 aldehyde (**5**). The aldol condensation between **4** and **5** proceeded rather slowly to give an easily separable mixture of the desired Felkin aldol (**6**)[11] and its C13-epimer (**7**). The ratio of the mixture varied in the range of 1 : 1.2 to 1 : 1.9 with a subtle change in reaction conditions but, unfortunately, **6** was always the minor product.[12] The stereochemistry of **6** and **7** was determined after their conversion to **8** and **9**, respectively. When **6** was treated with 2,3-dichloro-5,6-dicyano-1,4-benzoquinone (DDQ) in anhydrous CH_2Cl_2 at −10 °C, the oxidative acetalization[13] of the C15-*O*-3,4-dimethoxybenzyl (DMPM) group to the C13 hydroxy group proceeded smoothly to give **8**. Similarly, **7** gave **9**. The structures of **8** and **9** were determined by NMR, especially ^1H–^1H correlated spectroscopy (COSY) and nuclear Overhauser and

exchange spectroscopy (NOESY). In the latter, correlations of the benzylidene acetal proton with C13 and C15 protons in **8** were clearly observed, whereas these were seen with C12 and C15 protons in **9**.

The triethylsilyl (TES) protecting group was selectively removed with tetra-*n*-butylammonium fluoride (TBAF) in tetrahydrofuran (THF) in the presence of acetic acid (AcOH) at 0 °C to give the primary alcohol (**10**). This selective deprotection proceeded more cleanly with only AcOH in aqueous THF at room temperature. Conversion of **10** to the seco-acid (**3**) was carried out in the usual way. Dess–Martin oxidation[14] of **10** gave a crude aldehyde, which was subjected to the next reaction without purification. Sodium chlorite oxidation in the presence of 2-methyl-2-butene[15] and subsequent deprotection of the *tert*-butyldimethylsilyl (TBS) group with TBAF under acidic conditions easily gave **3**.

Lactonization of the Seco-Acid (3) to the 18-Membered Lactone (2) As pointed out in the synthetic study of erythronolide A,[5,16] among many ways of macrolactonization[17] the Yamaguchi method[6] is extremely effective especially in the presence of a large excess of 4-dimethylaminopyridine (DMAP).[18]

To efficiently synthesize macrolides *via* macrolactonization of the corresponding seco-acids, the high dilution technique is usually essential. However, such a technique should be unnecessary for cyclization of **3** which has favorably controlled conformation. In fact, **3** readily cyclized to the lactone (**2**) under usual acylation conditions *via* a mixed anhydride. When **3** was treated with Yamaguchi's 2,4,6-trichlorobenzoyl chloride[6] in the presence of triethylamine (Et_3N) in THF at room temperature, acylation proceeded slowly to give the mixed anhydride, which was dissolved in a 1 : 1 mixture of THF and benzene. To this solution an excess of DMAP was added at once with stirring to give the 18-membered lactone (**2**) quite smoothly in high yield.

The structures of **3** and **2** were confirmed by virtue of their COSY and NOESY, and correlations among many protons in the latter are shown in Fig 3. Finally, the observed vicinal proton coupling constants of the seco-acid methyl ester (**11**), prepared as a model of the mixed anhydride of **3** by treatment of the anhydride itself with methanol, and the lactone (**2**) were compared with the calculated values[19] of **3a** and **2a** as shown in Tables 1 and 2, respectively. There are no practical differences between the observed and calculated values except for the rather flexible C6–C7 bond of **11**. These data clearly substantiate reliability of the computation method as well as of the structural assignment of **2** and **3**.

In summary, we have demonstrated an example of the computational design of key intermediates and their efficient synthesis in the complex natural products synthesis, although in small-scale experiments. Further studies toward completion of a synthesis of **1** and development of an alternative concise and larger-scale synthesis are now in progress.

Experimental

(2*S*,3*S*,4*R*,5*S*,6*S*,7*R*,8*E*,10*S*,13*S*,14*R*,15*S*,16*S*,17*S*,18*E*,20*S*,21*Z*)-3,5-[(*S*)-3,4-Dimethoxybenzylidenedioxy]-15-(3,4-dimethoxybenzyloxy)-16-

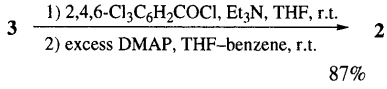

Chart 2

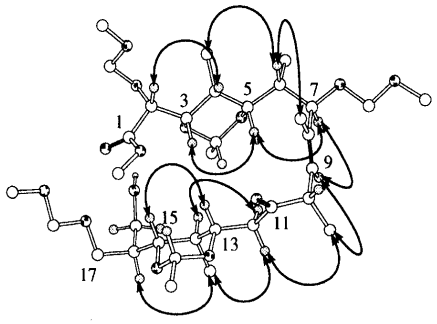

11

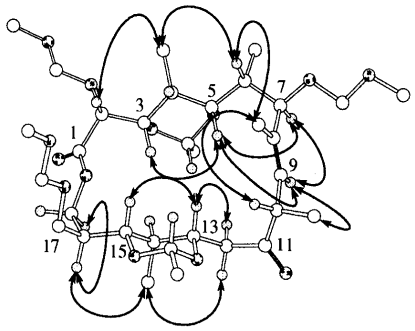

2

Fig. 3. NOESY Correlations in **11** and **2**

Table 1. Vicinal Proton Coupling Constants (*J*; Hz) of the Seco-Acid Methyl Ester

J_{H-H}	Obs (**11**)	Calcd (**3a**)
2–3	9.0	8.2
3–4	1.5	2.5
4–5	1.5	2.2
5–6	10.0	10.0
6–7	0	5.7
9–10	9.0	—
12–13	8.5; 4.0	9.2; 3.3
13–14	2.0	2.6
14–15	1.5	2.4
15–16	10.0	10.9
16–16′	4.2; 2.0	4.2; 2.3

Table 2. Vicinal Proton Coupling Constants (*J*; Hz) of the Lactone Derivatives

J_{H-H}	Obs (**2**)	Calcd (**2a**)
2–3	8.5	8.2
3–4	1.5	1.8
4–5	1.0	2.7
5–6	0	0
6–7	10.5	12.2
9–10	8.5	—
12–13	8.5; 6.0	9.1; 2.0
13–14	2.0	1.8
14–15	1.5	2.1
15–16	10.5	12.2
16–16′	1.5; 0.5	2.8; 0.5

[(1,1-dimethylethyl)dimethylsilyloxymethyl]-4,6,8,10,14,18,20-heptamethyl-13-hydroxy-1-triethylsilyloxy-2,7,17-trismethoxymethyloxy-8,18,21-tricosatrien-11-one (6) and (2*S*,3*S*,4*R*,5*S*,6*S*,7*R*,8*E*,10*S*,13*R*,14*R*,15*S*,16*S*,17*S*,18*E*,20*S*,21*Z*)-3,5-[(*S*)-3,4-Dimethoxybenzylidenedioxy]-15-(3,4-dimethoxybenzyloxy)-16-[(1,1-dimethylethyl)dimethylsilyloxy]-4,6,8,10,14,18,-20-heptamethyl-13-hydroxy-1-triethylsilyloxy-2,7,17-trismethoxymethyloxy-8,18,21-tricosatrien-11-one (7) A solution of **4** (139 mg, 208 μmol) in THF (1.5 ml) was added dropwise to a stirred 0.23 M solution of LHMDS in THF (1 ml, 230 μmol) at −78 °C under argon. After 1 h, a solution of **5** (39 mg, 68 μmol) in THF (0.5 ml) was added, and the solution was allowed to warm to −40 °C over 6.5 h. The reaction was quenched with saturated aqueous NH_4Cl, and the reaction mixture was extracted with Et_2O. The extract was washed with saturated aqueous NH_4Cl and brine, dried over Na_2SO_4, concentrated *in vacuo*, and chromatographed on a silica gel column, eluting with *n*-hexane–EtOAc (5 : 2—2 : 1), to give less polar **6** (22 mg, 26%; 29% based on the consumed **5**) and polar **7** (42 mg, 50%; 56% based on the consumed **5**) as colorless oils, and recovered **4** (56 mg, 40%) and **5** (4 mg, 11%). **6**: $[\alpha]_D^{18}$ +25° (c=0.74, $CHCl_3$). IR (neat) cm^{-1}: 3500, 2950, 1710, 1520, 1460, 1265, 1160, 1030, 840. ^{1}H-NMR (500 MHz, C_6D_6) δ: 0.15 (s, 3H), 0.17 (s, 3H), 0.73 (q, 6H, J=8.0 Hz), 1.05 (d, 3H, J=6.5 Hz, C20Me), 1.06 (s, 9H), 1.11 (t, 9H, J=8.0 Hz), 1.17 (d, 3H, J=7.0 Hz, C10Me), 1.31 (m, 9H, C6Me, C4Me, C14Me), 1.43 (s, 3H, C8Me), 1.62 (dd, 3H, J=1.0, 6.5 Hz, C23Me), 1.71 (s, 3H, C18Me), 2.11 (m, 1H, H6), 2.32 (m, 1H, H4), 2.36 (dd, 1H, J=3.0, 16.5 Hz, H12), 2.47 (m, 1H, H14), 2.65 (m, 1H, H16), 2.90 (dd, 1H, J=9.5, 16.5 Hz, H12), 3.25—3.35 (m, 1H, H10), 3.33 (s, 3H), 3.35—3.50 (m, 1H, H20), 3.39 (s, 3H), 3.42 (s, 3H), 3.43 (s, 3H), 3.45 (s, 3H), 3.54 (s, 3H), 3.60—3.70 (m, 2H, H16′), 3.66 (s, 3H), 3.92 (dd, 1H, J=4.5, 11.0 Hz, H1), 3.98 (dd, 1H, J=3.5, 11.0 Hz, H1), 4.06 (dd, 1H, J=1.0, 9.5 Hz, H5), 4.18 (s, 1H, H7), 4.22 (m, 1H, H2), 4.26 (dd, 1H, J=1.0, 8.5 Hz, H3), 4.30 (dd, 1H, J=1.5, 7.0 Hz, H15), 4.46 (d, 1H, J=7.0 Hz), 4.50 (d, 1H, J=9.5 Hz, H17), 4.59 (d, 1H, J=6.0 Hz), 4.74 (d, 1H, J=7.0 Hz), 4.75 (d, 1H, J=6.0 Hz), 4.76 (d, 1H, J=11.0 Hz), 4.78—4.88 (m, 1H, H13), 4.81 (d, 1H, J=11.0 Hz), 4.96 (d, 1H, J=6.5 Hz), 5.12 (d, 1H, J=6.5 Hz), 5.30 (ddq, 1H, J=9.5, 9.5, 1.5 Hz, H21), 5.34—5.43 (m, 2H, H9, H22), 5.63 (d, 1H, J=10.0 Hz, H19), 5.72 (s, 1H), 6.60—6.70 (m, 2H), 7.00—7.15 (m, 2H), 7.30—7.40 (m, 2H). ^{13}C-NMR (125 MHz, C_6D_6) δ: −5.32, −5.20, 4.80, 7.04, 7.61, 9.83, 10.36, 11.65, 13.06, 14.59, 16.34, 18.48, 21.46, 26.22, 30.69, 30.85, 36.68, 41.60, 44.60, 45.94, 46.68, 55.56, 55.60, 55.64, 56.14, 62.46, 63.19, 68.71, 74.16, 77.37, 78.26, 80.69, 80.98, 83.18, 83.26, 94.02, 95.37, 97.35, 102.60, 111.03, 111.93, 112.24, 112.39, 119.19, 120.30, 121.98, 125.85, 127.92, 128.10, 128.29, 131.33, 132.22, 132.78, 135.14, 135.26, 135.41, 149.77, 149.45, 150.31, 150.46, 210.57. FAB-MS *m/z* (%): 1247 (M^++1, 1.8), 1246 (M^+, 3.9), 1245 (M^+−1, 4.0), 439 (8.6), 409 (9.1), 349 (20), 281 (19), 253 (18), 227 (40), 211 (84), 166 (100), 115 (94), 73 (91). HR-MS Calcd for $C_{67}H_{113}O_{17}Si_2$ (M^+−1): 1245.7516. Found: 1245.7450. **7**: ^{1}H-NMR (500 MHz, C_6D_6) δ: 0.15 (s, 3H), 0.16 (s, 3H), 0.73 (q, 6H, J=8.0 Hz), 1.06 (s, 9H), 1.07 (d, 3H, J=6.5 Hz, C20Me), 1.10 (t, 9H, J=8.0 Hz), 1.17 (d, 3H, J=7.0 Hz, C10Me), 1.21 (d, 3H, J=7.0 Hz, C6Me), 1.28—1.34 (m, 6H, C4Me, C14Me), 1.45 (s, 3H, C8Me), 1.63 (dd, 3H, J=1.0, 6.5 Hz, C23Me), 1.75 (s, 3H, C18Me), 2.11 (m, 1H, H6), 2.32 (m, 1H, H4), 2.50—2.60 (m, 2H, H14, H16), 2.65 (dd, 1H, J=9.0, 16.0 Hz, H12), 2.72 (dd, 1H, J=2.0, 16.0 Hz, H12), 3.33 (s, 3H), 3.35—3.50 (m, 2H, H10, H20), 3.38 (s, 3H), 3.41 (s, 3H), 3.42 (s, 3H), 3.46 (s, 3H), 3.56 (s, 3H), 3.66 (s, 3H), 3.72 (dd, 1H, J=5.0, 10.0 Hz, H16′), 3.79 (dd, 1H, J=7.0, 10.0 Hz, H16′), 3.92 (dd, 1H, J=4.5, 11.0 Hz, H1), 3.97 (dd, 1H, J=3.5, 11.0 Hz, H1), 4.05 (d, 1H, J=9.5 Hz, H5), 4.18 (s, 1H, H7), 4.21 (m, 1H, H2), 4.26 (d, 1H, J=8.5 Hz, H3), 4.37 (dd, 1H, J=3.5, 3.5 Hz, H15), 4.40—4.50 (m, 3H, H13, H17, MOM), 4.58 (d, 1H, J=6.0 Hz), 4.70 (d, 1H, J=6.8 Hz), 4.74 (d, 1H, J=6.0 Hz), 4.76 (d, 1H, J=11.0 Hz), 4.83 (d, 1H, J=11.0 Hz), 4.96 (d, 1H, J=6.0 Hz), 5.11 (d, 1H, J=6.0 Hz), 5.33 (ddq, 1H, J=10.0, 10.0, 1.0 Hz, H21), 5.36—5.46 (m, 2H, H9, H22), 5.63 (d, 1H, J=10.0 Hz, H19), 5.72 (s, 1H), 6.60—6.80 (m, 2H), 7.00—7.15 (m, 2H), 7.30—7.40 (m, 2H). ^{13}C-NMR (125 MHz, C_6D_6) δ: −4.83, −4.73, 5.29, 7.55, 8.11, 10.32, 12.58, 12.95, 13.57, 15.14, 17.05, 18.96, 22.06, 26.73, 31.15, 31.39, 37.19, 42.61, 45.32, 46.72, 47.63, 56.07, 56.15, 56.68, 62.30, 63.66, 71.65, 74.35, 77.79, 78.71, 79.26, 81.28, 83.67, 83.74, 94.63, 95.75, 97.82, 103.13, 111.47, 112.36, 112.72, 112.81, 119.68, 120.70, 122.46, 126.01, 128.41, 128.60, 128.79, 132.50, 132.87, 133.57, 135.64, 135.84, 135.89, 150.23, 150.36, 150.71, 150.96, 212.28.

(2*S*,3*S*,4*R*,5*S*,6*S*,7*R*,8*E*,10*S*,13*S*,14*R*,15*S*,16*S*,17*S*,18*E*,20*S*,21*Z*)-3,5-[(*S*)-3,4-Dimethoxybenzylidenedioxy]-13,15-[(*S*)-3,4-dimethoxybenzylidenedioxy]-16-[(1,1-dimethylethyl)dimethylsilyloxymethyl]-4,6,8,10,14,18,20-heptamethyl-1-triethylsilyloxy-2,7,17-trismethoxymethyloxy-8,18,21-tricosatrien-11-one (8) DDQ (5.1 mg, 22 μmol) was added to a stirred solution of **6** (22 mg, 18 μmol) in CH_2Cl_2 (2 ml) at −10 °C under argon. After 40 min, saturated aqueous $NaHCO_3$ was added to quench the reaction, and the reaction mixture was extracted with Et_2O. The extract was washed with saturated aqueous $NaHCO_3$ and brine, dried over Na_2SO_4, concentrated *in vacuo*, and chromatographed on a silica gel column, eluting with *n*-hexane–EtOAc (2 : 1), to give recovered **6** (3.2 mg, 15%) and **8** as a colorless oil (17.5 mg, 80%; 93% based on the consumed **6**). $[\alpha]_D^{19}$ +32° (c=0.44, $CHCl_3$). IR (neat) cm^{-1}: 2950, 1715, 1520, 1460, 1265, 1165, 1035, 840. ^{1}H-NMR (500 MHz, C_6D_6) δ: 0.19 (s, 3H), 0.20 (s, 3H), 0.73 (q, 6H, J=8.0 Hz), 1.02 (d, 3H, J=7.0 Hz, C20Me), 1.07 (s, 9H), 1.11 (t, 9H, J=8.0 Hz), 1.15 (d, 3H, J=6.5 Hz, C10Me), 1.27 (d, 3H, J=6.5 Hz, C6Me), 1.29 (d, 3H, J=6.5 Hz, C4Me), 1.37 (s, 3H, C8Me), 1.38 (d, 3H, J=6.5 Hz, C14Me), 1.67 (d, 3H, J=5.5 Hz, C23Me), 1.75 (d, 3H, J=0.5 Hz, C18Me), 2.00—2.15 (m, 2H, H14, H6), 2.30 (m, 1H, H4), 2.32 (dd, 1H, J=5.0, 16.5 Hz, H12), 2.65 (m, 1H, H16), 2.95 (dd, 1H, J=7.5, 16.5 Hz, H12), 3.24 (s, 3H), 3.27 (s, 3H), 3.25—3.35 (m, 1H, H10), 3.42 (s, 3H), 3.425 (s, 3H), 3.43 (s, 3H), 3.48 (m, 1H, H20), 3.54 (s, 3H), 3.62 (s, 3H), 3.78 (dd, 1H, J=6.0, 10.0 Hz, H16′), 3.92 (dd, 1H, J=4.0, 11.0 Hz, H1), 3.98 (d, 1H, J=11.0 Hz, H1), 4.01 (dd, 1H, J=1.0, 10.0 Hz, H5), 4.03 (dd, 1H, J=1.0, 10.0 Hz, H15), 4.13 (s, 1H, H7), 4.18 (dd, 1H, J=3.0, 10.0 Hz, H16′), 4.18—4.25 (m, 3H, H2, H3, MOM), 4.54 (d, 1H, J=6.5 Hz), 4.60 (d, 1H, J=7.0 Hz), 4.69 (d, 1H, J=6.5 Hz), 4.75 (m, 1H, H13), 4.80 (d, 1H, J=5.0 Hz, H17), 4.97 (d, 1H, J=6.5 Hz), 5.12 (d, 1H, J=6.5 Hz), 5.35—5.45 (m, 2H, H21, H22), 5.57 (dd, 1H, J=0.5, 8.5 Hz, H19), 5.58 (d, 1H, J=10.0 Hz, H9), 5.69 (s, 1H), 5.71 (s, 1H), 6.60—6.75 (m, 2H), 7.20—7.40 (m, 4H). ^{13}C-NMR (125 MHz, C_6D_6) δ: −5.43, 4.80, 7.03, 7.56, 7.98, 9.72, 13.03, 13.26, 14.58, 16.24, 18.44, 21.50, 26.17, 26.19, 30.55, 30.86, 33.80, 36.49, 43.72, 46.83, 47.64, 55.46, 55.55, 55.60, 56.08, 60.41, 63.19, 77.80, 79.46, 82.00, 83.26, 94.53, 95.28, 97.37, 102.58, 110.95, 111.02, 111.83, 111.91, 119.18, 119.25, 122.34, 127.91, 128.10, 128.29, 132.49, 132.75, 134.89, 135.64, 135.66, 149.96, 150.50, 207.54. FAB-MS *m/z* (%): 1245 (M^++1, 1.8), 1214 (3.6), 281 (20), 253 (25), 211 (95), 151 (100), 137 (46). HR-MS Calcd for $C_{67}H_{113}O_{17}Si_2$ (M^++1): 1245.7516. Found: 1245.7430.

(2*S*,3*S*,4*R*,5*S*,6*S*,7*R*,8*E*,10*S*,13*R*,14*R*,15*S*,16*S*,17*S*,18*E*,20*S*,21*Z*)-3,5-[(*S*)-3,4-Dimethoxybenzylidenedioxy]-13,15-[(*S*)-3,4-dimethoxybenzylidenedioxy]-16-[(1,1-dimethylethyl)dimethylsilyloxymethyl]-4,6,8,10,14,18,20-heptamethyl-1-triethylsilyloxy-2,7,17-trismethoxymethyloxy-8,18,21-tricosatrien-11-one (9) DDQ (1.7 mg, 7.5 μmol) was added to a stirred solution of **7** (6.0 mg, 4.8 μmol) in CH_2Cl_2 (0.5 ml) at −10 °C under argon. After 30 min, work-up as described above gave recovered **7** (0.5 mg, 8.3%) and **9** as a colorless oil (5.0 mg, 84%; 91% based on the consumed **7**). ^{1}H-NMR (500 MHz, C_6D_6) δ: 0.16 (s, 3H), 0.17 (s, 3H), 0.73 (q, 6H, J=8.0 Hz), 1.04 (s, 9H), 1.07 (d, 3H, J=6.9 Hz, C20Me), 1.11 (t, 9H, J=8.0 Hz), 1.17 (d, 3H, J=6.8 Hz, C10Me), 1.30 (d, 3H, J=6.2 Hz, C6Me), 1.31 (d, 3H, J=6.0 Hz, C4Me), 1.44 (s, 3H, C8Me), 1.65 (d, 3H, J=6.6 Hz, C14Me), 1.74 (dd, 3H, J=0.5, 6.6 Hz, C23Me), 1.79 (s, 3H, C18Me), 1.98 (m, 1H, H14), 2.10 (m, 1H, H6), 2.30 (m, 1H, H4), 2.59 (m, 1H, H16), 2.82 (dd, 1H, J=6.8, 15.1 Hz, H12), 3.23 (s, 3H), 3.32 (s, 3H), 3.25—3.37 (m, 1H, H10), 3.41 (s, 3H), 3.42 (s, 3H), 3.43 (s, 3H), 3.38—3.48 (m, 1H, H20), 3.54 (s, 3H), 3.49—3.58 (m, 1H, H12), 3.61 (s, 3H), 3.80 (dd, 1H, J=5.7, 10.4 Hz, H16′), 3.92 (dd, 1H, J=4.6, 11.1 Hz, H1), 3.97 (dd, 1H, J=3.6, 11.1 Hz, H1), 4.04 (d, 1H, J=9.7 Hz, H5), 4.10 (dd, 1H, J=3.2, 10.4 Hz, H16′), 4.17 (s, 1H, H7), 4.18—4.27 (m, 2H, H2, H3), 4.28 (d, 1H, J=10.0 Hz, H15), 4.38 (d, 1H, J=6.9 Hz), 4.55 (d, 1H, J=6.4 Hz), 4.63—4.71 (m, 3H), 4.80 (d, 1H, J=5.2 Hz, H17), 4.97 (d, 1H, J=6.6 Hz), 5.11 (d, 1H, J=6.6 Hz), 5.52 (ddq, 1H, J=9.5, 9.5, 0.5 Hz, H21), 5.59 (m, 1H, H22), 5.62 (d, 1H, J=9.2 Hz, H19), 5.71 (s, 1H), 5.72 (d, 1H, J=10.0 Hz, H9), 6.01 (s, 1H), 6.60—6.75 (m, 2H), 7.30—7.50 (m, 4H).

(2*S*,3*S*,4*R*,5*S*,6*S*,7*R*,8*E*,10*S*,13*S*,14*R*,15*S*,16*S*,17*S*,18*E*,20*S*,21*Z*)-3,5-[(*S*)-3,4-Dimethoxybenzylidenedioxy]-13,15-[(*S*)-3,4-dimethoxybenzylidenedioxy]-16-[(1,1-dimethylethyl)dimethylsilyloxymethyl]-4,6,8,10,14,18,20-heptamethyl-1-hydroxy-2,7,17-trismethoxymethyloxy-8,18,21-tricosatrien-11-one (10) a) AcOH (2.4 μl, 42 μmol) and a 1.0 M solution of TBAF (21 μl, 21 μmol) were added to a stirred solution of **8** (17.5 mg, 14 μmol) in THF (0.5 ml) at 0 °C. After 3 h, the reaction was quenched with saturated aqueous $NaHCO_3$, and the reaction mixture was extracted with Et_2O. The extract was washed with saturated aqueous $NaHCO_3$ and brine, dried over Na_2SO_4, concentrated *in vacuo*, and chromatographed on a silica gel column, eluting with *n*-hexane–EtOAc (1 : 2), to give the recovered starting material (0.4 mg, 2.3%) and **10** as a colorless oil (13.8 mg, 87%; 89% based on the consumed **8**). $[\alpha]_D^{18}$ +52° (c=0.20, $CHCl_3$). IR (neat) cm^{-1}: 3500, 2925, 1710, 1520, 1460, 1260, 1160, 1030. ^{1}H-NMR (500 MHz, C_6D_6) δ: 0.19 (s, 3H), 0.20 (s, 3H), 1.02 (d, 3H, J=6.5 Hz, C20Me), 1.07 (s, 9H), 1.14 (d, 3H, J=7.0 Hz, C4Me), 1.16 (d, 3H, J=7.0 Hz, C10Me), 1.25 (d,

3H, *J*=6.5 Hz, C6Me), 1.39 (s, 3H, C8Me), 1.41 (d, 3H, *J*=6.5 Hz, C14Me), 1.67 (d, 3H, *J*=5.5 Hz, C23Me), 1.74 (s, 3H, C18Me), 2.00—2.10 (m, 2H, H6, H14), 2.18 (m, 1H, H4), 2.33 (dd, 1H, *J*=5.0, 16.5 Hz, H12), 2.43 (br, 1H, OH), 2.76 (m, 1H, H16), 2.97 (dd, 1H, *J*=8.0, 16.5 Hz, H12), 3.20 (s, 3H), 3.23 (s, 3H), 3.26 (s, 3H), 3.20—3.35 (m, 1H, H10), 3.42 (s, 3H×2), 3.47 (m, 1H, H20), 3.53 (s, 3H), 3.60 (s, 3H), 3.72 (m, 1H, H1), 3.78 (dd, 1H, *J*=6.0, 10.0 Hz, H16′), 3.87 (m, 1H, H1), 3.98 (dd, 1H, *J*=2.0, 10.0 Hz, H5), 4.03 (m, 1H, H2), 4.05 (dd, 1H, *J*=1.5, 10.0 Hz, H15), 4.06 (s, 1H, H7), 4.13—4.20 (m, 3H, H3, H16′, MOM), 4.54 (d, 1H, *J*=6.5 Hz), 4.55 (d, 1H, *J*=6.5 Hz), 4.69 (d, 1H, *J*=6.5 Hz), 4.72 (d, 1H, *J*=6.5 Hz), 4.77 (m, 1H, H13), 4.79 (d, 1H, *J*=5.0 Hz, H17), 4.92 (d, 1H, *J*=6.5 Hz), 5.35—5.47 (m, 2H, H21, H22), 5.55 (d, 1H, *J*=9.0 Hz, H19), 5.57 (d, 1H, *J*=9.0 Hz, H9), 5.64 (s, 1H), 5.71 (s, 1H), 6.60—6.80 (m, 2H), 7.20—7.40 (m, 4H). ^{13}C-NMR (125 MHz, C_6D_6) δ: −5.42, −5.37, 7.03, 8.01, 9.76, 13.03, 13.25, 14.54, 16.22, 18.43, 21.50, 26.19, 30.07, 30.86, 33.85, 36.30, 43.90, 46.84, 47.64, 53.28, 55.39, 55.47, 55.56, 55.58, 55.63, 56.07, 60.42, 61.46, 77.85, 77.94, 79.48, 79.66, 82.00, 82.32, 94.55, 95.27, 102.51, 102.55, 110.99, 111.85, 111.96, 119.18, 122.34, 125.44, 127.90, 128.19, 130.61, 132.46, 132.69, 134.87, 135.32, 135.67, 149.96, 150.53, 207.55. FAB-MS *m/z* (%): 1131 (M^++1, 10), 1130 (M^+, 7.1), 1114 (5.4), 1068 (4.0), 862 (5.3), 826 (5.5), 811 (7.8), 663 (5.5), 527 (9.2), 459 (8.8), 151 (100). HR-MS Calcd for $C_{61}H_{99}O_{17}Si$ (M^++1): 1131.6651. Found: 1131.6590.

b) AcOH (0.1 ml) was added to a stirred solution of **8** (2.8 mg, 2.25 μmol) in THF–H_2O (4 : 1, 0.5 ml) at room temperature. After 2 h, the reaction was quenched with saturated aqueous $NaHCO_3$, and work-up as described above gave **10** as a colorless oil (2.5 mg, 98%).

(2*R*,3*S*,4*R*,5*S*,6*S*,7*R*,8*E*,10*S*,13*S*,14*R*,15*S*,16*S*,17*S*,18*E*,20*S*,21*Z*)-3,5-[(*S*)-3,4-Dimethoxybenzylidenedioxy]-13,15-[(*S*)-3,4-dimethoxybenzylidenedioxy]-4,6,8,10,-14,18,20-heptamethyl-16-hydroxymethyl-11-oxo-2,7,17-trismethoxymethyloxy-8,18,21-tricosatrienoic Acid (3) A solution of **10** (13.8 mg, 12 μmol) in CH_2Cl_2 (0.5 ml) was added dropwise to a stirred solution of the Dess–Martin reagent (26 mg, 61 μmol) and pyridine (25 μl, 307 μmol) in CH_2Cl_2 (0.5 ml) at room temperature. After 9.5 h, saturated aqueous $NaHCO_3$ and saturated aqueous $Na_2S_2O_3$ were added to quench the reaction, and the reaction mixture was extracted with Et_2O. The extract was washed with brine, dried over Na_2SO_4, and concentrated *in vacuo*, to leave a crude aldehyde (16.2 mg).

A solution of $NaClO_2$ (11.0 mg, 122 μmol) and NaH_2PO_4 (22.0 mg, 183 μmol) in H_2O (2 ml) was added dropwise to a stirred solution of the above aldehyde (16.2 mg) and 2-methyl-2-butene (130 μl) in 2-methyl-2-propanol (0.8 ml) at room temperature. After 1 h, the reaction mixture was diluted with Et_2O, washed with brine, dried over Na_2SO_4, and concentrated *in vacuo* to leave a crude carboxylic acid (20.2 mg), a part of which was purified by silica gel chromatography. $[\alpha]_D^{21}$ +41° (*c*=0.21, $CHCl_3$). IR (neat) cm^{-1}: 3500—2400, 2925, 1740, 1715, 1520, 1460, 1260, 1160, 1030, 835, 740. ^{1}H-NMR (500 MHz, C_6D_6) δ: 0.19 (s, 3H), 0.20 (s, 3H), 1.03 (d, 3H, *J*=6.5 Hz), 1.09 (s, 9H), 1.17 (d, 3H, *J*=6.5 Hz), 1.22 (d, 3H, *J*=6.5 Hz), 1.36 (s, 3H), 1.40—1.45 (m, 6H), 1.67 (d, 3H, *J*=6.5 Hz), 1.73 (s, 3H), 1.98 (m, 1H), 2.07 (m, 1H), 2.15 (d, 1H, *J*=16.5 Hz), 2.35 (m, 1H), 2.63 (m, 1H), 2.91 (dd, 1H, *J*=8.5, 16.5 Hz), 3.20 (s, 3H), 3.20—3.60 (m, 2H), 3.30 (s, 3H), 3.43 (s, 3H×2), 3.49 (s, 3H), 3.53 (s, 3H), 3.62 (s, 3H), 3.75 (dd, 1H, *J*=6.5, 10.0 Hz), 3.94 (br, 1H), 3.96 (d, 1H, *J*=10.0 Hz), 4.00 (d, 1H, *J*=10.5 Hz), 4.06 (d, 1H, *J*=7.0 Hz), 4.18 (dd, 1H, *J*=3.0, 10.0 Hz), 4.22 (d, 1H, *J*=7.0 Hz), 4.51 (d, 1H, *J*=6.5 Hz), 4.65 (d, 1H, *J*=6.5 Hz), 4.68—4.81 (m, 6H), 5.38—5.48 (m, 3H), 5.53 (d, 1H, *J*=9.0 Hz), 5.61 (s, 1H), 5.63 (s, 1H), 6.60—6.80 (m, 2H), 7.20—7.40 (m, 4H). FAB-MS *m/z* (%): 1146 (M^++2, 5.2), 1145 (M^++1, 5.6), 1144 (M^+, 9.4), 926 (9.6), 803 (9.8), 743 (10), 688 (11), 550 (12), 413 (17), 337 (28), 149 (100).

AcOH (8.4 μl, 150 μmol) and a 1.0 M solution of TBAF (120 μl, 120 μmol) were added to a stirred solution of the above crude carboxylic acid (20 mg) in THF (1 ml) at room temperature. After 2 d, the reaction mixture was diluted with Et_2O, washed with brine, dried over Na_2SO_4, concentrated *in vacuo*, and chromatographed on a silica gel column, eluting with CH_2Cl_2–MeOH (10 : 1), to give **3** as a colorless solid (8.5 mg, 68%). $[\alpha]_D^{20}$ +81° (*c*=0.09, $CHCl_3$). IR (neat) cm^{-1}: 3500—2400, 2925, 1740, 1715, 1520, 1460, 1265, 1160, 1030, 805, 760. ^{1}H-NMR (500 MHz, C_6D_6) δ: 1.03 (d, 3H, *J*=6.5 Hz), 1.16 (d, 3H, *J*=6.5 Hz), 1.23 (d, 6H, *J*=6.5 Hz), 1.36 (s, 3H), 1.46 (d, 3H, *J*=6.5 Hz), 1.63 (dd, 3H, *J*=1.5, 6.5 Hz), 1.60—1.70 (m, 1H), 1.77 (d, 3H, *J*=1.0 Hz), 2.00—2.15 (m, 2H), 2.30—2.40 (m, 1H), 2.60—2.70 (m, 1H), 2.85 (dd, 1H, *J*=8.5, 16.5 Hz), 3.14 (s, 3H), 3.34 (s, 3H), 3.20—3.35 (m, 1H), 3.44 (s, 6H), 3.35—3.50 (m, 1H), 3.49 (s, 3H), 3.55 (s, 3H), 3.63 (s, 3H), 3.84 (dd, 1H, *J*=4.5, 11.5 Hz), 3.91 (dd, 1H, *J*=1.0, 10.5 Hz), 3.93 (dd, 1H, *J*=7.5, 11.5 Hz), 3.99 (d, 1H, *J*=9.5 Hz), 4.01 (d, 1H, *J*=9.5 Hz), 4.11 (d, 1H, *J*=7.0 Hz), 4.30—4.40 (m, 1H), 4.37 (d, 1H, *J*=6.5 Hz), 4.42 (d, 1H, *J*=10.0 Hz), 4.53 (d, 1H, *J*=10.0 Hz), 4.60—4.70 (m, 1H), 4.74 (d, 2H, *J*=6.5 Hz), 4.77—4.85 (m, 2H), 5.30—5.50 (m, 3H), 5.52 (d, 1H, *J*=9.0 Hz), 5.55 (s, 1H), 5.67 (s, 1H), 6.64 (d, 1H, *J*=8.0 Hz), 6.70 (d, 1H, *J*=8.0 Hz), 7.10—7.20 (m, 1H), 7.25—7.40 (m, 3H). ^{13}C-NMR (125 MHz, C_6D_6) δ: 7.22, 7.41, 9.67, 13.21, 13.56, 14.54, 16.35, 21.39, 30.84, 33.49, 36.09, 46.36, 46.69, 53.29, 55.63, 55.76, 56.07, 60.37, 65.27, 77.29, 79.88, 81.20, 82.31, 83.43, 94.58, 96.97, 102.44, 102.76, 110.67, 111.09, 111.59, 111.93, 119.34, 119.37, 122.64, 125.09, 127.91, 128.09, 128.29, 130.57, 132.32, 134.93, 135.34, 149.96, 150.30, 150.60, 178.63, 207.52. FAB-MS *m/z* (%): 1032 (M^++2, 2.7), 1031 (M^++1, 7.7), 1030 (M^+, 9.9), 968 (14), 784 (16), 753 (16), 690 (15), 440 (19), 391 (22), 230 (36), 136 (100). HR-MS Calcd for $C_{55}H_{82}O_{18}$ (M^+): 1030.5501. Found: 1030.5490.

(2*R*,3*S*,4*R*,5*S*,6*S*,7*R*,8*E*,10*S*,13*S*,14*R*,15*S*,16*S*)-2,7-Bismethoxymethyloxy-3,5-[(*S*)-3,4-dimethoxybenzylidenedioxy]-13,15-[(*S*)-3,4-dimethoxybenzylidenedioxy]-16-[(1*S*,2*E*,4*S*,5*Z*)-2,4-dimethyl-1-methoxymethyloxy-2,5-heptadienyl]-11-oxo-4,6,8,10,-14-pentamethyl-8-heptadecenolide (2) Et_3N (2.0 μl, 15 μmol) and 2,4,6-trichlorobenzoyl chloride (2.0 μl, 13 μmol) were added to a stirred solution of **3** (8.0 mg, 7.8 μmol) in THF (0.5 ml) at room temperature under argon. After 16.5 h, the reaction mixture was diluted with benzene (0.5 ml), then DMAP (2.4 mg, 20 μmol) was added , and the stirring was continued for 3 h. The reaction was quenched with saturated aqueous NH_4Cl, and the reaction mixture was extracted with Et_2O. The extract was washed with saturated aqueous NH_4Cl and brine, dried over Na_2SO_4, concentrated *in vacuo*, and chromatographed on a silica gel column, eluting with *n*-hexane–EtOAc (1 : 1), to give **2** as a colorless solid (6.8 mg, 87%). $[\alpha]_D^{20}$ +32° (*c*=0.37, $CHCl_3$). IR (neat) cm^{-1}: 2925, 2850, 1740, 1720, 1520, 1460, 1265, 1160, 1030, 810. ^{1}H-NMR (500 MHz, C_6D_6) δ: 0.94 (d, 3H, *J*=7.0 Hz, C10Me), 1.00 (d, 3H, *J*=6.5 Hz, C20Me), 1.40—1.50 (m, 1H, H14), 1.48 (s, 3H, C8Me), 1.58 (d, 3H, *J*=6.5 Hz, C6Me), 1.60 (d, 3H, *J*=6.5 Hz, C14Me), 1.65 (d, 3H, *J*=5.5 Hz, C23Me), 1.67 (s, 3H, C18Me), 1.73 (d, 3H, *J*=6.5 Hz, C4Me), 1.93 (m, 1H, H4), 1.98 (m, 1H, H6), 2.82 (dd, 1H, *J*=8.5, 13.5 Hz, H12), 2.98 (dd, 1H, *J*=6.0, 13.5 Hz, H12), 3.03 (m, 1H, H16), 3.08 (s, 3H), 3.23 (s, 3H), 3.31 (s, 3H), 3.28—3.36 (m, 1H, H10), 3.39 (s, 3H), 3.41 (s, 3H), 3.35—3.45 (m, 1H, H20), 3.45 (s, 3H), 3.56 (s, 3H), 3.88 (dd, 1H, *J*=1.0, 10.5 Hz, H15), 3.96 (dd, 1H, *J*=0.5, 11.5 Hz, H16′), 4.11 (d, 1H, *J*=10.5 Hz, H7), 4.37 (d, 1H, *J*=6.5 Hz), 4.35—4.41 (m, 1H, H13), 4.42 (d, 1H, *J*=1.5 Hz, H5), 4.45 (d, 1H, *J*=6.5 Hz), 4.53 (d, 1H, *J*=6.5 Hz), 4.60 (dd, 1H, *J*=1.5, 8.5 Hz, H3), 4.63 (d, 1H, *J*=8.5 Hz, H2), 4.64 (d, 1H, *J*=7.0 Hz), 4.66 (d, 1H, *J*=7.0 Hz), 4.68 (d, 1H, *J*=6.5 Hz), 4.92 (d, 1H, *J*=4.5 Hz, H17), 5.28 (d, 1H, *J*=8.5 Hz, H9), 5.31 (dd, 1H, *J*=1.5, 11.5 Hz, H16′), 5.40—5.51 (m, 2H, H21, H22), 5.61 (d, 1H, *J*=9.0 Hz, H19), 5.77 (s, 1H), 6.17 (s, 1H), 6.65 (d, 1H, *J*=8.0 Hz), 6.66 (d, 1H, *J*=8.0 Hz), 7.30—7.45 (m, 4H). ^{13}C-NMR (125 MHz, C_6D_6) δ: 7.49, 8.48, 11.10, 12.59, 12.91, 13.33, 14.31, 16.72, 21.24, 23.07, 29.77, 30.08, 30.16, 30.96, 35.23, 37.27, 39.74, 43.68, 44.77, 45.45, 55.35, 55.50, 55.56, 55.60, 55.83, 63.77, 78.25, 80.05, 81.86, 82.92, 85.78, 93.64, 94.44, 97.50, 102.43, 102.80, 110.90, 111.39, 111.95, 111.97, 119.31, 119.51, 122.52, 131.74, 132.41, 132.84, 133.57, 135.90, 136.04, 149.95, 150.20, 150.64, 150.91, 169.80, 207.75. FAB-MS *m/z* (%): 1014 (M^++2, 8.8), 1013 (M^++1, 16), 1012 (M+, 11), 663 (8.2), 211 (31), 154 (73), 136 (56), 45 (100). HR-MS Calcd for $C_{55}H_{81}O_{17}$ (M^++1): 1013.5473. Found: 1013.5440.

Methyl (2*R*,3*S*,4*R*,5*S*,6*S*,7*R*,8*E*,10*S*,13*S*,14*R*,15*S*,16*S*,17*S*,18*E*,20*S*,21*Z*)-3,5-[(*S*)-3,4-Dimethoxybenzylidenedioxy]-13,15-[(*S*)-3,4-dimethoxybenzylidenedioxy]-4,6,8,10,14,18,20-heptamethyl-16-hydroxymethyl-11-oxo-2,7,17-trismethoxymethyloxy-8,18,-21-tricosatrienoate (11) Et_3N (1.0 μl, 7.2 μmol) and 2,4,6-trichlorobenzoyl chloride (1.0 μl, 6.4 μmol) were added to a stirred solution of **3** (1.0 mg, 1 μmol) in THF (0.5 ml) at room temperature under argon. After 14 h, the reaction was quenched with MeOH, and the reaction mixture was diluted with Et_2O, washed with saturated aqueous NH_4Cl and brine, dried over Na_2SO_4, concentrated *in vacuo*, and chromatographed on a silica gel column, eluting with *n*-hexane–EtOAc (1 : 2), to give **11** as a colorless solid (0.7 mg, 70%). IR (neat) cm^{-1}: 3500, 2950, 2875, 1745, 1720, 1520, 1460, 1265, 1160, 1030, 805. ^{1}H-NMR (500 MHz, C_6D_6) δ: 1.00 (d, 3H, *J*=6.5 Hz, C20Me), 1.17 (d, 3H, *J*=7.0 Hz, C10Me), 1.23 (d, 6H, *J*=6.5 Hz, C6Me, C14Me), 1.28 (s, 3H, C8Me), 1.41 (d, 3H, *J*=6.5 Hz, C4Me), 1.62 (dd, 3H, *J*=1.5, 6.5 Hz, C23Me), 1.60—1.70 (m, 1H, H14), 1.77 (s, 3H, C18Me), 2.04 (dd, 1H, *J*=4.0, 16.5 Hz, H12), 2.00—2.10 (m, 1H, H6), 2.24 (m, 1H, H4), 2.65 (m, 1H, H16), 2.77 (m, 1H, OH), 2.86 (dd, 1H, *J*=8.5, 16.5 Hz, H12), 3.15 (s, 3H), 3.21 (m, 1H, H10), 3.28 (s, 3H), 3.30 (s, 3H), 3.42 (s, 3H), 3.43 (s, 3H), 3.40—3.50 (m, 1H, H20), 3.53 (s, 3H), 3.56 (s, 3H), 3.57 (s, 3H), 3.82 (m, 1H, H16′), 3.90 (m, 1H, H16′), 3.95 (dd, 1H, *J*=1.5, 10.0 Hz, H15), 3.98 (dd, 1H, *J*=1.0, 10.0 Hz, H5), 4.06 (s, 1H, H7), 4.11 (d, 1H, *J*=7.0 Hz), 4.39 (d, 1H, *J*=6.5 Hz), 4.43 (dd, 1H,

J=1.5, 9.0 Hz, H3), 4.52 (d, 1H, J=7.0 Hz), 4.56 (d, 1H, J=6.5 Hz), 4.66 (m, 1H, H13), 4.71 (d, 1H, J=9.0 Hz, H2), 4.72 (d, 1H, J=7.0 Hz), 4.77 (d, 1H, J=7.0 Hz), 4.78 (d, 1H, J=4.5 Hz, H17), 5.30—5.45 (m, 2H, H21, H22), 5.52 (d, 1H, J=9.0 Hz, H9), 5.54 (d, 1H, J=8.5 Hz, H19), 5.60 (s, 1H), 5.64 (s, 1H), 6.64 (d, 1H, J=8.0 Hz), 6.70 (d, 1H, J=8.0 Hz), 7.30—7.40 (m, 4H). FAB-MS m/z (%): 1045 (M^++1, 12), 1044 (M^+, 9.3), 1014 (4.3), 979 (9.7), 871 (8.2), 797 (13), 616 (11), 557 (14), 435 (16), 391 (15), 211 (22), 154 (78), 136 (95), 69 (100). HR-MS Calcd for $C_{56}H_{84}O_{18}$ (M^+): 1044.5658. Found: 1044.5710.

References and Notes

1) Schmitz F. J., Gunasekera S. P., Yalamanchili G., Hossain M. B., van der Helm D., *J. Am. Chem. Soc.*, **106**, 7251—7252 (1984).
2) Omura S., "Macrolide Antibiotics," Academic Press, Orlando, Florida, 1984.
3) More potent 13-deoxytedanolide was isolated from a Japanese sponge, *Mycale adhaerens*; Fusetani N., Sugawara T., Matsunaga S., Horita J., *J. Org. Chem.*, **56**, 4971—4974 (1991).
4) *a*) Yonemitsu O., *Yuki Gosei Kagaku Kyokai Shi*, **52**, 946—955 (1994); *b*) Matsushima T., Horita K., Nakajima N., Yonemitsu O., *Tetrahedron Lett.*, **37**, 385—388 (1996); *c*) Matsushima T., Mori M., Nakajima N., Maeda H., Uenishi J., Yonemitsu O., *Chem. Pharm. Bull.*, **46**, 1335—1336 (1998); *d*) Matsushima T., Mori M., Zheng B.-Z., Maeda H., Nakajima N., Uenishi J., Yonemitsu O., *ibid.*, **47**, 308—321 (1999); *e*) Matsushima T., Zheng B.-Z., Maeda H., Nakajima N., Uenishi J., Yonemitsu O. *Synlett*, **1999**, 780—782; *f*) Zheng B.-Z., Maeda H., Mori M., Kusaka S., Yonemitsu O., Matsushima T., Nakajima N., Uenishi J., *Chem. Pharm. Bull.*, **47**, 1288—1296 (1999); *g*) Taylor R. E., Ciavarri J. P., Hearn B. R., *Tetrahedron Lett.*, **39**, 9361—9364 (1998); *h*) Liu J.-F., Abiko A., Pei Z., Buske D. C., Masamune S., *ibid.*, **39**, 1873—1876 (1998); *i*) Roush W. R., Lane G. C., *Org. Lett.*, **1**, 95—98 (1999); *j*) Jung M. E., Karama U., Marquez R., J. *Org. Chem.*, **64**, 663—665 (1999); *k*) Jung M. E., Marquez R., *Tetrahedron Lett.*, **40**, 3129—3132 (1999); *l*) Smith A. B., III, Lodies S. A., *Org. Lett.*, **1**, 1249—1252 (1999).
5) *a*) Hikota M., Tone H., Horita K., Yonemitsu O., *J. Org. Chem.*, **55**, 7—9 (1990); *b*) *Idem*, *Tetrahedron*, **46**, 4613—4628 (1990); *c*) Hikota M., Sakurai Y., Horita K., Yonemitsu O., *Tetrahedron Lett.*, **31**, 6367—6370 (1990).
6) Inanaga J., Hirata K., Saeki H., Katsuki T., Yamaguchi M., *Bull. Chem. Soc. Jpn.*, **52**, 1989—1993 (1979).
7) *cf.* Stork G., Rychnovsky S. D., *J. Am. Chem. Soc.*, **109**, 1565—1567 (1987).
8) *a*) Goto H., Osawa E., *Tetrahedron Lett.*, **33**, 1343—1346 (1992); *b*) *Idem*, *J. Chem. Soc., Perkin Trans.*, **2**, 1993, 187—198; *c*) Goto H., Osawa E., Yamato M., *Tetrahedron*, **49**, 387—396 (1993).
9) Unless otherwise noted, numbering is based on that of **1**.
10) Denniff P., Whiting D. A., *J. Chem. Soc., Chem. Commun.*, **1976**, 712—713.
11) *cf.* Roush W. R., *J. Org. Chem.*, **56**, 4151—4157 (1991).
12) *a*) Heathcock C. H., Buse C. T., Kleschick W. A., Pirrung M. C., Sohn J. E., Lampe J., *J. Org. Chem.*, **45**, 1066—1081 (1980); *b*) Martin S. F., Lee W. C., Pacofsky G. J., Gist R. P., Mulhern T. A., *J. Am. Chem. Soc.*, **116**, 4674—4688 (1994); *c*) Oikawa M., Ueno T., Oikawa H., Ichihara A., *J. Org, Chem.*, **60**, 5048—5068 (1995).
13) Oikawa Y., Yoshioka T., Yonemitsu O., *Tetrahedron Lett.*, **23**, 889—892 (1982).
14) Dess D. B., Martin J. C., *J. Org. Chem.*, **48**, 4155—4156 (1983).
15) Bel B. S., Childers W. E., Jr., Pinnick H. W., *Tetrahedron*, **37**, 2091—2096 (1981).
16) Sakurai Y., Hikota M., Horita K., Yonemitsu O., *Chem. Pharm. Bull.*, **40**, 2540—2542 (1992).
17) *a*) Colvin E. W., Purcell T. A., Raphael R. A., *J. Chem. Soc., Chem. Commun.*, **1972**, 1031—1032; *b*) White J. D., Lodwig S. N., Trammell G. L., Fleming M. P., *Tetrahedron Lett.*, **1974**, 3263—3266; *c*) Mukaiyama T., Usui M., Saigo K., *Chem. Lett.*, **1976**, 49—50; *d*) Kurihara T., Nakajima Y., Mitsunobu O., *Tetrahedron Lett.*, **1976**, 2455—2458; *e*) Corey E. J., Hopkins P. B., Kim S., Yoo S., Nambiar K. P., Falck J. R., *J. Am. Chem. Soc.*, **101**, 7131—7134 (1979); *f*) Mitsunobu O., *Synthesis*, **1981**, 1—28; *g*) Boden E. P. Keck G. E., *J. Org. Chem.*, **50**, 2394—2395(1985).
18) *cf.* Höfle G., Steglich W., Vorbrüggen H., *Ang. Chem. Int. Ed. Engl.*, **17**, 569—583 (1978).
19) The calculated vicinal proton coupling constants were estimated by virtue of the Karplus calculation[20] on mean dihedral angles of vicinal protons taking into account the Boltzmann distribution of calculated conformers.
20) Jackmann L. M., Sternhell S., "Application of NMR Spectroscopy in Organic Chemistry," 2nd ed., Pergamon Press, New York, 1969, pp. 280—304.

Synthesis of Arnottin I through a Palladium-Mediated Aryl–Aryl Coupling Reaction

Takashi HARAYAMA,* Hirotake YASUDA, Toshihiko AKIYAMA, Yasuo TAKEUCHI, and Hitoshi ABE

Faculty of Pharmaceutical Sciences, Okayama University, Tsushima-Naka, Okayama 700–8530, Japan.
Received January 31, 2000; accepted March 24, 2000

6*H*-Dibenzo[*b*,*d*]pyran-6-one, 6*H*-benzo[*d*]naphtho[1,2-*b*]pyran-6-one, and their derivatives were prepared *via* the palladium mediated aryl–aryl coupling reaction of aryl *ortho*-halobenzoate. The short step synthesis of arnottin I (1) was achieved by this method.

Key words arnottin I; palladium reagent; biaryl coupling reaction

Arnottin I (**1**) was isolated from *Xanthoxylum arnottianum* MAXIM.,[1] and thereafter, the total synthesis of **1** was used to identify the chemical structure.[2] The core of its structure involves the 6*H*-benzo[*d*]naphtho[1,2-*b*]pyran-6-one skeleton which is the same as the gilvocarcins[3] and ravidomycin[4] (Chart 1). Since these compounds display biologically important properties[5] such as antitumor, antibacteria, or antivirus activity, our interests have been focused on the concise construction of the 6*H*-benzo[*d*]naphtho[1,2-*b*]pyran-6-one skeleton.[6]

Recently, we demonstrated the aryl–aryl coupling reaction of amide type biaryl compounds using a palladium reagent,[7] and its application to the synthesis of nitidine[8] and chelerythrine.[9] This coupling reaction can be expected to be useful for the formation of other biaryl compounds such as the ester-linked biaryl compounds.

In this paper, we describe a palladium-mediated aryl–aryl coupling reaction[10] for the effective construction of 6*H*-benzo[*d*]naphtho[1,2-*b*]pyran-6-one and the short step synthesis of arnottin I (**1**) as an application of this method.[11]

Internal Coupling Reaction of Phenyl Benzoate Derivatives In 1984, Ames and Opalko reported the intramolecular biaryl coupling reaction of both phenyl 2-bromobenzoate (**2**) and 2-bromophenyl benzoate (**3**).[12] In their report, the desired 6*H*-dibenzo[*b*,*d*]pyran-6-one (**4**)[12] was obtained from **2** using palladium (II) acetate ($Pd(OAc)_2$) (0.1 eq), triphenylphosphine (PPh_3), and sodium acetate (NaOAc) in *N*,*N*-dimethylacetamide (DMA), whereas **3** afforded no cyclized product **4** under the same reaction conditions (Chart 2).

In order to improve this unique biaryl coupling reaction, we investigated the reactivities of the corresponding iodo analogs **5**[13] and **6**,[14] which were supposed to be more highly reactive than the bromo compounds **2** and **3**. The results of the palladium-mediated reaction are summarized in Table 1. Initially, we examined $Pd(OAc)_2$ as a catalyst for the substrate **5**. It was found that the combination of a phosphine ligand and base was crucial for the yield of **4**. When PPh_3 was used as the ligand, sodium acetate gave a better result than silver carbonate (runs 1 and 2). While tri-(*o*-tolyl)phosphine ($P(2\text{-Tol})_3$) lead to lower yield of **4** (runs 3 and 4), a bidentate phosphine ligand, 1,3-bis(diphenylphosphino)-propane (DPPP) gave **4** in good yield when it was used with

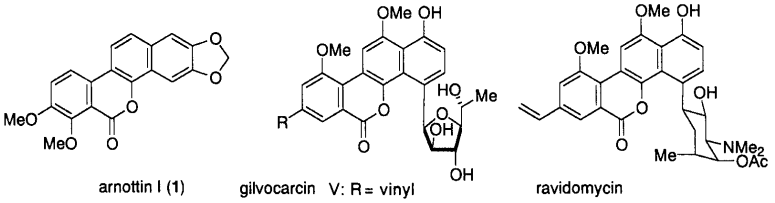

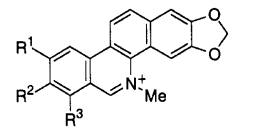

Chart 1

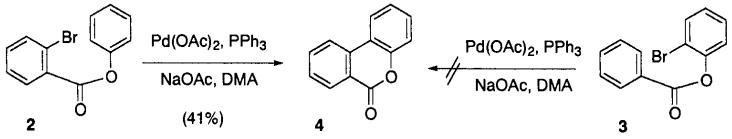

Chart 2

* To whom correspondence should be addressed. e-mail: harayama@pharm.okayama-u.ac.jp
© 2000 Pharmaceutical Society of Japan

NaOAc as the base (run 5). Interestingly, the best result was observed when no phosphine ligand was employed (run 7). The other catalysts such as bis(triphenylphosphine)palladium(II) chloride ($Pd(PPh_3)_2Cl_2$), palladium(II) acetylacetonate ($Pd(acac)_2$), and tetrakis(triphenylphosphine)palladium(0) ($Pd(PPh_3)_4$) afforded **4** in moderate yields (runs 8—11). On the other hand, the reaction of the ester **6** with $Pd(OAc)_2$, PPh_3, and NaOAc showed extremely poor reactivity (run 12).

Table 1. Cyclization Reaction of Phenyl *o*-Iodobenzoate (**5**) and *o*-Iodophenyl Benzoate (**6**)

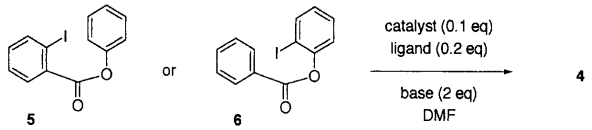

Run	Ester	Catalyst	Ligand	Base	Time (h)	Temp.	Yield (%) of **4**
1	**5**	$Pd(OAc)_2$	PPh_3	NaOAc	2	130 °C	73
2	**5**	$Pd(OAc)_2$	PPh_3	Ag_2CO_3	24	Reflux	38
3	**5**	$Pd(OAc)_2$	P(2-Tol)$_3$	NaOAc	4	Reflux	—[a]
4	**5**	$Pd(OAc)_2$	P(2-Tol)$_3$	Ag_2CO_3	24	Reflux	36
5	**5**	$Pd(OAc)_2$	DPPP	NaOAc	2	Reflux	75
6[b]	**5**	$Pd(OAc)_2$	DPPP[c]	iso-Pr_2NEt	2	Reflux	—[d]
7	**5**	$Pd(OAc)_2$	None	NaOAc	1	Reflux	84
8	**5**	$Pd(PPh_3)_2Cl_2$	None	NaOAc	1.5	130 °C	66
9	**5**	$Pd(acac)_2$	None	NaOAc	1.5	130 °C	68
10	**5**	$Pd(acac)_2$	PPh_3	NaOAc	2.5	130 °C	57
11	**5**	$Pd(PPh_3)_4$	None	NaOAc	4	130 °C	54
12	**6**	$Pd(OAc)_2$	PPh_3	NaOAc	2	Reflux	6

a) Phenyl benzoate was detected on TLC. *b*) See ref. 7. *c*) Bu_3P (0.1 eq) was added as an additive. *d*) Phenyl benzoate was isolated in 65% yield.

Table 2. Cyclization Reaction of 1-Naphthyl *o*-Iodobenzoate (7)

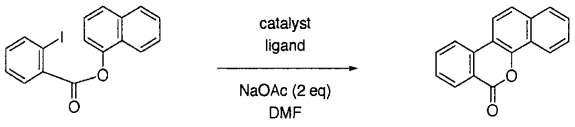

Run	Catalyst	(mol eq)	Ligand	(mol eq)	Time (h)	Temp.	Yield (%) of **8**
1	$Pd(OAc)_2$	(0.1)	PPh_3	(0.2)	3	150°C	55
2	$Pd(OAc)_2$	(0.1)	None	—	2	Reflux	51
3	$Pd(PPh_3)_4$	(0.1)	None	—	5	130°C	49
4	$Pd(PPh_3)_2Cl_2$	(0.1)	None	—	5	130°C	59
5	$Pd(PPh_3)_2Cl_2$	(0.2)	None	—	3.5	130°C	70
6	$Pd(acac)_2$	(0.1)	PPh_3	(0.2)	1.5	130°C	59
7	$Pd(acac)_2$	(0.1)	None	—	2.5	130°C	72

Internal Coupling Reaction of 1-Naphthyl 2-Iodobenzoate and 1-Naphthyl 2,3-Dimethoxy-6-iodobenzoate As preliminary experiments for the synthesis of arnottin I, the reactivity of both naphthyl esters **7** and **9** was examined. These substrates were prepared by the esterification of benzoic acid derivatives with 1-naphthol. As shown in Table 2, the conversion of the ester **7** into the biaryl coupling product **8** was observed in all runs. When $Pd(OAc)_2$ was employed with PPh_3, the cyclized product **8** was generated in 55% yield (run 1). It was found that the effect of the phosphine ligand was negligible (run 2). Also, changing the catalyst to $Pd(PPh_3)_2Cl_2$ or $Pd(PPh_3)_4$ did not have any notable effect (runs 3 and 4), but the use of 0.2 eq of the same catalyst lead to a slight improvement in the yield (run 5). While $Pd(acac)_2$ in the presence of PPh_3 gave **8** in only moderate yield (run 6), the best result was observed if this catalyst was used without the phosphine ligand (run 7).

Furthermore, our attempt at this coupling reaction of the ester-linked biaryl substrates was extended to the dimethoxy compound **9**. The results of the reaction are summarized in Table 3, in which results almost similar to those in Table 2 were observed. While the use of $Pd(OAc)_2$ gave **10** in moderate yields (runs 1 and 2), slightly higher yields were obtained when $Pd(PPh_3)_4$ or $Pd(PPh_3)_2Cl_2$ was employed (runs 3 and 4). In this case, $Pd(acac)_2$ worked the most effectively to give **10** in up to 79% yield (runs 5 and 6).

Synthesis of Arnottin I Since the palladium-mediated coupling reaction of the ester-linked biaryl compounds was successful as already described, we planned the total synthesis of arnottin I utilizing this method. Our concise synthetic route is outlined in Chart 3.

The preparation of a key compound **11** should be realized by condensation between the carboxylic acid **12**[15] and naphthol **13** which was easily derived from commercially available 6,7-dimethoxy-α-tetralone (**14**) *via* several steps as shown in Chart 4. Thus, the demethylation of **14** followed by

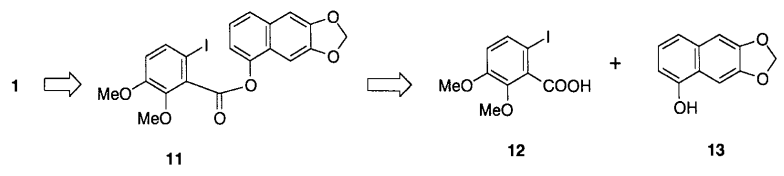

Chart 3

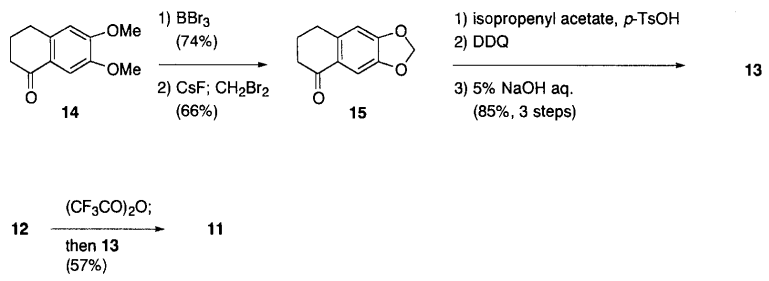

Chart 4

Table 3. Cyclization Reaction of 1-Naphthyl 6-Iodo-2,3-dimethoxybenzoate (**9**)

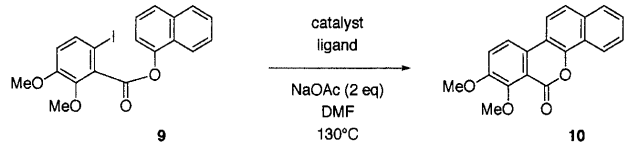

Run	Catalyst	(mol eq)	Ligand	(mol eq)	Time (h)	Yield (%) of **10**
1	$Pd(OAc)_2$	(0.2)	PPh_3	(0.4)	6.5	60
2	$Pd(OAc)_2$	(0.1)	None	—	16	58
3	$Pd(PPh_3)4$	(0.1)	None	—	5	64
4	$Pd(PPh_3)_2Cl_2$	(0.2)	None	—	10	65
5	$Pd(acac)_2$	(0.1)	PPh_3	(0.2)	3	79
6	$Pd(acac)_2$	(0.1)	None	—	4	76

Table 4. Cyclization Reaction of 6,7-Methylenedioxy-1-naphthyl 6-Iodo-2,3-dimethoxybenzoate (**11**)

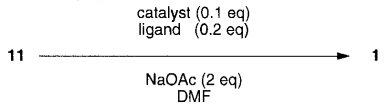

Run	Catalyst	Ligand	Time (h)	Temp. (°C)	Yield (%) of **1**
1	$Pd(PPh_3)_2Cl_2$	None	5	130	52
2	$Pd(acac)_2$	PPh_3	4	130	56
3	$Pd(acac)_2$	PPh_3	2	150	72
4	$Pd(PPh_3)_4$	None	3.5	130	58
5	$Pd(PPh_3)_4$	None	2	150	71

methylenation afforded **15**, and conversion into **13** was performed by Cushman's method[16] involving the enol acetate formation, dehydrogenation, and hydrolysis. The esterification of **12** with trifluoroacetic anhydride was carried out to afford **11** in 57% yield.

The results of the internal biaryl coupling reaction of **11** in the presence of palladium reagent are summarized in Table 4. The formation of arnottin I was observed in all runs. Although this reaction at 130°C gave only moderate yields of **1** (runs 1, 2, and 4), a slightly higher temperature resulted in satisfactory yields (runs 3 and 5). Spectral data obtained from the synthetic material were in agreement with those for the natural product.

Conclusion We found that aryl *o*-halobenzoates could cyclize to give 6*H*-dibenzo[*b*,*d*]pyran-6-one, 6*H*-benzo[*d*]-naphtho[1,2-*b*]pyran-6-one, and their derivatives using palladium reagent. The short step synthesis of arnottin I (**1**) was performed utilizing this internal aryl–aryl coupling reaction. Further studies on the mechanistic aspect and other application of this method are now underway in our laboratory.

Experimental

Melting points were measured with a Yanagimoto micro melting point hot-plate apparatus and are uncorrected. IR spectra were recorded on a JASCO A-102 spectrometer. NMR spectra were taken with a Varian VXR-500, VXR-200, or Hitachi R-1500 instrument with chemical shifts reported as δ ppm and couplings expressed in Hertz. Fast atom bombardment-mass spectra (FAB-MS) were obtained using a VG-70SE mass spectrometer. Elemental analyses were carried out on a Yanaco MT-5 CHN analyzer.

Phenyl 2-Iodobenzoate (**5**)[13] and 2-Iodophenyl Benzoate (**6**)[14] were prepared according to procedures reported in the literature.

1-Naphthyl 2-Iodobenzoate (7) To a solution of 2-iodobenzoic acid (1.12 g, 4.51 mmol) in dry tetrahydrofuran (THF) (20 ml) were added oxalyl chloride (0.79 ml, 9.02 mmol) and 2—3 drops of *N*,*N*-dimethylformamide (DMF) at 0 °C. After stirring for 1 h at room temperature, volatile materials were removed under reduced pressure to give a yellow residue which dissolved in dry pyridine (10 ml). To this mixture, 1-naphthol (617.6 mg, 4.28 mmol) was added, and stirred for 2 h at room temperature. The reaction mixture was poured into 10% HCl aqueous solution and extracted with AcOEt. The AcOEt layer was washed with 10% K_2CO_3 aqueous solution and brine, dried over Na_2SO_4, and concentrated. Purification by silica gel column chromatography with benzene-hexane (3 : 2) afforded **7** (1.40 g, 87%) as a colorless oil. IR ($CHCl_3$) cm^{-1}: 1760 (C=O). ^{1}H-NMR (60 MHz, $CDCl_3$) δ: 7.10—8.34 (11H, m). FAB-MS (positive ion mode) *m/z*: 375 $(M+1)^+$. *Anal.* Calcd for $C_{17}H_{11}IO_2$: C, 54.57; H, 2.96. Found: C, 54.29; H, 3.02.

1-Naphthyl 6-Iodo-2,3-dimethoxybenzoate (9) To a suspension of 6-iodo-2,3-dimethoxybenzoic acid (**12**)[15] (110.8 mg, 0.360 mmol) in dry benzene (3 ml) was added trifluoroacetic anhydride (0.06 ml, 0.425 mmol). After stirring for 2 h at 60 °C, a solution of 1-naphthol (51.8 mg, 0.359 mmol) in dry benzene (3 ml) was added to the mixture and stirred for 2 h at 60 °C. The reaction mixture was cooled to room temperature and then diluted with ether. After neutralization with 5% NaOH aqueous solution and extraction with ether, the obtained ether layer was washed with brine, dried over Na_2SO_4, and concentrated. Silica gel column chromatography of the residue with benzene gave pure **9** (112.9 mg, 72%). For the analytical sample, recrystallization with benzene–hexane was carried out that left colorless prisms, mp 107—108°C. IR (KBr) cm^{-1}: 1750 (C=O). ^{1}H-NMR (60 MHz, $CDCl_3$) δ: 3.90 (3H, s), 3.99 (3H, s), 6.78 (1H, d, J=8.8 Hz), 7.35—8.36 (8H, m). FAB-MS (positive ion mode) *m/z*: 435 $(M+1)^+$. *Anal.* Calcd for $C_{19}H_{15}IO_4$: C, 52.56; H, 3.48. Found: C, 52.39; H, 3.44.

6,7-Methylenedioxy-1-tetralone (15)[17] To a solution of BBr_3 (20 ml) in dry CH_2Cl_2 (150 ml) was added 6,7-dimethoxy-1-tetralone (17.5 g, 85 mmol) at 0 °C. After stirring for 1 h at 0 °C, the ice bath was removed and the reaction mixture was stirred for 2 h. Water (15 ml) was slowly added at 0 °C, and after the exothermic reaction ceased, a 5% NaOH aqueous solution was added to make the reaction mixture basic. The aqueous layer was washed with CH_2Cl_2, made acidic with conc. HCl aqueous solution, and extracted with ether. After washing with brine and dried over $MgSO_4$, the solvent was removed under reduced pressure to give a residue which was subjected to silica gel column chromatography with hexane–AcOEt (1 : 1). 6,7-Dihydroxy-1-tetralone[18] (11.3 g, 74%) was obtained as a pale yellow solid which was recrystallized with AcOEt–hexane that left pale yellow needles, mp 204—205 °C (lit.[18] mp 195 °C). IR (KBr) cm^{-1}: 3520, 3200 (-OH), 1660 (C=O). ^{1}H-NMR (60 MHz, CD_3OD) δ: 1.90—2.92 (6H, m), 4.82 (2H, s), 6.65 (1H, s), 7.36 (1H, s). FAB-MS (positive ion mode) *m/z*: 179 $(M+1)^+$. *Anal.* Calcd for $C_{10}H_{10}O_3$: C, 67.41; H, 5.66. Found: C, 67.26; H, 5.72.

CsF (47.5 g, 313 mmol) was added to a solution of 6,7-dihydroxy-1-tetralone (11.2 g, 62.6 mmol) in DMF (250 ml) and the resulting mixture was stirred for 3 h at room temperature. After dibromomethane (6.7 ml) was added, the mixture was stirred for 2 h at 100°C and cooled to room temperature. AcOEt was added to dilute the mixture, and then any undissolved solid was removed by filtration. The filtrate was washed with 5% NaOH aqueous solution and brine, dried over $MgSO_4$, and concentrated to give a residue which was subjected to silica gel column chromatography with benzene. Recrystallization with hexane was carried out to leave **15** (7.83 g, 66%) as colorless needles, mp 75—76 °C (hexane) (lit.[17] mp 74—76°C). IR (KBr) cm^{-1}: 1665, 1250, 1035. ^{1}H-NMR (200 MHz, $CDCl_3$) δ: 2.09 (2H, m), 2.59 (2H, t, J=6.6 Hz), 2.88 (2H, t, J=6.1 Hz), 6.00 (2H, s), 6.66 (1H, s), 7.47 (1H, s). FAB-MS (positive ion mode) *m/z*: 191 $(M+1)^+$. *Anal.* Calcd for $C_{11}H_{10}O_3$: C, 69.46; H, 5.30. Found: C, 69.57; H, 5.26.

6,7-Methylenedioxy-1-naphthol (13)[19] A mixture of **15** (1.90 g, 10 mmol), isopropenyl acetate (60 ml), and *p*-toluenesulfonic acid (*p*-TsOH) monohydrate (304 mg, 1.6 mmol) was refluxed for 3 h under an argon atmosphere. After cooling to room temperature, 2,3-dichloro-5,6-dicyano-1,4-benzoquinone (DDQ) (2.72 g, 12 mmol) was added to the mixture, which was stirred for 1 h at 90 °C. After cooling, the mixture was diluted with CH_2Cl_2, successively washed with 10% $NaHCO_3$, 5% HCl aqueous solution, and brine, then dried over $MgSO_4$. Evaporation of the solvent gave a residue which was dissolved in a mixture of ethanol (60 ml) and 10% NaOH aqueous solution (30 ml). The mixture was stirred for 90 min at 80 °C and then diluted with ether. The mixture was washed with 10% HCl aqueous solution and brine, and dried over $MgSO_4$. Evaporation of the solvent gave a crude residue which was purified by silica gel column chromatography with benzene to afford pure **13** (1.60 g, 85%) as colorless needles, mp 137—138 °C

(benzene–hexane) (lit.[19b] 124 °C, lit.[19c] 133—134 °C). IR (KBr) cm^{-1}: 3350, 1245, 1040. ^{1}H-NMR (500 MHz, $CDCl_3$) δ: 5.18 (1H, s), 6.04 (2H, s), 6.68 (1H, dd, J=7.5, 1.0 Hz), 7.09 (1H, s), 7.15 (1H, dd, J=8.0, 7.5 Hz), 7.26 (1H, d, J=8.0 Hz), 7.48 (1H, s). FAB-MS (positive ion mode) m/z: 189 $(M+1)^+$, 188 (M^+). *Anal.* Calcd for $C_{11}H_8O_3$: C, 70.21; H, 4.28. Found: C, 70.25; H, 4.47.

6,7-Methylenedioxy-1-naphthyl 6-Iodo-2,3-dimethoxybenzoate (11) To a suspension of **12**[15] (449.4 mg, 1.46 mmol) in dry benzene (6 ml) was added trifluoroacetic anhydride (0.42 ml, 2.97 mmol). After stirring for 2 h at 60 °C, a solution of **13** (274.5 mg, 1.46 mmol) in dry benzene (6 ml) was added to the mixture and stirred for 2 h at 60 °C. The reaction mixture was cooled to room temperature and then diluted with ether. After neutralization with 5% NaOH aqueous solution and extraction with ether, the combined ether layer was washed with brine, dried over Na_2SO_4, and concentrated. Silica gel column chromatography of the residue with benzene–hexane was carried out to leave pure **11** (293.8 mg, 57%) as colorless prisms, mp 175.5 °C. IR (KBr) cm^{-1}: 1750 (C=O). ^{1}H-NMR (500 MHz, $CDCl_3$) δ: 3.93 (3H, s), 4.01 (3H, s), 6.06 (2H, s), 6.81 (1H, d, J=8.5 Hz), 7.16 (1H, s), 7.37—7.39 (2H, m), 7.57 (1H, d, J=8.5 Hz), 7.59—7.62 (2H, m). FAB-MS (positive ion mode) m/z: 479 $(M+1)^+$. *Anal.* Calcd for $C_{20}H_{15}IO_6$: C, 50.23; H, 3.16. Found: C, 49.92; H, 3.22.

Typical Procedure for Internal Biaryl Coupling Reaction Base (0.882 mmol), phosphine ligand (0.076 mmol), and palladium reagent (0.037 mmol) were successively added to a solution of ester (0.368 mmol) in dry DMF (4 ml). The reaction mixture was then heated in an oil bath. After cooling to room temperature, the mixture was diluted with AcOEt. Undissolved materials were removed by filtration and then the filtrate was poured into 10% HCl aqueous solution. The organic layers were combined and washed with brine. Evaporation of the solvent gave a residue which was purified by silica gel chromatography with benzene–hexane.

6*H*-Dibenzo[*b*,*d*]pyran-6-one (**4**): Colorless needles, mp 92—94 °C (hexane) (lit.[20] 92—93 °C). IR (KBr) cm^{-1}: 1730 (C=O). ^{1}H-NMR (500 MHz, $CDCl_3$) δ: 7.36 (1H, td, J=8.0, 1.0 Hz), 7.39 (1H, dd, J=8.0, 1.0 Hz), 7.50 (1H, ddd, J=8.5, 7.5, 1.5 Hz), 7.60 (1H, td, J=7.5, 1.0 Hz), 7.84 (1H, ddd, J=7.5, 7.0, 1.5 Hz), 8.09 (1H, dd, J=8.0, 1.5 Hz), 8.15 (1H, d, J=8.0 Hz), 8.42 (1H, dd, J=8.0, 1.0 Hz). FAB-MS (positive ion mode) m/z: 197 $(M+1)^+$. *Anal.* Calcd for $C_{13}H_8O_2$: C, 79.58; H, 4.11. Found: C, 79.29; H, 4.41.

6*H*-Benzo[*d*]naphtho[1,2-*b*]pyran-6-one (**8**): Colorless needles, mp 191 °C (hexane) (lit.[21] mp 191 °C). IR (KBr) cm^{-1}: 1730 (C=O). ^{1}H-NMR (60 MHz, $CDCl_3$) δ: 7.37—8.57 (10H, m). FAB-MS (positive ion mode) m/z: 247 $(M+1)^+$. *Anal.* Calcd for $C_{17}H_{10}O_2$: C, 82.91; H, 4.09. Found: C, 82.74; H, 4.36.

7,8-Dimethoxy-6*H*-benzo[*d*]naphtho[1,2-*b*]pyran-6-one (**10**): Colorless needles, mp 185—187 °C (benzene). IR (KBr) cm^{-1}: 1740 (C=O). ^{1}H-NMR (500 MHz, $CDCl_3$) δ: 4.00 (3H, s), 4.05 (3H, s), 7.47 (1H, d, J=9.0 Hz), 7.56—7.64 (2H, m), 7.72 (1H, d, J=9.0 Hz), 7.86 (1H, d, J=8.0 Hz), 7.94 (1H, d, J=9.0 Hz), 7.99 (1H, d, J=9.0 Hz), 8.57 (1H, d, J=8.0 Hz). FAB-MS (positive ion mode) m/z: 307 $(M+1)^+$. *Anal.* Calcd for $C_{19}H_{14}O_4$: C, 74.50; H, 4.61. Found: C, 74.16; H, 4.72.

Arnottin I (**1**): Colorless prisms, mp 294—297 °C ($CHCl_3$) (lit.[2] mp 292—297 °C). IR (KBr) cm^{-1}: 1750. ^{1}H-NMR (500 MHz, $CDCl_3$) δ: 3.99 (3H, s), 4.03 (3H, s), 6.10 (2H, s), 7.14 (1H, s), 7.45 (1H, d, J=8.5 Hz), 7.54 (1H, d, J=8.5 Hz), 7.84 (1H, d, J=9.0 Hz), 7.85 (1H, s), 7.89 (1H, d, J=9.0 Hz).

Acknowledgement This work was supported in part by a grant-in-aid from the Ministry of Education, Science, Sports and Culture, Japan (No. 11672103 to T. H.). The authors are indebted to Professor T. Ishikawa, Faculty of Pharmaceutical Sciences, Chiba University, for providing us with the spectral data of arnottin I, and to the SC-NMR Laboratory of Okayama University for doing the high field NMR experiments.

References

1) Ishii H., Ishikawa T., Haginiwa J., *Yakugaku Zasshi*, **97**, 890—900 (1977).
2) Ishii H., Ishikawa T., Murota M., Aoki Y., Harayama T., *J. Chem. Soc., Perkin Trans. 1*, **1993**, 1019—1022.
3) Hatano K., Higashide E., Shibata M., Horii S., Mizuno K., *Agric. Biol. Chem.*, **44**, 1157—1163 (1980); Horii S., Fukase H., Mizuta E., Hatano K., Mizuno K., *Chem. Pharm. Bull.*, **28**, 3601—3611 (1980); Balitz D. M., O'Herron F. A., Bush J., Vyas D. M., Nettleton D. E., Grulich R. E., Brander W. T., Doyle T. W., Arnold E., Crardy J., *J. Antibiot.*, **34**, 1544—1555 (1981); Nakano H., Matsuda Y., Ito K., Ohkubo S., Morimoto M., Tomota F., *ibid.*, **34**, 266—270 (1981); Takahashi K., Yoshida M., Tomita F., Shirahata K., *ibid.*, **34**, 271—275 (1981).
4) Findlay J. A., Liu J.-S., Radics L., Rakhit S., *Can. J. Chem.*, **59**, 3018—3020 (1981); Sehgal S. N., Czerkawski H., Kudelski A., Pandev K., Saucier R., Vézina C., *J. Antibiot.*, **36**, 355—361 (1983).
5) Wei T. T., Chan J. A., Roller P. P., Weiss U., Stroshane R. M., White R. J., Byrne K. M., *J. Antibiot.*, **35**, 529—532 (1982); Wei T. T., Byrne K. M., Warnick-Pickle D., Greenstein M., *ibid.*, **35**, 545—548 (1982); Singh K., *ibid.*, **37**, 71—73 (1984).
6) Syntheses of gilvocarcins have been reported: Deshpande P. P., Martin O. R., *Tetrahedron Lett.*, **31**, 6313—6316 (1990); Matsumoto T., Hosoya T., Suzuki K., *J. Am. Chem. Soc.*, **114**, 3568—3570 (1992); Hosoya T., Takashiro E., Matsumoto T., Suzuki K., *ibid.*, **116**, 1004—1015 (1994), and references cited therein.
7) Harayama T., Akiyama T., Nakano Y., *Chem. Pharm. Bull.*, **45**, 1723—1725 (1997).
8) Harayama T., Akiyama T., Nakano Y., Shibaike K., *Heterocycles*, **48**, 1989—1993 (1998); Harayama T., Shibaike K., *ibid.*, **49**, 191—195 (1998).
9) Harayama T., Akiyama T., Kawano K., *Chem. Pharm. Bull.*, **44**, 1634—1636 (1996).
10) Review on palladium-mediated coupling reaction: Tsuji J., "Palladium Reagents and Catalysts," John Wiley and Sons Inc., New York, 1995, pp. 125—252; Knight D. W., "Comprehensive Organic Synthesis," Vol. 3, ed. by Trost B. M., Fleming I., Pergamon Press, Oxford, 1991, pp. 481—520.
11) A preliminary communication of this work has been published: Harayama T., Yasuda H., *Heterocycles*, **46**, 61—64 (1997).
12) Ames D. E., Opalko A., *Tetrahedron*, **40**, 1919—1925 (1984).
13) Singh A., Andrews L. J., Keefer R. M., *J. Am. Chem. Soc.*, **84**, 1179—1185 (1962).
14) Buchan S., McCombie H., *J. Chem. Soc.*, **1931**, 137—144.
15) Dyke S. F., Tiley E. P., *Tetrahedron*, **31**, 561—568 (1977).
16) Wang G., Cushman M., *Synth. Commun.*, **21**, 989—996 (1991).
17) Ninomiya I., Naito T., Ishii H., Ishida T., Ueda M., Harada K., *J. Chem. Soc., Perkin Trans 1*, **1975**, 762—764.
18) Momose T., Oya H., Ohkura Y., Iwasaki M., *Chem. Pharm. Bull.*, **2**, 119—122 (1954).
19) *a*) Takao N., Kamigauchi M., Sugiura M., Ninomiya I., Miyata O., Naito T., *Heterocycles*, **16**, 221—225 (1981); *b*) Dallacker F., Schneider P., *Chem. Ztg.*, **110**, 455—458 (1986); *c*) Zjawiony J., Peterson J. R., *Org. Prep. Proced. Int.*, **23**, 163—172 (1991).
20) Alo B. I., Kandil A., Patil P. A., Sharp M. J., Siddiqui M. A., Snieckus V., Josephy P. D., *J. Org. Chem.*, **56**, 3763—3768 (1991).
21) Chatterjea J. N., Bhakta S. C., Chattopadhyay A. K., *J. Indian Chem. Soc.*, **51**, 757—762 (1974).

Preparation of New Nitrogen-Bridged Heterocycles. 49.[1] A New Access to Thieno[3,4-*b*]indolizine Derivatives

Akikazu KAKEHI,* Suketaka ITO, Kazuyuki HIRATA, and Peng ZUO

Department of Chemistry and Material Engineering, Faculty of Engineering, Shinshu University, Wakasato, Nagano 380–8553, Japan. Received February 1, 2000; accepted February 28, 2000

The title compounds, together with 3-vinylindolizine-1-carbonitriles (4—56%), were prepared in 1—18% yields from the *S*-alkylation of pyridinium 1-[3-ethoxycarbonyl-1-[cyanomethylthio(thiocarbonyl)]]allylides with alkyl halides, followed by treatment of the resulting pyridinium salts with a base and then a dehydrogenating agent. In several reactions of pyridinium salts obtained from reaction of the allylides with benzylic halides, trace amounts of bis[1-cyano-9-(ethoxycarbonyl)thieno[3,4-*b*]indolizin-3-yl] disulfides with an interesting superimposed structure were also isolated. The structures of these compounds were confirmed by X-ray analyses.

Key words thieno[3,4-*b*]indolizine; 3-vinylindolizine; pyridinium allylide; cyclization; stacked structure; X-ray analysis

We recently reported the unexpected formation of ethyl 1-cyano-3-(methylthio)thieno[3,4-*b*]indolizine-9-carboxylates in the reactions of 1-[1-[cyanomethylthio(methylthio)methylene]-3-ethoxycarbonyl-2-propenyl]pyridinium bromides with a base and a dehydrogenating agent, and proposed a possible reaction mechanism.[1] In order to develop a general and effective preparative method for this type of heterocycle, we examined substituent effects and various reaction conditions such as bases, solvents, and reaction temperature. However, similar reactions of the salts obtained from pyridinium 1-[3-ethoxycarbonyl-1-[methylthio(thiocarbonyl)]]allylides and various alkylating agents, except bromoacetonitrile, gave exclusively 3-vinylindolizine derivatives and none of the desired thieno[3,4-*b*]indolizine derivatives. We then examined the use of pyridinium 1-allylides having a cyanomethylthio(thiocarbonyl) group on the ylidic carbanion for the synthesis of this type of compound. In this paper we report the preparation of the title compounds starting from pyridinium 1-[3-ethoxycarbonyl-1-[cyanomethylthio(thiocarbonyl)]]allylides with various alkylating agents, and of by-products, bis[1-cyano-9-(ethoxycarbonyl)thieno[3,4-*b*]indolizin-3-yl] disulfides, which have an interesting superimposed structure between the two indolizine rings in the molecule.

Results and Discussion

Reactions of Pyridinium 1-[3-Ethoxycarbonyl-1-[cyanomethylthio(thiocarbonyl)]allylides When pyridinium 1-[3-ethoxycarbonyl-1-[cyanomethylthio(thiocarbonyl)]]allylides (**1a—c**) were alkylated with various alkyl halides (**2a—e**), and the resulting *S*-alkylated pyridinium salts treated with 1,8-diazabicyclo[5.4.0]undec-7-ene (DBU) and then chloranil at 0 °C, the expected ethyl 3-alkylthio-1-cyanothieno[3,4-*b*]indolizine-9-carboxylates (**3a—o**) were formed in 1—18% yields as orange crystals with very strong fluorescence, together with ethyl 3-(2-alkylthio-3-cyanoindolizin-3-yl)acrylates (**4a—o**, 4—56%). Interestingly, another type of product, bis(1-cyano-9-ethoxycarbonylthieno[3,4-*b*]indolizin-3-yl) disulfides **5a**, **b** were also formed in the reactions of pyridinium allylides (**1a**, **b**) with benzylic halides (**2c—e**), but yields were very low (trace). These results are shown in Chart 1.

The structures of ethyl 3-alkylthio-1-cyanothieno[3,4-*b*]indolizine-9-carboxylates (**3a—o**) were determined by physical and spectral means and by spectral comparison with those (**3a**, **k**) prepared earlier by us.[1] The proton and methyl proton signals on the pyridine ring in the ^{1}H-NMR spectra of new compounds **3b—j**, **l—o** appeared at δ 6.43—9.19 and 2.14—2.75, respectively, and the chemical shifts were almostly parallel to those of the known **3a**, **k**. Their IR spectra showed a characteristic aromatic cyano (2183—2220 cm^{-1}) and a carbonyl absorption band (1664—1709 cm^{-1}). Since an alternative structural contribution (**3′**) for these thieno[3,4-*b*]indolizine derivatives (**3**) can be considered (see Chart 2), as seen in thieno[3,4-*a*]indolizine,[2] we carried out a single crystal X-ray analysis of **3g** in order to confirm this structure and to obtain further structural information. The ORTEP drawing[3] for **3g** is shown in Fig. 1. This structural data distinctly showed that thieno[3,4-*b*]indolizine has the structure **3** in preference to the alternative **3′**, because the S(1)–C(1) (1.751 Å) and the S(1)–C(2) bond length (1.727 Å) of **3g** are nearly parallel to or longer than the S–C bond lengths (1.714 Å) in thiophene[4] and the C(3)–C(10) bond length (1.431 Å) is longer than the C(1)–C(10) (1.389 Å) and the C(2)–C(3) bond length (1.371 Å). Furthermore, the C(3)–C(10) bond length (1.431 Å) of **3g** is clearly longer than those (1.370–1.411 Å) in an indolizine[5] and some 2,3-fused indolizines[6] but it is close to that (1.423 Å) in thiophene.[4]

The structures of the main products, ethyl 3-(2-alkylthio-1-cyanoindolizin-3-yl)acrylates (**4a—o**) were also confirmed by physical and spectral means. Compounds **4a**, **f**, **k** were in accord with authentic samples in all respects. The *trans* carbon–carbon double bond in products **4a—o** was indicated by an olefinic absorption band (1607—1622 cm^{-1}) in the IR spectra and by the presence of a set of AB type proton signals (near δ 6.7 and 7.8) with a 16.0 Hz coupling constant in the ^{1}H-NMR spectra. The elemental analyses of **4a—o** were also in accord with the composition of the proposed structures.

Similarly, the structures for the minor products, bis[1-cyano-9-(ethoxycarbonyl)thieno[3,4-*b*]indolizin-3-yl] disulfides (**5a**, **b**), were deduced by the absence of the alkylthio group and the presence of another thieno[3,4-*b*]indolizine moiety in the ^{1}H-NMR spectra, and their elemental analyses were in good accord with the structures. However, considerable up-field shifts for the protons on the pyridine ring in the ^{1}H-NMR spectra of **5a**, **b** were observed. For example, the

* To whom correspondence should be addressed. e-mail: akakehi@gipwc.shinshu-u.ac.jp

© 2000 Pharmaceutical Society of Japan

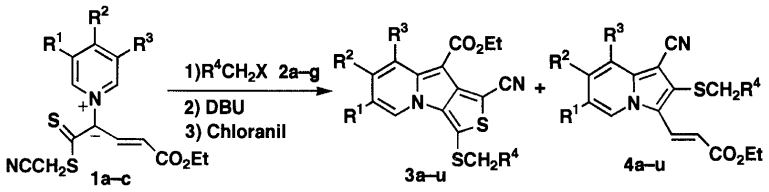

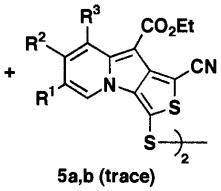

5	R^1	R^2	R^3
a	H	H	H
b	H	Me	H

2	R^4	X
a	H	I
b	Me	I
c	Ph	Br
d	C_6H_4Me-*p*	Cl
e	C_6H_4Br-*p*	Br

3,4	R^1	R^2	R^3	R^4	yield (%) 3	4
a	H	H	H	H	3	17
b	H	H	H	Me	8	29
c	H	H	H	Ph	10	12
d	H	H	H	C_6H_4Me-*p*	15	25
e	H	H	H	C_6H_4Br-*p*	7	30
f	H	Me	H	H	1	38
g	H	Me	H	Me	4	18
h	H	Me	H	Ph	8	56
i	H	Me	H	C_6H_4Me-*p*	2	31
j	H	Me	H	C_6H_4Br-*p*	4	33
k	Me	H	Me	H	3	45
l	Me	H	Me	Me	8	4
m	Me	H	Me	Ph	8	36
n	Me	H	Me	C_6H_4Me-*p*	18	8
o	Me	H	Me	C_6H_4Br-*p*	4	44

Chart 1

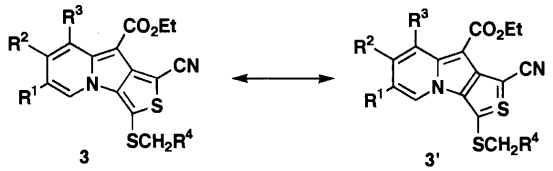

Chart 2

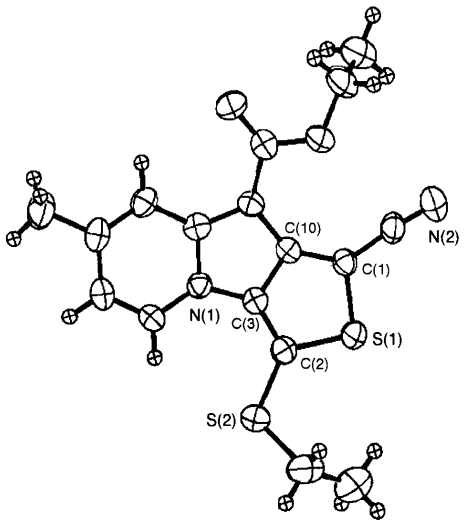

Fig. 1. ORTEP Drawing of Ethyl 1-Cyano-3-ethylthio-7-methylthieno-[3,4-*b*]indolizine-9-carboxylate (**3g**)

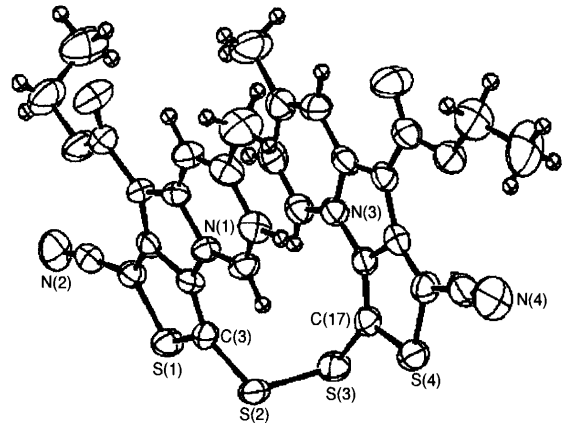

Fig. 2. ORTEP Drawing of Bis(1-cyano-9-ethoxycarbonyl-7-methylthieno[3,4-*b*]indolizin-3-yl Disulfide (**5b**)

^{1}H-NMR spectrum of **5a** showed only a set of signals at δ 6.46, 7.32, 8.14, and 8.16 attributable to the 6-, 7-, 8-, and 5-protons on the two thieno[3,4-*b*]indolizine rings, respectively. In comparison with those (δ 6.86, 7.47, 8.43, 9.07) of **3a**, the values are at higher magnetic field by 0.40, 0.15, 0.29, and 0.91 ppm, respectively, and a similar tendency was exhibited for disulfide **5b**. The order of the up-field shift in disulfides **5a**, **b** was 5-H>6-H>8-H>7-H. In view of the steric effect, disulfide can usually be expected to permit the two substituents to be as remote as possible. However, this obvious up-field shift of the pyridine proton signals prompted us to suspect a superimposed structure between the two thieno[3,4-*b*]indolizine rings in **5a**, **b**. The structures of disulfides were finally confirmed by X-ray analysis of **5b**. The ORTEP[3] and PLUTO drawings[7] for **5b** are shown in Figs. 2 and 3. As shown in Fig. 3, the two thieno[3,4-*b*]indolizine rings are superimposed, as judged by the least-square plane (15.3°) and a C(2)–S(2)–S(3)–C(17) torsion angle (90.9°). The reason for the acquisition of this interesting stacked structure in disulfides 5**a**, **b** is unclear, but favorable attractions between the cationic pyridine ring in a thieno[3,4-*b*]indolizine moiety and the anionic pyrrole ring in the other and *vice versa* may operate in this molecule. The contribution of such an ionic resonance structure for the indolizine ring is well known.[8]

Reaction Mechanism Since the transformation mechanism from 1-[1-substituted 2-(acylmethylthio)vinyl]pyri-

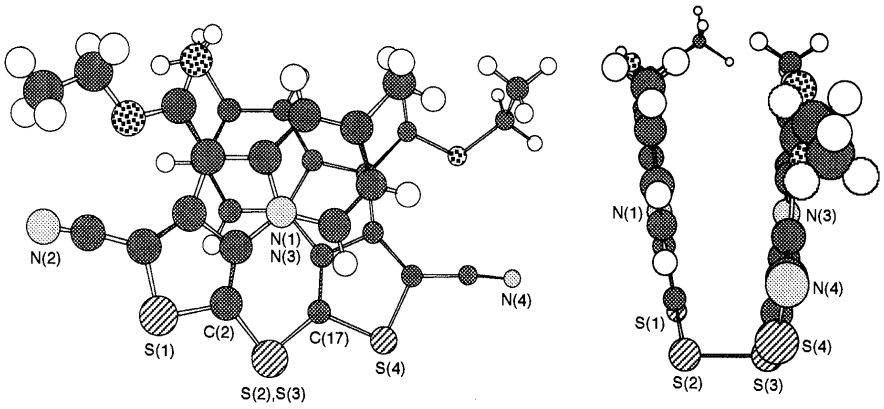

Fig. 3. PLUTO Drawing of Bis(3-cyano-9-ethoxycarbonyl-7-methylthieno[3,4-*b*]indolizin-3-yl) Disulfide (**5b**)

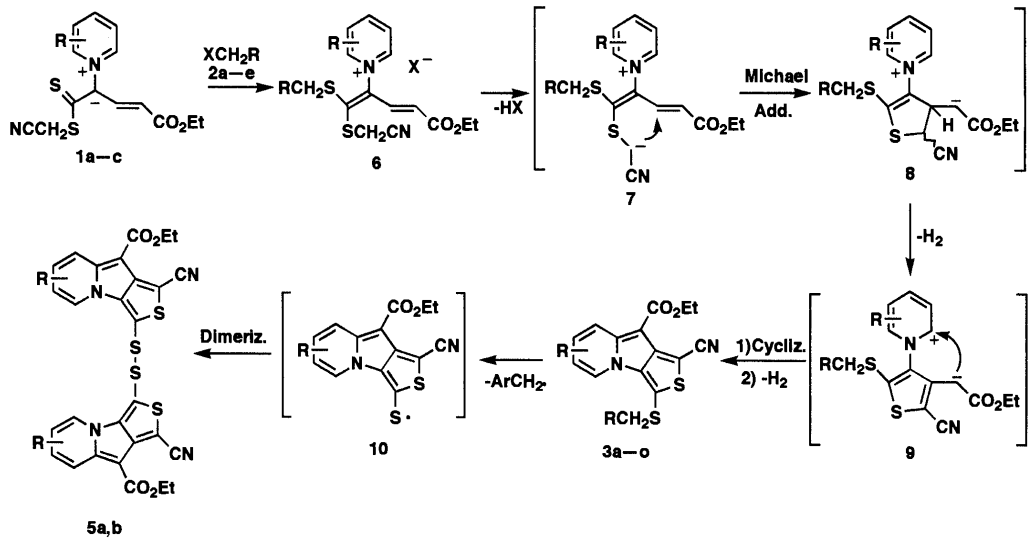

Chart 3

dinium halides to the corresponding indolizine derivatives is well established,[1,9] we describe here a possible formation mechanism (Chart 3) for ethyl 3-alkylthio-1-cyanothieno[3,4-*b*]indolizine-9-carboxylates (**3a**—**o**) and bis[1-cyano-9-(ethoxycarbonyl)thieno[3,4-*b*]indolizin-3-yl] disulfides (**5a**, **b**). Alkaline treatment of *S*-alkylated pyridinium salts **6**, formed from the reactions of pyridinium 1-allylides (**1a**—**c**) with halides **2a**—**e**, would provide the ethyl 3-alkylthio-1-cyanothieno[3,4-*b*]indolizine-9-carboxylates (**3a**—**o**) *via* intramolecular Michael addition of anion intermediates **7**, aromatization of the generated 2,3-dihydrothiophene derivatives **8**, followed by cyclization of the resulting 1,5-dipoles **9** and aromatization of the dihydroadducts. On the other hand, disulfides **5a**, **b** may be formed by homolytic fission of the sulfide linkage in 3-(benzylthio)thieno[3,4-*b*]indolizines (**3c**—**e**, **h**—**j**), and subsequent dimerization of radical component **10**, although no product derived from benzyl radicals could be detected.

Experimental

Melting points were measured with a Yanagimoto micromelting point apparatus and are not corrected. Microanalyses were carried out on a Perkin-Elmer 2400 elemental analyzer. The ^{1}H-NMR spectra were determined with a Hitachi R-600 spectrometer (60 MHz) in deuteriochloroform with tetramethylsilane used as an internal standard; the chemical shifts are expressed in δ values. The IR were taken with a JASCO FT/IR-5300 IR spectrophotometer.

Preparation of Pyridinium 1-[3-Ethoxycarbonyl-1-[cyanomethylthio-(thiocarbonyl)]allylides These pyridinium 1-[3-ethoxycarbonyl-1-[cyanomethylthio(thiocarbonyl)]allylides (**1a**—**c**) were prepared from the alkaline treatment of 1-(3-ethoxycarbonyl-2-propenyl)pyridinium bromides, carbon disulfide, and chloroacetonitrile in ethanol according to the procedure described earlier.[1,9] Some data of compounds **1a**—**c** are as follows:

Pyridinium 1-[3-Ethoxycarbonyl-1-[cyanomethylthio(thiocarbonyl)]]allylide (**1a**): 56%, yellow needles ($CHCl_3$–ether), mp 162—164 °C. IR (KBr) cm^{-1}: 2185, 1672, 1626. ^{1}H-NMR ($CDCl_3$) δ: 1.28 (3H, t, J=7.0 Hz), 4.24 (2H, q, J=7.0 Hz), 4.41 (2H, s), 4.49 (1H, d, J=15.0 Hz), 7.9—8.8 (5H, m), 8.38 (1H, d, J=15.0 Hz). *Anal.* Calcd for $C_{14}H_{14}N_2O_2S_2$: C, 54.88; H, 4.61; N, 9.14. Found: C, 54.91; H, 4.62; N, 9.10.

4-Methylpyridinium 1-[3-Ethoxycarbonyl-1-[(cyanomethylthio)thiocarbonyl]]allylide (**1b**): 46%, yellow needles ($CHCl_3$–ether), mp 145—147 °C. IR (KBr) cm^{-1}: 2243, 1687, 1635. ^{1}H-NMR ($CDCl_3$) 1.29 (3H, t, J=7.0 Hz), 2.78 (3H, s), 4.22 (2H, q, J=7.0 Hz), 4.40 (2H, s), 4.45 (1H, d, J=15.0 Hz), 7.8—8.6 (4H, m), 8.36 (1H, d, J=15.0 Hz). *Anal.* Calcd for $C_{15}H_{16}N_2O_2S_2$: C, 56.23; H, 5.03; N, 8.74. Found: C, 56.08; H, 5.06; N, 8.54.

3,5-Dimethylpyridinium 1-[3-Ethoxycarbonyl-1-[(cyanomethylthio)thiocarbonyl]]allylide (**1c**): 65%, orange needles ($CHCl_3$–ether), mp 143—145 °C. IR (KBr) cm^{-1}: 2241, 1689, 1620. ^{1}H-NMR ($CDCl_3$) 1.29 (3H, t, J=7.0 Hz), 2.59 (6H, s), 4.22 (2H, q, J=7.0 Hz), 4.39 (2H, s), 4.40 (1H, d, J=15.0 Hz), 8.0-8.5 (3H, m),, 8.32 (1H, d, J=15.0 Hz). *Anal.* Calcd for $C_{16}H_{18}N_2O_2S_2+H_2O$: C, 57.46; H, 5.42; N, 8.38. Found: C, 57.60; H, 5.47; N, 8.18.

Preparation of Thieno[3,4-*b*]indolizine and 3-Vinylindolizine Derivatives. General Method A chloroform solution (20 ml) of pyridinium 1-[(cyanomethylthio)thiocarbonyl]methylide (**1**, 2 mmol) was treated with alkyl halide (**2**, 2.4 mmol) at room temperature for 1 d. Evaporation of the

solvent from the reaction mixture, followed by the removal of the excess alkylating agent by washing three times with ether (each 20 ml) gave the corresponding pyridinium salt. The salt was again dissolved in chloroform (30 ml), and the solution was treated with DBU and then chloranil with stirring at 0 °C. The reaction mixture was allowed to react for a further 4 h under the same reaction conditions. The mixture was concentrated under reduced pressure and the residue was separated by column chromatography on alumina using ether and then chloroform. The separated portions were concentrated under reduced pressure. Recrystallization of crude products from chloroform–hexane gave the corresponding ethyl 3-alkylthio-1-cyanothieno[3,4-*b*]indolizine-9-carboxylates (**3a**—**o**) as orange crystals and ethyl 3-(2-alkylthio-1-cyanoindolizin-3-yl)acrylates (**4a**—**o**) as yellow crystals, respectively.

In the reactions of **1a**, **b** with benzyl halides (**2c**—**e**) trace amounts of bis[1-cyano-9-(ethoxycarbonyl)thieno[3,4-b]indolizin-3-yl] disulfides (**5a**, **b**) were also isolated, and recrystallization from chloroform afforded brown prisms.

Selected data for compounds **3a**—**o**, **4a**—**o** and **5a**, **b** are as follows:

Ethyl 1-Cyano-3-(methylthio)thieno[3,4-*b*]indolizine-9-carboxylate (**3a**): 3% (from **1a** and methyl iodide (**2a**)), mp 204—205 °C (Lit.[1] 203—205 °C).

Ethyl 1-Cyano-3-(ethylthio)thieno[3,4-*b*]indolizine-9-carboxylate (**3b**): 8% (from **1a** and ethyl iodide (**2b**)), mp 123—125 °C. IR (KBr) cm^{-1}: 2197, 1678. ^{1}H-NMR ($CDCl_3$) δ: 1.37, 1.50 (each 3H, t, J=7.0 Hz), 3.04, 4.54 (each 2H, q, J=7.0 Hz), 6.82 (1H, br t, J=7.0 Hz), 7.47 (1H, br dd, J=7.0, 9.0 Hz), 8.42 (1H, br d, J=9.0 Hz), 9.19 (1H, d, J=7.0 Hz). *Anal.* Calcd for $C_{16}H_{14}N_2O_2S_2$: C, 58.16; H, 4.27; N, 8.48. Found: C, 58.13; H, 4.27; N, 8.44.

Ethyl 3-Benzylthio-1-cyanothieno[3,4-*b*]indolizine-9-carboxylate (**3c**): 10% (from **1a** and benzyl bromide (**2c**)), mp 168—171 °C. IR (KBr) cm^{-1}: 2197, 1678. ^{1}H-NMR ($CDCl_3$) δ: 1.49 (3H, t, J=7.0 Hz), 4.11 (2H, s), 4.52 (2H, q, J=7.0 Hz), 6.61 (1H, br t, J=7.0 Hz), 6.9—7.6 (6H, m), 8.32 (1H, br d, J=9.0 Hz), 8.82 (1H, d, J=7.0 Hz). *Anal.* Calcd for $C_{21}H_{16}N_2O_2S_2$: C, 64.26; H, 4.11; N, 7.14. Found: C, 64.16; H, 4.36; N, 6.99.

Ethyl 1-Cyano-3-(*p*-methylbenzylthio)thieno[3,4-*b*]indolizine-9-carboxylate (**3d**): 15% (from **1a** and *p*-methylbenzyl chloride (**2d**)), mp 170—172 °C. IR (KBr) cm^{-1}: 2200, 1668. ^{1}H-NMR ($CDCl_3$) δ: 1.50 (3H, t, J=7.0 Hz), 2.22 (3H, s), 4.09 (2H, s), 4.54 (2H, q, J=7.0 Hz), 6.60 (1H, br t, J=7.0 Hz), 6.99 (4H, s), 7.40 (1H, br dd, J=7.0, 9.0 Hz), 8.35 (1H, br d, J=9.0 Hz), 8.81 (1H, d, J=7.0 Hz). *Anal.* Calcd for $C_{22}H_{18}N_2O_2S_2$: C, 65.00; H, 4.46; N, 6.89. Found: C, 65.06; H, 4.44; N, 6.85.

Ethyl 3-(*p*-Bromobenzylthio)-1-cyanothieno[3,4-*b*]indolizine-9-carboxylate (**3e**): 7% (from **1a** and *p*-bromobenzyl bromide (**2e**)), mp 169—171 °C. IR (KBr) cm^{-1}: 2204, 1664. ^{1}H-NMR ($CDCl_3$) δ: 1.51 (3H, t, J=7.0 Hz), 4.04 (2H, s), 4.54 (2H, q, J=7.0 Hz), 6.60 (1H, br t, J=7.0 Hz), 6.7—7.6 (5H, m), 8.36 (1H, br d, J=9.0 Hz), 8.75 (1H, d, J=7.0 Hz). *Anal.* Calcd for $C_{21}H_{15}BrN_2O_2S_2$: C, 53.51; H, 3.21; N, 5.94. Found: C, 53.71; H, 3.16; N, 5.95.

Ethyl 1-Cyano-7-methyl-3-(methylthio)thieno[3,4-*b*]indolizine-9-carboxylate (**3f**): 1%, (from **1b** and methyl iodide (**2a**)), mp 172—174 °C. IR (KBr) cm^{-1}: 2193, 1680. ^{1}H-NMR ($CDCl_3$) δ: 1.50 (3H, t, J=7.0 Hz), 2.44, 2.67 (each 3H, s), 4.54 (2H, q, J=7.0 Hz), 6.69 (1H, dd, J=7.0, 2.0 Hz), 8.21 (1H, br s), 8.95 (1H, d, J=7.0 Hz). *Anal.* Calcd for $C_{16}H_{14}N_2O_2S_2$: C, 58.16; H, 4.27; N, 8.48. Found: C, 58.11; H, 4.43; N, 8.37.

Ethyl 1-Cyano-3-ethylthio-7-methylthieno[3,4-*b*]indolizine-9-carboxylate (**3g**): 4%, (from **1b** and ethyl iodide (**2b**)), mp 121—124 °C. IR (KBr) cm^{-1}: 2195, 1680. ^{1}H-NMR ($CDCl_3$) δ: 1.37, 1.49 (each 3H, t, J=7.0 Hz), 2.46 (3H, s), 3.03, 4.53 (each 2H, q, J=7.0 Hz), 6.67 (1H, dd, J=7.0, 2.0 Hz), 8.22 (1H, br s), 9.09 (1H, d, J=7.0 Hz). *Anal.* Calcd for $C_{17}H_{16}N_2O_2S_2$: C, 59.28; H, 4.68; N, 8.13. Found: C, 59.13; H, 4.62; N, 8.09.

Ethyl 3-Benzylthio-1-cyano-7-methylthieno[3,4-*b*]indolizine-9-carboxylate (**3h**): 8%, (from **1b** and benzyl bromide (**2c**)), mp 192—194 °C. IR (KBr) cm^{-1}: 2199, 1680. ^{1}H-NMR ($CDCl_3$) δ: 1.49 (3H, t, J=7.0 Hz), 2.40 (3H, s), 4.11 (2H, s), 4.50 (2H, q, J=7.0 Hz), 6.43 (1H, dd, J=7.0, 2.0 Hz), 6.9—7.4 (5H, m), 8.10 (1H, br s), 8.71 (1H, d, J=7.0 Hz). *Anal.* Calcd for $C_{22}H_{18}N_2O_2S_2$: C, 65.00; H, 4.46; N, 6.89. Found: C, 64.75; H, 4.36; N, 7.14.

Ethyl 1-Cyano-7-methyl-3-(*p*-methylbenzylthio)thieno[3,4-*b*]indolizine-9-carboxylate (**3i**): 2%, (from **1b** and *p*-methylbenzyl chloride (**2d**)), mp 182—185 °C. IR (KBr) cm^{-1}: 2195, 1672. ^{1}H-NMR ($CDCl_3$) δ: 1.49 (3H, t, J=7.0 Hz), 2.23, 2.40 (each 3H, s), 4.06 (2H, s), 4.52 (2H, q, J=7.0 Hz), 6.44 (1H, dd, J=7.0, 2.0 Hz), 6.99 (4H, s), 8.15 (1H, br s), 8.68 (1H, d, J=7.0 Hz). *Anal.* Calcd for $C_{23}H_{20}N_2O_2S_2$: C, 65.69; H, 4.79; N, 6.66. Found: C, 65.98; H, 4.61; N, 6.45.

Ethyl 3-(*p*-Bromobenzylthio)-1-cyano-7-methylthieno[3,4-*b*]indolizine-9-carboxylate (**3j**): 4%, (from **1b** and *p*-bromobenzyl bromide (**2e**)), mp 182—185 °C. IR (KBr) cm^{-1}: 2199, 1668. ^{1}H-NMR ($CDCl_3$) δ: 1.50 (3H, t, J=7.0 Hz), 2.44 (3H, s), 4.04 (2H, s), 4.54 (2H, q, J=7.0 Hz), 6.44 (1H, dd, J=7.0, 2.0 Hz), 6.7—7.5 (4H, m), 8.14 (1H, br s), 8.58 (1H, d, J=7.0 Hz). *Anal.* Calcd for $C_{22}H_{17}BrN_2O_2S_2$: C, 54.44; H, 3.53; N, 5.77. Found: C, 54.24; H, 3.62; N, 5.70.

Ethyl 1-Cyano-6,8-dimethyl-3-(methylthio)thieno[3,4-*b*]indolizine-9-carboxylate (**3k**): 3%, (from **1c** and methyl iodide (**2a**)), mp 235—237 °C (Lit.[1] mp 235—237 °C).

Ethyl 1-Cyano-3-ethylthio-6,8-dimethylthieno[3,4-*b*]indolizine-9-carboxylate (**3l**): 8%, (from **1c** and methyl iodide (**2a**)), mp 149—151 °C. IR (KBr) cm^{-1}: 2197, 1697. ^{1}H-NMR ($CDCl_3$) δ: 1.36, 1.48 (each 3H, t, J=7.0 Hz), 2.32, 2.74 (each 3H, s), 3.05, 4.54 (each 2H, q, J=7.0 Hz), 7.08 (1H, br s), 8.98 (1H, br s). *Anal.* Calcd for $C_{18}H_{18}N_2O_2S_2$: C, 60.31; H, 5.06; N, 7.81. Found: C, 60.03; H, 4.90; N, 7.72.

Ethyl 3-Benzylthio-1-cyano-6,8-dimethylthieno[3,4-*b*]indolizine-9-carboxylate (**3m**): 8%, (from **1c** and benzyl iodide (**2c**)), mp 184—186 °C. IR (KBr) cm^{-1}: 2220, 1705. ^{1}H-NMR ($CDCl_3$) δ: 1.46 (3H, t, J=7.0 Hz), 2.14, 2.70 (each 3H, s), 4.05 (2H, s), 4.50 (2H, q, J=7.0 Hz), 6.94 (1H, br s), 7.0—7.3 (5H, m), 8.50 (1H, br s). *Anal.* Calcd for $C_{23}H_{20}N_2O_2S_2$: C, 65.69; H, 4.79; N, 6.66. Found: C, 65.58; H, 4.79; N, 6.64.

Ethyl 1-Cyano-6,8-dimethyl-3-(*p*-methylbenzylthio)thieno[3,4-*b*]indolizine-9-carboxylate (**3n**): 18%, (from **1c** and *p*-methylbenzyl chloride (**2d**)), mp 161—165 °C. IR (KBr) cm^{-1}: 2214, 1701. ^{1}H-NMR ($CDCl_3$) δ: 1.47 (3H, t, J=7.0 Hz), 2.15, 2.22, 2.71 (each 3H, s), 4.03 (2H, s), 4.52 (2H, q, J=7.0 Hz), 6.97 (5H, br s), 8.52 (1H, br s). *Anal.* Calcd for $C_{24}H_{22}N_2O_2S_2$: C, 66.33; H, 5.10; N, 6.45. Found: C, 66.09; H, 4.98; N, 6.32.

Ethyl 3-(*p*-Bromobenzylthio)-1-cyano-6,8-dimethylthieno[3,4-*b*]indolizine-9-carboxylate (**3o**): 4%, (from **1c** and *p*-bromobenzyl bromide (**2e**)), mp 126—130 °C. IR (KBr) cm^{-1}: 2212, 1709. ^{1}H-NMR ($CDCl_3$) δ: 1.50 (3H, t, J=7.0 Hz), 2.18, 2.75 (each 3H, s), 4.02 (2H, s), 4.54 (2H, q, J=7.0 Hz), 7.01 (1H, br s), 6.7—7.5 (4H, m), 8.43 (1H, br s). *Anal.* Calcd for $C_{23}H_{19}BrN_2O_2S_2$: C, 55.31; H, 3.83; N, 5.61. Found: C, 55.09; H, 3.92; N, 5.69.

Ethyl 3-[1-Cyano-2-(methylthio)indolizin-3-yl]acrylate (**4a**): 17% (from **1a** and methyl iodide (**2a**)), mp 145—146 °C (Lit.[10] mp 145 °C and Lit.[1] mp 142—143 °C).

Ethyl 3-[1-Cyano-2-(ethylthio)indolizin-3-yl]acrylate (**4b**): 29% (from **1a** and ethyl iodide (**2b**)), mp 112—114 °C. IR (KBr) cm^{-1}: 2205, 1696, 1607. ^{1}H-NMR ($CDCl_3$) δ: 1.30, 1.36 (each 3H, t, J=7.0 Hz), 3.12, 4.32 (each 2H, q, J=7.0 Hz), 6.78 (1H, d, J=16.0 Hz), 6.86 (1H, br t, J=7.0 Hz), 7.28 (1H, br dd, J=7.0, 9.0 Hz), 7.68 (1H, d, J=9.0 Hz), 8.00 (1H, d, J=16.0 Hz), 8.36 (1H, d, J=7.0 Hz). *Anal.* Calcd for $C_{16}H_{16}N_2O_2S$: C, 63.98; H, 5.37; N, 9.33. Found: C, 63.90; H, 5.35; N, 9.43.

Ethyl 3-[2-Benzylthio-1-cyanoindolizin-3-yl]acrylate (**4c**): 12% (from **1a** and benzyl bromide (**2c**)), mp 151—153 °C. IR (KBr) cm^{-1}: 2211, 1694, 1620. ^{1}H-NMR ($CDCl_3$) δ: 1.38 (3H, t, J=7.0 Hz), 4.23 (2H, s), 4.31 (2H, q, J=7.0 Hz), 6.68 (1H, d, J=16.0 Hz), 6.82 (1H, br t, J=7.0 Hz), 7.0—7.5 (6H, m), 7.70 (1H, d, J=9.0 Hz), 7.85 (1H, d, J=16.0 Hz), 8.32 (1H, d, J=7.0 Hz). *Anal.* Calcd for $C_{21}H_{18}N_2O_2S$: C, 69.59; H, 5.01; N, 7.73. Found: C, 69.83; H, 5.23; N, 7.48.

Ethyl 3-[1-Cyano-2-(*p*-methylbenzylthio)indolizin-3-yl]acrylate (**4d**): 25% (from **1a** and *p*-methylbenzyl chloride (**2d**)), mp 147—149 °C. IR (KBr) cm^{-1}: 2214, 1690, 1609. ^{1}H-NMR ($CDCl_3$) δ: 1.37 (3H, t, J=7.0 Hz), 2.28 (3H, s), 4.20 (2H, s), 4.32 (2H, q, J=7.0 Hz), 6.63 (1H, d, J=16.0 Hz), 6.77 (1H, br t, J=7.0 Hz), 6.9—7.5 (5H, m), 7.69 (1H, d, J=9.0 Hz), 7.83 (1H, d, J=16.0 Hz), 8.32 (1H, d, J=7.0 Hz). *Anal.* Calcd for $C_{22}H_{20}N_2O_2S$: C, 70.19; H, 5.35; N, 7.44. Found: C, 70.18; H, 5.33; N, 7.47.

Ethyl 3-[2-(*p*-Bromobenzylthio)-1-cyanoindolizin-3-yl]acrylate (**4e**): 30% (from **1a** and *p*-bromobenzyl bromide (**2e**)), mp 147—149 °C. IR (KBr) cm^{-1}: 2211, 1696, 1609. ^{1}H-NMR ($CDCl_3$) δ: 1.38 (3H, t, J=7.0 Hz), 4.19 (2H, s), 4.32 (2H, q, J=7.0 Hz), 6.65 (1H, d, J=16.0 Hz), 6.7—7.5 (6H, m), 7.72 (1H, d, J=9.0 Hz), 7.80 (1H, d, J=16.0 Hz), 8.34 (1H, d, J=7.0 Hz). *Anal.* Calcd for $C_{21}H_{17}BrN_2O_2S$: C, 57.15; H, 3.88; N, 6.35. Found: C, 57.14; H, 3.84; N, 6.41.

Ethyl 3-[1-Cyano-7-methyl-2-(methylthio)indolizin-3-yl]acrylate (**4f**): 38%, (from **1b** and methyl iodide (**2a**)), mp 148—150 °C (Lit.[1] mp 147—149 °C.

Ethyl 3-[1-Cyano-7-methyl-2-(ethylthio)indolizin-3-yl]acrylate (**4g**): 18%, (from **1b** and ethyl iodide (**2b**)), mp 126—128 °C. IR (KBr) cm^{-1}: 2211, 1707, 1622. ^{1}H-NMR ($CDCl_3$) δ: 1.28, 1.35 (each 3H, t, J=7.0 Hz), 2.45 (3H, s), 3.16, 4.34 (each 2H, q, J=7.0 Hz), 6.76 (1H, d, J=16.0 Hz), 6.84 (1H, dd, J=7.0, 2.0 Hz), 7.49 (1H, br s), 8.04 (1H, d, J=16.0 Hz), 8.32 (1H, d, J=7.0 Hz). *Anal.* Calcd for $C_{17}H_{18}N_2O_2S$: C, 64.94; H, 5.77; N, 8.91.

Found: C, 64.97; H, 5.75; N, 8.73.

Ethyl 3-[2-Benzylthio-1-cyano-7-methylindolizin-3-yl]acrylate (**4h**): 56%, (from **1b** and benzyl bromide (**2c**)), mp 133—136 °C. IR (KBr) cm^{-1}: 2216, 1699, 1616. ^{1}H-NMR ($CDCl_3$) δ: 1.38 (3H, t, J=7.0 Hz), 2.44 (3H, s), 4.23 (2H, s), 4.31 (2H, q, J=7.0 Hz), 6.64 (1H, d, J=16.0 Hz), 6.84 (1H, dd, J=7.0, 2.0 Hz), 7.27 (5H, s), 7.48 (1H, br s), 7.85 (1H, d, J=16.0 Hz), 8.23 (1H, d, J=7.0 Hz). *Anal.* Calcd for $C_{22}H_{20}N_2O_2S$: C, 70.19; H, 5.35; N, 7.44. Found: C, 70.24; H, 5.37; N, 7.37.

Ethyl 3-[1-Cyano-7-methyl-2-(*p*-methylbenzylthio)indolizin-3-yl]acrylate (**4i**): 31%, (from **1b** and *p*-methylbenzyl chloride (**2d**)), mp 138—140 °C. IR (KBr) cm^{-1}: 2214, 1701, 1616. ^{1}H-NMR ($CDCl_3$) δ: 1.36 (3H, t, J=7.0 Hz), 2.29, 2.44 (each 3H, s), 4.21 (2H, s), 4.32 (2H, q, J=7.0 Hz), 6.60 (1H, d, J=16.0 Hz), 6.81 (1H, dd, J=7.0, 2,0 Hz), 7.12 (4H, s), 7.48 (1H, br s), 7.84 (1H, d, J=16.0 Hz), 8.23 (1H, d, J=7.0 Hz). *Anal.* Calcd for $C_{23}H_{22}N_2O_2S$: C, 70.74; H, 5.68; N, 7.17. Found: C, 71.01; H, 5.76; N, 7.15.

Ethyl 3-[2-(*p*-Bromobenzylthio)-1-cyano-7-methylindolizin-3-yl]acrylate (**4j**): 33%, (from **1b** and *p*-bromobenzyl bromide (**2e**)), mp 131—133 °C. IR (KBr) cm^{-1}: 2209, 1698, 1613. ^{1}H-NMR ($CDCl_3$) δ: 1.38 (3H, t, J=7.0 Hz), 2.45 (3H, s), 4.17 (2H, s), 4.34 (2H, q, J=7.0 Hz), 6.62 (1H, d, J=16.0 Hz), 6.85 (1H, dd, J=7.0, 2.0 Hz), 7.0—7.5 (5H, m), 7.82 (1H, d, J=16.0 Hz), 8.25 (1H, d, J=7.0 Hz). *Anal.* Calcd for $C_{22}H_{19}BrN_2O_2S$: C, 58.03; H, 4.21; N, 6.15. Found: C, 58.09; H, 4.23; N, 6.01.

Ethyl 3-[1-Cyano-6,8-dimethyl-2-(methylthio)indolizin-3-yl]acrylate (**4k**): 45%, (from **1c** and methyl iodide (**2a**)), mp 117—119 °C (Lit.[1] 116—119 °C.

Ethyl 3-[1-Cyano-2-ethylthio-6,8-dimethylindolizin-3-yl]acrylate (**4l**): 4%, (from **1c** and ethyl iodide (**2b**)), mp 113—115 °C. IR (KBr) cm^{-1}: 2213, 1715, 1613. ^{1}H-NMR ($CDCl_3$) δ: 1.27, 1.39 (each 3H, t, J=7.0 Hz), 2.36, 2.74 (each 3H, s), 3.06, 4.36 (each 2H, q, J=7.0 Hz), 6.90 (1H, d, J=16.0 Hz), 6.91 (1H, br s), 8.04 (1H, d, J=16.0 Hz), 8.09 (1H, br s). *Anal.* Calcd for $C_{18}H_{20}N_2O_2S$: C, 65.83; H, 6.14; N, 8.53. Found: C, 65.78; H, 6.16; N, 8.57.

Ethyl 3-[2-Benzylthio-1-cyano-6,8-dimethylindolizin-3-yl]acrylate (**4m**): 36%, (from **1c** and benzyl bromide (**2c**)), mp 132—134 °C. IR (KBr) cm^{-1}: 2220, 1705, 1618. ^{1}H-NMR ($CDCl_3$) δ: 1.38 (3H, t, J=7.0 Hz), 2.33, 2.72 (each 3H, s), 4.19 (2H, s), 4.34 (2H, q, J=7.0 Hz), 6.74 (1H, d, J=16.0 Hz), 6.90 (1H, br s), 7.28 (5H, s), 7.84 (1H, d, J=16.0 Hz), 8.00 (1H, br s). *Anal.* Calcd for $C_{23}H_{22}N_2O_2S$: C, 70.74; H, 5.68; N, 7.17. Found: C, 70.56; H, 5.63; N, 7.22.

Ethyl 3-[1-Cyano-6,8-dimethyl-2-(*p*-methylbenzylthio)indolizin-3-yl]acrylate (**4n**): 8%, (from **1c** and *p*-methylbenzyl chloride (**2d**)), mp 121—125 °C. IR (KBr) cm^{-1}: 2214, 1701, 1622. ^{1}H-NMR ($CDCl_3$) δ: 1.34 (3H, t, J=7.0 Hz), 2.29 (6H, s), 2.71 (3H, s), 4.12 (2H, s), 4.34 (2H, q, J=7.0 Hz), 6.72 (1H, d, J=16.0 Hz), 6.88 (1H, br s), 7.15 (4H, s), 7.85 (1H, d, J=16.0 Hz), 8.03 (1H, br s). *Anal.* Calcd for $C_{24}H_{24}N_2O_2S$: C, 71.26; H, 5.98; N, 6.93. Found: C, 71.44; H, 6.00; N, 6.73.

Ethyl 3-[2-(p-Bromobenzylthio)-1-cyano-6,8-dimethylindolizin-3-yl]acrylate (**4o**): 44%, (from **1c** and *p*-bromobenzyl bromide (**2e**)), mp 139—141 °C. IR (KBr) cm^{-1}: 2213, 1709, 1615. ^{1}H-NMR ($CDCl_3$) δ: 1.38 (3H, t, J=7.0 Hz), 2.32, 2.72 (each 3H, s), 4.11 (2H, s), 4.34 (2H, q, J=7.0 Hz), 6.68 (1H, d, J=16.0 Hz), 6.90 (1H, br s), 7.0—7.5 (4H, m), 7.78 (1H, d, J=16.0 Hz), 8.00 (1H, br s). *Anal.* Calcd for $C_{23}H_{21}BrN_2O_2S$: C, 58.85; H, 4.51; N, 5.97. Found: C, 58.94; H, 4.42; N, 5.97.

Bis[1-cyano-9-(ethoxycarbonyl)thieno[3,4-*b*]indolizin-3-yl] Disulfide (**5a**): Trace, (from **1a** with **2c—e**), mp 266—268 °C. IR (KBr) cm^{-1}: 2206, 1680. ^{1}H-NMR ($CDCl_3$) δ: 1.51 (6H, t, J=7.0 Hz), 4.52 (4H, q, J=7.0 Hz), 6.46 (2H, br t, J=7.0 Hz), 7.32 (2H, br dd, J=7.0, 9.0 Hz), 8.14 (2H, br d, J=9.0 Hz), 8.16 (2H, d, J=7.0 z). *Anal.* Calcd for $C_{28}H_{18}N_4O_4S_4$: C, 55.80; H, 3.01; N, 9.30. Found: C, 56.00; H, 3.08; N, 9.02.

Bis[1-cyano-9-ethoxycarbonyl-7-methylthieno[3,4-*b*]indolizin-3-yl] Disulfide (**5b**): Trace, (from **1b** with **2c—e**), mp 268—273 °C. IR (KBr) cm^{-1}: 2204, 1682. ^{1}H-NMR ($CDCl_3$) δ: 1.51 (6H, t, J=7.0 Hz), 2.34 (6H, s), 4.52 (4H, q, J=7.0 Hz), 6.16 (2H, dd, J=7.0, 2.0 Hz), 7.89 (2H, br s), 7.94 (2H, d, J=7.0 Hz). *Anal.* Calcd for $C_{30}H_{22}N_4O_4S_4$: C, 57.12; H, 3.52; N, 8.88. Found: C, 56.92; H, 3.41; N, 8.59.

Crystallography of Ethyl 1-Cyano-3-ethylthio-7-methylthieno[3,4-*b*]-indolizine-9-carboxylate (3g) A single crystal (0.24×0.30×0.66 mm) grown from $CHCl_3$–hexane was used for the unit-cell determinations and the data collections of a Rigaku AFC5S four-circle diffractometer, with graphite-monochromated MoK_α radiation (λ=0.71069 Å). Crystal data of **3g**: $C_{17}H_{16}N_2O_2S_2$; M=344.46; triclinic, space group P$\bar{1}$ (#2), Z=4 with a=11.773 (2) Å, b=18.871 (2) Å, c=7.610 (2) Å, α=100.52° (1), β=96.47° (1), γ=88.77° (1); V=1651.8 (5) Å^3, and $D_{calc.}$=1.385 g/cm^3. All calculations were performed using the TEXSAN program.[11] The structure was solved by a direct method (MITHRIL).[12] The non-hydrogen atoms were refined anisotropically, and the hydrogen atoms were refined isotropically. The final R- and R_w-factors after full-matrix least-squares refinements were 0.059 and 0.061 for 4049 (I>2.00σ(I)) observed reflections, respectively.

Crystallography of Bis(1-cyano-9-ethoxycarbonyl-7-methylthieno[3,4-*b*]indolizin-3-yl) Disulfide (5b) A single crystal (0.14×0.26×0.48 mm) grown from $CHCl_3$–hexane was used for the unit-cell determinations and the data collections of a Rigaku AFC5S four-circle diffractometer, with graphite-monochromated MoK_α radiation (λ=0.71069 Å). Crystal data of **5b**: $C_{30}H_{22}N_4O_4S_4$; M=630.77; triclinic, space group P$\bar{1}$ (#2), Z=2 with a=10.930 (4) Å, b=14.033 (4) Å, c=10.340 (4) Å, α=92.42° (3), β=108.11° (3), γ=72.18° (3); V=1432.6 (9) Å^3, and $D_{calc.}$=1.462 g/cm^3. All calculations were performed using the TEXSAN program.[11] The structure was solved by a direct method (MITHRIL).[12] The non-hydrogen atoms were refined anisotropically, and the hydrogen atoms were attached at the idealized position and not refined. The final R- and R_w-factors after full-matrix least-squares refinements were 0.065 and 0.065 for 3008 (I>2.00σ(I)) observed reflections, respectively.

References

1) For part 48 of this series, see Kakehi A., Ito S., Sa H., *Chem. Pharm. Bull.*, **47**, 1607—1613 (1999).
2) Matsumoto K., Uchida T., Aoyama K., Nishikawa M., Kuroda T., Okamoto T., *J. Heterocylc. Chem.*, **25**, 1793—1801 (1988).
3) Johnson C. K., "ORTEP II, Report ORNL-5138," Oak Ridge National Laboratory, Oak Ridge, Tennessee, 1976.
4) "Kagaku Binran," ed by Chem. Soc. Jpn., Maruzen, Chap. 15, p II-657.
5) Pritchard R. G., *Acta Cryst.*, **C44**, 1150—1152 (1988).
6) Kakehi A., Ito S., Sakurai T., Urushido K., *Chem. Pharm. Bull.*, **39**, 1949—1951 (1991); Kakehi A., Kitajima K., Ito S., Takusagawa N., *Acta Cryst.*, **C49**, 604—607 (1993); *idem*, *ibid.*, **C49**, 1230—1232 (1993); *idem*, *ibid.*, **C50**, 139—141 (1994); Kakehi A., Ito S., Muranaka H., *Bull. Chem. Soc. Jpn.*, **67**, 2795—2802 (1994); Kakehi A., Ito S., Hayashi S., Fujii T., *ibid.*, **68**, 3573—3580 (1995).
7) Motherwell S., Clegg W., PLUTO program for plotting molecular and crystal structures. University of Cambridge, England, 1978.
8) Galbraith A., Small T., Barnes R. A., Boekelheide V., *J. Am. Chem. Soc.*, **83**, 453—458 (1961).
9) Kakehi A., Ito S., Yonezu S., Maruta K., Yuito K., Shiohara M., Adachi K., *Bull. Chem. Soc. Jpn.*, **60**, 1867—1879 (1987); Kakehi A., Ito S., Ohno Y., Shiba S., Kamata S., *ibid.*, **60**, 3713—3720 (1987); Kakehi A., Ito S., Kinoshita N., Abaka Y., *ibid.*, **61**, 2055—2062 (1988).
10) Maseda C., Sone M., Tominaga Y., Natsuki R., Matsuda Y., Kobayashi G., *Yakugaku Zasshi*, **94**, 839—843 (1974).
11) "TEXSAN TEXRAY, Structure Analysis Package," Molecular Structure Corporation, 1985.
12) Gilmore, C. J., *J. Appl. Cryst.*, **17**, 42—46 (1984).

Salicylic Acid Derivatives Form Stable Complexes with Scandium(III) Ion in Aqueous Solution

Naciye TÜRKEL* and Ulviye ÖZER

Department of Chemistry, Faculty of Arts and Sciences, Uludağ University 16059 Bursa, Turkey.
Received October 18, 1999; accepted February 8, 2000.

The stability constants of 5-nitrosalicylic acid (5-NSA) and 5-sulfosalicylic acid (5-SSA) complexes of Sc(III) were determined by potentiomeric pH titration. ML and ML_2 type first and second complexes were observed in the solutions of 5-NSA and 5-SSA with Sc(III) at 25 °C in I=0.1 M ionic medium. The stability constants of Sc(III)–5NSA and Sc(III)–5SSA systems were also investigated by spectrophotometry to determine the stoichiometries of the complexes formed in the reactions. Our results showed that Sc(III)–5SSA complexes are more stable than the Sc(III)–5NSA complexes in aqueous solutions.

Key words salicylic acid; scandium; stability constant; potentiometry

Scandium's chemical and physical features are similar to those of lanthanides. But it was suggested that scandium is a typical first transition series metal rather than being a lanthanide.[1] Sc(III) is the first member of the Sc, Y, La, Ac group. Transition metals have a very high tendency to form metal–ligand complexes with various mono and dihydroxy phenolic compounds. The formation of ML, ML_2 and ML_3 type complexes of Al(III)–5NSA and Al(III)–5SSA were reported previously.[2,3]

Sc(III) has a strong tendency to form hydroxo species in aqueous solution.[4] The complex forming tendency of Sc(III) with various ligands such as disodium 1,2-dihydroxy benzene 3,5-disulfonic acid (TIRON), 2,3-dihydroxy benzoic acid (2,3-DHBA) and salicylic acid (SA) was analyzed previously.[5,6] The complex formation between 5-NSA (H_2L), 5-SSA (H_2L^-) and Sc(III) has not been investigated so far.

We have analysed the formation and the stabilities of the 5-NSA and 5-SSA complexes of Sc(III) at t=25 °C in I= 0.1 M ionic medium in this study. The formation of complexes of Sc(III) with 5-NSA and 5-SSA, together with the dissociation constants of the ligand, were investigated using potentiometric and spectrophotometric methods.[6—8] The effects of electron attracting groups such as -nitro and -sulfo groups of the ligands on the stabilities of the Sc(III) complexes have not been reported previously. Hence 5-NSA and 5-SSA were used in our studies as ligands.

The potentiometric titration curves of the Sc(III)–5NSA system in 1 : 1 mol ratio exhibit inflection points at m (mmol base/mmol metal)=2.0 and m=3.25 (Fig. 1-II). The formation of an ML type complex of Sc(III) with 5-NSA may be suggested from the drops in the buffer regions of the titration curves, from inflection points at m=2.0 and from hydrolysis of the Sc(III) complex of 5-NSA in 1 : 1 mol ratio, between m=3.0—4.0. Inflection points on potentiometric titration curves were observed at m=4.0 and m=5.0 for the Sc(III)–5NSA system in 1 : 2 mol ratio (Fig. 1-III). The formation of an ML_2 type complex of Sc(III) with 5-NSA is one of the possibilities. Moreover, continued drops on pH readings after m=4.0 suggest that hydrolysis of an ML_2 type complexes is initiated in the system.

The potentiometric titration curve of Sc(III)–5SSA in 1 : 1 mol ratio exhibits inflection points at m=3.0 and m=4.0 (Fig. 2-II). The formation of an ML type complex of Sc(III)–5SSA was assumed. A drop in the pH values in the buffer regions and inflection points at m=3.0 were observed between m=3.0 and m=4.0; this reflects the formation of a 1 : 1 Sc(III)–5SSA complex.

When Sc(III) metal ion and 5-SSA are present at 1 : 2 mol ratio, inflection points on the potentiometric titration curves were observed at m=5.0 and m=6.0, respectively (Fig. 2-III). This result suggests that an ML_2 type complex formed gradually in the m=0.0—6.0 range. At the beginning, two moles of titrated protons are dissociated from the sulfo groups between m=0.0 and 2.0 while the other titrated protons dissociated between m=2.0 and m=4.0 are from the carboxylate groups. Two moles of protons which are dissociated between m=4.0 and m=6.0 at the final stage are from the phenolic groups.

The degree of formation, ($\bar{n}$) values, were evaluated both for Sc(III)–5NSA and Sc(III)–5SSA complexes that are present in 1 : 2 mol ratios. Then the formation curves were drawn (Figs. 3 and 4). It has been noticed that, the number of ligands per Sc(III) ion ($\bar{n}$) is approximately equal to 1.85.

The formation of an ML and an ML_2 type complex was assumed from the potentiometric titrations curves. In order to validate these assumptions, the stoichiometries of the formed complexes were investigated by the spectrophotometric method. For the potentiometric titration curves of 5-NSA alone, 1 : 1 and 1 : 2 mol ratios of Sc(III) and 5-NSA were prepared at pH ranges 2.40—3.98 and 2.20—5.00 respectively. Then, the spectrum of 5-NSA alone and solutions of Sc(III)–5NSA that are present at defined pH values and in different mol ratios were compared. After that, maximum absorbance values were determined for each species, at OD_{395}. The formation of ML and ML_2 type complexes was demonstrated using Job's diagram of Sc(III) and 5-NSA solutions in different mol ratios. In order to identify the stoichiometries of complexes formed between Sc(III) ion and the 5-SSA ligand, spectra were recorded at different pH values, as in the Sc(III)–5SSA solutions. Job's diagrams were drawn at OD_{260} for pH=3.5 and pH=4.5 and maximum absorbances were observed at X_M=0.5 and X_M=0.3 values in Job's diagram respectively.

It was concluded that Sc(III) ions form ML, ML_2 type complexes with 5-NSA and 5-SSA. The results obtained from the potentiometric data (β) are given in Table 1. The

* To whom correspondence should be addressed. e-mail: nturkel@uu20.bim.uludag.edu.tr
© 2000 Pharmaceutical Society of Japan

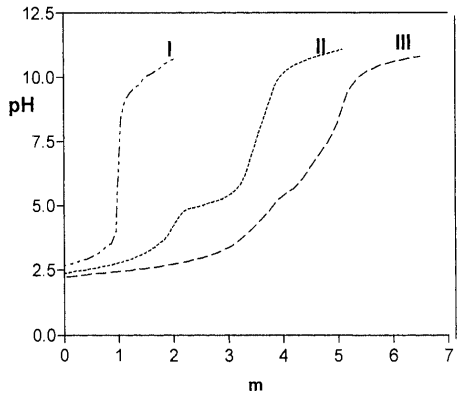

Fig. 1. Potentiometric Titrations of Sc(III)–5NSA System in 0.1 M KNO_3 at 25 °C with Different Molar Ratios of 5-NSA to Metal Ion

I, ligand alone; II, Sc(III)–5NSA (1 : 1); III, Sc(III)–5NSA (1 : 2).

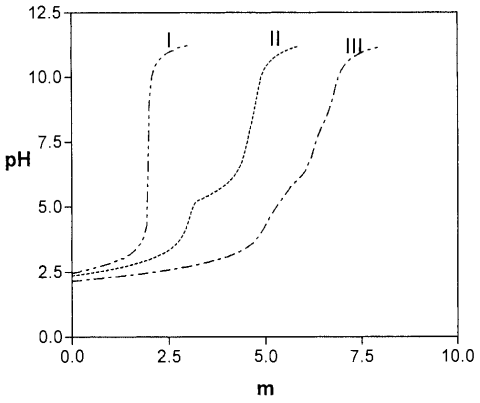

Fig. 2. Potentiometric Titrations of Sc(III)–5SSA system in 0.1 M KNO_3 at 25 °C with Different Molar Ratios of 5-SSA to Metal Ion

I, ligand alone; II, Sc(III)–5SSA (1 : 1); III, Sc(III)–5SSA (1 : 2).

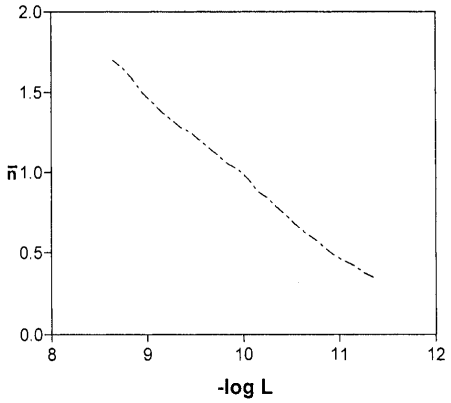

Fig. 3. Degree of Formation, $\bar{n}$, as a Function of $-\log L$ of Sc(III)–5NSA Complex

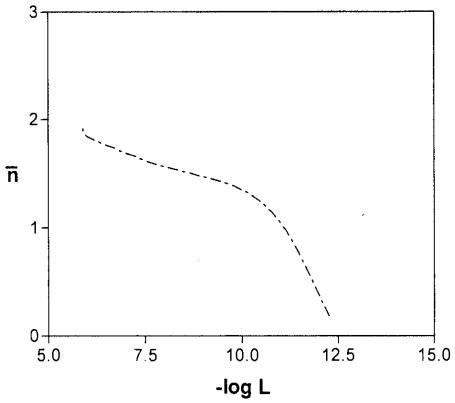

Fig. 4. Degree of Formation, $\bar{n}$, as a Function of $-\log L$ of Sc(III)–5SSA Complex

Table 1. Stability Constants of the Complexes ML, ML_2 and the Dissociation Constants of 5-NSA and 5-SSA at 25 °C and I=0.1

Ligands	Equilibrium	$-\log K_a$ [a]	$\log \beta$ [b]	$-\log K_{hyd.}$ [c]
5-NSA (H_2L)	$H_2L \rightleftharpoons H^+ + HL^-$	2.20		
	$HL^- \rightleftharpoons H^+ + L^{2-}$	10.10		
	$Sc^{3+} + L^{2-} \rightleftharpoons ScL^+$		10.93±0.05	
	$ScL^+ + OH^- \rightleftharpoons ScL(OH)$			5.10±0.09
	$Sc^{3+} + 2L^{2-} \rightleftharpoons ScL_2^-$		16.47±0.05	
	$ScL_2^- + OH^- \rightleftharpoons ScL_2(OH)^{2-}$			6.65±0.03
5-SSA (H_2L^-)	$H_2L^- \rightleftharpoons H^+ + HL^{2-}$	2.42		
	$HL^{2-} \rightleftharpoons H^+ + L^{2-}$	11.90		
	$Sc^{3+} + L^{3-} \rightleftharpoons ScL$		12.23±0.03	
	$ScL + OH^- \rightleftharpoons ScL(OH)^-$			5.21±0.03
	$Sc^{3+} + 2L^{3-} \rightleftharpoons ScL_2^{3-}$		18.06±0.03	
	$ScL_2^{3-} + OH^- \rightleftharpoons ScL_2(OH)^{4-}$			3.18±0.05

a) $-\log K_a$ is calculated as described previously.[7] Numbers show the acidity constants of the ligands. *b*) $-\log \beta$ is calculated as described previously.[6] It shows the stability constants of the formed complexes in the reaction. *c*) $-\log K_{hyd.}$ is the hydrolysis constant of Sc(III)–5NSA(1 : 1, 1 : 2) and Sc(III)–5SSA (1 : 1, 1 : 2).[6]

dissociation constants of the ligands were determined under the same experimental conditions as described previously[7] and are also given in Table 1.

5-NSA is more acidic than 5-SSA when their acidities are compared with each other. The reason for this is that the -nitro and -sulfo groups weaken the O–H bond by attracting electrons with inductive and resonance effects which results in the dissociation of a proton in a relatively easy way. It is also known that -nitro groups are more a electron attracting group than -sulfo group. These results suggest that the stabilities of complexes of Sc(III) formed with 5-SSA is higher than the stabilities of complexes of Sc(III)–5NSA.

Experimental

All the chemicals used in this study were of analytical reagent grade. 5-NSA (Aldrich, 99% purity) and 5-SSA (Merck) used in this study, were used as received, since Gran's plot of the ligand potentiometric study requires high purity.[9] The determination of acid dissociation constants of these ligands was explained previously.[7] Three different stock solutions of scandium(III) (7.2×10^{-3}, 1.44×10^{-3} and 2.88×10^{-3} M, respectively) were prepared from $Sc(NO_3)_3$ (Aldrich, 99% purity) for potentiometric studies. A known quantity of HNO_3 (Merck, 100% purity, d=1.52) was added to the

stock solution of Sc(III) to avoid hydrolysis. The stock solutions of scandium(III) (1×10^{-3}—1×10^{-4} M) were prepared from Sc_2O_3 (Aldrich, 99.9% purity) for spectrophotometric studies since the nitrate ion absorbs in the UV/VIS region of the spectrum.[4] The concentrations of the stock solutions were then checked by EDTA titration.[10]

CO_2 free 0.1 M NaOH stock solution was prepared with NaOH purchased from Merck Co. and was standardized with potassium hydrogen phthalate.[4] In order to maintain the ionic strength at constant level, 0.1 M KNO_3 was added at definite amount. All solutions were prepared under CO_2 free, nitrogen atmosphere and in double distilled water, at 25.0±0.10 °C, in a water jacketed titration cell. At least three different titrations were carried out for each Sc(III)–L system.

Instrumentation The pH was measured by a Schott-pH meter instrument, equipped with combined electrode. The titration solution was kept free from carbon dioxide and oxygen by continious bubbling of purified nitrogen and was presaturated by passing nitrogen through the titration cell. The electrode system was calibrated by the method of Harned and Owen,[11] so the pH-meter readings could be converted into hydrogen concentrations. In all cases the temperature was kept constant, at 25.0±0.10 °C, by means of a B. Braun Termomix UB Termostat.

Absorption spectra of the samples were measured using a Shimadzu UV-2100 Spectrophotometer. The stoichiometry of these complexes was determined by Job's method.[12] This allows the stoichiometry of the complexes to be defined by taking UV/VIS spectra of the metal ion and ligand system in definite mol ratios of metal ions and ligands. Thus, the results of the potentiometric studies were also validated by Job's method.

Calculations A computer program was devised for the computation and refinement of the formation constants using previously described equations.[8] First, the stability constants of Sc(III)–5NSA and Sc(III)–5SSA complexes that are in 1 : 1 and 1 : 2 stoichiometries of 5-NSA and 5-SSA to metal ion were determined using the part I and II of the program.[6] Then the stability constants of the complexes were determined using the derived equations. The twelve possible titrations were analysed mathematically (Table 1). All thermodynamic parameters are expressed in molar scale.

The values of $\bar{n}$, (the average number of ligand(s) bound per mole of metal ion)[13] and a log L (a free concentration of anionic form of the ligand) were computed in the third part of the computer program for the analysed two systems.

References

1) Cotton F. A., Wilkinson G., "Advanced Inorganic Chemistry," 5th ed. John Wiley and Sons, New York,1988.
2) Perlmutter-Hayman B., Tapuhi E., *Inorg. Chem.*, **16**, 2742 (1977).
3) Öhman L. O., Sjoberg S., *Acta. Chem. Scand., Ser. A*, **37**, 875—880 (1983).
4) Akalın S., Özer U., *J. Inorg. Nucl.Chem.*, **33**, 4171—4181 (1971).
5) Smith R. M., Martell A. E., Motekaitis R. J., "NIST Critically Selected Stability Constants of Metal Complexes Database, Version 4.0," Texas A and M University, College Station, Texas, 1997.
6) Türkel N., "Stabilities of Some Sc(III) Coordination Ions and Compounds in Aqueous Solution," Ph. D. Thesis, Uludağ University, Bursa, Turkey ,1997.
7) Aydın R., Özer U., Türkel N., *Turkish J. Chem.*, **24**, 428—436 (1997).
8) Rossotti F. J. C., Rossotti H., "The Determination of Stability Constants," Mc Graw Hill, New York 1961.
9) Rossotti F. J. C., Rossotti H., *J. Chem. Ed.*, **42**, 375—378 (1965).
10) Schwarzenbach G., Flaschka H., "Complexometric Titrations," Interscience Publishers, New York, 1969.
11) Harned H. S., Owen B. B., "The Physical Chemistry of Electrolytic Solutions," 2nd ed., Reinhold Publ, New York, 1950, p. 523.
12) Merritt W., Settle D., "Instrumental Methods of Analysis," 6th ed., Van nostrand, New York, 1981.
13) Mont G. E, Martell A. E., *J. Am. Chem.Soc.*, **88**, 1387 (1966).

Micellar Electrokinetic Chromatography (MEKC) Separation of Furanonaphthoquinones from *Tabebuia impetiginosa*

Junko KOYAMA,* Izumi MORITA, Akari KINO, and Kiyoshi TAGAHARA

Kobe Pharmaceutical University, Higashinada-ku, Kobe 658–8558, Japan.
Received December 2, 1999; accepted March 9, 2000

The separation of nine furanonaphthoquinones by micellar electrokinetic chromatography (MEKC) is described. The running electrolytes used in this method were 0.03 M sodium dodecyl sulphate (SDS) in 0.09 M borate buffer (pH 9) containing 10% methanol, with an applied voltage of 20 kV. Application of this technique in the determination of the main furanonaphthoquinones, 5-hydroxy-2-(1-hydroxyethyl)naphtho[2,3-*b*]furan-4,9-dione, 8-hydroxy-2-(1-hydroxyethyl)naphtho[2,3-*b*]furan-4,9-dione, and 2-(1-hydroxyethyl)naphtho[2,3-*b*]furan-4,9-dione, of *Tabebuia impetiginosa* is demonstrated in this paper.

Key words micellar electrokinetic chromatography; furanonaphthoquinone; Bignoniaceae; *Tabebuia impetiginosa*

In a continuation of our work on quinones that occur widely in the plant kingdom and that may have biological activities, we have developed a simple and rapid micellar electrokinetic chromatography (MEKC) method to separate and determine furanonaphthoquinones.

HPLC methods for the separation of some naturally occurring furanonaphthoquinones have already been developed.[1—3] We describe here the development of a simple and rapid method for separating and determining nine furanonaphthoquinones by MEKC using sodium dodecyl sulphate (SDS) in borate buffer containing 10% methanol as the electrolyte. This separation method has also been applied to analyze the extract of *Tabebuia impetiginosa* (Bignoniaceae) containing cytotoxic furanonaphthoquinones.[4]

T. impetiginosa is the national flower of Brazil and is widespread in Brazil and other South American countries. This plant has been used as a folk remedy for the prevention and treatment of cancer.[5,6] In the course of our screening for antitumor-active furanonaphthoquinones, it was found that 5-hydroxy-2-(1-hydroxyethyl)naphtho[2,3-*b*]furan-4,9-dione, 8-hydroxy-2-(1-hydroxyethyl)naphtho[2,3-*b*]furan-4,9-dione, and 2-(1-hydroxyethyl)naphtho[2,3-*b*]furan-4,9-dione have selectivity towards antitumor activity compared to normal cells.[7]

Experimental

Materials Naphtho[2,3-*b*]furan-4,9-dione (**1**), 2-acetylnaphtho[2,3-*b*]-furan-4,9-dione (**4**), and 7,8-dihydroxynaphtho[2,3-*b*]furan-4,9-dione (**8**) were synthesized by the application of a tandem-directed metalation on *N,N*-dimethylbenzamide and 3-furaldehyde.[8] 2-Methylnaphtho[2,3-*b*]furan-4,9-dione (**2**) and 2-ethylnaphtho[2,3-*b*]furan-4,9-dione (**3**) were synthesized according to Lee's method.[9] 8-Hydroxy-2-methylnaphtho[2,3-*b*]furan-4,9-dione (**9**) was synthesized by Friedel–Crafts reaction.[10] 2-(1-Hydroxyethyl)naphtho[2,3-*b*]furan-4,9-dione (**5**), 5-hydroxy-2-(1-hydroxyethyl)-naphtho[2,3-*b*]furan-4,9-dione (**6**) and 8-hydroxy-2-(1-hydroxyethyl)naphtho[2,3-*b*]furan-4,9-dione (**7**) were isolated from the bark of *T. impetiginosa*.[4]

Procedure for MEKC MEKC analyses were carried out on a Beckman P/ACE System 5000 apparatus (Fullerton, CA, U.S.A.) equipped with a UV detector set at 254 nm and a Beckman untreated fused-silica capillary (570 mm×75 μm i.d.; 500 mm effective length).

The analytical conditions were as follows: sampling time—5 s (hydrodynamic mode; 0.5 p.s.i.); applied constant voltage—20 kV; column temperature—20 °C. The electrolyte was a buffer solution prepared by mixing 0.09 M boric acid solution with appropriate volumes of 0.09 M sodium tetraborate solution (pH 9) followed by the addition of 0.03 M SDS and 10% methanol. Standard solutions for each furanonaphthoquinone were prepared by dissolving compounds in the electrolyte at a concentration of *ca.* 10 ppm.

Sample Preparation of *T. impetiginosa* Extracts Powdered bark (10 g) of *T. impetiginosa* was exhaustively extracted in a Soxhlet apparatus with chloroform (100 ml) for 10 h. After concentration, the residue was diluted with methanol to 100 ml. This solution was passed through a 0.45 μm filter. After centrifugation, 1 ml of the methanol solution was diluted to 10 ml with borate buffer (pH 9) yielding the sample for MEKC analysis.

Results and Discussion

We have studied the application of MEKC to the isolation of furanonaphthoquinone derivatives, and found that owing to the phenolic (and hence weak acidic) or neutral nature of furanonaphthoquinones, the weak alkaline condition of borate buffer as eluent could give a good resolution. It is well known that when the buffer concentration increases, the electro-osmotic flow decreases, and therefore the migration times increase. In the case of SDS, as the concentration of SDS increased, the migration time increased. The pH dependence of the migration times of 2-methylnaphtho[2,3-*b*]furan-4,9-dione were examined with 0.03 M borate buffer containing 0.03 M SDS in the pH range 5.5—10. At pH values over 9, the migration time becomes long; the peak obtained at pH 8 was the sharpest. After examining a series of buffer solutions differing in pH, composition, buffer concentration, and SDS

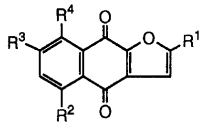

		R^1	R^2	R^3	R^4
1	naphtho[2,3-*b*]furan-4,9-dione	H	H	H	H
2	2-methylnaphtho[2,3-*b*]furan-4,9-dione	CH_3	H	H	H
3	2-ethylnaphtho[2,3-*b*]furan-4,9-dione	CH_2CH_3	H	H	H
4	2-acetylnaphtho[2,3-*b*]furan-4,9-dione	$COCH_3$	H	H	H
5	2-(1-hydroxyethyl)naphtho[2,3-*b*]-furan-4,9-dione	$CH(OH)CH_3$	H	H	H
6	5-hydroxy-2-(1-hydroxyethyl)-naphtho[2,3-*b*]furan-4,9-dione	$CH(OH)CH_3$	OH	H	H
7	8-hydroxy-2-(1-hydroxyethyl)-naphtho[2,3-*b*]furan-4,9-dione	$CH(OH)CH_3$	H	H	OH
8	7,8-dihydroxynaphtho[2,3-*b*]-furan-4,9-dione	H	H	OH	OH
9	8-hydroxy-2-methylnaphtho[2,3-*b*]-furan-4,9-dione	CH_3	H	H	OH

Chart 1

* To whom correspondence should be addressed. e-mail: j-koyama@kobepharma-u.ac.jp
© 2000 Pharmaceutical Society of Japan

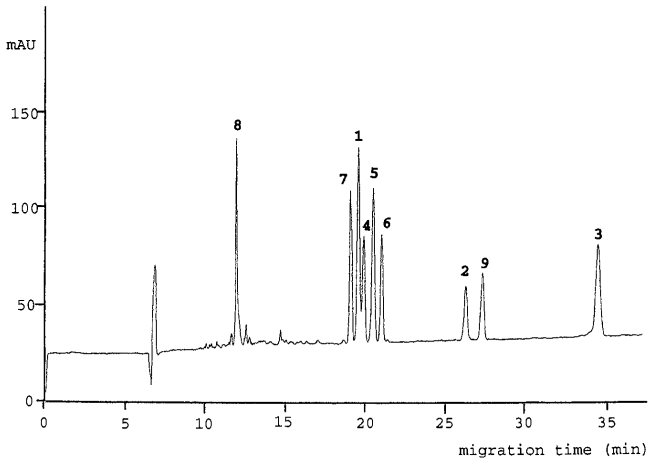

Fig. 1. Electropherogram Showing the Separation of Furanonaphthoquinones Using 0.09 M Borate Buffer (pH 9) Containing 0.03 M SDS and 10% Methanol

Peaks are identified by substance number as indicated on the Chart 1.

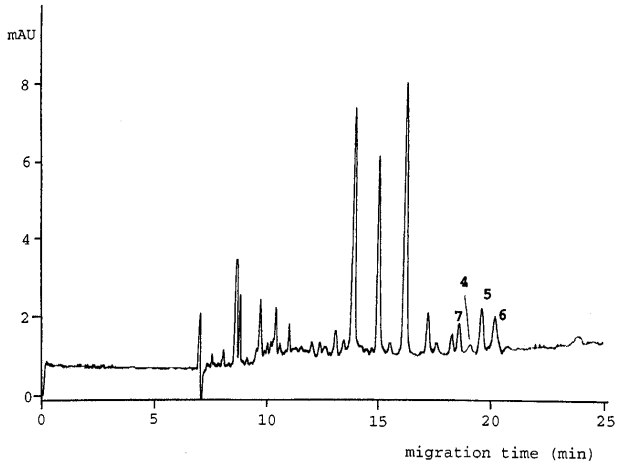

Fig. 2. Separation of a $CHCl_3$ Extract of *T. impetiginosa* Using 0.09 M Borate Buffer (pH 9) Containing 0.03 M SDS and 10% Methanol

4, 2-acetylnaphtho[2,3-*b*]furan-4,9-dione; **5**, 2-(1-hydroxyethyl)naphtho[2,3-*b*]furan-4,9-dione; **6**, 5-hydroxy-2-(1-hydroxyethyl)naphtho[2,3-*b*]furan-4,9-dione; **7**, 8-hydroxy-2-(1-hydroxyethyl)naphtho[2,3-*b*]furan-4,9-dione.

concentration, it was found that 0.09 M borate buffer (pH 8) containing 0.03 M SDS and 10% methanol could resolve the eight furanonaphthoquinones (**2**—**9**). Under the same conditions, the peaks of **1** and **7** overlapped, but increasing the pH to **9** gave good resolution. Figure 1 shows the electropherogram of a mixture of nine furanonaphthoquinones, and all components were well separated. In the separation of these furanonaphthoquinones, although the hydrophobic interaction with micelles is the main factor, borate complexation has some effect on the migration order of the molecules. When a hydroxyl group is present at the peri position of the carbonyl group, a strong internal hydrogen bond is formed between the hydrogen of the hydroxyl and the carbonyl group, and therefore the carbonyl can no longer interact with the buffer.[11] The migration time of 7,8-dihydroxynaphtho[2,3-*b*]furan-4,9-dione (**8**) is 11.98 min and it is the shortest. This could be explained by borate complexation with an ortho-dihydroxyl group that would provide a negative charge without forming a SDS micell.

The extract solution of *T. imptiginosa* was analysed with

Table 1. Reproducibility of Migration Times and Areas of Furanonaphthoquinones

Compound	Migration time (min)	RSD (%)	RSD of areas (%)
1	19.82	0.10	1.17
2	26.21	0.73	1.77
3	34.51	0.19	1.97
4	19.98	0.12	0.44
5	20.45	0.12	1.10
6	20.96	0.05	1.13
7	19.11	0.04	1.78
8	11.98	0.35	1.32
9	27.45	0.46	2.58
In a $CHCl_3$ extract of *T. impetiginosa*			
4	19.12	1.34	
5	19.53	1.45	
6	20.18	1.88	
7	18.51	1.32	

0.09 M borate buffer (pH 9)–0.03 M SDS–10% methanol and a good result was obtained. An electropherogram of *T. impetiginosa* extract is shown in Fig. 2. Among the peaks, **4**, **5**, **6** and **7** were identified by spiking with those of standards. In the comparison of MEKC with HPLC for the analysis of the extract of *T. impetiginosa*, MEKC has better resolution for **6** and **7**.

For quantitative analysis, the correlations between the peak area and the sample concentrations (**5**, **6**+**7**) were studied.

The curves (peak-area ratios, Y, *vs.* concentration, x, μg/ml) were constructed in the range of 5—50 μg/ml for **5** and 1.5—75 μg/ml for [**6**+**7**]. The sample (a mixture of **6** and **7**) for the calibration graph was isolated from *T. impetiginosa*, and the mixture could not be resolved by column chromatography (CC) or preparative thin layer chromatography (PTLC), so it was used as a mixture. We confirmed that the ratio of area of **6** and **7** was equal to the ratio of quantity of **6** and **7** by using HPLC analysis[3] (**6** : **7**=5 : 4). The regression equations of these curves and their correlation coefficients were calculated as follows: **5**, $Y=4947x+3391$ ($r=0.997$); [**6**+**7**], $Y=137606x-365355$ ($r=0.999$).

The extraction recovery was tested by adding known amounts of **5** and [**6**+**7**]. The recoveries of **5** were 80—92% and that of [**6**+**7**] 98—102%.

The reproducibilities, expressed as relative standard deviation (RSD), of this method calculated on the basis of peak area over three replicate injections are shown in Table 1. For a series of three consecutive injections, the migration time reproducibility for individual compound was between 0.04 and 1.88% RSD. In conclusion, the MEKC described here has proved to be a useful technique for investigating mixtures of furanonaphthoquinones as it is rapid, simple and reproducible.

References

1) Steinert J., Khalaf H., Rimpler M., *J. Chromatogr. A*, **693**, 281—287 (1995).
2) Steinert J., Khalaf H., Rimpler M., *J. Chromatogr. A*, **723**, 206—209 (1996).
3) Wagner H., Kreher B., Lotter H., Hamburger M. O., Cordell G. A., *Helv. Chim. Acta*, **72**, 659—667 (1989).
4) Fujimoto Y., Eguchi T., Murasaki C., Ohashi Y., Kakinuma K., Takagaki H., Abe M., Inazawa K., Yamazaki K., Ikekawa N., Yoshikawa O.,

Ikekawa T., *J. Chem. Soc., Perkin Trans. 1*, **1991**, 2323—2327.
5) Abbott B. J., Hartwell J., Leiter J., Perdue R. E. Jr., Schepartz S. A., *Cancer Res.*, **27B**, 190—199 (1967).
6) Hartwell J. L., *Lloydia*, **31**, 71—170 (1968).
7) Hirai K., Koyama J., Pan J. P., Simamura E., Shimada H., Yamori T., Sato S., Tagahara K., Turuo T., *Cancer Detect Prev.*, **23**, 539—550 (1999).
8) Koyama J., Okatani T., Tagahara K., Suzuta Y., Abst. Japanese-United States Congress for Pharmaceutical Science, Honolulu, 1987, December 2—7, p. 142.
9) Hayashi T., Smith F. T., Lee K. H., *J. Med. Chem.*, **30**, 2005—2008 (1987).
10) Koyama J., Toyokuni I., Kino A., Tagahara K., *Heterocycles*, **48**, 1631—1638 (1998).
11) Gil M. I., Ferreres F., Barberan F. A. T., *J. Liquid Chromatogr.*, **18**, 3007—3019 (1995).

Conversion of Quassinoids for Enhancement of Inhibitory Effect against Epstein–Barr Virus Early Antigen Activation. Introduction of Lipophilic Side Chain and Esterification of Diosphenol

Sadaaki TAMURA,[a] Narihiko FUKAMIYA,[a] Xiao-Yang MOU,[b] Teruo MUKAINAKA,[b] Harukuni TOKUDA,[b] Hoyoku NISHINO,[b] Kiyoshi TAGAHARA,[c] Kazuo KOIKE,[d] Kuo-Hsiung LEE,[e] and Masayoshi OKANO*,[a]

Department of Interdisciplinary Studies of Natural Environment, Faculty of Integrated Arts and Sciences, Hiroshima University,[a] 1–7–1 Kagamiyama, Higashi-Hiroshima 739–8521, Japan, Department of Biochemistry, Kyoto Prefectural University of Medicine,[b] Kawaramachi-dori, Kamigyo-ku, Kyoto 602–0841, Japan, Faculty of Pharmaceutical Sciences, Kobe Pharmaceutical University,[c] 1–19–1 Motoyamakita-machi, Higashinada-ku, Kobe 658–8558, Japan, School of Pharmaceutical Sciences, Toho University,[d] 2–2–1 Miyama, Funabashi, Chiba 274–8510, Japan, and Division of Medicinal Chemistry and Natural Products, School of Pharmacy, University of North Carolina,[e] Chapel Hill, N. C. 27599–7360, U.S.A. Received January 5, 2000; accepted February 8, 2000

Introduction of a senecioyl group into shinjulactones B and C, and esterification of the diosphenol moiety in brusatol and brucein A enhanced inhibitory effect against Epstein–Barr virus early antigen activation.

Key words quassinoid conversion; lipophilic side chain; diosphenol esterification; inhibitory effect against Epstein–Barr virus early antigen activation

Several natural products including flavonoids,[1] steroids,[2] triterpenoids,[3] triterpenoid saponins,[4] and quinones[5] have been investigated for their inhibitory effects on 12-*O*-tetradecanoylphorbol 13-acetate (TPA)-induced Epstein–Barr virus early antigen (EBV-EA) activation and, thus, potential antitumor promoting agents.

Recently, we reported the inhibitory activities of 59 natural quassinoids[6,7] and 3 derivatives[8] isolated from plants of the Simaroubaceous family, such as *Brucea* (*B.*) *javanica*, *B. antidysenterica*, *Picrasma ailanthoides*, and *Ailanthus* (*A.*) *altissima*, and 5 semisynthetic variations.[9] Every quassinoid tested showed inhibitory activity. The most potent ones were aglycones with carbonyl and hydroxyl groups in ring A, a methylenoxy bridge between C-8 and C-13, and an ester side chain at C-15. In contrast, several analogous glycosides, which have these same moieties, showed only moderate activity. The least active quassinoids lacked the methylenoxy bridge and the ester side chain. From the above results, we were interested in the effect of the lipophilic side chain on the inhibitory activity against EBV–EA activation, and so we investigated structure improvement for the less active quassinoids.

In the previous paper,[10] we reported the isolation of bruceanic acids A, B, C, and D. All these compounds may be obtained by oxidative degradation of diosphenol in bruceantin, bruceantarin, bruceantinol, and desacetylbruceantinol, respectively, of which isolation was reported by Kupchan *et al.*[11] Therefore, we were interested in the effect of protected diosphenol for its inhibitory activity against EBV–EA activation.

In this paper, we report the introduction of a lipophilic senecioyl group into shinjulactones B (**1**) and C (**2**), introduction of an ethylsuccinyl group into the diosphenol moiety of brusatol (**5**) and brucein A (**6**) for protection, and their inhibitory activities against EBV–EA activation.

Results and Discussion

Shinjulactone B (**1**) and shinjulactone C (**2**) were isolated from *A. altissima* as colorless amorphous solids. Compounds **3** and **4** were obtained as colorless solids by esterification of **1** and **2** using senecioyl chloride. The molecular formulae of **3** ($C_{24}H_{28}O_8$) and **4** ($C_{25}H_{28}O_8$) were confirmed by high resolution MS spectra. The position of esterification in **3** and **4** was confirmed as C-20 from big differences in the two ^{1}H-NMR signals between 20-CH_2 of **1** (δ 3.92 and 4.08) and that of **3** (δ 4.36 and 4.65), and also between 20-CH_2 of **2** (δ 4.03 and 4.07) and that of **4** (δ 4.56 and 4.61), respectively.

Bruceoside D (**5**) and bruceoside E (**6**) were obtained, respectively, as colorless amorphous solids from *B. javanica*. Compounds **5** and **6** were converted, respectively, into compounds **7** and **8** by acid hydrolysis using *p*-toluenesulfonic acid in MeOH. Compounds **7** and **8** were confirmed, respectively, as brusatol and brucein A by ^{1}H- and ^{13}C-NMR spectral comparison with those of the authentic compounds.

Compounds **7** and **8** were converted into compounds **9** and **10** by esterification using monoethylsuccinyl chloride. The molecular formulae of **9** ($C_{32}H_{40}O_{14}$) and **10** ($C_{32}H_{42}O_{14}$) were confirmed by high resolution MS spectra. The positions of esterification in **9** and **10** were confirmed, respectively, as C-3 according the big differences of the two ^{13}C-NMR sig-

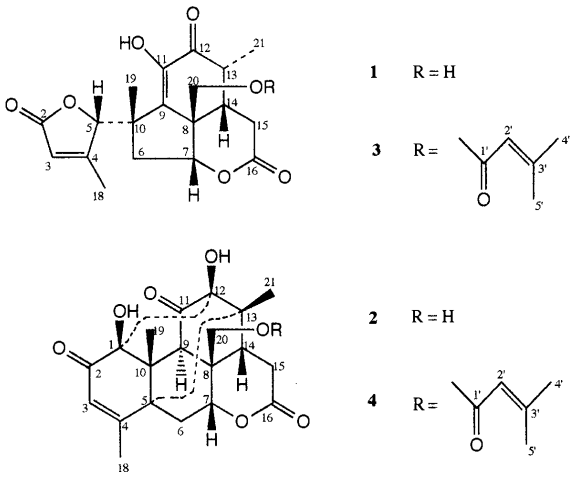

Fig. 1. Introduction of Senecioyl Group into **1** and **3** to Afford **2** and **4**

* To whom correspondence should be addressed. e-mail: okano@hiroshima-aki-u.ac.jp

© 2000 Pharmaceutical Society of Japan

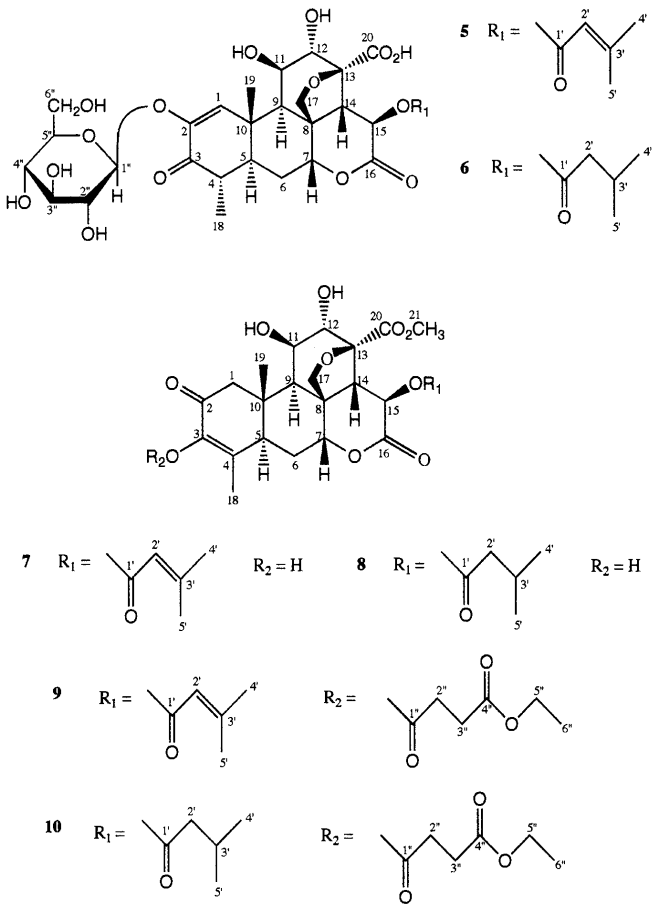

Fig. 2. Acid Hydrolysis of **5** and **6** to Afford **7** and **8**, and Esterification of 7 and **8** to Afford **9** and **10**

Table 1. Inhibitory Effects of Quassinoids (**1**—**6**, **9** and **10**) against TPA-Induced EBV–EA Activation

Compound	%EBV–EA Positive Cells					IC_{50}
	Compound concentration (mol ratio/32 pmol TPA)					
	1000	500	100	10	0[a)]	
Shinjulactone B (**1**)	3.1 (70)[b)]	18.4	30.5	36.1	40	445
Shinjulactone C (**2**)	0 (80)[b)]	4.4	21.8	28.4	40	145
Senecioate of **1** (**3**)	0.9 (70)[b)]	16.7	29.4	35.4	40	395
Senecioate of **2** (**4**)	0 (80)[b)]	3.9	20.5	28.2	40	115
Bruceoside D (**5**)	0 (80)[b)]	2.5	9.4	14.3	40	7.8
Bruceoside E (**6**)	0 (80)[b)]	1.6	8.2	12.8	40	7.3
Ethylsuccinate of **7** (**9**)	0 (80)[b)]	0	1.0	4.3	40	5.6
Ethylsuccinate of **8** (**10**)	0 (80)[b)]	0	0.9	4.1	40	5.5

a) Control. *b*) Values in the parentheses are viability percentage of Raji cells.

nals between C-4 of **7** (δ 128.3) and that of **9** (δ 142.6), and also between C-4 of **8** (δ 128.2) and that of **10** (δ 142.6).

In Table 1, senecioyl esters at C-15 (**3** and **4**) of compounds **1** and **2** showed higher inhibitory activity against EBV–EA activation than those of the starting materials. This fact indicates that the introduction of a lipophilic side chain is very important for enhancement of the inhibitory activity of quassinoids.

Ethylsuccinyl esters at C-3 (**9** and **10**) of compounds **7** and **8** showed the highest inhibitory activity against EBV–EA activation, as shown in Table 1. This fact indicates that the esterification of diosphenol is very important for enhancement of the inhibitory activity of quassinoids.

Materials and Methods

General Experimental Procedures Melting points were determined on an MRK air-bath type melting point apparatus and are uncorrected. Specific rotations were obtained on a JASCO DIP-370 digital polarimeter (length= 0.5 dm). IR spectra were recorded on a JASCO IR-810 spectrophotometer and UV spectra were obtained on a Hitachi 320-S or Shimadzu UV 3101 PC spectrophotometer. ^{1}H- and ^{13}C-NMR spectra were determined on JEOL JNM-A400 or Varian VXR-500 instruments in C_5D_5N using tetramethylsilane (TMS) as an internal standard. Mass spectra (MS) were recorded on a Hitachi M-80 instrument. Precoated silica gel plates (Merck, $60F_{254}$) of 0.25 mm thickness were used for analytical TLC, and plates of 1 mm thickness were used for preparative TLC. Components on TLC were detected using a UV lamp (254 and 365 nm). Analytical HPLC was performed on a Tosoh liquid chromatograph equipped with a UV detector set at 254 nm and a reverse-phase column (TSK-gel ODS-80Ts) using a mixed solvent of MeOH–H_2O. Preparative HPLC was carried out on a Tosoh or Gilson liquid chromatograph equipped with a reverse-phase column (Lichrosorb RP-18) at 254 nm using the same solvent as used for analytical HPLC.

Compound 1 This compound (**1**, shinjulactone B) was isolated as a colorless amorphous solid from *A. altissima*.[12,13] ^{1}H-NMR (C_5D_5N) δ: 1.05 (3H, d, J=7 Hz, 13-Me), 1.60 (3H, s, 10-Me), 1.95 (3H, d, J=1 Hz, 4-Me), 3.92 (1H, d, J=12 Hz, 20-H$_\alpha$), 4.08 (1H, d, J=12 Hz, 20-H$_\beta$).

Compound 2 This compound (**2**, shinjulactone C) was isolated as a colorless amorphous solid from *A. altissima*.[12,14] ^{1}H-NMR (C_5D_5N) δ: 1.05 (3H, s, 10-Me), 1.28 (3H, s, 13-Me), 1.98 (3H, s, 4-Me), 4.03 (1H, d, J=12 Hz, 20-H$_\alpha$), 4.08 (1H, d, J=12 Hz, 20-H$_\beta$).

Compound 3 Senecioyl chloride (33 mg, 0.28 mM) dissolved in $CHCl_3$ (0.3 ml) was added dropwise into compound **1** (20 mg, 0.055 mM), dissolved in C_5H_5N (1.2 ml) at 0 °C, and stirred at room temperature (24 °C) for 6 d. Then, MeOH (2 ml) was added to the reaction mixture for quenching. The reaction product was isolated first by preparative TLC (EtOAc–Et_2O, 50 : 50, v/v) and then by preparative HPLC (MeOH–H_2O, 60 : 40, v/v) to afford compound **3** (2.9 mg, 0.0065 mM, yield 11.8%) as a colorless amorphous solid, mp 186—188 °C. UV λ_{max}^{MeOH} nm (ε): 277 (8200). IR (KBr) cm^{-1}: 3400 (OH), 1760 (γ-lactone C=O), 1710 (C=O), 1680 (α,β-unsaturated C=O). ^{1}H-NMR (C_5D_5N) δ: 1.12 (3H, d, J=6.8 Hz, 13-Me), 1.60 (3H, s, 10-Me), 1.94 (3H, s, 4-Me), 4.36 (1H, d, J=12 Hz, 20-H$_\alpha$), 4.65 (1H, d, J=12 Hz, 20-H$_\beta$), 1.78 (3H, s, 3′-Me), 2.19 (3H, s, 3′-Me), 5.81 (1H, s, 2′-H). ^{13}C-NMR (C_5D_5N) δ: 12.5 (C-21, Me), 16.2 (C-18, Me), 24.0 (C-19, Me), 63.8 (C-20, CH_2), 20.2 (C-4′, Me), 27.1 (C-5′, Me), 115.6 (C-2′, CH), 158.9 (C-3′, C), 165.9 (C-1′, C=O). HREIMS m/z: 444.1793 (M^+) ($C_{24}H_{28}O_8$, error 1.1).

Compound 4 Senecioyl chloride (64 mg, 0.54 mM) dissolved in $CHCl_3$ (0.3 ml) was added dropwise into compound **2** (10 mg, 0.0267 mM) dissolved in C_5H_5N (2.0 ml) at 0 °C and stirred at 45—50 °C for 24 h. Then, MeOH (2 ml) was added into the reaction mixture for quenching. The reaction product was isolated by preparative HPLC (MeOH–H_2O, 50 : 50, v/v) to afford compound **4** (3.9 mg, 0.0085 mM, yield 31.9%) as a colorless amorphous solid, mp 296—298 °C (dec.). UV λ_{max}^{MeOH} nm (ε): 221 (15280). IR (KBr) cm^{-1}: 3400 (OH), 1760 (γ-lactone C=O), 1710 (C=O), 1660 (α,β-unsaturated C=O). ^{1}H-NMR ($CDCl_3$) δ: 0.99 (3H, s, 10-Me), 1.02 (3H, s, 13-Me), 2.08 (3H, s, 4-Me), 4.07 (1H, d, J=12 Hz, 20-H$_\alpha$), 4.13 (1H, d, J=12 Hz, 20-H$_\beta$), 1.91 (3H, s, 3′-Me), 2.17 (3H, s, 3′-Me), 5.65 (1H, s, 2′-H). ^{13}C-NMR ($CDCl_3$) δ: 12.1 (C-19, Me), 13.9 (C-21, Me), 20.4 (C-18, Me), 61.6 (C-20, CH_2), 23.2 (3′-Me), 27.5 (3′-Me), 114.7 (C-2′, CH), 158.9 (C-3′, C), 165.4 (C-1′, C=O). HREIMS m/z: 456.1780 (M^+) ($C_{25}H_{28}O_8$, error 0.3). ^{1}H-NMR (C_5D_5N) δ:1.14 (3H, s, 10-Me), 1.31 (3H, s, 13-Me), 2.01 (3H, s, 4-Me), 4.56 (1H, d, J=12 Hz, 20-H$_\alpha$), 4.61 (1H, d, J=12 Hz, 20-H$_\beta$), 1.69 (3H, s, 3′-Me), 2.13 (3H, s, 3′-Me), 5.74 (1H, s, 2′-H).

Compound 5 This compound (**5**, bruceoside D) was isolated as a colorless amorphous solid from *B. javanica*.[15] ^{1}H- and ^{13}C-NMR (C_5D_5N) spectra coincided with those of the authentic bruceoside D.

Compound 6 This compound (**6**, bruceoside E) was isolated as a colorless amorphous solid from *B. javanica*.[15] ^{1}H- and ^{13}C-NMR (C_5D_5N) spectra coincided with those of the authentic bruceoside E.

Compound 7 A mixture of compound **5** (64 mg, 0.0957 mM) and *p*-toluenesulfonic acid (18 mg) was dissolved in MeOH (6 ml) and stirred under reflux condition for 20 h. Then, the reaction mixture was subjected to preparative HPLC (MeOH–H_2O, 40 : 60, v/v) to afford compound **7** (brusatol, 24.3 mg, 0.0467 mM, yield 48.8%) as a colorless amorphous solid,

mp 249—251 °C. UV λ_{max}^{MeOH} nm (ε): 227 (7350). ^{1}H-NMR (C_5D_5N) δ: 1.67 (3H, s, 10-Me), 1.95 (3H, d, J=1.2 Hz, 4-Me), 3.76 (3H, s, OMe), 1.63 (3H, s, 3′-Me), 2.15 (3H, s, 3′-Me), 5.85 (1H, s, 2′-H). ^{13}C-NMR (C_5D_5N) δ: 13.4 (C-18, Me), 15.8 (C-19, Me), 42.5 (C-5, CH), 52.4 (OMe), 128.3 (C-4, C), 146.0 (C-3, C), 193.0 (C-2, C=O), 20.2 (3′-Me), 27.0 (3′-Me), 116.0 (C-2′, CH), 158.4 (C-3′, C), 165.4 (C-1′, C=O). The ^{1}H- and ^{13}C-NMR spectra of compound **7** coinsided with those of brusatol.[8]

Compound 8 A mixture of compound **6** (80 mg, 0.119 mM) and *p*-toluenesulfonic acid (23 mg) was dissolved in MeOH (6 ml) and stirred under the reflux condition for 20 h. Then, the reaction mixture was subjected to preparative HPLC (MeOH–H_2O, 45 : 55, v/v) to afford compound **8** (brucein A, 23.4 mg, 0.0448 mM, yield 37.6%) as a colorless amorphous solid, mp 144—146 °C. UV λ_{max}^{MeOH} nm (ε): 278 (5120). ^{1}H-NMR (C_5D_5N) δ: 1.62 (3H, s, 10-Me), 1.94 (3H, d, J=1.6 Hz, 4-Me), 3.83 (3H, s, OMe), 0.95 (3H, d, J=6.8 Hz, 3′-Me), 0.97 (3H, d, J=6.4 Hz, 3′-Me). ^{13}C-NMR (C_5D_5N) δ: 13.3 (C-18, Me), 15.7 (C-19, Me), 128.2 (C-4, C), 146.0 (C-3, C), 193.0 (C-2, C=O), 22.4 (3′-Me), 22.5 (3′-Me), 25.9 (C-3′, CH), 43.3 (C-2′, CH_2), 171.7 (C-1′, C=O). The ^{13}C-NMR spectrum of compound **8** coincided with that of brucein A.[16]

Compound 9 Monoethylsuccinyl chloride (7.69 mg, 0.0467 mM) dissolved in $CHCl_3$ (0.1 ml) was added dropwise into compound **7** (brusatol, 24.3 mg, 0.0467 mM), dissolved in C_5H_5N (1.0 ml), and stirred at 24 °C for 17 h. Then, the reaction mixture was subjected to preparative HPLC (MeOH–H_2O, 50 : 50, v/v) to afford compound **9** (9.7 mg, 0.0149 mM, yield 32%) as a colorless amorphous solid, mp 200—202 °C. UV λ_{max}^{MeOH} nm (ε): 222 (11090). IR (KBr) cm^{-1}: 3420 (OH), 1740 (ester C=O), 1710 (C=O), 1675 (α,β-unsaturated C=O), 1640 (C=C). ^{1}H-NMR (C_5D_5N) δ: 1.77 (3H, s, 10-Me), 1.80 (3H, s, 4-Me), 3.75 (3H, s, OMe), 1.66 (3H, s, 3′-Me), 2.14 (3H, s, 3′-Me), 5.85 (1H, s, 2′-H), 1.12 (3H, t, J=6.8 Hz, 6″-Me), 2.80 (2H, t, J=6.4 Hz, 2″-CH_2), 3.05 (2H, t, J=6.4 Hz, 3″-CH_2), 4.12 (2H, q, J=6.8 Hz, 5″-CH_2). ^{13}C-NMR (C_5D_5N) δ: 14.2 (C-18, Me), 15.8 (C-19, Me), 52.3 (OMe), 142.6 (C-4, C), 146.6 (C-3, C), 189.9 (C-2, C=O), 20.2 (3′-Me), 27.0 (3′-Me), 115.9 (C-2′, CH), 158.5 (C-3′, C), 168.2 (C-1′, C=O), 14.3 (C-6″, Me), 29.0 (C-2″, CH_2), 29.1 (C-3″, CH_2), 60.7 (C-5″, CH_2), 170.8 (C-4″, C=O), 172.2 (C-1″, C=O). HREIMS *m/z*: 648.2417 (M^+) ($C_{32}H_{40}O_{14}$, error 0.1).

Compound 10 Monoethylsuccinyl chloride (6.08 mg, 0.0369 mM) dissolved in $CHCl_3$ (0.1 ml) was added dropwise into compound **8** (brucein A, 19.3 mg, 0.0369 mM) dissolved in C_5H_5N (1.0 ml) and stirred at 24 °C for 24 h. Then, the same amount of monosuccinyl chloride was added into the reaction mixture and the reaction was continued in the same way. This procedure was repeated twice. Finally, the reaction mixture was subjected to preparative HPLC (MeOH–H_2O, 50 : 50, v/v) to afford compound **10** (7.2 mg, 0.0111 mM, yield 30%) as a colorless amorphous solid, mp 204—206 °C. UV λ_{max}^{MeOH} nm (ε): 246 (11650). IR (KBr) cm^{-1}: 3400 (OH), 1740 (ester C=O), 1710 (C=O), 1660 (α,β-unsaturated C=O), 1635 (C=C). ^{1}H-NMR (C_5D_5N) δ: 1.75 (3H, s, 10-Me), 1.80 (3H, s, 4-Me), 3.82 (3H, s, OMe), 0.95 (3H, d, J=6.4 Hz, 3′-Me), 0.98 (3H, d, J=7.2 Hz, 3′-Me), 2.22 (1H, m, 3′-H), 2.35 (2H, m, 2′-CH_2), 1.12 (3H, t, J=7.2 Hz, 6″-Me), 2.81 (2H, t, J=6.8 Hz, 2″-CH_2), 3.06 (2H, t, J=6.8 Hz, 3″-CH_2), 4.12 (2H, q, J=7.2 Hz, 5″-CH_2). ^{13}C-NMR (C_5D_5N) δ: 14.2 (C-18, Me), 15.8 (C-19, Me), 52.3 (OMe), 142.6 (C-4, C), 146.5 (C-3, C), 189.9 (C-2, C=O), 22.4 (C-4′, Me), 22.5 (C-5′, Me), 25.9 (C-3′, CH), 43.3 (C-2′, CH_2), 171.7 (C-1′, C=O), 14.3 (C-6″, Me), 29.0 (C-2″, CH_2), 29.0 (C-3″, CH_2), 60.7 (C-5″, CH_2), 170.8 (C-4″, C=O), 172.2 (C-1″, C=O). HREIMS *m/z*: 650.2587 (M^+) ($C_{32}H_{42}O_{14}$, error 1.5).

EBV–EA Activation The inhibition of EBV–EA activation was assayed using a literature method described in literature.[17] The cells were incubated at 37°C for 48 h in a medium containing butyric acid (4 nM), TPA (32 pM), and various amounts of test compound. Smears were made from the cell suspension and the EBV–EA inducing cells were stained by means of an indirect immunofluorescence technique.[18]

In each assay, at least 500 cells were counted, and the number of stained cells (positive cells) was recorded. Triplicate assays were performed for each data point. The EBV–EA inhibitory activity of the test compound was compared with that of the control experiment with butyric acid plus TPA. In the control experiments, the EBV–EA activities were ordinarily around 40%, and these values were taken as a positive control. The viability of the cells was assayed by the trypan-blue staining method. For the determination of cytotoxicity, the cell viability was required to be more than 60%.[19]

Acknowlegments This study was supported in part by Grants-in-Aid from the Ministry of Education, Science and Culture, and from the Ministry of Health and Welfare. The authors thank Dr. T. Sai, Kobe Pharmaceutical University, for her measurement of MS spectra.

References

1) Konoshima T., Takasaki M., Kozuka M., Inada A., Nakanishi T., Tokuda H., Matsumoto T., *Shoyakugaku Zasshi*, **43**, 135—141 (1989).
2) Inada A., Nakanishi T., Konoshima T., Kozuka M., Nishino H., Iwashima A., *Shoyakugaku Zasshi*, **44**, 215—218 (1990).
3) Diallo H., Vanhaelen H., Vanhaelen-Fastre R., Konoshima T., Kozuka M., Tokuda H., *J. Nat. Prod.*, **53**, 879—881 (1989).
4) Tokuda H., Konoshima T., Kozuka M., Kimura T., *Cancer Lett.*, **40**, 309—317 (1988).
5) Konoshima T., Kozuka M., Koyama J., Okatani T., Tagahara K., Tokuda H., *J. Nat. Prod.*, **52**, 987—995 (1989).
6) Okano M., Fukamiya N., Tagahara K., Tokuda H., Iwashima A., Nishino H., Lee K. H., *Cancer Lett.*, **94**, 139—146 (1995).
7) Kubota K., Fukamiya N., Tokuda H., Nishino H., Tagahara K., Lee K. H., Okano M., *Cancer Lett.*, **113**, 165—168 (1997).
8) Rahman S., Fukamiya N., Tokuda H., Nishino H., Tagahara K., Lee K. H., Okano M., *Bull. Chem. Soc. Jpn.*, **72**, 751—756 (1999).
9) Rahman S., Fukamiya N., Ohno N., Tokuda H., Nishino H., Tagahara K., Lee K. H., Okano M., *Chem. Pharm. Bull.*, **45**, 675—677 (1997).
10) Toyota T., Fukamiya N., Okano M., Tagahara K., Chang J. J., Lee K. H., *J. Nat. Prod.*, **53**, 1526—1532 (1990).
11) Kupchan S. M., Britton R. W., Lacadie J. A., Ziegler M. F., Sigel C. W., *J. Org. Chem.*, **40**, 648—654 (1975).
12) Okano M., Fukamiya N., Tagahara K., Cosentino M., Lee T. M. Y., Natschke S. M., Lee K. H., *Bio-Org. Med. Chem. Lett.*, **6**, 701—706 (1996).
13) Furuno T., Ishibashi M., Naora H., Murae T., Hirota H., Tsuyuki T., Takahashi T., Itai A., Iitaka Y., *Bull. Chem. Soc. Jpn.*, **57**, 2484—2489 (1984).
14) Ishibashi M., Tsuyuki T., Murae T., Hirota H., Takahashi T., Itai A., Iitaka Y., *Bull. Chem. Soc. Jpn.*, **56**, 3683—3793 (1983).
15) Ohnishi S., Fukamiya N., Okano, M., Tagahara K., Lee K. H., J. *Nat. Prod.*, **58**, 1032—1038 (1995).
16) Sakaki T., Yoshimura S., Ishibashi M., Tsuyuki T., Takahashi T., Honda T., Nakanishi T., *Bull. Chem. Soc. Jpn.*, **58**, 2680—2686 (1985).
17) Ito Y., Yanase S., Fujita J., Harayama T., Takashima M., Imanaka H., *Cancer Lett.*, **13**, 29—37 (1981).
18) Henle G., Henle W., *J. Bacteriol.*, **91**, 1248—1256 (1966).
19) Ohigashi H., Takamura H., Koshimizu K., Tokuda H., Ito Y., *Cancer Lett.*, **30**, 143—151 (1986).

Two 3,4-seco-Lupane Triterpenes from Leaves of *Acanthopanax divaricatus* var. *albeofructus*

O-Jin Oh,*[a] Seung-Yeup Chang,[b] Chang-Soo Yook,[c] Ki-Sook Yang,[a] Sang-Yong Park,[d] and Toshihiro Nohara*[d]

College of Pharmacy, Sookmyung Women's University,[a] Chungpa-dong 2-ka, Seoul 140–742, Korea, Korea Food and Drug Administration,[b] 5 Nokbun-dong, Seoul 122–704, Korea, College of Pharmacy, Kyung-Hee University,[c] 1 Hoegi-dong, Seoul 132–702, Korea, and Faculty of Pharmaceutical Sciences, Kumamoto University,[d] 5–1 Oe-honmachi, Kumamoto 862–0973, Japan. Received January 11, 2000; accepted Feburuary 14, 2000

Two 3,4-seco-lupane triterpenoids (1, 2) were isolated from the leaves of *Acanthopanax divaricatus* var. *albeofructus* (Araliaceae). Based on the spectroscopic data, the chemical structures of 1 and 2 were characterized as 24-hydroxychiisanogenin and 22α-hydroxychiisanogenin, respectively. 1 was a new compound and 2 was isolated for the first time from the natural source, although it had been obtained as an enzymatically hydrolyzed artifact from 22α-hydroxychiisanoside.

Key words *Acanthopanax divaricatus* var. *albeofructus*; Araliaceae; 3,4-seco-lupane triterpene; 24-hydroxychiisanogenin; 22α-hydroxychiisanogenin

In previous papers, we reported the isolation and characterization of two lupane triterpenoids, chiisanogenin and chiisanoside, from the leaves of *Acanthopanax divaricatus* Seemann var. *albeofructus* C. S. Yook *et* T. H. Kim and two lignoids, *l*-sesamin and *l*-savinin, from the root bark of this plant,[1,2] and five new lupane triterpenoids, acantrifoside A, and acankoreosides A, B, C and D, from *A. trifoliatus*[3] and *A. koreanum*.[3—5] In a continuing study on *Acanthopanax* species, we report here the isolation and structural determination of two additional 3,4-seco-lupane triterpenoids, named 24-hydroxychiisanogenin (**1**) and 22α-hydroxychiisanogenin (**2**), as minor components of the leaves of *A. divaricatus* var. *albeofructus*.

24-Hydroxychiisanogenin (**1**), obtained as colorless needles, mp 250—252 °C (MeOH), $[\alpha]_D$ +61.0° (MeOH), showed absorption bands due to hydroxyl groups at 3425 cm^{-1}, carbonyl groups at 1711 cm^{-1} and C=C groups at 1643 cm^{-1} in the IR spectrum. The negative FAB-MS exhibited a molecular ion peak due to $[M-H]^-$ at *m/z* 499 ($C_{30}H_{44}O_6$–H). The ^{1}H-NMR spectrum (in pyridine-d_5) showed signals due to four tertiary methyl groups at δ 1.00, 1.04, 1.05 and 1.67, four olefinic protons at δ 4.62 (1H, br s), 4.91 (1H, br s), 5.12 (1H, br s) and 5.58 (1H, br s), two oxygen-bearing methine protons at δ 3.69 (1H, d, J=7.8 Hz) and 4.62 (1H, d, J=6.8 Hz), and two oxygen-bearing methylene protons at δ 4.43 (1H, d, J=14.5 Hz) and 4.62 (1H, d, J=14.5 Hz), as illustrated in Table 1. Signals due to one tertiary methyl group appeared at δ 1.67 and two exomethylene protons with geminal coupling suggested the presence of an isopropenyl group. Moreover, a total of thirty carbon signals observed in the ^{13}C-NMR spectrum (Table 1) and distortionless enhancement by polarization transfer (DEPT) experiment suggested the presence of two carboxyl groups, two disubstituted double bonds, two oxygen-bearing methine carbons, one oxygen-bearing methylene carbon, five methine carbons, eight methylene carbons and four methyl carbons. All ^{13}C-NMR data of **1** were very similar to those of chiisanogenin (**3**) isolated from the leaves of this plant, except for the absence of one tertiary methyl carbon signal of C-24 observed in **3** and the presence of one oxygen-bearing methylene carbon signal at δ 67.2 in **1**. Furthermore, taking into consideration the molecular ion peaks of both compounds, it was suggested that one tertiary methyl carbon at C-24 in **3** was replaced by one oxygen-bearing methylene carbon in **1**. This conclusion was supported by a significant downfield shift of the C-4 signal (5.2 ppm) by an α-effect of hydroxylation shift, upfield shifts of the C-5 signal (4.2 ppm) and C-23 signal (2.9 ppm) by β-effect, and downfield effects of the C-6 (1.8 ppm) and C-10 (0.5 ppm). Moreover, the ^{1}H-NMR signals of olefinic protons at δ 5.12 (1H, br s, H-23*a*) and 5.58 (1H, br s, H-23*b*) shifted downfield (0.12 and 0.48 ppm, respectively). Measurements of two-dimensional (2D) NMR spectra of **1** enabled the respective signals to be assigned. Based on the above spectroscopic data, **1** was determined to be 1(*R*)-1α,11α,24-trihydroxy-3,4-seco-lupa-4(23),20(30)-dien-3,28-dioic acid 3,11-lactone.

22α-Hydroxychiisanogenin (**2**), obtained as colorless needles, mp 243—245 °C (MeOH), $[\alpha]_D$ +92.1° (MeOH), showed absorption bands due to hydroxyl groups at 3462, 3377 cm^{-1}, carbonyl groups at 1697 cm^{-1} and C=C groups at 1643 cm^{-1} in the IR spectrum. The negative FAB-MS also exhibited a molecular ion peak due to $[M-H]^-$ at *m/z* 499 ($C_{30}H_{44}O_6$–H). The ^{1}H-NMR spectrum (in pyridine-d_5) showed signals due to five tertiary methyl groups, four olefinic protons and three oxygen-bearing methine protons,

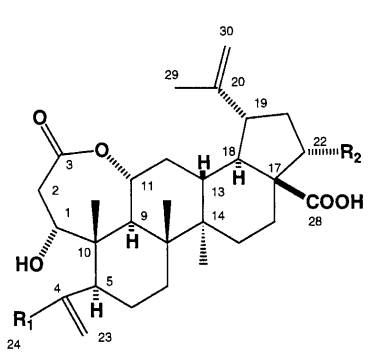

1 : R_1 = CH_2OH R_2 = H
2 : R_1 = CH_3 R_2 = OH
3 : R_1 = CH_3 R_2 = H

* To whom correspondence should be addressed. e-mail: none@gpo.kumamoto-u.ac.jp

© 2000 Pharmaceutical Society of Japan

Table 1. ^{1}H- and ^{13}C-NMR Data for Compounds **1** and **2** in Pyridine-d_5 (δ in ppm, 400 MHz)

C	**1**		**2**	
	δ_C	δ_H	δ_C	δ_H
1	70.9 d	3.69 (1H, d, J=8.1 Hz, H-1β)	70.4 d	3.66 (1H, d, J=8.0 Hz, H-1β)
2	38.4 t	3.07 (1H, d, J=14.5 Hz, H-2α) 2.75 (1H, dd, J=8.1, 14.5 Hz, H-2β)	38.7 t	3.05 (1H, d, J=14.9 Hz, H-2α) 2.76 (1H, dd, J=8.0, 14.9 Hz, H-2β)
3	172.8 s	—	173.1 s	—
4	152.9 s	—	147.6 s	—
5	45.4 d	2.74[a)]	49.4 d	2.86 (1H, d, J=12.9 Hz, H-5α)
6	26.9 t	1.56,[a)] 1.88[a)]	25.1 t	1.06,[a)] 1.37[a)]
7	32.6 t	1.12,[a)] 1.34[a)]	32.4 t	1.15,[a)] 1.34[a)]
8	41.6 s	—	42.1 s	—
9	44.2 d	2.73 (1H, d, J=9.5 Hz, H-9α)	44.0 s	2.70[a)]
10	44.6 s	—	44.1 s	—
11	75.5 d	4.62 (1H, d, J=6.8 Hz, H-11β)	75.4 d	4.58[a)]
12	33.5 t	1.73,[a)] 2.58[a)]	33.6 t	1.80,[a)] 1.64[a)]
13	35.3 d	2.88 (1H, m, H-13β)	35.0 d	3.01[a)]
14	42.2 s	—	41.6 s	—
15	29.6 t	1.10,[a)] 1.73[a)]	29.0 t	1.17,[a)] 1.74[a)]
16	32.9 t	1.49,[a)] 2.56[a)]	26.9 t	2.30 (1H, m), 2.43[a)]
17	56.3 s	—	62.4 s	—
18	49.6 d	1.63[a)]	49.6 d	1.68[a)]
19	47.8 d	3.48 (1H, m, H-19β)	47.9 d	3.55 (1H, m, H-19β)
20	150.5 s	—	150.9 s	—
21	31.0 t	1.47,[a)] 2.20[a)]	41.8 t	1.69,[a)] 2.57[a)]
22	37.3 t	1.51,[a)] 2.21[a)]	75.2 d	4.71 (1H, d, J=3.2 Hz, H-22β)
23	111.0 t	5.12 (1H, br s, H-23*a*) 5.58 (1H, br s, H-23*b*)	113.8 t	4.95 (1H, br s, H-23*a*) 5.06 (1H, br s, H-23*b*)
24	67.2 t	4.43 (1H, J=14.2 Hz, H-24*a*) 4.62 (1H, J=14.9 Hz, H-24*b*)	23.5 q	1.80 (3H, s)
25	18.6 q	1.05 (3H, s)	19.0 q	0.94 (3H, s)
26	17.9 q	1.00 (3H, s)	17.8 q	0.99 (3H, s)
27	13.7 q	1.04 (3H, s)	13.7 q	1.11 (3H, s)
28	178.7 s	—	178.4 s	—
29	18.9 q	1.67 (3H, s)	18.7 q	1.88 (3H, s)
30	110.6 t	4.62 (1H, br s, H-30*a*) 4.91 (1H, br s, H-30*b*)	110.9 t	4.62 (1H, br s, H-30*a*) 4.98 (1H, br s, H-30*b*)

All assignments of ^{1}H and ^{13}C signals were made by ^{1}H–^{1}H COSY(Correlation Spectroscopy), HMQC (^{1}H-Detected Multiple Quantum Coherrence Spectrum) and HMBC (^{1}H-Detected Multiple-bond Heteronuclear Multiple Quantum Coherrence Spectrum) spectra. *a)* Overlapped signals.

as illustrated in Table 1. Signals due to two tertiary methyl groups appeared at δ 1.80 and 1.88, and four exomethylene protons with geminal coupling suggested the presence of an isopropenyl group. Moreover, a total of thirty carbon signals observed in the ^{13}C-NMR spectrum (Table 1) indicated the presence of two carboxyl, two disubstituted double bonds, three oxygen-bearing methine carbons, five methine carbons, seven methylene, and five methyl carbons. The ^{13}C-NMR data of **2** were also very similar to that of **3**, except for signals due to the DE ring moiety. One methylene carbon signal at δ 37.3 in **3** was replaced by one oxygen-bearing methine carbon signal at δ 75.2 in **2**. The position of one oxygen-bearing methine carbon was deduced at C-22 by comparison of chemical shifts of the ^{13}C-NMR data of **2** with that of **3**: significant downfield shifts at C-21 (10.8 ppm) and C-17 (6.1 ppm) and an upfield shift at C-16 (5.7 ppm). Moreover, this location was verified by ^{1}H-detected multiple-bond heteronuclear quantum coherrence spectrum (HMBC), that is, one oxygen-bearing methine proton at δ 4.71 (1H, d, J= 3.2 Hz) had cross peaks with C-18, C-19 and C-28, and the configuration at H-21 was determined to be β scince H-21 possessed cross peaks with H-19β, not with H-18α, in the nuclear Overhauser and exchange spectroscopy (NOESY). Therefore, hydroxylation occurred at C-22 with an α-configuration, and **2** was characterized as 22α-hydroxychiisanogenin.

To the best of our knowledge, **1** was a new compound and **2** was isolated for the first time from a natural source, although the latter had previously been obtained as an enzymatically hydrolyzed artifact from 22α-hydroxychiisanoside.[6)]

Experimental

Melting points (uncorrected) were measured using a Boetius micromelting point apparatus. Optical rotations were determined on a JASCO DIP-1000 KUY polarimeter (l=0.5). IR spectra were obtained with a Hitachi 270-30 type spectrophotometer. FAB-MS were obtained in a glycerol matrix in the positive and negative ion mode using JEOL JMS-DX300 and JMS-DX303HF instruments. NMR spectra were measured in pyridine-d_5 on a JEOL λ-400 spectrometer, and chemical shifts were relative to tetramethylsilane (TMS). Column chromatography (CC) was carried out on silica gel 60 (0.040—0.063 mm, Merck). TLC was performed on precoated silica-gel $60F_{254}$ (Merck) and RP-$18F_{254S}$ plates (Merck).

Plant Material The leaves of *A. divaricatus* var. *albeofructus* were harvested at Cheonan-gun, Chungcheongnam-do Province of Korea, in September 1995 and were botanically identified by one of the authors, Prof. Yook, C. S.; the specimen has been deposited in the Herbarium of the College of Pharmacy, Kyung-Hee University.

Isolation The dried leaves of *A. divaricatus* var. *albeofructus* (500 g) were repeatedly extracted with 70% MeOH to give an extract (121 g), a part of which (37 g) was chromatographed on Diaion HP-20P (Mitsubishi Chem.

Ind. Co., Ltd., Japan) by elution with H_2O, 20%, 40%, 60%, 80% MeOH and MeOH, succesively. A fraction eluted with 80% MeOH was subsequently chromatographed on silica gel (Merck Co.) using the gradient elution of $CHCl_3$–MeOH–H_2O (10 : 1 : 0→7 : 3 : 0.5) to give six fractions. Fraction 1 was chromatographed on a reverse phase column, Chromatorex ODS (30—50 μm, Fuji Silysia Chem. Ind. Co., Ltd., Japan), using gradient elution from 65% MeOH to 80% MeOH to give **1** (32 mg) and **2** (610 mg).

24-Hydroxychiisanogenin (**1**): Colorless needles, mp 250—252 °C (from MeOH); $[\alpha]_D^{28}$ +61.0°(c=0.30 in MeOH); IR ν_{max} (KBr) cm^{-1}: 3425 (OH), 2947 (aliphatic CH), 1711 (carbonyl), 1643 (C=C); negative FAB-MS *m/z*; 499 $[M-H]^-$; ^1H- and ^{13}C-NMR: see Table 1.

22α-Hydroxychiisanogenin (**2**): Colorless needles, mp 243—245 °C (from MeOH); $[\alpha]_D^{28}$ +92.1°(c=1.03 in MeOH); IR ν_{max} (KBr) cm^{-1}: 3462, 3377 (OH), 2942 (aliphatic CH), 1697 (carbonyl), 1643 (C=C); negative FAB-MS *m/z*; 499 $[M-H]^-$; ^1H- and ^{13}C-NMR: see Table 1.

Acknowledgements The authors would like to thank Dr. Dong-Hyuk Shin of Dong-Wha Pharm. Ind. Co., Ltd. in Korea for NMR measurements.

Reference

1) Oh O. J., Chang S. Y., Kim T. H., Yang K. S., Yook C. S., Park S. Y, Nohara T., *Natural Medicines*, **54**, 29—32 (2000).
2) Yook C. S., Leem J. Y., Hahn D. R.. The abstract papers of The 4th International Symposium of Plant Biosystematics, Biological Approaches and Evolutionary Trends in Plants, Kyoto, Japan, 1993, pp. 53—54.
3) Yook C. S., Kim I. H., Hahn D. R., Nohara T., Chang S. Y., *Phytochemistry*, **49**, 839—843 (1998).
4) Chang S. Y., Yook C. S., Nohara T., *Phytochemistry*, **50**, 1369—1374 (1999).
5) Chang S. Y., Yook C. S., Nohara T., *Chem. Pharm. Bull.*, **46**, 163—165 (1998).
6) Shirasuna K., Miyakoshi M., Mimoto S., Isoda S., Satoh Y., Hirai Y., Ida Y., Shoji J., *Phytochemistry*, **45**, 579—584 (1997).

The '2+1' Construction of Homooxacalix[3]arenes Possessing Different Substituents on Their Upper Rims

Kazunori TSUBAKI, Koichiro MUKOYOSHI, Tadamune OTSUBO, and Kaoru FUJI*

Institute for Chemical Research, Kyoto University, Uji, Kyoto 611–0011, Japan.
Received January 13, 2000; accepted February 7, 2000

Several homooxacalix[3]arenes possessing different substituents on their upper rims were synthesized in yields of 7—20% by a condensation reaction between the *p*-substituted phenol dimer and monomer under acidic high-dilution conditions.

Key words homooxacalix[3]arene; host compound; molecular recognition; calixarene

Calixarenes have been extensively investigated in supramolecular and molecular recognition chemistry over the past two decades.[1] In contrast to calixarenes, homooxacalix[3]arenes have received little attention despite their unique structural features, such as a cavity composed of an 18-membered ring, C_3-symmetry, and a limited number of possible conformations (*i.e.* cone and partial cone).[2] Homooxacalix[3]arenes are dissymmetric molecules with unique features, when the three substituents at the upper rim are different and the conformational mobility between the cone and the partial cone is restricted. Only a few methods for synthesizing homooxacalix[3]arenes, involving cyclotrimerization of 2,6-bis-(hydroxymethyl)phenols as a monomer unit, have been reported.[3—5] Although this method is a very simple one-step procedure for these interesting macrocycles, a serious drawback is that it can provide only homooxacalix[3]arenes with identical substituents on their upper rims. Recently, we reported a stepwise construction of homooxacalix[3]arenes based on cyclization of the corresponding linear trimers.[6] Although this method is the first synthetic pathway to homooxacalix[3]arenes bearing different substituents on their upper rims, many reaction steps are required to obtain the desired molecule. A low overall yield is also unavoidable. In this paper, we report an alternative method for synthesizing a variety of homooxacalix[3]arenes with different substituents on their upper rims based on the condensation reaction between *p*-substituted phenol dimers and a monomer under acidic high-dilution conditions.

The known acetonides **2**,[6,7] prepared from 4-substituted 2,6-bis-(hydroxymethyl)-phenols **1**,[5,6,8] were chlorinated with CCl_4–PPh_3 to yield the corresponding benzylchlorides **3**. We previously reported that acetonides **2** were converted to the benzylbromides with CBr_4–PPh_3,[6] but it was difficult to separate the benzylbromide from CBr_4. The replacement of CBr_4 with CCl_4 gave better yields of the corresponding chloride. Alkylation of **2** with 1.1 eq of chlorides **3** gave the corresponding dimers **4**—**9** in good yields, as shown in Chart 1.

Using dimers **4**—**9** and monomer **1** as coupling components, homooxacalix[3]arenes **10**—**19**, with different substituents on their upper rims, were synthesized. A mixture of the dimer, 1.1 eq of monomer, 5 eq of $KClO_4$ and a catalytic amount of $HClO_4$[9] in 1,2-dimethoxyethane (DME) were stirred under high-dilution conditions at room temperature for 2 d to afford the desired homooxacalix[3]arenes in 7—20% yields. The results of the cyclization to a variety of homooxacalix[3]arenes **10**—**19** are summarized in Table 1. The mechanism of this condensation may be similar to that postulated by Hampton and co-workers.[5]

In general, the present synthetic route to homooxacalix[3]arenes with different substituents on their upper rims gives a better yield than that involving cyclization of the linear trimer. For example, **19** was synthesized in 6 steps in 12.4% overall yield from **1** through the '2+1' condensation route, but in 2.3% overall yield in 9 steps by the latter route.[6]

In conclusion, we present a method for synthesizing a vari-

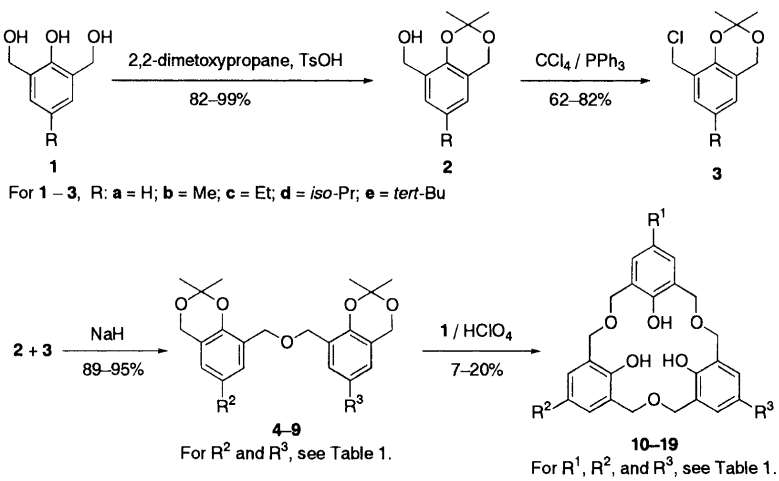

Chart 1

* To whom correspondence should be addressed. e-mail:
© 2000 Pharmaceutical Society of Japan

Table 1. The '2+1' Cyclization to the Homooxacalix[3]arenes

Entry	Monomer	Dimer	R^1	R^2	R^3	Product	Yield, %
1	**1a**	**4**	H	Me	Et	**10**[a]	8
2	**1a**	**5**	H	Me	*iso*-Pr	**11**	9
3	**1a**	**6**	H	Me	*tert*-Bu	**12**	9
4	**1a**	**7**	H	Et	*iso*-Pr	**13**	10
5	**1a**	**8**	H	Et	*tert*-Bu	**14**	10
6	**1a**	**9**	H	*iso*-Pr	*tert*-Bu	**15**	7
7	**1b**	**7**	Me	Et	*iso*-Pr	**16**	14
8	**1b**	**8**	Me	Et	*tert*-Bu	**17**	16
9	**1b**	**9**	Me	*iso*-Pr	*tert*-Bu	**18**	13
10	**1c**	**9**	Et	*iso*-Pr	*tert*-Bu	**19**[a]	20

a) Known, see ref. 6.

ety of homooxacalix[3]arenes with different substituents on their upper rims, using a '2+1' fragmentation condensation reaction. The present method should be useful for the synthesis of chiral homooxacalix[3]arene derivatives, and might contribute to the field of host–guest chemistry.

Experimental

General Melting points are uncorrected. ^{1}H-NMR spectra were taken at 200 MHz in $CDCl_3$ with chemical shifts being reported as δ ppm from tetramethylsilane as an internal standard and coupling constants are expressed in hertz. All extractive organic solutions were dried over anhydrous sodium sulfate. Flash column chromatography was carried out with silica-gel 60 spherical (40—100 μm).

General Procedure for the Preparation of Benzylchlorides 3 The conversion of the acetonide **2c** to the benzylchloride **3c** is typical. A solution of the acetonide **2c** (100 mg, 0.45 mmol) and triphenylphosphine (141 mg, 0.54 mmol) in carbon tetrachloride (2 ml) was refluxed for 4 h. Triphenylphosphine (23.6 mg, 0.09 mmol) and carbon tetrachloride (3 ml) was added to the reaction mixture and further refluxed for 14 h. The solution was evaporated under reduced pressure. Ether was added to the residue and the resulting suspension was filtered to remove triphenylphosphine oxide. The filtrate was evaporated under reduced pressure and the residue was purified by preparative TLC on silica-gel with hexane/EtOAc=20/1 as an eluent to afford the benzylchloride **3c** (88.5 mg, 82%). IR (neat) cm^{-1}: 2964, 1485, 1268, 1135. ^{1}H-NMR ($CDCl_3$) δ: 1.20 (3H, t, J=7.6), 1.55 (6H, s), 2.56 (2H, q, J=7.6), 4.59 (2H, s), 4.83 (2H, s), 6.78 (1H, br s), 7.07 (1H, br s). HR-MS: Calcd for $C_{13}H_{17}Cl^{35}O_2$ (M^+) 240.0917. Found: 240.0921, Calcd for $C_{13}H_{17}Cl^{37}O_2$ (M^+) 242.0888. Found: 242.0883. *Anal.* Calcd for $C_{13}H_{17}ClO_2$: C, 64.86; H, 7.12. Found: C, 64.72; H, 6.98.

3d: Yield: 62%. IR (neat) cm^{-1}: 2960, 1485, 1268, 1131. ^{1}H-NMR ($CDCl_3$) δ: 1.21 (6H, d, J=6.9), 1.57 (6H, s), 2.82 (1H, hep, J=6.9), 4.60 (2H, s), 4.83 (2H, s), 6.80 (1H, br s), 7.09 (1H, br s). HR-MS: Calcd for $C_{14}H_{19}Cl^{35}O_2$ (M^+) 254.1074. Found: 254.1062.

3e: Yield: 78%. mp 55—57 °C; IR (KBr) cm^{-1}: 2964, 1485, 1375, 1272. ^{1}H-NMR ($CDCl_3$) δ: 1.28 (9H, s), 1.56 (6H, s), 4.61 (2H, s), 4.84 (2H, s), 6.95 (1H, d, J=2.3), 7.25 (1H, d, J=2.3). HR-MS: Calcd for $C_{15}H_{21}Cl^{35}O_2$ (M^+) 268.2130. Found: 268.1210. *Anal.* Calcd for $C_{15}H_{21}ClO_2$: C, 67.03; H, 7.88. Found: C, 67.15; H, 7.93.

General Procedure for the Preparation of Dimers 4—9. The preparation of dimer **4** from **2b** and **3c** is typical. To a solution of the acetonide **2b** (9.8 g, 46.6 mmol) in dimethylformamide (DMF, 65 ml) was added portionwise sodium hydride (60% dispersion in mineral oil, 2.1 g, 52.5 mmol) at 0 °C and the suspension was further stirred for 10 min. A solution of the benzylchloride **3c** (12.3 g, 51.1 mmol) in DMF (10 ml) was added dropwise to the suspension, and the resulting mixture was stirred for 2 d at ambient temperature. The reaction mixture was poured into ice-cold water and extracted with EtOAc. The organic layer was washed with water (4 times), brine, and dried over $MgSO_4$. Concentration of the extract under reduced pressure gave the residue, which was subjected to silica-gel column chromatography with hexane/EtOAc=5/1 to afford dimer **4** (17.2 g, 89%). IR (neat) cm^{-1}: 2993, 2856, 1483, 1246, 1137. ^{1}H-NMR ($CDCl_3$) δ: 1.20 (3H, t, J=7.7), 1.52 (12H, s), 2.27 (3H, s), 2.58 (2H, q, J=7.7), 4.59 (4H, s), 4.82 (2H, s), 4.84 (2H, s), 6.72 (2H, br s), 7.17 (2H, br s). HR-MS: Calcd for $C_{25}H_{32}O_5$ (M^+) 412.2250. Found: 412.2241. *Anal.* Calcd for $C_{25}H_{32}O_5$: C, 72.79; H, 7.82. Found: C, 72.81; H, 7.84.

5: Yield: 92%. IR (neat) cm^{-1}: 2957, 1484, 1373, 1246, 1140. ^{1}H-NMR ($CDCl_3$) δ: 1.21 (6H, d, J=6.9), 1.53 (12H, s), 2.27 (3H, s), 2.84 (1H, hep, J=6.9), 4.59 (4H, s), 4.82 (2H, s), 4.84 (2H, s), 6.71 (1H, br s), 6.75 (1H, br s), 7.16 (1H, br s), 7.20 (1H, br s). HR-MS: Calcd for $C_{26}H_{34}O_5$ (M^+) 426.2406. Found: 426.2388. *Anal.* Calcd for $C_{26}H_{34}O_5$: C, 73.21; H, 8.03. Found: C, 73.16; H, 8.02.

6: Yield: 95%. IR (neat) cm^{-1}: 2953, 2861, 1484, 1272, 1140. ^{1}H-NMR ($CDCl_3$) δ: 1.29 (9H, s), 1.52 (6H, s), 1.53 (6H, s), 2.27 (3H, s), 4.59 (2H, s), 4.60 (2H, s), 4.82 (2H, s), 4.85 (2H, s), 6.71 (1H, br s), 6.90 (1H, br s), 7.18 (1H, br s), 7.36 (1H, br s). HR-MS: Calcd for $C_{27}H_{36}O_5$ (M^+) 440.2563. Found: 440.2553. *Anal.* Calcd for $C_{27}H_{36}O_5$: C, 73.61; H, 8.24. Found: C, 73.59; H, 8.19.

7: Yield: 91%. mp 57—59 °C; IR (KBr) cm^{-1}: 2960, 1486, 1375, 1250, 1125. ^{1}H-NMR ($CDCl_3$) δ: 1.20 (3H, t, J=7.6), 1.21 (6H, d, J=6.8), 1.53 (12H, s), 2.57 (2H, q, J=7.6), 2.84 (1H, hep, J=6.8), 4.60 (4H, s), 4.84 (4H, s), 6.73 (2H, br s), 7.20 (2H, br s). HR-MS: Calcd for $C_{27}H_{36}O_5$ (M^+) 440.2563. Found: 440.2566. *Anal.* Calcd for $C_{27}H_{36}O_5$: C, 73.61; H, 8.24. Found: C, 73.37; H, 8.25.

8: Yield: 95%. mp 91—93 °C; IR (KBr) cm^{-1}: 2963, 1486, 1375, 1273, 1127. ^{1}H-NMR ($CDCl_3$) δ: 1.20 (3H, t, J=7.6), 1.29 (9H, s), 1.52 (6H, s), 1.53 (6H, s), 2.57 (2H, q, J=7.6), 4.61 (4H, s), 4.84 (2H, s), 4.85 (2H, s), 6.72 (1H, br s), 6.89 (1H, br s), 7.20 (1H, br s), 7.37 (1H, br s). HR-MS: Calcd for $C_{28}H_{38}O_5$ (M^+) 454.2719. Found: 454.2682. *Anal.* Calcd for $C_{28}H_{38}O_5$: C, 73.98; H, 8.42. Found: C, 73.97; H, 8.45.

9: Yield: 93%. mp 145—147 °C; IR (neat) cm^{-1}: 2958, 1486, 1375, 1273, 1135. ^{1}H-NMR ($CDCl_3$) δ: 1.21 (6H, d, J=6.8), 1.29 (9H, s), 1.53 (12H, s), 2.83 (1H, hep, J=6.8), 4.61 (2H, s), 4.62 (2H, s), 4.84 (2H, s), 4.85 (2H, s), 6.75 (1H, br s), 6.89 (1H, br s), 7.23 (1H, br s), 7.39 (1H, br s). HR-MS: Calcd for $C_{29}H_{40}O_5$ (M^+) 468.2876. Found: 468.2873. *Anal.* Calcd for $C_{29}H_{40}O_5$: C, 74.33; H, 8.60. Found: C, 74.17; H, 8.63.

General Procedure for the Preparation of Homooxacalix[3]arenes 10—19 To a stirred solution of dimer (1.00 g), monomer (1.1 eq) and $KClO_4$ (5.0 eq) in DME (200 ml, dried over molecular sieves 4A) was added 70% $HClO_4$[9] (50 μl for 1.00 g of dimer). The reaction mixture was stirred at room temperature for 2 d and then K_2CO_3 (0.3 g) was added to the solution. Most of the DME was evaporated under reduced pressure, diluted with EtOAc and washed with 1 N HCl aq, water (2 times), brine and dried over Na_2SO_4. The solvent was evaporated under reduced pressure and the residue was roughly purified by column chromatography on silica-gel (100 ml) with $CHCl_3$ as an eluent and further purified by column chromatography on silica-gel (70 ml) with hexane/EtOAc=5/1 as an eluent followed by recycling preparative HPLC (Japan Analytical Industry Co., Ltd. LC-908) using JAIGEL-1H (20×600 mm) and JAIGEL-2H (20×600 mm) columns under conditions of 3.5 ml/min of flow rate with $CHCl_3$ detected by UV (254 nm) and RI (refractive index) to afford the desired homooxacalix[3]arene.

11: mp 138—139 °C (from MeOH); IR (KBr) cm^{-1}: 3338, 2865, 1614, 1488, 1075. ^{1}H-NMR ($CDCl_3$) δ: 1.17 (6H, d, J=6.9), 2.22 (3H, s), 2.79 (1H, hep, J=6.9), 4.68—4.72 (12H, m), 6.78 (1H, t, J=7.4), 6.93 (2H, s), 6.98 (2H, s), 7.11 (2H, d, J=7.4), 8.56 (2H, s), 8.80 (1H, s). HR-MS: Calcd for $C_{28}H_{32}O_6$ (M^+) 464.2199. Found: 464.2187. *Anal.* Calcd for $C_{28}H_{32}O_6$: C, 72.39; H, 6.94. Found: C, 72.56; H, 7.03.

12: mp 91—92 °C (from MeOH–H_2O); IR (KBr) cm^{-1}: 3353, 2955, 1603, 1488, 1075. ^{1}H-NMR ($CDCl_3$) δ: 1.25 (9H, s), 2.21 (3H, s), 4.65—4.75 (12H, m), 6.78 (1H, t, J=7.6), 6.93 (2H, s), 7.11 (2H, d, J=7.6), 7.13 (2H, s), 8.57 (2H, s), 8.80 (1H, s). HR-MS: Calcd for $C_{29}H_{34}O_6$ (M^+) 478.2355. Found: 478.2338. *Anal.* Calcd for $C_{29}H_{34}O_6$: C, 72.78; H, 7.16. Found: C, 72.78; H, 7.21.

13: mp 63—66 °C (from $CHCl_3$–MeOH); IR (KBr) cm^{-1}: 3343, 2959, 1614, 1487, 1076. ^{1}H-NMR ($CDCl_3$) δ: 1.17 (6H, d, J=7.1), 1.17 (3H, t, J=7.3), 2.52 (2H, q, J=7.3), 2.79 (1H, hep, J=7.1), 4.71 (12H, br s), 6.78 (1H, t, J=7.4), 6.95 (2H, s), 6.98 (2H, s), 7.12 (2H, d, J=7.4), 8.57 (2H, s), 8.80 (1H, s). HR-MS: Calcd for $C_{29}H_{34}O_6$ (M^+) 478.2355. Found: 478.2357. *Anal.* Calcd for $C_{29}H_{34}O_6$: C, 72.78; H, 7.16. Found: C, 72.50; H, 7.11.

14: mp 127—129 °C (from MeOH); IR (KBr) cm^{-1}: 3351, 2960, 1602, 1489, 1076. ^{1}H-NMR ($CDCl_3$) δ: 1.15 (3H, t, J=7.6), 1.25 (9H, s), 2.52 (2H, q, J=7.6), 4.70 (4H, s), 4.71 (4H, s), 4.72 (4H, s), 6.78 (1H, t, J=7.3), 6.95 (2H, s), 7.12 (2H, d, J=7.3), 7.14 (2H, s), 8.58 (2H, s), 8.81 (1H, s). HR-MS: Calcd for $C_{30}H_{36}O_6$ (M^+) 492.2512. Found: 492.2537. *Anal.* Calcd for $C_{30}H_{36}O_6$: C, 73.15; H, 7.37. Found: C, 72.95; H, 7.27.

15: mp 76—78 °C (from MeOH–H_2O); IR (KBr) cm^{-1}: 3349, 2957, 1603, 1488, 1074. ^{1}H-NMR ($CDCl_3$) δ: 1.16 (6H, d, J=6.8), 1.24 (9H, s), 2.79 (1H, hep, J=6.8), 4.72 (12H, br s), 6.78 (1H, t, J=7.8), 6.98 (2H, s), 7.12 (2H, d, J=7.8), 7.13 (2H, s), 8.58 (2H, s), 8.81 (1H, s). HR-MS: Calcd for $C_{31}H_{38}O_6$ (M^+) 506.2668. Found: 506.2687. *Anal.* Calcd for $C_{31}H_{38}O_6$: C,

73.49; H, 7.56. Found: C, 73.75; H, 7.80.

16: mp 79—81 °C (from $CHCl_3$–MeOH); IR (KBr) cm^{-1}: 3351, 2959, 1613, 1487, 1082. ^{1}H-NMR ($CDCl_3$) δ: 1.16 (6H, d, J=6.8), 1.10—1.30 (3H, m), 2.21 (3H, s), 2.51 (2H, q, J=7.8), 2.78 (1H, hep, J=6.8), 4.65—4.70 (12H, m), 6.92 (2H, s), 6.94 (2H, s), 6.97 (2H, s), 8.57 (3H, s). HR-MS: Calcd for $C_{30}H_{36}O_6$ (M^+) 492.2512. Found: 492.2502. *Anal.* Calcd for $C_{30}H_{36}O_6$: C, 73.15; H, 7.37. Found: C, 73.14; H, 7.33.

17: mp 85—87 °C (from MeOH–H_2O); IR (KBr) cm^{-1}: 3352, 2960, 1612, 1488, 1081. ^{1}H-NMR ($CDCl_3$) δ: 1.14 (3H, t, J=7.6), 1.24 (9H, s), 2.21 (3H, s), 2.51 (2H, q, J=7.6), 4.67 (4H, s), 4.68 (4H, s), 4.70 (4H, s), 6.92 (2H, s), 6.95 (2H, s), 7.13 (2H, s), 8.57 (3H, s). HR-MS: Calcd for $C_{31}H_{38}O_6$ (M^+) 506.2668. Found: 506.2684. *Anal.* Calcd for $C_{31}H_{38}O_6$: C, 73.49; H, 7.56. Found: C, 73.61; H, 7.69.

18: mp 83—86 °C (from MeOH–H_2O); IR (KBr) cm^{-1}: 3353, 2957, 1612, 1488, 1081. ^{1}H-NMR ($CDCl_3$) δ: 1.16 (6H, d, J=6.9), 1.24 (9H, s), 2.21 (3H, s), 2.79 (1H, hep, J=6.9), 4.65—4.75 (12H, m), 6.93 (2H, s), 6.97 (2H, s), 7.13 (2H, s), 8.57 (3H, s). HR-MS: Calcd for $C_{32}H_{40}O_6$ (M^+) 520.2825. Found: 520.2803.

References and Notes

1) For reviews on calixarenes; *a*) Gutsche, C. D. "Calixarenes" the Royal Society of Chemistry; Cambridge; *b*) Gutsche, C. D. "Calixarenes Revisited" the Royal Society of Chemistry, 1998.
2) a) Araki K., Inaba K., Otsuka H., Shinkai S., *Tetrahedron*, **49**, 9465—9478 (1993); *b*) Araki K., Hashimoto N., Otsuka H., Shinkai S., *J. Org. Chem.*, **58**, 5958—5963 (1993); *c*) Takeshita M., Shinkai S., *Chem. Lett.*, **1994**, 125—128; *d*) Matsumoto H., Nishio S., Takeshita M., Shinkai S., *Tetrahedron*, **51**, 4647—4654 (1995); *e*) Masci B., *ibid.*, **51**, 5459—5464 (1995); *f*) Araki K., Inada K., Shinkai S., *Angew. Chem. Int. Ed. Engl.*, **35**, 72—74 (1996); *g*) Ikeda A., Suzuki Y., Yoshimura M., Shinkai S., *Tetrahedron*, **54**, 2497—2508 (1998); *h*) Ohkanda J., Shibui H., Katoh A., *Chem. Commun.*, **1998**, 375—376; *i*) Tsubaki K., Tanaka K., Kinoshita T., Fuji K., *ibid.*, **1998**, 895—896.
3) Dhawan B., Gutsche C. D., *J. Org. Chem.*, **48**, 1536—1539 (1983).
4) Zerr P., Mussrabi M., Vicens J., *Tetrahedron Lett.*, **32**, 1879—1880 (1991).
5) Hampton P. D., Bencze Z., Tong W., Daitch C. E., *J. Org. Chem.*, **59**, 4838—4843 (1994).
6) Tsubaki K., Otsubo T., Tanaka K., Fuji K., Kinoshita T., *J. Org. Chem.*, **63**, 3260—3265 (1998).
7) Freeman J. H., *J. Am. Chem. Soc.*, **74**, 6257—6260 (1952).
8) Clark D. A., Riccardis F. D., Nicolaou K. C., *Tetrahedron*, **50**, 11391—11426 (1994).
9) Particular care should be taken when handling perchloric acid and related compounds. Especially, it must be kept in mind that heating the reaction mixture might cause a hazardous explosion.

α-Bromo-α,α-difluoroallyl Derivatives as Synthetic Intermediate: Nucleophilic Substitution of α-Bromo-α,α-difluoroallyl Derivatives in the Presence of Palladium Catalysts

Masayuki KIRIHARA,* Tomofumi TAKUWA, Maiko OKUMURA, Takahiro WAKIKAWA, Hiroki TAKAHATA, Takefumi MOMOSE, Yoshio TAKEUCHI, and Hideo NEMOTO*

Faculty of Pharmaceutical Sciences, Toyama Medical and Pharmaceutical University, Sugitani 2630, Toyama 930–0194, Japan. Received January 21, 2000; accepted March 21, 2000

The palladium catalyzed nucleophilic substitution of α-bromo-α,α-difluoroallyl derivatives turned out to be an efficient method for the preparation of several fluorinated organic molecules. Several soft carbon nucleophiles regioselectively reacted with 3-bromo-3,3-difluoropropene (BDFP) to give the 3-substituted 1,1-difluoroalkenes. Phenylzinc chloride and tributylphenyltin afforded 1-fluoro-1,3-diphenylpropene. The radical bromination of 3-substituted 1,1-difluoroalkenes provided 1-substituted BDFPs, and a 1-substituted BDFP reacted with carbon nucleophiles to give 1,3-disubstituted 3,3-difluoroalkenes. For the reaction of nitrogen nucleophiles with BDFP, an amine and the sodium salts of the carbamates reacted with BDFP at the γ-position. However, the sodium salts of the sulfoneamide predominantly attacked at the α-position.

Key words 3-bromo-3,3-difluoropropene; α-bromo-α,α-difluoroallyl derivative; difluoroallyl-palladium

The introduction of a *gem*-difluoromethylene moiety (CF_2) into organic molecules has provided us with attractive results in a wide range of application fields.[1] This moiety has been recognized as an isopolar-isosteric substitute for oxygen and used as one strategy for the modification of biologically active compounds.[2] Some building blocks have been developed to introduce CF_2 into organic compounds.[1] Among them, 3-bromo-3,3-difluoropropene (BDFP) and its derivatives (**1**) are some of the most important ones. The *gem*-difluoroallylic metal species, available by treatment of **1** with alkyllithium,[3] zinc-metal[4] or indium-metal,[5] react with carbonyl compounds to afford *gem*-difluorohomoallyl alcohols. Tellier *et al.* reported that the treatment of **1** with organometallic reagents in the presence of copper and lithium salts gives various 1,1-difluoroalkenes.[6] (Chart 1). This method is quite important because 1,1-difluoroalkenes are critical for certain mechanism-based enzyme inhibitors, and they can function as bioisosteres for aldehydes and ketones.[2]

In this paper, we report that α-bromo-α,α-difluoroallyl derivatives (**1**) are versatile fluorinated building blocks through palladium catalyzed nucleophilic substitutions (Chart 2).

The 1,1-difluoroalkenes were obtained from the reaction of BDFP (**1a**) with several soft nucleophiles in the presence of 4 mol% palladium acetate and 16 mol% triphenylphosphine. These results are summarized in Table 1. Interestingly, the 3-substituted 1,1-difluoroalkenes (**2**) (γ-substitution) were the only isolated products, and the 3-substituted 3,3-difluoroalkenes (**2'**) (α-substitution) were not obtained in all cases. This reaction might be an excellent method for synthesizing the 1,1-difluoroalkenes.

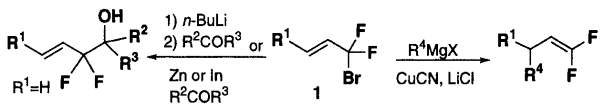

Chart 1

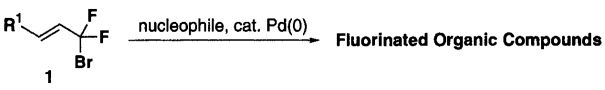

Chart 2

The reaction might proceed through the (difluoroallyl)palladium complex (**4**), which is formed by the oxidative addition of **1** to Pd(0) (generated from palladium acetate and triphenylphosphine), as a reaction intermediate (Chart 3). Shi *et al.* reported that the reaction of the 3,3-difluoroallyl acetates with nucleophiles in the presence of Pd(0) catalysts caused γ-substitution which produced the 1,1-difluoroalkenes and also postulated a similar mechanism.[7]

We then examined the reaction of **1a** with phenylzinc chloride or tributylphenyltin in the presence of the Pd(0) catalyst. In these cases, we did not obtain **2e** but 1-fluoro-1,3-diphenylpropene (**5**). These results are consistent with the reaction of the 3,3-difluoroallyl acetates with nucleophiles in

Table 1.

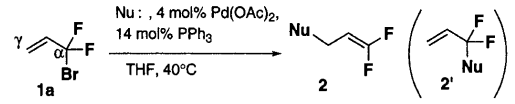

Entry	Nucleophile	Products
1	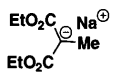	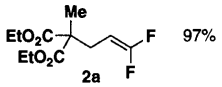 97%
2	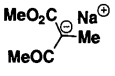	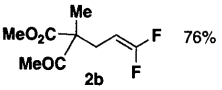 76%
3	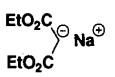	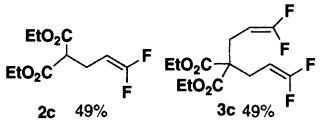
4	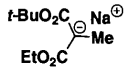	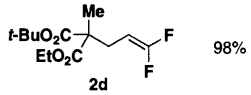 98%

2c 49% 3c 49%

2a 2b 2d

* To whom correspondence should be addressed. e-mail: kirihara@ms.toyama-mpu.ac.jp

© 2000 Pharmaceutical Society of Japan

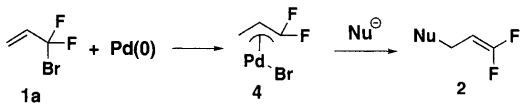

Chart 3

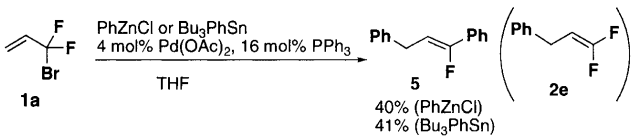

Chart 4

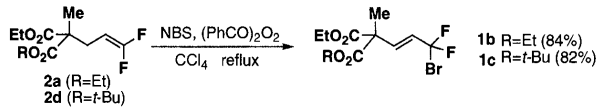

Chart 5

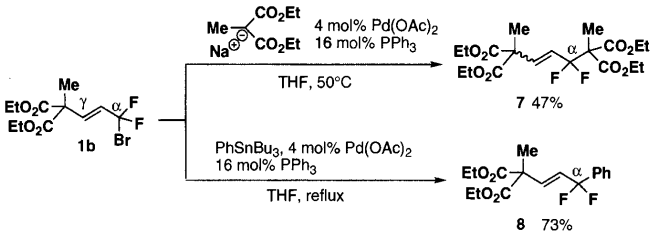

Chart 6

the presence of Pd(0) catalysts.[7] Phenylzinc chloride or tributylphenyltin reacted with allylpalladium at its fluorinated terminus to afford the 3,3-difluoro-3-phenylpropene (**6**) and a further *SN*2′ reaction of **6** with another equivalent of phenylzinc chloride or tributylphenyltin afforded **5** (Chart 4).

Next, we examined the radical bromination of **2** and found that 1-substituted BDFPs (**1b**, **c**) were selectively obtained (Chart 5).[8,9]

Interestingly, the palladium catalyzed nucleophilic substitution of **1b** afforded the 1,3-disubstituted 3,3-difluoroalkenes (**7**, **8**) (α-substitution) as the sole products in these cases (Chart 6).[10]

On the basis of these results, the steric effect plays an important role in the regioselectivity of this reaction. Although Shi *et al.* explained that the γ-selectivity of the nucleophilic substitution of **9** was only due to an electronic effect, the steric effect can not be ignored. There is the possibility that nucleophiles attack the less hindered carbon. For the reaction of tributylphenyltin, a further *SN*2′ reaction of **8** was prevented by the steric hindrance (Chart 7). Further investigation of the regioselectivity of the palladium-catalyzed nucleophilic substitution of **1** is currently in progress.

It is notable that the BDFP (**1a**) acts as the dication equivalent (**10**) in these successive reactions (Chart 8).

We then examined the reaction of **1** toward the several nitrogen nucleophiles in the presence of a palladium catalyst. As shown in Table 2, **1** regioselectively reacted with an

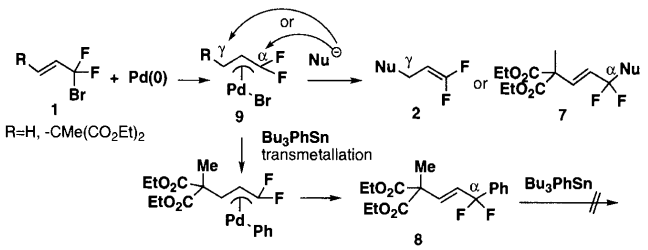

Chart 7

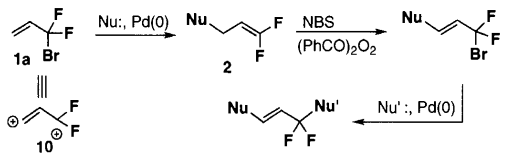

Chart 8

Table 2.

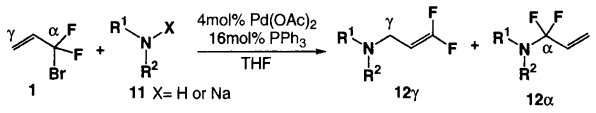

Entry	**11**	Products	Yield[a]
1	**11a**	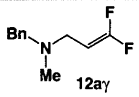 **12aγ**	75%
2	**11b**	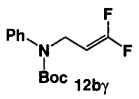 **12bγ**	71%
3	**11c**	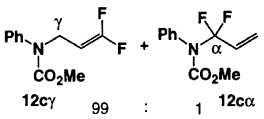 **12cγ** 99 : 1 **12cα**	83%
4	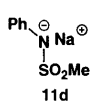 **11d**	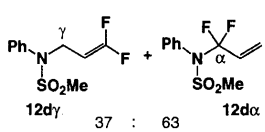 **12dγ** 37 : 63 **12dα**	86%
5	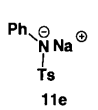 **11e**	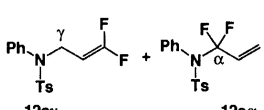 **12eγ** 21 : 79 **12eα**	100%

a) Combined yield.

amine and the sodium salt of the carbamates (entries 1—3) at its γ-position. Interestingly, the α-position of **1** was predominantly attacked in the cases of the sodium salts of the sulfoneamide (entries 4 and 5). The reason for these interesting regioselectivities still remains unknown.

In conclusion, we found that the α-bromo-α,α-difluoroallyl derivatives (**1**) are very important building blocks for the preparation of several fluorinated organic compounds (Chart 9).

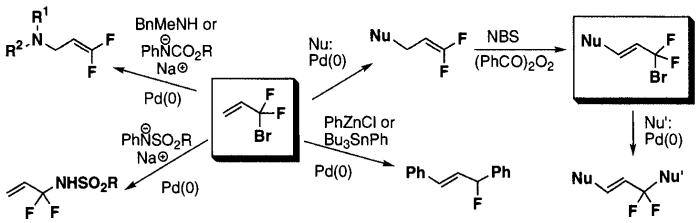

Chart 9

Experimental

The infrared spectra were measured using a Perkin–Elmer 1600 series Fourier transform (FT)-IR spectrophotometer. The ^{1}H- and ^{19}F-NMR spectra were obtained using a JEOL GX270, Varian Gemini 300 or Varian UNITY plus 500 instrument with tetramethylsilane (for ^{1}H) and chlorotrifluoromethane (for ^{19}F) as the internal standards. The mass spectra (MS) and high-resolution mass spectra (HR-MS) were measured on a JEOL JMS D-200 spectrometer. Column chromatography was performed on silica gel (Merck Kieselgel 60). Phenylzinc chloride was prepared according to the literature.[11]

General Procedure for the Palladium Catalyzed Nucleophilic Substitution of 1 To a solution of palladium acetate (9 mg, 0.04 mmol) and triphenylphosphine (42 mg, 0.16 mmol) in tetrahydrofuran (THF) (5 ml) was added **1** (1.00 mmol), and the mixture was stirred for 10 min at room temperature. A THF (1 ml) solution of a carbon nucleophile (2.00 mmol) was then added to the mixture and stirred for 2 h at 40 °C. Water (5 ml) was added to the mixture and the resulting mixture was extracted with dichloromethane (20 ml×3). The combined organic extract was dried over anhydrous magnesium sulfate, filtered, and the solvent was removed *in vacuo*. The residue was purified using chromatography on silica gel (*n*-hexane–ethyl acetate) to give **2**.

Diethyl 2-(3,3-Difluoroprop-2-enyl)isobutan-1,3-dioate (**2a**): A colorless oil. IR (neat) cm^{-1}: 1731. ^{1}H-NMR ($CDCl_3$) δ: 1.23 (6H, t, J=7.1 Hz), 1.38 (3H, s), 2.52 (2H, dt, J=8.3, 1.7 Hz), 4.07—4.23 (5H, m); ^{19}F-NMR ($CDCl_3$) δ: −85.77 (1F, d, J=40.7 Hz), −89.25 (1F, dd, J=40.7, 24.9 Hz). MS *m/z*: 250 (M^+). HR-MS Calcd for $C_{11}H_{16}F_2O_4$: 250.1016 (M^+). Found: 250.1002.

Methyl 2-Acetyl-5,5-difluoro-2-methylpent-4-enoate (**2b**): A colorless oil. IR (neat) cm^{-1}: 1748, 1717. ^{1}H-NMR ($CDCl_3$) δ: 1.28 (3H, s), 2.09 (3H, s), 2.32—2.56 (2H, m), 3.68 (3H, s), 4.04 (1H, dtd, J=24.0, 8.1, 2.5 Hz). ^{19}F-NMR ($CDCl_3$) δ: −85.54 (1F, d, J=39.8 Hz), −89.25 (1F, dd, J=39.8, 24.0 Hz). MS *m/z*: 206 (M^+). HR-MS Calcd for $C_9H_{12}F_2O_3$: 206.0754 (M^+). Found: 206.0755.

Diethyl 2-(3,3-Difluoroprop-2-enyl)propane-1,3-dioate (**2c**): A colorless oil. IR (neat) cm^{-1}: 1748. ^{1}H-NMR ($CDCl_3$) δ: 1.21 (6H, t, J=7.1 Hz), 2.50 (2H, td, J=7.4, 1.4 Hz), 4.10—4.25 (5H, m). ^{19}F-NMR ($CDCl_3$) δ: −86.30 (1F, dd, J=41.6, 6.5 Hz), −88.80 (1F, ddd, J=41.6, 25.0, 7.4 Hz). MS *m/z*: 236 (M^+). HR-MS Calcd for $C_{10}H_{14}F_2O_4$: 236.0824 (M^+). Found: 236.0837.

Diethyl 2,2-Di(3,3-difluoroprop-2-enyl)propane-1,3-dioate (**3c**): A colorless oil. IR (neat) cm^{-1}: 1747. ^{1}H-NMR ($CDCl_3$) δ: 1.23 (6H, t, J=7.1 Hz), 2.55 (4H, dt, J=8.4, 1.5 Hz), 4.00—4.22 (6H, m). ^{19}F-NMR ($CDCl_3$) δ: −85.00 (2F, d, J=39.8 Hz), −88.60 (1F, dd, J=39.8, 24.0 Hz). MS *m/z*: 312 (M^+). HR-MS Calcd for $C_{13}H_{16}F_4O_4$: 312.0985 (M^+). Found 312.0981.

tert-Butyl Ethyl 2-(3,3-Difluoroprop-2-enyl)isobutan-1,3-dioate (**2d**): A colorless oil. IR (neat) cm^{-1}: 1734; ^{1}H-NMR ($CDCl_3$) δ: 1.26 (3H, t, J=7.3 Hz), 1.36 (3H, s), 1.45 (9H, s), 2.50 (2H, d, J=8.4 Hz), 4.09—4.27 (3H, m); ^{19}F-NMR ($CDCl_3$) δ: −86.38—−86.70 (1F, m), −89.60—−90.00 (1F, m). MS *m/z*: 222 (M^++H−*tert*-Bu). HR-MS Calcd for $C_9H_{12}F_2O_4$: 222.0704 (M^++H−*tert*-Bu). Found: 222.0790.

(*Z*)-1-Fluoro-1,3-diphenylpropene (**5**): A colorless oil. IR (neat) cm^{-1}: 3030, 1482, 760, 738. ^{1}H-NMR ($CDCl_3$) δ: 3.56 (2H, dd, J=7.9, 1.7 Hz), 5.52 (1H, dt, J=36.1, 7.9 Hz), 7.20—7.44 (8H, m), 7.50—7.53 (2H, m); ^{19}F-NMR ($CDCl_3$) δ: −121.04 (1F d, J=39.1 Hz). MS *m/z*: 212 (M^+). HR-MS Calcd for $C_{15}H_{12}F$: 212.1001 (M^+). Found: 212.1006.

(3,3-Difluoroprop-2-enyl)methylbenzylamine (**12a**γ): A colorless oil. IR (neat) cm^{-1}: 1746. ^{1}H-NMR ($CDCl_3$) δ: 2.21 (3H, s), 3.06 (2H, dt, J=7.8, 1.7 Hz), 3.50 (2H, s), 4.40 (1H, dtd, J=24.8, 7.8, 2.5 Hz), 7.24—7.36 (5H, m). ^{19}F-NMR ($CDCl_3$) δ: −85.65 (1F, d, J=41.6 Hz), −88.54 (1F, dd, J=41.6, 24.8 Hz). MS *m/z*: 197 (M^+). HR-MS Calcd for $C_{11}H_{13}F_2N$: 197.1016 (M^+). Found: 197.1031.

N-Phenyl-*N*-(3,3-difluoroprop-2-enyl)methoxyformamide (**12b**γ): A colorless oil. IR (neat) cm^{-1}: 2978, 1746, 1700, 1392, 1367, 1251, 1166. ^{1}H-NMR ($CDCl_3$) δ: 1.36 (9H, s), 4.15 (2H, dt, J=7.3, 1.9 Hz), 4.31—4.46 (1H, m), 7.09—7.30 (5H, m). ^{19}F-NMR ($CDCl_3$) δ: −86.53 (1F, d, J=77.8 Hz), −87.98—−88.22 (1F, dd-like) . MS *m/z*: 269 (M^+). HR-MS Calcd for $C_{14}H_{17}F_2NO_2$: 269.1227 (M^+). Found: 269.1187.

A 99:1 mixture of *N*-Phenyl-*N*-(3,3-difluoroprop-2-enyl)methoxyformamide (**12c**γ) and *N*-Phenyl-*N*-(1,1-difluoroprop-2-enyl)methoxyformamide (**12c**α): A colorless oil. IR (neat) cm^{-1}: 2955, 1747, 1706, 1447, 1386, 1294, 697. ^{1}H-NMR ($CDCl_3$) δ: 3.70 (3H, s), 4.26 (2H, d, J=7.5 Hz), 4.39—4.54 (1H, dt-like), 7.15—7.64 (5H, m). ^{19}F-NMR ($CDCl_3$) δ: −74.87 (0.01F, d-like), −80.29 (0.01F, dd-like), −88.27 (0.99F, dd, J=37.9, 24.9 Hz), −86.35 (0.99F, d, J=37.9 Hz). MS *m/z*: 227 (M^+). HR-MS Calcd for $C_{11}H_{11}F_2NO_2$: 227.0758 (M^+). Found: 227.0740.

(3,3-Difluoroprop-2-enyl)(methylsulfonyl)phenylamine (**12d**γ): A colorless oil. IR (neat) cm^{-1}: 1748, 1734, 1653, 1559, 1154, 758, 668. ^{1}H-NMR ($CDCl_3$) δ: 2.90 (3H, s), 4.25—4.45 (3H, m), 7.29—7.40 (5H, m). ^{19}F-NMR ($CDCl_3$) δ: −84.65—−84.79 (1F, m), −87.34—−87.59 (1F, m). MS *m/z*: 247 (M^+). HR-MS Calcd for $C_{10}H_{11}F_2NO_2S$: 247.0479 (M^+). Found: 247.0511.

(1,1-Difluoroprop-2-enyl)(methylsulfonyl)phenylamine (**12d**α): A colorless oil. IR (neat) cm^{-1}: 3025, 1490, 1415, 1351, 1231, 1165, 1127, 978, 775, 756, 732, 694, 659. ^{1}H-NMR ($CDCl_3$) δ: 3.20 (3H, s), 5.45 (1H, d, J= 10.8 Hz), 5.74 (1H, dt, J=17.1, 2.0 Hz), 5.89—6.03 (1H, m), 7.33—7.46 (5H, m). ^{19}F-NMR ($CDCl_3$) δ: −72.86 (2F, d, J=9.3 Hz). MS *m/z*: 247 (M^+). HR-MS Calcd for $C_{10}H_{11}F_2NO_2S$: 247.0479 (M^+). Found: 247.0491.

A 21 : 79 mixture of (3,3-Difluoroprop-2-enyl)[(4-methylphenyl)sulfonyl]-phenylamine (**12e**γ) and (1,1-Difluoroprop-2-enyl)[(4-methylphenyl)sulfonyl]phenylamine (**12e**α): A colorless oil. IR (neat) cm^{-1}: 3064, 1747, 1700, 1684, 1653, 1597, 1559, 1489, 1453, 1368. ^{1}H-NMR ($CDCl_3$) δ: 2.43 (12/5H, s), 2.46 (3/5H, s), 4.17—4.34 (3/5H, m), 5.57—5.84 (8/5H, m), 6.39 (4/5H, dd, J=16.5, 1.6 Hz), 7.01—7.94 (9H, m). ^{19}F-NMR ($CDCl_3$) δ: −89.05—−89.01 (1.58F, d-like), −102.32—−105.42 (0.42F, m). MS *m/z*: 323 (M^+). HR-MS Calcd for $C_{16}H_{15}F_2NO_2S$: 323.0792 (M^+). Found: 323.0872.

General Procedure for the Radical Bromination of 2 A mixture of **2a** (1.00 g, 4.00 mmol), *N*-bromosuccinimide (NBS) (2.14 g, 12.0 mmol) and benzoyl peroxide (9.00 mg, 0.037 mmol) in carbon tetrachloride (20 ml) was refluxed under an inert atmosphere for 24 h. The reaction mixture was filtered and the resulting filtrate was concentrated *in vacuo*. The residue was purified by silica gel chromatography (*n*-hexane : ethyl acetate = 100 : 1) and gave **1b** (1.11 g, 84%).

(*E*)-Diethyl 2-(3-Bromo-3,3-difluoroprop-1-enyl)isobutane-1,3-dioate (**1b**): A pale yellow oil. IR (neat) cm^{-1}: 2985, 1736, 964. ^{1}H-NMR ($CDCl_3$) δ: 1.27 (3H, t, J=7.1Hz), 1.58 (3H, s), 4.23 (4H, q, J=7.1 Hz), 5.98 (1H, dt, J=15.9, 9.7 Hz), 6.66 (1H, dt, J=15.9, 2.3 Hz). ^{19}F-NMR ($CDCl_3$) δ: −45.88 (2F, dd, J=9.7, 2.3 Hz). MS *m/z*: 331 (M^++H for ^{81}Br), 329 (M^++H for ^{79}Br). HR-MS Calcd for $C_{11}H_{15}{}^{79}BrF_2O_4$: 328.0322 ($M^+$). Found: 328.0165.

(*E*)-*tert*-Butyl Ethyl 2-(3-Bromo-3,3-difluoroprop-1-enyl)isobutane-1,3-dioate (**1c**): A pale yellow oil. IR (neat) cm^{-1}: 2985, 1736, 964. ^{1}H-NMR ($CDCl_3$) δ: 1.28 (3H, t, J=7.0 Hz), 1.46 (9H, s), 1.55 (3H, s), 4.23 (4H, q, J=7.0 Hz), 5.97 (1H, dt, J=16.1, 10.1 Hz), 6.62—6.73 (1H, m). ^{19}F-NMR ($CDCl_3$) δ: −46.33 (2F, dd, J=28.7, 10.1 Hz), MS *m/z*: 257 (M^+−CO_2*tert*-Bu for ^{81}Br), 255 (M^+−CO_2*tert*-Bu for ^{79}Br). HR-MS Calcd for $C_8H_{10}{}^{79}BrF_2O_2$: 254.9832 (M^+−CO_2*tert*-Bu). Found: 254.9859.

Diethyl 2,6-Di(ethoxycarbonyl)-5,5-difluoro-2,6-dimethylhept-3-ene-1,7-dioate (7) Using the procedure similar to the general procedure for the palladium catalyzed nucleophilic substitution of BDFP, **7** (100 mg, 47% as a mixture of *E* and *Z* isomers, *E* : *Z* = 4.6 : 1) was obtained from **1b** (165 mg, 0.50 mmol) as a pale yellow oil. IR (neat) cm^{-1}: 2983, 1737, 1661, 1617, 1448, 928. ^{1}H-NMR ($CDCl_3$) δ: 1.19—1.27 (18H, m), 4.11—4.24 (8H, m), 5.82 (4.6/5.6H, dd, J=33.3, 11.5 Hz), 6.18 (1/5.6H, dd, J=22.3, 12.5 Hz) 7.02 (1/5.6H, d, J=12.5 Hz), 7.41 (4.6/5.6H, d, J=11.5 Hz). ^{19}F-NMR

($CDCl_3$) δ: −93.53 (2/5.6F, d, J=22.3 Hz), −101.16 (9.2/5.6F, d, J=33.3 Hz). *Anal.* Calcd for $C_{19}H_{28}F_2O_8$: C, 54.02; H, 6.68. Found: C, 54.24; H, 6.55.

Diethyl 2-(3,3-Difluoro-3-phenyl-1-enyl)isobutane-1,3-dioate (8) To a solution of **1b** (165 mg, 0.500 mmol), palladium acetate (3.4 mg, 0.010 mmol) and triphenylphosphine (7.9 mg, 0.030 mmol) in THF (12 ml) was added tributylphenyltin (220 mg, 0.60 mmol) in THF (4 ml) under an inert atmosphere, and the resulting mixture was heated under reflux for 24 h. The reaction mixture was poured onto a mixture of ether (30 ml) and 33% aqueous potassium fluoride (30 ml) and then the organic phase was separated. The aqueous layer was extracted with ether (30 ml×3). The combined organic phase was washed with brine, dried over anhydrous magnesium sulfate, filtered, and the solvent was removed *in vacuo*. The residue was purified using chromatography on silica gel (*n*-hexane : ethyl acetate=10 : 1) gave **8** (119 mg, 73%) as a yellow oil. IR (neat) cm^{-1}: 2984, 1735, 1674, 1452, 973. ^{1}H-NMR ($CDCl_3$) δ: 1.17 (6H, t, J=7.1 Hz), 1.51 (3H, s), 4.13 (4H, q, J=7.1 Hz), 5.84 (1H, dt, J=16.3, 9.4 Hz), 6.44 (1H, dt, J=16.3, 2.7 Hz), 7.34—7.44 (5H, m). ^{19}F-NMR ($CDCl_3$) δ: −91.68 (2F, dd, J=9.4, 2.7 Hz). MS *m/z*: 326 (M^+). HR-MS Calcd for $C_{17}H_{20}F_2O_4$: 326.1330 (M^+). Found: 326.1359.

Acknowledgement This work was supported in part by the Foundation for the Promotion of Higher Education in Toyama Prefecture.

References and Notes

1) Tozer M. J., Herpin T. F., *Tetrahedron*, **52**, 8619—8683 (1996).
2) Blackburn G. M., England D. A., Kolkmann F., *J. Chem. Soc., Chem. Commun.*, **1981**, 930—932; Blackburn G. M., Kent D. E., Kolkmann F., *J. Chem. Soc., Perkin Trans. 1*, **1984**, 1119—11125; Chambers R. D., Jaouhari R., O'Hagan D., *Tetrahedron*, **45**, 5101—5108 (1989); Blackburn G. M., Jakeman D. L., Ivory J. A., Williamson M. P., *Bioorg. Med. Chem. Lett.*, **4**, 2573—2578 (1994); Burke T. R. Jr., Smyth M. S., Otaka A., Nomizu M., Roller P. P., Wolf G., Care R., Shoelson S. E., *Biochemistry*, **33**, 6490—6494 (1994).
3) Seyferth D., Simon R. M., Sepelak D. J., Klein H. A., *J. Org. Chem.*, **45**, 2273—2274 (1980); Seyferth D., Simon R. M., Sepelak D. J., Klein H. A., *J. Am. Chem. Soc.*, **105**, 4634—4639 (1983).
4) Yang Z., Burton D. J., *J. Fluorine Chem.*, **44**, 339—343 (1989); Yang Z., Burton D. J., *J. Org. Chem.*, **56**, 1037—1041 (1991).
5) Kirihara M., Takuwa T., Takizawa S., Momose T., *Tetrahedron Lett.*, **38**, 2853—2854 (1997).
6) Tellier F., Baudry M., Sauvétre R., *Tetrahedron Lett.*, **38**, 5989—5992 (1997).
7) Shi G., Huang X., Zhang F., *Tetrahedron Lett.*, **36**, 6305—6308 (1995).
8) A similar selectivity was observed during the radical bromination of 1,1-difluoro-2-phenylthio-1-propene; Jeong I. H., Kim M. S., Kim B. T., *Synth. Commun.*, **29**, 235—241 (1999).
9) Although the fluorine atom can stabilize an α-carboradical, its stabilizing effect is very low; Smart B. E., "Organofluorine Chemistry: Principles and Commercial Applications," ed. by Banks R. E., Smart B. E., Tatlow J. C., Plenum Press, New York, 1994, pp. 57—88. The steric effect might play an important role in the radical bromination of **2**.
10) We also synthesized methyl 2-aceto-5-bromo-5,5-difluoro-2-methylpent-3-enoate (**1d**) by the radical bromination of **2b**, and confirmed that **1d** exclusively reacted with nucleophiles at the α-position to afford the 1,3-disubstituted BDFP (**13**, **14**) in the presence of the palladium catalyst. However, we could not obtain a pure sample of them (**1d**, **13**, **14**) due to their instability (Chart 10).

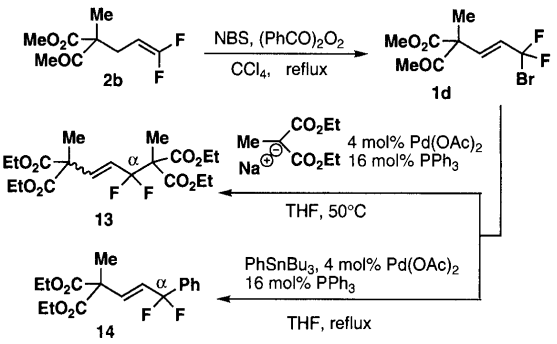

Chart 10

11) Minato A., *J. Org. Chem.*, **56**, 4052—4056 (1991).

Saponins of Plants of Panax Species Collected in Central Nepal, and Their Chemotaxonomical Significance. III.[1)]

Osamu TANAKA,*,[a] Eyong-Chae HAN,[b] Hiroyuki YAMAGUCHI,[c] Hiromichi MATSUURA,[c] Toshiyuki MURAKAMI,[d] Toshio TANIYAMA,[d] and Masayuki YOSHIKAWA[d]

Institute of Pharmaceutical Sciences, Faculty of Medicine, Hiroshima University,[a] Hiroshima 734–8551 Japan, Korea Wild Ginseng Research Institute,[b] 3RI Daegi, Wangsan, Gangnung City, 210–917 Korea, Health Care Institute of Wakunaga Pharmaceutical Co. Ltd.,[c] Shimokotachi, Kohda-cho, Takata-gun, Hiroshima 739–1195 Japan, and Kyoto Pharmaceutical University,[d] Misasagi, Yamashina-ku, Kyoto 607–8414 Japan. Received January 24, 2000; accepted February 24, 2000

***Panax pseudo-ginseng* subsp. *pseudo-ginseng* has a carrot like root with a small rhizome. It was shown that the saponin composition of roots and rhizomes of this subspecies collected in Tibet and China was extremely poor. From the roots and rhizomes collected in Central Nepal, (specimen-PNct), only a small amount of an oleanolic acid saponin, β-D-glucopyranosyl-oleanolate (2) was isolated together with a polyacetylene-alcohol, panaxynol (3). In another specimen (specimen-PNs), also collected in Central Nepal, two oleanolic acid saponins, stipleanoside R2 (4) and chikusetsusaponin IV (5) were detected. No dammarane saponin was identified in either specimen. *P. pseudo-ginseng* subsp. *himalaicus* (Subsp-H) has a big rhizome with a small round root. From rhizomes and roots of this subsp. collected in Central Nepal (specimen-HNct), a fairly large amount of dammarane saponins, ginsenosides-Rb_1 (6), -Rd (7), -Re (9) and -Rg1 (10), gypenoside XVII (8), notoginsenoside-R_1 (11), majonoside-R2 (12) and pseudo-ginsenoside-F_{11} (13) were isolated, while no oleanane saponin (oleanolic acid saponin) was identified in this subsp. Based on the present and previous studies, medicinal evaluation and chemogeographical correlation of Himalayan *Panax* spp. are discussed.**

Key words saponin; *Panax pseudo-ginseng*; Araliaceae; Himalayan *Panax*; ginsenoside; chemotaxonomy

In the Central and Eastern Himalayas, South-Western China and Japan, several wild *Panax* species which have a close taxonomical relationship with each other are found. In 1970, Hara designated these Asian wild plants as subspecies or varieties of *P. pseudo-ginseng*; *Panax pseudo-ginseng* WALL. subsp. *pseudo-ginseng* HARA (tentatively named Subsp-P), *P. pseudo-ginseng* WALL. subsp. *himalaicus* HARA (tentatively named Subsp-H), *P. pseudo-ginseng* WALL. var. *bipinatifidus* HARA, *P. pseudo-ginseng* WALL. var. *angustifolius* HARA and *P. pseudo-ginseng* WALL. subsp. *japonicus* HARA (=*P. japonicus* C. A. MEYER).[2)] Of these species, Subsp-P has a carrot-like fleshy root with a small rhizome, growing rarely in the Himalayas, while Subsp-H and most of the other Asian wild *Panax* spp. have a long developing rhizome with a small round root.

From ginseng (*P. ginseng* C. A. MEYER, North-Eastern Asia), the well-known oriental traditional medicine, a number of biologically active dammarane saponins named ginsenosides were isolated together with an oleanane saponin, ginsenoside-Ro (=chikusetsusaponin V, a glucuronide-saponin of oleanolic acid, **1**).[3)] Comparative studies on saponins of *Panax* spp. have been extensively conducted.[4—6)] It has been revealed that the saponin content of a specimen of Subsp-P collected at Nielamu, Tibet was very low.[7)] For further confirmation of the saponin composition of this subsp., the present authors have investigated the specimens of Subsp-P growing near Kathmandu, Central Nepal where Hara and coworkers collected the specimens for their taxonomical studies.

For Subsp-H, which abundantly grows in the Eastern and Central Himalayas, a close relationship between the saponin-composition and locality of plants has been observed.[1,8—18)] In order to obtain further evidence on this chemogeographical observation, the present authors have conducted isolation, identification and analysis of saponins of a specimen of Subsp-H collected near Kathmandu, Central Nepal.

Results and Discussion

Because only small amounts of materials were available, the identification was carried out only for the major saponins (content or yield: >0.01%), as in the case of previous studies on Himalayan *Panax* spp.[1,7—10)]

TLC and HPLC of extracts of Subsp-P roots with small rhizomes, collected at Chautara, near Kathmandu, Central Nepal (specimen-PNct, 34.3 g) suggested a much lower saponin content than other *Panax* spp. Repeated chromatography of this extract afforded an oleanolic acid saponin, β-D-glucopyranosyl-oleanolate (**2**, yield: 0.052%, Fig. 1) which was previously isolated from Chinese *P. japonicus* C. A. MEYER var. *angustifolius* (Burk.) CHENG et CHU[19)] *etc.*, while no ginseng major dammarane saponins, ginsenosides-Rb_1, -Rb_2, -Rc, -Rd (and their malonylated saponins), -Re and -Rg_1 were detected (Fig. 2). Together with **2**, a polyacetylene-alcohol, panaxynol[20,21)] (**3**, Fig. 1) already obtained from ginseng and several other *Panax* spp., was isolated and identified in a yield of 0.028%.

For saponins from the roots and small rhizomes of Subsp-P collected at Mt. Shioupuri near Kathmandu, Central Nepal (specimen-PNs), identification was conducted only by comparison of TLC and HPLC due to shortage of material (roots: about 12 g, rhizomes: about 0.2 g). Two oleanolic acid saponins, stipleanoside R2 (**4**) and chikusetsusaponin IV (**5**) (Fig. 1) were detected together with a trace amount of unidentified saponins. Saponin (**4**) has been isolated from the rhizomes of *P. stipleanatus* growing in South China,[22)] and compound (**5**) has been isolated from the rhizomes of Japanese *P. japonicus*[23)] and several Himalayan and Chinese *Panax* spp. The amounts of these saponins in specimen-PNs were determined by HPLC[24)]; **4**: 0.10% in roots and 0.13% in rhizomes and **5**: 0.16% in both roots and rhizomes. Ginseng

* To whom correspondence should be addressed. e-mail: shoyaku@mb.kyoto-phu.ac.jp

© 2000 Pharmaceutical Society of Japan

Table 1. Yields (%) of Major Saponins from Rhizomes of *Panax Pseudo-ginseng* subsp. *himalaicus* Collected in Central and Eastern Himalaya

	West ←						→ East
	HNg	HNcm	HNct	HNd	HBt	HBp	HBk
Dammarane saponins							
20(*S*)-Protopanaxadiol-type							
Ginsenoside-Rb_1 (**6**)	5.00*	1.70*	0.62	0.7	0.3	0.05	1.1
Ginsenoside-Rb_3 (**14**)	0.09	0.16	—	—	—	—	—
Ginsenoside-Rd (**7**)	0.94	2.20	0.20	0.1	0.2	0.07	—
Gypenoside-XVII (**8**)	0.39	0.11	0.095	0.08	—	0.03	—
Others	0.17	0.10	—	—	—	0.05	—
20(*S*)-Protopanaxatriol-type							
Ginsenoside-Re (**9**)	0.12	0.18	0.10	0.3	—	0.1	—
Ginsenoside-Rg_1 (**10**)	0.46	0.19	0.51	0.2	0.4	1.2	—
Ginsenoside-Rg_2 (**15**)	—	—	—	0.03	—	—	—
Notoginsenoside-R1 (**11**)	0.06	—	0.16	0.2	—	—	—
Notoginsenoside-R2 (**16**)	—	—	—	0.09	—	—	—
Others	—	—	—	0.02	0.1	0.02	—
Ocotillol-type							
Pseudo-ginsenoside-F_{11} (**13**)	—	—	0.036	0.01	0.07	—	—
24(*S*)-Pseudo-ginsenoside-F_{11} (**17**)	0.10	0.06	—	0.06	—	—	—
Majonoside-R2 (**12**)	0.10	—	0.19	0.1	—	—	—
Others	—	—	—	0.02	0.24	0.02	—
Dammarane saponin total	7.43	4.7	1.91	1.91	1.31	1.54	1.1
Oleanane saponins							
Chikusetsusaponin-IVa (**18**)	—	—	—	0.04	1.7	1.8	0.6
Chikusetsusaponin-IV (**5**)	—	—	—	—	—	—	0.3
Chikusetsusaponin-V (**1**)	—	—	—	0.5	0.4	0.1	7.3
Pseudo-ginsenoside-RT1 (**19**)	—	—	—	0.4	—	5.12	—
Others	—	—	—	—	—	0.12	—
Oleanane saponin total	0	0	0	0.94	2.1	7.13	8.2

Specimen-HNb[11]: collected at Ghorapani, the western foot of Mt. Annapurna, Central Nepal, altitude 2743 m. Specimen-HNcm[11]: collected at Chame, the eastern foot of Mt. Annapurna, Central Nepal, altitude 2700 m. * The quantitative HPLC analysis[24] indicated that 29% of **6** occurred as the malonyl ester, malonyl-ginsenoside-Rb_1, which was also isolated from HNg.[11] Specimen-HNct: collected at Chautara near Kathmandu, Central Nepal, altitude 3050 m. Specimen-HNd[11]: collected between Dhunche and Singkunba near Kathmandu, Central Nepal, altitude 2500 m. Specimen-HBt[10]: collected at Tzatogang, Western Bhutan, altitude 3100 m. Specimen-HBp[10] collected between Pari-la and Gasa, Western Bhutan, altitude 3550—2600 m. Specimen-HBk[8,9]: collected at Khosa, Western Bhutan, altitude 1800 m.

major dammarane saponins were not detected in roots or rhizomes.

As mentioned, Subsp-P has a carrot-like root, similar to the well-known traditional medicine, ginseng. For example, American ginseng (*P. quinquefolius* L.) and notoginseng (*P. notoginseng* (Burk.) CHEN cultivated in Yunnan, China). Previously, Subsp-P was erroneously concluded to be a wild type of notoginseng, however, the present study coupled with previous studies[7,25] confirmed that the saponin content and composition of Subsp-P are very low and poor, being clearly different from ginseng and most other *Panax* spp. This evidence suggests that this subsp. may have no ginseng-like medicinal value. Recently, DNA analysis of Himalayan and Japanese *Panax* spp. indicated that on the phylogenic tree, Subsp-P forms a separate group with a large distance from other Himalayan types, as well as Japanese types.[25] Hara's proposal (*vide supra*)[2] that all Himalayan and Japanese races must be designated as subspecies or varieties of *P. pseudo-ginseng*, should be reinvestigated.

Regarding Subsp-H, from rhizomes with small roots (total 25.3 g) collected at Chautara, Sindhu Chouk District near Kathmandu, Central Nepal (specimen-HNct), the following dammarane-saponins were isolated and identified (Table 1, Fig. 1); saponins of 20(*S*)-protopanaxadiol; ginsenosides-Rb_1[26] (**6**, yield: 0.62%) and -Rd[26] (**7**, yield: 0.20%) and gypenoside-XVII[27] (**8**, yield: 0.095%), saponins of 20(*S*)-protopanaxatriol; ginsenosides-Re[28] (**9**, yield 0.10%) and -Rg_1[29] (**10**, yield 0.51%) and notoginsenoside-R_1[30] (**11**, yield: 0.16%) and ocotillol-type saponins (Table 1); majonoside-R2[31] (**12**, yield 0.19%) and pseudo-ginsenoside-F_{11}[32] (**13**, yield 0.036%). Saponins **6**, **7**, **9** and **10** are known as the major ginseng biologically active principles, and **11** has been isolated from notoginseng and several *Panax* spp. Furthermore, the content of these saponins in specimen-HNct were quantitatively determined by HPLC analysis[33]: **6**: 0.85%, **9**: 0.25%, and **10**: 0.77% (Fig. 2). Saponin **8** has been isolated from *Gynostemma pentaphyllum* and also from several *Panax* spp. Ocotillol-type saponins, **12** and **13** have been isolated from *Panax* spp. growing wild in South-Western China and the Himalayas. It was reported that **12** was also isolated from Vietnamese ginseng (*P. vietnamensis* HA et GRUSHV.) in a yield of more than 5%,[34] and the biological activities of this saponin have been extensively investigated.[35] Oleanolic acid saponin was not isolated from this specimen.

As in the case of wild *Panax* spp. in South-Western China and Japan,[3—6] it has been disclosed that the content and composition of saponins in Subsp-H in the Himalayas are highly diverse, depending upon the locality (Table 1). It has been reported that specimens-HNg and -HNcm, collected around Mt. Annapurna, Nepal near the western limit of distribution of *Panax* spp., contain a significant amount of ginseng dammarane saponins without oleanolic acid saponin (oleanane saponin).[11] It appears that on going from the west to the east, the contents of dammarane saponins decrease, while those of oleanolic acid saponins increase. With regards a specimen collected between Dunche and Singkuba near

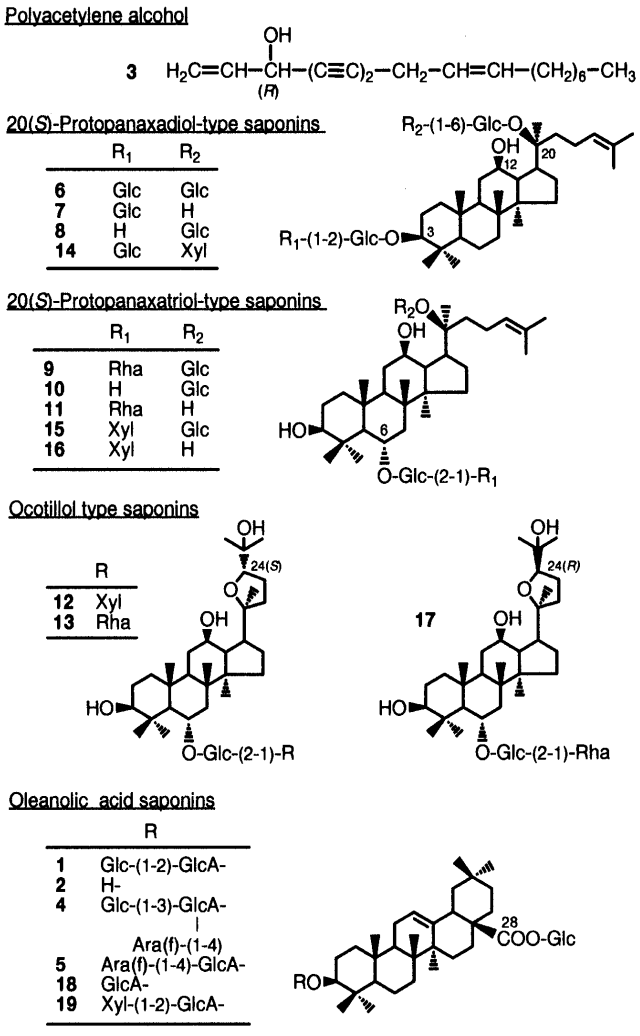

Glc: β-D-glucopyranosyl, Rha: α-L-rhamnopyranosyl, Xyl: β-D-xylopyranosyl
GlcA: β-D-glucuronyl, Ara(f): α-L-arabinofuranosyl

Fig. 1

Kathmandu (specimen-HNd in the previous study),[1] several oleanolic acid saponins such as chikusetsusaponins were isolated in a total yield of 0.94% together with a significant amount of dammarane saponins. In the present study, from specimen-HNct collected at another area near Kathmandu, dammarane saponins were identified without oleanolic acid saponin, as in the case of specimens-HNg and -Hncm. It is suggested that the areas near Kathmandu may be a chemo-geographical borderline of distribution of Subsp-H with and without oleanolic acid saponins. Comparison of the pharmacological activities of specimens-HNg and -Hncm, as well as specimens-HNct and Hnd, with those of ginseng, American ginseng, notoginseng and Vietnamese ginseng would be an attractive research subject. It should be emphasized that for utilization of these wild plants as a medicine, cultivation of the selected specimen must preserve natural resources, as well as supply sufficient amounts of medicinal materials with constant quality.

It has been demonstrated that rhizomes of Subsp-H collected in the Eastern Himalayas, the Singalila Range of Darjeeling, India[12—18] and Bhutan (specimens-HBt, -HBp and -HBk, Table 1)[8—10] contain large amounts of oleanolic acid saponins (yields: 2—8%) together with relatively small

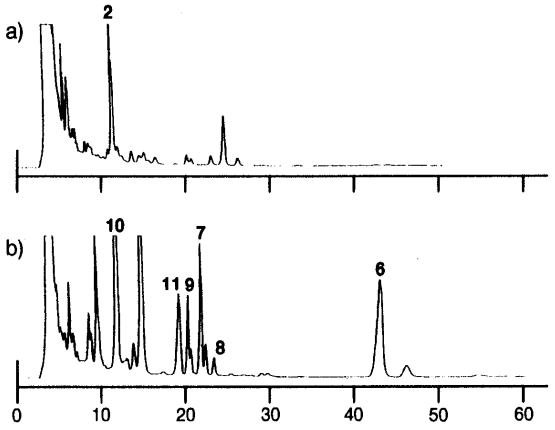

Fig. 2. HPLC Chromatogram

a) Specimen-PNct. b) Specimen-HNct. Conditions for HPLC Chromatograph: Shimadzu LC-10A; column: YMC-Pack A-612 (NH_2) (150×60 mm); mobile phase: 0.05 M phosphate buffer (pH 2.6)–CH_3CN (18 : 82); flow rate: 1.3 ml/min; detection: UV 202 nm, 0.08 AUFC.

amounts of dammarane saponins, being similar to most *Panax* spp. growing wild in South-Western China and Japan.[3—6] The pharmacological activities of these Subsp-H from the Eastern Himalayas may be similar to those of Chinese and Japanese "Chikusetsu-ninjin" (*P. japonicus*=*P. pseudo-ginseng* subsp. *himalaicus*), being different from those of ginseng. It is also suggested that *Panax* spp., specimens-HBt, -HBp and -HBk from the Eastern Himalayas may be taxonomically distinct from specimens-HNg, -HNcm and -HNct from the Central Himalayas.

Experimental

Plant Material 1) Specimen-PNct: collected at Chautara, Sindhu Chouk District (north-eastern area of Kathmandu, Nepal, elevation 3050 m) in June, 1998 by Mr. Rajan Sakya, Himalayan Herbs Collection & Conservation, P. O. Box 10949, Kathmandu, Nepal. This specimen was supplied to us by Mr. Hideo Fujii, Hideo-Fuji Co. Ltd., 4–2–34 Takatanobaba, Shinjuku-ku, Tokyo 169–0075. A voucher specimen is deposited at Himalayan Herbs Collection & Conservation. 2) Specimen-PNs: collected near the top of Mt. Shioupuri (northern area of Kathmandu, Nepal, elevation 2500 m) in August, 1988 by Dr. Eyong-Chae Han, Korea Wild Ginseng Research Institute, 3RI Daegi, Wangsan, Gangnung City, 210–917 Korea. A voucher specimen is deposited at Korea Wild Ginseng Research Institute. 3) Specimen-HNct, collected at Chautara, Sindhu Chouk District (north-eastern area of Kathmandu, Nepal, elevation 3050 m) in June, 1998 by Mr. Rajan Sakya, Himalayan Herbs Collection & Conservation. This specimen was supplied by Mr. Hideo Fujii, Hideo-Fuji Co. Ltd. A voucher specimen is deposited at Himalayan Herbs Collection & Conservation.

Isolation of 2 and 3 from Specimen-PNct The rhizomes of specimen-PNct (34.3 g, collected in Central Nepal) were cut and extracted four times with MeOH under reflux. Evaporation of the solvent under reduced pressure provided the MeOH extract (11.0 g, 32.1%). The MeOH extract (10.8 g) was partitioned into AcOEt–H_2O (1 : 1, v/v) solution. Removal of the solvent under reduced pressure from the AcOEt–soluble portion and aqueous phase yielded 1.3 g (3.8%) and 9.2 g (26.8%) of residue, respectively.

The AcOEt extract (1.2 g) was separated by normal-phase silica gel column chromatography [BW-200 (Fuji Silysia Chemical, Ltd., 100 g), *n*-hexane–AcOEt (15 : 1→10 : 1→3 : 1, v/v)→MeOH], reversed-phase silica gel column chromatography [Chromatorex ODS DM1020T (Fuji Silysia Chemical, Ltd., 15 g), MeOH–H_2O (80 : 20, v/v)→MeOH], and HPLC [MeOH–H_2O (80 : 20, v/v)] to give panaxynol (**3**, 13 mg, 0.028%).

The H_2O extract (9.2 g) was separated by reversed-phase silica gel column chromatography [1) 100 g, H_2O→MeOH→$CHCl_3$–MeOH–H_2O (6 : 4 : 1, v/v); 2) 15 g, MeOH–H_2O (60 : 40→70 : 30, v/v)→MeOH] and HPLC [YMC-Pack ODS-A (YMC Co., Ltd., 250×20 mm i.d.), MeOH–H_2O (60 : 40, v/v)] to give β-D-glucopyranosyl-oleanolate (**2**, 18 mg, 0.052%). The known compounds (**2**, **3**) were identified by comparison of authentic

samples.

Analysis of Neutral and Acidic Saponins of Rhizomes and Roots of Specimen-PNs The roots (11.906 g) was extracted 5 times with 60 ml of 70% MeOH at room temperature for 20 min and the combined extracts were concentrated to dryness below 40 °C. An aqueous suspension of the residue was chromatographed on a small column of highly porous polymer (MCI-gel CHP20P, 75—150 μm, 1×10 cm, Mitsubishi Chemical Industry) by eluting with H_2O, 40% MeOH and then MeOH (200 ml each). The MeOH eluate was concentrated to dryness and the residue (saponin fraction) was dissolved in 70% MeOH and subjected to quantitative analysis by HPLC according to the reported procedures[24]; on a ODS column, Ultron N-C18 (Chromato Packing Center, Kyoto, Japan) and on a column of Ultron NH_2 (Chromato Packing Center, Kyoto, Japan).

Qualitative analysis of saponins was carried out by TLC on Kiesel gel $60F_{254}$ (Merck) developing with H_2O saturated 1-BuOH, 1-BuOH–AcOH–H_2O (4 : 1 : 5, v/v, upper phase) or $CHCl_3$–MeOH–H_2O (65 : 35 : 10, v/v, lower phase), visualized with H_2SO_4.

Saponins in rhizomes (0.202 g) were also analyzed by the same procedures as above.

Isolation of Dammarane-Type Saponins from Specimen-HNct The rhizomes of specimen-HNct (25.3 g, collected in Central Nepal) were cut and extracted four times with MeOH under reflux. Evaporation of the solvent under reduced pressure provided the MeOH extract (7.8 g, 30.8% from natural medicine). The MeOH extract (7.5 g) was partitioned into a 1-BuOH–H_2O (1 : 1, v/v) solution. Removal of the solvent under reduced pressure from the 1-BuOH-soluble portion yielded 3.6 g (14.2%) of residue. The 1-BuOH extract (3.4 g) was subjected to normal-phase silica gel column chromatography [100 g, $CHCl_3$–MeOH–H_2O (7 : 3 : 1, lower layer→65 : 35 : 10, lower layer→6 : 4 : 1, v/v)→MeOH] to give seven fractions [fr. 1 (357 mg, 1.4%), fr. 2 (135 mg, 0.5%), fr. 3 (619 mg, 2.4%), fr. 4 (373 mg, 1.5%), fr. 5 (434 mg, 1.7%), fr. 6 (1088 mg, 4.3%), fr. 7 (387 mg, 1.5%)]. Fraction 3 (600 mg) was separated by reversed-phase silica gel column chromatography [20 g, MeOH–H_2O (1 : 1, v/v)→MeOH] and HPLC [MeOH–H_2O (60 : 40, v/v)] to give ginsenoside-Rg_1 (**10**, 128 mg, 0.51%), majonoside R2 (**12**, 47 mg, 0.19%), and pseudo-ginsenoside-F_{11} (**13**, 9 mg, 0.036%). Fraction 4 (373 mg) was separated by reversed-phase silica gel column chromatography [15 g, MeOH–H_2O (60 : 40→80 : 20, v/v)→MeOH] and HPLC [1) MeOH–H_2O (60 : 40, v/v); 2) MeOH–H_2O (85 : 15, v/v)] to give notoginsenoside-R1 (**11**, 41 mg, 0.16%), ginsenosides-Re (**9**, 26 mg, 0.10%) and -Rd (**7**, 50 mg, 0.20%), and gypenoside-XVII (**8**, 24 mg, 0.095%). Fraction 6 (600 mg) was purified by HPLC [MeOH–H_2O (75 : 25, v/v)] to give ginsenoside-Rb_1 (**6**, 156 mg, 0.62%). Those known dammarane-type saponins were identified by comparison of their physical data ($[\alpha]_D$, IR, ^{1}H-NMR, ^{13}C-NMR) with reported values and authentic samples.

Quantitative Analysis of Specimens-PNct and -HNct The method of HPLC quantitative analysis was basically the same as described in our previous paper.[33] Thus, powdered ginseng (<100 mesh, PNct 0.7897 g, HNct 0.5396 g) was extracted with 60% aqueous MeOH (20 ml) three times for 30 min. After removal of the solvent from the aqueous MeOH extracts under reduced pressure, the residue was dissolved in H_2O (10 ml) and then the water solution was subjected to Sep-Pak C18 column, which was eluted with H_2O (20 ml), 40% aqueous MeOH (20 ml), and MeOH (20 ml). The MeOH-eluted fraction was concentrated under reduced pressure and the residue was dissolved in 0.05 M phosphate buffer (pH 2.6)–CH_3CN (18 : 32, 1 ml), which was subjected to HPLC analysis. HPLC conditions: chromatograph: Shimadzu LC-10A; column: YMC-Pack A-612 (NH_2) (150×6 mm i.d.); mobile phase: 0.05 M phosphate buffer (pH 2.6)–CH_3CN (18 : 32); flow rate: 1.3 ml/min; detection: UV 202 nm, 0.08 AUFS.

Acknowledgments We are grateful Mr. Hideo Fujii, Hideo-Fuji Co. Ltd., Tokyo, Japan for kind supply of plant specimens.

References and Notes

1) Part II: Morita T., Kong Y. C., But P. P., Ng K. H., Yip T. T., Kasai R., Tanaka O., *Chem. Pharm. Bull.*, **34**, 4368—4372 (1986).
2) Hara H., *Journ. Jap. Bot.*, **45**, 197—212 (1970).
3) Tanaka O., Kasai R., "Progress in the Chemistry of Organic Natural Products," ed. by Herz W., Griesebach H., Kirby G. H., Tamm Ch., Springer-Verlag, Wien, New York, 1984, Vol. 46, pp. 1—76.
4) Tanaka O., *Pure & Appl. Chem.*, **62**, 1281—1284 (1990).
5) Tanaka O., *Gakujutsu Geppo*, **44**, 590—596 (1991).
6) Tanaka O., *Gakujutsu Geppo*, **47**, 607—614 (1994).
7) Morita T., Zhou J., Tanaka O., *Chem. Pharm. Bull.*, **34**, 4833—4835 (1986).
8) Kondo N., Shoji J., Tanaka O., *Chem. Pharm. Bull.*, **21**, 2702—2711 (1973).
9) Kondo N., Shoji J., *Chem. Pharm. Bull.*, **23**, 3282—3285 (1975).
10) Tanaka O., Morita T., Kasai R., Kinouchi J., Sanada S., Ida Y., Shoji J., *Chem. Pharm. Bull.*, **33**, 2323—2330 (1985).
11) Namba N., Matsushige K., Morita T., Tanaka O., *Chem. Pharm. Bull.*, **34**, 730—738 (1986).
12) Shukla Y. N., Thakur R. S., *Phytochemistry*, **24**, 1091—1092 (1985).
13) Shukla Y. N., Thakur R. S., *Phytochemistry*, **25**, 2201—2203 (1986).
14) Shukla Y. N., Thakur R. S., *Planta Med.*, **54**, 367—368 (1988).
15) Shukla Y. N., Thakur R. S., *Phytochemistry*, **27**, 3012—3014 (1988).
16) Shukla Y. N., *Planta Med.*, **55**, 396 (1989).
17) Shukla Y. N., Thakur R. S., *Phytochemistry*, **29**, 239—241 (1990).
18) Shukla Y. N., Thakur R. S., *Phytochemistry*, **31**, 1046—1048 (1992).
19) Wang Z., Jia Z.-J., Zhu Z.-Q., Yang C.-R., Zhou J., Kasai R., Tanaka O., *Acta Botanica Sinica*, **27**, 618—624 (1985).
20) Takahashi M., Yoshikura M., *Yakugaku Zasshi*, **86**, 1053—1056 (1966) and references cited therein.
21) Bernart M. W., Hallock Y. F., Cardellina J. H., Boyd M. R., *Tetrahedron Lett.*, **35**, 993—994 (1994).
22) Yang C.-R., Jiang Z. D., Zhou J., Kasai R., Tanaka O., *Acta Botanica Yunnanica*, **7**, 103—108 (1985).
23) Kondo N., Shoji J., Nagumo N., Komatsu N., *Yakugaku Zasshi*, **89**, 846—850 (1969).
24) Yamaguchi H., Kasai R., Matsuura H., Tanaka O., Fuwa T., *Chem. Pharm. Bull.*, **36**, 3468—3473 (1988).
25) Watanabe T., Kawaguchi K., Suzuki J., Yoshikawa T., Takano A., Isoda S., Kohda H., Malla K. J., *Natural Medicines*, **52**, 426—433 (1998).
26) Sanada S., Kondo N., Shoji J., Tanaka O., Shibata S., *Chem. Pharm. Bull.*, **22**, 421—428 (1974).
27) Takemoto T., Arihara S., Nakajima T., Okuhira M., *Yakugaku Zasshi*, **103**, 1015—1023 (1983).
28) Sanada S., Kondo N., Shoji J., Tanaka O., Shibata S., *Chem. Pharm. Bull.*, **22**, 2407—2412 (1974).
29) Nagai Y., Tanaka O., Shibata S., *Tetrahedron*, **27**, 881—892 (1971).
30) Zhou J., Wu M., Taniyasu S., Besso H., Tanaka O., Saruwatari T., Fuwa T., *Chem. Pharm. Bull.*, **29**, 2844—2850 (1981).
31) Morita T., Kasai R., Tanaka O., Zhou J., Yang T.-R., Shoji J., *Chem. Pharm. Bull.*, **30**, 4341—4346 (1982).
32) Tanaka O., Yahara S., *Phytochemistry*, **17**, 1353—1358 (1978).
33) Yoshikawa M., Fukuda Y., Hatakeyama S., Murakami N., Yamahara J., Taniyama T., Hayashi T., Kitagawa I., *Yakugaku Zasshi*, **113**, 460—467 (1993).
34) Duc N. M., Kasai R., Ohtani K., Ito A., Nham N. T., Yamasaki K., Tanaka O., *Chem. Pharm. Bull.*, **41**, 2010—2014 (1993).
35) *a*) Huong N. T. T., Matsumoto K., Yamasaki K., Duc N. M., Nham N. T., Watanabe H., *Pharmcol. Biochem. Behav.*, **57**, 285—291 (1997); *b*) Huong N. T. T., Matsumoto K., Yamasaki K., Watanabe H., *Life Sci.*, **61**, 395—402 (1997) and references cited therein.

Reactivity of an *o*-Indoloquinone to 1- and 2-Azadienes

Vania BERNARDES GÉNISSON,[a] Pascal NEBOIS,[a] Monique DOMARD,[b] and Houda FILLION*,[a]

Laboratoire de Chimie Organique[a] and Laboratoire de Chimie Physique[b], Faculté de Pharmacie, Université Claude Bernard Lyon 1, 8, Avenue Rockefeller, F-69373 Lyon Cedex 08, France.
Received January 24, 2000; accepted March 22, 2000

The cycloaddition reactions of *o*-indoloquinone 4 to azadienes are described. With 1-azadiene 2, quinone 4 works as a dienophile to give the directly aromatized cycloadduct 6. In contrast, when 2-azadiene 3 is used, the cycloaddition occurs with CO-4, indicating that this system functions as a hetero-dienophile.

Key words Diels-Alder; *o*-indoloquinone; 1-azadiene; 2-azadiene

Quinones are very interesting compounds with fascinating chemistry. Moreover, some of them are used as therapeutic agents or are recognized as enzyme cofactors or electron carriers in redox biological systems. Since the advent of the Diels-Alder reaction, *p*-quinones have been the subject of extensive investigations directed toward cycloadditions with numerous dienes.[1] In contrast, *o*-quinones have received much less attention due to their instability. Most of the cycloaddition reactions concerning *o*-quinones were performed with carbodienes.[2—5] Recently, our group was the first to show the ability of benzofuran-4,5-diones as suitable dienophiles with 2-ethoxybut-2-enal *N*,*N*-dimethylhydrazone to give the directly aromatized furoquinoline-4,5-diones.[6] In order to obtain analogues of pyrroloquinolinequinone (PQQ),[7] a redox cofactor of quinoproteins known to participate in several physiological processes, we planned to investigate the hetero Diels-Alder reactions between 1-azadienes **1**[6] or **2**[8] and 2-azadiene **3**[9] toward *o*-indoloquinone **4** (Chart 1).

The synthesis of **4** was achieved in two steps. Thus the ester **5b**[10] was readily prepared from the commercially available acid **5a** and then oxidized with Frémy's salt to give *o*-quinone **4**[11] in 85% overall yield (Chart 2). Surprisingly, the cycloaddition reaction of **4** with the electron-rich azadiene **1** attempted in tetrahydrofuran (THF) at room temperature failed. The starting quinone was completely decomposed and no trace of a cycloadduct was evident. In contrast, the use of azadiene **2** in the same conditions afforded the directly aromatized cycloadduct **6**[12] (42% yield) through a spontaneous elimination of dimethylamine. Neither a primary adduct nor a dihydro derivative was observed. The regiochemistry of **6** was assigned by analogy with the cycloadditions of electron-rich dienes and *o*-indoloquinones.[5] In order to explain this regiochemistry, we calculated the HOMO and LUMO frontier molecular orbital coefficients by the density functional theory (DFT) method with the hybrid B3LYP functional[13] using the GAUSSIAN 94 package[14] with basis set 6-31 G*. The results indicated that the larger HOMO coefficients of azadienes **1** and **2** are located at C-4, while those of the LUMO for quinone **4** are situated at C-7 (Table). Therefore, the assigned regiochemistry for compound **6** is in good agreement with calculations. In contrast, these latter cannot explain the difference in reactivity of azadienes **1** and **2** toward quinone **4**, based on their similar $3p_z$ orbital coefficient values. The failure encountered with azadiene **1** remains inexplicable.

On the other hand, the behavior of quinone **4** toward 2-azadiene **3** was completely different (Chart 2). The reaction carried out in THF at room temperature for 40 min showed on thin-layer chromatography (TLC) the disappearance of the starting material and the formation of two diastereomers which were purified by column chromatography on silica gel. When maintained for 24 hours at room temperature, they were both spontaneously converted into a single, more polar compound **7**. Structural assignment of the latter was made from its spectral data. Due to its poor solubility in $CDCl_3$, all NMR experiments were performed in dimethylsulfoxide (DMSO). The ^{1}H-NMR spectrum exhibited an AB system (6.58 and 6.26 ppm, J=9.9 Hz) and two signals at 11.08 ppm

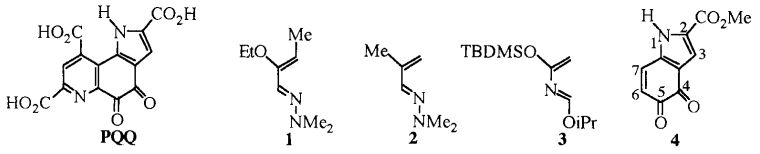

Chart 1

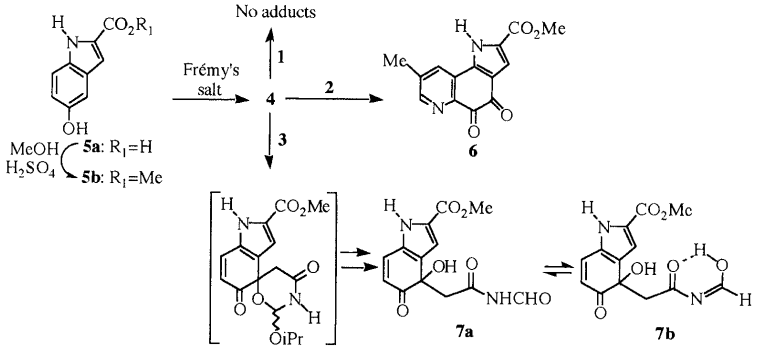

Chart 2

* To whom correspondence should be addressed. e-mail: fillion@cismsun.univ-lyon1.fr
© 2000 Pharmaceutical Society of Japan

Table 1. Frontier Molecular Orbital Coefficients of Compounds **1** to **4** Calculated by the DFT Method

		$2p_z$	$3p_z$
Azadiene **1**	N-1	0.186	0.133
(HOMO)	C-4	0.297	0.234
Azadiene **2**	N-1	0.196	0.136
(HOMO)	C-4	0.282	0.233
Azadiene **3**	C-1	0.077	0.101
(HOMO)	C-4	0.393	0.330
o-Indoloquinone **4**	C-6	0.180	0.203
(LUMO)	C-7	0.250	0.247

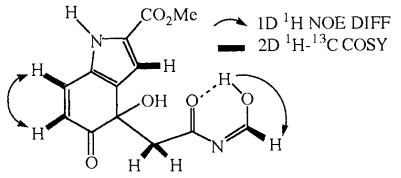

Fig. 1. 1D ^{1}H NOE DIFF and 2D ^{1}H–^{13}C COSY Correlations in **7b**

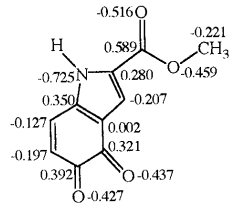

Fig. 2. Electron Densities of **4** Calculated by the DFT Method

(d, 1H, J=9.6 Hz) and 8.84 ppm (d, 1H, J=9.6 Hz). The ^{1}H-NMR spectrum with D_2O indicated the presence of three exchangeable protons at 12.54 (NH), 11.08 (N=C-OH), and 5.85 ppm (4-OH). ^{13}C-NMR distortionless enhancement by polarization transfer (DEPT) showed four CH, one CH_3, and one CH_2. We propose the structure **7b**[15] for compound **7**, since we are aware that an equilibrium exists with the imide form **7a**. It was previously reported for analogous structural produtcs that such an equilibrium is solvent dependent.[16] Therefore, in a polar solvent like DMSO, the equilibrium would be totally displaced to the enolic form **7b** which may be stabilized through an intramolecular hydrogen bonding. Then, both the 1D ^{1}H nuclear Overhauser effects difference (NOE DIFF) and 2D ^{1}H–^{13}C correlation spectroscopy (COSY) experiments are in aggreement with this structure (Fig. 1). In order to confirm this, we calculated the optimized molecular geometry of compound **7** by the semiempirical PM3 method. The calculated distances were found to be compatible with the NOE DIFF results and with the presence of the hydrogen bonding ($d_{O\cdots H}$=1.81 Å). A probable mechanism to explain the formation of **7** is that *o*-quinone **4** does not function as a carbodienophile but as a heterodienophile. Thus the activated 2-azadiene **3** adds to CO-4 of quinone **4** to give diastereomeric spiro intermediates that are not stable and open to yield compound **7**. Similar [4+2] cycloadditions on the carbonyl of a quinone were previously reported to occur between electron-rich carbodienes and *o*-benzoquinones[17] or a 2-azadiene and a naphthoquinone.[18] Calculations by the DFT method[13] of electron densities of C-4 (−0.332) and C-5 (−0.397) (Fig. 2) agree with the preferred nucleophilic attack of C-4 of azadiene **3** on C-4 of quinone **4**.

This work describes the first example of cycloaddition reactions of an *o*-indoloquinone with heterodiene systems. *o*-Quinone **4** can react either as a carbodienophile or as a heterodienophile. Moreover, its cycloaddition reaction with 1-azadiene **2** illustrates a new synthetic approach to a PQQ analogue.

References and Notes

1) For reviews on Diels-Alder reactions with quinones, see Finley K. T., "The Chemistry of Quinonoid Compounds," Vol. 2, ed. by Patai S., Rappoport Z., Wiley, New York, 1988, pp. 537—717.
2) For Diels-Alder reactions of o-benzoquinones, see (*a*) Nair V., Kumar S., *Synlett*, **1996**, 1143—1147; (*b*) Nair V., Kumar S., Tetrahedron, **55**, 11017—11026 (1999).
3) For Diels–Alder reactions of *o*-naphthoquinones, see (*a*) Fieser L. F., Dunn J. T., *J. Am. Chem. Soc.*, **59**, 1016—1021 (1937); (*b*) Bradsher C. K., Brown F. C., Leake P. H., *J. Am. Chem. Soc.*, **78**, 4400—4405 (1956); (*c*) Davies W., Ennis B. C., *J. Chem. Soc.*, **1959**, 915—918; (*d*) Paquet J., Brassard P., *Can. J. Chem.*, **67**, 1354—1358 (1989); (*e*) Lion C., Hocquaux M., Amouzegh P., Philippe M., Henrion J.-C., Caron E., Briand S., *Bull. Soc. Chim. Belg.*, **104**, 557—561 (1995); (*f*) Chernov S. V., Shul'ts E. E., Gatilov Y. V., Bagryanskaya I. Y., Tolstilov G. A., *Russ. J. Org. Chem.*, **33**, 619—631 (1997).
4) For Diels-Alder reactions of 3-methylbenzofurane-4,5-dione, see Lee J., Li J.-H., Oya S., Snyder J. K., *J. Org. Chem.*, **57**, 5301—5312 (1992) and references therein.
5) For Diels-Alder reactions of *o*-indoloquinones, see (*a*) Cai P., Snyder J. K., Chen J.-C., Fine R., Volicer L., *Tetrahedron Lett.*, **31**, 969—972 (1990); (*b*) Somei M., Fukui Y., Hasegawa M., *Heterocycles*, **41**, 2157—2160 (1995).
6) Nebois P., Cherkaoui O., Benameur L., Fillion H., Fenet B., Tetrahedron, **50**, 8457—8464 (1994).
7) (*a*) Salisbury S. A., Forrest H. S., Cruse W. B. T., Kennard O., *Nature*, **280**, 843—844 (1979); (*b*) Duine J. A., Frank J., Jr., Van Zeeland J. K., *FEBS Lett.*, 1979, **108**, 443—446 (1979).
8) Waldner A., *Helv. Chim. Acta*, **71**, 486—492 (1988).
9) (*a*) Bayard Ph., Sainte F., Beaudegnies R., Ghosez L., *Tetrahedron Lett.*, **29**, 3799—3802 (1988); (*b*) Gouverneur V., Ghosez L., *Tetrahedron Lett.*, **32**, 5349—5352 (1991); (*c*) Ghosez L., Bayard Ph., Nshimyumukiza P., Gouverneur V., Sainte F., Beaudegnies R., Rivera M., Frisque-Hesbain A.-M., Wynants C., *Tetrahedron*, **51**, 11021—11042 (1995).
10) Bergel F., Morrison A. L., *J. Chem. Soc.*, **1943**, 49.
11) The bright orange *o*-quinone **4** was very unstable over silica gel or alumina. It was used in the Diels-Alder step without purification. ^{1}H-NMR (300 MHz, DMSO-d_6) δ: 13.0 (1H, broad s), 7.32 (1H, d, J=10.0 Hz), 7.07 (1H, s), 6.2 (1H, d, J=10.0 Hz), 3.79 (3H, s). IR (KBr) cm^{-1}: 3250, 1690, 1660.
12) ^{1}H-NMR (300 MHz, DMSO-d_6) δ: 12.90 (1H, s), 8.55 (1H, s), 8.50 (1H, s), 7.16 (1H, s), 3.91 (3H, s), 2.40 (3H, s). IR (KBr) cm^{-1}: 3240, 2960, 1725, 1670, 1650.
13) (*a*) Lee C., Yang W., Parr R. G., *Phys. Rev.*, **B 37**, 785—789 (1988); (*b*) Becke A. D., *J. Chem. Phys.*, **98**, 5648—5652 (1993).
14) GAUSSIAN 94 (Revision C.3), Gaussian, Inc., Pittsburgh, PA, 1995.
15) Compound **7** was obtained in 70% yield. mp 190 °C (dec.). ^{1}H-NMR (300 MHz, DMSO-d_6) δ: 12.54 (1H, s), 11.08 (1H, d, J=9.6 Hz), 8.84 (1H, d, J=9.6 Hz), 7.02 (1H, s), 6.58 (1H, d, J=9.9 Hz), 6.26 (1H, d, J=9.9 Hz), 5.85 (1H, s), 3.81 (3H, s), 2.99 (1H, d, J=15.4 Hz), 2.79 (1H, d, J=15.4 Hz). ^{13}C-NMR (75 MHz, DMSO-d_6) δ: 193.4 (C), 170.6 (C), 162.9 (CH), 160.6 (C), 141.7(C), 140.1 (CH), 123.8 (C), 118.1 (C), 115.8 (CH), 112.2 (CH), 71.7 (C), 51.6 (CH_3), 45.7 (CH_2). IR (KBr) cm^{-1}: 3450, 3250, 3200, 2960, 1740, 1690, 1660. HRMS *m/z*: 292.0672 (Calcd for $C_{13}H_{12}O_6N_2$: 292.0695).
16) Uflyand I. E., Ryabukhin Y. I., Gorbunova M. O., Kovaleva T. V., Starikov A. G., Dimukhamedov A. I., Sheinker V. N., *J. Gen. Chem. USSR*, **60**, 1466—1472 (1990).
17) For the cycloadditions of electron-rich carbodienes to *o*-quinones to give spiropyran derivatives see: Nair V., Kumar S., *J. Chem. Soc., Perkin Trans. 1*, **1996**, 443—447 and references therein.
18) Echavarren A. M., Stille J. K., *J. Am. Chem. Soc.*, **110**, 4051—4053 (1988).